MANUFACTURING ESPIONAGE: FROM THE FRONT OFFICE TO THE FACTORY FLOOR

BY

ANKU ADHIKARI

DISSERTATION

Submitted in partial fulfillment of the requirements
for the degree of Doctor of Philosophy in Computer Science
in the Graduate College of the
University of Illinois Urbana-Champaign, 2022

Urbana, Illinois

Doctoral Committee:

Professor Marianne S. Winslett, Chair
Professor Carl A. Gunter
Professor Paris Smaragdis
Dr. Sun Sumei, Institute for Infocomm Research, A*STAR

ABSTRACT

This dissertation identifies and addresses new data security problems for manufacturing environments and their associated commercial office spaces. The work includes novel attacks and defenses for the factory floor and front office, as well as an architecture for securely sharing data all along the manufacturing supply chain.

Security needs for storing and sharing manufacturing data. Even back in 2015 when digitization was in its infancy, manufacturers already produced more data than any other sector of industry. The subsequent push toward Manufacturing 4.0, with its smart factories driven by big data, has intensified the need to extract value from manufacturing data that can drive innovation and efficiency improvements. One crucial component of this is the ability to share data securely, starting at the factory floor, continuing on up throughout the supply chain and across all the enterprises in a manufacturing federation. Any weak link in this chain of organizations constitutes a threat that can have a major negative impact for organizations all along the chain. This dissertation explains the reasons for the move towards integration of information about high-value manufactured products, and investigates how data can be retrieved securely from machines on the factory floor and converted into snapshots of data packets called "digital threads" that give fine-grained insight into the processes happening on the factory floor at any point of time. The challenge is to support secure extraction, processing, storage and secure sharing for huge amounts of manufacturing data in a trustless environment with multiple players. The dissertation outlines several key threats to digital threads that have not been fully addressed in previous work on securing provenance information, and proposes digital-threads-as-a-service (DTaaS) as a potential way to ameliorate several of the open issues. The dissertation proposes a hybrid data architecture framework to provide integrity and immutability support for managing digital threads as they are generated, stored and appropriately shared all along the supply chain, from factory floor to end user.

Side-channel vulnerabilities on factory floors. Even before the data leaves the factory floor for intended sharing and storage, the sounds made by machines on a factory floor can leak data that gives away manufacturing secrets. This dissertation explores pathways for intellectual property theft during the design and machining process of a product, and demonstrates the vulnerability through acoustic and electromagnetic side-channel attacks that can reconstruct the product design and manufacturing process for simple objects with high accuracy and precision.

Novel eavesdropping pathways in office spaces. A front office that is air-gapped and secured against traditional attacks can still be vulnerable to data exfiltration attacks. This dissertation demonstrates vulnerabilities that exist in almost all commercial buildings today as a side effect of building code requirements. In particular, the dissertation exposes a novel covert channel attack that exploits the building's own physical infrastructure to leak data throughout the building and beyond. Based on acoustic transducers, this novel audio attack supports wide bandwidth eavesdropping channels. The dissertation also proposes and experimentally evaluates several methods to defend against such an attack.

To Ama and Bua.

With your love and support, you have erased many barriers to show me the limitless skies.

To my love Danny.

For motivating me throughout this endeavor and being my strength every step of the way.

ACKNOWLEDGMENTS

I am deeply indebted to my amazing advisor Prof. Marianne Winslett, without whose guidance this endeavor would not have been possible. Prof. Winslett has countless times gone above and beyond for me, by being not just an advisor but also a mentor and inspiration. Her strong support and openness to unusual research problems has allowed me to pursue a much more adventurous path of research than I ever would have imagined.

I sincerely thank my committee members Prof. Paris Smaragdis, Prof. Carl Gunter and Dr. Sun Sumei, whose expert technical guidance and advice were vital in driving this interdisciplinary research work in the right direction. I am especially grateful to Prof. Smaragdis, who has time and again patiently addressed my many questions about audio signals and provided technical guidance and hardware design suggestions for the pipe attack. I am grateful to have had the opportunity to collaborate with Prof. Gunter in some of my research projects and publications, where he has shared security expertise and insights beyond the box. I am also thankful for the opportunity to collaborate with Dr. Sun Sumei, who organized factory visits and welcomed me to events and brainstorming sessions that have provided me with a much better understanding of smart manufacturing of the future.

I thank Prof. Andrew Singer, who generously shared his communication and information theory expertise to push the pipe attack work to completion, pointing me to theorems and algorithms I could use to gain better insights and fill in the missing pieces in the puzzle. Special thanks also goes to Prof. Douglas Jones for the vital resources, audio expertise and advice he gave us throughout the factory phone attack project and also during the design and analysis phase of the pipe attack project, giving us insight into the initial pipe results and audio equipment recommendations for system design. I am also grateful to Prof. William P. King, who headed the initial projects on manufacturing data security and took us on field trips to factories, which eventually led me down the path of investigating security problems for manufacturing spaces. Special thanks to people at Datum Tools and Manufacturing, who gave us a detailed factory tour that helped us build our case study.

I am extremely grateful to those who came forward to help us when Covid pandemic challenges closed down most buildings and brought our pipe attack research to a standstill. I deeply appreciate the generosity of Laura Kalman, who let me use her buildings to run our experiments and complete the pipe attack research. I also appreciate the help of my grand-advisor Prof. Gio Wiederhold at the beginning of the pandemic. Studying his buildings allowed us to understand pipe layouts, perform initial testing and verify attack feasibility during the early stage of the pipe attack work. I also

thank Dustin and the other helpful individuals who gave us building tours and provided access to spaces that allowed us to collect investigative data samples and understand how information moved through pipes.

I am thankful to the colleagues and interns I collaborated with during the course of my PhD. Samuel Guo made important contributions to the experimental calculations for the pipe attack project, while still an undergraduate. I learned so much from Thi Ngoc Tho Nguyen, who showed herself to be an expert coder for audio signal processing under tight deadlines during the factory phone attack project. Undergraduate intern Kushagra Madan analyzed EMF signals from factory machines, and interns Anurag Bharadwaj, Ankur Sharma and Trevor Bush did deep dives into defenses for audio attacks and automating the factory phone attack analysis. I thank Dr. Yao Chen for many useful discussions, and for his pointers during the system design stage of the pipe project. I also thank Babu Ramachandran, who advised me through the hardware design process for retrofittable sensors, including guidance on how to make them compact and thermally resistant.

Lastly but most importantly, I could not have undertaken this journey without the continued love and support of my family. My husband Danny has been my strong pillar of support, providing me with motivation, caffeination, and home-cooked nourishment, especially when I had to burn the midnight oil. My little bundle of joy, my daughter Anya who arrived in the middle of my PhD journey, has unknowingly taught me time management and given me the little push I needed to bring this dissertation to its completion. Despite their busy schedules, my sisters Anju and Aditi have jumped at any opportunity to help me, lending me their garage and yard space to build and house long pipe runs during Covid closures, babysitting my little one when deadlines approached, and ensuring that I kept up with my health and exercise. And finally, the unconditional love and support of my parents Amod (Bua) and Bina (Ama) gave me the motivation and courage to embark on this journey. To them I dedicate this dissertation.

TABLE OF CONTENTS

Chapter 1: INTRODUCTION

1.1 MANUFACTURING 4.0

We are in the midst of the fourth revolution in manufacturing in recorded history, *Manufacturing 4.0*, as illustrated in Figure 1.1. This ongoing revolution is based on the capture and analysis of data generated during the entire lifecycle of a manufactured object, from its birth among the machines on a factory floor, through its incorporation into larger products, journey to its end-users, usage, maintenance, and eventual death and disposal. The resulting succession of digital snapshots paints a complete picture of a manufactured object's lifecycle, which we call a *digital thread*. An object's digital thread can contain information about its source, design, materials that went into it, manufacturing process, quality assurance, certification and testing, purchase, usage log, and maintenance records.

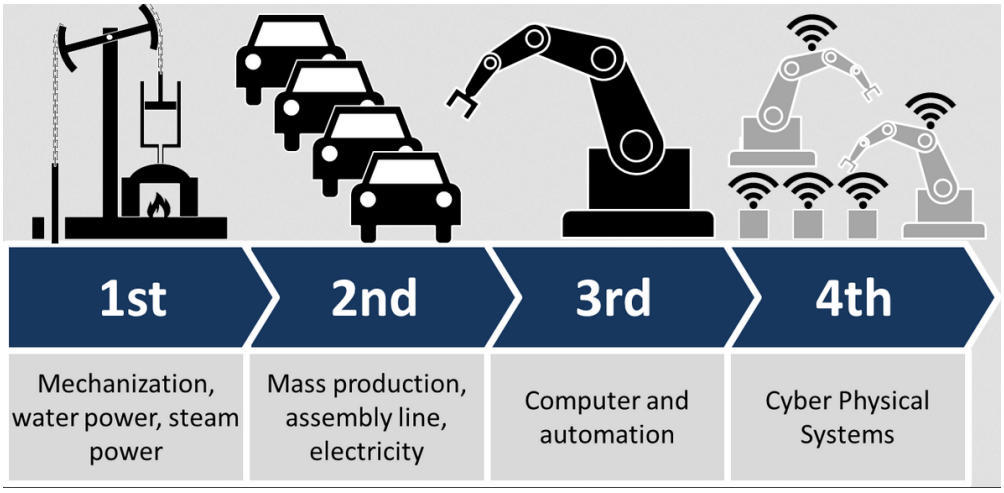

Figure 1.1: The Four Industrial Revolutions

Digital threads can be analyzed to produce insights that can improve the efficiency of a factory's manufacturing processes and the quality of the products it produces, while also reducing product design cycle time and increasing customer satisfaction. The data and its associated infrastructure can also be used to reduce human errors, deal with risks associated with rising costs and supply constraints, reduce latency in order processing and subpart movement, and improve the efficiency of outsourcing and manufacturing.

In a futuristic Manufacturing 4.0 environment, we could even envision an advanced decentralized architecture that supports contractable machines, factory floors, and/or complete business enterprises, each working as an independent business entity, bidding for contracts during downtime, and automatically processing tasks. All of these entities would work together towards an end goal

product, recording and using data generated during the process that is shared with authorized parties in the federation.

To deliver on any of these promises, Manufacturing 4.0 must capture massive amounts of data on the factory floor and as the product moves along the supply chain. To store and analyze the data, the factory's previously siloed and sequestered operational technology (OT) systems must be connected to the company's broader IT infrastructure. Further, Manufacturing 4.0 must reduce the barriers to data sharing along the supply chain, in part through the adoption of federated components such as distributed ledgers instead of centralized, monolithic information architectures.

1.2 SECURITY IMPLICATIONS OF MANUFACTURING 4.0

Today's attacks against the manufacturing sector are typically motivated by financial gain through extortion; the use, sale, or exposure of stolen data; or both. These motivations are realized through a combination of *theft*, as of intellectual property or processes; *disruption*, as of a manufacturing process; and *sabotage*, as of products or reputation [1]. The interconnection of IT and OT systems required for Manufacturing 4.0 exposes the OT systems on the factory floor to the same kinds of cybersecurity threats long faced by IT systems, which OT systems were never designed to withstand.

Cyberattacks against manufacturing were already widespread almost a decade ago: in 2014, 21% of manufacturers reported a loss of intellectual property (IP) [2]. These observed losses may have been the tip of the iceberg, as 69% of all 2012 data breaches were carried out within a few hours, but 64% of breaches took months or years to detect [3]. As Manufacturing 4.0 spread, so did the number of manufacturing cyberattacks. The Industrial Control Systems Cyber Emergency Response Team (ICS-CERT), operated by the US Department of Homeland Security, responded to 50% more incidents in the manufacturing sector in 2015 than in 2014 [4, 5]. By 2021, Fortinet's survey of OT leaders found that nine out of 10 organizations had experienced at least one intrusion in the past year, and 63% had three or more intrusions (2021 State of Operational Technology and Cybersecurity Report, available at [6]. The most common intrusions were malware (57% of surveyed OT leaders) and phishing (58%). In addition, 42% experienced insider breaches, up from 18% in 2020. These numbers will only continue to grow as the Manufacturing 4.0 revolution proceeds.

1.3 OVERVIEW OF THIS DISSERTATION

This dissertation focuses on data management and security requirements that are unique to manufacturing, though some of our results are also applicable to traditional IT environments.

Chapter 2 focuses on the security and sharing requirements for digital threads. Digital threads

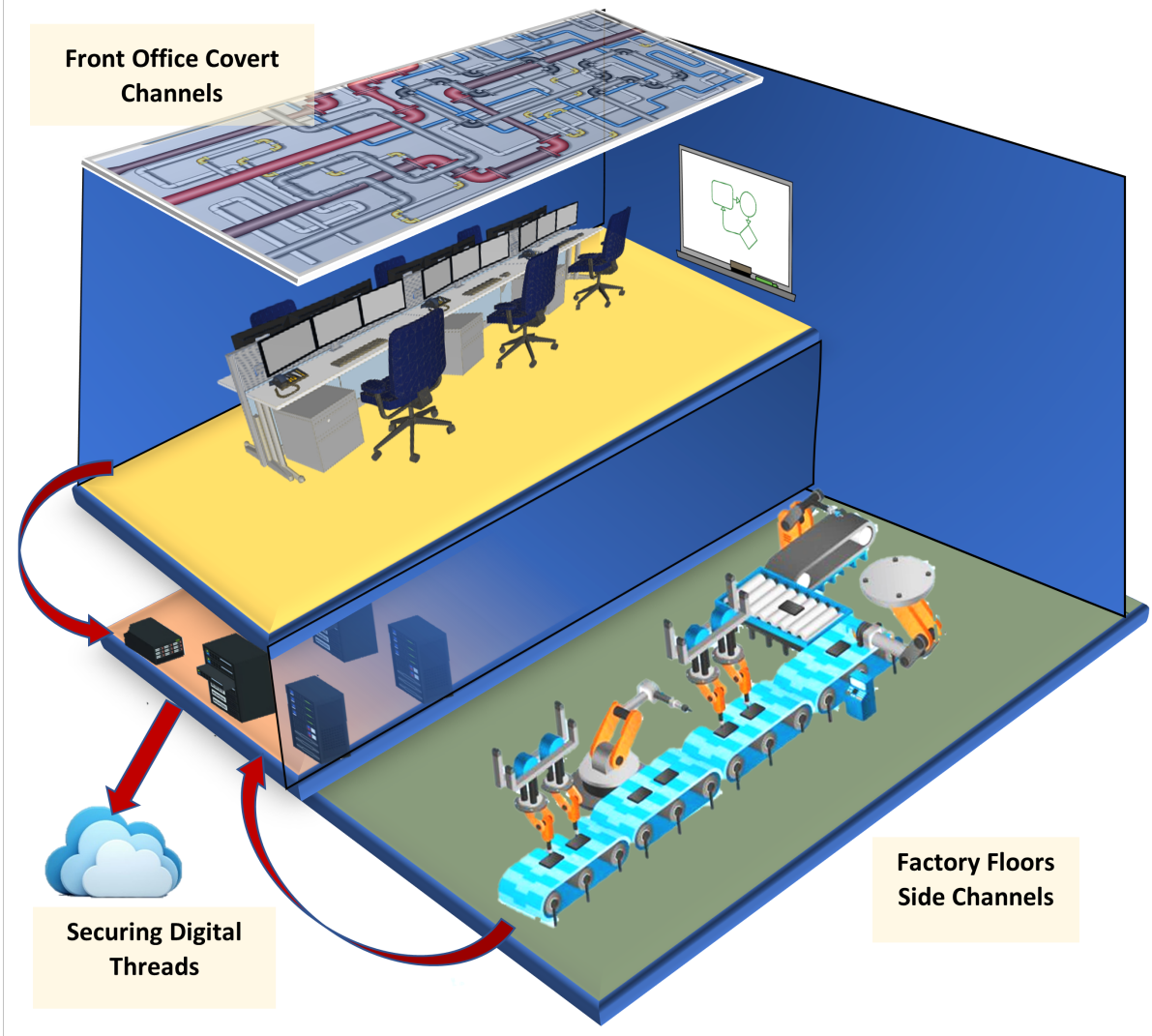

Figure 1.2: Overview of Research Focus Areas

allow stakeholders to collaborate by adding information to a thread and sharing thread information as needed with each other. The thread may be contained within an enterprise or stretch across many stakeholders who supply subparts, provide certification and testing services, or handle outsourced steps in the manufacturing process. Selected data about a particular product, production batch or an order may be shared with others within a federation as contractually required.

The data capture and management mechanism for digital threads must be fast and tightly coupled to the activity that generates the data, as otherwise it could add lag time to the manufacturing process, increase the factory down time, and reduce the factory yield. As fine-grained real-time data from real-time processes on the factory floor can reveal manufacturing intellectual property secrets,

the newly generated information must be kept safe from prying eyes while it is being transmitted from the factory floor to its long-term home, e.g., by using a secure channel or encrypting the data before transmission [7]. To appreciate the sensitivity of this data, consider that even the smallest manufacturer has its own "secret sauce", i.e., proprietary manufacturing process tricks that make its products a compelling value proposition in their market niche.

Chapter 2 analyzes the suitability of the methods available today for securely managing the wide variety of data produced by the manufacturing sector, and performs a case study of a real factory. The chapter then proposes a hybrid data management architecture based on the threats to the different types of information on the factory floor and when, how, and by whom the information is to be used. The proposed hybrid information architecture is based on decentralized blockchains, cloud-based WORM storage, and ordinary cloud storage [8], and can be retrofitted to factories as they adopt Manufacturing 4.0.

Chapter 3 examines a novel attack on factory floor data. The data that is relevant for digital threads includes not only digital communications between machines and their controllers, but also data generated by sensors attached to machines that measure aspects of the quality of the manufacturing process, using signals such as temperature, pressure, vibration, and sound. For example, consider a microphone sensor capturing sound data from a 3D printer or CNC mill. This data could be collected to support short-term predictive maintenance and likely product quality by analyzing the change in sound of moving machine parts, a technique long employed by human operators of machines of all types. However, Chapter 3 shows that this same information can reveal proprietary information with long-term value about how a high-value part was designed and manufactured [9].

Important product, design, and contractual secrets can leak from a factory's front office as well as from the factory floor. Chapter 4 demonstrates that building structure and construction elements that are required by the International Building Code can be used to exfiltrate information about sensitive business and manufacturing data. The chapter identifies novel covert channels that are present in essentially all commercial spaces, due to the pipes required in commercial buildings to transport water, gas, and other materials for manufacturing processes, fire sprinkler systems, heating and air conditioning systems, and water cooler, maintenance, and restroom plumbing. The chapter demonstrates an attack that shows how this infrastructure can be exploited to exfiltrate information from front office spaces, with high data bandwidth. The attack works regardless of whether the front office network is air-gapped, and can be implemented in a manner that is almost undetectable by traditional bug-sweeping methods.

Chapter 5 presents our conclusions and directions for future work.

Chapter 2: SECURE STORAGE AND SHARING OF MANUFACTURING DATA

In this chapter, we discuss the essential characteristics of digital threads and present examples of how analysis of digital threads can be used to benefit manufacturers. We describe how data flowing through machines and processes within a factory and collaborators within the manufacturing federation can have different features and use cases and propose a classification system for that data. We analyze the suitability of the methods available today for securely managing data produced by the manufacturing sector, through the lens of a case study of a real factory. We also propose a hybrid data architecture based on how different types of manufacturing data are stored, used, and shared, with an eye to the needs of the long tail of small and medium manufacturing enterprises.

2.1 DIGITAL THREADS

Manufacturing is widely viewed as being far behind the state of the art in terms of information technology (IT) capabilities and usage. In spite of this lag, in 2011 manufacturing already generated more data each year than any other sector of the US economy, and manufacturing's data volume has increased sharply since then [10]. The upward trend occurs because major manufacturers of high-value products all around the globe have determined that it is worthwhile to collect extensive data about the way that their products are designed, made, used, and maintained. The manufacturers can analyze this data to devise improvements to their designs and processes, reduce time to market, and radically improve the efficiency and effectiveness of their operations and the value of their products.

As a running example, consider a representative airplane built by Alice's Aircraft, an imaginary competitor to Boeing, Lockheed, and Airbus. Each plane produced by Alice's Aircraft has over a million individual parts made in thousands of factories, some of which belong to large companies with professional IT security staff, but many of which are mom-and-pop specialty vendors with special manufacturing expertise but minimal IT expertise and little or no understanding of IT security issues. The design of the plane itself is a many-year process that produces extensive data, from the specification and design of individual pieces through to simulation codes and test results. The manufacture of most parts of the plane will be contracted out to other vendors, who in turn choose their own vendors for subparts. Each high-value part of the plane is associated with information about its design, manufacture, transport, and usage in the plane. Instrumentation continually generates data about the life of the key parts of the plane during the plane's initial testing and subsequent flights.

The airplane's usage data is already used today to help guide maintenance, and the maintenance

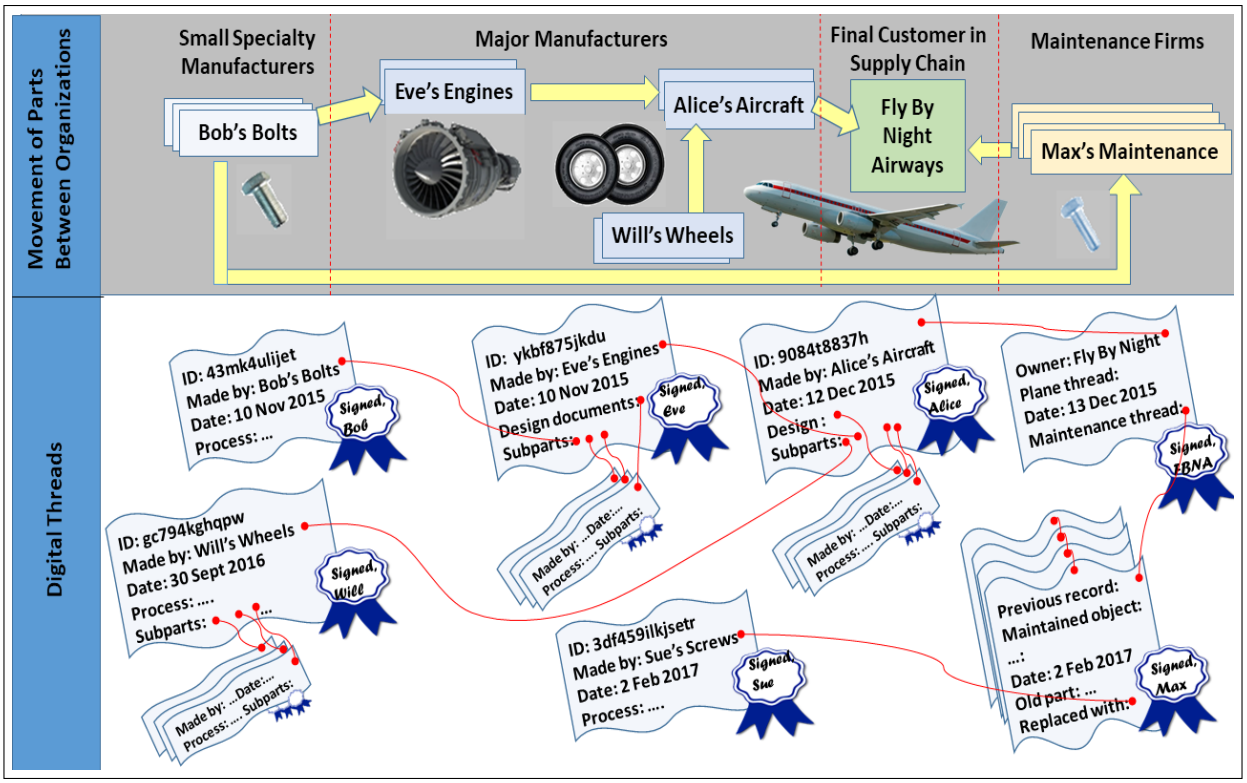

Figure 2.1: Digital threads generated during product lifecycle of a plane

process generates yet more data about the parts of the plane. But the airplane's designers and part manufacturers know relatively little about how their products are actually used and how well they bear up under usage. In part, this is because information captured during a product's deployment and maintenance is not automatically fed back to the original designers of the product and its subparts. Major manufacturers recognize that this extensive information could be used proactively to help identify and correct defects and make improvements, and could be used to guide the next generation of design. These data analytics can potentially produce such compelling cost savings and product improvement opportunities that major manufacturers are now working to integrate this information throughout each high-value manufactured item's lifetime, across all of its subparts (see, e.g., [11]).

The collection of all this life history information for an atomic part is called its digital thread. The digital thread for a more complex part, such as an engine, consists of the life history information about the engine as a whole, plus the digital threads for all its subparts. When appropriately secured and shared, a digital thread can provide indisputable accountability information linking factories to their products and prevent stakeholder disputes in supply chain; allow stakeholders to distinguish counterfeit goods from originals; and support forensic investigations by providing a traceable record with manufacturing settings for a part that fails.

2.1.1 Information in a Digital Thread

Consider a particular plane that Fly By Night Airways has purchased from Alice's Aircraft. Suppose that vendor Eve's Engines wins the contract to build the plane's engines, and Eve contracts out the manufacture of a specialty bolt in the engine assembly to a small company, Bob's Bolts. As shown in Figure 2.1, the plane's digital thread includes information generated during design, manufacturing, usage, and maintenance. The design-related information in the thread may include multiple versions of requirements documents, specifications, design documents, change orders, simulation code, and simulation results. These documents will primarily be generated in the offices of companies with well-trained IT staff. Information generated for the plane's digital thread during manufacturing comes primarily from machines on the factory floor, describing the physical objects produced and assembled there and the process used to accomplish that. For example, if the machines on Bob's factory floor are of recent vintage, they will spew forth detailed information about the manufacturing process used on each machine for each bolt. If the machines are old – thirty year old machines are not at all uncommon – Bob may have attached sensors to them to capture similar information. The digital thread for a part may also include information about the logistics of the movement of the completed part from the factory to its customer. Similarly, an engine's thread describes how it was assembled from its subparts on Eve's factory floor. This elaboration of threads continues all the way up the supply chain until the completed plane itself is delivered to Fly By Night. The factory floors are likely to have rudimentary IT security at best, for reasons discussed below, and small companies like Bob's Bolts are unlikely to employ any IT professionals at all. After delivery, the plane's thread continues to grow. Sensors will automatically capture and record extensive usage information during the plane's flights, throughout the many years of the plane's deployment. Fly By Night will own this usage data, parts of which it will want to share with its local maintenance contractor, Max's Maintenance. Max's records show what was done to the plane, along with why, when, where, how, and by whom. Throughout the plane's lifetime, Max will replace and upgrade old parts; each new part will come with its own thread, so that new subthreads will be continually be added to the plane's thread. While some parts of the thread may reach the end of their useful lifetime, so that it is appropriate to delete them, most of the thread must remain available for the entire lifetime of the plane.

2.1.2 Analytics for Digital Thread Data

Big data aficionados will immediately imagine potential uses of data analytics for digital threads. For example, Fly By Night pays for the plane's maintenance and hence has a high incentive to reduce these costs. Guided by data analytics, Fly By Night can pressure Alice's Aircraft and its

suppliers to help it achieve this goal, by altering designs and manufacturing processes as appropriate. For example, which bolt suppliers' products are failing fastest in a given location in an engine? Is there evidence that this failure is due to a bad batch of bolts from that supplier, which should be proactively replaced? If so, Eve's Engines might want to query the digital threads of her engines to identify the current locations in all her engines of the bolts made by that supplier on that date. Or are all suppliers' bolts failing prematurely in that engine location, perhaps indicating a vibration problem that needs to be addressed by altering the design of that part of the engine, and by increasing the frequency at which maintenance replaces the bolts in that location in engines with the old design? As another example taken from existing state-of-the-art aircraft maintenance: are there patterns of sensor readings during flight that indicate that a particular engine part is going to fail soon and should be replaced proactively? As a security-oriented example, if it becomes known that a particular version of the firmware for a specific factory floor machine was compromised, Fly By Night Air could query the threads for its planes to find out which of them currently contain parts that were made by machines that had that version of the firmware, and take appropriate remedial action. Support for sophisticated analytics like these examples requires a big-data approach.

2.1.3 Digital Thread Challenges

The potential advantages of being able to support analytics over digital threads are impressive, but two major hurdles stand in the way: lack of standards for information representation and access, and problems with trustworthiness.

Standard Information Representation Much of the information that constitutes a digital thread is already being collected today in a haphazard and piecemeal manner, but it is not being made available across different phases of a part's lifetime, across organizational boundaries, or in an appropriate format. To realize the analytics potential of digital threads, once the information in a subthread is generated, it must be stored for the lifetime of its parent thread in such a manner that appropriate parties can find it and use it in analytics. There are no standards yet for what information must be included in a thread, what format the information should be in, or how to find particular information, and hence no way to perform the kind of analytics described above. A systematic, efficient way to search through threads in a highly distributed environment is required, and some portion of thread contents should be represented in such a way that at least one major current analytics paradigm (SQL, map-reduce, statistical packages) can be applied to key parts of the thread contents. Major manufacturers like Alice's Aircraft are moving towards specifying such standards internally, and requiring their vendors to comply with them and share the data. Small manufacturers like Bob's Bolts want to avoid a balkanization of standards, i.e., being required to

supply slightly different information in a different format to every customer, as that would be a nightmare for a small company with little IT expertise. Manufacturers are beginning to discuss sector-wide standards for what information to include in a thread and how to represent it, through forums such as the Digital Manufacturing & Design Innovation Institute (dmdii.uilabs.org) and NIST's digital thread efforts (see www.nist.gov/el/msid/infotest/digital-thread-manufacturing.cfm).

Trustworthiness Use of digital threads will expose manufacturers and their customers to additional threats [12]. Already in 2014, the manufacturing sector was the target of 27% of cyberattacks, which is the second highest among critical infrastructure sectors [13]. For reasons explained below, the factory floor is the weakest link in terms of manufacturers' IT security, so attacks will continue to rise as more factories connect their industrial control systems to the internet; the current attack rate was up from 5% and 15% of cyberattacks in 2010 and 2013, respectively [14] [15]. To clarify the current extent of connectivity as of 2014: Bob's Bolts probably received Eve's bolt spec by fax.

Manufacturers' biggest trust-related concern about digital threads is confidentiality, i.e., theft of intellectual property, which is already rampant for high-value parts. As one example, during the maiden flight of the first F35 aircraft, all data generated during the flight was stolen in real time, along with the operating system for the plane [16]. The theft could allow rival manufacturers to duplicate the product without the high expense of first designing it, and could also pose a threat to the plane's future operations, by making its code available up front to attackers for an analysis of potential vulnerabilities.

Easier access to digital thread information could make critical design and manufacturing information easier to steal. As one example, the manufacturing spec for any subpart implicitly gives some information about the part it fits into. If an adversary obtains enough information about engine subparts, the adversary starts to understand the engine itself. Thus by stealing subpart thread information from many small manufacturers like Bob with poor IT security, an attacker can learn a lot about a more heavily guarded part like an engine.

Bob also has information he does not want stolen. Every manufacturer has some sort of secret sauce, a kind of manufacturing process savvy that is their competitive advantage. In Bob's case, this might be the settings on his factory floor machines, the exact composition of materials, and the exact series of steps taken to produce each bolt. In theory, all this information should go into the thread. For Bob, it is critical that such details not reach his competitors, either directly or via casual comments from his customers or his own suppliers, throughout the lifetime of the thread.

Eve can freely choose her suppliers. She would not want her competitors to know who her suppliers are, and in general, Alice's Aircraft does not have the right to learn who Eve's suppliers are. Yet as we have seen, there can be legitimate reasons for Alice, Fly By Night, or Max's Maintenance to want to do analytics over parts of plane threads that might directly or implicitly

identify Eve's and Bob's suppliers and customers.

More generally, guidelines for which company's analytics tasks should be allowed to see which parts of a thread are murky at best. For example, consider the question of which bolts are failing prematurely, as determined by maintenance records. Eve's engines may be sold to many companies and maintained not just by Max, but by a patchwork of different companies at different airports. If Eve can see records from all of them, she will learn a lot about the practices of the competitors of Fly By Night and Max, which she might leak to them. If Eve also manufactures other products (e.g., bolts), the maintenance records for her engines may leak information about her competitors in those product lines. These concerns arise whenever thread information is shared across organizational boundaries, not just in the case of maintenance.

Though confidentiality is currently their greatest concern, manufacturers are aware that it is important that the information in digital threads be trustworthy in other ways. When thread information is generated, it must be correctly and completely captured, including metadata, and stored properly. As one example, often high-value parts are repeatedly measured by machines on the factory floor as they are produced; if threads contain incorrect measurements, that could cause havoc on the factory floor or when parts reach their customers. Once stored, the information in the thread must be protected against tampering and destruction, and must be easily available when needed. Since many manufactured parts are long-lived, the digital thread must be appropriately secured against bit rot and key compromise. Finally, there should be ways to audit compliance with all of the above, without compromising confidentiality.

2.2 UNIQUE THREATS FOR DIGITAL THREADS

2.2.1 Managing Provenance Information

A digital thread provides provenance information, i.e., information about where an object comes from. The computer science research community has a long-term interest in managing provenance information, including two annual forums on that topic (Theory and Practice of Provenance (TAPP), and International Provenance and Annotation Workshop (IPAW)).

Digital threads share many of the characteristics of other types of provenance information: the threads are read-and-append-only; the thread for a particular object can be thought of as forming a directed acyclic graph; and threads can contain highly heterogeneous types of information coming from many different organizations. Digital threads differ in that traditional provenance research has focused primarily on how to record and manage the provenance of digital artifacts, such as computer logs and the data products resulting from scientific workflows.

However, because high-value manufactured objects are uniquely identifiable, the impact of moving from digital objects to physical objects is less than one might expect. Many of the digital thread trustworthiness issues outlined above are issues for other types of provenance information, and solutions have already been proposed for many of them. For example, researchers recognize that all provenance information should be correctly, completely and efficiently captured when generated [17, 18], and have proposed techniques to protect captured provenance information against tampering and forgery [19, 20]. Researchers also recognize the complexity of the confidentiality and authorization policies that will be needed for provenance information, and the information-flow-related challenge of determining whether a particular data access can inappropriately leak information about provenance or vice versa [21, 22, 23]. Some researchers argue that the potential heterogeneity and complexity of provenance information and their associated confidentiality requirements may be best handled by using semantic web techniques [22, 24]. Researchers have also proposed systems to support reasoning about provenance information and the systems that manage it [25] and have devised an approach for secure tracking of manufactured goods during transport [26].

2.2.2 Factory Floor Vulnerabilities

The biggest challenge not addressed by previous work on making provenance information trustworthy is how to secure the factory floor so that thread-related information cannot be altered or stolen once it has been generated. Major manufacturers employ experts in IT security, who understand office environments well but have minimal understanding of the role of IT's counterpart on the factory floor, Operational Technology (OT), and what the security issues are there. (The long tail of important small manufacturers is even worse off.)

As one example, designs are normally transmitted to factory floor machines in the clear, without a digital signature [27]. Thus any tampering with the transmitted design will not be detected, and designs can be stolen by eavesdroppers. As another example, thread information may lie around in multiple places for long periods, expanding the window of vulnerability for inappropriate disclosure.

A second challenge in securing the factory floor stems from manufacturers' aversion to any disruption of factory floor operations. Every minute that an operating factory line must be shut down represents a financial loss for the manufacturer. The result is an "if it ain't broke, don't fix it" attitude. For this reason, software on the factory floor, including the PCs attached to modern factory floor equipment, is rarely if ever patched or upgraded [12]. This attitude will change once the cost of disrupting operations to update software clearly exceeds the expected costs of not doing so; how to update in a way that minimizes downtime is an interesting open question.

Another result of aversion to production delays is that when a machine on the factory floor

breaks down, often it is accessed remotely over the internet to speed up repair. Remote access is an attractive opportunity for an attacker. An on-site visit for repair is hardly better, as the PC controller for a machine generally has a single password, which is likely to be taped to the screen. Thus a casual walk across the factory floor can reveal passwords for many machines. Further, the repair process may begin with the insertion of a USB device, bringing any sort of malware with it.

Major manufacturers are very aware of Stuxnet [28], and are quite concerned over the possibility of malware getting into the firmware of their machines and destroying the machines, thereby shutting down factory lines for lengthy periods. They are also aware that repair of factory floor machines is a potential vector for introduction of such malware, and current repair practices pose a security risk. Major manufacturers are particularly concerned about the vulnerability of their smaller suppliers. The design of trustworthy approaches to rapid repair and trustworthy, user-friendly factory OT environments are open problems.

Overall, attitudes among manufacturers in 2014, when this chapter was first drafted, were reminiscent of those in the electrical power grid community a decade or so earlier. That community has made major changes since vulnerabilities of SCADA systems became well known [29] and power companies had to pay ransom to avoid blackouts [30]. Since 2014, the manufacturing community has begun to evolve under similar pressures.

2.2.3 Access Control and Confidentiality

The second unaddressed threat for digital thread trustworthiness lies in confidentiality. Previous work has recognized [21] and addressed the problem of ensuring that only certain parties can examine particular parts of a digital thread [19]. But the extent of the need for fine-grained control, the need to support currently unanticipated uses, the strong requirement for usability, the many organizations accessing the thread, and the inherent conflicts of interest in many of these organizations mean that it will be very hard for the owner of a piece of information in the thread to settle on a reasonable authorization policy or keep that policy up to date. It would be unrealistic to assume that small manufacturers could correctly set up and use, for example, a public key infrastructure with attribute-based security to control future access to thread data they generate. Designing a scalable and user-friendly solution to this issue remains an open problem.

2.3 CASE STUDY

2.3.1 Datum Tool & Manufacturing Today

Our case study is based on Datum Tool & Manufacturing (datumtoolandmanufacturing.com)

Figure 2.2: Snapshots of a factory: Datum Tools & Manufacturing

in South Elgin, Illinois. This 33-year-old company is a full service machine shop that specializes in precision machining of specialty parts made of metal, such as valves, end caps, and nozzles. Like other small US family-owned machine shops, the company has automated tools and computational support but no cyber-physical or data analytics support beyond what is built into individual factory floor machines. We refer to the company today as Datum 3.0.

Through factory visits and interactions with the owner and employees, we gained a high level understanding of Datum 3.0's data flows and processes. Figure 2.2 shows several internal process stations at Datum 3.0, as well as processes that are outsourced to other factories they cooperate with. In brief, raw materials are procured and stored until needed for an order (1). Then they go through an iterative process of material removal that includes cutting to length, turning on a lathe and milling (both computer-controlled), grinding, and finally polishing (2-5, 7). The next step is heat treatment and plating, which are outsourced to another company (6). In-progress orders are tracked and moved between stations manually (8), and measurement to check whether a part is within tolerances is also manual. Protective waxing (9) is the final step before packing and shipping (10); the product is also shipped to and from the outsourced plating service.

Like most other long-lived machine shops, Datum 3.0 has recurrent similar orders from another business/factory, and most of Datum 3.0's orders come from a subset of their regular customers.

2.3.2 Datum 4.0 in the Future

When Manufacturing 4.0 technology becomes cost-effective for small manufacturers, we can imagine automated movement of material between process stations, automated measurement, and/or

automated tracking of the progress of orders. Automated just-in-time ordering of materials could be done in the background based on analytics over the digital thread, by predicting likely reorders based on order histories. Analytics could potentially help to schedule tasks to machines more efficiently as well.

On the IoT side, sensors on the factory floor machines could detect from audio when bits and other cutting and grinding edges are getting dull, even before a human can recognize the change in sound or a low-quality pass through the machine has been made. As another example, we have been told that an expert human can tell from the sound a machine makes how high quality the part will be that it produces, e.g., how close to tolerances. Perhaps an automated version of this analysis could trace back the causes of poor performance, using the classic indicators of audio and vibration. Audio and vibration could also be used to detect future failures before they occur, so that, for example, predictive maintenance could allow an out-of-calibration problem to be fixed before it causes down time and delays order delivery.

2.3.3 Data Features and Use Cases

Manufacturing is a diverse sector and the data that must be collected for sharing and analytics can vary based on the use case and the data features. The best way to handle a particular kind of data generated at a factory will depend on its size, arrival rate, threat model, how often it will be read and by whom, its anticipated lifetime, the information technology capabilities and infrastructure of the factory, and the cost and benefits of outsourcing data storage and/or analytics. The following data features are key determining factors in evaluating the suitability of particular data management solutions:

1. Granularity of data
2. Volume of data
3. Access controls (whether the data is only visible internally within the manufacturer, or externally visible to certain parties)
4. Read/write/update process and frequency
5. Storage ownership, volatility and availability
6. Threat model for security and privacy (within the company or externally within a federation)

The discussion that follows is based on six use cases for Datum 4.0, which we characterize in terms of these attributes:

- UC2.1: *Microphones and/or accelerometers near moving machine parts, for predictive maintenance analytics based on audio and/or vibration.* Very high volume and velocity; short read-once lifetime unless being used to train a new predictive maintenance model; internal access; as a side channel, can leak manufacturing IP, design IP, factory activities.

- UC2.2: *Thermometer senses 3D printer bed temperature, to support the quality assurance certification that the product was processed without exceeding a certain temperature.* Low to medium volume and velocity; very long read-once lifetime if contractually required for forensic purposes; internal or external access; side-channel leak of proprietary information, potential motivation to tamper.

- UC2.3: *Minute angle readings from a CNC mill as it grinds through raw metal to shape a bolt, for correlation with usage data about bolt lifetimes and eventual analytics for process improvement.* Very high volume and velocity; very long read-once lifetime; internal access; side-channel leak of proprietary information.

- UC2.4: *Tagging of raw material source and composition as part of a complete digital thread verifying source and supporting certification requirements to satisfy contractual terms of a many-part product manufactured by a federation.* Low volume and velocity; very long read-multiple lifetime; internal and external access within federation; incentives for tampering and theft (supplier information can be very attractive to competitors).

- UC2.5: *Product measurements for/from outsourcing,* as in the outsourced chrome treatment step (8) in Figure 2.2, to help both parties verify that the correct thickness of chrome was applied. Low volume and velocity, short read-rarely lifetime, access by two parties; incentives for tampering and perhaps for theft.

- UC2.6: *Product shipment tracking, for verifiable delivery.* Low volume and velocity, long read-rarely lifetime, access by three or more parties, modest incentives for tampering and theft (reveals customer names to competitors).

The distinction between data that is only internally visible within a manufacturer and data that is externally visible is fundamental for storage and handling. Externally visible data is made available to one or more members of the manufacturing federation such as logistics companies, suppliers of materials and services, customers, customers' customers, and so forth, as contractually or legally required, while other data is not made visible. In fact, many other key data characteristics tend to divide along the internal/external visibility line.

In general, tampering is a low-level threat for data that is only visible internally; when such tampering occurs, it is most likely attributable to human error or a malicious insider. Data that

is only visible internally often can reveal IP, so theft is a concern. Internal-only data includes much high-volume, high-velocity data that can be fed into analytics models (read-once) or used to construct them (read-multiple).

Typical internal-only data includes fine-grained sensor data used for predictive maintenance and process improvement, as in UC2.1 and UC2.3; such data provides a fine-grained snapshot of sensitive factory floor processes at each moment.

There is no need for expensive, high-end approaches to protect internal-only data against tampering, and repudiation is not an issue. This suggests that simple, readily available approaches to ensure confidentiality while also providing access for analytics are best. The most inexpensive approach is to consume the data immediately on a well-secured machine in immediate proximity to the factory floor, and then discard the data, but this is impractical for most manufacturers, for two reasons. Most manufacturers do not patch or update their computer software, both because patches often lead to factory downtime, and because no patches are available for old heavy machinery software anyway. Further, most manufacturers do not use authentication facilities to limit access to computers on the factory floor, as quick access by a variety of people is often needed. Eventually proximity badges may help with this problem, but not until the authentication system is seamlessly integrated with the factory floor software.

If the value of sensor side-channel information to competitors is significant, then it is better to use cloud-based storage and services for data that is intended to be only visible internally, even though a large volume of data must be transmitted. Even ordinary cloud storage and services will provide better facilities to ensure confidentiality than most small manufacturers can provide. The data must be kept private during transmission, e.g., by using a secure channel.

Use cases UC2.2 and UC2.4-6 involve externally-visible data, i.e., information that the factory has agreed to share with its collaborators. In all four of these use cases, there is a significant incentive for tampering to avoid blame from collaborators when things go wrong.

For use cases UC2.4, UC2.5 and UC2.6, since the data is likely to be of low volume and velocity, data management methods that provide distributed trustworthy information sharing, such as blockchains, can be considered. For example, suppose Datum receives a shipment of steel bars under UC2.4. Datum can record this fact and the provenance of the shipment on a blockchain. If the shipper and supplier have entered their own information about the shipment on the same or other blockchains, then Datum can verify those entries and reference them in its own entry.

In UC2.6, the product shipment tracking data volume from any single manufacturer will be low, but the aggregate volume across all customers of a shipper may be very high. Given that the threat levels are relatively low, a blockchain-based approach seems too expensive. We prefer to see a system like that provided by shippers today, where anyone possessing an appropriate token can see the logistics details for the order associated with that token. These systems are based on traditional

database management technology. If data integrity and availability are of high concern, the shipper could charge an additional small fee to guarantee data availability for a fixed period of time, e.g., by archiving the records on WORM storage for a fixed period of time.

For UC2.5, in theory Datum can record on a blockchain the dimensions of the product being sent for plating. In theory, the plating company can do the same when it completes the order and ships it back; and a smart contract could automate payment when the shipment is received. However, the recipient of shipped goods may dispute that the posted measurements actually correspond to the shipment received, and the blockchain cannot resolve this problem.

Further, if the order is large then the volume of data may be too high to be practical for a blockchain. Also, Datum may not wish to make its product's dimensional data visible to others. The computer security community has a bag of tricks for this situation, such as zero-knowledge proofs and other forms of secure multi-party computation, but it is not clear that they would be a cost-effective solution to this problem. We return to these points in the next use case.

UC2.2 is particularly interesting, as it combines high volume and velocity with integrity and availability concerns for temperature data. Putting the data on the blockchain would address the latter two concerns, even if the manufacturer closes its doors tomorrow, but is impractical for scalability reasons.

We propose a hybrid solution: the data itself can go on low-cost cloud-based WORM storage owned by the manufacturer, while a token corresponding to the data can be included on the blockchain. The token leaks minimal information about the manufacturing process, allaying potential confidentiality concerns. Upon conditions that can also be spelled out in the blockchain, certain parties have the contractual right to present the token to the manufacturer and be given access to the data.

2.4 DATA ARCHITECTURE FOR SECURE MANAGEMENT OF DIGITAL THREADS

In this section, we propose a hybrid data architecture based on how different types of manufacturing data are stored, used, and shared, with an eye to the needs of the long tail of small and medium manufacturing enterprises. The resulting three tier architecture includes a tier of conventional cloud-based storage and services for high-volume, high-velocity, short-lifetime, sensitive data typified by sensor data from the factory floor. A second tier uses blockchains for low-volume data that must be shared with others, has a long lifetime, and may have high incentives for tampering. The third tier is for high-volume long-lifetime sensitive data that is sensitive, must be shared, and may have high incentives for tampering. This tier employs cloud WORM storage for the data itself, plus a blockchain entry that includes a token allowing retrieval of information from the WORM if

certain specified conditions are met.

We point out shortcomings in the technology available today for realizing our proposed hybrid architecture. In particular, we identify a need for low-cost IoT-based systems to capture, identify, preprocess, encrypt and transmit factory floor data to the corresponding data storage subsystem. Our proof-of-concept design and implementation focuses on practical, cost-effective data capture systems for all three tiers, and can be easily retrofitted to today's factories.

2.4.1 Related Data Management Technologies

The Linux Foundation's open-source Hyperledger data management framework for manufacturing is based on blockchain technology [31]. The Hyperledger initiative is in its early stages and has so far, through protocols such as Hyperledger Fabric, addressed limited use case scenarios [32], focusing mainly on data that is shared in the supply chain. Such data and its threat model are a good match for blockchains, but shared supply chain data is only a small portion of a digital thread.

Much other fine-grained data from a factory floor can be valuable for manufacturing analytics, but is a poor match for blockchains, due to its volume, velocity, and mismatch with the blockchain threat model. Even with scalability improvements with modifications such as BitCoin-NG, yet bottlenecks still lie in the network diameter size and node processing power [33]. Further, much factory-floor data is of interest only to the factory and will never be shared with others, making the non-repudiation capabilities of blockchains irrelevant.

At the other end of the spectrum, traditional file systems and databases scale up and out well and can provide fine-grained control over data access through their front ends. However they are vulnerable to classical attacks. These problems can be reduced by the use of WORM storage for data that must be retained long-term. WORM storage can be thought of as a file system that understands mandatory retention periods and allows each file to be written only once, alteration not being permitted and only deletion possible at end of retention period. WORM storage focuses on making writes efficient for large volumes of data that might be hardly read. Using the WORM facilities offered by public clouds, e.g., by Amazon [34], can further enhance its tamper-proof properties. While researchers have investigated ways to leverage WORM storage to provide tamper-evident indexes for data lookup and even tamper-evident relational databases, publicly available cloud WORM facilities are still just file systems. As brute force search is impractical, there is no trustworthy way to find a particular piece of information on WORM storage based on part of its content. In other words, WORM storage alone does not guarantee availability, because it does not support fine-grained content-based lookup.

2.4.2 Hybrid Data Architecture Design

The Datum use cases suggest a three-tiered data architecture:

1. Traditional cloud-based storage and analytics services for high-volume, short-lifetime data that is not shared with others. This includes the vast majority of factory sensor data, which is at low risk for tampering but may be an appealing target for theft.

2. Blockchains for low-volume long-lifetime shared data. This data may be at risk for tampering, but theft is less of a concern.

3. A combination of cloud-based WORM storage and blockchains for high-volume shared data. Here the blockchain contains a token and conditions on when the token can be used. When the conditions are fulfilled, presentation of the token to the manufacturer grants the presenter with access to a particular data item that resides on WORM storage.

Figure 2.3 depicts the WORM-blockchain tier of the system. The WORM layer includes a blockchain element because even if data has been placed on WORM storage, there is no guarantee that anyone can find it. The WORM-blockchain combination overcomes this problem by placing the relevant lookup information on the blockchain.

For example, DELL EMC sells a WORM storage system where each stored file can only be retrieved by presenting a hash of its contents [35]. If this hash and appropriate metadata, e.g., a part ID and manufacturer name, are placed on a public blockchain, then anyone who knows the part ID can, in theory, find the part ID on the blockchain and use the associated hash to retrieve the file about that part from the supplier's WORM storage in the cloud. The use of the blockchain ensures that the required token cannot be lost or tampered with, and reduces the availability problem to the need to quickly find a blockchain record by its content, which is already on researchers' agendas.

Hybrid WORM-blockchain storage may not offer the desired confidentiality and availability if a manufacturer divests a division, is acquired, or shuts down; if the WORM cloud provider shuts down; or the relevant blockchain is abandoned. These are interesting issues for future work.

2.4.3 Proof-of-concept Implementation for Datum 4.0

This section describes the design, implementation, and experimental results from a proof-of-concept implementation of the hybrid architecture, aimed at enterprises like Datum 4.0.

A key requirement is the ability for a manufacturing federation to be able to adopt Manufacturing 4.0 without minimal or no modifications to existing factory floor machines, and at low cost. One option that meets these requirements is to implement the Manufacturing 4.0 data capture facilities

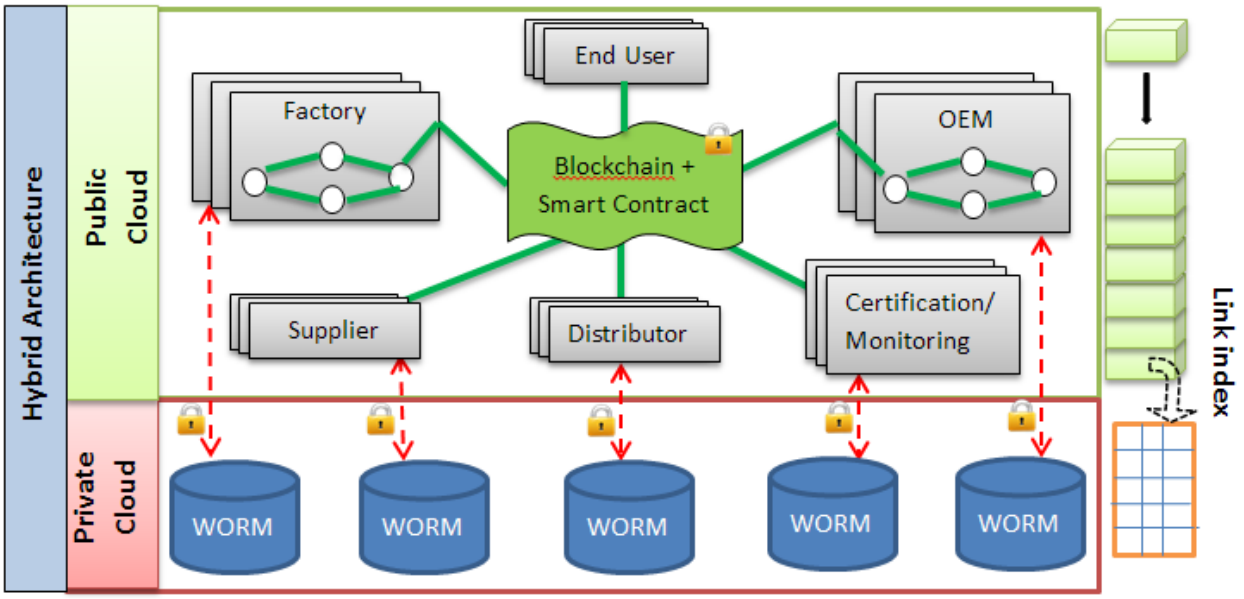

Figure 2.3: WORM-Blockchain Hybrid Storage Tier

using an overlay of simple IoT-enabled compute units, such as Raspberry Pi boards or Particle Photon boards. By listening to sensors and to communications without interfering with current operations, these boards can collect digital thread data and send it to the cloud for storage and future analytics.

We need two separate data paths for data captured and stored for the manufacturer's internal applications (predictive maintenance, data analytics, process monitoring and improvements) and data that is shared externally within the manufacturing federation according to contractual and legal requirements. To reduce security issues, we isolate these two data paths from each other and from the manufacturer's other data systems by implementing them as two separate subsystems, one for manufacturer-internal data and one for the federation's external blockchain, supported by different dedicated IoT compute units at the factory floor machines. These are shown in Figures 2.4 and 2.5.

The internal data storage IoT subsystem supports internal data capture. For this subsystem, we chose the Particle Photon board as a compute unit, due to its small footprint that makes it easy to retrofit to legacy equipment, its built-in encryption support, and good cloud integration and testing options. We integrated the Particle Photon board with a temperature sensor (TMP 36), microphone (Electret Microphone Amplifier MAX9814), and an IMU sensor unit (the MinIMU-9 v5 with a gyroscope, accelerometer, and compass). The entire system cost US$50.40. We used AES and RSA to encrypt the data from the sensors before sending it to an Amazon Web Services cloud for storage. The Photon Particle board comes with built-in support for the Device cloud. As we wanted to evaluate its compatibility with other clouds, we decoupled its existing links with the Device

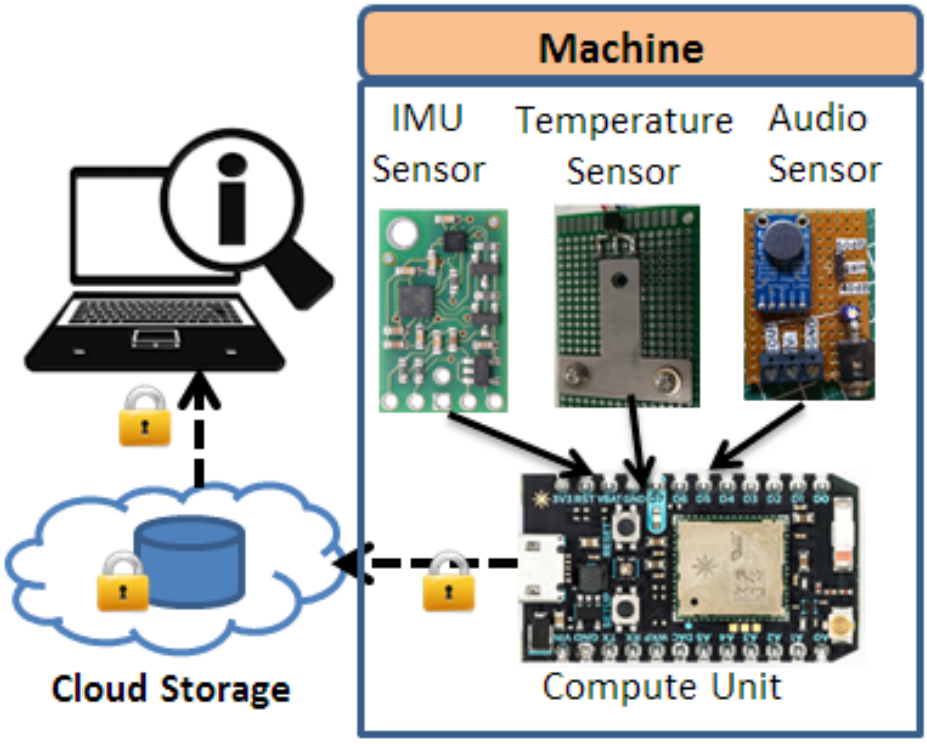

Figure 2.4: Capture and Storage of IoT Data Intended for Manufacturer Internal Use Only

cloud and linked it with the AWS cloud instead. Our prototype design takes into consideration the machine temperature, power source, space clearance for sensor attachment and legacy machine compatibility. We used standard AWS cloud facilities, but in a production version, AWS's WORM cloud storage can be used.

Our implementation of the data capture system for externally shared data runs the Ethereum blockchain protocol on a US$40 Raspberry Pi 3B+ connected to several sensors ranging from $5 to $17. This system can also be retrofitted to existing machines on the factory floor. We chose the Raspberry Pi because support for integrating blockchains with the Photon Particle board was lacking, making it difficult to use the Photon for externally shared data.

The externally-shared data implementation includes two Raspberry Pi 3B+ boards that collect data from five virtual pieces of Datum factory floor equipment: the CNC mill, steel cutting, the raw material area, a factory-floor computer, and shipping. The testbed also includes a laptop running three blockchain miners for Datum, and a second laptop to support the external chrome plating service. When raw material arrives, the incoming smart contract goes to the raw material miner. When the material is processed at a piece of equipment, additional information is collected either manually or by automated measurements from the sensors/actuators connected to the Raspberry Pi unit, and appended to the blockchain. Smart contract conditions can be set up in the server and the miner can fetch and check conditions through it. All pieces of equipment must be connected to a

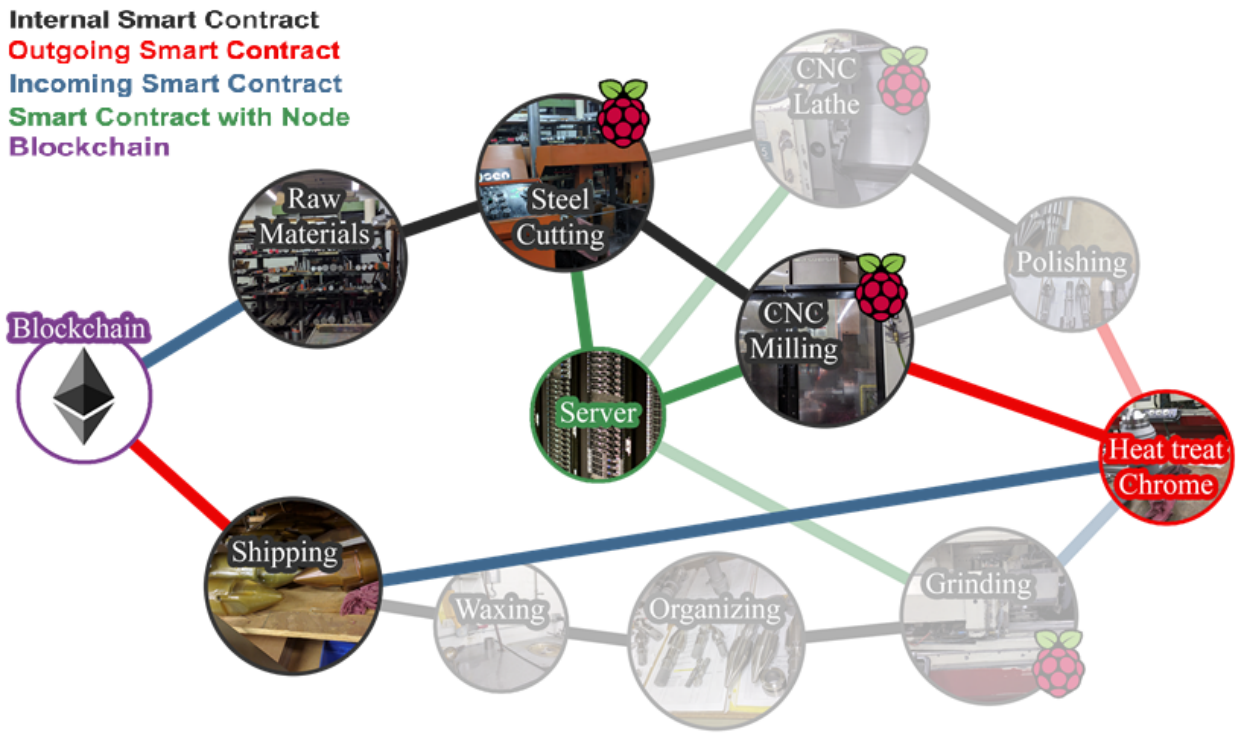

Figure 2.5: External Manufacturing Federation Blockchain IoT Subsystem for Datum 4.0

miner.

Results from Implementation Overall, both the internal and external data capture systems worked well, up to the data transfer limits imposed by the hardware. We did observe issues with the stability of the Photon board connection in general and had to manually reset the connection if the device was idle for long. This could be remedied in a production system by implementing automated reset support.

Today's small-footprint IoT compute units are resource constrained. A Raspberry Pi's processor is considered fairly powerful for a small computer, but its I/O throughput is limited. In a Raspberry Pi and most other IoT-capable compute units, the Ethernet and all USB data go through a single USB 2.0/3.0 pipe, placing a hard limit on the volume of data coming into the system and going out to the blockchain. The theoretical upper limit on throughput for the latest model of Raspberry Pi 3 is 40 Mbits/sec by WiFi or 300 Mbits/sec by gigabit LAN. Once a factory approaches that limit, it would either need to use multiple systems in parallel, or upgrade to an implementation that uses more powerful (and more expensive) hardware.

Memory and processing speed constraints may also dictate that the blockchain block sizes processed remain small, so that they do not delay the manufacturing process. In particular, the need to support cryptographic protocols for confidentiality requires both the blockchain mechanism

and cryptographic protocols to be low-cost. The overhead of handling multiple sensors and preprocessing their data places additional burdens on the system.

Overall, these limits further emphasize the need for a WORM-blockchain tier of storage for low-cost deployments. There is generally a tradeoff between affordability and compute power as well, and small-budget factories will require a cost-benefit analysis.

2.5 DTAAS: MANAGING HYBRID DATA ARCHITECTURES

It is unreasonable to expect small and medium manufacturers to acquire IT security expertise, even in the long term. We believe that the best way forward for providing trustworthy digital threads is to provide professionally managed IT and analytics services for them. We call this digital-threads-as-a-service (DTaaS). Major manufacturers can provide DTaaS using an internal cloud managed by their IT staff, while smaller manufacturers can purchase DTaaS at low cost from a neutral vendor, which may rely on a public or private cloud. We envisage that for each piece of information uploaded to a thread, the manufacturer will transmit it over a secure channel with an indication of which thread (product item) it is to be associated with. The DTaaS provider will sign and store the new entry, and link it into its thread. The DTaaS provider will also provide metadata management services for the important information about the new entry, including who provided it, what manufactured item it is associated with, a timestamp, and additional metadata that will be used to search threads or used in the analytics supported by the DTaaS provider.

The DTaaS provider will provide search facilities over the metadata and control access to the thread data and analytics results, with input from the information owner. For customers willing to pay for them, the DTaaS provider can provide additional assurances and facilities at additional cost, such as storing thread entries encrypted, encrypting certain fields in its database of metadata, keeping thread entries or metadata on cloud WORM storage [36] (e.g., using EMC's Centera, Network Appliance's SnapLock, and archival products from HP's StorageWorks and IBM's TotalStorage) to make it hard to tamper with, and supporting additional metadata and more sophisticated analytics.

The resulting centralization of thread information makes the thread repository and its access interface an attractive target for attack, but the repository can be hardened against attack and regularly audited, so that the weakest links along the supply chain are no longer very weak.

DTaaS can reduce the vulnerability window at thread information generation time by getting newly generated information off the factory floor as quickly as possible. All subsequent access to information in the thread can go through a narrow DTaaS interface with professionally managed software. If factories delete their local copies of thread data once the DTaaS provider has confirmed receipt, then the window for theft is greatly narrowed.

2.6 CONCLUSIONS

Digital thread data about a product and the process used to manufacture it can be used to verify the provenance of the product and support analytics to improve the efficiency of the manufacturing process. When shared within a manufacturing federation, it can facilitate the end-to-end lifetime tracking of a product and provide support to analytics that could improve efficiency all along the supply chain. However, unless appropriately protected, digital thread data could also reveal manufacturing IP secrets, thus giving away the manufacturer's "secret sauce" and competitive edge.

Practical and modular implementations of IoT-enabling hardware, along with a flexible and secure data architecture, are needed to make the digital thread vision for Manufacturing 4.0 ready for deployment. However, manufacturing data and its potential applications are very diverse, making some data management solutions not suitable if applied alone.

In this chapter we explored the wide range of data that can be collected during the life-cycle of a product. We examined trust issues in information sharing and proposed data management methods that are more suitable for manufacturing, based on how that data is stored, used and shared. Building on our case study of a small manufacturer, we proposed a hybrid data architecture that couples a decentralized low-volume data sharing system such as blockchain with a centralized high volume internal data management system such as WORM. Our proof-of-concept design and implementation focused on a practical, cost-effective solution that can be easily retrofitted to factories today to make it Industry 4.0 capable, with minimal modifications to factory floor machines.

Chapter 3: SIDE-CHANNEL VULNERABILITIES ON FACTORY FLOORS

Hackers have noticed the large amount of valuable information available in the cyber-physical systems on factory floors. In addition to straightforward data theft, a determined adversary can, in theory, take advantage of side-channel attacks based on electromagnetic leaks, acoustic emissions, timing information, light emission, and power consumption [37, 38, 39, 40, 41, 42]. The leaked information can be used to compromise systems and to obtain or infer sensitive data. For example, researchers have successfully partially compromised Diffie-Hellman exponents, factored RSA keys, and broken other cryptosystems by measuring the amount of time required to perform private key operations [43, 44, 45].

Defending against side-channel attacks requires a level of security more advanced and more comprehensive than updating an operating system or installing security patches. Despite the efficacy of firewalls and anti-virus software, manufacturers currently have no effective way to protect against information leakage from their factory floor equipment.

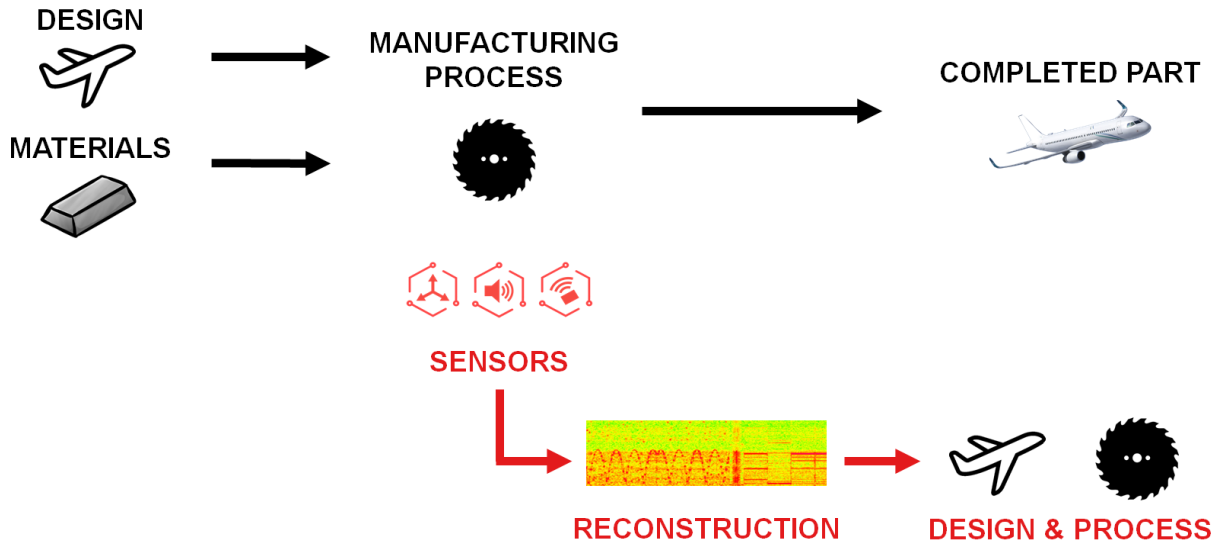

Figure 3.1: High Level System and Attack Model. Designs and raw materials are the inputs to a manufacturing process that produces completed parts. By placing phone sensors near the manufacturing process and analyzing the data they collect, the side-channel attack reconstructs the design and the manufacturing process.

In a modern factory, nearly everyone on the manufacturing floor carries a smartphone or similar electronic device. These devices are programmable and come with a growing number of embedded sensors, including a microphone, accelerometer, magnetometer, gyroscope, GPS, and camera. These sensors can capture side-channel information regardless of the level of information technology or security sophistication on the factory floor and inside the manufacturing equipment.

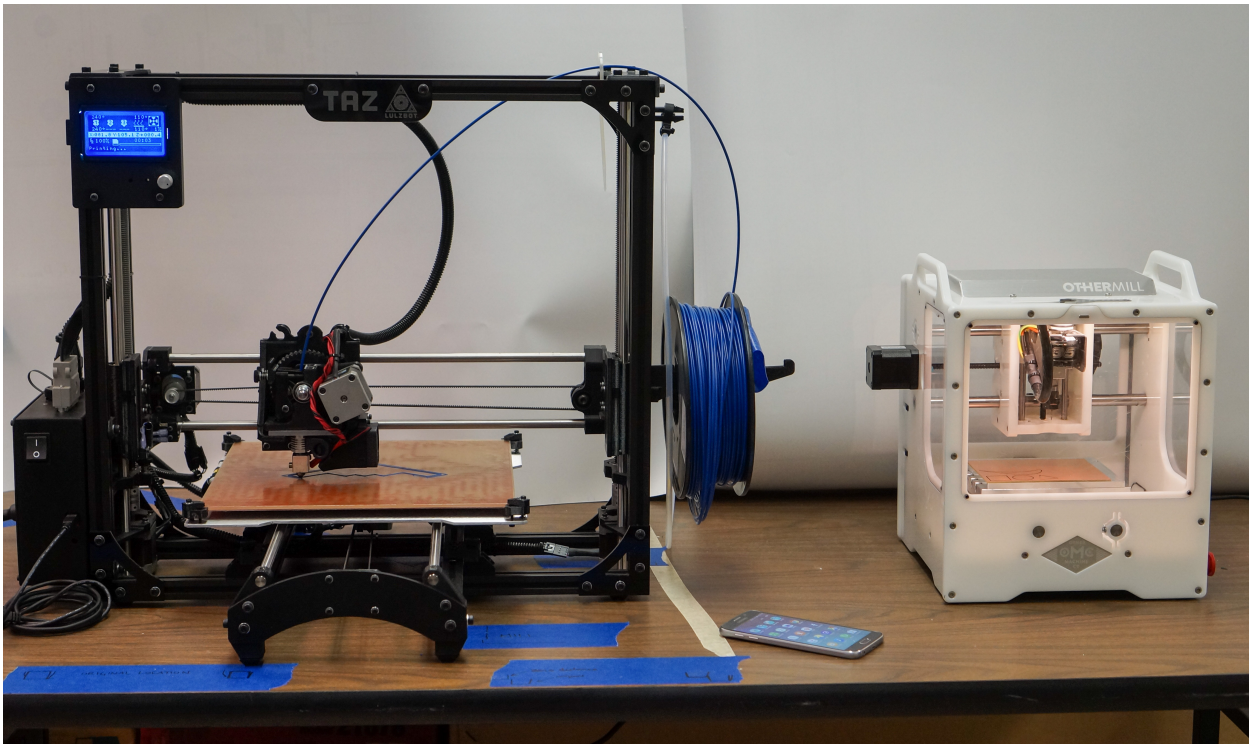

Figure 3.2: Attack Setup. For the phone attack, a phone placed on the same table as a 3D printer (left) or CNC mill (right) records the readings of its sensors. For the phone call attack, an attacker on the other end of a call records the call's audio.

This chapter presents a novel attack in which a phone's sensors are deliberately or inadvertently used to capture sensitive information from manufacturing equipment, as shown in Figure 3.1. We capture the relevant sensor data by deliberately or accidentally placing an attack-enabled phone close to, on top of, or inside a piece of manufacturing equipment while the machinery is fabricating the target object. Figure 3.2 shows this setup. Alternatively, the relevant audio can be recorded by deliberately or accidentally making or receiving a phone call while standing next to the machinery or by installing malware on any other nearby device that has a microphone.

We provide methods that use the captured data to reconstruct a model of the object being manufactured along with its manufacturing process parameters. We demonstrate the attack on both additive and subtractive manufacturing using a 3D printer and a CNC mill. We demonstrate the reconstruction process with a 3D printer and discuss ways to reduce the attack's effectiveness.

This chapter's contributions are:

- *New techniques.* We show that the data captured by acoustic and magnetic sensors embedded in a phone can be used to identify specific manufacturing equipment and manufacturing processes, including reconstructing manufactured objects and reproducing the processes used to make them.

- *New understanding.* We demonstrate the feasibility of applying side-channel attacks to manufacturing equipment: in particular, 3D printers and CNC mills. The fundamentally different operating modes of these two types of manufacturing equipment indicate that the attack may be broadly applicable across many types of manufacturing equipment.

- *Implementation and evaluation of reconstruction method.* We provide a method for reconstructing manufactured objects and the processes used to make them; the method is based on machine learning and signal processing. We show that the method accurately reconstructs previously unseen objects.

In the remainder of the chapter, Section 3.1 provides background information and discusses the motivations of potential attackers. Section 3.2 describes the attack model and reconstruction method. Section 3.3 provides experimental results, and Section 3.4 offers recommendations for defending against the attacks and raising the cost of reconstruction.

3.1 BACKGROUND

Traditional high-value discrete manufacturing relies heavily on subtractive processes: equipment is used to cut, chip, and grind away excess material to form the desired product. Interest is high in the potential for new additive manufacturing processes, which deposit material layer by layer to form objects. Our attack and reconstruction methods target both additive and subtractive manufacturing, represented in our experiments by a 3D printer and CNC mill, respectively.

The manufacturing sector has a rich history of research on obtaining information about a manufacturing process from its acoustic emissions. Recordings have been used to judge parameters including tool wear, tool breakage, chatter, chip formation mechanism, material removal regime, sheet metal material hardness, sheet metal thickness, and the identity of the metal or alloy being machined [46, 47, 48, 49, 50, 51, 52]. Our reconstruction methods use acoustic information for less benign purposes.

Until the recent advent of ransomware, IP theft was by far the most common motive behind attacks on factories, especially for high-value products. Attackers targeted product design information, manufacturing process information, or both. The advantage of stealing design information is clear, but many manufacturers' competitive advantage largely lies in the fact that they know how to manufacture a given design better, faster, or cheaper than their competitors do. Process information may include the details of what materials are used and what machines are used and in what order, plus all the settings of those machines: which tool head was used, its rotation rate, the material feed rate, and so forth.

When a phone illicitly records data on the factory floor, its owner could be intentionally carrying

out corporate espionage, or she could be an unwitting dupe with a compromised application or even the innocent maker or receiver of a phone call at an ill-advised moment. In these latter cases, she may have been targeted by a third party such as a rival manufacturer, or swept up in a large net cast by a well-financed backer of economic espionage such as a nation-state. For example, a nation-state hacker might be seeking to increase the competitiveness of its manufacturing sector, gain the ability to manufacture objects viewed as important for the national interest, or learn about its rivals' capabilities and activities.

Such motivations may have been behind the theft of the design for Lockheed Martin's US F-35 Lightning II fighter jet, stolen by hackers allegedly supported by the Chinese government[1]. The US and Israeli governments allegedly unleashed STUXNET, which targeted the programmable logic controllers of Iran's nuclear centrifuges, causing them to self-destruct. Allegedly, the Chinese government has financed the large-scale theft of industrial IP [53] and the Iranian government has sponsored IT intrusions overseas [54]. The US and Israeli governments have been attributed as potential sources of the Flame malware, apparently designed to increase situational awareness of Iran's technical capabilities and activities [55]. In addition to gathering files likely to contain technical information, Flame collected data from the sensors of the devices it infected.

Our approach to factory floor snooping leverages the fact that sensor spyware could spread to anyone's phone and export the data it captures for subsequent analysis and reconstruction of manufacturing activities. While Flame targeted Windows PCs, similar malware can be constructed for phone applications. For example, Cai et al. [56] highlight the capabilities of modern mobile devices for snooping on users by sniffing their smartphone's sensors. The Shedun Android malware provides a framework for automatically downloading and installing undesired new applications and for serving potentially malicious adware; security researchers consider Shedun nearly impossible to remove completely. DroidKungFu, targeted at users in China, offers similar capabilities for the automatic installation of malicious new applications.

With over a thousand new infections per day as of this writing, malware like Shedun and DroidKungFu provides a channel to reach factory employees. The malware may even be present when a phone is first purchased; Indian phone manufacturer Gionee has been accused of this[2]. Once a malicious app has been installed, its recording function could be activated by a geofence around the factory, and could run in the background of another app with appropriate permissions, such as a game.

Al Faruque et al. [57] recognized that thermal side channels can be used to infer activities taking place inside a 3D printer. Closer to our work, they also investigated the possibility of attacking

[1] "Chinese hackers stole F-35 fighter jet blueprints in Pentagon hack, Edward Snowden documents claim": http://goo.gl/Vnvbs2.

[2] "Wenn der Spion in der Hosentasche steckt" (If the Spy Is in Your Pants Pocket), *Die Welt*, 12 October 2014.

manufacturing machinery via audio recordings. They placed a microphone close to additive manufacturing equipment to record fabrication runs, then used machine learning to reconstruct the low-level instructions (G-code) used to manufacture the object, with an accuracy of 89.72% in reproducing the as-designed object's perimeter.

While Al Faruque et al. used a high-quality microphone located in a specific location in a controlled environment, our work uses ordinary mobile phones that may be located anywhere near the machine or in the user's hand and can target machinery located in any environment, including public fabrication labs. We employ different reconstruction methods from Al Faruque et al., and our experiments show that we reconstruct perimeters more accurately; however, we also suggest different measures of accuracy that we believe to be more revealing. A final difference is that because G-code is quite low level, reproducing the same object on a different model or type of machine requires nontrivial extra work to rewrite the G-code. For that reason, we provide a higher-level reconstruction suitable for translation into G-code for a variety of machines.

3.2 RECONSTRUCTION

Different fabrication machines have different process parameters. For example, a grinding wheel can run at different speeds. The wheel could be touching the object being made, or could be away from it, e.g., while repositioning the wheel to a different location on the object. The object could be moving past the wheel at different rates. The same machine could use grinding wheels with different levels of grit. To accurately reproduce a manufacturing process, we need to specify the values for all of its parameters.

As no single piece of research can reconstruct all process parameters for all major types of equipment, we focus on key parameters related to the location of the tool head with respect to the object being fabricated and its direction of travel. These location and direction parameters are important for both additive and subtractive manufacturing, and must be specified to control machines as disparate as a 3D printer and a CNC mill. Further, while prior research in the manufacturing community has concluded that many aspects of fabrication have inherent acoustic signatures, no signatures that specify these parameters have been established in previous work.

We describe tool head location and direction with respect to the platform of a machine, which defines an implicit XY plane and an associated Z axis. Different machines have different constraints in traversing this space, and reconstruction can take advantage of these constraints to simplify the task. For example, a typical 3D printer builds up an object in horizontal layers. At any given layer, the printer head moves in an XY plane and can trace any angle in that plane with respect to the X axis. The printer slowly works its way up the Z axis, emitting a characteristic sound from this

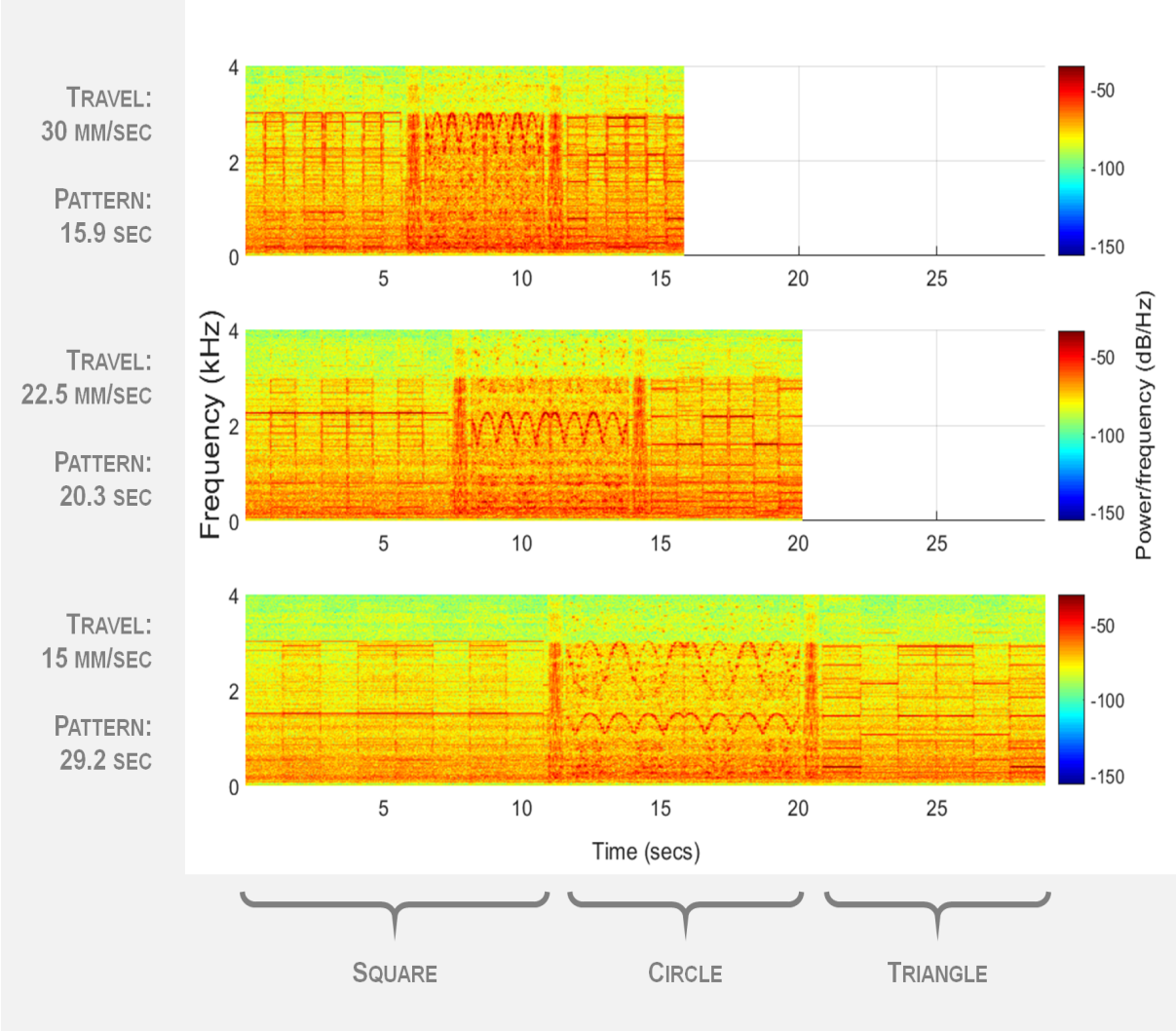

Figure 3.3: Audio Magnitude Spectrograms of a 3D Printer. The printer is making the same three geometric primitive objects, a square, circle, and triangle, at three different feed rates (15, 22.5, and 30 mm/sec). The increase in head travel speed changes the spectrogram in a systematic way.

movement. Further, in an object with multiple layers, each layer must either overlap the previous layer or have its own support material, so a layer's shape is constrained by the previous layer. Likewise, a subtractive manufacturing operation generally removes material adjacent to material it has already removed, and subtractive methods typically also work in layers. We take advantage of this layer-focused machine behavior by restricting our attention to the XY plane for a fixed value of Z, i.e., a given layer. Our reference and training data and validation experiments use nearly-planar objects: 3D prints two layers thick and shallow cuts with the mill.

Any planar figure that can be manufactured by machines like CNC mills and 3D printers can be specified as a sequence of tool head movements to be made at particular angles to the X axis

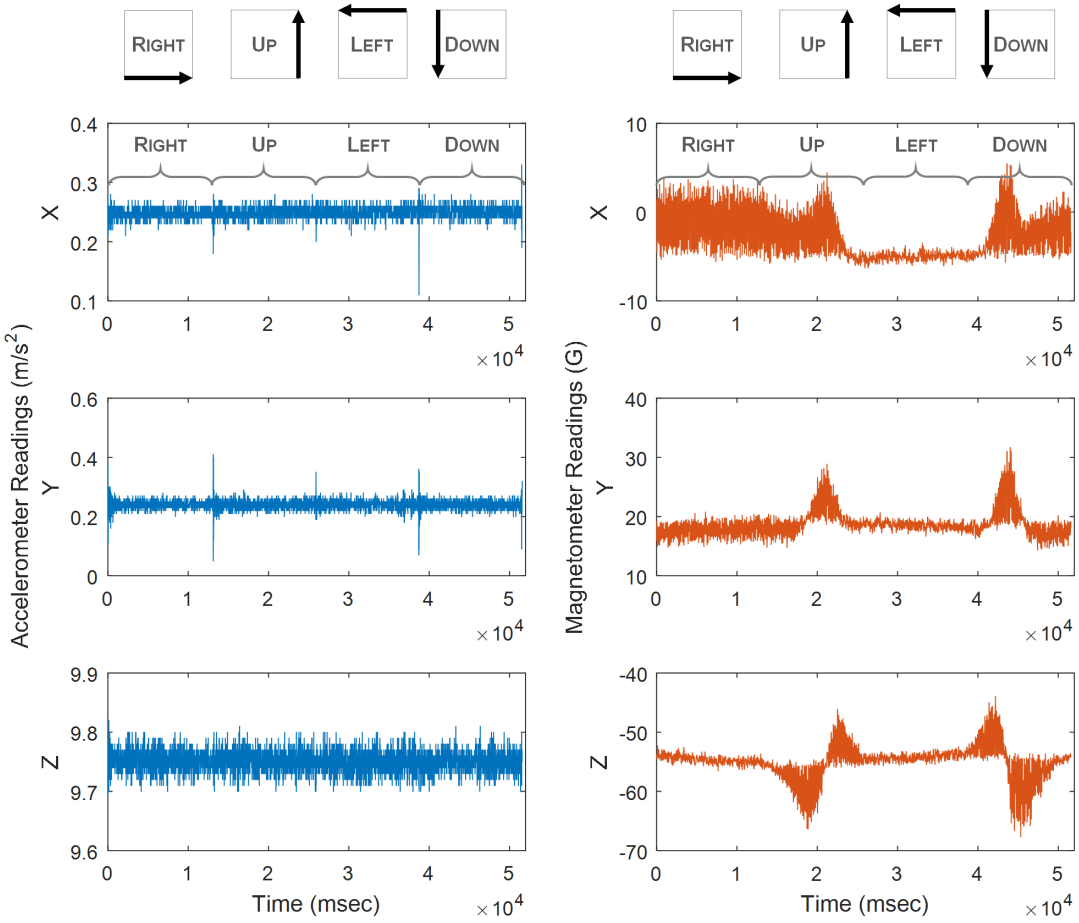

Figure 3.4: Raw Sensor Data from the Three Axes of the Accelerometer and Magnetometer While 3D Printing a Square. The readings vary predictably, providing additional information not fully captured in audio recordings. We found readings from the magnetometer to be more accurate than those from the accelerometer in explaining tool head movement.

for particular straight-line distances (with curves described by short tangential segments). We reconstruct both these angles and the distances. As it can be hard to visualize the tool head trajectories and phone placements we discuss, readers may wish to refer to the videos of our printer and mill in action, and an example reconstruction session, at `https://goo.gl/FijZ9T`.

The 3D printer head can travel at different speeds (feed rates). As shown in Figure 3.3, the printer's audio signature for a particular angle changes in a systematic way as the feed rate changes. Zooming in on these high-resolution figures, we see that the pattern in the figure's three spectrograms compresses in time and shifts up in frequency as the feed rate increases, though the human eye quickly recognizes that the high-level pattern is unaffected. For this reason, we focus on the printer's default feed rate of 30 mm/sec.

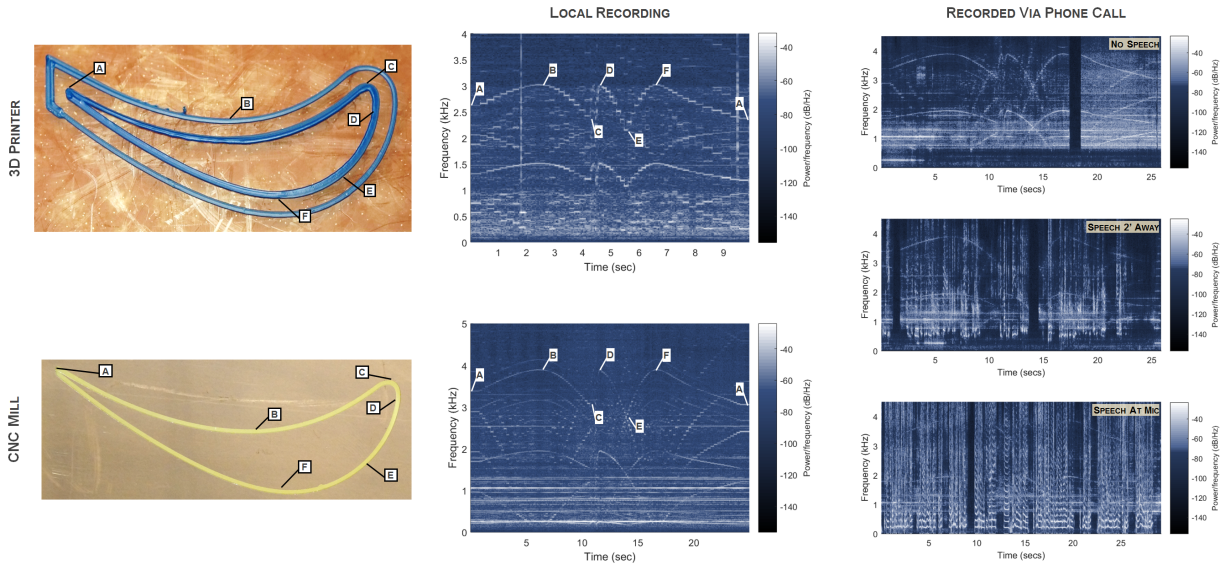

Figure 3.5: Comparison of Spectrograms. The spectrograms are taken from the 3D printer recorded locally (center top), the CNC mill recorded locally (center bottom), and the CNC mill recorded on the other end of a phone call (right column). The right column compares three phone call recordings: no speech (right top), speech 2 ft from the recording microphone (right center), and speech directly at the receiving microphone (right bottom). The annotations illustrate how the spectrograms correspond to the fabrication processes. The spectrograms from recordings of the fabrication of the same turbine blade shape display a trace in a consistent shape, even across different machines; each contains sufficient information to reconstruct the shape. Additionally, while speech overlaps with the frequencies that indicate machining, the traces are not fully obscured.

Figures 3.4 and 3.5 show example data from the phone accelerometer, magnetometer, and microphone. The reconstruction method uses audio and magnetometer data when both are available and just audio otherwise. When multiple reconstructed objects are consistent with the results produced by signal processing and machine learning, the reconstruction method uses a search process, domain constraints, and human assistance to rule out unlikely and impossible reconstructions.

We reconstruct the angle of travel of the machine tool head by comparing its audio to examples in a prerecorded reference library. We found that angles that are just a few degrees apart have very different audio signatures, so the recordings for the library need to include each angle that might be used to fabricate a target object. These recordings could be obtained from a similar machine model that the attacker plans to use to fabricate stolen designs or processes. Alternatively, as discussed in Section 3.3, the necessary calibration pattern could be hidden in the design of an object fabricated on a machine belonging to the victim or a third party, and recorded in an attack launched specifically to gather that information for the library. The result is a library of audio signatures that the machine produces for each angle of movement.

To build an audio signature library, we first use a cell phone to record the sound that the machine

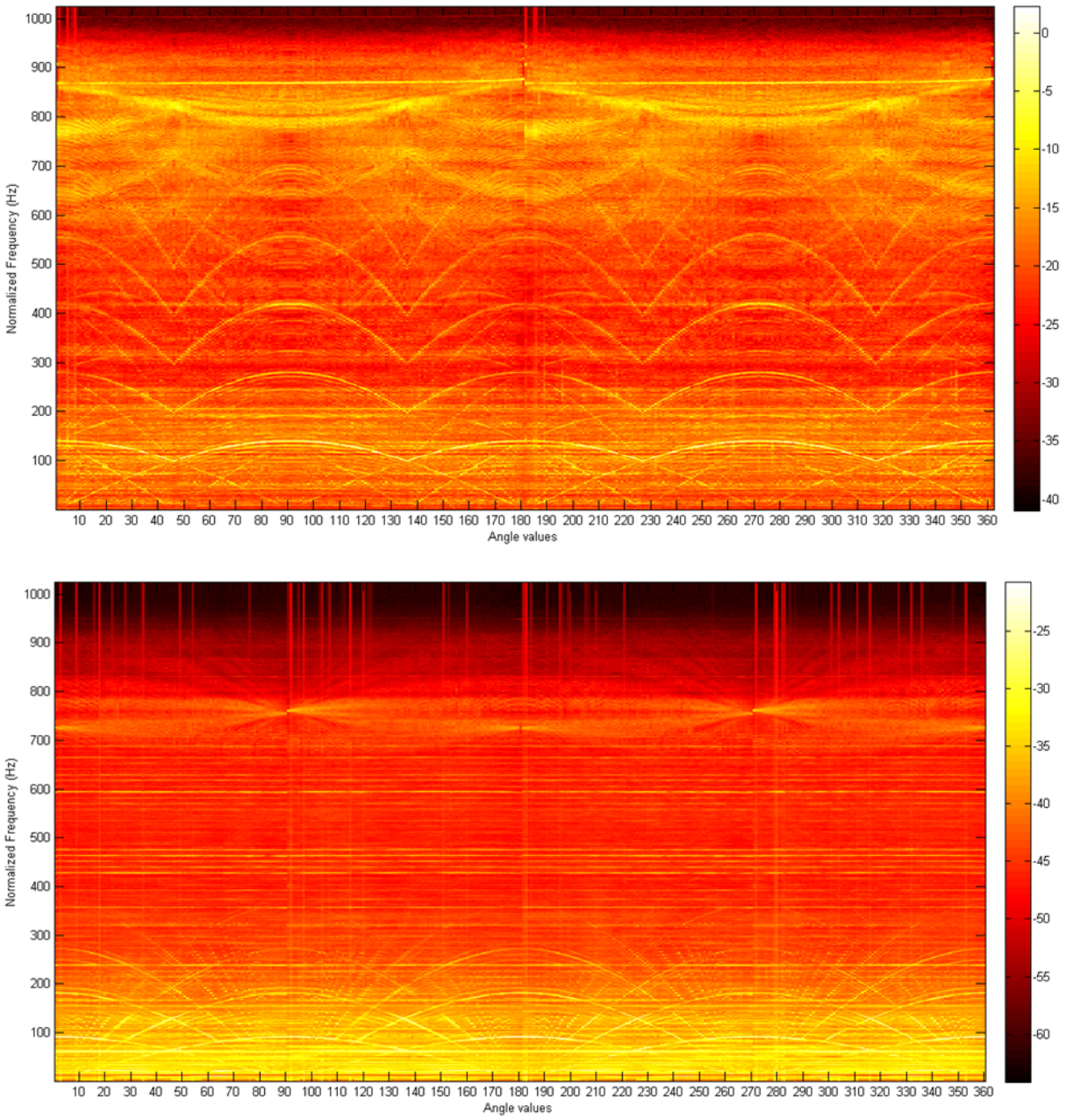

Figure 3.6: Example Magnitude Spectrograms for Audio Data. Juxtaposed magnitude spectrograms of 360 different angles of machine head travel with a 3D printer (top) and CNC mill (bottom). This data is used in a reference library during reconstruction.

produces when it moves along potential angle of interest. In this study, we used 1 degree of resolution, recording angles from 0 to 359 degrees. The sampling rate of the cell phone recording was 44100 samples/second, the default.

The second step is to transform the recorded audio from the time domain to the frequency domain

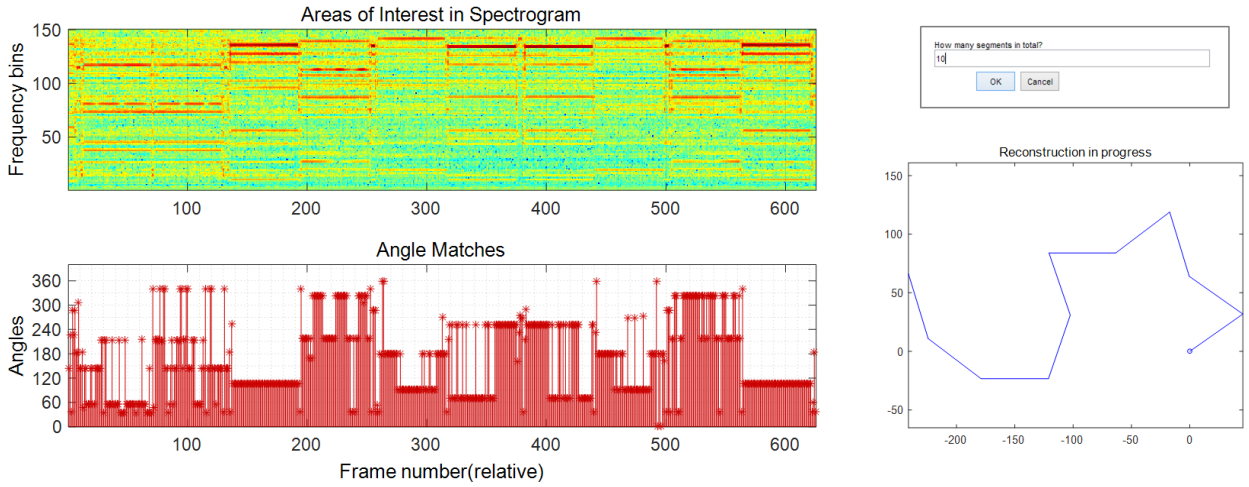

Figure 3.7: In-progress Reconstruction of a 3D-Printed Star, with Spectrogram Above and Matched Filter Beneath. Changes of tool head direction are visible as yellowish vertical bars in the spectrogram. The audio has been segmented and the search for a reconstruction that satisfies domain constraints is underway. The reconstruction at the lower right will be automatically rejected because it is not a closed figure; the first erroneous angle is off by 180 degrees, and its mirror image will be considered later in the search.

using a short time Fourier transform (STFT), and then produce a magnitude spectrogram. We used the Matlab function *spectrogram* for this purpose, with a Hann (Hanning) window of length 2048 samples, an overlap of 25% between successive windows, and 2048 frequency points. The use of overlapping Hanning windows is a standard technique in audio processing that helps to reduce the noise in the signal by smoothing it out. The use of 2048 frequency points gave sufficient resolution for reconstruction.

When recordings are made in a manufacturing environment, the audio contains background noise whose energy spreads across all frequency bands, and in general the background noise energy tends to decrease as the frequency increases. We found that for reconstruction to succeed, it is important to reduce this background noise, especially at low frequencies, to emphasize the useful content of the audio signal. Thus the third step in building the audio library is to perform noise normalization in the frequency domain. We estimate the background noise covariance matrix Rnn based on a portion of the recording when the machine is idle. Assuming noise is uncorrelated across frequencies, we use Rnn to normalize the signal spectrogram as follows:

$$X_{white} = diag\left(\frac{1}{\sqrt{diag(Rnn)+\epsilon}}\right) \times X, \tag{3.1}$$

where X is the magnitude spectrogram for the recording, and $\epsilon = 1 \times e^{-8}$ is a constant used to avoid dividing by zero. To further reduce the effect of background noise and unwanted interference

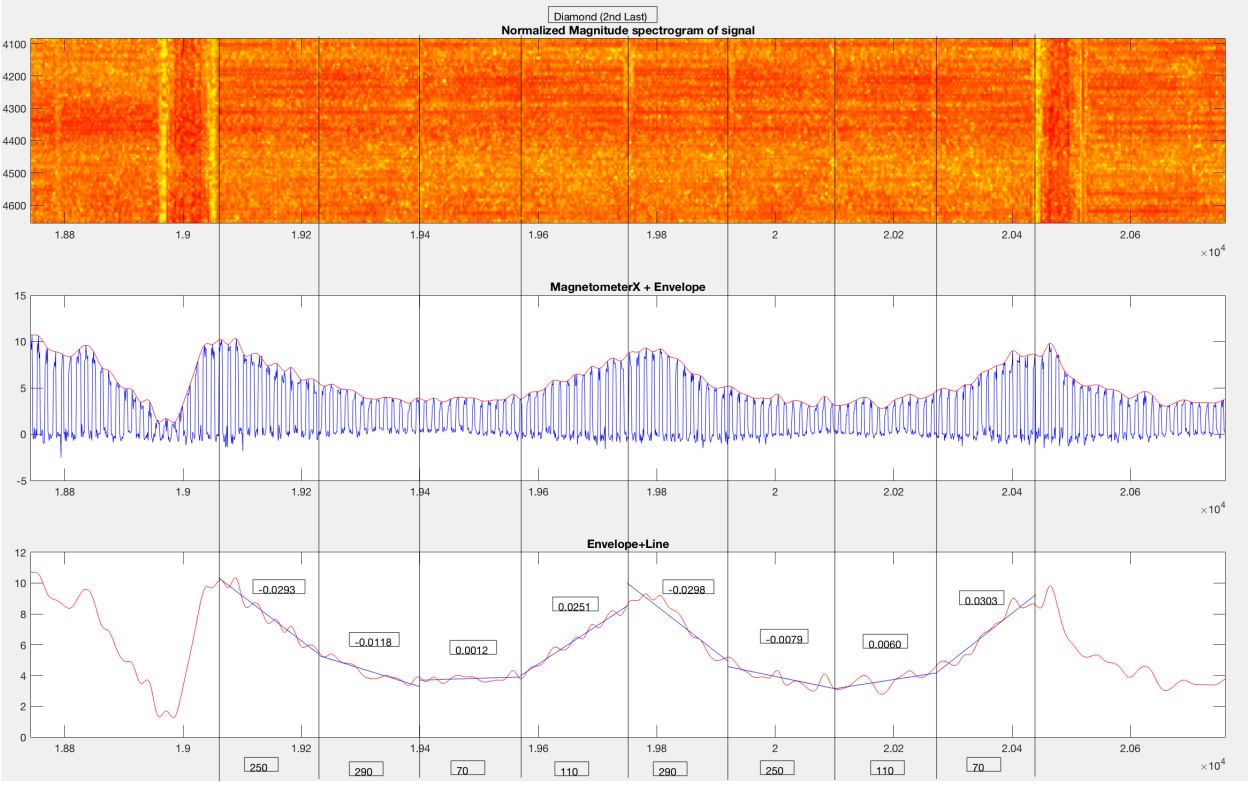

Figure 3.8: Segmented Audio Magnitude Spectrogram, Magnetometer Signal in the X Dimension, and Regression Lines for Each Segment. The 3D printer is fabricating a 2-layer diamond shape, and the sign of the slope of each regression line indicates whether the angle for that segment lies above or below the printer platform's X axis. The magnitude of a segment's peaks indicates how far forward on the platform that segment's fabricated line lies, which can be helpful for establishing a canonical orientation for the object being manufactured.

in the library, we average all the frames of the signal of the same angle along the time dimension of the spectrogram. The result is 360 frames, corresponding to the 360 angles of movement illustrated in Figure 3.6. Each frame is the audio signature of the machine head at a particular angle across frequencies.

Figure 3.6 shows that most of the information needed to decide what angle the machine is moving at is concentrated at low frequency bands. Further, signal artifacts such as aliasing are visible at high frequency bands. Therefore we select only frequencies below a cutoff frequency f_c for further processing, saving the results in the reference library. We also record the domain constraints specific to that machine, such as its platform size and the value of f_c.

After these signal processing steps, the audio of each 3D printer angle a appears very similar to that of the three other angles created by mirroring the given angle in each quadrant of the plane $(\pm a, 180 \pm a)$; this introduces ambiguity into reconstruction. Similarly, each mill angle sounds like 15 other angles, produced by mirroring across the X and Y axes and the ± 45 and ± 135 degree

lines. We suspect that more sophisticated audio signal processing techniques that can pick out the secondary tones visible in our spectrograms (and audible to a keen ear) can be used to tell these angles apart, but that remains for future work, and we rely on two other disambiguation techniques described later: magnetometer data and a search process that exploits domain constraints. For simplicity, the discussion that follows is written as though the library contains just one reference angle audioclip for each set of ambiguous angles, e.g., only first quarter angles for the 3D printer. However, for ease of incorporating new domain constraints and information from other sensors, our actual implementation retains reference data for all angles.

With the reference library in hand and a target object to reconstruct from its fabrication audio, we begin by cleaning up the audio by applying the same first four signal processing steps as for reference audioclips: define overlapping frames, produce a magnitude spectrogram, normalize with respect to background noise, and retain only the relevant frequency band. Then we find the most likely angle for each frame of the cleaned-up audio by comparing it to all of the reference library's angle frames and finding the one it is most correlated with. More precisely, we use a custom matched filter function[3] to compute the correlation between the audio frame and each of the reference library frames; this is a standard technique for comparing two audio samples. The result is one value for each combination of a target audio frame and a library angle. For each target audio frame, we select the library angle with the highest cross correlation value for that frame: this is our best guess angle for that moment of the fabrication. Then we present the results to the user, as shown in Figure 3.7's screenshot of our interactive reconstruction framework. The screen shows the spectrogram of the target audio, aligned along the time axis with a matched filter visualization, where the height of each match head indicates the reference library angle selected for that frame in the audio. When magnetometer data is not available, this completes the automated signal processing phase of the reconstruction.

Next, the search phase begins, with optional human assistance to steer the framework's search process. To prepare for this role, a user requires only brief training in how to recognize changes of angles and the start/stop of tool work in audio magnitude spectrograms.

In our current framework implementation, the user has two tasks. First is to click on the points in the audio at which the tool head changes its angle; these points can be seen quite easily as the edges of the vertical bars in the spectrogram. The identified points divide the manufactured object into a series of straight-line tool head runs, which we call *segments*. From watching a video of the 3D printer, framework users learned several constraints that were useful to them during segmentation. The first two are generic to 3D printing: the printer begins and ends each run with a particular movement sequence; and the printer fabricates a 1-layer bounding box around all the closed figures

[3]For an explanation of matched filters, see goo.gl/Nrjojv.

it will subsequently construct during the run. Users also observed a third constraint specific to the 2-layer objects we were building: after fabricating the first layer of an object, the tool head retraces its path in reverse to construct the second layer. Together, these three constraints helped the user identify the first and last segment of each fabricated object.

The duration of each segment multiplied by the machine's feed rate gives the physical length of each linear segment in the reconstructed shape, so the accuracy of segmentation affects the accuracy of the final reconstruction. In our experiments, we did not focus on trying to get segment lengths exactly right. We expect that signal processing techniques can be used to automate segmentation in the future, and may be more accurate than a human.

The interactive framework automatically shows the user-selected segment boundaries superimposed on the spectrogram and its accompanying matched filter timeline. The most common matched filter head height in a segment is the best guess angle for that segment. For example, the third and tenth segments of the audio in Figure 3.7 will have only one suggested angle, while the sixth and seventh will have two.

The user's second task is to provide optional guidance to speed up the search process. For example, suppose that the first choice angles for all segments do not produce a reconstruction. While the search process can automatically identify the segments with the most uncertainty in the matches, and automatically identify the second most likely angle for each, the user can also guide this process by clicking on the matched filter head heights (angles) that she would like the search to consider next. This flexibility is particularly useful when the framework does not have a full set of domain constraints. For example, we implemented a domain constraint that the tool head must move at different angles in adjacent segments. Without this constraint, the framework might assign the same angles to segments 6 and 7 in Figure 3.7, but the user could click to force the use of different angles.

Each matched filter head height may correspond to several different mirrored angles in the reference library. Thus in our experiments, a k-sided 3D-printed object has an audio-only reconstruction search space of roughly 4^k potential objects. (When magnetometer readings are available, the search space shrinks to roughly 2^k, as explained below.) Fortunately, manufacturing domain constraints allow us to prune away most of the search space. We implemented two constraints generic to 3D printing. The first constraint is that a layer should not cross over itself. More precisely, each segment in a layer should intersect exactly two other segments, one at each of its endpoints, except that the first and last can intersect either one or two other segments. The second constraint is that at the end of a segment, the printer head should change its angle of travel rather than continuing in a straight line or (unless it is the end of a layer) doubling back on itself. We implemented a third constraint specific to the kinds of objects we were building: each object layer should form a closed figure in the plane. The framework automatically explores the search space not eliminated by these

constraints and displays the resulting reconstructions to the user, who can accept or reject them. If unhappy with all the reconstructions shown, the user can click on additional matched filter head heights for a segment, so that additional angles will be considered.

In theory, a phone's magnetometers could tell us whether each nearby motor in a machine is accelerating, decelerating, or holding steady, and for how long; from that information we could determine the exact path the tool head traces. In practice, however, we only found magnetometer data useful for reliably distinguishing between angles a and $-a$ for the 3D printer. This means that when we have both magnetometer and audio data for a fabrication run on the 3D printer, each angle appears very similar to only *one* other angle, its mirror image across the X axis. In other words, de facto, with the phone located near the corner of the printer, its magnetometer registers the machine platform's forward and back movement during fabrication, but does not pick up a signal from the machine's other motors and movements.

To illustrate the disambiguation, consider the example three-dimensional magnetometer signal in Figure 3.8, which was recorded with the phone lying flat near the corner of the printer. If the peaks of the magnsetometer signal in the dimension most closely aligned with the machine platform's Y axis are decreasing in a segment where the machine head traverses angle a, then the peaks of the magnetometer signal in that dimension will be increasing as the machine head traverses angle $-a$. More precisely, our algorithm for processing magnetometer data uses the magnetometer's dimension with the strongest signal overall (X for the 3D printer, Z for the mill). Then for that dimension in each segment, the algorithm identifies the peaks in the magnetometer's magnetic field strength measurements. Our implementation uses the Matlab function *envelope*$(x, np,' peak')$, which uses spline interpolation over local maxima separated by at least np samples; $np = 8$ worked well for our phone's magnetometer data. Then we find the regression line that minimizes the peak points' average squared distance to the line. Our implementation uses the Matlab function *polyfit*$(x, y, 1)$, which returns the coefficients for a line $p(x)$ that is a best fit (in a least-squares sense) for the data in y. If the slope of the resulting line is negative, then the angle is between 0 and 180 degrees. If the slope is positive, then the angle is between 180 and 360 degrees. Intuitively, a positive slope means that the platform of the printer is moving toward the phone. A negative slope means that the platform is moving away from the phone. A slope very close to zero (with respect to the amplitude of the signal) means that the platform is not moving closer to or further away from the phone. We found that background noise normalization was not helpful in analyzing the magnetometer data for either the printer or the mill.

We found that the sound associated with travel at a particular angle to the X axis did not depend on where the tool head was located on the Y axis, so audio for the reference library and target objects could be recorded with the tool head anywhere on the machine platform and the phone anywhere nearby. In contrast, magnetometer readings fall off with the cube of the distance to the

source, and we found that the phone needs to be within a foot of the platform to pick up useful data. Magnetometer readings are also sensitive to the phone's orientation; flipping the phone around essentially reverses its reading. Still, as long as the phone's orientation remains approximately the same while recording, its magnetometer readings will reliably distinguish between a and $-a$. More generally, we expect that the best way to use magnetometer data will vary greatly for different types of machines, depending on the configuration of their motors and where it is natural to set down a phone. For example, if our phone had picked up on the head's side-to-side movement only, then we would have been able to distinguish between a and $180 - a$, rather than registering only the movement of the platform forward and back. In fact, when we printed an entire platform full of diamond shapes, the phone's magnetometer did seem to register additional information (perhaps generated at the tool head) while a diamond was printed in the extreme corner of the platform, very close to the phone. When magnetometer data is not available (e.g., an audio-only recording, the phone changing orientation during recording as the user moves around, or the magnetometer being too far away to pick up readings), each angle still appears similar to three others, its mirror images across the X and Y axes.

We found that analysis of the phone's accelerometer data did not improve the accuracy of reconstruction, so we used only audio and magnetometer data in the experiments. The accelerometer data does indicate the times at which the tool head changes direction at a segment intersection, which can be incorporated in the future to segment the data from the other sensors. Further analysis may reveal additional information the reconstruction method could utilize.

For a particular reconstruction task, additional domain or product constraints may be useful. For example, a reconstructed object should not extend beyond the machine's platform. If we know the general shape of the item being manufactured, such as a turbine blade, this context can inform the reconstruction process. If all constraints are met, we show the reconstructed object to the user; otherwise we move on to the next candidate reconstruction.

3.3 EXPERIMENTAL RESULTS

Setup. We conducted experiments with the Lulzbot Taz 5 3D printer and Other Machine Co. Othermill CNC mill shown in Figure 3.2, hereafter referred to as the "printer" and the "mill." The X axis of each machine is controlled by a stationary stepper motor that drives a carriage on which the tooling (the printer's extruder and the mill's spindle) rides. The Y axis of each machine is controlled by a second stationary stepper motor that moves the platform. The printer's Z axis is controlled by two stepper motors, one on each end, that raise and lower the full X axis. The mill's Z axis is controlled by a single stepper motor that controls the height of the spindle relative to the X carriage,

which remains fixed in height. All experiments in this section used the printer's default feed rate, 30mm/second.

We built an Android app that monitors and records the sensor data on a phone and used it to record the audio and magnetometer data used in reconstruction. The audio is collected at a 44100 Hz sampling rate.

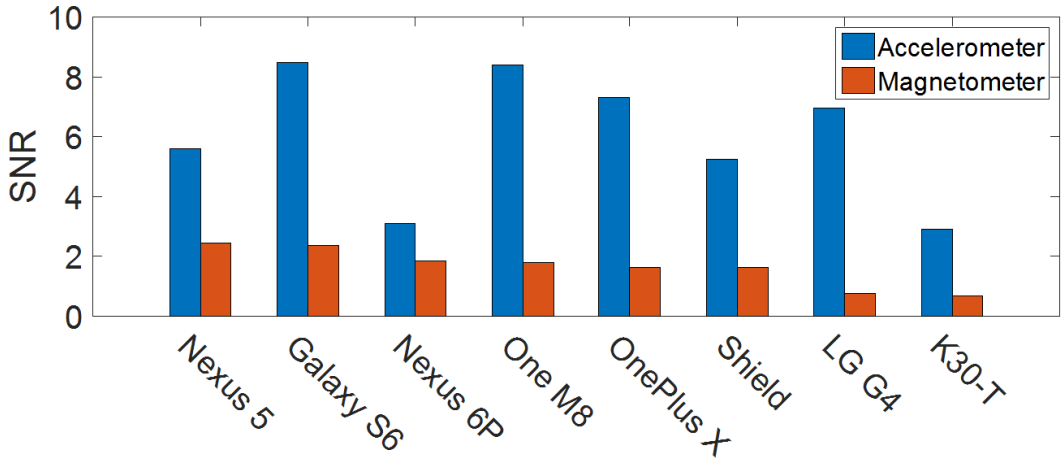

Figure 3.9: Signal-to-noise ratio (SNR) of the Accelerometer Y Axis and Magnetometer Z Axis Readings on Different Devices. The Samsung Galaxy S6, with the highest SNR for its accelerometer and second-highest SNR for its magnetometer, is the best overall.

3.3.1 Data Quality with Different Devices

To evaluate the quality of the sensor data produced by different devices, we installed the recording app on seven smartphones and one tablet, listed in Table 3.1. To ensure a fair comparison across devices, we placed each device with its lower right corner 2.5 centimeters from the rear left corner of the printer. Then we enabled the app's recording function while the printer fabricated a simple geometric shape resembling a trapezoid. The printed object and its process parameters were identical in each trial.

We compared the signal to noise ratio (SNR) of the accelerometer and magnetometer in each device. The Samsung Galaxy S6 performed the best overall, with the highest accelerometer SNR and second-highest magnetometer SNR. Surprisingly, the Nexus 6P, the newest model, had the second-lowest accelerometer SNR. The full results are shown in Figure 3.9. The placement of the sensors inside each device varies. While our other experiments suggest that for the accelerometer this variation will have a negligible impact on the reconstruction quality compared to the impact of the variation inherent in the sensor, the magnetometer works at a much shorter range, and it may be

affected. In evaluating the other sensors' data quality, we focused on the Galaxy S6.

Manufacturer	Model	OS	Form
HTC	One M8	Android 6.0	Phone
Huawei	Nexus 6P	Android 6.0	Phone
LG	G4	Android 5.1	Phone
LG	Nexus 5	Android 5.1	Phone
OnePlus	X	Android 5.1	Phone
Samsung	Galaxy S6	Android 5.1	Phone
Lenovo	K30-T	Android 4.4	Phone
Nvidia	Shield	Android 5.1	Tablet

Table 3.1: Compared Devices

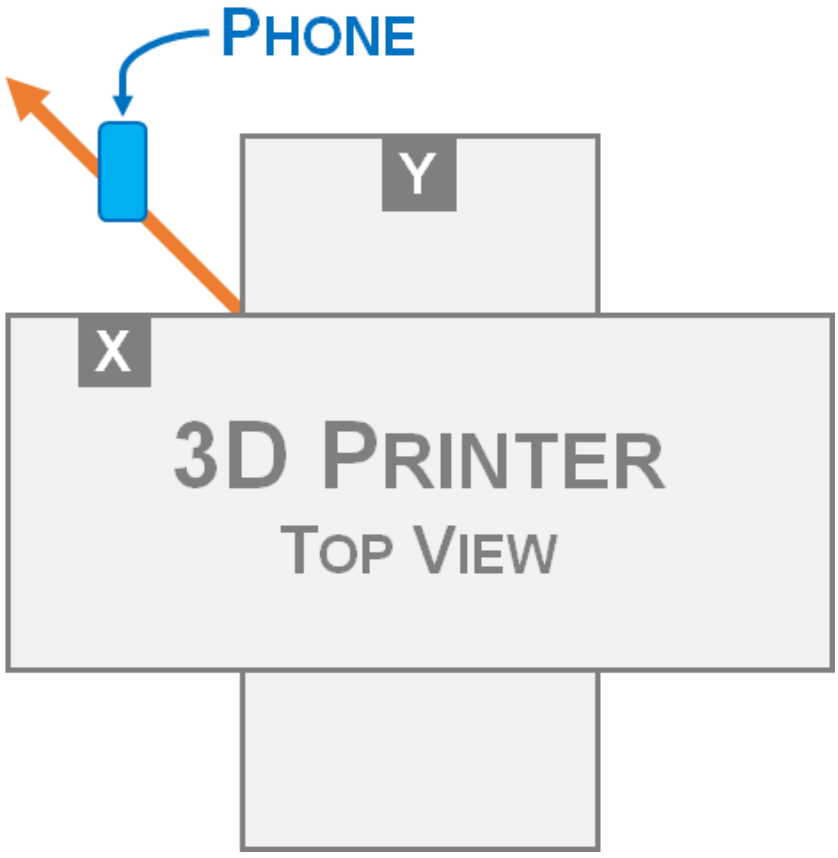

Figure 3.10: Setup for Testing the Quality of Sensor Recordings at Different Distances from the Printer. Starting from the rear left corner, approximately midway between the X and Y motors, the phone was moved away at a 135° angle.

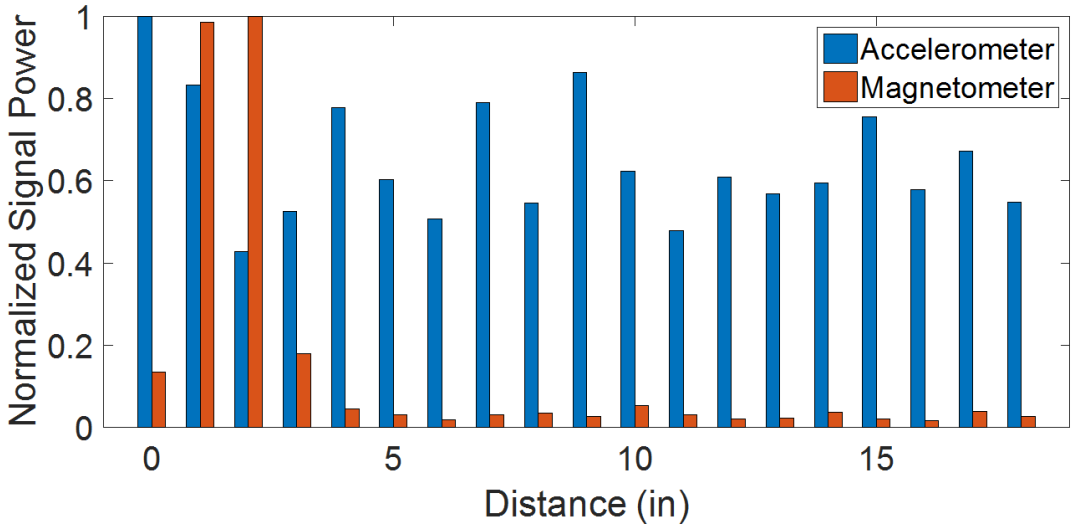

Figure 3.11: Signal Power of a Phone's Sensor Recordings at Different Locations from the Machine. While the magnetometer readings drop off sharply with distance, the accelerometer readings are strong at all locations on the table.

3.3.2 Data Quality at Different Locations

To determine the impact of distance on data quality, we compared readings from the Samsung Galaxy S6 at different locations relative to the 3D printer. Beginning at the rear left corner, the phone was used to record the same fabrication activity (a simple 45-degree line) as its distance from the printer was incremented by 2.5 cm. We moved the phone away from the printer in a line approximately 135 degrees from horizontal so that it remained approximately equidistant from the X and Y motors, as illustrated in Figure 3.10.

We calculated the signal power of the accelerometer and magnetometer readings at each location as a measurement of the effect of distance, as shown in Figure 3.11. The accelerometer, which was measuring the movement of the table the printer was placed on, had strong readings at all distances from 0 to 18 inches. The readings decreased slightly with distance, but the output was clear at all distances. In contrast, the magnetometer was measuring a magnetic field, and the strength of a magnetic field drops with the distance cubed. The magnetometer readings were unusable at distances greater than 4 inches. This limitation affects our ability to use magnetometer data to distinguish between mirrored angles.

3.3.3 Data from Different Machines

While the data generated by the 3D printer and mill is similar enough that our reconstruction methods can be applied to both, the data is also distinct. More generally, each machine has a unique

signature, and types of machines will have distinct sounds corresponding to their manufacturing processes. For example, the sound of a mill's spindle spinning and tool cutting is absent in audio from a 3D printer. The spindle noise alone is sufficient to distinguish between the printer and the mill used in our experiments. Additionally, each motor of a machine has a signature. Though they are nominally identical, depending on the configuration of the machine, each motor moves a different amount of weight. This distinction is already apparent within our printer and mill: the machine's X and Y motors are nominally identical but display distinct signatures. The frequencies at which the motors emit noise, as a function of the work they are doing, allows us to differentiate between different machine models. While this technique would also work to distinguish between different models of the same machine type—say, two printers instead of a printer and a mill—a more complex technique would be needed to distinguish between two same-model machines.

To substantiate these claims, we compared recordings of the 3D printer with recordings from the mill. The mill's and printer's X and Y movements are driven by similar motors in similar configurations, and we found that the mill's movements exhibit a clear, consistent, and uniquely identifiable audio signature, analogous to that of the 3D printer. We demonstrate this signature in Figure 3.5, comparing the spectrograms of the same turbine blade shape made on the printer and on the mill. The trace is shifted in frequency on the two machines, since each motor on each machine has its own signature, but the two traces exhibit the same pattern.

These results suggest that a recording of a simple calibration pattern is all that is needed to train either of our reconstruction methods on most 3D printers and desktop mills, as well as other types of subtractive manufacturing methods operated by stepper motors. This calibration pattern could be hidden in the interior of an object and designed to look like typical 3D printer infill, or hidden in the toolpath of a subtractive manufacturing operation. If the attacker asks the operator to manufacture this object and makes a recording, she now has all the information necessary to reconstruct objects and machining conditions from that machine.

3.3.4 Data Quality in a Phone Call Attack

The previous sections focused on the case where phone sensor data was captured by a malicious phone application. If the data was instead captured during a phone call, the audio signal will have been altered by the phone's noise reduction. Conveniently, the key audio frequencies of factory floor machinery tend to lie in the same range as the human voice, so the phone's noise reduction does not simply remove the signal.

We tested the phone call attack on both the printer and mill. The results from each recording, while noisier, are clear and consistent with the audio recorded directly on a phone located near the machine. For example, the frequency magnitude spectrogram in Figure 3.5 shows that the same

pattern is visible whether a recording is made next to the mill or recorded through a phone call. We also tested the phone call attack while people were speaking. Figure 3.5 shows the difference in the audio when a person is speaking two feet from the device next to the machine and speaking directly into the microphone of the device far from the machine; even though the speech overlaps the information-rich regions of the spectrogram, the trace is not obscured completely and the shape is still clearly visible.

While reconstruction following a phone call attack must rely on audio only, this method greatly broadens the scope of the attack. Capturing information from multiple sensors at once requires an appropriate app to be present on the phone; in contrast, the phone call attack allows any phone to capture factory audio with no prior preparation beyond the attacker being prepared to record the call on the remote end. More generally, an audio-only attack can be executed using any device with a microphone, which expands the attack to not only phones but also tablets, laptops, and other computers, either through malware or by recording a voice-over-IP call.

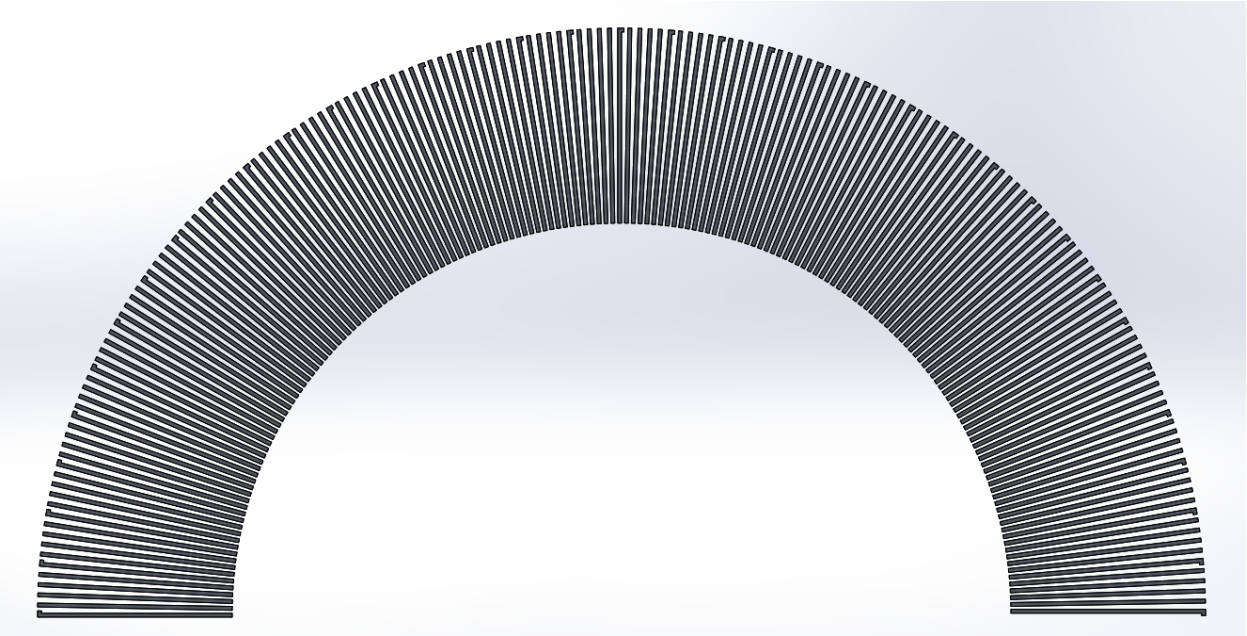

Figure 3.12: The Fan Shape Fabricated to Provide Example Audio for the Reference Library.

3.3.5 Accuracy of Reconstruction

All training and test data for the reconstruction methods was recorded using a Samsung Galaxy S6 placed within 4 inches of the printer, i.e., close enough to collect usable magnetometer data. We did not try to place the phone in the exact same position for each run.

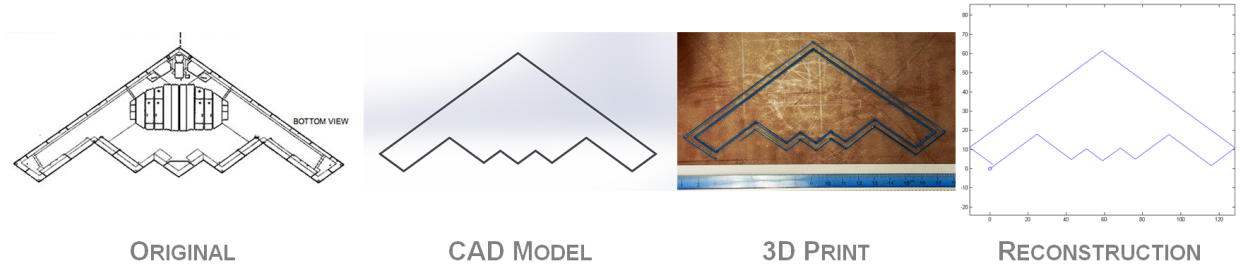

Figure 3.13: Results from Reconstructing an Airplane. The original design model (far left); the CAD design (center left); the fabricated object (center right); and the reconstructed model (far right).

We built the interactive framework using Matlab, Adobe Audition, and Python. For both the printer and the mill, we constructed the reference library from the audio of one pass of the machine head over the left-hand half of the 2-layer planar fan shape shown in Figure 3.12; this shape has 360 different angles of machine head travel in each mirrored half. A spectrogram of the resulting library is shown in Figure 3.6. As mentioned earlier, to prune the reconstruction search space for the signal processing method, we implemented three domain constraints in the signal processing interactive framework: the reconstructed object layer should be within .5 feed units of being a closed planar object with no mid-segment self-crossings, and there should be a change of angle at the end of each segment.

The framework's user was an EE Master's student with no prior experience with 3D printers or mills and no prior experience in audio analysis. She prepared for her reconstruction tasks by watching and listening to videos of a 3D printer and mill traversing a square, circle, triangle, and turbine blade outline (see `https://goo.gl/FijZ9T`). From examining the resulting spectrograms, she learned to recognize the visual signatures in the spectrogram corresponding to the start and stop of the machine's work on an object, the vertical bars where the machine head changed its direction of travel, and tool head up/down. She practiced by using the framework to reconstruct the triangle and square made by the 3D printer and the mill; due to angle ambiguities, her results included the actual objects as well as their mirror reflections, which we find acceptable for all reconstructions. We anticipate that crowdsourced workers with the same training as our user could segment the data equally well. To test this claim, a second-year computer science undergraduate with no prior experience with signal processing or audio also experimented with segmenting, and found it easy.

We tested the reconstruction effectiveness on the 3D-printed outlines of a star, an airplane, and a gun. Our user had never seen any of these designs before.

The resulting reconstructions, along with the original design, are shown in Figures 3.13 and 3.14, and we discuss their accuracy below.

The user reconstructed all three objects, plus their mirror reflections. However, she described the airplane, which was a B2 stealth bomber, as a "fish mouth" and was quite dissatisfied with the result, even revisiting the matched filter diagram to consider second-choice values for angles and look for other potential reconstructions. In other words, our user successfully reconstructed a mystery object, even though the mystery object was not something she could recognize in real life so she was not assisted by context. For the gun, our user reconstructed the original object, but did not a priori prefer it to variants produced by mirroring the angles in the very short segments of the gun.

Table 3.2 shows the length of each side and degree of each angle in the original and reconstructed objects. On average, angles are within a degree of the actual.

For the mill, we correctly reconstructed all angles in a square (not shown in the table); for a triangle, we reconstructed one angle exactly and the other two with 1 degree of error. The other objects in the table are from the 3D printer, and have similar accuracy in angle reconstruction.

As we currently perform segmentation manually, error in computing segment lengths is independent of the segment lengths and reflects human judgment and focus. The framework's user was off by approximately 1mm on average in indicating segment lengths for the plane and the star. This error could probably be reduced, as our main concern was getting the angles right and slightly-too-short segments do allow fully accurate angle reconstruction. We were highly accurate in perimeter reconstruction, the measure used by [57]. However, this measure is quite sensitive to the segment lengths of the target object, as the total error in manual segmentation is directly proportional to the number of segments, rather than to their lengths.

Even with fully-automated reconstruction, non-expert users could provide useful guidance during reconstruction. For example, we could hear someone clicking a pen in one of the machine recordings. The click was quite distinct from ordinary machine sounds, and we knew that it did not indicate a machine event such as an angle change; but signal processing techniques or a regression model might have been fooled by it. More generally, when machine learning and signal processing fail due to irrelevant background or foreground noise, a human may be able to salvage the reconstruction.

3.4 RECOMMENDATIONS

We designed and tested a defense that obfuscates the acoustic emissions from manufacturing equipment by playing recordings during production. Since noise reduction has been studied extensively[4], instead of playing a random signal, we chose to play recordings of variations of the part being produced that have small dimensional deviations from it. The attacker would still be able to determine the general shape of item being manufactured, which may provide situational

[4]For an introduction to the topic, see goo.gl/IFnJ0r.

Object	Reconstructed		Actual		Error	
	Angle	Length (mm)	Angle	Length (mm)	End Gap (mm)	Angle
Triangle 3 sides, 0.0348s/frame	16	20.6970	15	20	0.05013	1
	135	20.3462	135	20		0
	255	20.3462	255	20		0
Star 10 sides, 0.0348s/frame	35	59.8668	36	66.15 (all)	2.5119	1
	325	61.1012	326			1
	107	61.1012	106			1
	37	61.1012	38			1
	179	61.7184	178			1
	109	59.8668	110			1
	251	59.2497	250			1
	179	59.2497	182			3
	323	61.1012	322			1
	253	61.7184	254			1
B2 plane 12 sides, 0.0348s/frame	36	31.4916	36	31.32	4.2312	0
	324	21.4884	324	23.42		0
	36	10.3737	36	11.29		0
	324	10.7442	324	12.04		0
	36	10.3737	36	12.04		0
	324	10.3737	324	11.29		0
	36	22.9704	36	23.42		0
	324	28.5277	324	31.32		0
	36	15.5606	36	16.22		0
	144	91.1405	144	94.29		0
	216	89.6585	216	94.29		0
	324	15.5606	324	16.22		0
Diamond 4 sides, 0.0348s/frame	250	49.36	250	50	1.3436	0
	290	49.05	290	50		0
	70	49.83	70	50		0
	110	49.99	110	50		0
Gun 12 sides, 0.0348s/frame	73	42.2551	74	47.38	0.9093	1
	149	8.4510	150	10.43		1
	79	3.4969	79	4.60		0
	90	7.8682	90	9.71		0
	0	118.314	0	132.38		0
	270	14.5708	270	17.51		0
	180	69.9395	180	78.72		0
	270	9.3253	270	10.59		0
	288	4.0798	287	4.86		1
	180	22.4389	180	25.53		0
	253	32.3470	254	37.25		1
	172	23.0217	172	24.49		0

Table 3.2: Angles and Segment Lengths for the Original and Reconstructed Figures. The triangle is from the mill and the other shapes are from the 3D printer.

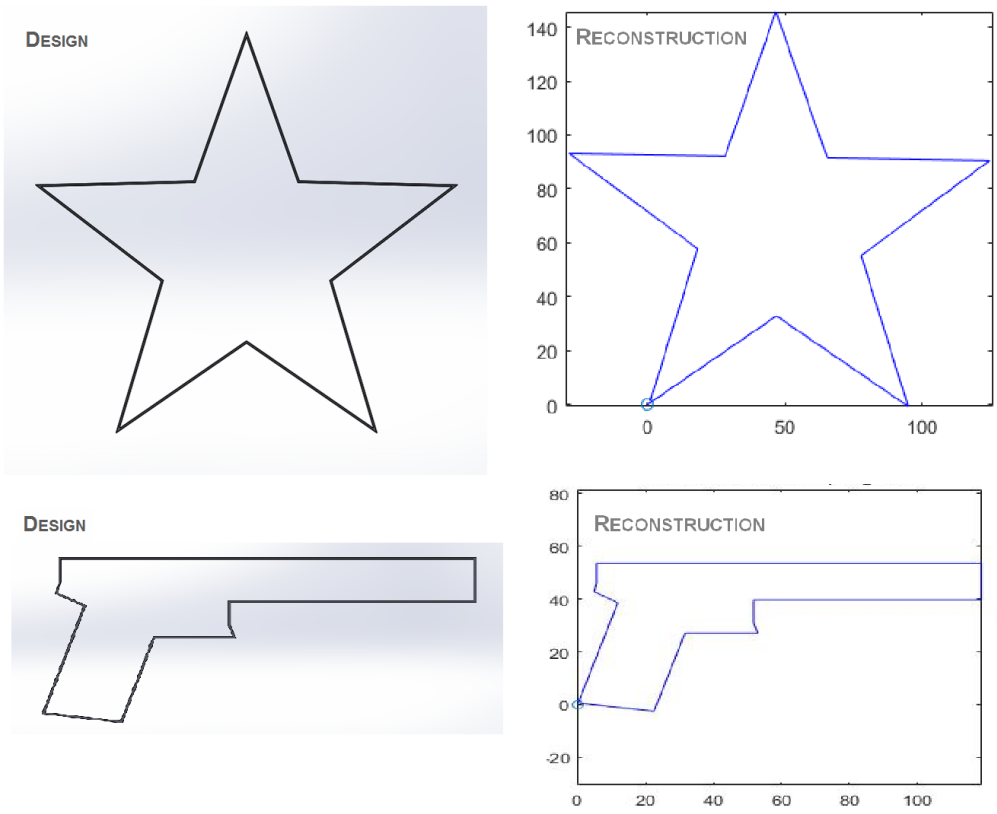

Figure 3.14: Original Design and Reconstructed Shape for the Star (top) and Gun (bottom).

awareness about a manufacturer's capabilities and the current activities in their factory. On the other hand, obfuscation can make it harder for the attacker to separate the target audio stream from the others and reconstruct the object's exact dimensions or process parameters. Because often the small details of the process or design are exactly the information that an attacker would like to obtain, it is worthwhile to make them harder to identify. For example, in high-value manufacturing, there may be a hundred wrong ways to make an object and one way to make it correctly. Obfuscation could greatly raise the cost of finding the right method, though this kind of obfuscation has inherent limits: since every speaker has a unique acoustic signature, in principle a set of played-back recordings could be identified as such and peeled away, revealing the desired audio within. However, if the obfuscation greatly increases the cost of the attack, it will make many kinds of manufacturing espionage not worth the price.

To test this hypothesis, we selected eleven similar turbine blade profiles and scaled them so that the print time was approximately the same. The first ten were recorded as they printed individually. The audio recordings from these prints were combined and aligned with a slight stagger at the beginning, and the resultant composite audio was played while the eleventh profile printed. Analysis of the composite audio shows that while the fundamental frequencies were reproduced, the harmonics

were lost during the combination step. In the eleventh recording, the fundamentals from the first ten turbine blades obscure the data necessary to reconstruct the eleventh, but the harmonics from the eleventh appear clearly; this harmonic data is sufficient for an audio reconstruction. In future work, we will experiment with combining the audio tracks in a way that preserves the harmonics and matches other features such as amplitude, to obfuscate the recording to a state that will significantly raise the cost of reconstruction.

Limiting the electromagnetic field generated by manufacturing machinery can raise the cost of reconstruction by making it expensive or impossible for reconstruction methods to determine which quadrant an angle of travel lies in. Since magnetometer readings drop off with the cube of the distance from the source, one option is to increase the size of a machine's enclosure. We tested this hypothesis with a large high-end new-model mill at the Digital Manufacturing Design and Innovation Institute, and found that when the phone was placed on the machine's enclosure, the magnetometer was too far away from the motors to pick up useful readings.

When it is not practical to enlarge an enclosure, improving motor shielding can help. For example, recent research on interference shielding has shown that polymer-matrix composites are effective for electromagnetic interference shielding due to their light weight, resistance to corrosion, flexibility, and modest cost. These composites have been used for many purposes (see, e.g., [58]). Additionally, researchers have shown that composites such as carbon nanofiber-polymer can provide effective shielding for the frequency range of $8.2 - 12.4GHz$ [59]. We suggest the use of composites to cover the stepper motors in manufacturing equipment with a shield thin enough that the motor is not damaged by excessive heat retention, but thick enough to protect it from broadcasting sensitive information to an adversary.

3.5 CONCLUSIONS

Factory floors produce vast quantities of proprietary data that can be stolen by adversaries intent on learning about manufacturing process specifications, product designs, and factory activities. Nation-states' activities to obtain this kind of information have grown over the years, and attacks on the manufacturing sector have become common. Using a CNC mill and a 3D printer to represent subtractive and additive manufacturing, respectively, we demonstrated that ordinary mobile phones can effectively capture these machines' acoustic and electromagnetic information on a factory floor, and the recordings can be used to reconstruct the objects being manufactured and the processes used to make them.

As both additive and subtractive manufacturing tend to be layer-oriented, we adopted a layer-oriented approach to reconstruction, using 3D printer data to reconstruct the shape and process

information for three previously unseen manufactured objects. Our method uses signal processing and machine learning techniques, coupled with an interactive framework that uses manufacturing domain constraints and a non-expert human to help guide the reconstruction process. Experiments showed that the method was highly accurate in reconstructing a star, a gun, and an airplane shape from recordings of a 3D printer, even though the human did not recognize the airplane as such after reconstruction.

As mobile phones are ubiquitous, so is the potential for carrying out phone-based attacks, regardless of the state of IT security in a factory floor's systems. Phone recordings may be made deliberately by an attacker or inadvertently by an individual with a compromised application on their phone or other microphone-enabled device. Good audio data can even be captured in the background of a phone call placed or received on the factory floor. For these reasons, we recommend that manufacturers consider obfuscating the side-channel signals emanating from their equipment by playing audio recordings of similar but flawed processes and shielding tool head motors or enlarging machines' enclosures. Most importantly, manufacturers should consider asking their employees and visitors to leave their phones at the factory door.

Chapter 4: THE PIPE ATTACK: AN UBIQUITOUS DATA EXFILTRATION PATHWAY IN COMMERCIAL SPACES

Fire sprinkler pipes running just above the ceiling of every room, water pipes zigzagging around obstacles on their way to a kitchen or washroom, gas pipes supplying fuel to the furnaces that keep occupants warm: pipes are such a normal part of building design that we rarely think about them. Yet these same pipes also pose a vulnerability not previously investigated by the security community, because as prisoners observed long ago, a tap on a pipe can be heard quite far away. Under the assumption that some form of signaling through building pipes can serve as the basis of a practical data exfiltration attack – the *pipe attack* – the key research questions become:

- What kinds of pipes can be used to exfiltrate data?
- Where can a pipe attack transmitter and receiver be placed in a building? How obvious is the installation process, and the installed devices themselves?
- How should the transmitter and receiver be designed? What kind of signals should they transmit? How should the transmitter and receiver be powered? Can they be soundproofed? Can they be retrieved after the attack has accomplished its goals?
- How can an attacker get the data to be exfiltrated to the transmitter and retrieve it from the transmitter?
- What kind of data can be exfiltrated – text, audio, video? What kind of bitrate can be supported, and under what conditions?
- How can we detect that a pipe attack is taking place? Can we quickly find its transmitter?
- What can be done to prevent the pipe attack or make it less effective, through computer science and/or new construction methods? How expensive will these defenses be?

In this chapter, we address each of these questions. We show that in any environment where an attacker can gain access to pipes, the attacker can attach to the pipe a small, removable, unobtrusive vibrating mechanism similar to a bone-conducting headphone, and use it to transmit wide-bandwidth data to a small receiver located elsewhere in the building or at its perimeter. Whether filled with gasses or water, the pipe acts as a wave guide that speeds signals on their way. The transmission path can run long distances across floors and even between floors, along a straight run or through many turns and twists. The narrower the pipe and the fewer intersections along the way, the better the signal travels, often even growing louder along the way to its destination.

The pipe attack matters because it can exfiltrate data from air-gapped spaces that are secured against remote network based attacks. Our implementation of the attack provided a covert channel of roughly 1Kbps for distances of up to 170ft. The maximum possible transmission distance is greater than that distance, as signals do not attenuate much and in fact often amplify as they pass through the pipe system. This attack can be carried out during normal busy hours for the building, as it is not impacted by environmental noise and can use frequencies above the range of human hearing. The attack is applicable to all commercial buildings and many residences, and does not require the attacker or a confederate to be nearby while the attack is underway, unlike most other covert channel data exfiltration methods. The attack is also hard to prevent and defend against, especially with a high-budget attacker.

In the remainder of the chapter, we first present our threat model and assumptions in Section 4.1. Then we examine what is known about the transmission of sound through pipes, metal, and water in Section 4.2. We also summarize previously proposed data exfiltration methods in that section. To evaluate the applicability of the attack, it is crucial to understand how fire sprinkler systems and other building pipes are laid out, which in turn is governed by the building codes and by construction cost considerations. We review this material in Section 4.3. After a discussion of pipe materials in Section 4.4, we apply sprinkler layout rules to the problem of transmitter and receiver placement in Section 4.5. We consider the issue of getting data to the transmitter and from the receiver in Section 4.6, and camouflaging the devices in Section 4.7.

Next we move on to the pipe attack itself. Section 4.8 considers potential options for the design and implementation of a pipe attack transmitter and receiver, and presents details about the most effective implementation that we found. In Section 4.9, we describe the real-world buildings and pipelines as well as the laboratory-conditions pipelines that we used for the experiments.

Section 4.10 presents our measurements of the bandwidth and effectiveness of such pipes as covert communication channels in existing large buildings. Section 4.11 analyzes the capacity of the channels tested.

In Section 4.12, we argue that the pipe attack transmitter and receiver are hard for humans and bug-sweepers to detect. We also propose and experimentally evaluate a variety of methods of defense, none of which prove fully satisfactory. In Section 4.13, we discuss ways to detect an ongoing attack, and Section 4.14 presents an efficient method to find an attacker's transmitter on the pipe while an attack is underway.

4.1 THREAT MODEL AND ASSUMPTIONS

The Threat The threat is that an attacker desires to exfiltrate high-value data in an air-gapped

environment where the data cannot be physically removed by easier means, e.g., via electronic transfer, on a portable device such as a memory stick, or via phone images. Such data might include, for example, audio or video footage, transcripts, or planning and design documents about matters of national or international security or strategy, or regarding very high value IP. Example physical environments include secure buildings such as embassies, computing facilities, and military, energy, and defense facilities. The attacker may be seeking to further national interests or pursuing personal gains, such as financial rewards.

Assumptions We assume that the attacker, a confederate, or an unwitting dupe of the attacker has physical access to the pipes in the building and is willing and able to attach to the pipes a small transmitter at the location from which the data is to be exfiltrated. Of most relevance are the sprinkler system pipes, which are usually easily accessible just above the suspended ceiling in every area of every room of every commercial building.

As discussed in detail in a subsequent section, we assume that the attacker has a means of capturing and transferring the data to the transmitter for exfiltration, whether through physical or electronic upload by a confederate or dupe or via a covert surveillance device such as Amazon's fake sprinkler heads that record audio and video.

We also assume that the attacker or a confederate has physical access to the pipes at another location in the building (e.g., a restroom, maintenance closet, or office down the hall), and attaches to them a small receiver from which the data is to be exfiltrated. The path between the transmitter and receiver must consist of pipes of diameter at most 3", as is true for rooms on the same sprinkler system on a floor of a building. We assume that the attacker, a confederate, or an unwitting dupe has a means of obtaining the data once it reaches the receiver, e.g., physical retrieval or another offloading mechanism.

4.2 RELATED RESEARCH

4.2.1 Sound Transmission through Pipes and Water

Though our work is unique in focusing on the security vulnerabilities posed by pipes, their use as a communication channel has drawn the interest of scientists and engineers for centuries. The first written record of this suggested use is in Sir Francis Bacon's unfinished utopian novel *New Atlantis* [60], published posthumously in 1627. Indeed, from the early 1800s until the telephone became popular, air-filled pipes were the standard means of communication at a distance in ships, submarines, cars, planes, and high-end homes and offices [61], reportedly at distances of up to

300 feet. Our work exploits similar techniques over similar distances, though for less upstanding purposes.

Pipe-based musical instruments demonstrate how pipes filled with air and open at one or both ends can resonate at some acoustic frequencies. The air inside the pipe carries the acoustic signal forward through the pipe [62]. As discussed later, we also observed resonance phenomena in fire sprinkler system pipes.

Communication through water has a long history of research. Underwater acoustic communication is crucial for maritime and navigation applications, where prior research has investigated multi-path propagation and channel characteristics of sea water that is under pressure. However, the extensive research on open sea underwater communication does not carry over to a water pipe setting. Compared to open waters, a water pipe is a hybrid medium where acoustic signals travel through the inner and outer pipe surfaces as well as through the water. In effect, a pipe acts as a waveguide, so signals propagate much further than in open water.

Researchers have examined the use of wave signals in acoustic, wireless, ultrasound, and other forms to analyse water, oil, and gas pipes and cables for application-specific purposes [63, 64, 65, 66, 67, 68, 69, 70, 71, 72, 73, 74, 75, 76, 77, 78, 79, 80, 81, 82]. In particular, acoustic signals can be helpful in detecting and localizing leaks and other structural health issues in water and gas pipes, and ultrasound is particularly useful for structural health monitoring of pipes and, more broadly, metal structures in general (e.g., [83, 84, 85, 86]). Generally, the idea is to use the metal structure, pipe, and/or the medium inside the pipe as a signal conductor. The signals are transmitted by communicating hardware sensors on the metal surface or inside a pipe. In the case of pipes, the pipe and medium provide a waveguide channel for communication.

Acevedo et al. [63] experimented with remote monitoring of pipe status using communication hardware and low cost sensors installed inside a water pipe. As part of their work, they experimented with communication between piezoelectric sensors mounted inside the pipe. Their experimental setup evaluated the frequency response of audible range (20Hz to 20kHz) sine sweep wave transmissions using a laboratory setup consisting of a small piece of cast iron pipe that measured 40cm in its longest section and had just two 90 degree bends. They found that sound frequencies in the 2-3 KHz range travelled well in the pipe. Since their setup involved a very small pipe in a laboratory environment, we cannot generalize directly from their experiments to real office buildings, but we found the frequency response information from this work useful as a starting point in our own work.

In other work, Jin et al. [65] evaluated the potential of a steel pipe for transmission of data. They used the pipe as a signal conductor for transmission along the surface and as a waveguide, employing sensors inside and on the surface of the pipe for transmission. In their experiments using a water-filled stainless steel pipe and transmitting data using sensors along the surface of the pipe, they were able to achieve a data rate of up to 100K bits per second with a mean bit error rate of

0.129. This work is in the spirit of our own, but their experiments focused on a 1.5 meter long steel pipe that was closed at only one end, making it hard to generalize to our setting of transmitting and receiving on the surface of building pipes, which are much longer and are closed at both ends. This work and that of Acevedo et al. considered transmitters and receivers inside the pipe as well as on its surface, while for reasons discussed later, we consider only surface mounts.

A technical report by Erickson et al. [87] investigates the feasibility of using gas pipes for communication between robotic devices inside the pipe. The authors investigated two scenarios. In the first, the gas-filled pipeline was treated as a waveguide, with the transmitter and receiver segments placed inside the pipe and transmitting transverse electromagnetic (TEM) waves through the pipe. In the second setup, the pipe was used as a conductor and signals were injected and transmitted through the surface of the pipe. When tested with a 24 inch diameter pipeline that was 0.9 miles long, both methods demonstrated good transmission of certain wave frequencies. When the transmitter and receiver were inside the pipe, the authors were able to support frequencies up to the 6 GHz range, with signal strength strong enough to support creating a connection with a 802.11b (2.5GHz) modem. When the transmitter and receiver were on the surface of the pipe, the authors were able to transmit signals below 1KHz frequency for the full 0.9 mile pipeline distance, though with more attenuation and more power required than for the first setup. This suggests that surface transmission would only be practical over long distances if amplifiers are placed regularly along the pipe. Although this work is based on gas pipelines using electromagnetic signals, we can use similar methodologies for evaluating the communication potential of water-filled pipes.

Researchers have evaluated the physical characteristics of underground water pipes as a communication channel [67, 68, 69]. One of the earlier works in this area studies the possible modes that propagate through buried iron water pipes as acoustic waves disperse [67] and shows how dispersion and attenuation varies for each signal mode. One of the interesting takeaways from this paper is their experimental setup, where to simulate the sound of water gushing out of a leaking pipe, they flush mounted a transmitter that is a tapping device consisting of a simple solenoid-controlled steel tip with a controllable tapping rate (0-5 kHz bandwidth) and force. To receive the signals, they used four accelerometers spaced at equal distances down the pipe. While this setup might not simulate the most accurate water leakage sounds, it is relevant in helping us understand that vibrations caused by direct tapping on the pipe surface can propagate over long distances.

The contents of a pipe affect how far and fast sound can travel through it. The speed of sound in water at 20 degrees Celsius is 1481 meters per second, which is about four times faster than in air (343 m/s). This is because water has a higher density and is less compressible than air. Sound travels faster through a medium that is more rigid, bounces back slower after compression and compresses less [68]. However, water being less compressible and denser than air also means that transmission of sound through water requires more energy than for the same signal to propagate through air. The

speed of sound increases in warmer temperatures (higher kinetic energy). Overall, our experiments showed that at normal indoor temperatures, sound propagated slightly better through water-filled pipes than through air-filled ones, although both worked quite well.

Regarding theoretical models of signal propagation through pipes, Maltseva et al. [69] analyzed the phase shift distortion and dispersion undergone by an acoustic wave as it propagates through a pipe, and built a theoretical model for it. Similarly, Kondis [68] provided a detailed mathematical analysis of the acoustic propagation characteristics of water-filled pipes. His analysis uses properties such as pipe material, pipe thickness and dimensions, and properties of the filled fluid, as well as the frequency and duration characteristics of the excitation acoustic signal. These works demonstrate that it is extremely complex to model the physics of acoustic transmission in water pipes once fittings, intersections, and turns are taken into consideration, and convinced us to take an empirical approach. While our focus is on transmission rate, distance, and signal clarity in existing building pipe systems, we do where appropriate reference the parameter interactions in the theoretical models of Kondis. To evaluate the communication potential of a pipe-based communication channel, we consider the bandwidth, frequency ranges, speed of transmission, distance of transmission, attenuation rate and bit rate, among other factors.

With one exception, the work cited in this subsection is based on laboratory experiments with pipes a meter or two long and very few if any fittings, intersections, and turns. (The exception is the .9 mile 24 inch pipeline [87] discussed earlier, which is also very different from building pipes.) These differences make it hard to confidently generalize from the prior work on structural health monitoring to what bit rate we may expect from pipes in large commercial spaces.

4.2.2 Structural Health Monitoring

Structural health monitoring typically uses ultrasound to identify potential areas of structural weakness in metal, such as in bridge, tunnel, and building superstructure. A number of recent works in this area have focused on allocating a separate channel in the ultrasound to return the results of the monitoring, and on potential communication protocols for use on that channel.

Low power usage is often a key consideration for structural health monitoring, and so reported single-frequency bit rates are low. For example, researchers have reported 21 bps at 6.35W [73], 100 bps at 5-10mW [75, 76], and 170 bps at 224mW [88]. For data exfiltration purposes, in general an attacker would like to have significantly higher bit rates than these, though they suffice for basic signaling.

When power is not such a concern, reported rates include 100 bps [65], 250 bps [74], 470 bps [82], 2K-10K bps [79, 80], and 20K-40K bps [78]. Again, ideally an attacker would like a higher bit rate, though these bit rates already pose concerns for sensitive locations such as embassies.

The work cited in this subsection typically involves small-scale laboratory experiments with short pieces of metal, which make it hard to confidently generalize from the prior work on structural health monitoring to what bit rate we may expect from pipes in large commercial spaces.

4.2.3 Data Exfiltration Methods for Air-gapped Spaces

We discuss previously proposed data exfiltration methods that work in buildings with air-gapped networks. Overall, the pipe attack does not require the attacker or receiving device to be in close vicinity during the attack, and does not require line of sight or have other limitations for capturing data remotely. On the other hand, we require the receiving location to be within the same pipe network, with no pipes wider than 3" along the path from transmitter to receiver; this requirement is usually satisfied by any two rooms on the same floor and wing of a multi-story building, via the fire sprinkler system; and by stacked rooms with water supply lines in multistory buildings, such as restrooms and janitor closets. Our approach has been shown to work at up to 170ft distances in real-world buildings, and it is compatible with many kinds of data sniffers/eavesdroppers at the transmitter side.

Previously proposed data exfiltration attacks for air-gapped buildings can be classified into methods that use acoustic, electromagnetic, electric, thermal and optical methods. We discuss each of these below.

Acoustic Methods Acoustic exfiltrations methods capture activity details from the noise emitted by computer components such as fans and hard disk drives. These attacks can use malware to control the fan and disk speed and movements, and hide data in that signal. The captured data is then transmitted to a nearby acoustic device (phone, speaker, headphone, microphone), which the attacker uses to record and exfiltrate the data from an air-gapped network.

In the Mosquito attack [89], Guri et al. use malware that changes speakers (or headphones) to act like microphone input devices, by changing the audio chip settings. These reversed speakers use speaker-to-speaker communication at ultrasonic frequencies to capture and send data stealthily between passive devices up to 9 meters apart, at 10 - 166 bps. Suggested countermeasures for Mosquito include making substantial hardware changes to audio devices/drivers, making software malware detection and change protections, and using ultrasonic jammers to secure areas. The simplest and easiest mitigations could be to disable changes to the audio hardware in UEFI/BIOS, or to simply eliminate speakers in devices in secure areas. Another attack [90] also uses speaker-to-microphone channels to transmit data up to 11 meters away at audible frequencies and ultrasonic frequencies, achieving a bitrate of 6.7kbps and 140bps respectively. However, the audible frequency range attacks are detectable by humans (500Hz and above range). In general, the pipe attack works

at greater distances, as long as the pipe network runs between the transmitter and receiver with relatively narrow pipes (under 3" diameter).

In the Fansmitter attack [91], Guri et al. use malware to control the speed of the fan in a computer (CPU, GPU or chassis fan) and hide and exfiltrate data to a nearby or remote microphone (smartphone). The attack works at distances of 1-8 meters, in presence of reasonable background sounds, at rates of 1bps per fan being controlled by the malware. Countermeasures proposed in this work include detecting, audio jamming, noise-blocking chassis, quieter fans, monitoring for malware, and most preferably changing to water-based cooling systems instead. Fansmitter might be easy to detect with monitoring (or hearing) the fan's fluctuating speeds. Again, the pipe attack works offers higher data rates at greater distances.

The Diskfiltration attack [92] exploits a covert acoustic channel through the noise from hard disk drives by using malware to control the drive's actuator arm to modulate data that is captured by a nearby audio device. Diskfiltration was able to transmit up to 2 meters with a bit rate of 3bps. This method does not work on solid state disk drives, which can be an easy countermeasure in secure buildings.

In the Inkfiltration attack [93], Briseno et al. use malware to alter printers to create imperceptible patterns on documents being printed, generating acoustic signals while doing so. These sounds are captured by a nearby acoustic recording device (up to 4m away), with a bit rate of around 0.5bps. Compared to this attack, the pipe attack has a higher bit rate at greater distances.

The CD-LEAK attack [94] uses a malware-infected computer to covert acoustic signals from optical CDs/DVDs, which is then captured by a nearby audio receiver (phone, computer, microphone). CD-LEAK experiments show a data rate of 0.8 to 3.5 signals per second at a distance of 1.5 to 8m.

The GAIROSCOPE attack [95] uses malware to generate ultrasonic tones in the resonant frequency of a MEMS gyroscope, and exfiltrates data via a speaker-to-gyroscope covert channel by sending attack audio signals that oscillate the gyroscope. Gyroscopes generally require low permissions for access and are not as well protected as other smartphone sensors such as the microphone; this weakness makes this malware-assisted attack convenient. Experiments for the GAIROSCOPE attack shows that it works for 0-200cm distance with bit rates of 1-8bps. In an earlier work that also uses gyroscopes for eavesdropping, Michalevsky et al. captured speech using the MEMS gyroscope of a smartphone [96] at the resolution of $<$200Hz, sufficient to identify the speaker (50% success rate) and understand some parts of speech (26% when speaker is unknown, 65% when speaker is known). Compared to these attacks, the pipe attack has a higher bit rate at greater distances, and works in buildings where cell phones are not allowed.

A few attacks use sensor-based side channels on smartphones to capture acoustic data. One attack uses the phone's accelerometer to eavesdrop on the speaker on the same phone [97]. Using a spy app that employs deep learning methods to recognize and reconstruct the speech on the received

accelerometer side channel data recordings, it can achieve 78% accuracy in differentiating 10 digits and 70% accuracy in recognizing 20 speakers when the phone is placed on a table. Other researchers have also extracted sound from smartphone sensor side channels (e.g., [98, 99, 100, 101], and a prior work from our research group using audio and magnetometer side channels to steal factory IP secrets [9]. The AirViber attack [102] uses malware-generated vibration covert channels to vary the speed of the internal fans in a computer, which can be sensed by the accelerometer of a nearby smartphone placed on the same table surface. Again, the pipe attack works in secure buildings where smartphones are not allowed.

Optical Methods A historically well-known data exfiltration method is to use a laser microphone to eavesdrop by pointing at a vibrating device that is close to a sound source [103]. As far back as 1880, Alexander Graham Bell developed the photophone, a telecommunication device that can transmit speech on a beam of light up to 213m away, a precursor to the CDs, DVDs and fiber optic communications of today [104]. The underlying principle is that when a laser beam hits anything that vibrates, it starts to vibrate too and capturing this can give us information on the source sound of the vibrations. Léon Theremin built a popular war-time spying gadget using a variant of this technique (infrared beams), called the Buran Eavesdropping device [105]. In 1984, Ralph Muscatell filed the first patent for a laser microphone [106].

Today, laser-based eavesdropping through glass and walls is a fairly well known technique, with spying devices commercially available [107] and instructions for building such devices also readily available [108]. A version has even been patented that captures sounds by observing the vibrations of particles in free air (U.S. patent 7,580,533), without the need for glass or another reflective surface, although the device does not seem to be commercially available. In general, today's laser microphones can capture sound with a low distortion of 8% [109], and reach distances of up to 400m [107], although at greater distances and oblique angles, distortion makes it practical only to separate and perhaps recognize individual speakers, not reconstruct their conversations.

Compared to the pipe attack, these vibration-and-laser-based exfiltration methods have the advantage of not requiring the presence of a confederate or dupe inside the building, as long as the target data is already available as sounds in an appropriate room. Like the pipe attack, they cannot be detected with an RF scanner, can be started and stopped at will, and humans cannot see or hear them if the devices avoid the human-audible and human-visible frequencies and are camouflaged from view. Laser-based microphones also have the advantage of being able to move data through open air and beyond the building perimeter, unlike the pipe attack. On the other hand, the pipe attack does not require line-of-sight or the presence of walls or windows, which is important since purpose-built high-security buildings and rooms typically do not have windows and are constructed with walls that do not easily vibrate.

When line of sight is available and the weather is good, a laser microphone can be used from far away, e.g., 400 meters for today's Spectra Laser Microphone M+, whereas the pipe attack works within a single piping system (up to 52,000 square feet in the case of a sprinkler system) and requires a wired or wireless repeater to transfer data between two physically separate pipe systems, such as a sprinkler system and the potable water supply lines. Further, the laser approach can only capture data that is already audible within a room, e.g., a conversation, so it is not as well suited for exfiltrating digital data. The pipe attack is also immune to bad weather and rippled window glass, and cannot be detected with an infrared scanner (although neither can the Spectra Laser Microphone M+, according to the marketing brochure for its "innovatory beam modulation technology"). Both attacks can be mitigated with small devices that inject noise directly into each piping system and each window, respectively. The two approaches can be combined by using the pipe attack to move data from a windowless room such as a conference room to another room that has a window, and from there to outside the building. High-security buildings can increase the cost of such attacks through glass by installing white-noise vibrating devices on their window glass.

With the Visual Microphone, Davis et al. [110] use high speed video to capture minute vibrations on everyday objects (tissue paper, water bottles, potted plants, bags of chips, and so on) that leak audio data from their environment. The experiments used a 400mm lens camera to recover sounds from 3-4m away. The pipe attack works over greater distances and does not require line-of-sight access, but the Visual Microphone has the advantage of moving the data outside the building. As with laser microphones, the two techniques can be combined.

The Lamphone attack [111] uses covert optical methods to capture the vibrations of a desk light lamp bulb and recover speech and sound from the vicinity. Lamphone can recover sounds at intelligible levels when the source is 10-35 meters from the light. Unlike the pipe attack, Lamphone requires line-of-sight between the attacker's device and the electro-optical sensor used for capturing the vibrations on the light source. On the other hand, the attacker can be outside a clear window, so Lamphone can be used to move data out of a building, unlike the pipe attack. Other vibrating devices in close proximity, such as a fan or air conditioner, can make it difficult for Lamphone to work or limit the quality of the extracted signals. As with other approaches that work through a window, Lamphone could be combined with the pipe attack to move data to a room with a window, turned into vibrations in that room, and then exfiltrated using Lamphone.

Electromagnetic and Magnetic Methods Researchers have used malware [112, 113] to tweak the current in wires to control EMF generation and leak data from air-gapped computers, achieving a bandwidth of up to 480bps and at up to 9m distance. Researchers have also used malware to send data to infected phones in the vicinity through FM signals [114]. CPU and memory buses have also been exploited to exfiltrate data at GSM, UMTS and LTE frequencies, at bit rates of 1-2bps and

distances up to 30m [115]. USB has also been used to generate EMF to exfiltrate data in air gapped places [116] at 160-640bps.

Compared to these signaling methods, the pipe attack offers higher bit rates over greater distances. Further, the EMF emission attacks can be prevented by reducing emissions using shielding devices, insulation around secure areas, and prohibiting bringing USB devices and mobile phones into the building. All EMF attacks also require malware-based modifications and anti-malware defenses can be effective in preventing these.

Magnetic side channels can leak data that can be captured by magnetometers in smartphone devices, as demonstrated by previous work [101, 117]. However, magnetometers' effectiveness drops rapidly with distance, so this attack only is practical within a few centimeters of the sound source, as discussed in [9]. Distance based protection and magnetic shielding to reduce emissions can be employed as defenses, as can a ban on mobile phones.

CMOS devices have been shown to leak information about underlying computations through EMF side channels, presenting a threat to cryptography and revealing otherwise secure computations [118]. This is orthogonal to the pipe attack, which seeks to move data much longer distances.

Electric Methods Electric signatures emitted by a smartphone being charged by a USB device can be captured by an electric side-channel in the USB charging cable to leak information about the location of button presses on a smartphone screen that a user is interacting with [119]. On-chip power monitors can be built on FPGA chips to analyze powerline patterns that leak information and break timing protections for RSA cryptographic measures running on the computer [120].

The PowerHammer attack [121] uses conducted emisssions to send information about CPU utilization by modulating, encoding and transmitting over the powerline. In the powerline based attack called PowerMitter, malware based control of CPU utilization is used to change the electromagnetic emissions of the power supply [122].

These techniques are orthogonal to the pipe attack, which seeks to move data much longer distances and is applicable in environments that ban mobile phones.

Thermal Methods Monitoring thermal signatures in a computer can give insight into the activity performed by a user, as demonstrated in the ThermalBleed attack [123], where various cache and physical memory accesses were shown to display differentiating thermal signatures. Similarly, the thermal signature emanating from the servers in a data center can leak information such as runtime and usage information [124]. An attacker has to be present within centimeters of the device to capture the thermal radiation patterns for these attacks, and as temperatures take a long time to change, the effective data bitrate is only 1-40 bits per hour. Similarly, the BitWhisper attack [125] exploits heat emissions using built in thermal sensors, transmitting data as thermal changes at

the rate of 1-8 bits per hour. Compared to these attacks, the pipe attack works over much larger distances and offers higher bit rates.

4.3 BUILDING CODES AND FIRE SPRINKLER SYSTEMS

After a brief overview of building codes, in this section we explain the different types of fire sprinkler systems and how they work. For our purposes, sprinkler systems can be characterized by what material they are filled with, when they are filled with it, what they protect, how their pipes are laid out, and what their pipes are made of. Readers who are already familiar with fire sprinkler systems may wish to skip to the next section.

This section is full of "weasel words": *generally*, *usually*, *normally*, *typically*. Every building code rule has its exceptions, construction abounds with both literal and figurative corner cases, new specialty products and materials are continually introduced, different jurisdictions adopt and modify different building codes, and different building inspectors have different opinions on what is permissible. However, these details do not really matter here, as we seek not to build fire-safe buildings, but to exploit them. This section accurately depicts what an attacker can expect to find overall in a building's sprinkler system.

4.3.1 Building Codes

Building codes worldwide devote much of their space to rules intended to ensure fire safety. Under the *prescriptive* approach, the building code lays out a set of construction rules that suffice to guarantee certain safety provisions in the event of a fire, based on empirical evidence from past fires and from research results. Under the *performance-based* approach, the burden is on the building designer to show through calculation and simulation that the building's occupants will have a certain amount of time to escape before they are overcome by smoke and flames, and the building's structure will not collapse. Often both prescriptive and performance-based approaches are allowed in a particular jurisdiction, at the discretion of fire officials.

Prescriptive building codes generally require fire sprinkler systems in commercial buildings. However, performance-based codes, such as the pan-European Eurocodes [126], do not. Nonetheless, sprinkler systems greatly reduce the chance that a fire will spread enough to overcome people before they can escape, and that a fire will cause structural collapse. Thus although performance-based codes do not require the use of fire sprinkler systems, the *voluntary* inclusion of a sprinkler system in a building design will tend to greatly reduce the expense of the structural parts of the building, the expense of materials used to protect the structural members from fire, and the size of the structural members and their fireproofing. This in turn frees up space in the building, which

provides more freedom and flexibility to the building designer for a given budget, and will generally also leave more floor space for building occupants. Since these incentives all strongly encourage the use of sprinkler systems in performance-based designs, we assume that building designers in jurisdictions governed by performance-based codes will choose to include sprinkler systems.

The discussion that follows is based on the provisions of the prescriptive codes that require sprinklers, as they serve as a baseline for what to expect.

Almost all jurisdictions in the US and Canada have adopted a version of the National Fire Protection Association Standard for the Installation of Sprinkler Systems (NFPA 13) [127]. This standard is referenced in the broader International Fire Code (IFC) [128] and in the International Building Code (IBC) [129].The IBC and its sister standard for one- and two-family homes, the International Residential Code (IRC) [130], require fire sprinkler systems in almost all new construction and remodeling over a certain size, both commercial and residential.

Jurisdictions that adopt the IBC, IRC, IFC, and NFPA 13 often add local amendments that can weaken or strengthen their fire code provisions. Most local jurisdictions in the US and Canada have *not* adopted the IRC's requirement for sprinklers in small-scale residential construction, but *do* require sprinkler systems for all but the smallest commercial buildings. Building codes in China also require sprinkler systems in large or tall commercial buildings [131]. NFPA's and NFPA-13's influence is global, and the discussion that follows is based on the IBC and NFPA 13.

4.3.2 Wet and Dry Sprinkler Systems

The material that a sprinkler system uses to put out fires will be water unless the system is in a high-hazard area where another material would be more effective, such as in an aircraft hangar. The water can be in the pipes connected to the sprinkler heads all the time (a *wet* system) or only in case of fire (a *dry* system). A wet system is the preferred approach unless the pipes are subject to freezing or the area being protected contains valuable material that could be badly damaged by water, such as in a computer room or an art museum. In a dry system, the pipes are pressurized with air or nitrogen; if a sprinkler head activates, the gas rushes out and then water follows behind. If the system is for a high-hazard area such as a chemical plant, where a fire could spread extremely quickly, a *deluge* system is needed, where all sprinkler heads turn on at once. Otherwise, only the sprinkler heads that overheat will turn on.

Popular TV shows and movies have given us the impression that, as the NFPA puts it, "When a fire occurs, every sprinkler will activate and everything in the house will be ruined." In fact, 85% of the time, only the sprinkler closest to the fire turns on, spraying water on the fire and putting it out [132].

The IBC dictates sprinkler system requirements according to the use of the area that the sprinkler

system will protect. For our purposes, it suffices to consider light-hazard and ordinary-hazard usage. Office and residential space will normally be light-hazard, while factories, restaurant kitchens, and enclosed parking garages will normally be ordinary-hazard. (Factories that work with dangerous materials are not ordinary-hazard, and must meet a higher standard.) As the hazard level grows, the IBC requires sprinkler heads to be located closer together and/or to emit more water. In turn, this means that higher hazard levels must use larger diameter pipes to supply the needed water pressure; this impacts the effectiveness of the pipes for signal transmission, because wider pipes are less effective as waveguides. In light-hazard and ordinary-hazard settings, sprinkler heads will normally be spaced approximately 15 feet apart in each direction in each room. Further, there will be a sprinkler head within 6-7.5 feet of the wall around the perimeter of each room.

Sprinkler heads activate when the ambient air reaches a certain temperature, usually set hotter than a hot water heater (140 degrees Fahrenheit). Rising temperatures make a liquid stored in the sprinkler head expand, breaking the little glass ampule that encloses the liquid. When that ampule breaks, the water or gas in the sprinkler head rushes out.

For areas containing valuable material, such as a computer server room or art, a dry *preaction* system may be used. A preaction system requires two positive inputs before water will start to flow, such as a signal from a smoke alarm in addition to an overheated sprinkler head.

4.3.3 Pipe System Layout

Commercial buildings normally have a large pipe called a *standpipe* that goes vertically through the building, typically through a stairwell. The fire department can attach a hose to the standpipe at the bottom of the building, often without needing to go into the building, and connect the other end of the hose to a nearby hydrant to boost water pressure.

Water for the sprinkler system and for other uses can flow through the same standpipe or *riser* (vertical pipe), but typically the sprinkler system in a commercial building will have its own separate standpipe. That way its water pressure is not diluted from other usage, which is important because high water pressure is key for designing a low-cost sprinkler system. In our situation, the separation of the two systems means that the sprinkler system will not have noise from running water. In many jurisdictions, if the sprinkler system has its own separate standpipe, then that standpipe can be connected directly to the water main outside the building, bypassing the water meter entirely. This is interesting for our purposes, as it opens up the possibility of transmitting data all the way out of the building, rather than having transmission end at the water meter.

Each sprinkler system standpipe can service up to 52,000 square feet. The pipes that connect directly to sprinkler heads are called *branch lines*, and NFPA 13 requires them to be 1 inch or greater in diameter. Branch lines are tied together on a single floor with (usually larger) pipes called

cross mains. Larger-yet *feed mains* connect the cross mains to the riser or standpipe on that floor. To minimize construction costs, generally the smallest diameter pipes are used that will supply the required flow rate (typically a minimum of 7 pounds per square inch) at the sprinkler heads furthest from the riser that serves the sprinkler. Each pipe fitting (connection between two or more lengths of pipe) has a small negative effect on the flow of water, and the NFPA provides tables that allow engineers to convert each fitting to an equivalent length of pipe when computing pressure at a sprinkler head.

The art and science of laying out sprinkler systems is based on a combination of NFPA 13 hard requirements for sprinkler head spacing and coverage, minimum required water pressure at each sprinkler head, and minimum-height-above-floor requirements; and soft requirements, such as the need to route pipes around obstacles such as ductwork and beams, to ensure that strong structural members are in the right locations to support pipe hangers for the pipes, and to minimize the cost of material, fabrication, and installation.

In new construction, sprinkler systems are normally installed after structural, heating, ventilation, air conditioning, plumbing, and electrical work is completed. To dodge the artifacts left by these tradespeople, branch lines and cross mains normally run *underneath* all these other obstacles. As a result, in an office environment, the branch line that feeds a sprinkler head is normally located just above the ceiling.

The diameters of the branch lines, cross mains, and feed main are determined by the need to provide a certain amount of water pressure at each sprinkler head. To a first approximation, the number of sprinkler heads that can be serviced by a pipe of a particular diameter is predetermined, whether the pipe is a branch line, cross main, or feeder main. For example, NFPA 13 limits 1 inch branch lines to service 10 sprinkler heads, about 150 feet.

On a single floor of a building, the sprinkler pipes will be laid out as a tree, a loop, or a grid.

In a tree layout, the pipes form a tree (in the usual computer science sense of the word), with the standpipe connection at the root of the tree. A tree layout provides exactly one path to each sprinkler head from the riser supplying the sprinkler system on that floor. Every building we have been able to examine in the course of this research has had a tree layout.

In a loop layout, there are two paths to each sprinkler head. In a grid layout, there are many paths. The advantage of a loop or grid layout is that the designer can achieve the required water pressure at each sprinkler head using smaller diameter pipes than in a tree system. Smaller diameter pipes are cheaper, take up less room above the ceiling, and are less likely to require a redesign and rebuild of the sprinkler system when the interior is remodeled in the future.

In theory, the smaller diameter pipes of a loop or grid topology may be more effective waveguides than the larger pipes of the tree topology. Further, the shortest path between a transmitter and receiver might be much shorter in a loop or grid than in an equivalent tree topology. However, the

more intersections a sprinkler system has, the less distance the signal from a transmitter can travel before its signal becomes so attenuated as to be undetectable. Further, signals that take different paths through the grid may interfere with each other, making it harder to decode the transmission. This suggests that a loop or grid topology is not necessarily more effective than a tree topology for transmission of vibrations. Since we did not locate any buildings with loop or grid topologies, we were unable to investigate these questions empirically.

4.4 PIPE MATERIALS

Water supply lines for fire sprinkler systems can be made of various forms of steel and iron, copper, or CPVC. Buildings a century old may still have cast iron in parts of their sprinkler systems. Steel eventually replaced cast iron for that purpose in part because of its lighter weight, which makes it easier to install and requires less expensive and bulky hangars and supports for installation. Black (non-galvanized) steel is the most popular sprinkler pipe material today in commercial buildings, and it is also used for natural gas lines.

CPVC is a plastic with a high melting temperature that can be cut, joined, and installed in a manner very similar to PVC. Since 1985, CPVC has been allowed in many jurisdictions for light-hazard sprinkler systems. CPVC is lighter weight than steel and much quicker and easier to cut to size and install, which in turn lowers construction costs. This is making it popular in those jurisdictions that allow its use in sprinkler systems. We did not find any buildings that use CPVC for sprinkler systems, so we experimented with that material under laboratory conditions.

Old plumbing tends to use copper water supply pipes for non-sprinkler use, because copper lasts well, is relatively easy to work with, and used to be quite affordable. In many jurisdictions, new construction and remodels use PEX instead of copper, because PEX is very flexible, which makes it quicker and easier to install than copper. PEX melts at too low a temperature for use in sprinkler systems in commercial buildings, as does PVC, which warps just from carrying hot potable water. Since any sprinkler system is safer than none, NFPA 13D does now allow PEX in single-family home fire sprinkler systems. We did not come across any buildings that use more than a tiny bit of PEX.

As low-density residential fire sprinkler system requirements are adopted in more jurisdictions, the pipe attack will become quite practical for those settings. Until then, the attack can be used with residential water supply lines or gas lines, although unlike fire sprinkler systems, these pipes are not normally present in every room.

4.5 TRANSMITTER AND RECEIVER PLACEMENT OPTIONS

The ubiquity of fire sprinkler systems in commercial buildings throughout the developed world makes them ideal for the pipe attack. Sprinkler heads are generally spaced 6-15 feet apart in every room of the building, with pipes located very close to the sprinkler heads, so an attacker's transmitter can be placed within a few feet of any desired location in the building, as long as the attacker has access to the pipe. Since sprinklers do not operate unless there is a fire, the water or air inside sprinkler pipes is stationary, and building codes require the water or air inside the pipes to meet strict pressure standards. Thus these pipes provide a very stable medium for wave propagation, undisturbed by noise from flow-based environmental changes that other water and gas pipes are subject to.

4.5.1 Ceiling Types

Three types of ceilings are used in most commercial and residential buildings: suspended ceilings, finished ceilings and open ceilings.

Suspended Ceiling Suspended ceilings are the most popular finishing material for many types of commercial buildings, because they make it so easy to repair and update mechanical systems and to move walls and remodel spaces for new tenants. Suspended ceilings have a metal support grid that holds acoustic tiles.

Given a suspended ceiling, an attacker can install a transmitter or receiver on a branch line in a few minutes: stand on a desk or ladder, pop up the acoustic tile next to a sprinkler head, superglue the device to the top of the sprinkler pipe, and drop the tile back in place. The acoustic tile even provides additional soundproofing, so the data transmission can create more ambient noise than with an open ceiling. Any employee or visitor with a few minutes alone in a room should be able to complete the installation without drawing the attention of others, assuming that a ladder, desk, bookcase, or other furniture is at hand that is tall enough to allow the attacker to reach above the ceiling. Otherwise, an attacker can disguise herself as a maintenance worker, tradesperson, or janitor and install the device, or bribe an authentic such worker to install it.

Finished Ceiling Finished ceilings are the norm in residential settings and can be found in commercial spaces as well. To maintain an attractive appearance when the ceiling is finished with drywall or another material, normally each sprinkler head is concealed by a color-matched cover plate that will be pushed out of the way by water if the sprinkler head ever activates. The finished ceiling prevents an attacker from easily reaching the branch line to install a transmitter or receiver.

To install a receiver or transmitter above a finished ceiling, one approach is for the attacker to follow the relatively intrusive and obvious procedure normally used to replace a damaged or painted (paint is never allowed on sprinkler heads) sprinkler head: turn off the sprinkler system's main water valve, unscrew the sprinkler head in question, use a bucket to catch the water that comes out, attach the receiver or transmitter to the branch line or directly to the new sprinkler head, install the new sprinkler head, and re-pressurize the system.

An easier approach is for the attacker to reach a fire sprinkler pipe through an existing hole in the finished ceiling that was cut for another mechanical system, such as a modern recessed light that can be popped back up through the ceiling, leaving a hole wide enough to reach through. In the absence of such holes, the attacker may be able to maneuver through the more awkward holes left by installing smoke detectors, ordinary light fixtures, or fans.

If the ceiling offers no convenient holes, the simplest approach is to use a hole saw drill attachment to drill through the drywall near a sprinkler head, reach through the hole to install the device on the pipe, then fill the hole with a cover plate or fake device such as a smoke detector. The cover allows easy access for subsequent removal or replacement of the device. If it would draw the attention of others to use the hole saw, the attacker could bribe or masquerade as a tradesperson.

While it is also possible for the attacker to patch the ceiling using the piece of drywall from the hole saw, that would be unwise. It would take quite a few minutes to tape the edge of the patch, apply drywall mud, wait for it to dry, smooth it, add a second coat if needed, then prime and paint it. More importantly, it would be very hard to exactly match the existing paint color, and painting the entire ceiling would take even more time. For these reasons, a cover plate would usually be a better option than repairing the ceiling.

Open Ceilings Not every building has a finished or suspended ceiling. Factories and very modern and very old-fashioned spaces often have an open ceiling, where pipes and wiring are out in the open instead of being concealed behind other materials. With a ladder of the right height, pipe access is easy in these cases.

4.5.2 Receiver Placement Options

All the sprinkler pipes attached to one standpipe form a single interconnected network, and with a sufficiently strong signal from the transmitter, the attacker should theoretically be able to transmit between any two points in that network. Sufficiently large buildings will have two or more separate standpipes and sprinkler systems, and we will not be able to transmit signals between the separate systems. So once the transmitter is in place, the attacker's receiver must be installed somewhere on the same fire sprinkler system.

Conveniently for the attacker, to minimize construction costs, the building will be designed with as few separate sprinkler systems as possible for its footage (maximum 52,000 square feet per system in the US). This means that in a building of less than 52,000 square feet, all the sprinkler pipes will be interconnected, making it theoretically possible for the attacker to install the receiver on a sprinkler pipe in any room of the building.

In buildings larger than 52,000 square feet, usually construction costs will be minimized by putting a riser in each stairwell of the building, and using the riser to supply water to the sprinkler heads in the 52,000 square feet nearest to that stairwell, with similar coverage on each floor. This means that an attacker can, in theory, place the receiver in any room relatively close by on the same floor, or in the rooms stacked above or below it on other floors.

4.5.3 Transmission Between Floors

Our experiments presented later show that it is harder in practice to transmit signals between different floors than the equivalent distance across a single floor, because the fire sprinkler risers in multistory buildings are much larger in diameter than the branch lines, cross feeds, and main feeds that traverse each floor. Further, sounds may escape the pipes, echo, and be amplified by the hard surfaces in the stairwell, making them more noticeable to passersby. Thus we do not consider it practical for an attacker to send signals between floors using the sprinkler system. For example, an attacker would probably not be able to use a fire sprinkler system riser to transmit from an upstairs office in a high-rise down to a first-floor publicly-accessible restroom without attracting attention.

To transmit between floors, other types of pipes may be more useful. To minimize construction costs, generally water coolers, restrooms, and maintenance closets will be stacked one above the other in a building. Water supply lines, usually made of copper, run vertically between them, and are much narrower than the risers that supply the sprinkler system. Attacker access to water supply lines is somewhat limited (e.g., underneath restroom sinks), but the narrower size and vertical configuration of water supply lines running between stacked restrooms, water coolers, radiators, and maintenance closets make the water supply lines a more effective and accessible transmission route than fire system risers.

On the other hand, water supply lines do have the disadvantage of intermittent noise from water flow, and the need for the attacker to install additional equipment that can pass data between the fire sprinkler system and other water supply lines.

Putting these two options together, if necessary to get signals downstairs, an attacker can transmit signals through the fire sprinkler system to a receiver in a restroom on the same floor as the transmitter, transfer the data from that receiver to a transmitter on a water supply line in the restroom, then transmit to a receiver in a restroom on a distant floor, e.g., first floor public restroom.

A less appealing option to move data between floors and between rooms on the same floor is to use HVAC pipes. Hot water and steam radiators heat a building by having hot water, often from a boiler in the basement, circulate up through the building on loops that reach each radiator. Both modern and old-fashioned radiators rely on metal pipes filled with water or a mixture of water and glycol, which prevents the water from freezing in cold weather. Each radiator loop is typically separated by a pair of check valves that prevents backflow.

In experiments not reported here, we found that signals traveled well in the metal pipes between a pair of check valves but not past them. However, engineers typically install check valves of the same diameter as the pipe serving a radiator, while in fact the check valve should be one size smaller than the pipe [133]. This suggests that a determined adversary who only has access to radiator pipes (e.g., an HVAC contractor) could install trojan check valves that appear to be the same diameter as the pipe, are actually one size smaller internally, and devote the extra space to a hidden device that repeats the incoming signals on the other side of the check valve.

4.5.4 Non-commercial Buildings

Most jurisdictions require fire sprinkler systems in existing commercial buildings and in certain types of high-density residential buildings, such as highrises. However, the current NFPA standards require fire suppression systems in all new-construction residences. Because of the impact on residential construction costs, most jurisdictions have not adopted these latest standards yet.

As these standards are adopted in more jurisdictions, the attacks discussed in this chapter can be used to move data between any two points in a residence. Meanwhile, in buildings without fire sprinkler systems, such as one- and two-family private residences, transmitters and receivers can be attached to water supply lines or gas lines in kitchens and bathrooms.

4.5.5 Pipe Interior versus Pipe Surface Mount

Unless an attacker is involved in the installation, maintenance, test, or repair of pipes within the target building, it will not be practical for the attacker to install transmitters or receivers inside its pipes. For example, except when a fire sprinkler system is being installed, modified, or repaired, an attacker would have to drain, refill, and repressurize the system in order to install a transmitter or receiver inside its pipes. These relatively disruptive activities would draw unwanted attention, even from occupants who are normally oblivious to the building's infrastructure.

Attackers also would face the long-term challenge of supplying power to devices installed inside sprinkler pipes, which do not contain moving water that might be harnessed for energy.

Given these considerations, we assume that the attacker will mount the transmitter and receiver

on the outside of the pipe. For an attacker who does not want to endanger the building's inhabitants or compromise their comfort, the outside mount has the advantage of not affecting the functionality of the fire suppression, plumbing, heating, ventilation, and cooling systems that the pipe supports. Further, if the attack is of limited duration, an outside mount allows the transmitter and receiver to be removed at the end of the attack. If the devices are not direct-wired, or if data must be offloaded manually from the receiver, then the outside mount offers additional advantages for battery replacement, device swapping, and data removal.

4.6 GETTING DATA TO AND FROM THE TRANSMITTER AND RECEIVER

In a typical office environment, the transmitter and receiver will be above the dropped ceiling, hidden behind sprinkler pipes. That raises the question of how to get data to and from the transmitter and receiver. While this is not the focus of our research, we outline possibilities in this section, and discuss means of detecting them in Section 4.12. No doubt additional and better options for data transfer to the receiver reside in the arsenal of spy devices used by nation-states.

The attacker might be interested in audio, video, and/or still photos of objects (computer screens, open files, other paperwork) and activities (meetings, phone calls, people) in the room, or in digital data that is accessible in the environment, such as files or cryptographic keys.

One option is for the attacker to rely on data sent to the transmitter from surveillance devices. For example, a search on Amazon reveals a variety of small surveillance devices, including cameras and audio recorders that are simply tiny as well as those incorporated into light bulbs, smoke detectors, clocks, USB plug receptacles, entry door viewers, and pens – along with devices that promise to detect them. We return to the latter point in our discussion of detection of the pipe attack.

The second alternative is for the attacker to personally upload data to the transmitter from the room in question, using a wireless connection. This requires access or a confederate, and also runs a risk of detection, as discussed later.

The third option is for the data to be exfiltrated to be already included in the transmitter at the time it is installed. For example, files could have been loaded onto the transmitter in advance from a computer, e.g., using a USB connection, or transferred from a phone using Bluetooth. Alternatively, a camera or audio recorder incorporated into the transmitter could have been used to capture the data before the transmitter was installed.

Finally, the transmitter could include an integrated microphone or camera as part of the device. This would work best with an open ceiling.

Retrieving data from a receiver will be easier for the attacker than getting it to the transmitter, as the attacker will have been able to choose the receiver's location with that need in mind. For

example, the receiver may be near a sprinkler head in a public restroom, inside a maintenance closet, or in an office that the attacker has rented on the same floor as the transmitter. If the attacker cannot directly access the receiver through legitimate access to the building or by posing as a tradesperson or maintenance worker, then the attacker will need to hire or bribe such an individual to change out the receiver or extract its data, e.g., in the guise of monitoring water usage efficiency, checking the health of the sprinkler system, or another ruse.

4.7 DEVICE CAMOUFLAGE

We designed our transmitter and receiver to be as small as possible with the supplies and equipment (e.g., soldering iron) readily available to us at low cost over the internet. An attacker with more financial resources, patience, and skill would be able to construct much smaller versions of our devices. But even at their current size, we hypothesized that the transmitter and receiver could be easily camouflaged to look like ordinary parts of a sprinkler system.

To test this hypothesis, we photographed the sprinkler system pipes in several buildings that we had access to, as well as newly purchased pipes and fittings from large hardware stores. As can be seen in Figure 4.1, although all of the pipes and fittings except the faux fitting, the sprinkler head and the bell fitting it connects to were made of what is known as black steel, they differed greatly in color and sheen, ranging from medium brown through bright gray to black.

We chose one particular fitting to imitate, a T fitting that fits on the same 1-inch diameter pipe as found in most branch lines. We built a removable version of the fitting out of an ordinary 1-inch PVC T fitting, removed its 3-dimensional markings and visible seams, and added faux 3-dimensional markings and seams identical to those found on black steel T fittings. Then we added texture and color to make the faux fitting look like a newly manufactured black steel T fitting, as shown in Figure 4.1. We chose to make the faux fitting black, but the same approach can be used to create a version in any other shade of color. When installed on the pipe, the seams that allow the fitting to be attached to and removed from a branch line look like ordinary pipe seams, and we believe that the faux fitting is indistinguishable from a real black steel fitting, to the untrained eye. Only upon touching the fitting does it become apparent that the fitting is not made of black steel.

In buildings with open ceilings, the building owners often choose to paint the pipes and their hangers and the faux fitting should be painted to match. The fire code permits this; only the sprinkler heads themselves must remain unpainted.

A short length of black steel or camouflaged PVC pipe fits into the camouflaged T, to hold the transmitter or receiver. As shown in Figure 4.1, the pipe can end in a cap or include a (non-functional) sprinkler head. However, the pipes in Figure 4.1 are much longer than necessary to hold

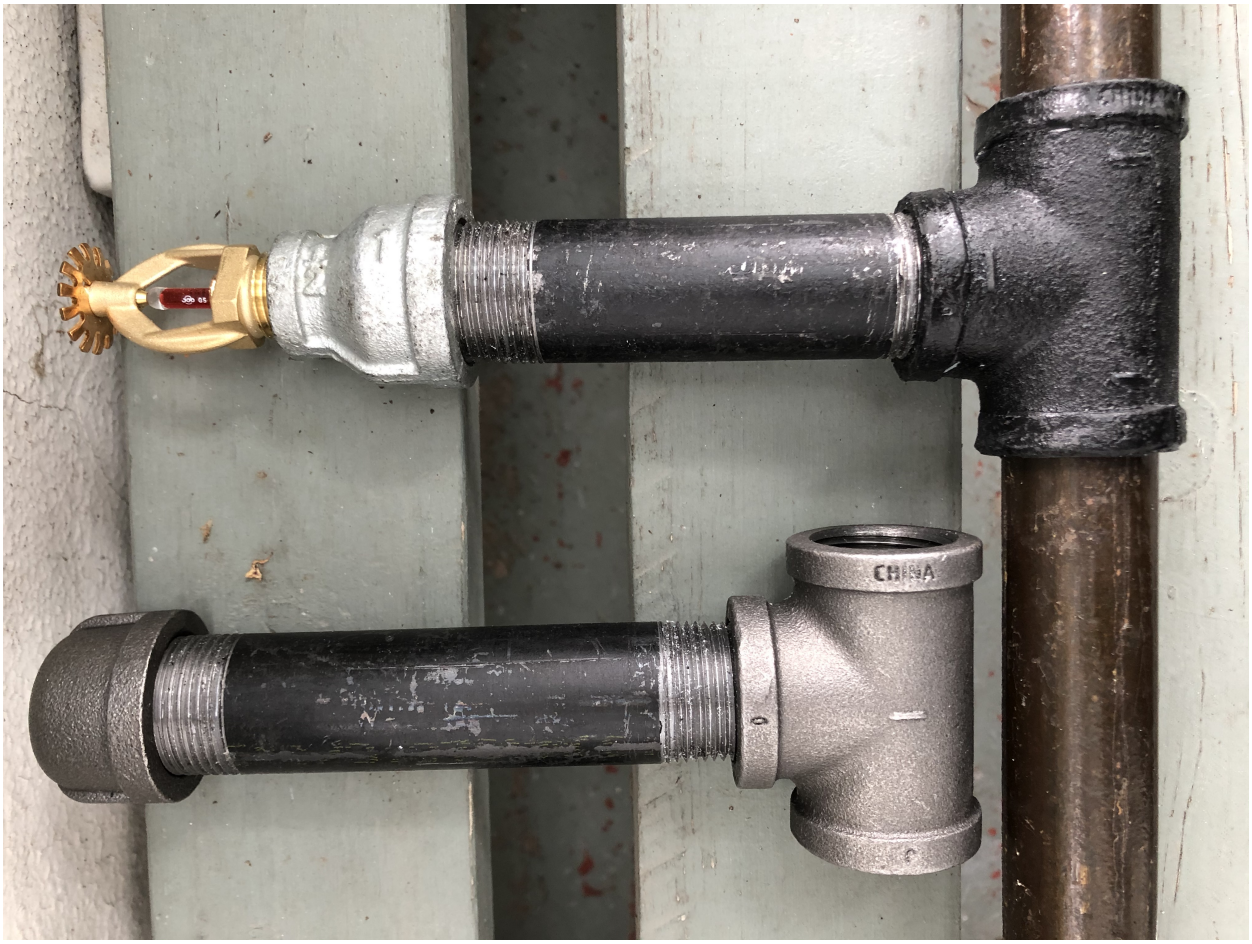

Figure 4.1: Pipes and Fittings. In spite of the wide variety of colors and levels of sheen, all of these are black steel except the sprinkler head itself, the bright silver galvanized steel bell fitting that the sprinkler head is attached to, and the faux T fitting at upper right.

a transmitter or receiver. Figure 4.2 shows the shortest length of pipe that held the receiver we built, roughly 3.5 inches, using black steel and uncamouflaged PVC. We used a snapfit PVC T fitting as the base here, to allow us to insert and remove the transmitter without removing the cap; however, a real installation should instead use a faux T fitting instead of a snapfit.

The pipe that houses the transmitter or receiver can end in a cap, as shown in Figure 4.2; a plug; a sprinkler head; or a pressure gauge or other device. A trained eye will recognize the oddness of a pipe stub being present at such a random location in the sprinkler system. To anyone else who pokes their head above the suspended ceiling, even in a newly constructed building, the faux fitting and pipe will look like just another pipe in a morass of mechanicals (see Figure 4.3 (upper photo)). Even with an open ceiling, the faux fitting and pipe stub will fit into the crowd of mechanicals (see Figure 4.3 (lower photo)).

Most of the 3.5” of pipe length was needed to hold the batteries for our unit, which were separate

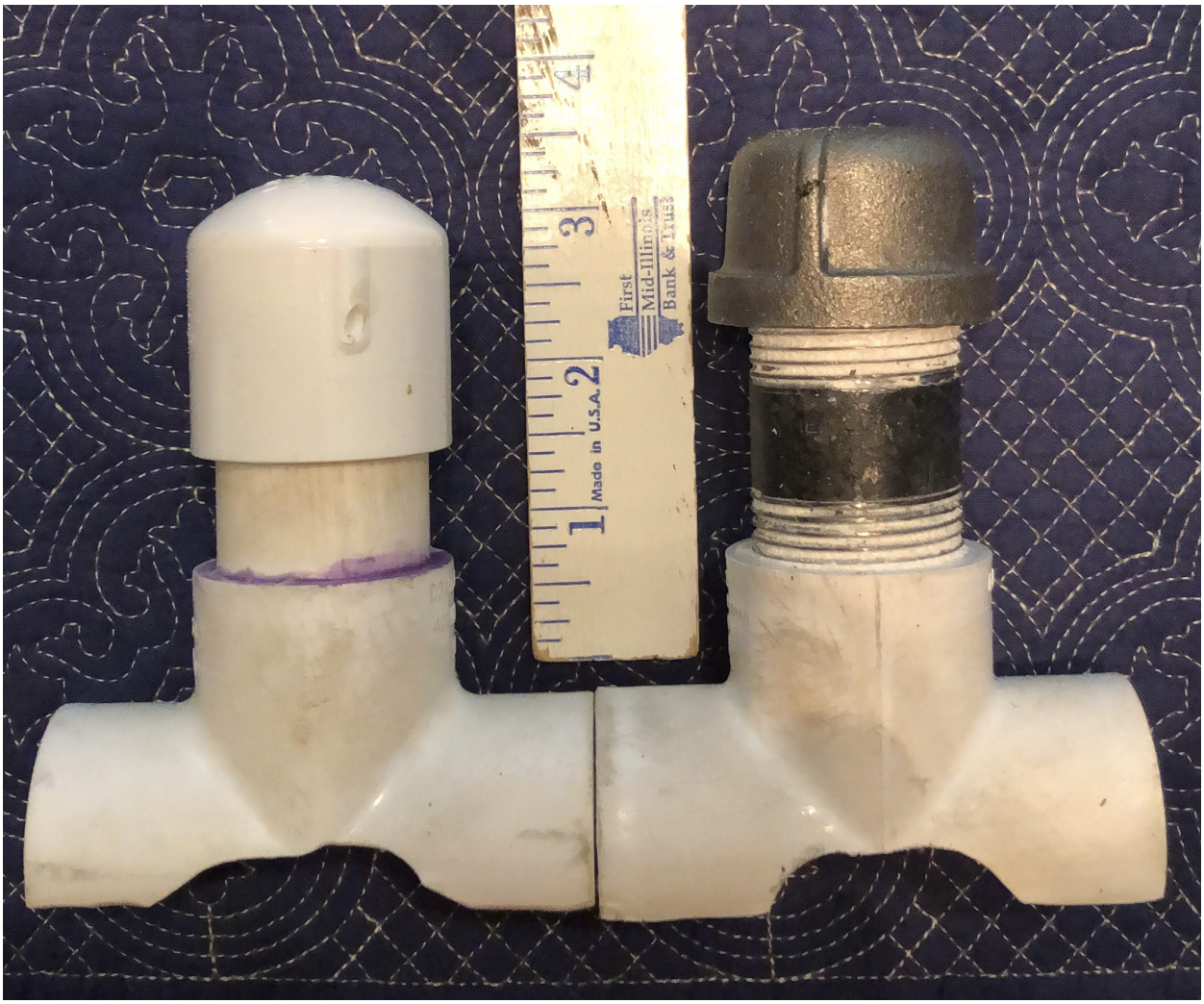

Figure 4.2: Pipe Length Required to Hold Receiver.

from the main circuit board. Figure 4.4 shows the snap fittings from Figure 4.2 installed on black steel pipe, together with the receiver itself and a piece of rock wool. This pipe length required to hold the receiver shown was built using 1 inch diameter PVC and black steel. An implementation with integrated batteries could use a much shorter pipe than the 3.5" we required.

We inserted the receiver in the faux fitting on a real branch line and tested it to ensure that the receiver was working under those conditions.

So far we have focused on visual camouflage, but auditory camouflage can also be helpful. In a real deployment, the transmitter and receiver might be able to use stronger signal transmissions without detection by nearby observers if the devices were well soundproofed. As a poor man's version of this, we experimented with packing the empty space in the pipe stub with rock wool insulation, but found that it did not significantly reduce the apparent sound of the transmission for

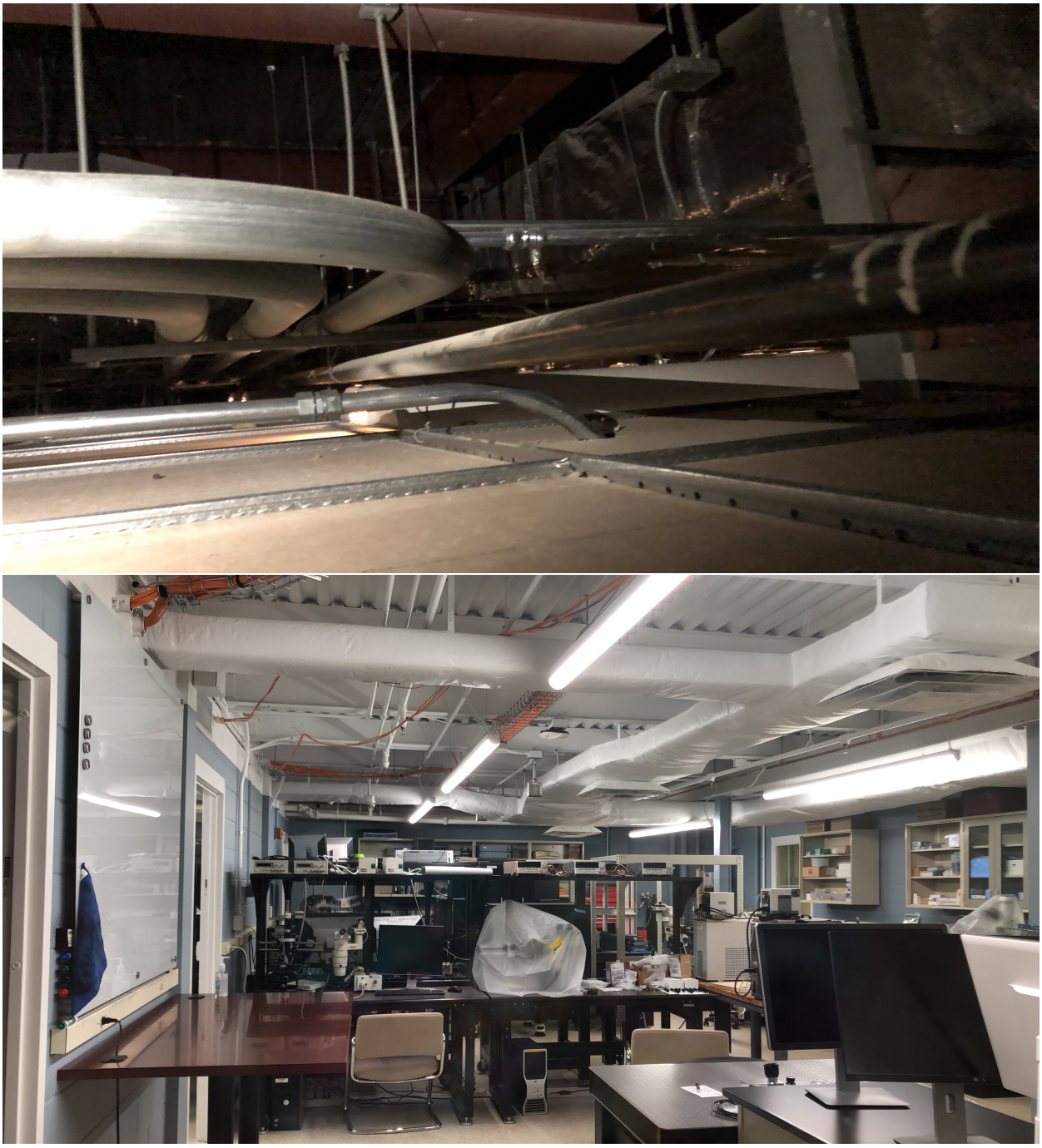

Figure 4.3: Mechanical Systems Above a Suspended Ceiling (upper photo) and Below an Open Ceiling (lower photo).

an external observer. No doubt an attacker with access to a wider variety of soundproofing materials would be able to reduce signal leakage.

Figure 4.4: Snap Fitting Installed on Black Steel Pipe with Receiver and Rockwool

4.8 KEY DESIGN AND IMPLEMENTATION DECISIONS

The first key design decision is what form of signals to send, and we conducted experiments to determine what was most effective.

One option is to use acoustic transmissions. To test this approach, we flush-mounted a mini-speaker to the surface of a riser that ran through a closet in a stairwell in a highrise building, then wrapped the speaker in high density foam for soundproofing and to reduce signal loss and leakage to air. As the receiver, we used a microphone flush mounted to the pipe surface in a closet in the same stairwell on an adjacent floor. This first receiver captured the intended signals, i.e., those that traveled through the pipe. To evaluate signal leakage, we dangled a second microphone in the air at the same height as the first, but at a 1 foot distance from the pipe. This second receiver was intended to capture signals received from the air surrounding the pipe, either due to leakage of vibrations from the pipe or else directly from the transmitter one floor away. We found that the second receiver picked up strong signals, especially directly from the transmitter itself. Much of the transmitter's

signal was lost through the air, which made the transmission audible to nearby humans and also impractical for long distance transmission.

A second option is to send vibrations through the pipe by attaching a transducer that converts audio signals to mechanical vibrations. As the transmitter, we experimented with different models of bone conduction headphones, which are essentially electro-mechanical transducers that produce subtle taps on the surface of the pipe. In the same test environment as described above, this transmission method showed much less signal leakage through the air to the second receiver, so much so that the signals were inaudible to a human standing next to the pipe on either floor. We concluded that mechanical transmission is much more suitable for covert messages than acoustic transmission.

The next question was exactly which hardware to use for the transmitter and receiver. We evaluated several transmitter and receiver pairs for their sensitivity, bandwidth, hardware noise and environmental noise handling abilities.

4.8.1 Transmitter Hardware Comparison

The winner on the transmitter side was the Adafruit 8 ohm bone conductor transducer. We amplified its signals using the TPA2016 Adafruit Class D audio amplifier with AGC, a breakout board audio amplifier which has a small form factor.

The Adafruit audio amplifier is 22mm x 28mm and the Adafruit bone conductor transducer is 14mm x 21.5mm; this small form factor is a big help in making the transmitter easy to hide and camouflage when mounted on a branch line or other small pipe.

We also experimented with a commercially available Aftershokz wireless Bluetooth bone conductor headphone (AS600). However, the Bluetooth frame rate was rather low, which limited the potential transmission quality and rate. We also experimented with a wired version, Aftershokz Sportz Titanium. This model achieved similar audio signal magnitudes for most frequencies as the Adafruit bone conductor when analyzed on the receiver side, but there was more noise in the circuit, some repeating along some intervals as shown in Figure 4.5(a) versus Figure 4.5(b).

4.8.2 Receiver Hardware Comparison

We experimented with half a dozen receivers, and obtained best results using a Traderplus professional contact microphone pickup, intended for use with musical instruments such as guitars and violins. This pickup contains a piezoelectric element encased to eliminate interference from environmental noise. We tried several other models of commercially available microphone pickups:

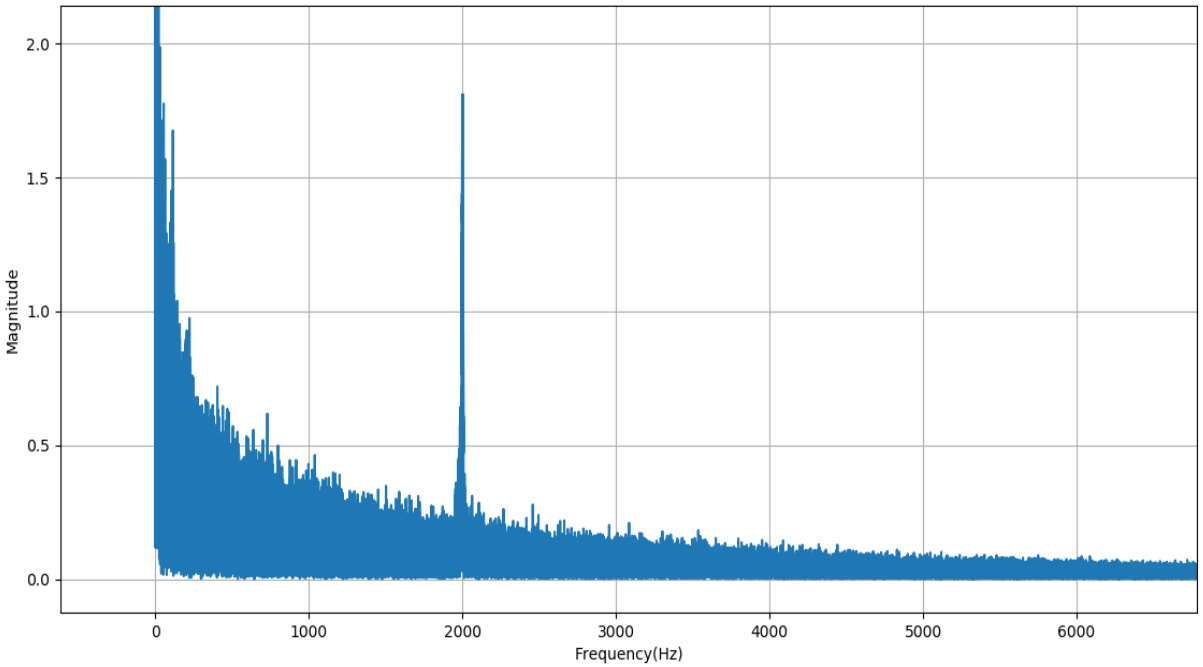

(a) Circuit Noise from Adafruit Bone conductor Transmitter with Traderplus Contact Microphone Receiver (Zoomed in)

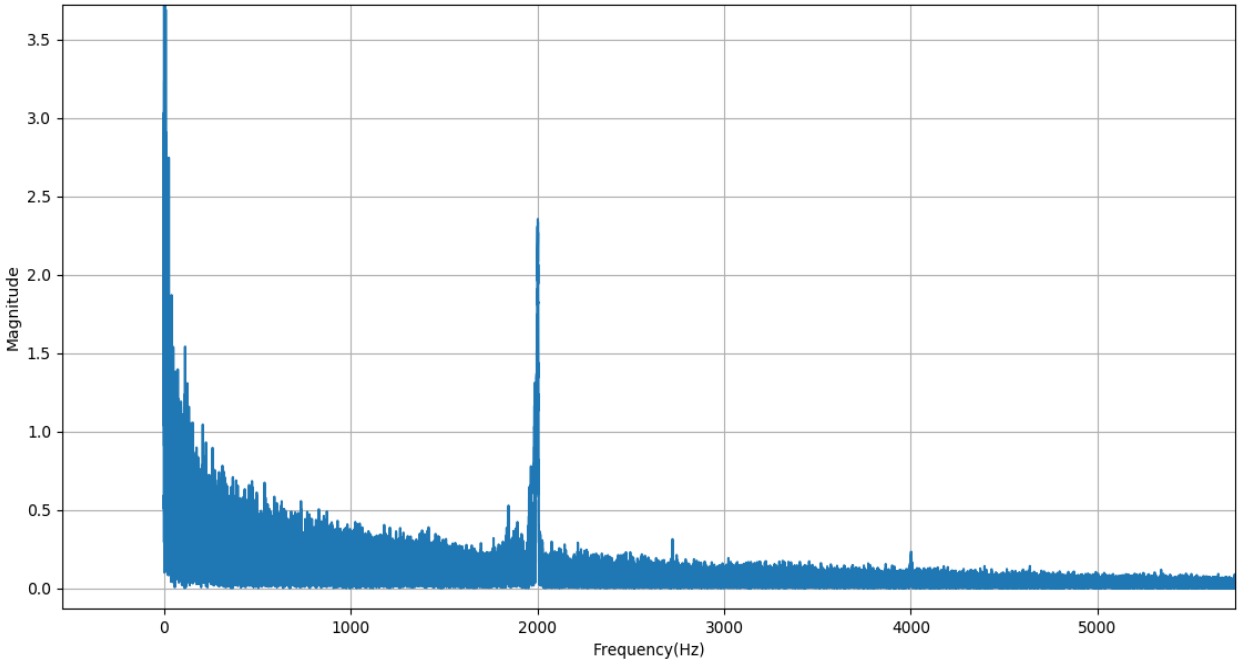

(b) Circuit Noise from Aftershokz Sportz Titanium (Wired) Bone Conductor Transmitter AS600 with Traderplus Contact Microphone Receiver (Zoomed in)

Figure 4.5: Circuit noise FFT from Various Transmitter- Receiver Pairs. A 5-second 2000Hz pulse was transmitted along a standalone 3 feet long pipe section where transmitter and receivers were flush mounted

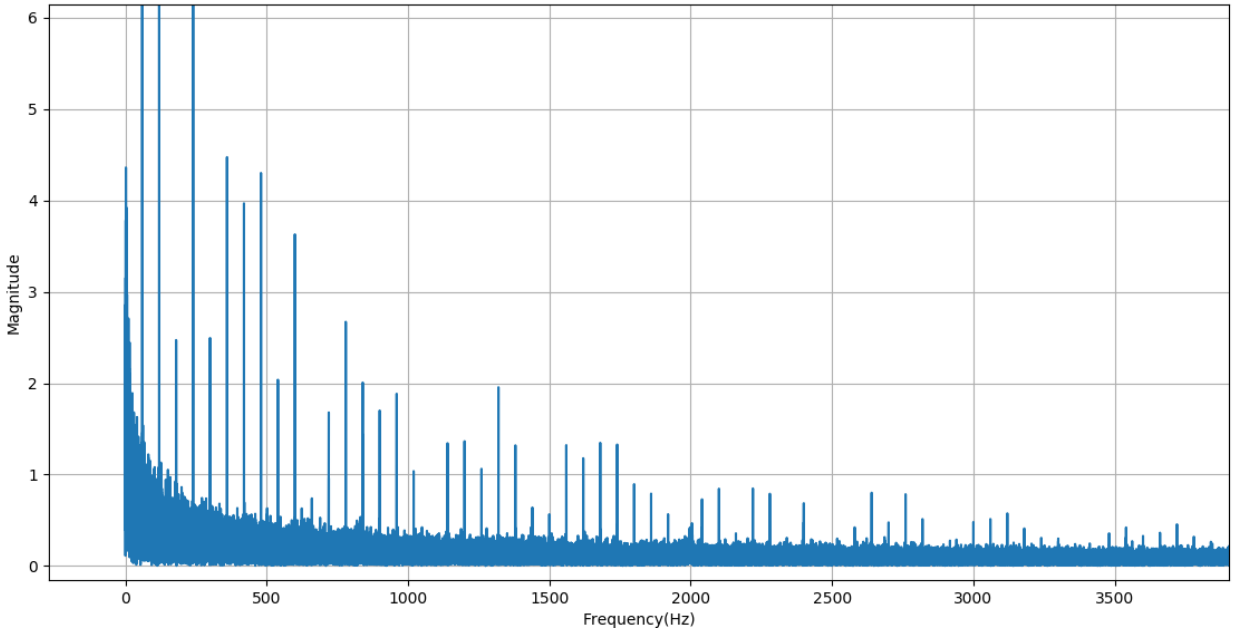

(c) Circuit Noise from Aftershokz Sportz Titanium (Wired) Bone Conductor Transmitter AS600 with Knowles BU-23173-000 Accelerometer Receiver (Zoomed in)

Figure 4.5 (cont.)

1. Peterson Tuners Pitch Grabber Pickup
2. Donner Acoustic Guitar Pickup Transducer TP-1
3. Drfeify Portable Universal Pickup
4. Greenten Piezo Pickup Soft Saddle Transducer
5. Musiclily Guitar Under Saddle Piezo Bridge Pickup
6. Jiuwu Plastic guitar violin pickup

We found that some were less sensitive, some picked up more environmental noise, some added more noise to the circuit themselves, and some broke so easily that they were not suitable for use in experiments that required repositioning of the device in different buildings and at different distances along a given sprinkler system.

We also experimented with medical and mechanical stethoscopes, together with a dual microphone built into a stethoscope-microphone device. We used the Omron Sprague Rappaport medical stethoscope and connected both the ear pieces to a Boya dual microphone, using heat-shrinks to hold it together. We connected the microphone jack to a laptop to receive the data. We also experimented with a Pittsburgh Mechanical Stethoscope in the same stethoscope-microphone setup.

Between the two, the mechanical stethoscope performed better at capturing signals and also had a smaller surface that could be flush mounted against the pipe more snugly. However, both the medical and mechanical stethoscope-microphone setup were only sensitive to signals below 5KHz frequencies and often picked up substantial low frequency noise from the environment at 1KHz, as shown in Figure 4.6. As they handle a smaller bandwidth range compared to the piezo pickups (20Hz-20KHz) and picked up much overlapping noise within that bandwidth, we did not consider them further.

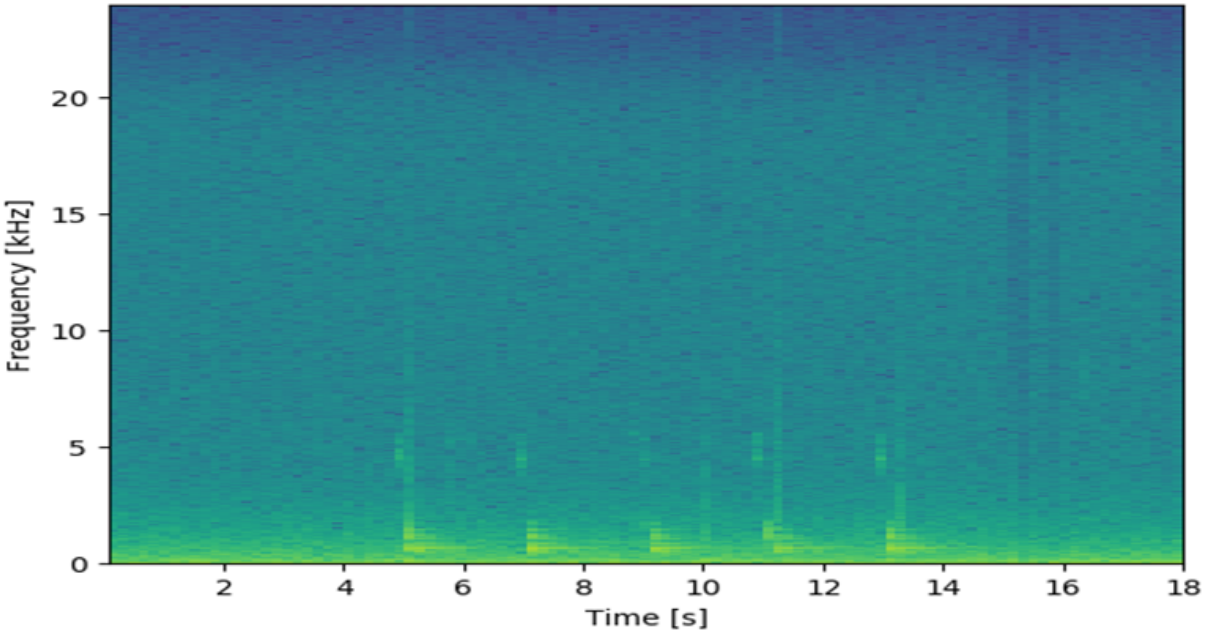

Figure 4.6: Spectrogram of Received Signal Using Pittsburgh Mechanical Stethoscope. Transmitted signal is a set of five chirp signals (20KHz to 0Hz linearly descending signal) separated by 1 second of silence. Transmitter is an Aftershokz Wireless Bone Conductor headphone.

For the receiver, we also experimented with an accelerometer (Knowles BU-23173-000) plus amplifier. This had a smaller form factor and higher sensitivity than the stethoscope, but it picked up strong interference from environmental noise, as shown in Figure 4.5(c), and missed certain frequencies, e.g., 2000Hz signals.

4.8.3 Processing Device Comparisons

For the processing unit used for sending the audio files to the transmitter and recording and post-processing the received audio sample from the receiver, we compared the performance of a laptop and a phone in terms of the audio noise it adds to the setup. For the laptop we used a Lenovo Thinkpad X230 laptop (Intel(R) Core(TM) i5-3320M CPU @ 2.60GHz), and for the phone we

used a Samsung Galaxy S8 (Qualcomm MSM8998 Snapdragon 835 (10 nm)). We used the same transmitter (Adafruit bone conductor with amplifier) and receiver (Traderplus contact microphone) for connecting to each of these devices, and transmitted the same 5-second 2KHz pulse.

Figure 4.7 shows a comparison of the FFT of the received audio clip. We see more noise over the lower end of the spectrum in the audio received by the phone (Figure 4.7b), as compared to the received audio in the laptop (Figure 4.7a). The phone records receiving a slightly higher magnitude of the transmitted 2KHz signal compared to the laptop, as it has a higher maximum volume it can achieve. As an attacker, however, we prefer to use a processing device that injects less noise into the setup and optimizes available bandwidth better. Signal amplification can always be achieved by pre-processing at the transmitter or receiver ends if needed. All factors considered, the laptop emerges as the winner as a processor unit for our experimental setup.

4.8.4 The Best Configuration

Our experiments in this chapter use the best performing transmitter, receiver and processing unit with respect to bandwidth utilization and noise impact on the circuit. Given the 20kHz constraint, our final hardware configuration, shown in Figure 4.9, was:

- Transmitter: Adafruit 8 ohm bone conductor transducer (14mm x 21.5mm) with TPA2016 Adafruit Class D audio amplifier with AGC (22mm x 28mm)
- Receiver: TraderPlus Piezo professional contact microphone pickup, intended for guitars and violins
- Processor: Lenovo Thinkpad X230 laptop (Intel i5-3320M CPU @ 2.60GHz)

Figure 4.9 shows the final versions of the transmitter and receiver. The logical connection of the Adafruit transmitter and Traderplus receiver to the pipes and the processing unit is shown in Figure 4.8. The arrows indicate the direction of flow of audio data through this system.

The laptop holds prerecorded sequences of tones, music, or speech, which are sent to the transmitter at a user-determined volume. The amplifier in the transmitter circuitry amplifies the audio signal and sends it to the bone conductor transducer that converts it into mechanical vibrations. As discussed below, to allow easy repositioning, in our experiments we snugly flush mounted the bone conductor transducer on the pipe using a self-adhering bandage.

The transmitter translates the target audio clip to mechanical taps on the pipe surface. The pipe conducts these vibrations to the location where the receiver circuitry with its piezo pickup is flush mounted on the pipe surface and snugly attached using a self-adhesive bandage, as discussed below.

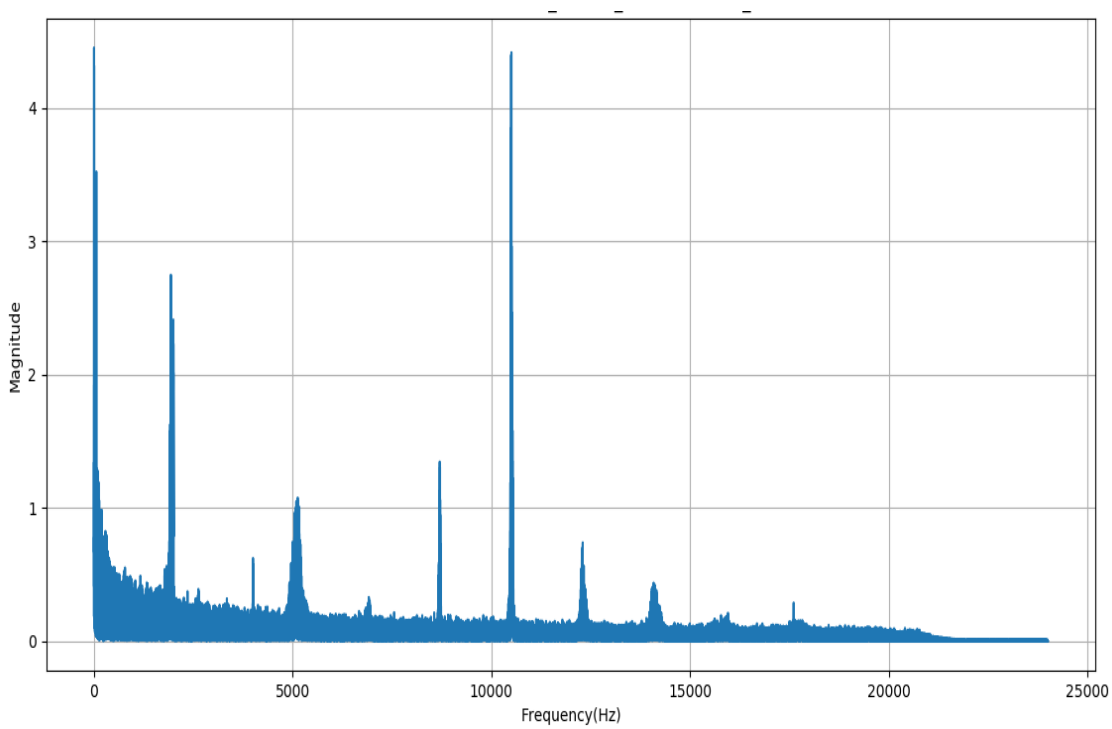

(a) Circuit Noise FFT from Laptop Connected to Receive 2KHz Pulse Recording (Zoomed in)

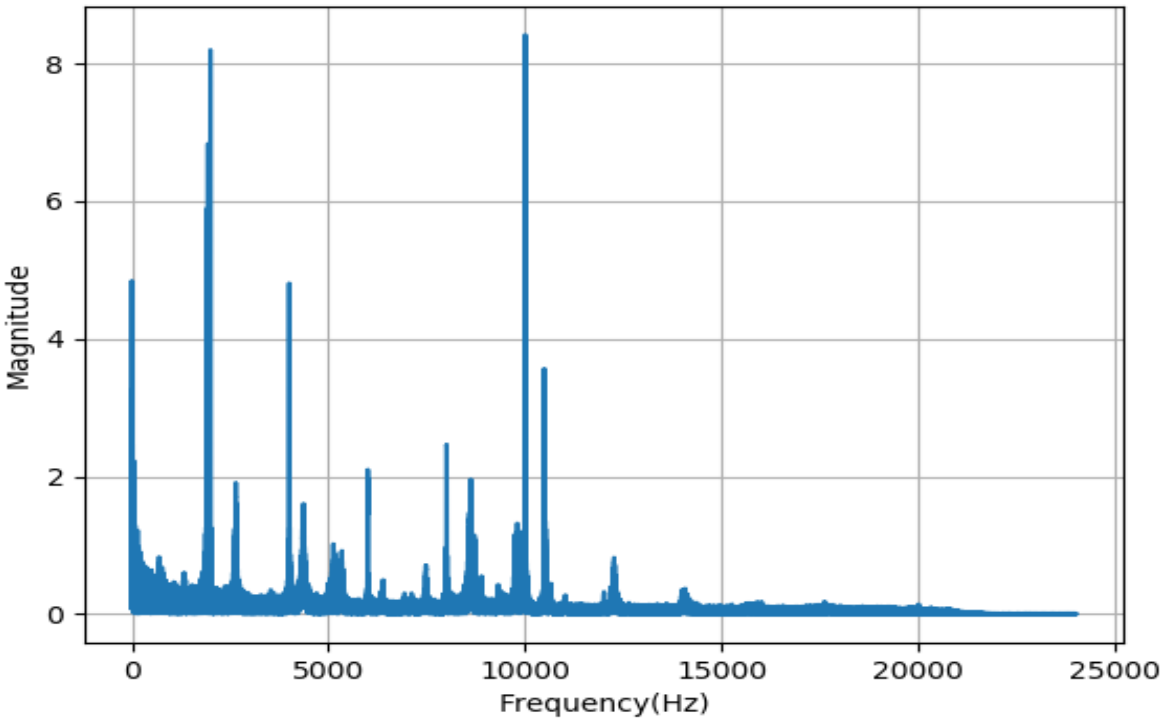

(b) Circuit Noise FFT from Phone Connected to Receive 2KHz Pulse Recording (Zoomed in)

Figure 4.7: Circuit Noise (FFT) Difference from Using Laptop Versus Phone to Receive a 2KHz Pulse. The same transmitter (Adafruit bone conductor with amplifier) and receiver (Traderplus contact microphone) were used in both setups.

The pickup receiver is connected to the processing laptop through the audio port. The signal picked up by the receiver is sent to the laptop, which records it and performs postprocessing to analyze the received audio clip.

Since there is a single audio port in the Lenovo laptop, we used a speaker-headphone splitter at the audio port to split the audio output to the transmitter from the audio input coming in from the receiver. We wrote multithreaded code in Python to separate the play and record threads in the laptop, synchronized to start the play first followed by the recording in parallel for each test file. We created and analyzed FFTs and spectrograms of recordings, and extracted the frequency and magnitude of the major signal peak in the FFT for each single-tone audioclip.

We ran each experiment on a variety of pipes in different buildings. On each pipe, we moved the receiver closer to/further away from the transmitter, to test transmission at different distances along the pipe.

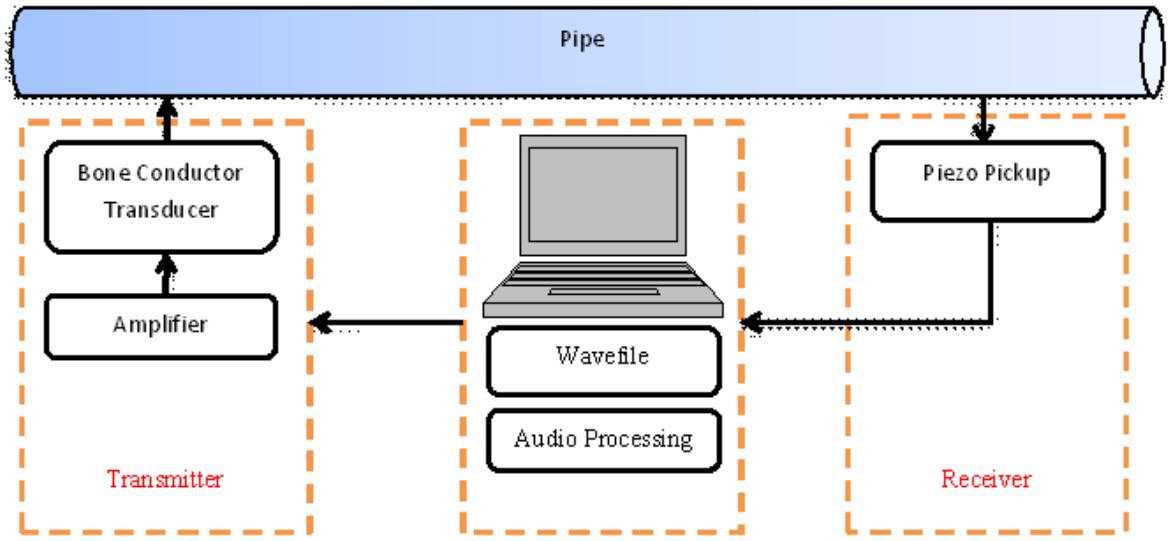

Figure 4.8: Pipe Attack Setup with Adafruit Transmitter (Bone Conductor+Amplifier) and Traderplus Receiver.

The physical connection between the pipes and the transmitter and receiver was a significant challenge, because the devices needed to be easily repositionable. Audio experts told us that the best results would be obtained by supergluing the devices to the pipe. This approach would also be attractive for an attacker, as superglue dries very quickly and its residue is transparent. Because pipes are curved, we found that the superglued devices could easily be removed afterward by firmly rotating the device in place. This quick and easy removal would also be a plus for attackers who wished to remove all obvious signs of their presence, or needed to swap in a new device

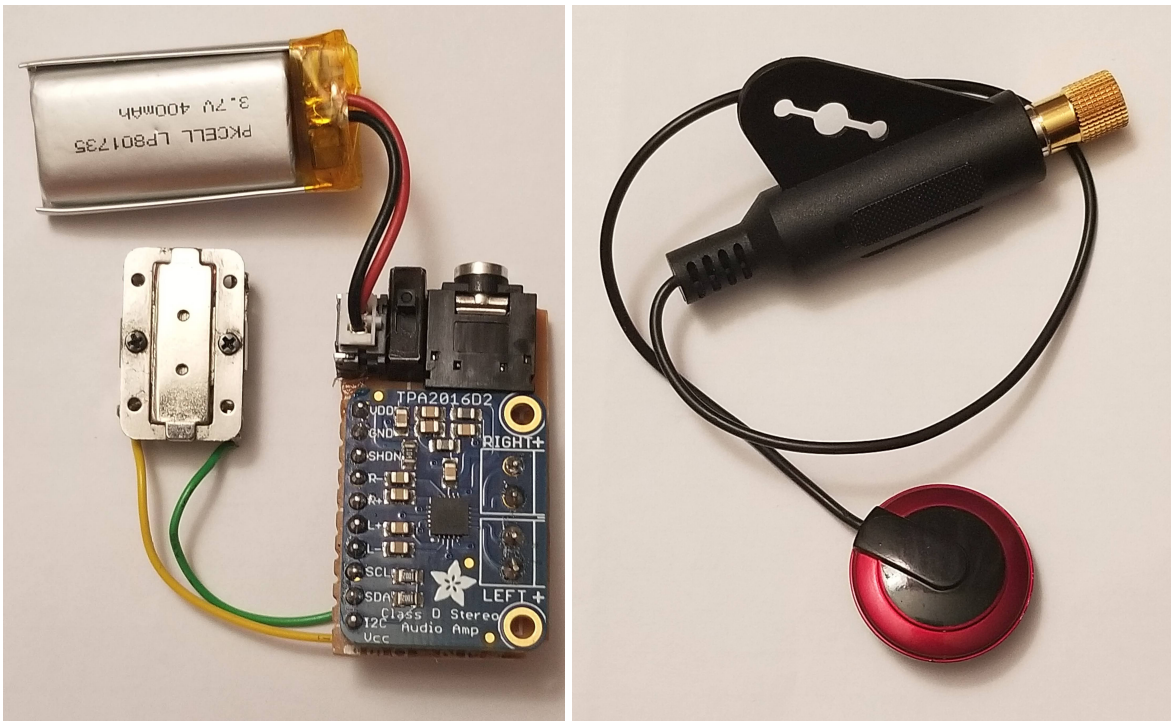

(a) Adafruit Bone Conductor Transmitter (b) Traderplus Piezo Pickup Receiver

Figure 4.9: Best Configuration of Transmitter and Receiver – Adafruit Transmitter and Traderplus Receiver

with fresh batteries. However, we found that the act of removal was too violent for the delicate soldered connections between the subcomponents of the devices, and in some cases too violent for the components themselves as well. Given the need to frequently reposition the devices to take measurements on different pipes and at different distances, lengthy resoldering of tiny connections and mail-ordering new components after repositioning was impractical.

To enable repositioning without damage, we switched to using stretchy self-adhesive bandages, available from all major drugstores. More specifically, we used Walgreens brand Self-Adherent Wrap. Compared to superglue, this looser attachment surely resulted in less signal going from the transmitter into the pipe, and more signal escaping into the environment. On the receiving end, the looser connection of the pickup to the pipe would have reduced the captured signal as well. Thus our experimental results should be viewed as an understatement of the results that could be obtained in practice by an attacker using superglue.

4.9 BUILDINGS AND PIPELINES TESTED

We evaluated the effectiveness of pipe transmissions in six pipes located in three buildings: an

old commercial building with both wet and dry sprinkler systems (Old Commercial), a new commercial office and laboratory building with wet sprinklers (New Commercial), and an old single-family residence with new plumbing (Residence). We describe each location below. The pipe types, sizes and lengths that we used in each building are described in Table 4.1.

New Commercial. Built in the 2000s, this sprawling commercial building has over 200,000 square feet of space spread across four floors and a basement, as well as a partial fifth floor. As befits its size, the building has multiple separate sprinkler systems, each made of black steel and each laid out in a tree topology. We conducted our experiments in one wing of the building, which is served by a single sprinkler system that we estimate as covering 50,000 square feet. This wing primarily has dropped ceilings with acoustic tiles, and houses office and lab space with a relatively open floor plan. We mapped the topography of the sprinkler system in the wing, which follows an almost identical pattern on all floors. We took measurements on one floor of the wing and in two of the stairwells near the wing, one of which housed the riser that served the wing, and the other of which held a smaller riser that served another section of the building. Figure 4.10 illustrates the relevant portion of this building's sprinkler system layout.

Old Commercial. Built in the 1910s, this commercial building has been remodeled and repurposed multiple times over the years. Today it offers a modern open floor plan with open ceilings and a 40,000 square footprint on each of two floors and a basement. The basement and first floor have a wet sprinkler system, and the second floor has a dry sprinkler system filled with air. The sprinkler system pipes are black steel. Each floor uses a tree topology. The building's first floor ceilings are very high, so for safer access, we took measurements in the basement and on the second floor.

Residential. Built in the first decade of the 1900s, this residential building has a 2,000 square foot footprint on each of three floors and a basement. The building has no sprinkler system. Water supply lines in the house are copper pipes installed in the 1990s. The natural gas supply lines running along the ceiling of its basement are made of black steel.

Table 4.1 summarizes the test environment in these buildings, including pipe types, sizes, and lengths. For sales and building code purposes, pipes are normally characterized by their nominal internal diameter; we report our empirical measurements of the external diameters in this table, using a digital caliper. For example, we worked with 1.66" outer diameter pipes, which correspond to a 1.25" inner diameter. Similarly, 1" internal diameter corresponds to 1.32" outer diameter, and 2.5" inner diameter corresponds to 2.875" outer diameter.

When appropriate buildings were not available to us for a particular experiment, we built our own pipeline for the experiment. CPVC is approved for use in some jurisdictions for fire sprinkler systems, but no building we had access to used CPVC pipes for any purpose, so we built our own CPVC pipeline. Since CPVC is very similar to PVC in terms of material and workability, but PVC is much cheaper and fittings for it are more readily available in hardware stores, we also built a

Name	Pipe Description	Pipe Material / Outer Diameter	Pipe Contents	Distances Measured
RG	Residential Gas Pipe 50ft long, with branches	Black Steel 1.04”	Natural Gas	20ft, 30ft, 40ft
RW	Residential Water Supply 40ft long, with branches	Copper 1.04”	Water	20ft, 30ft, 40ft
OCS	Old Commercial Wet Sprinkler 170ft, with branches	Black Steel 1.05” to 1.65”	Water (pressurized)	20ft, 40ft, 60ft, 80ft, 100ft, 120ft, 170ft
OCDS	Old Commercial Dry Sprinkler 90ft, no branches	Painted Steel Pipe 1.93”	Air	20ft, 50ft, 60ft, 90ft
NCS	New Commercial Wet Sprinkler Multibranch with crossmains	Black Steel 1.30” to 1.90” branch lines, 2.88” crossmain	Water (pressurized)	10ft, 50ft, 80ft, 116ft (adjacent branch lines) 161ft (non-adjacent branch lines separated by crossmain)
NCR	New Commercial Riser (combination wet) 6-floor standpipe	Painted Steel 4”	Water (pressurized)	30.3ft, 45.6ft, 61.2ft

Table 4.1: Measurement Locations for the Pipe Attack

PVC pipeline. In this laboratory setting, we could easily cut up the PVC and CPVC pipes and reconfigure and reconnect them with different fittings.

More precisely, we built three indoor pipelines, each approximately 30 feet in length, using 3/4-1” inner diameter PVC and CPVC. We outfitted these with a variety of PVC, metal, and CPVC fittings and filled them with air or water. We used solvent-based connections wherever possible, employing Oatley PVC primer and sealant to connect the pipes to their fittings. This setup is shown in Figure 4.21 and discussed in more detail later.

For experiments to evaluate the effect of different couplings, we built an outdoor pipeline roughly 42.5 feet long, using two 21 foot lengths of 1.25” inner diameter Schedule 10 black steel pipe (slightly larger than the 1” diameter used for most branch lines), outfitted with a variety of couplings approved for use in wet sprinkler systems. Both Schedule 10 and Schedule 40 black steel pipes are rated for use in fire sprinkler systems. We chose Schedule 10 over Schedule 40 because Schedule 10 pipes weigh less, cost less, and have lower freight delivery charges. The fire rated schedule 10 pipes that we purchased have a groove joint at the ends and require grooved couplings to join one pipe to the other, or to connect to an adapter that allows access to non-grooved fittings. Grooved couplings are also used in the New Commercial building, and are quite popular because of the speed and ease with which they can be used to assemble black steel sprinkler systems.

For our experiments, we connected the two 21 foot pipes with a grooved coupling in the middle. We used an additional grooved coupling at each end of the pipe to interface with the fittings and adaptors needed to connect the pipes to a water source and drain it. This experimental setup is

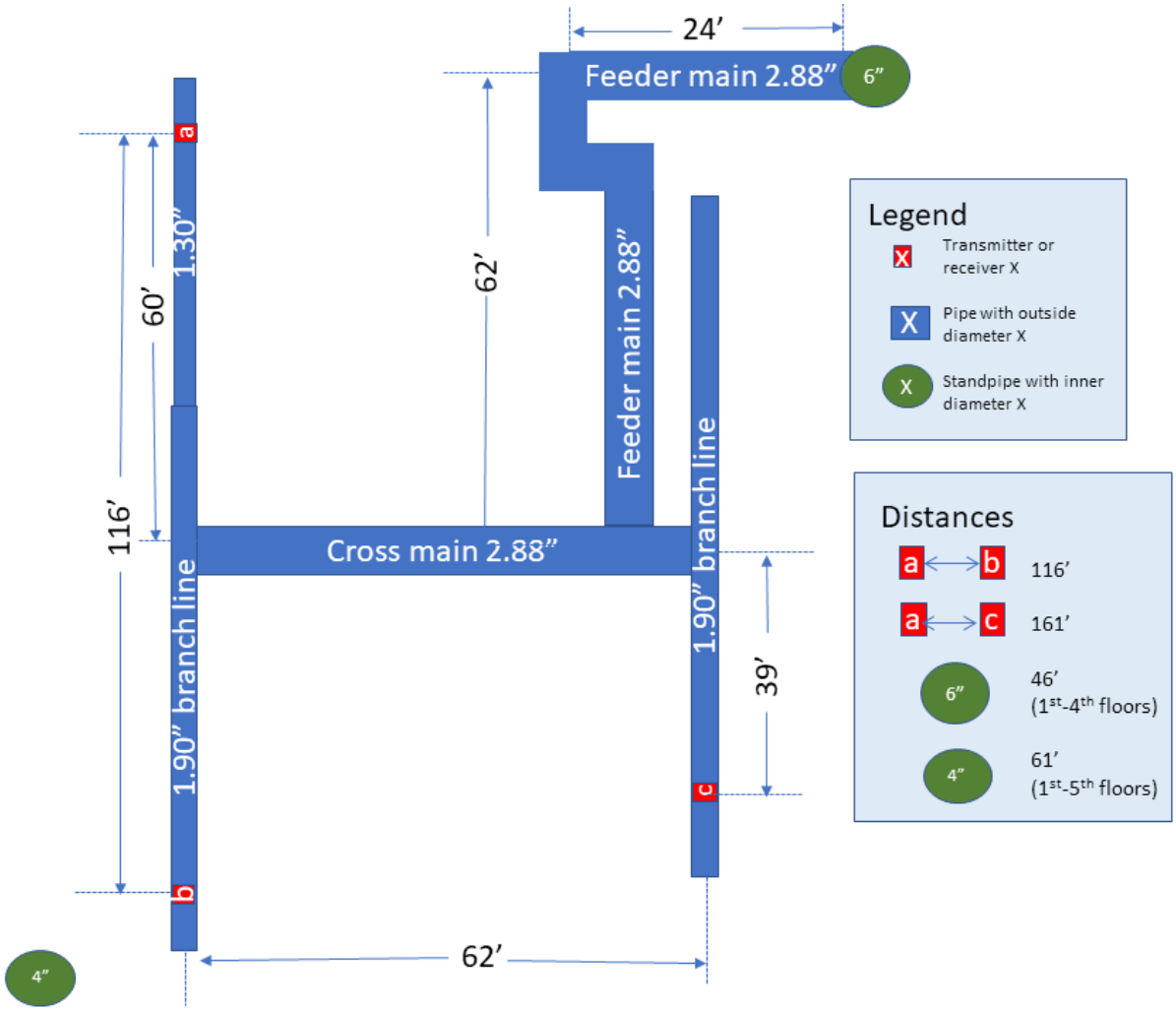

Figure 4.10: Layout and External Diameter of Fire Sprinkler Pipes Tested at New Commercial Building Locations NCS and NCR. Not shown are the dozens of branch lines that intersect the pipe pathways used in the tests, or the many small twists and turns to dodge other mechanicals.

shown in Figure 4.24.

4.10 EXPERIMENTAL RESULTS

Our experiments evaluated several characteristics of the communication between the transmitter and receiver:

- Best frequency bands for each pipeline, and bandwidth available
- Attenuation and/or signal strength changes for different pipeline over distances
- Covertness of setup and environmental signal leaks

4.10.1 Warmup: Recognizing Famous Recordings

As a warmup during initial testing of our hardware, we used the Adafruit transmitter to send recordings of well-known pop songs over long distances in the New Commercial building, and used the Shazam app to recognize the signals collected by the Traderplus receiver. This is a much easier task than recognizing arbitrary transmissions: Shazam has prior knowledge of a vast library of previously recorded songs, and has previously analyzed those recordings using machine learning. Thus Shazam only needs to map each received song to the closest match in its library, which is much easier than accurately recognizing arbitrary signals.

These experiments use the Residential and Old Commercial pipelines RG, RW, OCS, and OCDS locations (described in Table 4.1). Shazam recognizes songs by comparing fingerprints of an audioclip's frequencies and peak amplitudes, taken over a succession of sliding windows, to those previously computed and stored in its library. The details of the algorithm, such as its understanding of the temporal ordering of the fingerprints, do not matter for our purposes.

Overall, with the laptop set to 50-100% of maximum volume, Shazam was able to correctly recognize the transmitted songs from audio clips 3-5 seconds in length, on all pipelines tested. Figure 4.11 presents snapshots of the song 'Hey Jude' by the Beatles, as it arrived at the transmitter, along with spectrograms for the transmitted recording. Figure 4.12 presents snapshots and associated spectrograms of the transmitted and recognized speech "I have a dream", by Martin Luther King.

These results gave us confidence in the hardware setup, and we then moved on to more challenging benchmarking.

4.10.2 Frequency Response and Bandwidth

In theory, an attacker can broadcast information in parallel on all frequencies that are within the range of the attacker's transmitter and receiver. However, not all frequencies will work equally well. Some may tend to be absorbed or distorted by the pipe along the way, or interfere with other frequencies, so that the signals become indistinguishable from signals in other frequencies, fade out faster, or even grow louder along the way. Such changes can make the attack more noticeable and reduce the maximum practical distance for sending messages that can be accurately interpreted.

To characterize the ability of a pipeline to act as a communication channel for different signal frequencies, we evaluate its frequency response, which will determine the bandwidth that the communication channel can support at a particular volume. In response to a stimulus signal, frequency response measures the output produced by the system in terms of the amplitude and phase for different signal frequencies. To evaluate our pipelines' frequency response, we generated audio files (lossless wave files) containing signals of different frequencies, which we converted to

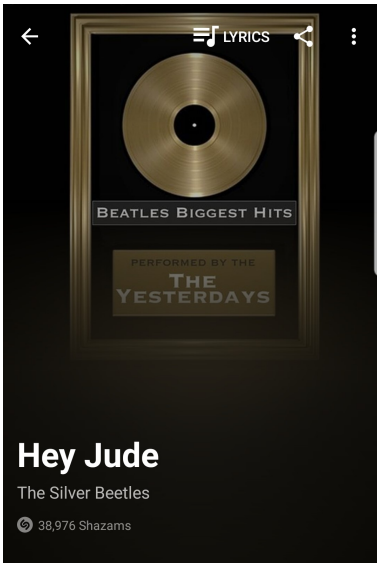

(a) Shazam's Identification Snapshot

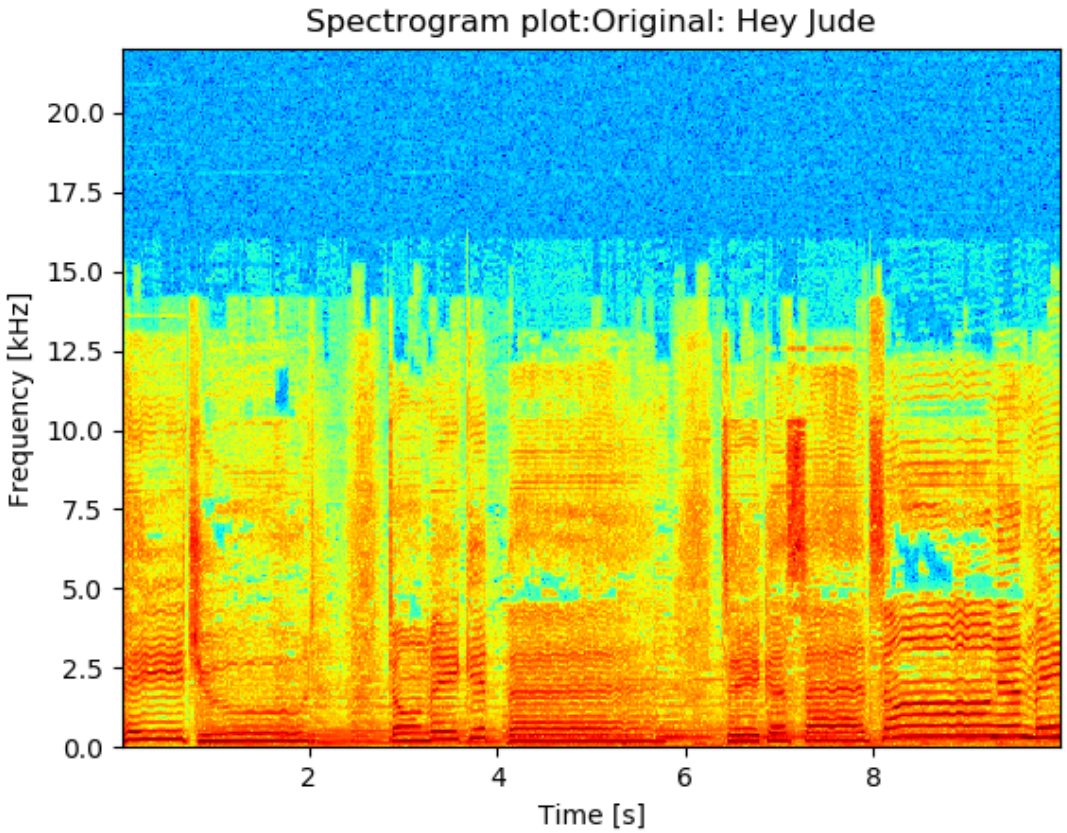

(b) As Transmitted: Hey Jude

Figure 4.11: Spectrogram of the Song 'Hey Jude' after Transmission. Pipes are as described in Table 4.1.

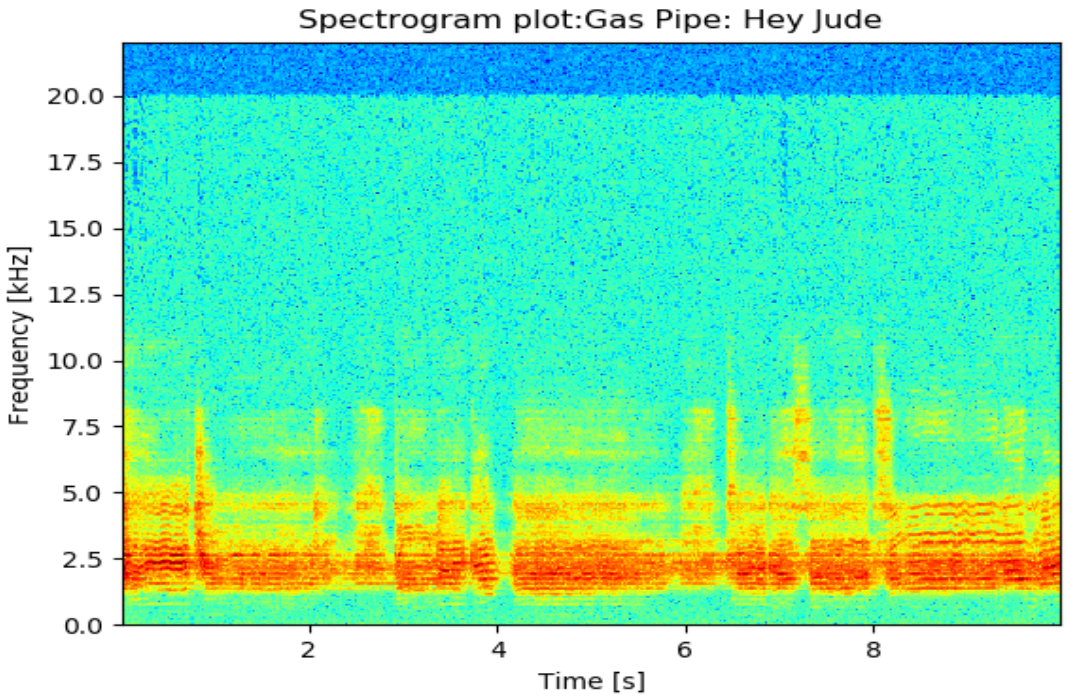

(c) As Received: Gas-filled Black Steel Pipe, Location RG at 40ft

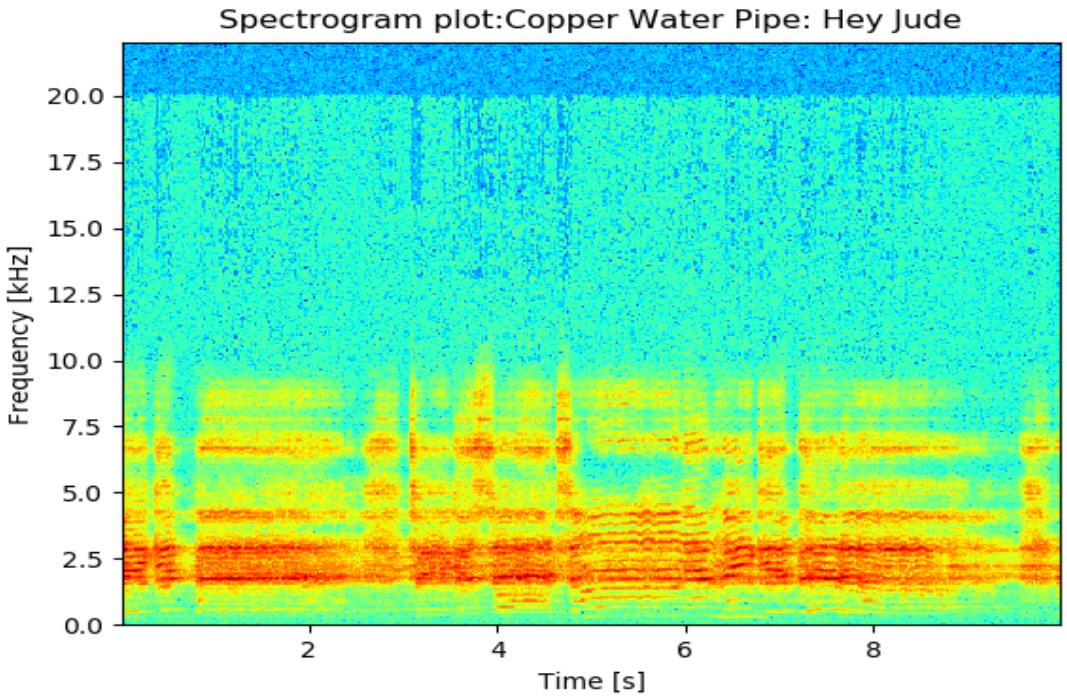

(d) As Received: Water-filled Copper Pipe, Location RW at 40ft

Figure 4.11 (cont.)

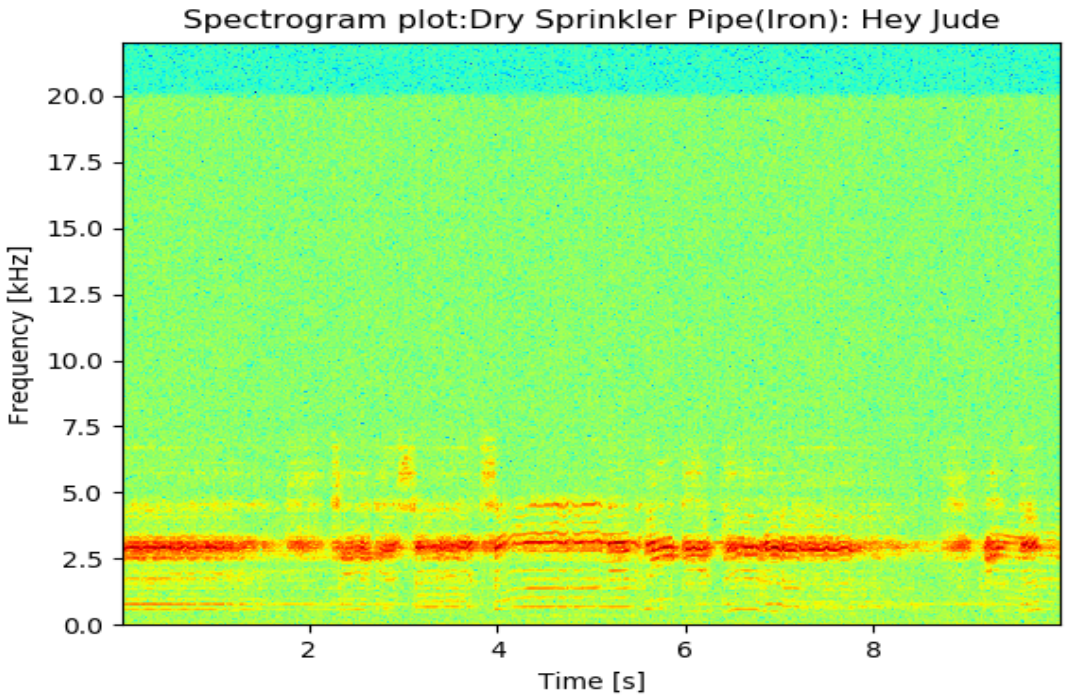

(e) As Received: Air-filled Black Steel Pipe, Location OCDS at 90ft

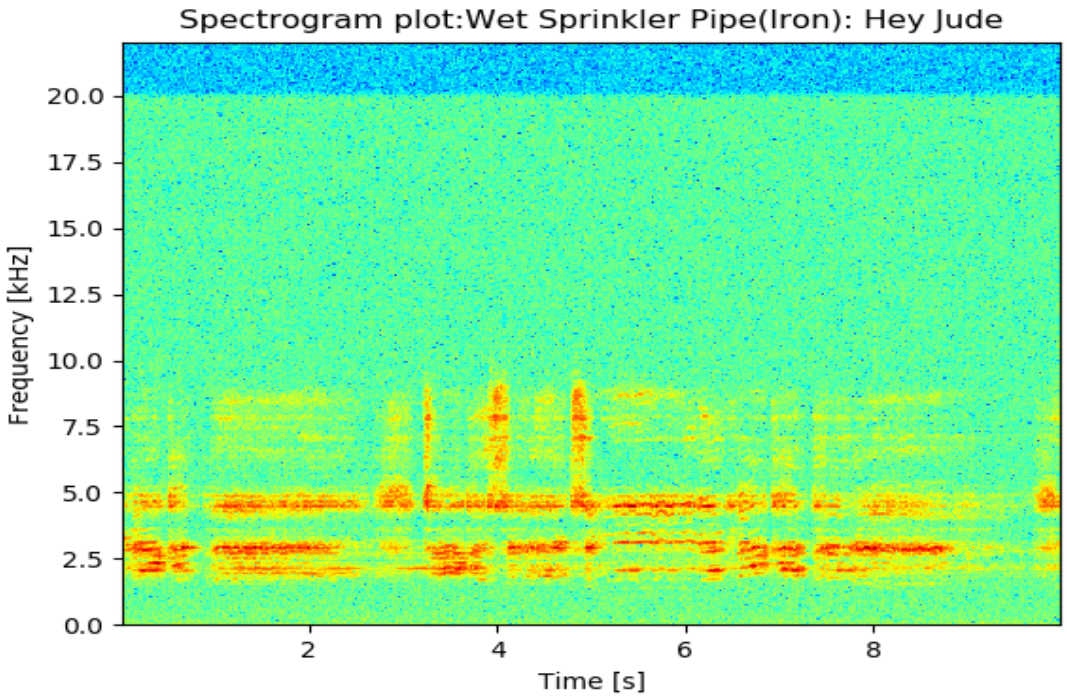

(f) As Received: Water-filled Black Steel Pipe, Location OCS at 170ft

Figure 4.11 (cont.)

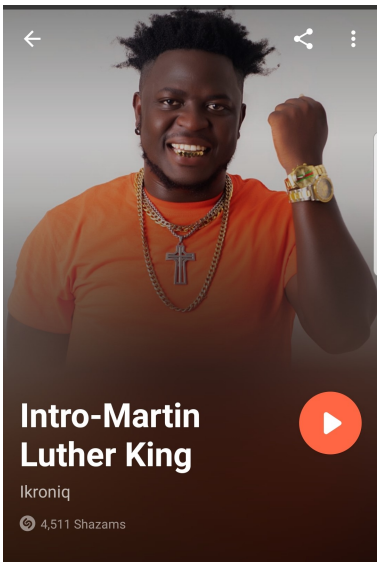

(a) Shazam's Identification Snapshot

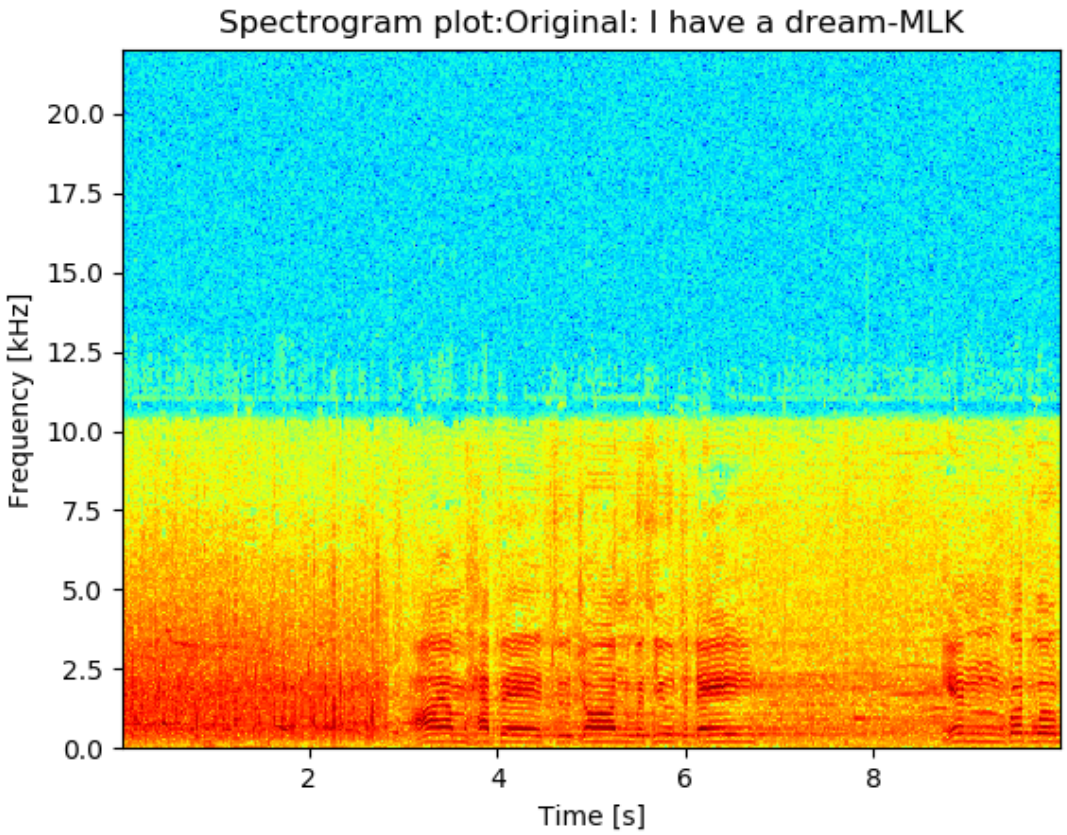

(b) As Transmitted: I Have a Dream

Figure 4.12: Results for 'I have a dream' speech by Martin Luther King, as recognized by Shazam. Pipes are described in Table 4.1.

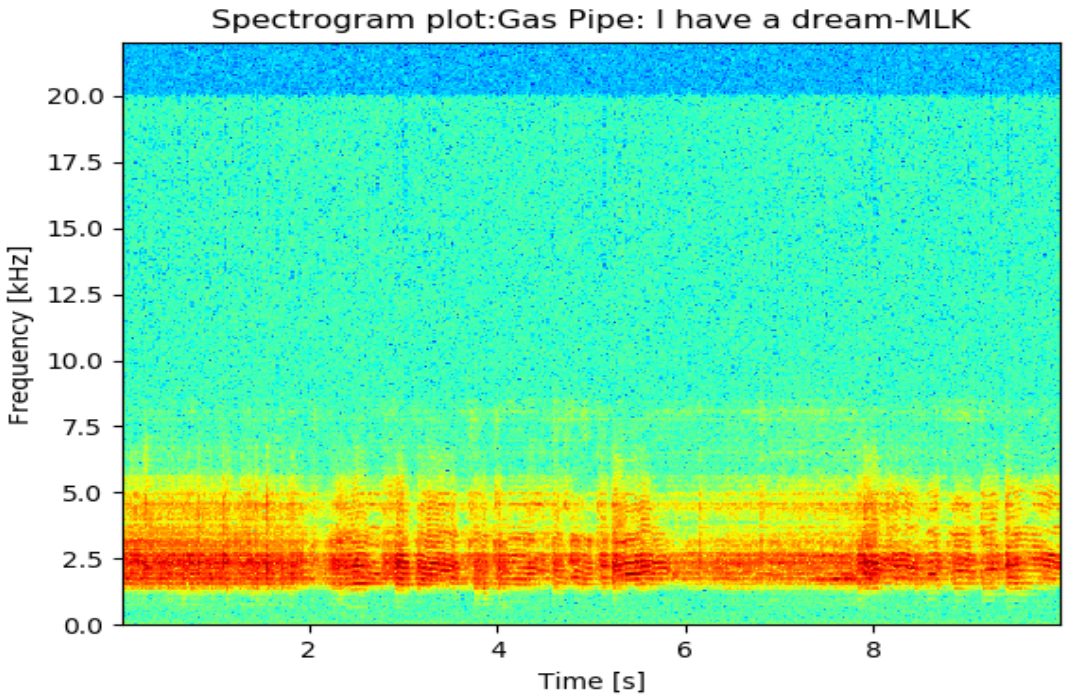

(c) As Received: Gas-filled Black Steel Pipe, Location RG at 40ft

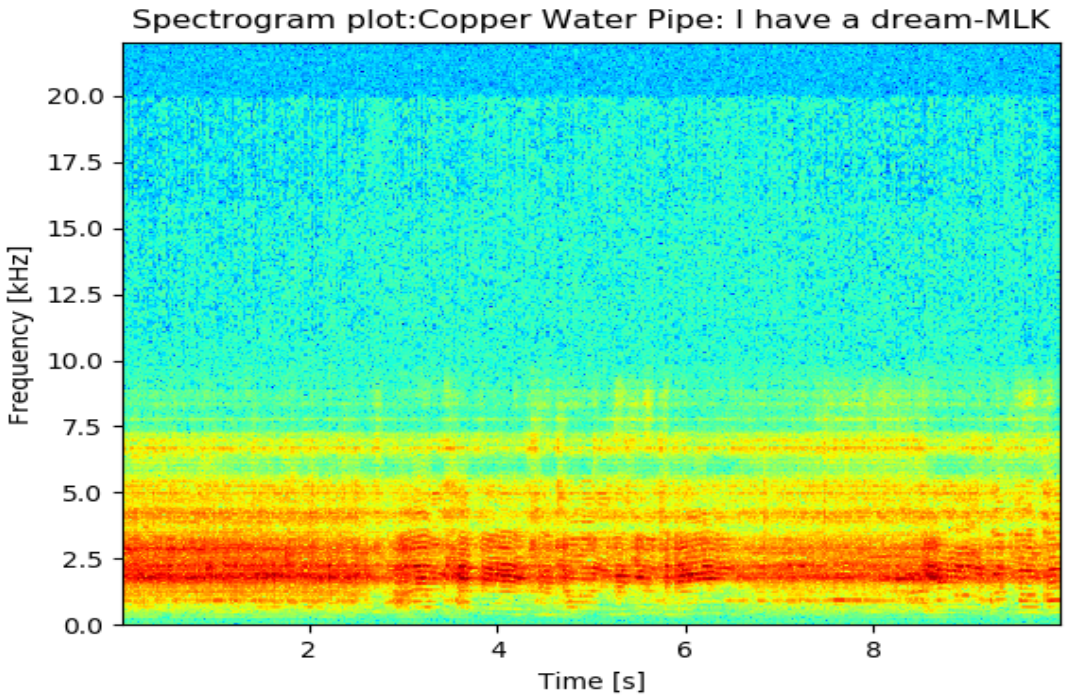

(d) As Received: Water-filled Copper Pipe, Location RW at 40ft

Figure 4.12 (cont.)

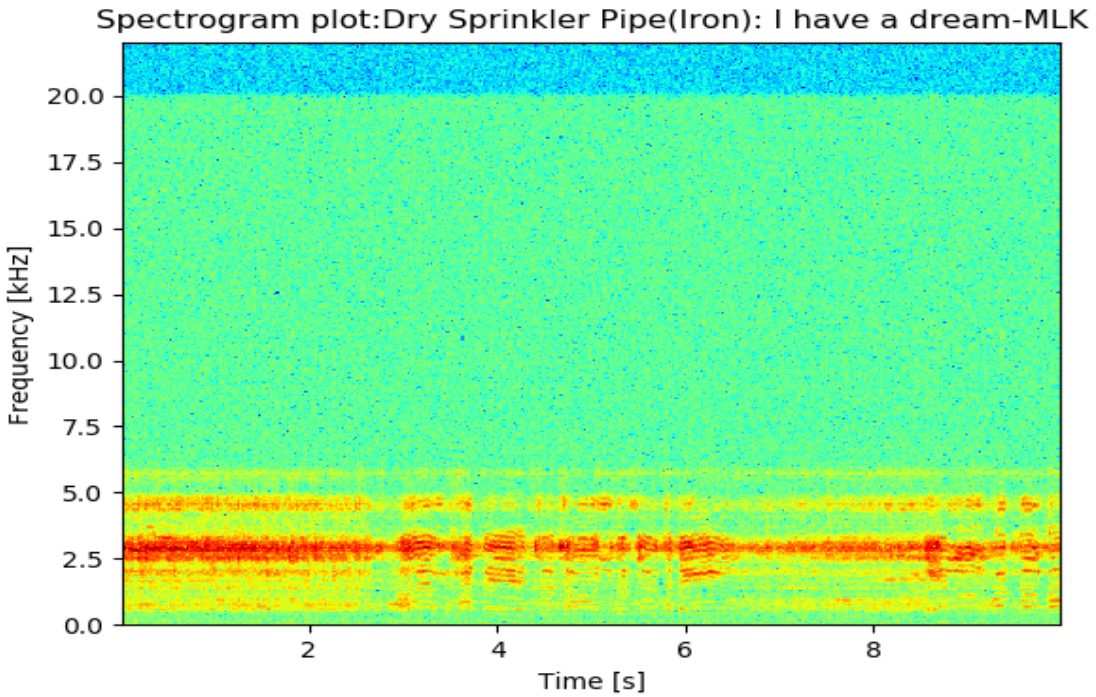

(e) As Received: Air-filled Steel Pipe, Location OCDS at 90ft

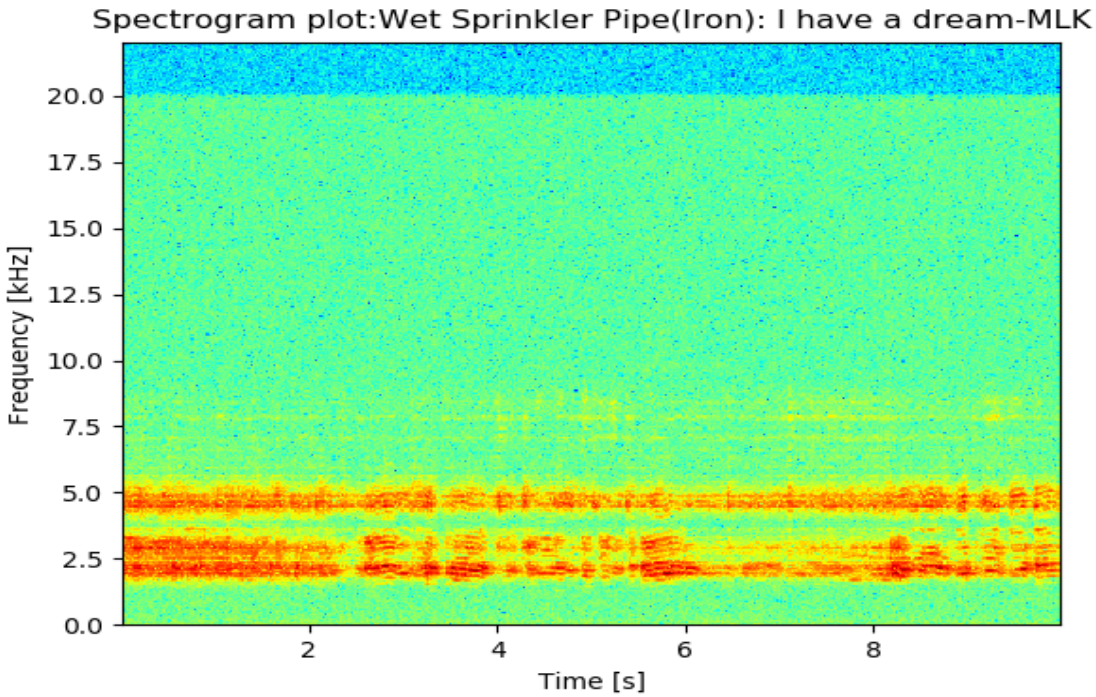

(f) As Received: Water-filled Black Iron Pipe, Location OCS at 170ft

Figure 4.12 (cont.)

vibrations in the bone-conduction transmitter. The resulting signals arrived at the receiver down the pipe, as shown in Figure 4.8, and were sent back to the laptop, where we recorded and analyzed them.

We evaluated the frequency response for the 1Hz-20KHz range. This range is supported by most commercially available audio devices (speakers, headphones, microphones), which are built for supporting the human audible frequency spectrum, 20Hz to 20KHz. Note, however, that the prior work on communication through building structures for structural monitoring purposes used ultrasound. Thus although our transducer and audio devices do not go beyond 20KHz, the available bandwidth to an attacker will go beyond our tested range if more sophisticated attack hardware is available.

Our evaluation method uses single frequency waves of 1 second in length, preceded and followed by 0.5 second silence, corresponding to an audio file of 2 seconds duration. We tested each frequency that is a multiple of 100, from 0Hz to 20000Hz, at a sample rate of 44100Hz. We measured the signal at multiple distances for each tested pipe.

We use the following *bandwidth condition* to determine whether a particular single frequency is convenient for attackers to use: given pipe noise and other attenuation, when the transmitter sends frequency f, is f the major frequency in the signal seen by the receiver? More precisely, is frequency f within 5Hz of being the main peak in the frequency domain, after we perform a Fast Fourier Transform on the received audio clip, at all measurement locations along the pipe? If so, we include f in the attacker's bandwidth, and determine how much f attenuates or changes in magnitude as it passes along the pipe.

We use this strict condition to simplify the extraction of the best frequencies, though more complex signal processing methods could extract a wider range of signals that may not arrive as a peak. However, more advanced signal extraction techniques might require a more detailed understanding of the building pipe material, structure and other information that an attacker often will not have.

When a frequency signal does not arrive as the major peak, this could be due to noise in the pipe or environment causing distortion or attenuation, or due to the properties of the pipe itself and the way it handles propagation of waves of certain frequency. When the noise ceiling of the environment is high and overlaps with the signal frequency, it can drown out the signal, making it hard to identify as a major peak.

To visualize the frequency bandwidth available to an attacker for the locations we evaluated, we generate a scatter plot to show frequencies that are received successfully at different distances, i.e., frequency signals that satisfy the bandwidth condition. Figure 4.13 shows the received frequencies that satisfy the bandwidth condition and their received magnitude at different distances along the pipes. Locations and details of the pipes are listed in Table 4.1. Frequencies that were not detectable

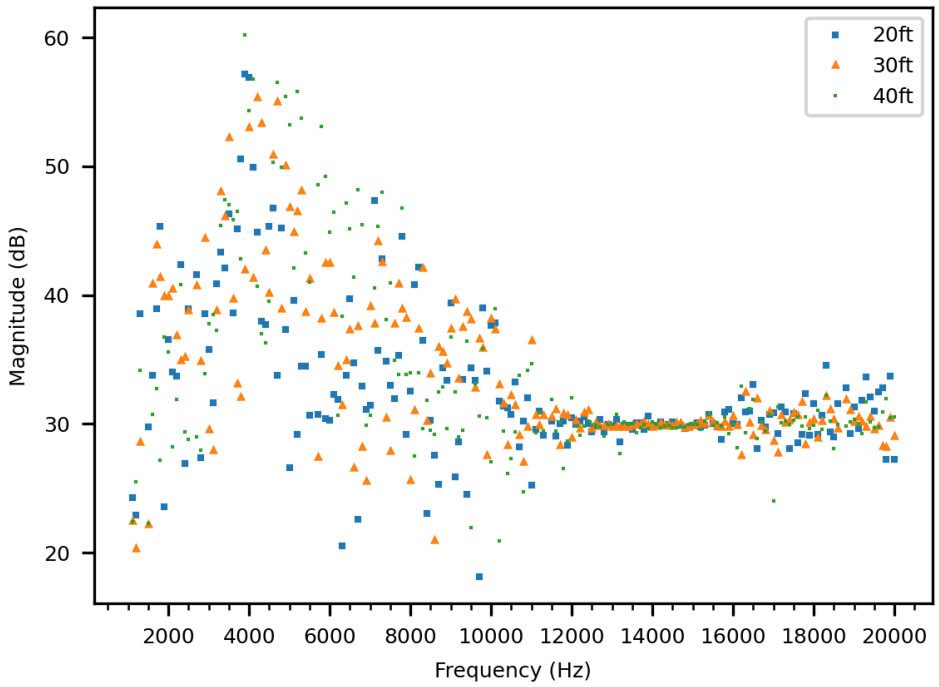

(a) Residential Black Steel Gas Pipe

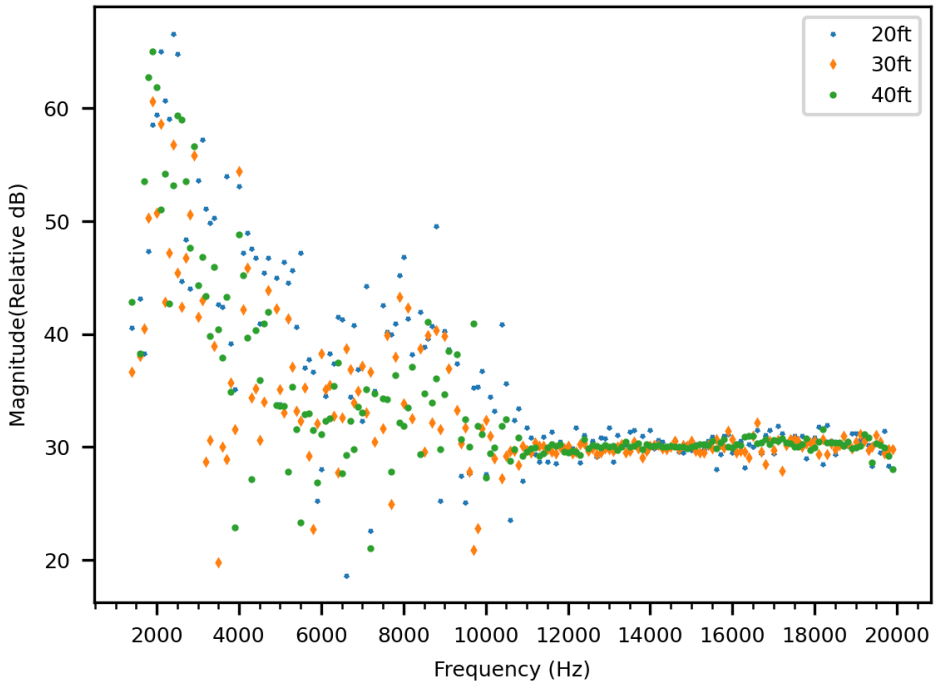

(b) Residential Copper Water Pipe

Figure 4.13: Frequencies Satisfying Bandwidth Conditions After Transmission Through Residential Building, Old Commercial Building and New Commercial Building Pipes at Various Distances

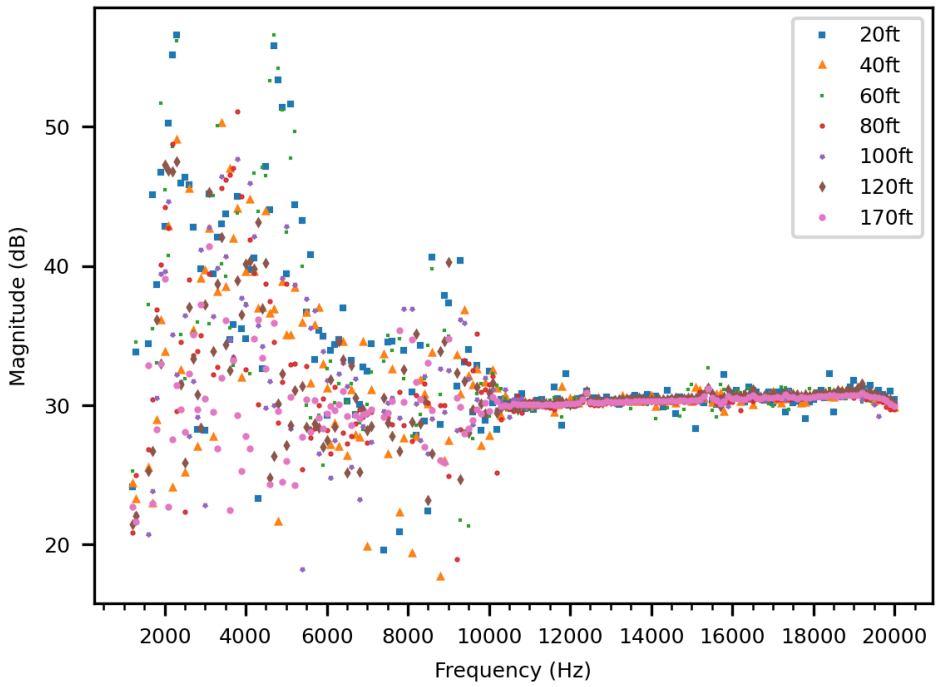

(c) Old Commercial Building Wet Sprinkler Pipe

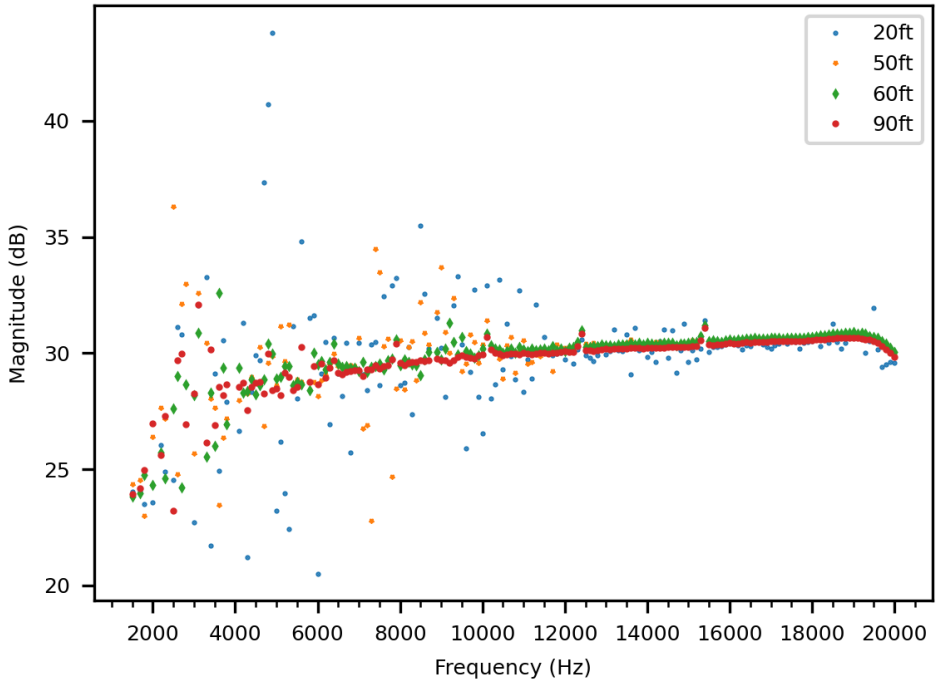

(d) Old Commercial Building Steel Dry Sprinkler Pipe

Figure 4.13 (cont.)

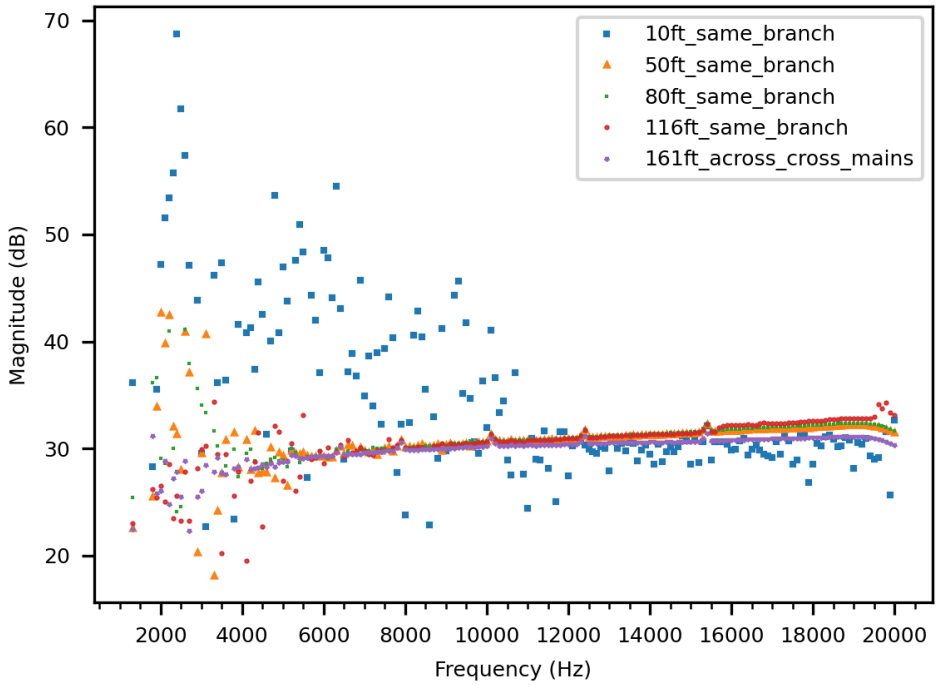

(e) New Commercial Building Black Steel Sprinkler Single-floor Pipe Runs

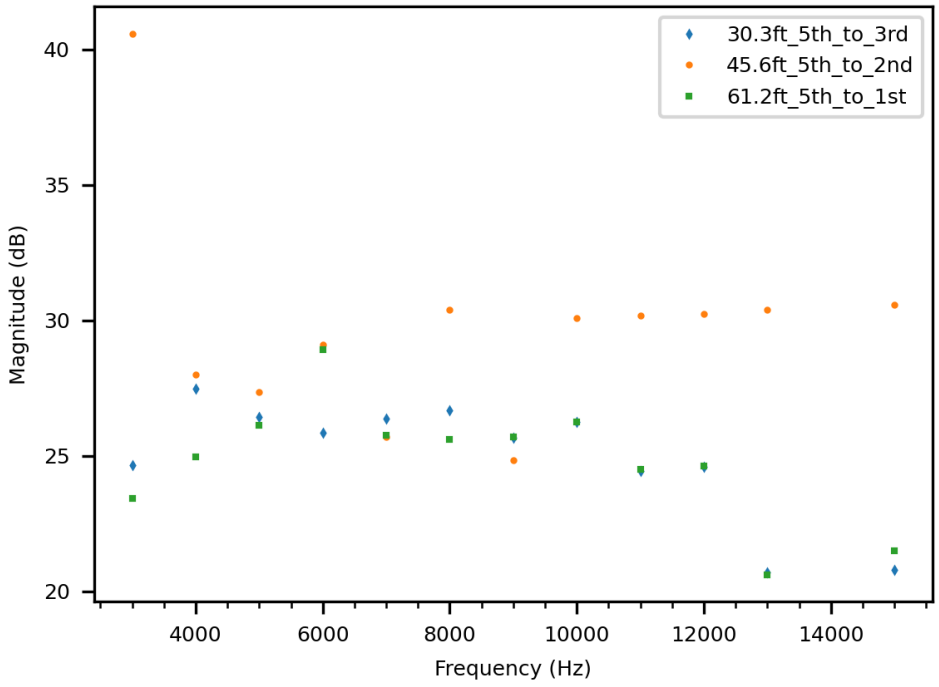

(f) New Commercial Building 4” Wet Standpipe/Riser (Every 1000Hz Only), from 1st to 5th Floors

Figure 4.13 (cont.)

as a major peak signal at the receiver side are excluded from the figure.

Figure 4.13 shows that certain frequencies are much higher in magnitude than the others, whether this is due to pipe resonance frequency, the way certain frequencies bounce due to the structure of the pipe pathways or simply an effect due to environmental noise. Though we expected a clear attenuation trend with distance across the pipes, Figure 4.13 shows that that is not the case; many frequencies' signals decrease in strength at first but then increase in magnitude as they pass through the pipe. We hypothesize that the increases are due to constructive interference between the waves at certain points in the pipe.

In all buildings and pipe runs except the 6" standpipe, we successfully transmitted and received many frequencies at the longest distances available. The longest pipe run was 170ft in OCS along a black steel wet sprinkler pipe; the pipe run was exposed and was relatively straight, though with many fittings. The second longest but much more twisting pipe run was in the NCS concealed wet sprinkler system, where we transmitted 161ft from one branch line end, through a larger cross main, then to the end of the furthest branch off the cross main. In addition to the twists and turns, this pipe run included dozens of intersections with other branch lines and the short pipe runs that connect sprinkler heads to branch lines. Thus the signal transmitted well across complex pipe structures on a single floor. Further, the de facto limit of about 150' per typical branch line (10 sprinklers of standard coverage, spaced 15' apart) means that an attacker should be able to transmit and receive along the full length of any branch line, as well as anywhere within a single-floor sprinkler system run in a building with four (as in the measured wing of NCS) or more floors. Finally, since the figure shows that signals at many frequencies hold their magnitude well at the maximum distances measured, the maximum potential distance for successful transmission is certainly not limited to 161'.

The least successful transmission in Figure 4.13 was for the NCR 4" wet risers. These pipes pass through multiple floors, with large feeder mains tying into them at each floor. We found the standpipe to have a lot of low frequency noise, coupled with serious attenuation and ambient leakage issues for the frequencies we tested. We tested at this location using signals at multiples of 1000Hz, and only 3KHz-13KHz and 15KHz satisfied the bandwidth condition. Upon reception, the 4" standpipe also had the lowest magnitude signals overall for the frequencies tested. The NC 6" standpipe was even worse, and is not shown in the figure. As attackers, we would avoid these pipes.

Note also that transmissions on the adjacent floor branch lines and cross main could not be picked up on the risers in the stairwell. This means that the risers are not good locations for receivers intended to pick up transmissions on the adjacent floor.

Comparing the results across all pipe materials, diameters, and internal pipe contents, we see that all the pipes with less than 3" diameter successfully supported transmission of high frequency signals across relatively long distances, with little attenuation as the frequency and distance increase.

The 4” and 6” pipes failed to meet this standard.

An attacker would often prefer to be able to place the receiver entirely outside the building, for easier pickup of the transmitted data. In our experience, transmissions did not travel well through the water meter. We also had the opportunity to test a roughly 100’ outdoor underground copper water supply line that ran between Residence’s main building and an outbuilding. We found that signals did not transmit well along that pipe run. Thus our experiments focus on indoor pipes of less than 3” diameter, and especially on sprinkler system pipes, since they allow an attacker to place a receiver and transmitter in essentially any room or hallway.

4.10.3 Best Frequencies for Attackers

An attack should be easy to configure, hard to detect, and have a low signal loss and error rate. There are three factors that an attacker must consider when designing the attack:

- A preconfigured attack should use frequencies that are known to work well in most pipes, as details regarding the sprinkler system pipes and layout are usually not available.
- The attacker should use frequencies that people are unlikely to overhear, which is trivial with ultrasound but requires attention with equipment like ours.
- To maximize battery life and reduce the risk of detection, the attacker should use the lowest volume/power that allows successful reception of the signal.

In theory, the first and last of these three parameters can be calibrated by firmware during attack setup. We provide a poor-man’s guide to the best choices in the subsections that follow.

4.10.4 Frequencies That Work for Most Pipes

As an attacker, we prefer frequencies that consistently perform well regardless of pipe material, pipe structure, building structure, environmental noise in the pipe and at all distances along the pipe. To arrive at this global view of an attacker’s preferred bandwidth, Figure 4.14 shows the frequencies that satisfy the bandwidth condition at all tested transmission distances for all tested pipes that run within a single building floor (RG, RW, OCS, OCDS, NCS).

In Figure 4.14, frequencies that satisfy the bandwidth condition (regardless of the magnitude of the signal received) are depicted as colored bands in a broken bar plot derived from the data in Figure 4.13. White spaces in the frequency band show frequencies that do not satisfy the bandwidth condition. Horizontal stretches of solid color for a pipe run and vertically across multiple pipe runs

indicate a stretch of bandwidth where the attack works well for all pipes. Overall, many frequencies work well, as shown by the colored regions without white space across all pipes. The longest stretch of contiguous good frequencies for all buildings is in the 12KHz to 18KHz bandwidth range (12kHz-20kHz for commercial spaces).

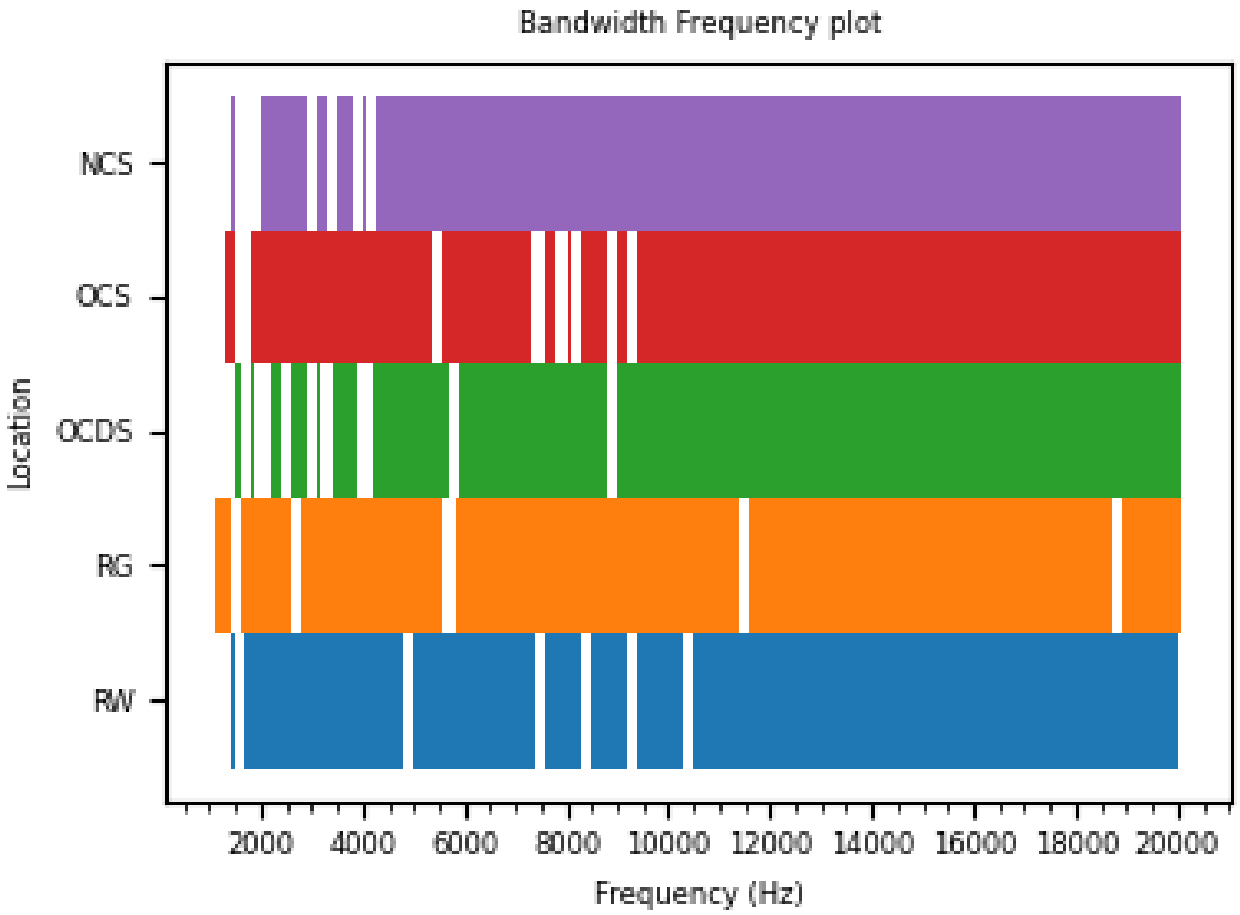

Figure 4.14: Frequencies That Satisfy the Bandwidth Condition at All Distances.

4.10.5 Frequencies Least Noticeable to Human Ears

The human audible frequency range is generally considered to be 20Hz to 20KHz [134]. Within this audible range, human ears are most sensitive to the frequencies from 2KHz to 5KHz [135].

Above this spectrum, human ears tend to become less sensitive as the frequency increases, and the upper frequency range of human hearing is generally 15-17Hz [136]. This limited range has been documented scientifically by much prior research and medically linked to the cochlear structure in human ears [136, 137]. This upper range and the entire audible bandwidth also drops and reduces respectively as we age [138].

For a quick verification that frequencies at the higher end of this range will be difficult for most people to hear, we evaluated the audible ranges for 8 volunteer test subjects aged from 20s to 60s. In this small evaluation, we found frequencies above 12KHz were not audible to 2 out of 8 volunteers, above 14KHz were not audible to 3 out of 8 volunteers, above 15KHz were not audible to 7 out of 8 volunteers, and above 16.3KHz were not audible to any volunteers.

Though our evaluation was within the range of standard human hearing (20Hz-20KHz), an attacker who desires to go undetected would strategically prefer to use the upper frequency ranges (15KHz-20kHz) that most people cannot hear, and avoid the most sensitive ranges of 2KHz to 5KHz. As shown in Figure 4.14, there is a large stretch of contiguous frequencies in the upper bandwidth range of 12KHz to 18KHz that are supported well by all pipes over all distances. Thus an attacker will strategically prefer to use these transmission-friendly upper frequency ranges.

4.10.6 Lowest Possible Transmission Volume and Power

During the initial setup phase of an attack, the attacker can determine the lowest possible transmission volume that provides good reception, for each frequency that the attacker plans to use. As mentioned earlier, this check could also help to avoid any locally noisy frequencies. For buildings with consistent pipe noise, the attacker could also make an initial recording of the noise and employ noise removal techniques to improve signal detection. However, none of our tested pipes were very noisy at high frequencies, even when a group of children were building with Legos in OCS and we expected to have to rerun the experiments.

To estimate the lowest volume/power at which transmissions could be made and still be intelligible above the background noise of a pipe, we transmitted a linear chirp descending from 20kHz to 1Hz along the maximum distance of each building pipe run. For RW and RG, which are 40' residential runs, a minimum laptop volume setting of 6 (peak loudness of 22.8dBA, a bit softer than a whisper) sufficed for the graph of the signal to be clearly visually differentiated from the background noise. For OCS, OCDS, and NCS, a minimum laptop volume of 10 (peak loudness of 30.5dBA, about as loud as a quiet rural area) was required, while the New Commercial 4" standpipe required a laptop volume of 30 or higher.

These are the volumes being injected into the pipe. To minimize leakage of the signal into the air at the point of transmission, soundproofing would be important in a real attack, especially if the contact between a flat transducer and the curved pipe is not perfect. Our implementation of the transmitter did not include any soundproofing. In our experience, some signal also leaks into the air along the pipe run, but the transmitter was the main point of leakage.

4.10.7 Hiding the Signal Using Other Modulation Methods

We encoded the information being transmitted as a signal of a certain frequency, i.e., the data lies in the frequency domain. However, an attacker might obtain higher throughput or a stealthier attack by using other domains to send the data. Some traditionally used modulation methods in communication employ forms of amplitude, frequency or phase based modulation. Drawing inspiration from stegnanography, time based modulation or hiding the data in other modulation patterns could be employed by an ambitious attacker. An attacker could, for example, time the subsequent signals so that the information lies in the timing gap between the signals instead of the particular frequency being sent, change the phase of the signals so that different phases indicate different symbol values, change the magnitude of the signal to indicate different data, and so on. However, as our experiments did not find consistent attenuation trends as the transmission distance increases, and in fact may even amplify at some locations along a complex piping system, magnitude based modulation would not be well suited to this application. Phase based modulation, timing based stegnanography to hide the signal, and their variations show promise, along with frequency based modulation methods.

4.11 CHANNEL CAPACITY ANALYSIS

Given the empirical results summarized in Figure 4.13, we can derive an upper bound on the channel capacity for each individual frequency in each pipe run, and for the channel capacity of each pipe run as a whole. To closely approach these upper bounds in practice would require the use of a communication protocol with excellent error correction.

For individual single-frequency channels in the presence of noise, we have the Shannon-Hartley Theorem [139]:

$$C = B \log_2(\frac{S+N}{N}), \tag{4.1}$$

where C is the channel capacity in bits per second; B is the bandwidth of the channel in hertz; S is the received signal power; and N is the total noise power over the bandwidth.

In this formula, we set $S+N$ to be the power spectral density of the entire signal coming through the pipe (i.e., the intended signal S plus the noise N). We obtain N from the power spectral density of the signal coming through the pipe when no transmission was taking place, applied across the bandwidth. For this we used a .5 second recording of the sound on the pipe before each frequency was transmitted. Finally, B is the bandwidth of the channels being used, e.g.1KHz for a single frequency channel, 19kHz for all frequencies upto 19KHz.

We focused on the maximum distance transmission for each pipe tested and determined the

highest-capacity frequency across all frequencies tested in Figure 4.13. Table 4.2 gives the details. In all real-world settings tested except the 4" standpipe and the residential gas line, the highest-capacity frequency was close to 20KHz. The distribution was very flat, i.e., the capacity of the best frequency differs little from that of the worst. In all real-world pipe runs except the standpipe, the highest-capacity frequency can be used to transfer roughly 15 bits per second in our implementation. The standpipe capacity is less than 12Kbps, making it unattractive to an attacker. The outdoor laboratory pipe runs performed slightly better than the indoor pipe runs.

Pipe Run	Pipe Type	Highest-Capacity Frequency (Hz)	Highest 1Hz Channel Capacity (bps)	Total (Kbps) Capacity	51-Channel Capacity (bps)
OCS	170' Wet Sprinkler	19,600	15.496	77.497	776.77
OCDS	90' Dry Sprinkler	19,600	15.456	77.297	775.70
NCS (across cross-mains)	161' Wet Sprinkler	19,600	15.604	78.039	782.74
NCS (contiguous branch)	116' Wet Sprinkler	19,800	16.671	83.376	808.41
NCR	62' 4" Riser	15,000	2.523	12.619	15.14
RG	50' Gas Pipe	16,200	15.870	79.367	767.28
RW	40' Water Supply	19,200	15.474	77.386	769.63
Indoor Lab	30' Water CPVC	19,600	15.298	76.508	769.55
Indoor Lab	30' Air CPVC	17,400	15.306	76.546	770.91
Outdoor Lab	42.5' Victaulic 75	19,600	18.667	93.354	902.57
Outdoor Lab	42.5' Victaulic 005	19,300	19.187	95.953	947.09

Table 4.2: For 15KHz-20KHz Bandwidth, the Highest-capacity Channel Frequency at Maximum Distance, Pipe Capacity Ignoring Interference, and Pipe Capacity with 51 Non-interfering Channels

We can directly estimate each pipe run's total capacity using the empirical data collected to evaluate the Bandwidth Condition for each frequency. From this data, we know the signal dispersion for each frequency at each distance measured along each pipe run. Given a set of frequencies that are spaced far enough apart that that they do not interfere with each other according to the dispersion data, the total capacity of that set is the sum of the individual orthogonal channel capacities computed according to the Shannon-Hartley Theorem for each frequency. While this estimate understates the total maximum capacity of the pipe run, it also has an advantage: the lack of interference makes the attacker's task of interpreting the received signal much easier.

Figure 4.15 shows the dispersion patterns of the frequencies with the *most* dispersion in NCS at 10', 80', and 161'; the patterns in other pipe runs and at other distances were similar. (We do not consider the 4" standpipe in this section, because its diameter is too large for the pipe attack to be effective.) As suggested in the figure, a frequency separation distance of 80Hz would be needed to ensure that no frequency in the range 15K-20KHz would overlap with any other at any measured distance during transmission.

We consider the slightly larger separation of 100Hz and consider channels between 15K-20KHz in multiples of 100Hz, to be used in parallel without interference. Applying the Shannon-Hartley Theorem to each of the 51 frequencies in the target range and adding up their capacities, we obtain

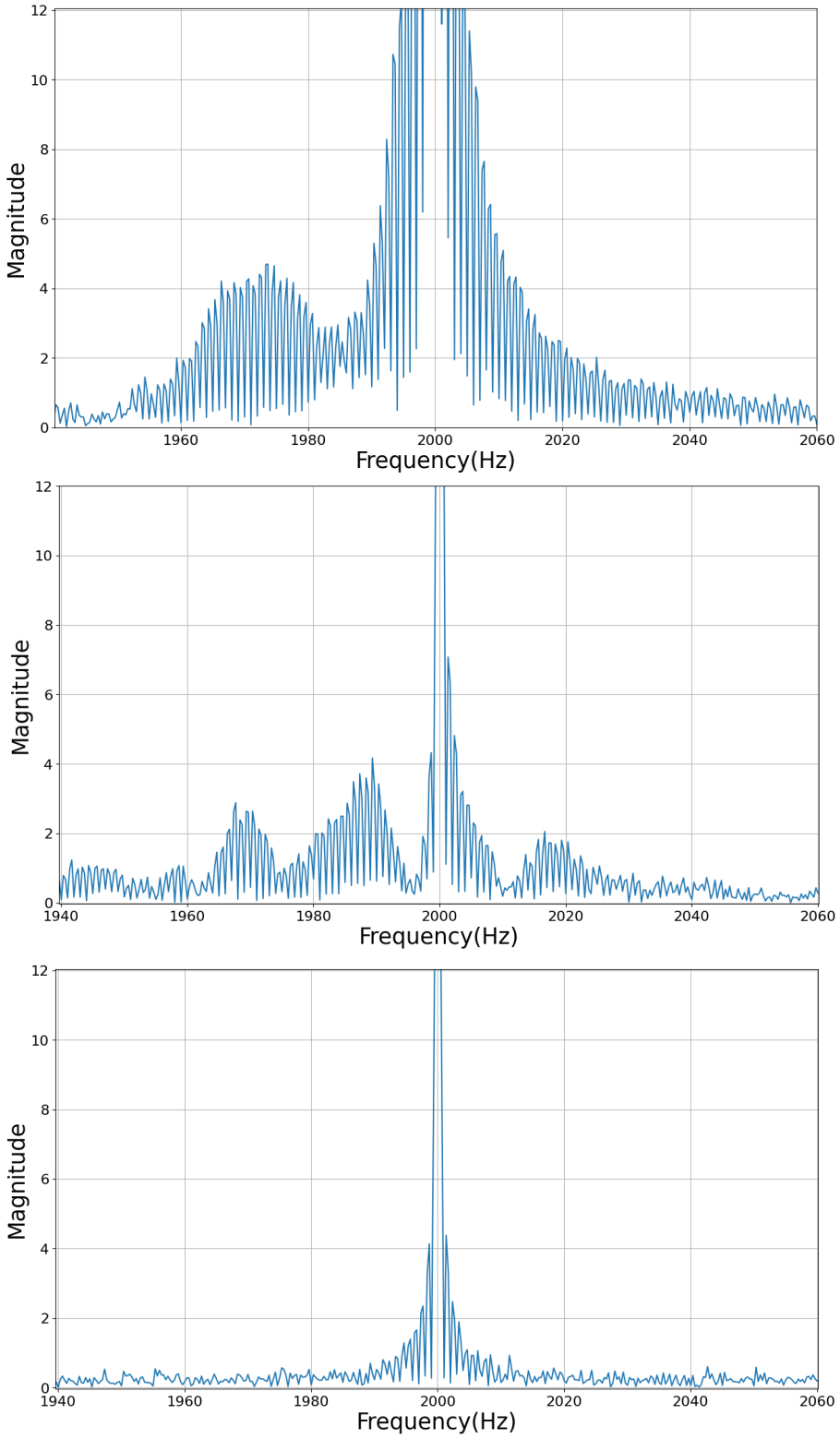

Figure 4.15: Dispersion Patterns of the Frequencies with the Most Dispersion at 10’ (top), 80’ (center), and 161’ (bottom) in NCS.

the estimated total capacity of roughly 770bps per real-world pipe run, shown in the last column of Table 4.2, given sufficient device power. If an attacker uses the minimum 80Hz separation required for non-interference, they will have 61 channels instead of 51. We estimate that the 10 additional channels will boost the capacity of each pipe run to 924bps.

A separation distance of 100Hz is more than needed to avoid interference, but a small transmitter is unlikely to have enough power to transmit on every non-interfering frequency at the same time, unless the transmitter is hardwired or the attack is of quite short duration. Further, parallel transmission on all 51 frequencies would be about 15dB louder than the same transmission on a single frequency, which means it would seem roughly three times as loud to a human. As the number of channels increases, at some point the increase in sound leakage from the pipes might draw human attention, though in many environments, device power constraints are more likely to be the limiting factor.

4.11.1 Power-Limited Channel Capacity

In practice, the power budget of the transmitter and how it is divided across the frequency channels dictates how much of the channel capacity can be utilized in a multi-channel communication medium such as a piping system. In our case, the power budget must also consider the maximum volume allowable to ensure stealthiness in the attack environment. Further, power should only be allocated to channels that fall within the attacker's preferred bandwidth, 15KHz-20KHz.

Each frequency channel has an associated signal to noise ratio (SNR). Intuitively, when dividing and allocating the total power across a set of frequency channels, the channels with more favorable SNRs should be allocated more power. To determine an upper bound on the power-limited information carrying capacity across all frequencies for a pipe run, the theoretical tool of choice is the Water Filling Theorem [139], also known as the Water Pouring Theorem.

Water filling is a standard channel equalization technique that is designed to optimize power usage and data capacity in communication systems. We can think of the process as that of pouring water into a pot with a very uneven bottom, i.e., areas of different depth at its base. When we pour water into the pot, the water level at the top will eventually be level across the entire pot, but each area of the pot will have a different depth of water.

Drawing the analogy that the water is the power, the total volume of water corresponds to the total power of the system. The varying water depth in different areas of the pot is analogous to the different SNRs in different channels, which require different power allocations to maximize the overall capacity. The deepest areas in the allocation are the channels whose noise and gain allows them to use power the most efficiently. We can view the water depth for a particular channel as a function of the SNR for that channel's frequency.

For a multichannel system, the total capacity is the sum across the individual channels' power-limited capacity calculated using the Water Filling Theorem. Channels with a poor SNR may not receive any power at all. As the total power increases, a channel that had zero allocation may begin to receive some power, so the fraction of power allocated to each channel changes in a non-linear manner, in general.

More precisely, we have:

> **Water Filling Theorem.** Assume an allocation $P_1, \ldots, P_n$ of total power budget $P = \sum_{1 \leq i \leq n} P_i$ across n non-interfering channels with gain-to-noise ratios $\frac{1}{\lambda_1}, \ldots, \frac{1}{\lambda_n}$. Then the total information transfer rate across the channels is maximal iff the following holds for all $1 \leq i, k \leq n$: if $P_i > 0$, then $P_i + \lambda_i \leq P_k + \lambda_k$.

Let us look at this in more detail. The total achievable throughput for a given power budget is the sum of the individual rates of the non-interfering channels:

$$C = \sum_{i=1}^{n} log_2(1 + \mathrm{SNR}_i(P_i)), \tag{4.2}$$

where the signal-to-noise ratio $\mathrm{SNR}_i(P_i)$ for channel i when that channel is allocated a certain power level P_i is a function of its gain. For simplicity, let us assume that the normalized noise N_0 is the same for all channels. Then the SNR for channel i will depend on the power allocated to it:

$$\mathrm{SNR}_i(P_i) = \frac{G_i P_i}{N_0}. \tag{4.3}$$

The Water Filling Theorem maximizes the throughput summed over all n channels given individual channel gains G_i, while satisfying the constraint that the total power allocated to the channels must sum to P. Using formulas 4.2 and 4.3 and applying the constraint that the power allocations sum to P, we can write this maximization problem as:

$$\begin{aligned} \underset{P_i}{\text{maximize}} \quad & \sum_{1 \leq i \leq n} \log_2(1 + \frac{G_i P_i}{N_0}) \\ \text{subject to the constraints} \quad & P = \sum_{1 \leq i \leq n} P_i, \\ & P_i \geq 0, \forall 1 \leq i \leq n. \end{aligned} \tag{4.4}$$

This convex optimization problem has been well-studied in the literature. We used the solution approach recommended in [140, 141], which simplifies the problem into a bisection search algorithm for α parameters such that:

$$P_i = \frac{1}{\alpha} - \frac{N_0}{G_i}. \tag{4.5}$$

In our calculations, we considered simultaneous transmission across the $n = 51$ non-interfering channels at 100Hz separation in the 15KHz-20KHz band of interest to an attacker. We compute the gain G_i for channel i from the transmission and receiving power averages across all readings in the experiments presented in the previous section. Let S_i^0 be channel i's signal values received immediately adjacent to the transmitter (zero distance), averaged across separate measurements. Let S_i^{dj} be the signal values received in the jth reading taken at distance d from the transmitter. Then channel i's gain is the ratio of those two signal values, averaged across all the measurements taken at each distance:

$$G_i = \frac{1}{n_D}\Big(\sum_{1 \le d \le D} \frac{1}{R_d}\Big(\sum_{1 \le j \le R_d} \frac{S_i^{dj}}{S_i^0}\Big)\Big), \tag{4.6}$$

where R_d is the number of readings taken at distance d, up to the maximum distance D measured for that pipe run; and n_D is the number of locations along the pipe run at which measurements were taken. Note that R_d is the same for all frequencies measured at a particular location.

We compute the normalized noise N_0 per pipe location by measuring the noise signal power spectral density from the spectrum observed in the .5 seconds before a signal is transmitted on the pipe. We normalize the noise power spectral density values by dividing by the highest amplitude signal observed. Then we average the normalized noise power spectral density signals observed in all readings at a location across all frequency channels. To convert the power spectral density to noise power, we multiply it by the 51 non-interfering 1Hz channels' total bandwidth of interest (15KHz to 20KHz). We compute N_0 separately for each location along the pipe run.

We compute the SNR of each channel in a pipe run as the ratio of the signal power (P_{signal}) and noise power (P_{noise}) measured empirically over each frequency channel in the 15kHz to 20KHz bandwidth, and averaged across all readings for each channel. Signal and noise power are obtained using their respective power spectral densities. Then we define the total power budget P using the median SNR among all the frequency channels for that pipe run. The SNR in dB ($\mathrm{SNR_{dB}}$) scale used for obtaining the power budget for each pipe run is shown in the third column of Table 4.3. The total power budget is obtained from $\mathrm{SNR_{dB}}$ using formula 4.8.

As shown in Table 4.3, the real-world pipe runs have $\mathrm{SNR_{dB}}$ values of 42-44. These are excellent values, the equivalent of a 5-bar signal on a mobile phone, and far higher than the 20-25 recommended for wireless data and voice traffic. The exception is the 4 inch riser, whose negative $\mathrm{SNR_{dB}}$ means that its noise power exceeds that of its signal. This confirms that the riser is not a good communication medium.

$$\mathrm{SNR}_{\mathrm{dB}} = 10 \log_{10} \frac{P_{signal}}{P_{noise}} \tag{4.7}$$

$$P = 10^{\mathrm{SNR}_{\mathrm{dB}}/10} \tag{4.8}$$

Pipe Run	Pipe Type	$\mathrm{SNR}_{\mathrm{dB}}$	N_0	Total Capacity (bps)
OCS	170' Wet Sprinkler	44.11	8.4e-3	694.90
OCDS	90' Dry Sprinkler	43.83	42.4e-3	454.37
NCS	161' Wet Sprinkler (across a cross main)	44.31	65.1e-3	359.18
NCS	116' Wet Sprinkler (along contiguous branch lines)	45.83	63.2e-3	429.89
NCR	62' 4" Riser	-2.47	10.1e-3	55.09
RG	50' Gas Pipe	42.87	1.3e-3	783.98
RW	40' Water Supply	43.36	0.46e-3	729.72
Indoor Lab	30' Water CPVC	43.62	52.3e-3	437.59
Indoor Lab	30' Air CPVC	43.70	62.8e-3	416.84
Outdoor Lab	42.5' Victaulic 005	55.59	27.4e-3	530.19
Outdoor Lab	42.5' Victaulic 75	54.25	61.3e-3	492.51

Table 4.3: Power-Limited Capacity of Each Pipe Run According to the Water Filling Theorem, for 15KHz-20KHz with SNR-based Total Power Limits

Table 4.3 presents the total channel capacity in the 15KHz-20KHz range according to the Water Filling Theorem, using our transmitter implementation with SNR based power limits. The pipe runs vary in power-limited capacity from 359bps for the 161' run to 783bps for the 50' gas pipe.

Most frequencies of interest to an attacker are above the range of human hearing, while the remainder are difficult for most humans to hear. By transmitting only on frequencies that humans do not hear, i.e., 17KHz and above, an attacker can fully utilize the 31 channels in that region while remaining stealthy. In the 15KHz-17KHz frequencies that some humans can hear, better soundproofing around the transmitter or as ceiling acoustic tiles would allow us to increase the volume without worrying about transmissions being audible at bystander level, thus creating a higher power budget and increasing the throughput.

Another potential way to raise the throughput is to use different methods of encoding the data in the signal. This has been explored in the literature on ultrasonic health monitoring for building skeletons, where researchers report a wide variety of bit transfer rates, many close to our range but some as high as 40Kbps per channel. Using more sophisticated hardware for the transmitter and receiver can also improve the quality of the signals received by improving the gain even at smaller volume levels, which will allow us to utilize more capacity. More sophisticated hardware may also allow us to support additional channels with a small amount of interference. Finally, noise

cancellation at the receiver side can also improve the quality of the signal and allow us to utilize more capacity.

4.12 DETECTION, LOCALIZATION & PREVENTION

No matter what an attacker may be able to do with them, buildings still need to have fire sprinklers. This section considers ways to reduce the effectiveness of pipe attacks, including detection and defensive measures for new and old construction. When defense is ineffective, detecting and localizing the attack location and prevention measures can be taken.

We explored the effectiveness of a number of potential defensive measures:

- CPVC. Though not present in any building we had access to, CPVC is approved as a fire sprinkler pipe material for some building usages in some jurisdictions. As a non-metallic material, CPVC might be impervious to the pipe attack.
- Check valves. We had noted in our experiments with radiator water supply loops that we were unable to send signals past a loop's backflow prevention valves.
- Flexible couplings. Victaulic, a major manufacturer of sprinkler system components, cites significant reductions in annoying vibrations if three flexible Victaulic couplings are included in a pipe run after the pipe emerges from a pump.
- Gaps along the pipe surface. If signals are traveling primarily through the pipe surface, then the signals might have difficulty in moving past gaps in the pipe surface.
- Ambient noise. Ambient noise either in the form of white noise or noisy room occupants might reduce the effectiveness of transmissions.
- Wider pipes. Since the pipe attack is less effective in wider sections of pipe, the inclusion of wider sections of pipe at periodic intervals might serve as a defense.
- Signal obfuscation. A defender could inject signals directly into the pipe to obfuscate an attacker's signal.
- Sound cancellation. A defender could install sound cancellation devices along the pipes.

In the remainder of the section, we consider each of these measures in turn, as well as traditional parameter securing methods using bug sweeping and localization of the transmitter. While the best of the bunch is signal obfuscation, we did not find any technique to be especially effective.

4.12.1 CPVC and PVC Pipes

Our initial understanding was that metal pipes were excellent conductors of vibrations, compared to other materials. To test the hypothesis that non-metalic pipes would not carry vibrations as well as metal does, we created three laboratory setups using PVC and CPVC pipes:

1. 1” inner diameter CPVC pipe run, 30 feet long
2. 1” inner diameter PVC pipe runs, 30 feet long
3. 3/4” inner diameter PVC pipe runs, 30 feet long

The two PVC pipe runs are shown in Figure 4.17 and the CPVC pipe run is shown in Figure 4.16.

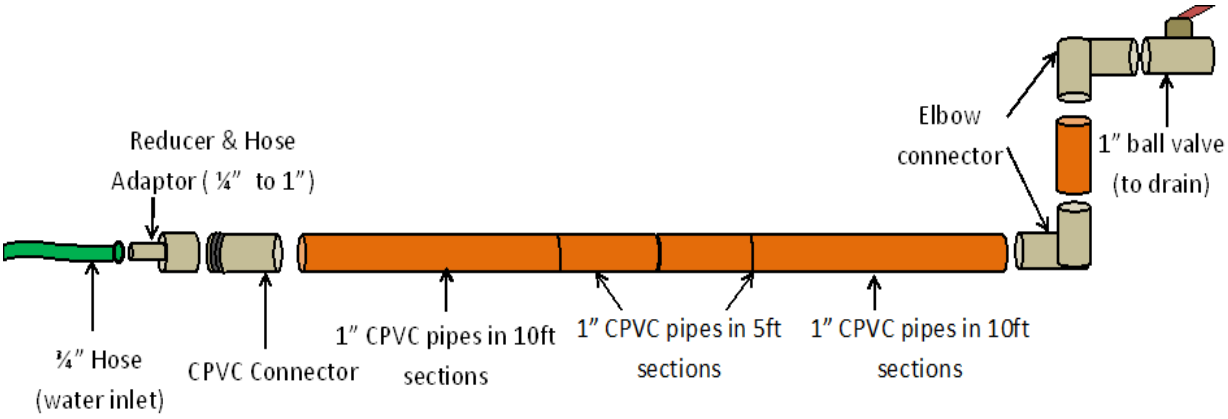

Figure 4.16: CPVC Pipeline

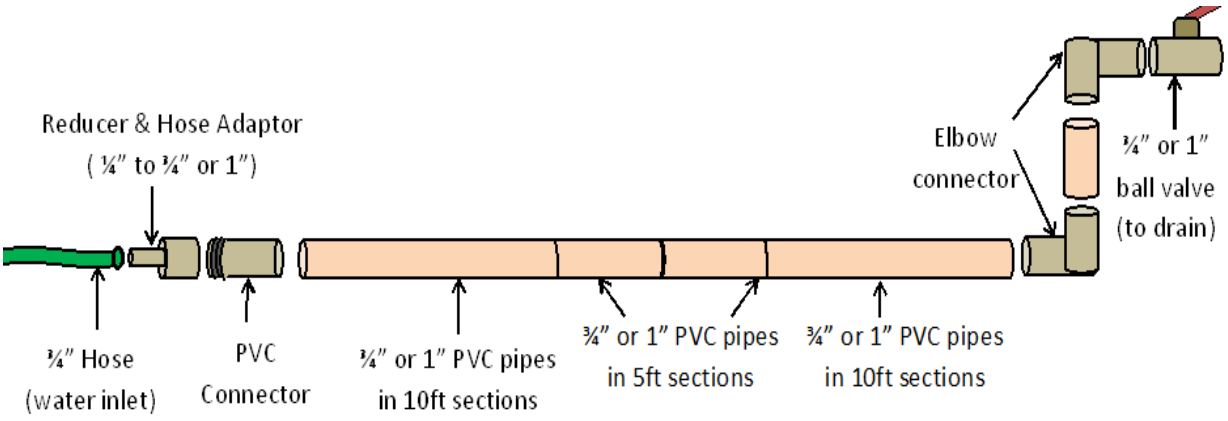

Figure 4.17: PVC Pipeline

In a nutshell, we found that the pipe attack worked very well with air- or water-filled CPVC and PVC. The results from experiments with 1” CPVC pipe reported in Figure 4.18 show that in

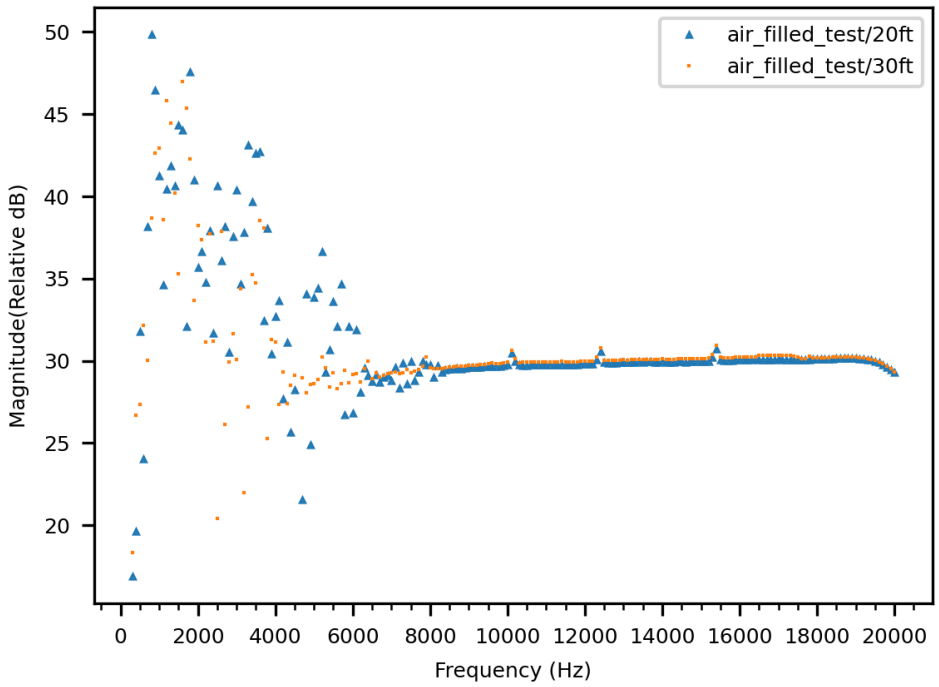

(a) Air-filled 1” Diameter CPVC Pipe

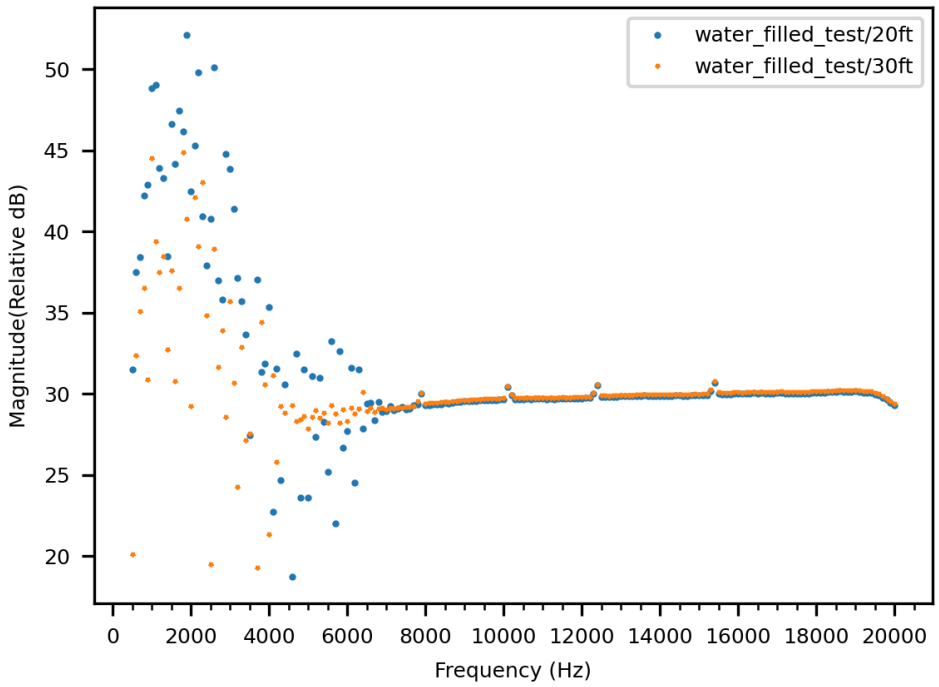

(b) Water-filled 1” Diameter CPVC Pipe

Figure 4.18: Frequencies Satisfying the Bandwidth Condition After Transmission Through 1” Diameter CPVC Pipes at Various Distances

general, frequencies above 500Hz pass through the CPVC pipe and can be received as a clear signal at the other end, satisfying the bandwidth condition. We also see the metal-pipe trend of signal magnitude slightly increasing with distance before starting to decline near the ultrasound range.

While not good news for defense, the effectiveness of CPVC and PVC for transmission meant that we did not have to use black steel for all experiments with fittings. This was convenient, because it is much easier and faster to saw up and reconfigure PVC and CPVC than black steel. Thus we used PVC pipe to test the effectiveness of check valves as a defense.

4.12.2 Check valves

We noted in early experiments with copper radiator water supply loops that we were unable to send signals past a loop's backflow prevention valves. We also observed that transmissions in the sprinkler system on a particular floor of a building do not seem to reach the riser that serves that floor, which is generally separated from the feeder main by a backflow prevention device. Based on these results, we hypothesized that the inclusion of check valves at regular intervals, e.g., at room boundaries, might reduce the effectiveness of the pipe attack.

To test this hypothesis we added check valves to the CPVC and PVC pipe run setups described earlier. We purchased the two check valves shown in Figure 4.19:

1. Homewerks Worldwide 1 inch Lead Free Brass FIP x FIP Swing Check Valve
2. Proline Series FIP x FIP PVC Check Valve

(a) Homewerks Worldwide Lead Free Brass FIP x FIP Swing Check Valve

(b) Proline Series FIP x FIP PVC Check Valve

Figure 4.19: Check Valves Tested as a Defense

The two check valves both prevent backflow, but are constructed of different materials (brass versus PVC) and use different internal mechanisms. We installed each valve at the center of the

CPVC and PVC pipe run setups (15 feet from each end), as shown in Figure 4.20 and 4.21. We attached the transmitter and receiver at opposite ends of each pipe run, 30' apart.

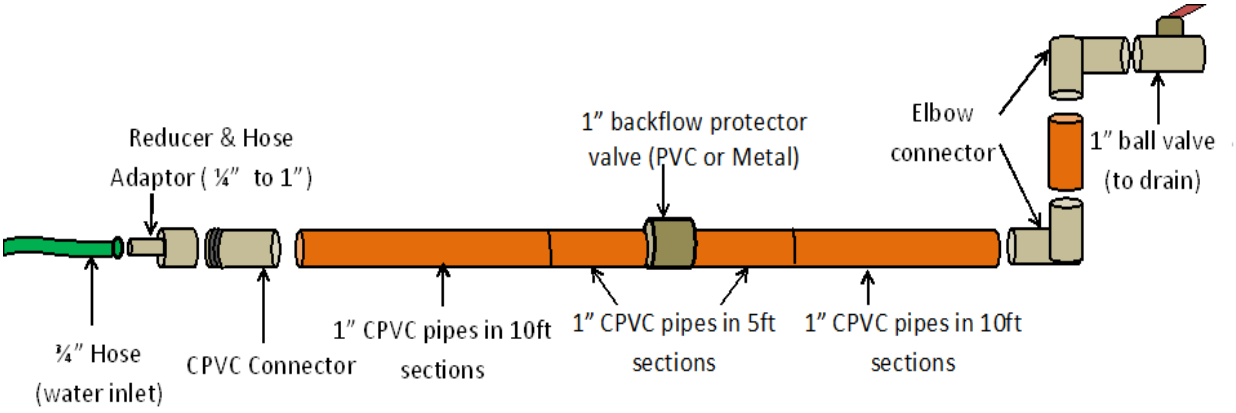

Figure 4.20: CPVC Check Valve Pipeline

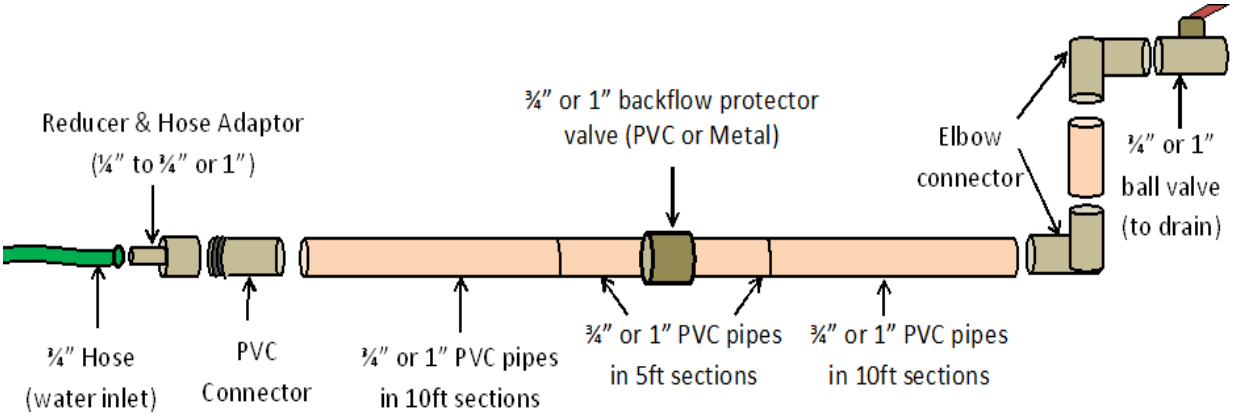

Figure 4.21: PVC Check Valve Pipeline

We measured the transmission of signals before and after the check valves were added to the pipeline, both when the pipes were filled with air and with water, and with the direction of transmission running with and against the check valve. For comparison, we sent the same signals through the pipe with a PVC threaded coupling in place of the check valve. Figure 4.22(a)–(f) shows that the presence of the Homewerks swing check valve has no discernable impact on the magnitude of low, medium, and high-frequency transmissions received in 3/4" PVC. We repeated the experiment with 1" air filled PVC pipe and the Proline Series PVC check valve, and also with transmission from the other end of the pipe. We determined that in all cases, the presence of the check valves did not significantly reduce the transmission of the intended signal in either direction along the pipes.

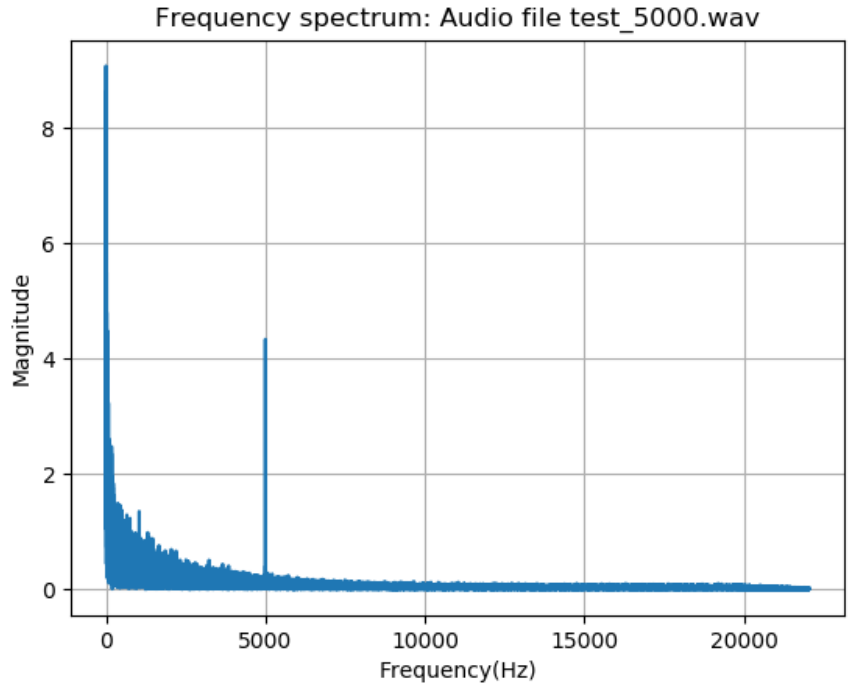

(a) 5KHz Signal Received in PVC Pipe Run without Check Valve

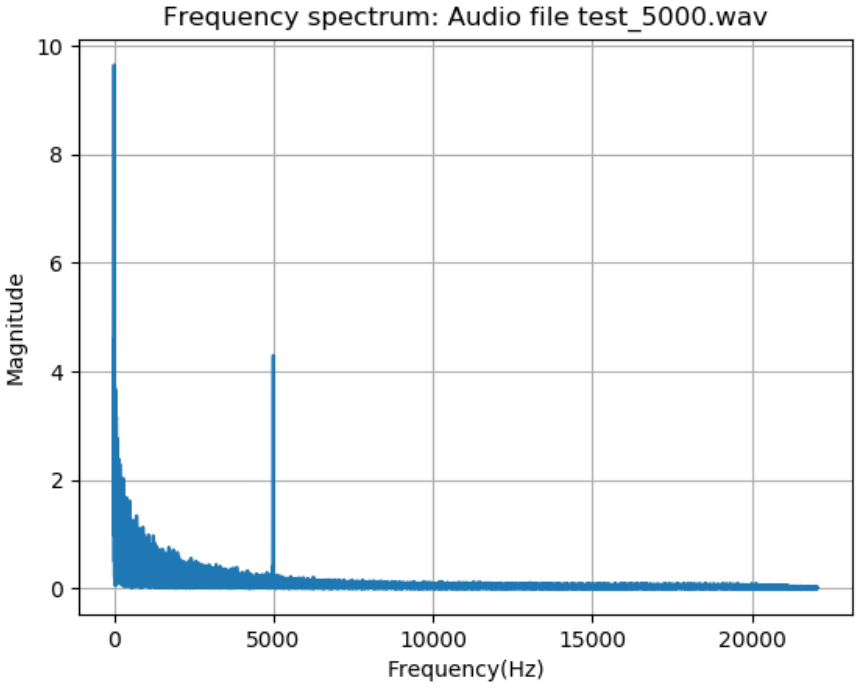

(b) Transmitted 5KHz Signal Received in PVC Pipe Run with Check Valve

Figure 4.22: 5KHz, 10KHz and 20KHz Signal Receptions in a 30' Water Filled PVC (3/4" internal diameter) Pipe Run with and without a Homewerks Check Valve at the Midpoint of the Run

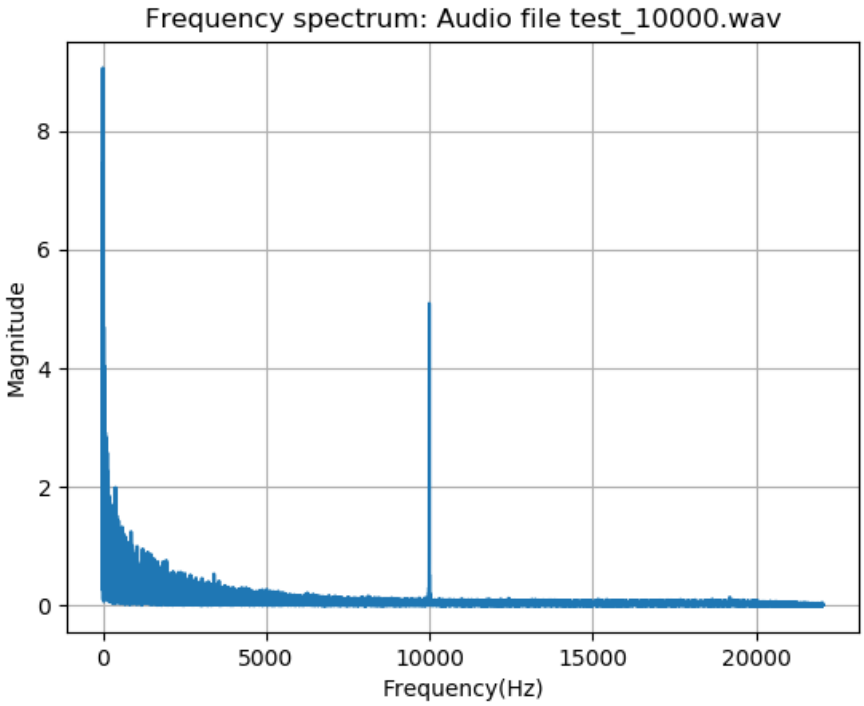

(c) 10KHz Transmission in PVC Pipe without Check Valve

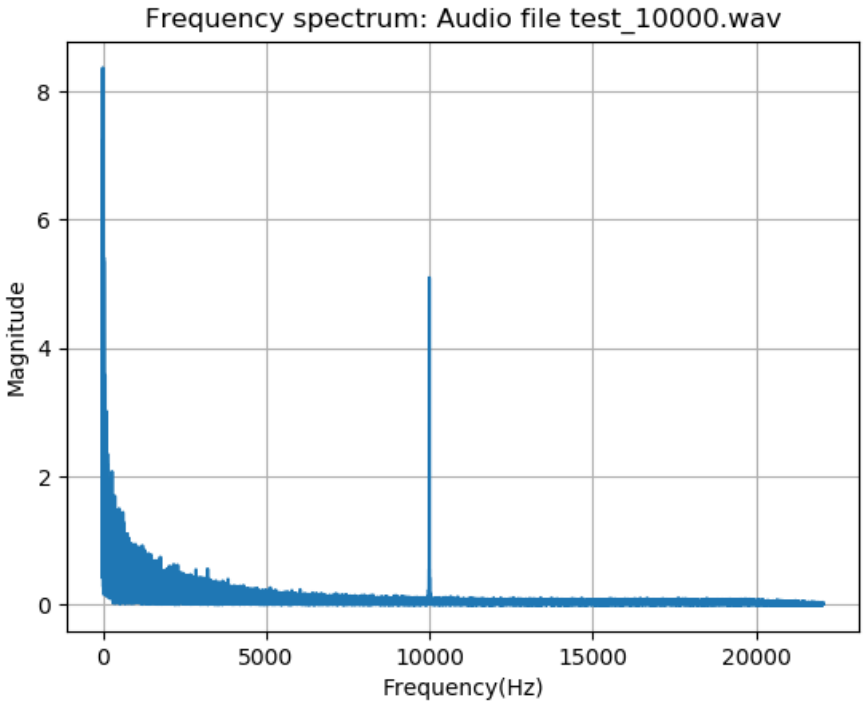

(d) 10KHz Transmission in PVC Pipe with Check Valve

Figure 4.22 (cont.)

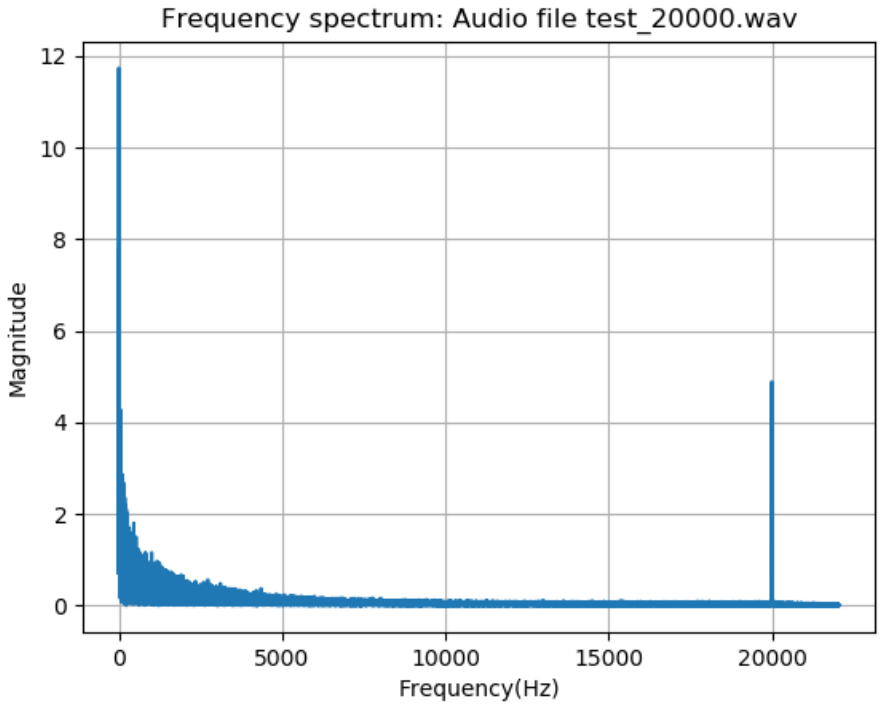

(e) 20KHz Transmission in PVC Pipe without Check Valve

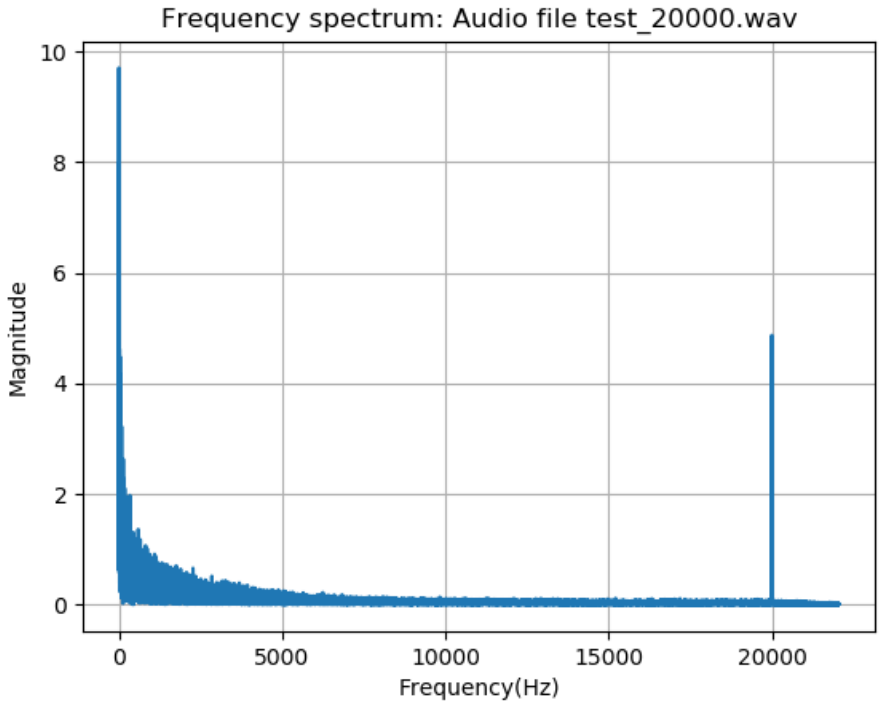

(f) 20KHz Signal Transmission in PVC Pipe with Check Valve

Figure 4.22 (cont.)

4.12.3 Flexible couplings and air gaps

When pumps are connected to metal pipes, the vibration of the pumps can be transmitted along the pipes, which can be extremely annoying for building occupants. Victaulic, a major manufacturer of sprinkler system couplings, markets their flexible couplings as a means of reducing this disturbance (see Figure 4.23). Victaulic's literature cites significant reductions in vibration if three flexible couplings are included in the pipe run after the pipe emerges from the pump, so we evaluated these couplings' potential as a defense against the pipe attack. For example, perhaps a buffer of three flexible couplings between rooms would suffice to prevent transmission.

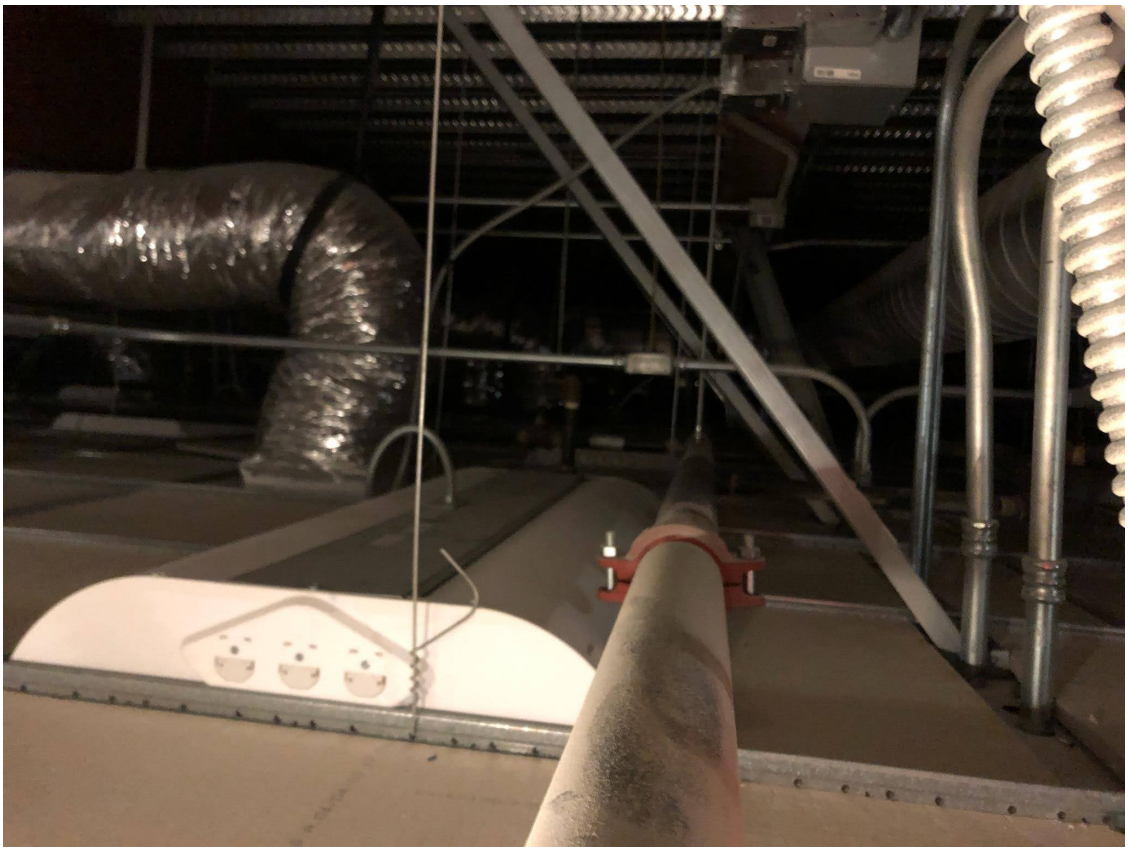

Figure 4.23: Red Victaulic Coupling in a Sprinkler Pipe Run in the New Commercial Building

As illustrated in Figure 4.25, Victaulic's grooved pipe coupling consists of a resilient elastomeric gasket encased inside a ductile iron housing. The gasket provides discontinuity for the vibrations travelling along the pipe and also offers a vibration absorption effect. The ductile iron housing of the coupling provides a strong structure to hold the pipes in place, while also providing a boundary for the gasket to prevent overstretching when the pipe moves. The coupling can only be used with pipes that have a groove machined into the end of the pipe, within close tolerances. The coupling fits around the ends of two pipes, and the bulges on the coupling's inner edges fit precisely into the

grooves on the pipe ends. The pipe ends are held apart from each other by the coupling.

Flexible pipe couplings such as Victaulic's have long been used in the shipbuilding industry to improve the comfort of passengers and crew and extend the lifetime of the ship. The couplings reduce noise, and the flexible joint prevents damaging stresses at the point where the pipes would otherwise touch [142]. Since Victaulic couplings are not rigid, the pipes can expand and contract in response to movements and changes in temperature in the environment. At a test conducted at NASA's Vibration and Acoustics Test Facility (VATF), the vibration attenuation effects using 4–12", 18", and 24" Victaulic flexible couplings installed on standard wall pressurized (300 psi/20 bar) carbon steel pipe outperformed that of double sphere rubber connectors and stainless steel braided pump connectors, when subjected to a frequency range of 10-2000Hz [143].

Our focus is on indoor sprinkler system, gas, and water supply pipes, which are significantly smaller than those tested by Victaulic. Further, we are interested in a much wider range of frequencies, from 100Hz to 20000Hz, and especially toward the higher end of this range.

Since our accessible buildings did not include flexible couplings in their sprinkler systems, we ran vibration transmission experiments using the outdoor laboratory 42' black steel pipe run and all of the couplings shown in Figure 4.25. The two Victaulic couplings in the figure are approved for use in fire sprinkler systems, while the flexible PVC coupling and rubber washers are not.

As shown in Figure 4.24, we connected the black steel pipes using three couplings: one at the center (approximately 21') and another at each end of the pipe run (approximately 0' and 42'), before the transitions to the valves and hose. In a real-world deployment, we would prefer to have the three couplings placed close to each other, but we did not have access to the machinery needed to cut and groove the ends of short lengths of pipe.

For each type of coupling in Figure 4.25, we ran tests using three of that type of coupling. We sent signals in the range of 100-20000KHz and evaluated how the signal changes in magnitude at various distances along the pipe.

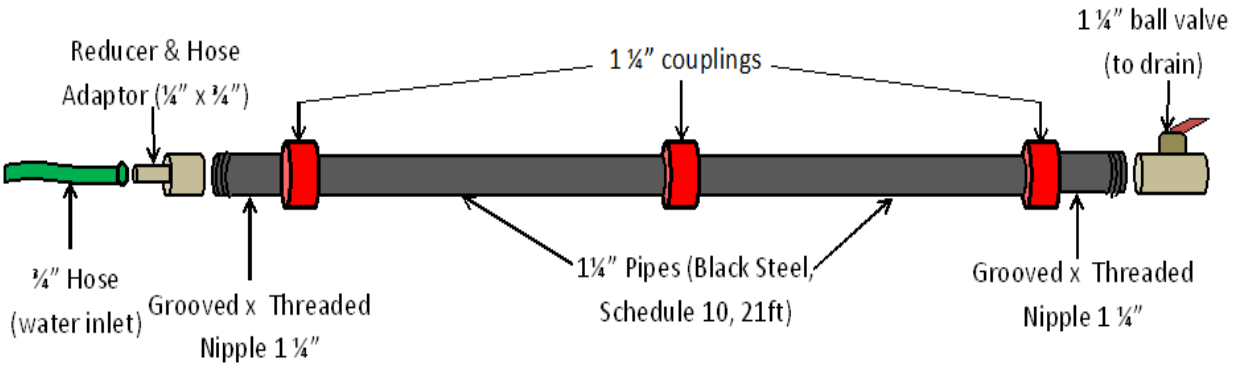

Figure 4.24: Black Steel Pipe Setup with Flexible Couplings

Results from individual couplings Figure 4.26 shows that all three couplings show several common characteristics in test results. For example, repeated small local maxima in magnitude are visible at regular intervals as the frequency increases. Further, for all three types, magnitudes

(a) Victaulic Style 005 Rigid Coupling

(b) Victaulic Style 75 Flexible Coupling

(c) Flexible PVC Coupling

(d) Flanged Rubber Washer

Figure 4.25: Couplings and Washers Tested

increase as we move from from 100Hz to 4000Hz and then remain high for frequencies above 4000Hz. Except for the lowest frequencies (100-400Hz), all tested frequencies satisfied the bandwidth criteria at all distances.

Beyond that, however, the choice of coupling does affect how the signal travels along the pipe. For example, as the signal travels along the pipe run with the Victaulic 75 flexible couplings, Figure 4.26a shows that the signal generally is higher in magnitude when received at 40ft and 42.5ft, across all frequencies. Signal magnitudes at 0ft and 10ft are on average the lowest across all frequencies. On the other hand, with the Victaulic 005 rigid coupling, Figure 4.26b shows that the signal increases in magnitude as it travels from 0ft to 20ft and then decreases a bit as it reaches the maximum distance of 42.5ft. With the flexible PVC coupling in Figure 4.25c, the magnitudes of the signals generally reach their maximum at 30ft and decrease slightly at 42.5ft. As in the indoor experiments, we believe the increases are due to constructive interference in the waves, causing the signal to amplify. With all three types of couplings, the amplitude of the signal at 0ft is among the lowest on average across all frequencies.

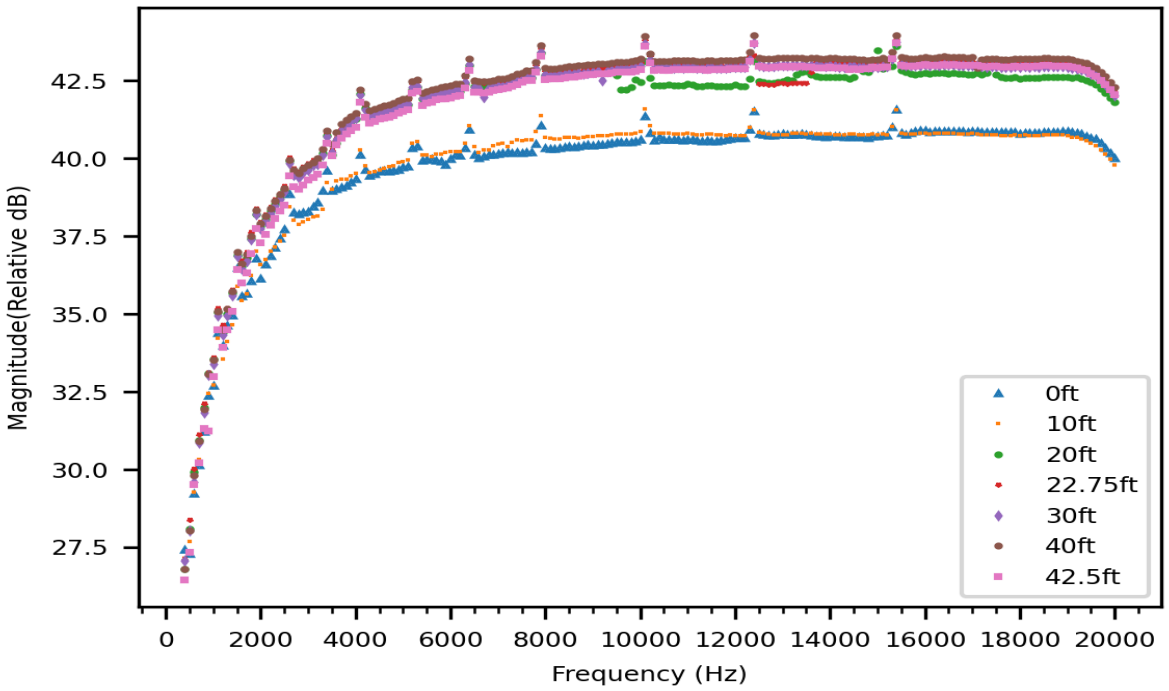

(a) Victaulic 75 Flexible Coupling

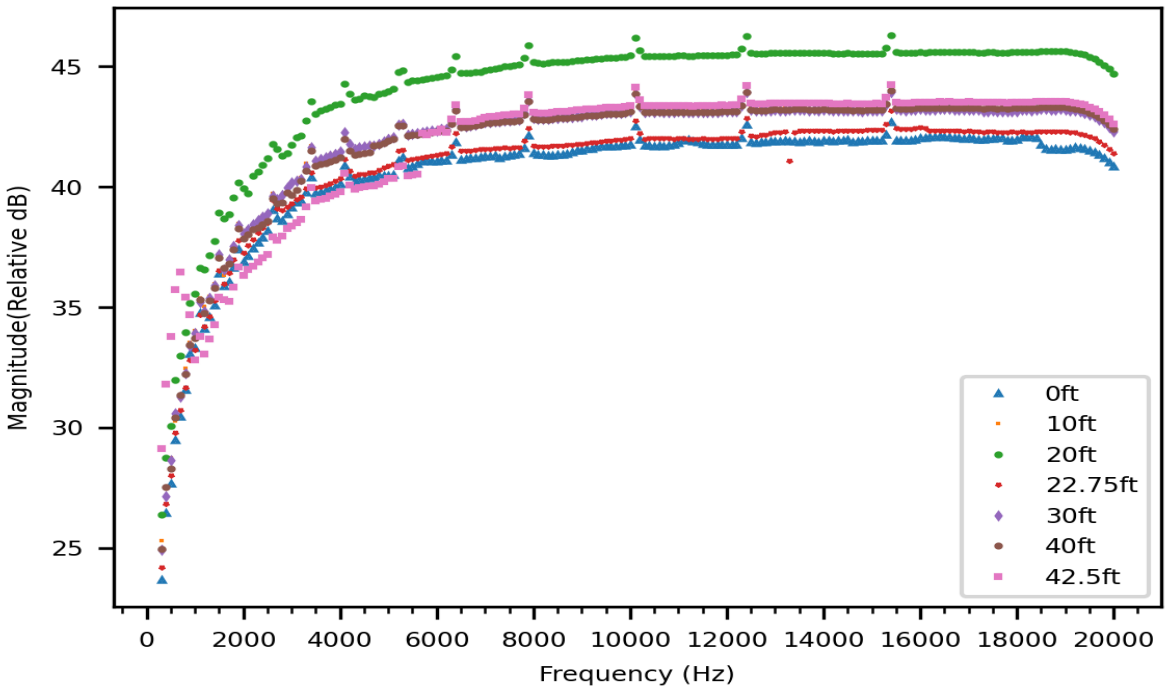

(b) Victaulic 005 Rigid Coupling

Figure 4.26: Received magnitudes for different frequencies with flexible and rigid couplings, at various distances

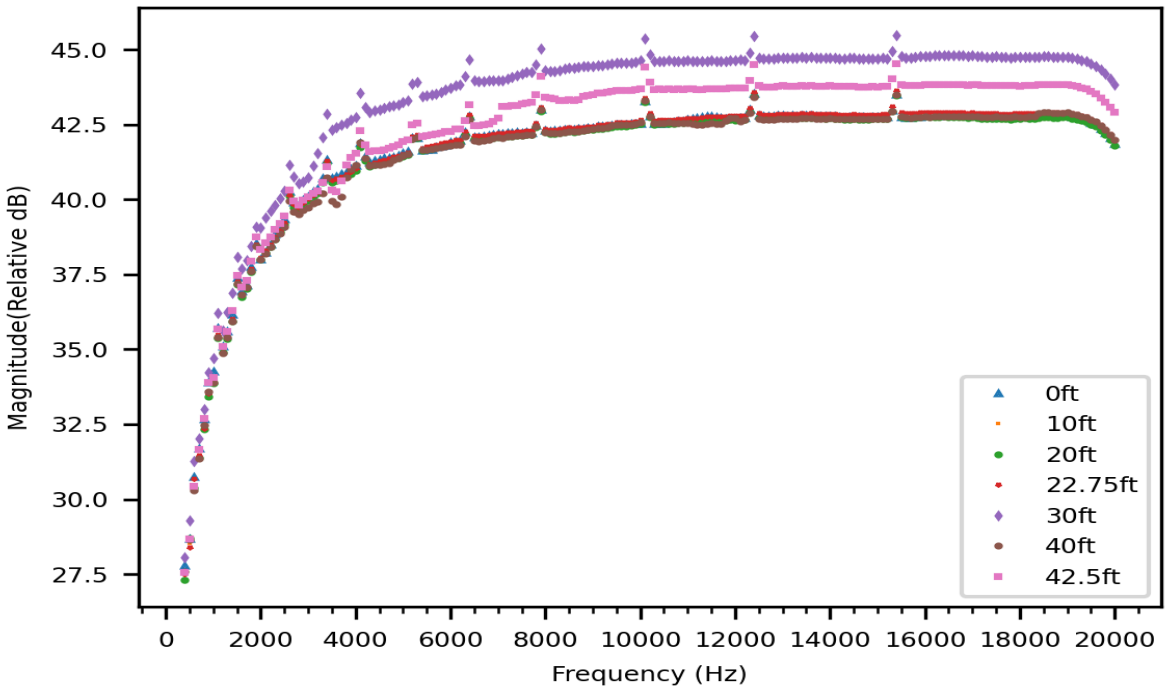

(c) Flexible PVC Coupling

Figure 4.26 (cont.)

Comparison across all couplings for a given distance Figure 4.27 shows that at a given distance, Victaulic 75 flexible couplings do slightly reduce the magnitude of the frequency signal overall. More precisely, at distances of 10ft, 20ft, and 30ft, the signal amplitude averages across all frequencies are smallest with the Victaulic 75. At 40ft, the flexible PVC coupling outperforms the Victaulic 75, but when the signals reach 42.5ft at the end of the pipe run, the Victaulic 75 again emerges as the winner in terms of dampening the magnitude. As expected, the Victualic 005 rigid coupling provides the least attenuation effect on the signals on average.

Unfortunately, the Victaulic 75's slight decrease in magnitude is not substantial enough to be a practical defense against the pipe attack, especially since we do not see a steady attenuation as the distance increases.

4.12.4 Gaps along the pipe surface

If signals are traveling primarily through the pipe surface, then the signals might have difficulty in moving past discontinuities in the surface that break the flow of the vibrations as they pass from the black steel surface to another material. We tested this hypothesis in the outdoor laboratory by

placing rubber washers between the pipe segments. More precisely, we flush mounted Everbilt 1-1/2" Sink Drain Pipe Flanged Rubber Washers, shown in Figure 4.25d, on the pipe ends before connecting the pipes with a coupling as in Figure 4.24. We used the washers with the flexible PVC coupling, Victaulic 005 rigid coupling and Victaulic 75 flexible coupling from Figure 4.25.

Figure 4.28 shows the results, as measured at distances of 10-40 feet. We can also see the signal magnitudes with and without washers for all coupling types in Figures 4.27a–4.27f, at distances of 10ft, 20ft, 30ft, 40ft and 42.5ft respectively.

Even though the washers provide a physical boundary between the metal parts, our results show that the washers do not absorb the vibrations. If anything, we see a small increase in signal strength when washers are added. On average across all signals and for most distances, the worst performing coupling and washer pair, i.e., the highest received signal magnitudes, is the Victaulic 005 rigid coupling with washer. The Victaulic 75 flexible coupling performs best in reducing signal strength overall, but this advantage decreases when the washer is added to the setup. We hypothesize that this may be because the washers conduct vibrations better than the small air gap that would otherwise be there. These results show that washers are not a viable defense.

4.12.5 Ambient Noise

We tested the hypothesis that ambient noise might reduce the effectiveness of transmissions, by playing white noise at a high volume on a speaker in close proximity to the transmitter in the Old Commercial building, and evaluating the quality of the signal received at the far end of the pipe run. We found that the white noise did not significantly obfuscate or hamper the signal. We also compared readings in a workshop where multiple machines were being run (drills, saws, mills, etc.) and school children were building with Legos. Neither noisy children nor loud white noise played next to the pipe noticeably impaired signal transmission. Far from constituting a defense, this suggests that the pipe attack may also be effective in noisy environments such as planes, trains, and factories.

4.12.6 Wider pipes

Among all the locations and pipes tested, the wider 4-6" pipes used for the standpipes in the New Commercial building showed by far the weakest performance in terms of satisfying the bandwidth condition, maintaining signal strength, and ambient sound leakage. Since the pipe attack is less effective in wider sections of pipe, the inclusion of wider sections of pipe at periodic intervals might serve as an effective defense. This could be implemented as a short balloon-shaped length of pipe

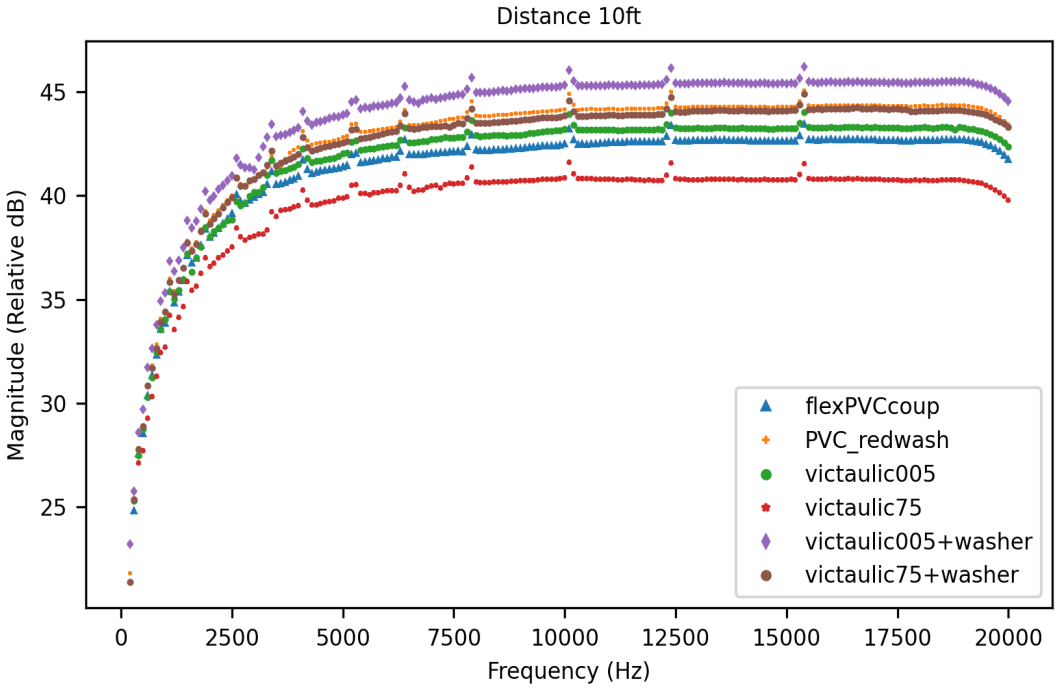

(a) Signal Magnitudes at 10ft, All Couplings

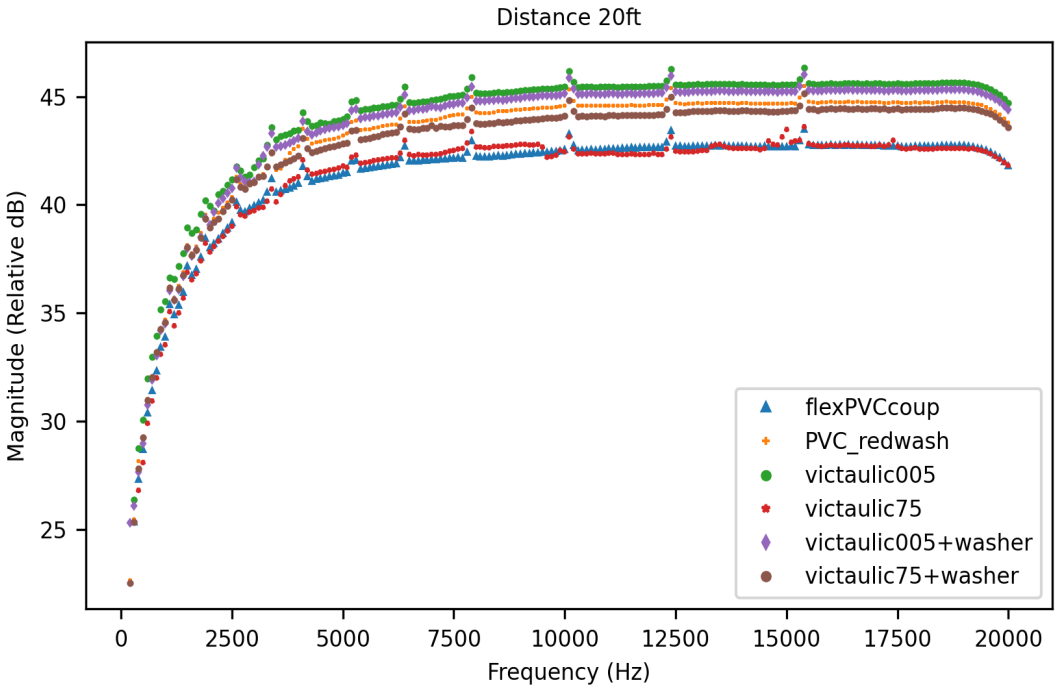

(b) Signal Magnitudes at 20ft, All Couplings

Figure 4.27: Comparative Effect on Magnitude of Different Couplings, for Transmissions of 10-42.5 Feet

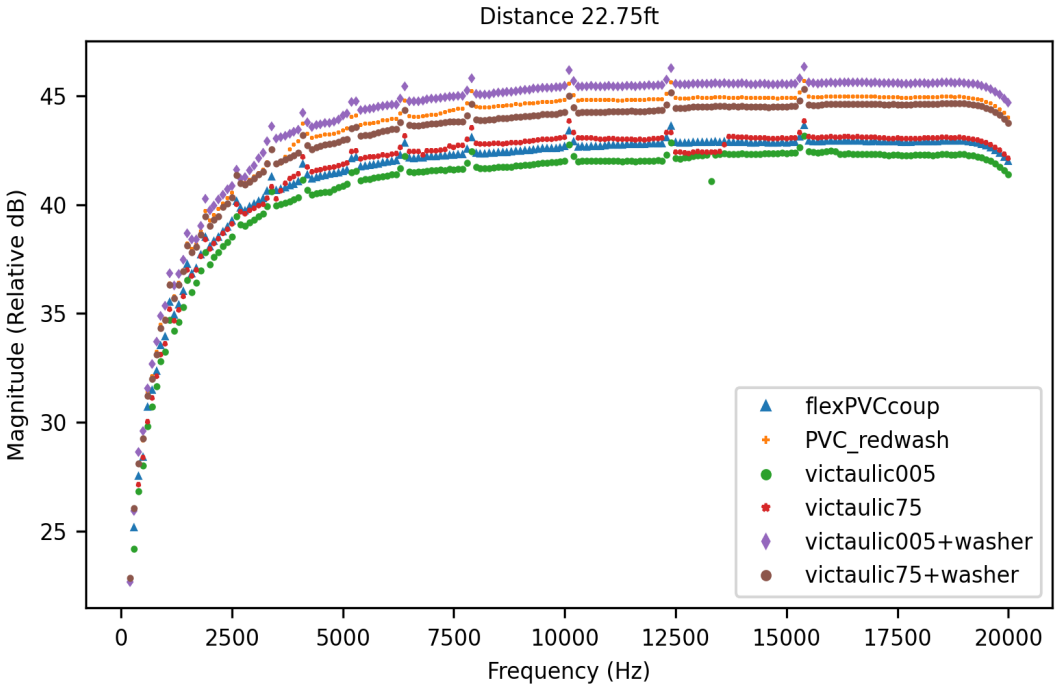

(c) Signal Magnitudes at 22.75ft, All Couplings

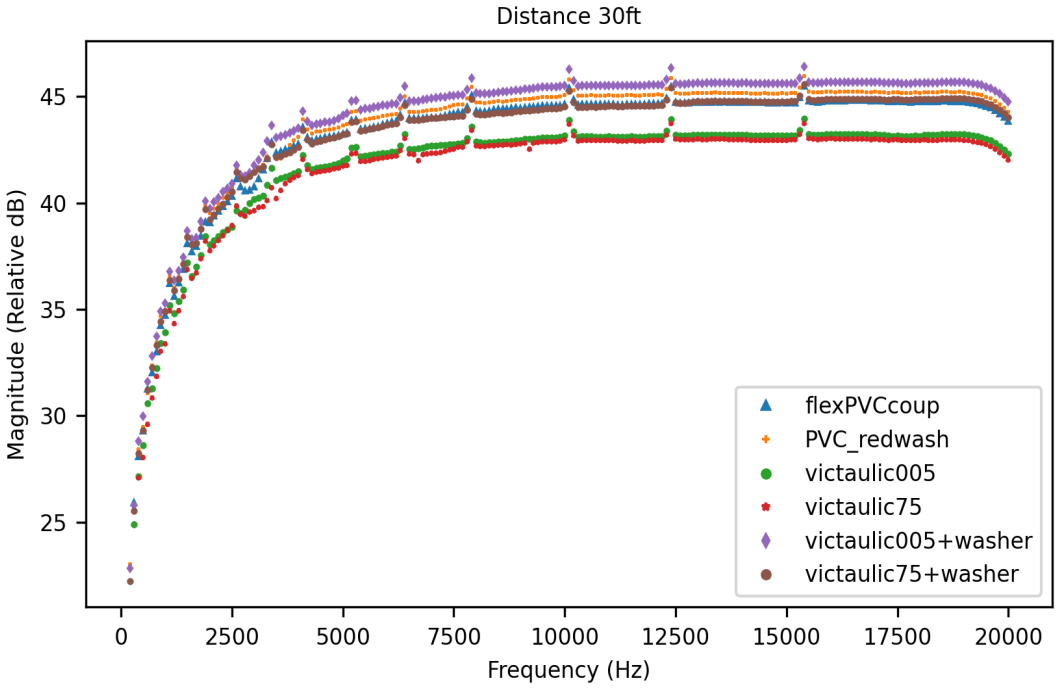

(d) Signal Magnitudes at 30ft, All Couplings

Figure 4.27 (cont.)

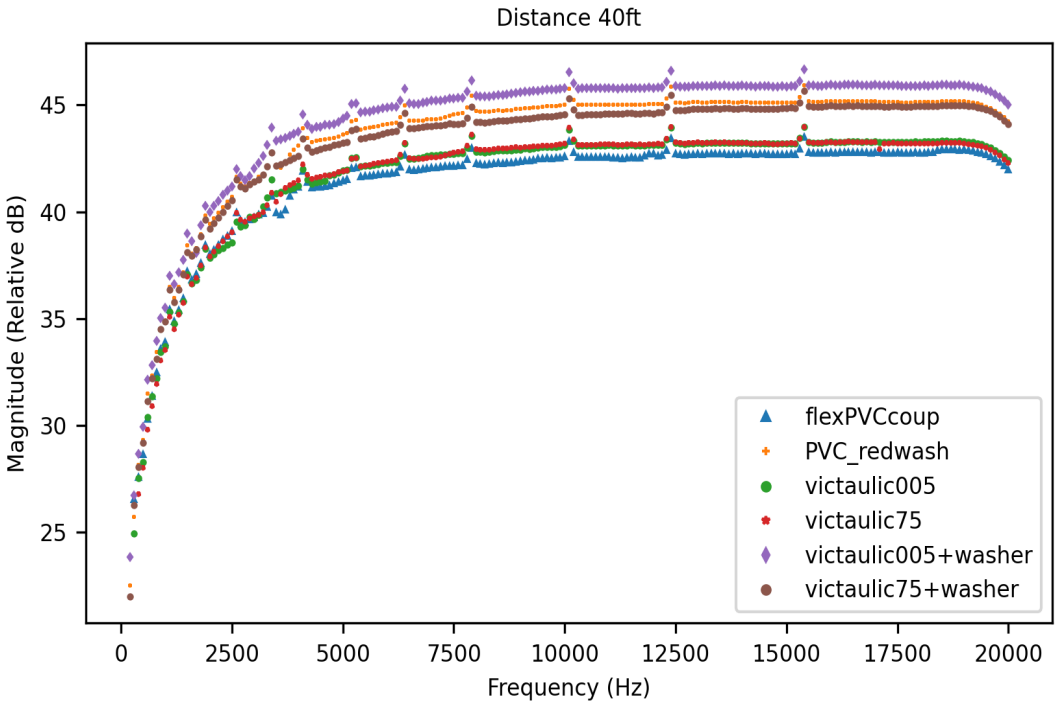

(e) Signal Magnitudes at 40ft, All Couplings

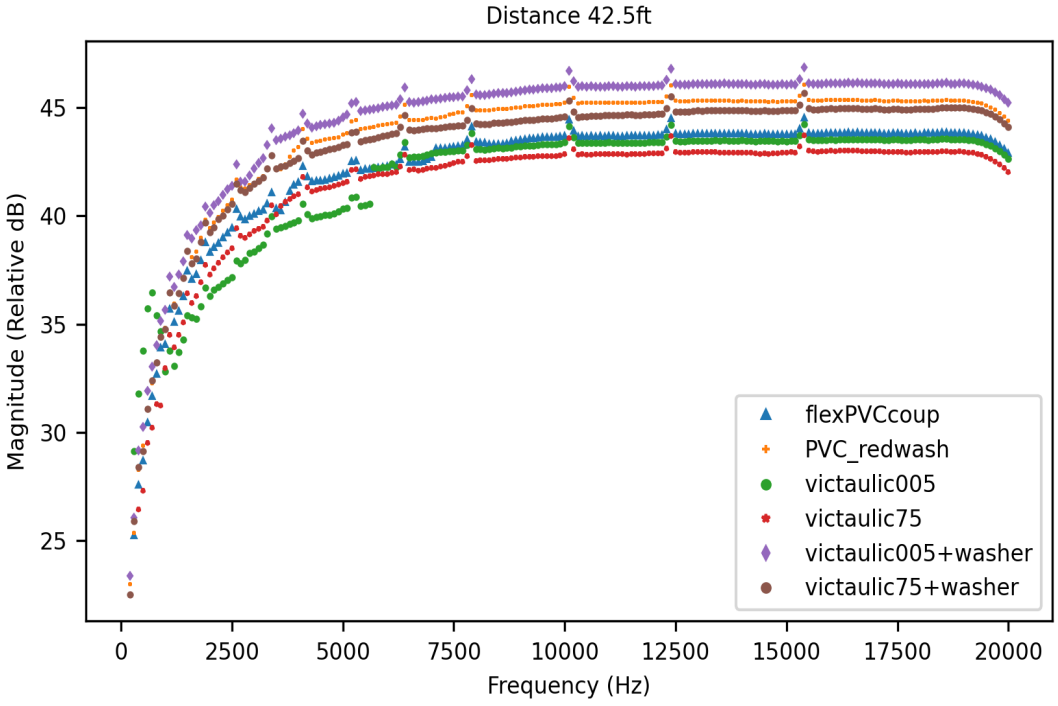

(f) Signal Magnitudes at 42.5ft, All Couplings

Figure 4.27 (cont.)

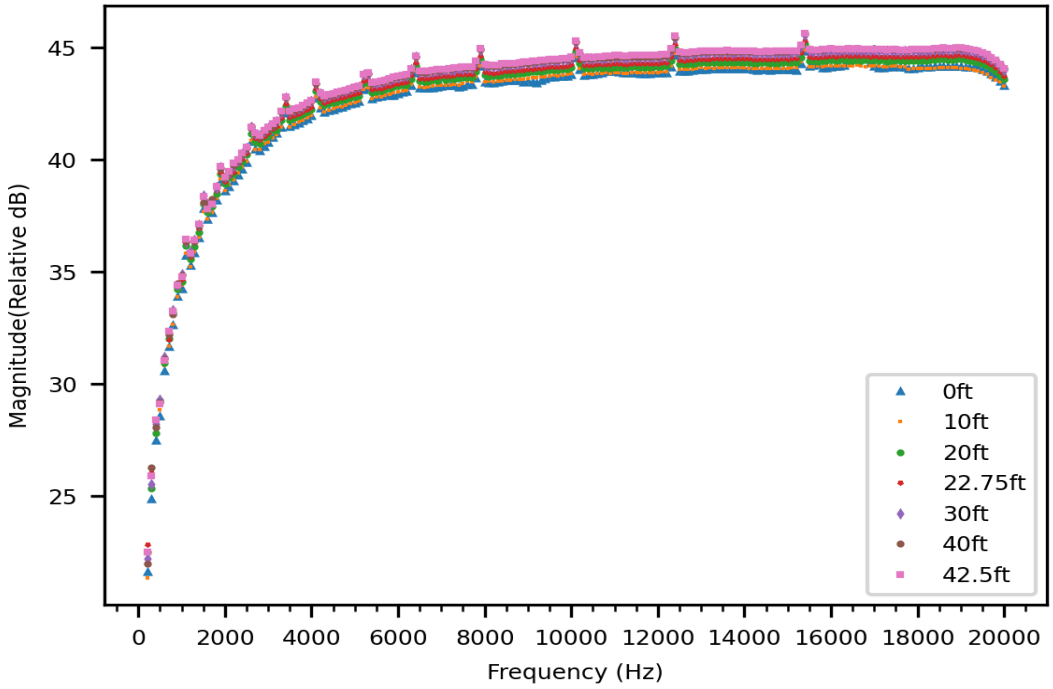

(a) Victaulic 75 Flexible Coupling with Washer

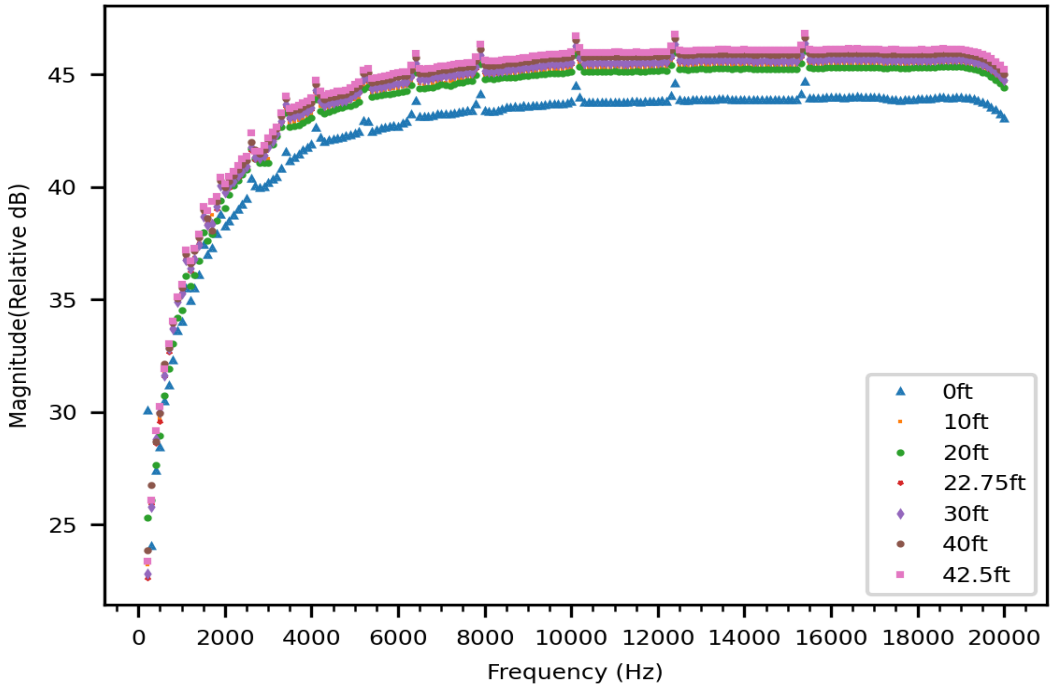

(b) Victaulic 005 Rigid Coupling with Washer

Figure 4.28: Effect on Signal Magnitude of Washers Paired with Black Steel Pipe Couplings

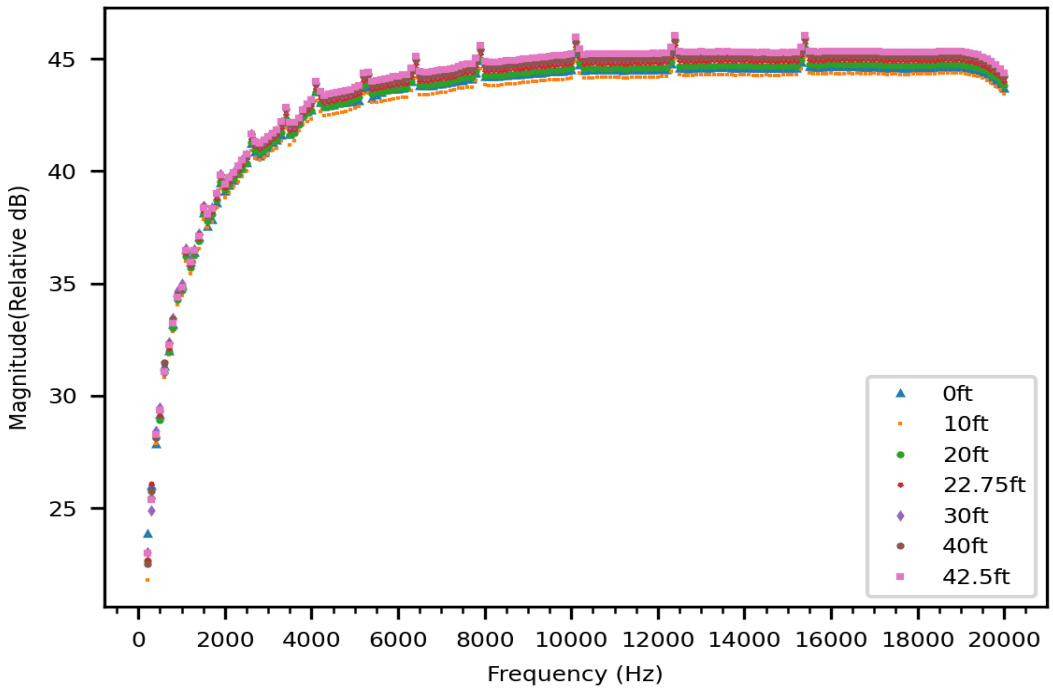

(c) Flexible PVC Coupling with Washer

Figure 4.28 (cont.)

or simply a diameter increasing adaptor in the middle of pipe runs, above room boundaries. We have not tested this defense.

The more obvious option of moving to wider pipes in general would not be a practical defense because of its impact on building construction. First, space is often at a premium along sprinkler pipe runs, with often less than 1” clearance between a suspended ceiling and the pipes above it. Second, wider steel pipes are much more expensive and weigh much more than narrower ones, so that they take longer to cut, are harder to maneuver into place, and are slower to install, all of which also drive up building construction costs. Third, water-filled pipes are already very heavy, and changing from a typical 1” branch line to a 4” diameter branch line would increase the pipe volume by a factor of 8. The 4” pipe would require much sturdier hanging hardware and increase the building dead load, which would also drive up construction costs.

4.12.7 Signal obfuscation

The best defense that we have identified is for defenders to inject noise or other signals directly into the pipe, to obfuscate an attacker’s signal. This would increase the cost of a successful attack

by making the signal harder to extract from the noise introduced on the pipe.

However, attaching defensive audio transmitting hardware would not be able to conceal the original signal sent by a resourceful and motivated attacker. Instead, this defense is likely to result in an arms race between highly motivated attackers and defenders of sensitive locations, such as embassies.

Audio researchers have worked hard to detect, distinguish, locate, and separate different sources of sound. For example, using methods such as described in [144], an attacker can analyze the received audio from a single microphone to distinguish the presence and location of an additional sound source (obfuscating signal) and eliminate it from the recording. Further, subtle fabrication imperfections arising during the manufacturing process could help in differentiating between signals from the attacker's and defender's devices [145], even if the devices have the same vendor, make and model. A motivated attacker with enough resources and time could still perform source identification and separation of acoustic vibrations to counter the effects of such obfuscation methods. Defensive sound injection would also add to construction and maintenance costs and might annoy occupants.

Another means of signal obfuscation is to add noise to pipes by moving the substances within them. For example, many buildings already contain water recirculating loops so that occupants on upper floors do not have to wait a long time for hot water to reach them, after turning on a faucet. The sound of moving water would mask subtle signals, while the sudden cessation of water movement would expose louder signals if the transmitter did not automatically adjust to the change in background noise. The air within dry sprinkler systems could be moved in the same way.

While easy to implement using existing technology, recirculation has several weak points as a defense. The constant sound of moving water or air can greatly irritate occupants. Moving water tends to wear pipes and damage imperfect ones, e.g., causing pinpoint leaks that can cause major damage under ordinary household water pressures. Further, water or air recirculating pumps are not currently used in fire sprinkler systems, and would need to be approved and possibly redesigned for that type of pipe system; in addition, the system's sprinkler head water pressures would have to be recalculated to ensure that the revised system still satisfies the building code. The pipe attack might still be possible using abandoned pipes, which are present in all old buildings, or using other types of metal structures that we have not evaluated, such as metal conduit, the building's steel skeleton, or the trays used to support wiring above hallways. Finally, recirculation would raise the cost of a successful attack, but as with computer-driven noise injection, it offers no theoretical guarantees of effectiveness and is likely to set off an arms race in high-stakes environments such as embassies.

4.12.8 Sound cancellation

A defender could install sound cancellation devices along the pipes as retrofitted defense hardware

that listens to the signal on a pipe and counters it with cancelling signals in real time. Although this could theoretically work as a defense against the pipe attack, there are technological and practical challenges in achieving such a design.

Today's noise-cancelling headphones are expensive and do not completely cancel all their noise. Their hardware must react at the speed of sound in air, which is 331.29 meters per second for dry air at 0 degrees Celsius. Sound travelling as vibrations on a steel pipe surface would be as fast as 3000 meters per second, or possibly even higher depending on the composition of the steel (our measured speed for one steel pipe run was 1466 meters per second). The need to react so quickly would pose an extra challenge for real-time response. The price of the resulting system would be so high that it would only be practical for very high-stakes environments.

4.12.9 Bug Sweeping

Today's bug-sweepers generally rely on detecting RF signals from a bug, recognizing its anomalous thermal image, or detecting the presence of semiconductors.

Many bug-sweepers look for RF signals, but this technique will not detect the pipe attack itself, because the attack does not rely on RF. If an attacker chooses to transfer data to a pipe attack transmitter using RF signals, then an RF bug sweep could detect that capability if the transmitter is not powered off at the time of the bug sweep. However, if the transmitter is specially designed to passively watch for RF signals without emitting any itself, then the transmitter itself would not be detected; and it might be hard to distinguish between an ordinary RF-enabled smart light bulb/plug and an attack-enabled bulb/plug that also sends data to the transmitter. The same considerations hold for pipe attack receivers.

To avoid detection by thermal imaging bug-sweepers, the transmitter/receiver housing (e.g., faux pipe stub) can be wrapped in mylar or the equivalent to prevent heat radiation from batteries, or direct wired to one of the many power supplies already present above the ceiling. Alternatively, the transmitter/receiver can be passive, i.e., not rely on a power supply at all; such transmitters were made and used during the 1950s (see https://www.cryptomuseum.com/covert/bugs/thing/index.htm).

Non-linear junction detectors (NLJDs) detect the presence of semiconductors even in devices that are powered off, by detecting harmonic signatures coming off of electronics that contain semiconductor junctions (diodes, transistors, circuit board connections). To fool NLJD bug sweepers, the standard countermeasure is to combine the device with an isolator that will absorb any energy that would otherwise have been reflected back to the NLJD (see https://en.wikipedia.org/wiki/Nonlinear_junction_detector#Countermeasures). We expect that this countermeasure would also work for pipe attack transmitters and receivers.

4.13 DETECTING AN ONGOING PIPE ATTACK

Given a target false positive and false negative rate, a defender can use signal processing techniques to decide whether an attacker's signal is on the pipe, or just noise. A defender can install a receiver device like ours on the pipe to listen and record the historical noise in the pipe when an attack is not underway, and use that data to build a model of normal pipe noise. Then the model can be compared to current readings to detect whether the differences in current and past pipe noise bandwidth and amplitude exceed a predefined acceptable threshold. If such an anomaly is detected, an alarm can be raised to notify authorities for further investigation and detection of the potential attack location on the pipe.

Any anomaly-based detection method will suffer from false alarms, missed actual attacks, or both. In the case of the pipe attack, false alarms might be caused by an electrician scraping nearby pipes while replacing a light fixture, remodeling down the hall that vibrates pipes, a New Year's Eve party that blasts music, the annual tests of the sprinkler system near the risers, or occasional ambient sounds that resonate with the pipes. The threshold for anomaly detection can be tuned to attempt to balance the significant annoyance and inconvenience caused by false alarms with the severity of the threat of exfiltration attempts.

A huge body of prior research work on anomaly-based intrusion detection offers methods to detect deviations from models of historical behavior (see, e.g., [146, 147] and the decades of subsequent research that built on their ideas). Similar methods can be applied to detect anomalies in noise patterns on pipes, as long as historical data of normal behavior is available and a model can be trained for detecting deviations from it.

However, an effective anomaly detection model must be trained to inspect and detect variations across all possible modulation patterns that might hold data. While our focus in this chapter has been on frequency modulation, other modulation approaches are also possible, as described in Section 4.10.7. A model that considers only frequency modulation might not detect any anomaly when the data is hidden in other domains, such as the timing between a pair of normal-seeming frequency signals. The vast number of methods in the communication field to modulate data and the variety of steganography methods to hide that data [148] magnify the challenges in building a model to detect the attack. Furthermore, if the attacker has the technical know-how to keep the signal magnitudes very close to those of the ambient pipe noise, then there is no theoretical guarantee that a defender will be able to recognize that a pipe attack is underway. Techniques to transmit data using signal masking close to the ambient noise ceiling are well known in the field of audio steganography [148]. At best, the attacker and defender are in an arms race.

Another weak point in the use of detection as a defensive technique is that by the time the pipe attack is detected, data is already being exfiltrated. By the time the transmitter is located and

disabled, even more data will have been exfiltrated. To reduce this loss in high-stakes environments, crossing the anomaly detection threshold could automatically activate a standby transmitter that would inject large amounts of noise, in an attempt to drown out the ongoing data transmission. Even that measure offers no theoretical guarantees of successful defense, however, and the additional noise will also make it harder to localize the attacker's transmitter.

A final weak point is that the model of normal behavior must be built from data collected when no attack is underway. Further, if the model needs to be updated over time to match shifts in normal pipe ambient noise, then that opens an opportunity for the attacker to include transmissions of gradually increasing magnitude in the evolving model.

4.14 LOCALIZING THE PIPE ATTACK TRANSMITTER

If a defender believes that a pipe attack is a credible threat, one defensive measure is to visually inspect every inch of the pipe runs until all unauthorized devices have been found and removed. With the typical suspended ceilings and the ease of camouflaging a transmitter, this will be a very slow process that must be repeated regularly. Making it worse, most buildings do not have blueprints of the exact sprinkler runs, so in a typical commercial environment, the defenders will have to pop up many irrelevant ceiling panels to trace the exact path of the pipes. Further, defenders often will not have good visual access in the crowded areas above suspended ceilings, let alone above finished ceilings. Hence manual localization methods are at best unpleasant and at worst impractical in environments with suspended or finished ceilings. With open ceilings, often the pipes are very high above the floor, with office furniture or industrial equipment beneath them. This makes it very difficult to run tall ladders underneath the pipes all along their runs. Finally, vertical pipes such as copper water supply lines that run between floors pose an additional challenge for inspection. On the other hand, regular inspections offer the possibility of preventing a pipe attack, as opposed to detecting the attack once exfiltration is already taking place.

Once a pipe attack transmission is underway, a defender can expedite the search for an attacker's transmitter by installing two or more receivers along the pipe run and using the difference in arrival time of the attacker's signal at the receivers to determine in which direction the transmitter lies along the pipe run. In the following sections, we propose how to do this using two receivers, and estimate the search time required in real building sprinkler pipe systems. We also present a method for localization using more than two receivers, examine when it could be employed, and estimate the search time it would require.

4.14.1 Localization Using Two Defensive Receivers

In this section, we use two microphones as receivers to find the location of the attacker's transmitter along a pipe run. We tested this method using our outdoor laboratory with 42.5' of black steel pipes connected by Victaulic 005 rigid couplings, illustrated in Figure 4.24.

For this experiment, we assume the attacker may use any signal in the supporting bandwidth, and so we evaluate localization using linear chirp signals (continuous from 20KHz down to 1Hz) of duration 500 milliseconds. We use the same transmitter and receiver as in Figure 4.9, i.e., the Adafruit bone conductor transducer as a transmitter and two TraderPlus piezo contact microphone pickups as the localization receiver devices for the defender.

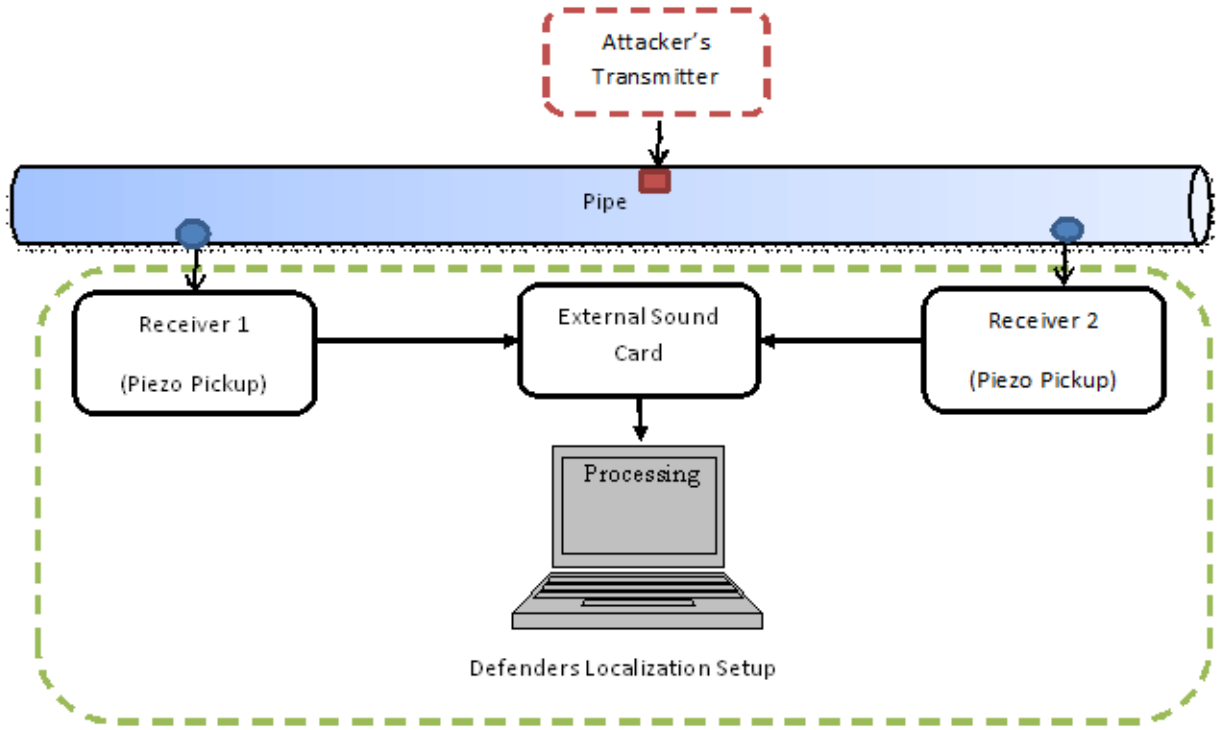

Figure 4.29: Localization Setup Using Two Receivers

We record the signal received at each receiver, and use the time difference of arrival (TDoA) of the signals to determine which receiver is closer to the attacker's transmitter. The TDoA calculation for fast travelling audio signals along a pipe is a time sensitive process, and the receivers' readings must be time synchronized for us to compare them. As shown in Figure 4.29, to provide this synchronization, we attach the receivers to the StarTech.com 7.1 USB external sound card, which takes two microphone channel inputs. We connect the external sound card to the laptop through a single USB port. We record and process the data in the laptop using Python's SciPy signal packages. The single USB connection for recording and two separate recording threads to support the receivers

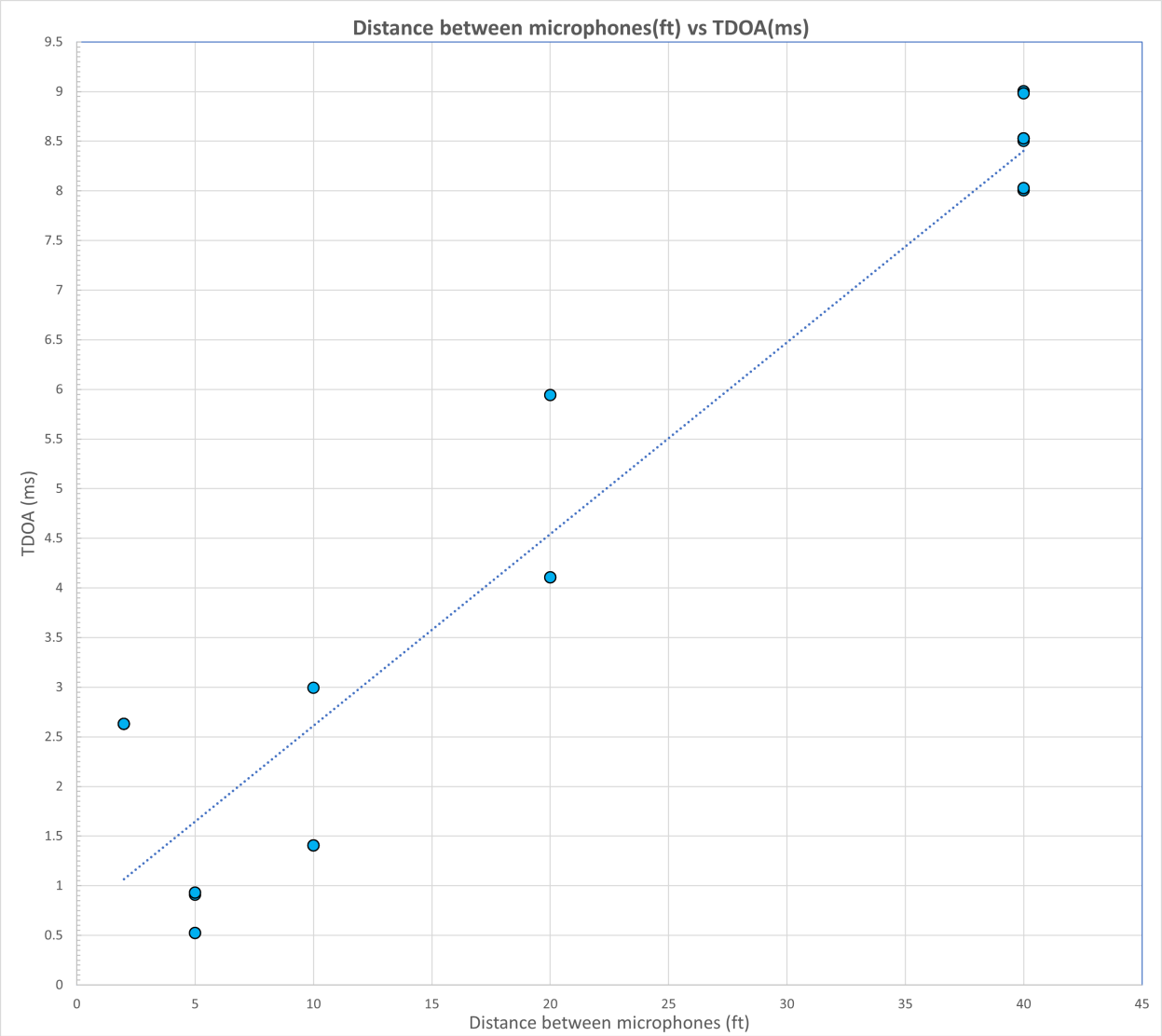

Figure 4.30: TDoA for Two Receivers at Various Distances

that start in parallel ensure that the recording starts at the same time and is synchronized.

After affixing the receivers to the pipe, we take 5.0 seconds of recordings and then find the lag between the two time series synchronized recordings, using signal cross correlation. For cross correlation we use Pearson Correlation Coefficients with mean suppression. Based on the difference in the lag values after signals are correlated, we find the time difference of arrival at the two receivers, which tells us which one is closer to the source of the sound.

If the attacker is using magnitude or phase based modulation instead of the frequency modulation that we employ, similar correlations across the magnitude or phase domain could be used to match signals across the receivers for accurate comparison and localization. Analysis in all generally used modulation domains would strengthen the defender against an ambitious attacker who is skilled in

hiding the data.

Our implementation is able to determine which receiver is closer to the transmitter as long as the transmitters are at least 2 feet apart from each other. At closer distances, the TDoA is so small as to be error-prone with our equipment.

This method works for localization if the attacker's transmitter is sending signals that change over time, i.e., not just continuous tones, while the defender's receivers are listening. Otherwise, the correlation based methods for finding TDoA will not work properly. Of course, in a real attack scenario, an attacker would prefer not to send continuous long tones, as the attacker would want to make good use of channel capacity and send data quickly.

We collected readings for TDoA on the 42.5ft pipe run with the receivers at 2ft, 5ft, 10ft, 20ft and 40ft separation distances from each other. We took five readings at each distance, and Figure 4.30 illustrates how the TDoA changes with the distance between the microphones. Many of the readings are highly consistent, so they overlap in the graph and look like a single data point, rather than appearing as five separate data points at each distance. The dotted line shows the roughly linear relationship between TDoA and the distance between the receivers for this pipe topology. The equation of the dotted line fits the following formula:

$$\text{TDoA} = 0.1931(\Delta D) + 0.6798, \tag{4.9}$$

where ΔD is the distance along the pipe run between the two receivers. Our measurements show an average speed of signal along the pipe of 1465.805 meters per second (4809.071 ft/sec), about five times faster than the 331.29 meters per second for dry air at 0 degrees Celsius.

Contrary to our expectations, the TDoA was consistently larger at 2 feet than at 5 feet. We do not know whether this was due to peculiarities of that pipe run, or other factors. Nonetheless, the TDoA calculation always correctly identified the direction of the signal with a 2' receiver separation, so we recommend that minimum separation distance in practice.

4.14.2 Classic Binary Search for Localization

Our first localization algorithm is inspired by the binary search algorithms normally used to find an element in a sorted array without duplicates. In classic binary search, we start by considering the entire array, from end point A to end point B. We compare the searched-for value to the value stored at the array midpoint. If they match, we are done. Otherwise, the search space end points move to the first half of the array if the middle element is greater than the value being searched for, else the second half of the array otherwise. Thus the search progresses by reducing the search space every iteration by half until it finds the element in $O(\log n)$ time worst case, for an array with n

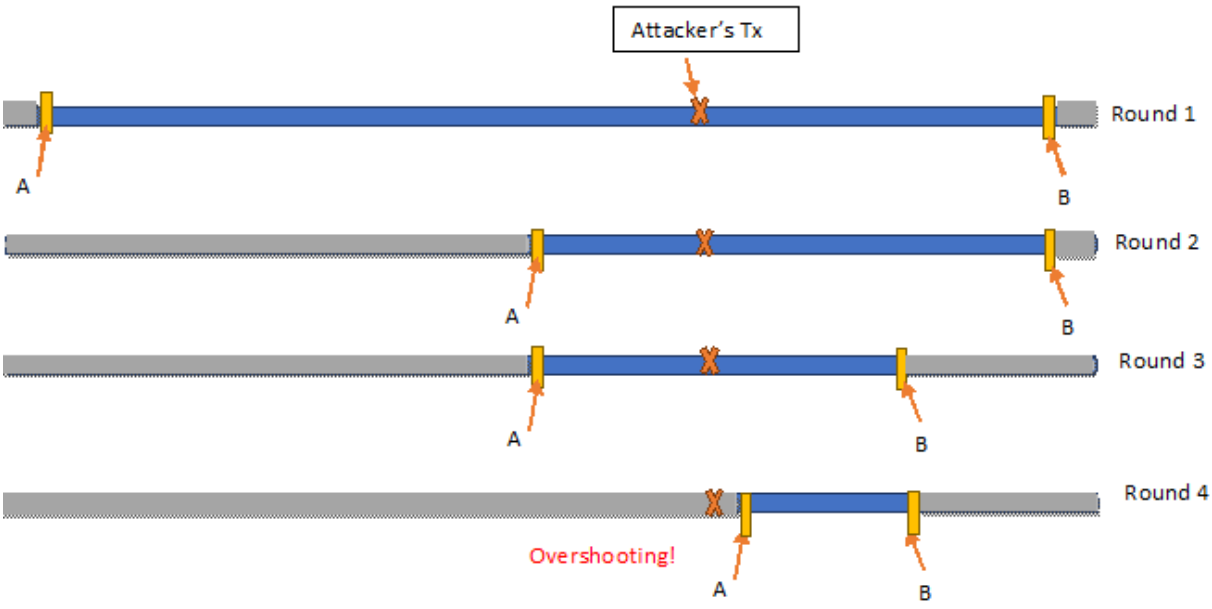

Figure 4.31: Example of Midpoint Overshooting When Traditional Binary Search is Used for Attack Localization Along Twisting Real-world Pipes

elements.

Binary search uses the notion of a midpoint. As our concept of the midpoint of a tree topology, in this section it suffices to define a **midpoint** as any point along the pipe that divides the search space, defined as the total pipe length, in half. We formalize this concept in a later section.

If we place two receivers at points A and B respectively in a pipe system with a tree topology, there is no guarantee that the attacker's transmitter lies between A and B, i.e., lies on any path through the pipe between A and B, even if A and B are initially placed at the far ends of pipe runs. In this case, classic binary search will stop when the TDoA is zero, i.e., when the two receivers are side by side or are equidistant from the intersection that leads to the transmitter. In the latter case, the search needs to be restarted with the two transmitters relocated to the ends of the pipe run that passes through the intersection halfway between A and B. Thus in a tree topology, we could start the search with A and B at the ends of the feeder main, use that search to identify the correct cross main, restart the search on that cross main, use its results to identify the correct branch line, then restart the search on that branch line. This iterative method is relatively slow, requires physical access to the ends of many pipe runs, and requires a method of time synchronization for receivers that are far apart (e.g., power line synchronization [149]).

We also face the danger of misidentifying and overshooting the midpoint. While the ends of pipe runs can usually be recognized visually once they are found, it is much harder to recognize the midpoint between two end points, given all the twists and turns that real-world pipes take to avoid

heating and cooling ducts, wiring conduits, and other obstacles along their route. Measurement discrepancies and difficulty of access can cause the defender to locate and advance the midpoint wrongly and overshoot the actual midpoints. If the attacker's device is near the actual overshot midpoint and the defender does not notice it by looking the "wrong way" down the pipe, this overshooting will eventually require backtracking and a redo of a portion of the search.

Figure 4.31 illustrates the overshooting problem with a straight pipe run. The third iteration of the search considers the two endpoints labeled 'A, round 3' and 'B, round 3'. Due to unseen twists and turns in the pipe or obstructions that make access difficult (not shown in the figure), the defender incorrectly chooses a midpoint for round 3, and round 4 starts with the endpoints labeled 'A, round 4' and 'B, round 4'. However, the process has overshot the correct midpoints, and so the transmitter does not lie between the two new endpoints. Subsequent rounds will move endpoint B closer and closer to the point labeled 'A, round 4', eventually converging there with a zero TDoA. Once the defender observes that there is in fact no transmitter at the point of convergence and no pipe intersection there to offer an alternative explanation, the defender will realize that the round 3 process overshot when it picked the point 'A, round 4' as the new midpoint. Then the search must backtrack and restart with 'A, round 4' and 'A, round 3' as the two new endpoints. Given the non-linearity of real-world pipe layouts and the prevalence of obstructions below them, the very real possibility of overshooting means an inefficient search with no guaranteed convergence within a certain amount of time for the defender.

Given all the drawbacks of classic binary search, we need a better search algorithm that converges within a reasonable time regardless of the starting points picked along the pipe runs.

4.14.3 Modified Binary Search for Localization

Instead of placing the defender's receivers at the ends of pipe runs, we can place them a small constant distance apart and move them as a unit during each iteration.

For the defender's convenience of installation and observation using a single ladder, it is best to place the receivers as close together as possible. Our experiments presented earlier showed that a minimum distance of 2 feet between the two receivers was required to correctly identify which receiver receives a signal first, so we recommend a 2 foot separation. A 2-foot separation also allows the defender to set up a ladder in a single location for each iteration, pop up adjacent ceiling tiles (their standard modern size is 2' by 2') to attach the receivers, and time-synchronize the receivers by plugging them into a single laptop. Further, with a 2' separation, we can assume that the defender will notice the transmitter if it is in between the two receivers, even if the transmitter is well camouflaged.

More generally, however, the transmitter separation can be any constant distance that allows

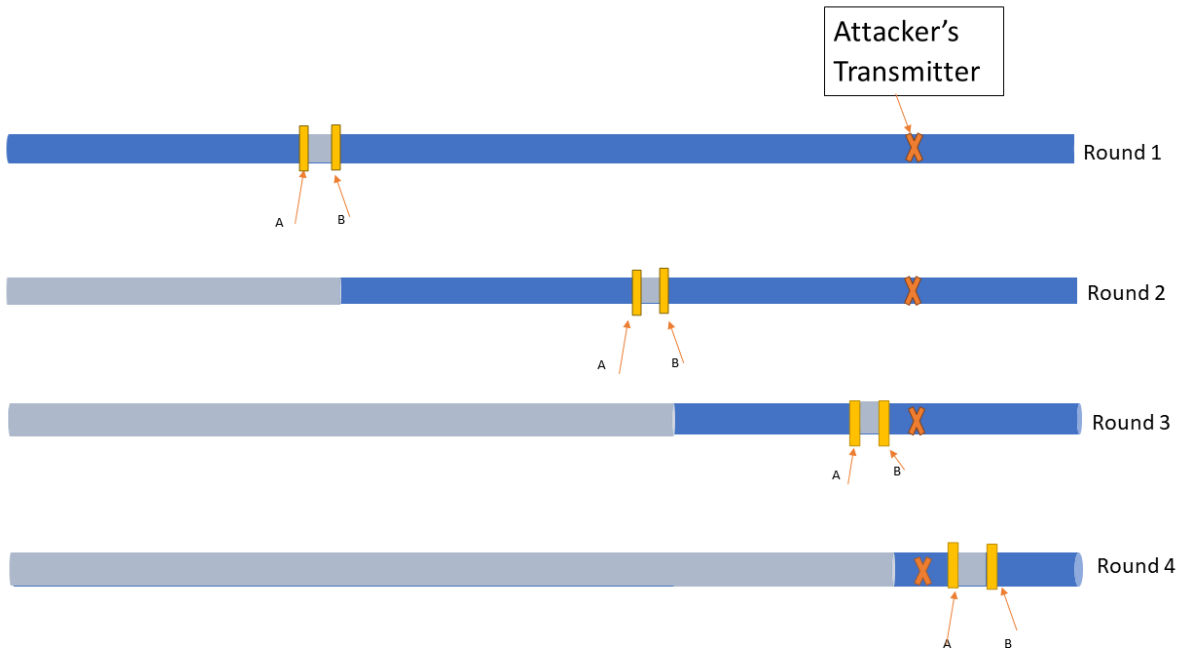

Figure 4.32: Example of the Modified Binary Search Localization Algorithm, with Localization Receivers a Fixed Constant Distance Apart and Repositioned Together

the defender to manually recognize any transmitters between the two receivers, avoid placing the transmitters where they will be separated from each other by a *large fitting*, i.e., an intersection of three or more pipes, and for which the defender's equipment can accurately compute the TDoA.

We assume that the defender only attaches the receivers to plain pipe, not to pipe fittings (i.e., two-, three-, or four-way intersections of pipes). A defender would find it hard to attach a receiver to the complex surface of a real-world pipe fitting. Further, signal reception might be affected by the double layer of material at the joint. The defender should instead use attachment points immediately adjacent to the fitting. As fittings are only a few inches long and are separated by at least short sections of plain pipe, such a point should always exist in real-world pipe systems.

As shown in Figure 4.32 with a straight pipe run, the modified binary search localization algorithm starts with the defender affixing her two receivers the minimum distance apart on a pipe at a starting location in the piping system, without any large fitting between them. A TDoA calculation tells the defender which direction the transmitter lies in, which is to the right in this case. The defender discards all of the search space to the left and moves both the receivers together to the remaining search space on the right, placing the receivers as close as possible to the midpoint of that space. She discards roughly half of the search space at each round of the search, until she sees the attacker's transmitter when she starts to attach her receivers in round 5 (not shown). If the defender had somehow not noticed the transmitter at that moment, then its signal would have arrived at both of

the defender's receivers at the same time, and the TDoA of zero would have told the defender to look around more carefully.

This algorithm has an expected and worst case search time of $O \log(n)$, where n is the total size in linear pipe feet of the search space, e.g., the total length of the sprinkler pipes in the target sprinkler system on the target floor of the building. The base of the logarithm is given by the largest-size fittings in the system, which is at most six for pipes in general and at most four for a sprinkler system.

To formalize this approach, we begin by defining the concept of a tree T that is an abstraction of the pipe system to be searched. Intuitively, the nodes of the tree represent the large pipe fittings and pipe run endpoints. To avoid the use of edge weights, we add enough additional nodes that the distance between two large fittings in T corresponds to the distance between those fittings in the real world.

More formally, let each real-world intersection of $k > 2$ pipes in the pipe system be represented by a unique node, and let I be the set of all such nodes. Further, let each endpoint in the real-world pipe system be represented by a unique node, and let E be the set of all such nodes. Without the possibility of confusion, we use X to refer to both a real-world intersection or endpoint and its representation in T. Then T is the smallest tree such that all members of $I \cup E$ are nodes of T, and nodes X and Y in $I \cup E$ are connected by a path of length d in T iff the real-world locations they represent are distance d apart along the pipe. (This representation will slightly stretch and shrink the real-world distances, according to the distance units chosen.)

We assume that the units of distance used for the edges of T are large enough that the defender's two receivers fit on a single edge (e.g., 2' long), and the distance units are small enough that a defender can visually recognize a transmitter placed in the location corresponding to that edge. In line with that assumption, the algorithm uses an oracle function TxHere(e) that returns TRUE if edge e contains the attacker's transmitter.

We also need to formalize the concept of the midpoint of a tree topology pipe system. Intuitively, a midpoint is a location on the plain pipe (not on a fitting) such that if the pipe is sliced in half at that point, an equal number of linear feet lie on each side of the cut. To formalize this concept, however, we must consider the case where the midpoint would ideally fall right on top of, say, a 3-way intersection of equal-length pipe runs. In that case, we cannot divide the search space in half. The best we can do is to cut the pipe system into two pieces that are roughly 1/3 and 2/3 of the size of the current system, respectively. Similarly, if the exact center of the pipe system falls at a 4-way intersection of equal-length pipes, then in the worst case, the best we can do is to cut the pipe system into two pieces, the smaller of which is roughly $1/d = 1/4$ the size of the original system.

More generally, we need to constrain midpoint selection to ensure that the two new search spaces are as equal in size as possible, even when there is a fitting at the center of the search space that

connects many pipes. A single-edge search space does not require further subdivision, so we define midpoints only for trees with at least two edges. Let size$(T) \geq 2$ be the number of edges in T, and define the degree of an edge $e = (n_1, n_2)$ as degree$(e) = \max(\text{degree}(n_1), \text{degree}(n_2))$. Then e is a **midpoint** of tree T if when we remove e from T, the smaller of the subtrees thus created, T', satisfies the following condition:

$$\text{size}(T') \geq \left\lfloor \frac{\text{size}(T) - 1}{\text{degree}(e)} \right\rfloor \tag{4.10}$$

Algorithm 4.1 formalizes the search for the attacker's transmitter, represented as an edge in T. The algorithm relies on the function FindMidpoint(T) to find the midpoint e of T, and the function FindTDoA(e) to determine the difference in arrival time at the defender's two receivers on edge e of the ongoing transmissions from the attacker's transmitter. The algorithm assumes that an attack is ongoing, the two receivers fit on a single edge, and the defender (the oracle) can recognize whether the attacker's transmitter is on a particular edge. Until that edge is found, the algorithm finds the midpoint of the remaining search space, checks the TDOA at that midpoint, and then repeats the process with the search space confined to whichever side of e was indicated by the test results.

Algorithm 4.1: Modified Binary Search Algorithm for Localization

Input: a tree T containing at least one edge and an attack underway;
Output: e, the edge corresponding to the position of the attacker's transmitter;
repeat
  if $size(T) = 1$ **then**
    return the sole edge in T;
  end
  $(n_1, n_2) \leftarrow e \leftarrow$ FindMidpoint(T);
  Let T_1, T_2 be the subtrees of T that are rooted at n_1 and n_2, respectively, when e is removed from T;
  $TDoA \leftarrow$ FindTDoA(e);
  if *TDoA* < 0 **then**
    $T \leftarrow T_1$;
  end
  if *TDoA* > 0 **then**
    $T \leftarrow T_2$;
  end
  return e;

Figure 4.33 shows an example where the attacker's transmitter lies on a side branch (other branches not shown). In the third round, the defender uses a midpoint just to the right of a 4-way intersection of pipes. The search then moves to the branch line in round 4, at which point the defender picks a midpoint where the attacker's transmitter is visible.

In the real world, defenders will not usually be able to identify and access exact midpoints, because real pipe runs are messy and the nearby ceiling and floor may be littered with obstacles. But the search will still conclude in logarithmic time as long as the defender is within some constant distance, say 10-20', of the true midpoint in the early rounds of the search. Starting at the feeder main, i.e., the largest pipe, then moving on to a narrower cross main, then the branch lines and finally a sprinkler drop is a good heuristic to avoid wasting time.

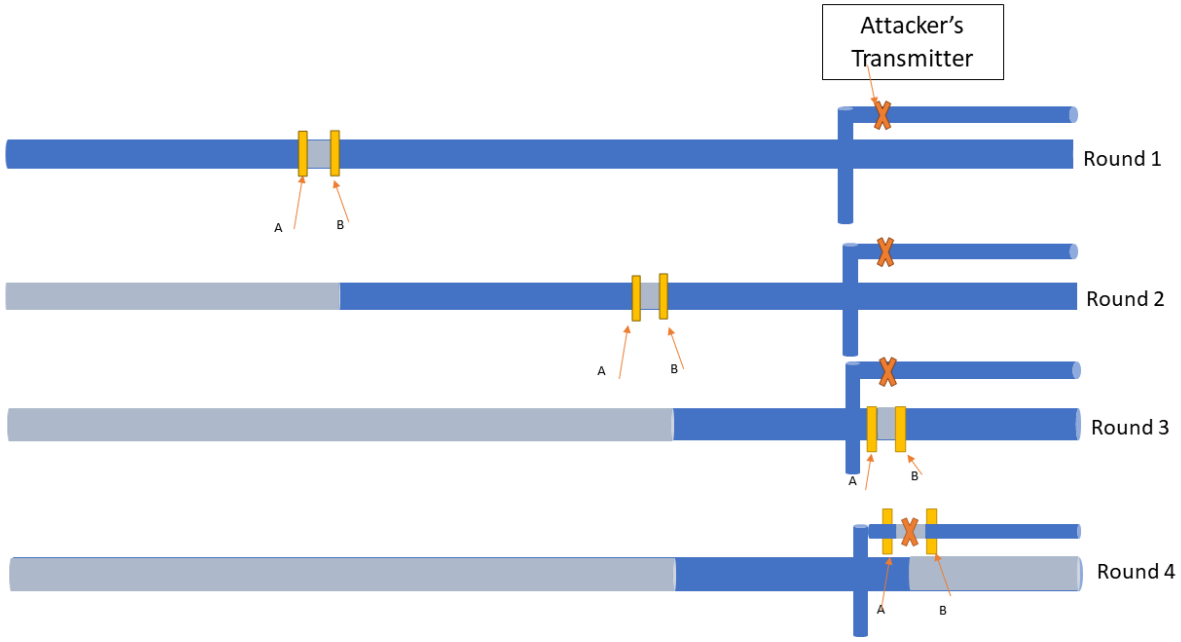

Figure 4.33: Example of the Modified Binary Search Localization Algorithm Identifying the Branch Line Where the Attacker's Transmitter is Located

4.14.4 Localization in Loop Topologies

With grid or loop pipe layouts, the search process becomes more complex. Consider a loop topology, as illustrated in Figure 4.34 without branch lines or the feeder main. We might think that all the defender needs to do to start the search is to visually examine any point on the loop, such as the arbitrary location marked in gray at the top of the figure. If the attacker's transmitter isn't there, then that short section of the loop can be eliminated from the search space, and the defender can then apply Algorithm 4.1 to search the remaining tree structure. However, this does not work, because the attacker's signals will still travel in both directions around the loop. Thus as Figure 4.34 shows, the calls to TDoA(e) in Algorithm 4.1 will still indicate the shortest path from e to the attacker's transmitter, even if that path travels through the edge that the defender has

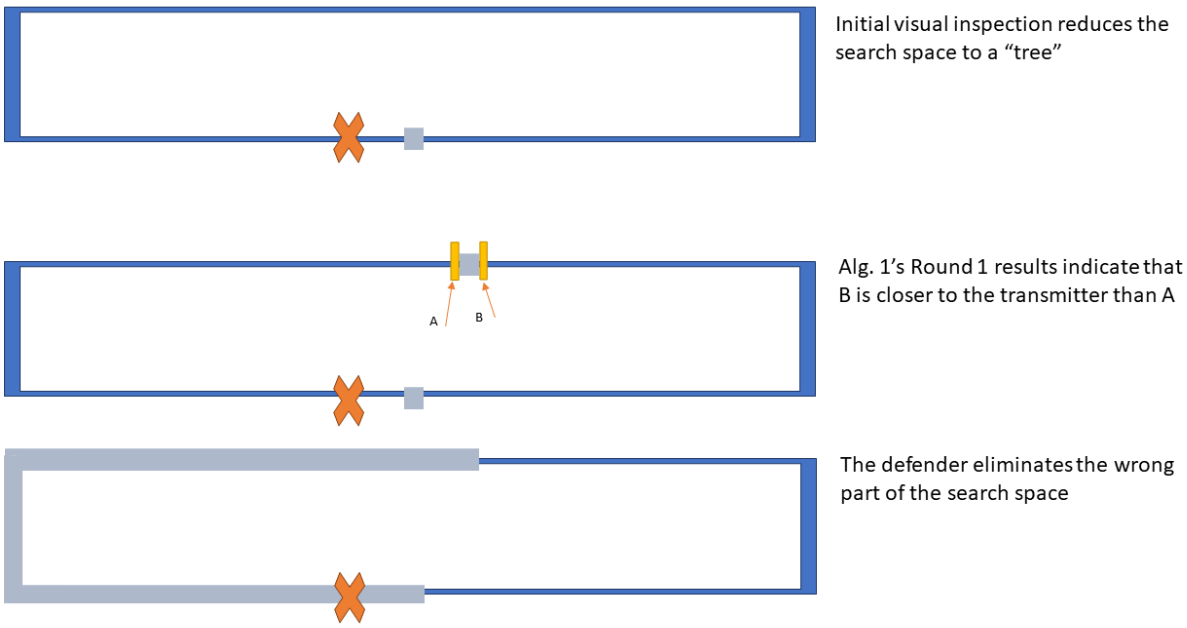

Figure 4.34: Localization in a Loop Topology Is Nontrivial

visually eliminated from the search space. Only a physical cut through the pipe would eliminate the forbidden route through that point. More generally, the defender needs to eliminate at least half of the loop from the search space before she switches to Algorithm 4.1, to avoid the TDoA misinterpretation problem illustrated in Figure 4.34.

Figure 4.35 shows that in a building whose occupants are concerned about a pipe attack, advance identification of a midpoint along the loop can eliminate this problem. More precisely, before any attack, the defenders can choose an arbitrary point as Noon, and then find the point on the loop that is equidistant from Noon in both directions – 6PM. At this location, a signal sent out from Noon will arrive at 6PM's two receivers with zero TDoA, and vice versa. We call this equidistant point *the loop midpoint*, without possibility of confusion with Algorithm 4.1's concept of a tree's size-based midpoint. If one of her two receivers would be atop a fitting when placed at Noon or 6PM, she should move those two locations slightly clockwise or counterclockwise around the loop to get them on plain pipe.

As shown in Figure 4.35, when an attack is underway, a defender can affix her two receivers at Noon or 6PM and run a "Round Zero" TDoA computation to determine which half-loop the attacker's transmitter lies in. With the correct half identified (marked with the light blue band in the figure), the defender can move on to Round 1 of Algorithm 4.1. In the figure, this is indicated by the location labelled as Round 1, and the attacker's signal is identified as coming from the half-circle

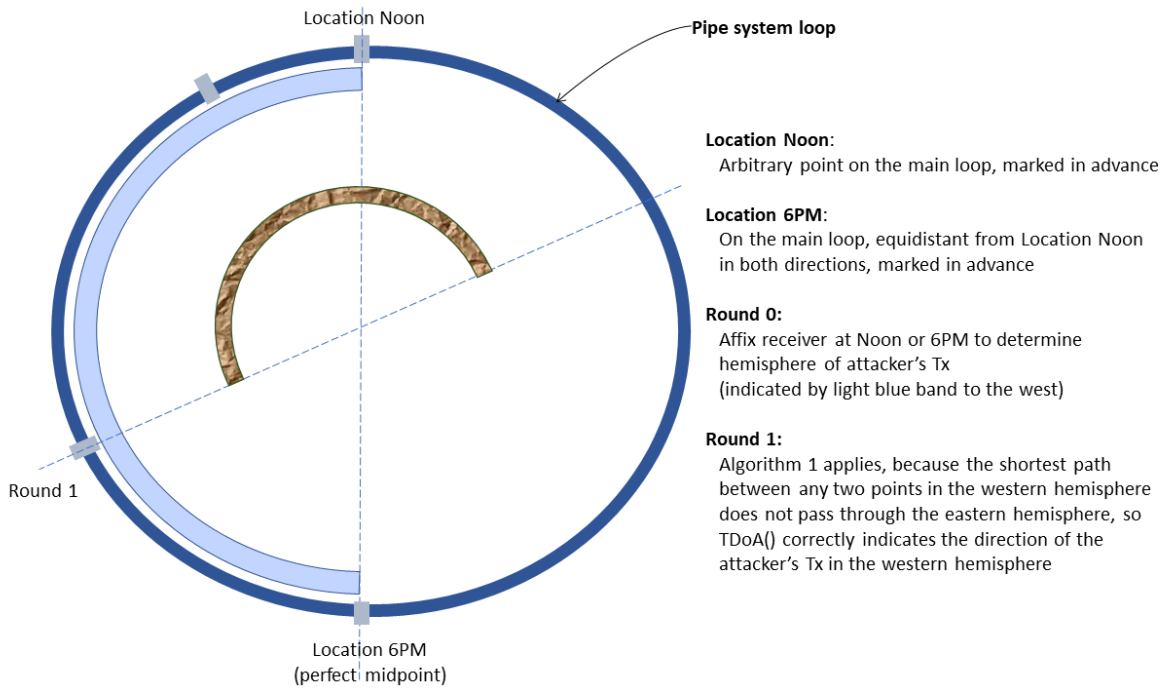

Figure 4.35: The Advantage of a Predetermined Initial Midpoint in a Loop Topology

above Round 1's location, indicated by a rocky brown band. The search then moves on to Round 2 as usual, considering only the portion of the loop in the intersection of the arcs indicated by the brown and light blue bands.

To find the loop midpoint, defenders can begin by choosing the point to be used as Noon, affixing two receivers there at the standard separation distance, attaching a transmitter at their best guess for 6PM, and then adjusting its location until the TDoA is zero. The magnitude of the TDoA at the receivers can help the defenders zero in on 6PM more quickly, as discussed in Section 4.14.7 below, although asymptotically one cannot do better than binary search.

Once the loop midpoint is found, the defenders need to permanently mark both Noon and 6PM and make a note of those locations, as they will be needed during any subsequent localization efforts. Ideally, the defenders should leave the receivers attached at Noon or 6PM, both for use in attack detection and to save time when an attack is underway.

If a loop midpoint has not been located in advance, then it will be harder to find the attacker's transmitter. Figure 4.36 shows how a series of seemingly-reasonable receiver placement decisions can stand between the defender and Algorithm 4.1. In Round 1 of this figure, the defender places her receivers at 6PM and determines that the transmitter lies in the half-loop indicated by the pale blue band. The defender then looks for the end of that half-loop, indicated by the white rectangle at Noon. With an attack ongoing, she is unable to find Noon by looking for a TDoA of zero from

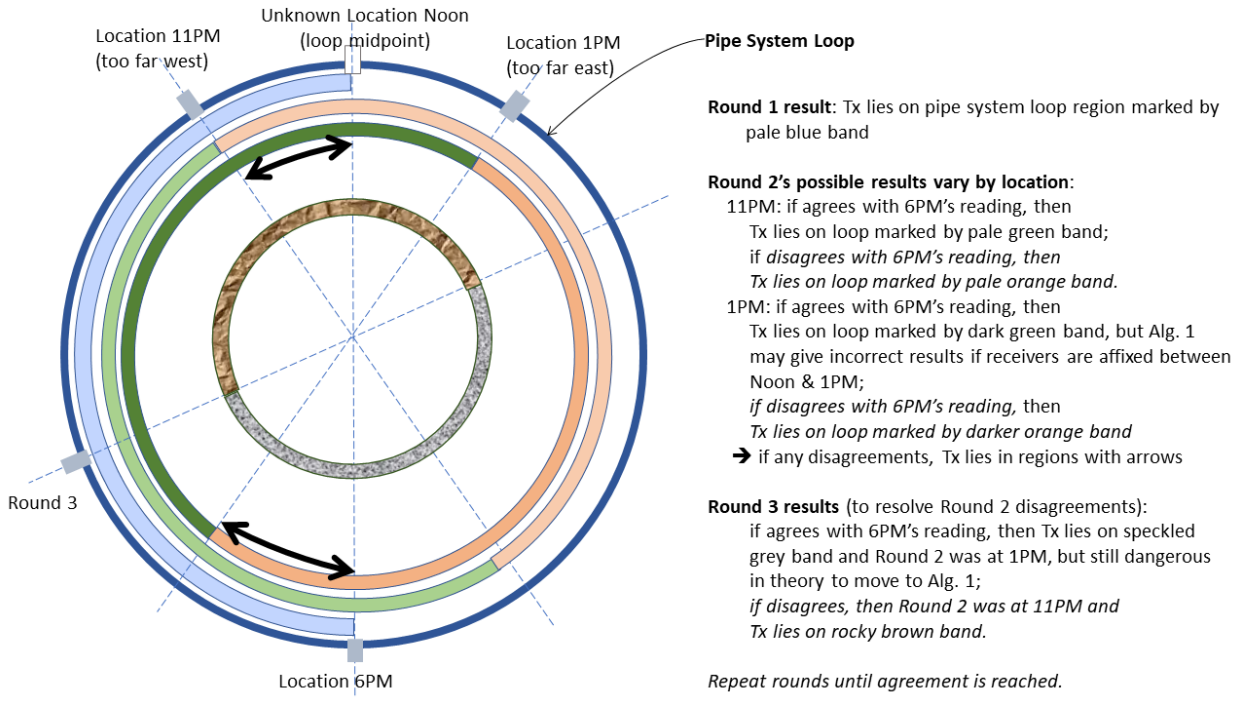

Figure 4.36: Receiver Localization in a Loop Topology without a Predetermined Initial Midpoint

her own signal. Instead she inadvertently places her receivers on one side or the other of Noon, indicated by locations 11PM and 1PM in Figure 4.36.

If the defender is at 11 PM and her TDoA reading agrees with that taken at 6PM, i.e., indicates that the attacker's transmitter lies south of 11PM and north of 6PM (light green band), then she can safely move on to Algorithm 4.1 with the subgraph between 6PM and 11PM. However, if she is at 1PM, then the same reading (transmitter to the west of 6PM and 1PM, dark green band) does not indicate that she can safely move on to Algorithm 4.1 with that tree, because more than half the loop lies to the west of 1PM and 6PM. Since the defender does not know whether she is at 11PM or 1PM, she cannot move on to the tree search algorithm in either case.

Similarly, if the defender is at 11PM (respectively 1PM) and her TDoA reading disagrees with the TDoA reading previously taken at 6PM, then the transmitter lies along the pale (respectively medium) orange band in Figure 4.36, and the attacker's transmitter lies within the upper (respectively lower) arc indicated by black arrows, i.e., the regions where the blue and orange arcs overlap. She does not know whether she is at 11PM or 1PM and cannot safely move on to Algorithm 4.1 in either case, since her best-effort descriptions of the relevant portion of the loop will include more than half the loop.

One might think that the defender could quickly resolve the situation with a third round as marked in Figure 4.36, but in theory n rounds may be required. TDoA readings inconsistent with that of

6PM indicate that the defender has overshot and must move her receivers away from the direction of receipt until her readings are consistent with those taken at 6PM, but even then she cannot be confident that she has eliminated at least half the loop from the search space and can safely move on to Algorithm 4.1 with the remaining portion of the topology.

Fortunately, the defender can almost surely avoid this problem in the real world. After inspecting the area at location 6PM and taking a TDoA reading, if its value is zero, then she knows that the attacker's transmitter is at location Noon and can confine the search to that approximate area. Otherwise, she should not try to cut the loop in half. Instead she should reduce it to roughly a quarter of its original length, by moving to approximately 9PM for her next reading. Without ever knowing quite where Noon is, she can then move on to Algorithm 4.1 and 7:30PM for the third reading, if the transmitter is determined to be south of 9PM; or else put her receivers at roughly 10:30PM and continue to iterate. In the worst case, the attacker's transmitter is just west of Noon, so all her readings will disagree with the 6PM reading until she finally sees the transmitter, without ever having moved to Algorithm 4.1. But it does not matter, because the TDoA misinterpretations that break Algorithm 4.1 will not affect her: she does not need the algorithm to help her roughly estimate the midpoint of the remaining search space. In this case, human judgment is less fragile than the algorithm's.

4.14.5 Localization in Grid Topologies

Grid topologies for sprinkler systems consist of one main loop plus additional pipe runs that start at one point on the loop and end at another point on the loop, without intersecting any other points of the loop or each other in between. The topology is still planar and each branch line (not shown in the figure) does not intersect any other branch line, chord, or loop point except at its root.

As Figure 4.37 shows, localization in a grid topology can be far more difficult than in a loop. In the figure, the defender has placed her receivers along the main loop, and her TDoA reading has told her that the shortest distance along the pipe from the attacker's transmitter to receiver A is less than the shortest distance from the transmitter to receiver B, but that information only allows her to rule out the gray areas of the grid, which is extremely unhelpful. Further, even though the remainder of the grid forms a tree, our experience with loops in the previous section showed that Algorithm 4.1 is not applicable to this tree: with more than half of each chord still in the tree, TDoA readings cannot be relied upon because the shortest path between the transmitter and the next measurement point may go through a gray area.

Although the placement in Figure 4.37 is particularly useless, most other placements also fail to reduce the grid to a tree that can take advantage of Algorithm 4.1, as shown in Figure 4.38. The placements at top left and bottom right do not cut across all the internal cycles. The remaining

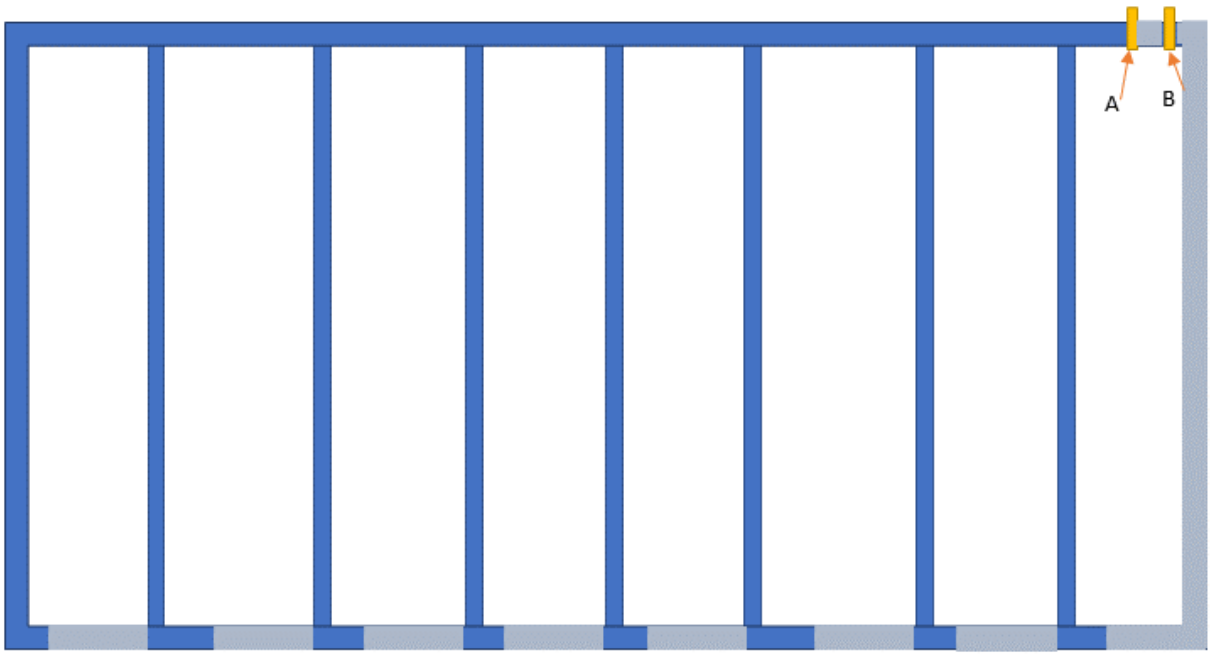

Figure 4.37: The Impact of Poor Receiver Placement During Localization in a Loop Topology

placements do result in trees, but the bottom left example cannot guarantee that the shortest path to the receiver in subsequent rounds would not go through a gray area. The remaining three placements do not suffer from that problem, but only because the attacker's signal reached receiver B first. If it had reached A first, then those placements would have the same problem as the bottom left example.

Our discussion of predetermined loop midpoints in the previous section suggests that the best approach is for the defender to use a predetermined receiver location whose initial readings can cut the loop and each of its chords in half lengthwise, before moving on to tree-style localization. As shown in Figure 4.39, the defender can do this in advance by using TDoA testing to identify the midpoints of each chord and of the two additional pipe runs that form the ends of the main loop (3PM and 9PM). With each of these chords and the end runs sliced exactly in half lengthwise, no shortest path between two locations along blue pipes goes through gray pipes, and vice versa. We assume that the midpoints do not fall on any large fittings.

Once the midpoints have been determined, the defender can leave her receivers in place at any one of the midpoints where the receivers are not on a fitting. When an attack is suspected, non-zero TDoA readings from that midpoint will tell the defender whether the attacker's transmitter lies in the blue or gray region above or below, respectively, the previously identified midpoints. After that initial TDoA test, Algorithm 4.1's binary search in the appropriate region will find the attacker's transmitter.

If the initial TDoA midpoint reading is zero, then the attacker's transmitter lies at one of the

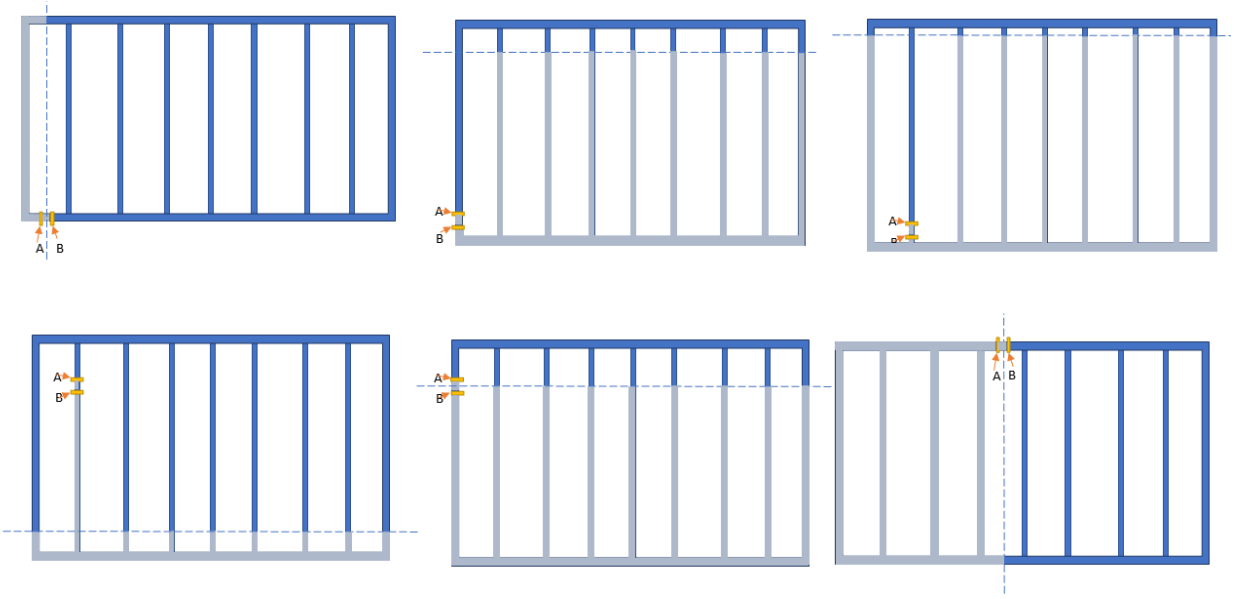

Figure 4.38: The Impact of Poor Receiver Placement in a Grid Topology

midpoints and the defender cannot exclude them from the search space or, in theory, move on to Algorithm 4.1. However, the defender can use a binary search along the length of the top or bottom of the main loop (no need to search past the corners in Figure 4.39) to learn which chord or end run holds the transmitter at its midpoint. During the binary search along the main loop, she can ignore any branch lines sprouting off the main loop, because she already knows that the transmitter lies elsewhere. Once the correct chord or end run has been identified, the defender can go directly to the appropriate midpoint and find the attacker's transmitter.

4.14.6 Localization Using More Than Two Microphones

If the defender has a complex pipe system to analyze, a localization method that uses additional receivers at fixed locations can be used to kick off the search and reduce the search time. With time-synchronized receivers scattered across the piping system (e.g., using power-line synchronization), the defender can record across all of the receivers to obtain the difference in time of arrival to all of the receivers and pinpoint the closest receiver to the source signal. For example, if receivers are installed near each intersection of a branch line with a cross main, a single round of the localization algorithm can pinpoint the transmitter to a particular branch line. In general, unless the receivers are very close together, the defender will need to employ mobile receivers to complete the search.

The use of additional receivers at fixed locations can reduce the search time by a factor of up to

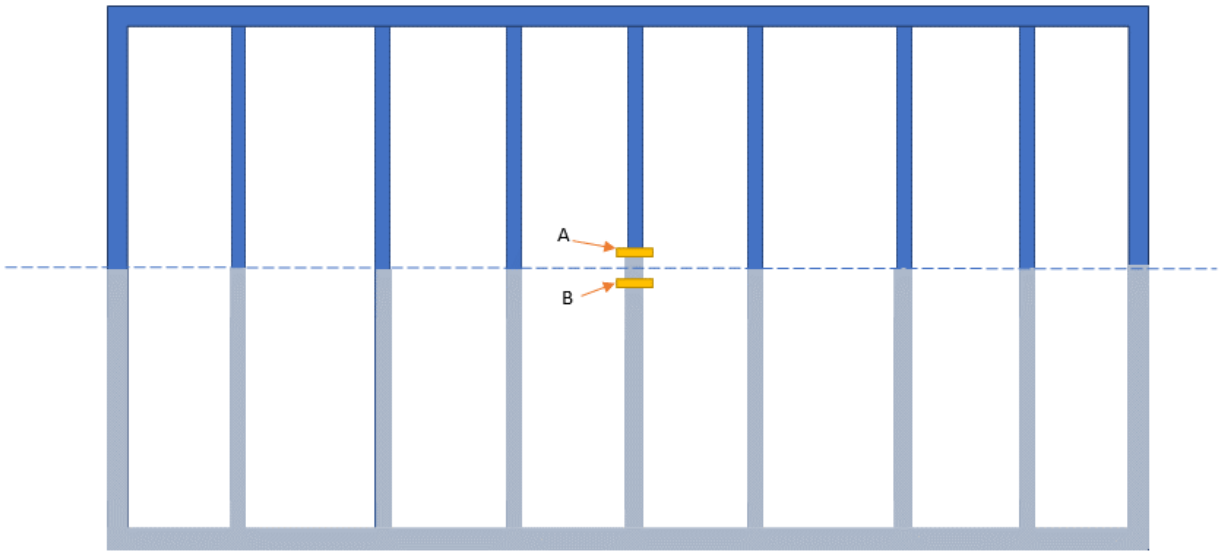

Figure 4.39: For Fastest Localization, Identify All Chord Midpoints in Advance

$n-1$, where n is the number of receivers used for localization.

If the defender deploys receivers at fixed locations, the defender must regularly check to ensure that the receivers have not been tampered with, moved, or compromised.

4.14.7 Interpolated Jump Based Binary Search

An interpolation based binary search algorithm that makes interpolated jumps to the next search point based on the difference in time of arrival seen at the receivers can be used to further reduce the search space and time spent. Based on the results shown in Figure 4.30, the distance between the receivers shows an approximately linear relationship with the TDoA between them. This means that if the attacker's transmitter is, for example, located very close to one of the defender's receivers, then the other localization receiver should see a signal whose TDoA is close to the TDoA corresponding to the distance d between the two receivers. If the attacker's transmitter is located in the middle of the search space between two localization receivers, the TDoA would correspond to roughly half the distance between the two receivers, $d/2$, instead. As the defender knows the distance d between her two localization receivers, the TDoA value can help the defender estimate the location of the attacker's transmitter more accurately than just assuming that the next iteration of the search should proceed from the midpoint of the current pipe run.

Interpolation estimates from a pair of fixed-location receivers at the ends of a feeder main or cross main at the start of the search can help to quickly find the most promising cross main or branch line, respectively, to search, and help the defender to estimate the best point along the pipe

to place mobile transmitters for continuing the search.

4.15 CONCLUSIONS

The requirements imposed on commercial spaces by the International Building Code have the unintended effect of ensuring that even a front office that is air-gapped and secured against traditional attacks is still vulnerable to wide-bandwidth data exfiltration through its pipes, using acoustic transducers attached to pipes. Through study of building codes along with audio transmission experiments in real-world buildings and an experimental testbed, we evaluated how vulnerable today's buildings are to pipe attacks. We evaluated the effectiveness of data transmission through experiments with pipes used in fire sprinkler systems (both wet and dry, black steel and CPVC), potable water pipes (copper, PVC, CPVC), black steel gas lines, and the copper pipes used in heating systems. In existing large buildings and also in an laboratory experimental setup, we measured how well these pipes serve as a covert data communication channel.

Our results demonstrate achievable throughput in the range of 15bps in the highest capacity frequency channel for each pipe run tested. The wide bandwidth of suitable frequencies for transmissions gives an attacker 51 non-interfering frequency channels spaced 100Hz apart in the range of 15KHz to 20KHz, above the range of most human hearing, and this is where we took our measurements. An attacker could use as many as 61 channels at 80Hz spacing, again without interference. The volume to transmit the maximum distance tested with those channels ranges from the equivalent of a whisper to a quiet rural area. When sufficient power is available, the channels can be used in parallel and their capacities sum to a total of approximately 770bps with 51 channels and 924bps with 61 non-interfering channels. To human perception, using all 51 channels at once makes the sound appear to be about three times louder than with a single channel transmission. These are the volumes at the pipe surface, rather than in the ambient air, but good soundproofing is still important to minimize ambient leakage and corresponding the possibility of detection.

We considered a wide variety of potential defenses, and evaluated the effectiveness of switching to CPVC, adding check valves, using flexible couplings, introducing air gaps between pipes, and increasing ambient white noise. None of these measures was effective as a defense. We recomment the injection of noise into the pipe to raise the cost of a successful attack, along with attack detection based on anomaly detection methods that use comparisons with historical data and consider a wide variety of potential attacker modulation methods.

Once an anomaly is detected in the pipe system, a localization method can be used to find the location of the attacker's transmitter along the pipe. We proposed a localization method that uses the time difference of arrival of the attacker's signal across two or more microphones to refocus the

search in the direction of the attacker's transmitter. We combined this with a modified binary search algorithm to find the attacker's device in $O\log(n)$ search time. This search algorithm works in realistic building piping systems that twist, turn, merge and branch in complicated ways, regardless of where the search begins. We suggested ways to speed up the search by using preinstalled receivers at fixed strategic locations, as well as interpolation based on the time delay of arrival to reduce localization time.

Chapter 5: CONCLUSION AND FUTURE WORK

5.1 CONTRIBUTIONS

Factory floors produce vast quantities of proprietary data that can be stolen by adversaries intent on learning about manufacturing process specifications, product designs, and factory activities. We have explored espionage methods that exploit these vulnerabilities, starting with the factory floor where the information is generated, on through the factory front office, and finally in the manufacturing federation where the information is shared, modified and consumed.

We began by exploring the wide range of data about a manufacturing product that will be generated, stored, shared and used during its life cycle. Our research contributions:

- We explained the concept of digital threads, which track all information about a manufactured item through its lifecycle, and identified the threats and challenges that are unique to digital threads for manufacturing data. These include manufacturers' front office IT security experts' lack of understanding of what actually happens on factory floors, manufacturers' aversion to any change in factory floor software, the realities of the factory floor equipment repair process, and the challenges of determining an appropriate access control policy to preserve the confidentiality of a digital thread.

- We developed a case study of a small real-world manufacturer, including a set of data use cases that can be used to evaluate potential information security architectures.

- To meet the security needs and threats identified for the case study and for other manufacturers, we proposed a hybrid data architecture that couples a decentralized low-volume data sharing system such as blockchain with a centralized high volume internal data management system such as WORM.

- We provided a proof-of-concept design and implementation of the proposed hybrid data architecture, including add-on hardware for factory floor machines. The result is a modular, practical and cost-effective solution that can be easily retrofitted to factories today to make them Industry 4.0 capable, with minimal modifications to factory floor machines.

Even in a factory where data is securely generated, stored and shared, there can be additional vulnerabilities on the factory floor. Our contributions in this area:

- We identified a novel side-channel vulnerability that can lead to factory secrets and manufacturing IP being leaked and stolen, by exploiting the sensors in phones carried onto the factory floor.

- Using a CNC mill and a 3D printer to represent subtractive and additive manufacturing, respectively, we demonstrated that ordinary mobile phones can effectively capture these machines' acoustic and electromagnetic information on a factory floor, and the recordings can be used to reconstruct the shape and manufacturing process information of objects being manufactured. Our reconstruction method uses signal processing and machine learning techniques, coupled together in an interactive framework where a non-expert human-in-the loop applies manufacturing domain constraints and guides the reconstruction process.

- We identified several methods for launching the attack. The first is for a confederate to record audio with their phone on the factory floor. A second option is to infect a factory worker's phone with malware that allows an attacker to record audio, either automatically or at will. As a third method, we demonstrated that the attack is effective even in the background of a phone call placed or received on the factory floor. This third approach allows attackers to carry out the attack remotely, without malware.

- We offered defenses against the phone attack, based on audio obfuscation of factory machines, physical shielding against EMF emanations, controlling the separation distance between humans and machines so that EMF emanations are negligible, and restricting usage of phones and other sensors on the factory floor.

The front offices of manufacturing facilities also house industrial secrets that can be irresistible to attackers. Our contributions:

- We determined that the requirements imposed on commercial spaces by the International Building Code have the unintended effect of ensuring that a front office that is air-gapped and secured against traditional attacks is still vulnerable to wide-bandwidth data exfiltration through its sprinkler system and other kinds of pipes.

- Our novel *pipe attack* for data exfiltration uses an acoustic transducer, such as those used in bone-conducting headphones, to transmit data through pipes. The transducer is physically attached to a pipe by a confederate or dupe, and a receiver attached to the same pipe system picks up the transmitted signals. We suggested a variety of methods for getting the data to be exfiltrated up to the transmitter.

- We demonstrated that data can be transmitted roughly equally effectively through the pipes used in fire sprinkler systems (both wet and dry, black steel and CPVC), potable water pipes (copper, PVC, CPVC), black steel gas lines, and the copper pipes used in heating systems.

- We designed and built a small and unobtrusive transmitter and receiver. We demonstrated that they transmitted data effectively in all pipes we tested of less than 4 inches inner diameter.

We showed that the pipe attack is ineffective in fire sprinkler system risers, because they are too wide. To transmit data between floors of a building, an attacker must use other types of pipes, such as the water supply lines that connect janitorial closets and restrooms stacked one above another in a building.

- Through empirical measurements in a variety of commercial and residential buildings, we determined that pipe transmissions using frequencies in the range of 15KHz-20KHz are hard for humans to overhear and are easy to a receiver to interpret, in the sense that the frequency transmitted is also the peak frequency received.

- We demonstrated throughput of approximately 15bps per frequency channel between 15KHz and 20KHz in 90-170 foot pipe runs in existing large commercial and residential buildings and in 30-42 foot pipe runs in laboratory settings. The transmission volume to traverse the maximum distance tested with those channels ranged from the equivalent of a whisper to the ambient noise in a quiet rural area. We found little to no drop in volume at the end of the pipe run, implying that the maximum distance for effective transmission is quite a bit higher.

- Through measurements of interference, we determined that attackers have 51 non-interfering frequency channels used in our measurements, spaced 100Hz apart in the range of 15KHz to 20KHz, above the range of most human hearing. The channels can be spaced 80Hz apart without interference, which would give an attacker 61 non-interfering frequency channels. When sufficient power is available, all non-interfering channels can be used in parallel. The capacities sum to a total of approximately 770bps over 51 channels for each real-world pipe run, and we estimate 924bps if 61 non-interfering channels are used. The previous work on communication through a building's structural skeleton suggests a variety of ways to push this bitrate higher. If all 51 channels are used in parallel, the apparent volume to a human bystander will be about three times higher than if a single channel is used.

- We proposed, built, and tested a wide variety of countermeasures.

  - The best defense we found is to raise the cost of a successful attack by injecting noise into the pipe, either directly through a transmitter or by circulating the water in the pipes. The latter will tend to wear out the pipes and both may create ambient sound that annoys building occupants. From a theoretical point of view, noise injection provides no guarantees against a successful attack, so it is likely to spark an arms race.

  - Defenses that we found ineffective include the use of other pipe materials (e.g., CPVC); the addition of extra check valves, flexible couplings, or air gaps along the pipes; a high level of ambient noise; using wider pipes throughout the sprinkler system

(unacceptable due to its negative impact on building design and construction costs), and sound cancellation (very expensive, as sound travels much faster through a sprinkler pipe's surface than through air). The resilience of the pipe attack to ambient noise suggests that it can be effective on the factory floor and in other noisy environments, as well as in the front office.

- As noise injection only raises the cost of a successful attack, building occupants who are concerned about data exfiltration should also use a receiver on the pipe and anomaly detection software to decide whether an attack is underway. They should also sweep for bugs, even though we argued that the pipe attack is relatively resilient against bug sweeping.
- To find a transmitter while an attack is underway, we proposed a localization method that uses two receivers attached to the pipe. In a linear pipe run, the time difference of arrival of the attacker's signal at the two receivers indicates the direction in which the transmitter lies. We incorporated the directional information from the pair of receivers into a modified binary search algorithm to find the attacker's device in a tree topology sprinkler system in $O\log(n)$ time worst case, where n is the length of the pipe system. Regardless of where the building occupants begin the search, this algorithm works in realistic building piping systems that twist, turn, merge and branch in complicated ways. We also proposed localization methods for the two other sprinkler system topologies, namely, loops and grids.
- We suggested ways to speed up the search for an attacker's transmitter by using preinstalled receivers at fixed strategic locations, as well as interpolation based on the time delay of arrival.

5.2 FUTURE WORK

Given the ease and ubiquity of the pipe attack for data exfiltration, one area for future work is on improved defenses against that attack. For example:

- Can the effectiveness of the pipe attack be reduced by incorporating short sections of wider pipe (perhaps with unusual shapes or configurations such as spherical) at key points in a pipe system, such as room, department, and organization boundaries?
- For highly secure facilities, are there alternative pipe materials that could perform satisfactorily during a fire while also dampening signal transmission?

- Could a new type of flexible coupling be introduced that satisfies fire safety requirements while also dampening signals in the 15KHz-20KHz range?
- Could unique topologies be introduced into sprinkler systems that raise the cost of an effective attack (as grid topologies and, to a lesser extent, loop topologies already do), at moderate cost during building construction? Intuitively, such topologies might behave like a large set of loops of different lengths.

To defend effectively against an attack, we must know the boundaries of where the attack is practical. This raises many questions for the pipe attack, including:

- With a custom transmitter, an attacker can extend the set of available transmission channels into the ultrasound range above 20KHz. Ultrasound has the advantage of being inaudible to humans, along with the disadvantage that transmission distance drops off rapidly as the frequency increases. In a sprinkler system and other building pipes, how many additional channels, over what distances, and with what data rates can an attacker take advantage of with non-interfering frequencies above 20KHz?
- Can the pipe attack work on electrical conduit, i.e., metal pipes that have wires running through them?
- How easy is it to take over the structural monitoring hardware and software already being installed in the steel skeletons of new buildings, and use it for data exfiltration? What sorts of data rates can an attacker obtain there?
- How easy is it to install new attack devices that use a building's metal skeleton, or even just its metal drywall studs, to transmit data? What kinds of transmission rates over what distances are practical?
- Can the pipe attack be modified to transmit data along the metal trays often used to carry cables and wiring above hallways?

The phone audio attack on the factory floor also raises unanswered research questions, but the situation is different there because manufacturers already know that personal phones are a security risk, and high-security facilities already prohibit workers from bringing personal phones into their buildings. Phones are banned because they can be used to photograph sensitive information and transport data of all types, not just audio. Yet workers are reluctant to part with their phones. Open questions include how we might prevent the exfiltration of data using phones: how to prevent the taking of photos in secure facilities, how to prevent recording of video and audio, how to prevent data upload.

Given the long lifetime of factory equipment, we cannot expect that equipment software will be maintained and patched by the software maker during the entire working life of the equipment, which may span 50 years. How can we put factory equipment in a bubble that protects it against new attacks against its underlying hardware and software (e.g., the operating system) and equipment-specific software, while simultaneously allowing remote access for repair purposes? Researchers have already been investigating ways to protect the USB ports ubiquitous on factory floor equipment, and the other parts of the system also need protection.

As technology advances, it is common to retrofit old equipment with new sensors to record data. How can we make sure that all sensors attached to a piece of equipment are authorized to be there, and none have been subverted?

This list of open research questions is not exhaustive: the creative adversarial mind can find many ways to steal a factory's secrets. A potentially bright spot is that as ransomware attacks continue to grow in popularity and insurers demand a stricter standard of computer security before insuring against business interruption, we expect that manufacturers will continually raise their defenses against ransomware. In many but not all cases, improving defenses against ransomware will have the side effect of increasing the cost of stealing manufacturers' intellectual property, the main focus of this work.

REFERENCES

[1] S. Zimmerman and D. Glavach, "Applying and assessing cybersecurity controls for direct digital manufacturing systems," in *Cybersecurity for Direct Digital Manufacturing Symposium*. NIST, 2015, pp. 51–64.

[2] "Kaspersky lab survey: One in every five manufacturing businesses has lost intellectual property to security breaches within the past year," Kaspersky Lab press release, August 2014.

[3] S. Widup, K. Maxwell, W. Baker, C. Porter, J. Jacobs, K. Thompson, M. Spitler, D. Hylender, S. Brannon, and K. Gilbert, "2013 data breach investigations report," Verizon, Tech. Rep., 2013.

[4] ICS Alert, "ICS-CERT Monitor September 2014 – February 2015," Department of Homeland Security (DHS) National Cyber-security and Communications Integration Center (NCCIC), Tech. Rep., March 2015.

[5] ICS Alert, "ICS-CERT Monitor November/December 2015," Department of Homeland Security (DHS) National Cyber-security and Communications Integration Center (NCCIC), Tech. Rep., May 2016.

[6] Fortinet, "2021 the state of operational technology and cybersecurity," Fortinet, Tech. Rep., 2021. [Online]. Available: https://www.fortinet.com/resources-campaign/operational-technology/2021-the-state-of-operational-technology-and-cybersecurity?utm_source=blog&utm_campaign=2021-the-state-of-operational-technology-and-cybersecurity

[7] A. Adhikari, A. Hojjati, J. Shen, J.-T. Hsu, W. P. King, and M. Winslett, "Trust issues for big data about high-value manufactured parts," in *2016 IEEE 2nd International Conference on Big Data Security on Cloud (BigDataSecurity), IEEE International Conference on High Performance and Smart Computing (HPSC), and IEEE International Conference on Intelligent Data and Security (IDS)*. IEEE, 2016, pp. 24–29.

[8] A. Adhikari and M. Winslett, "A hybrid architecture for secure management of manufacturing data in Industry 4.0," in *2019 IEEE International Conference on Pervasive Computing and Communications Workshops (PerCom Workshops)*, 2019, pp. 973–978.

[9] A. Hojjati, A. Adhikari, K. Struckmann, E. Chou, T. N. Tho Nguyen, K. Madan, M. S. Winslett, C. A. Gunter, and W. P. King, "Leave your phone at the door: Side channels that reveal factory floor secrets," in *Proceedings of the 2016 ACM SIGSAC Conference on Computer and Communications Security*. New York, NY, USA: ACM, 2016, pp. 883–894.

[10] J. Manyika, M. Chui, B. Brown, J. Bughin, R. Dobbs, C. Roxburgh, and A. Hung Byers, *Big data: The next frontier for innovation, competition, and productivity*. McKinsey Global Institute, 2011.

[11] C. Furstoss, "Digital thread: Creating a self-improving, brilliant factory," *CIO Review*, vol. 3, p. 12, 2013.

[12] J. Bisceglie, M. McGrath, D. Chesebrough, M. Fedak, J. Godwin, M. Gordon, L. John, C. Ortiz, C. Peters, and W. Barkman, "Cybersecurity for advanced manufacturing," *National Defense Industrial Association (NDIA) Manufacturing Division*, 2014.

[13] ICS Alert, "ICS-CERT Monitor," Department of Homeland Security, Tech. Rep., 2014.

[14] ICS Alert, "ICS-CERT Monitor," Department of Homeland Security, Tech. Rep., 2011.

[15] ICS Alert, "ICS-CERT Monitor," Department of Homeland Security, Tech. Rep., 2013.

[16] S. Freedberg, "Top official admits f-35 stealth fighter secrets stolen," *Breaking Defense*, vol. 20, 2013.

[17] R. Hasan, R. Sion, and M. Winslett, "Introducing secure provenance: problems and challenges," in *Proceedings of the 2007 ACM Workshop on Storage Security and Survivability*, 2007, pp. 13–18.

[18] D. J. Pohly, S. McLaughlin, P. McDaniel, and K. Butler, "Hi-fi: collecting high-fidelity whole-system provenance," in *Proceedings of the 28th Annual Computer Security Applications Conference*, 2012, pp. 259–268.

[19] R. Hasan, R. Sion, and M. Winslett, "Preventing history forgery with secure provenance," *ACM Transactions on Storage (TOS)*, vol. 5, no. 4, pp. 1–43, 2009.

[20] R. Lu, X. Lin, X. Liang, and X. Shen, "Secure provenance: the essential of bread and butter of data forensics in cloud computing," in *Proceedings of the 5th ACM Symposium on Information, Computer and Communications Security*, 2010, pp. 282–292.

[21] U. J. Braun, A. Shinnar, and M. I. Seltzer, "Securing provenance," in *Proceedings of the 3rd USENIX Workshop on Hot Topics in Security (HotSec'08)*. USENIX Association, 2008.

[22] B. Thuraisingham, T. Cadenhead, M. Kantarcioglu, and V. Khadilkar, *Secure data provenance and inference control with semantic web*. CRC Press, 2014.

[23] S. Chong, "Towards semantics for provenance security." in *Workshop on the Theory and Practice of Provenance*, 2009.

[24] J. J. Carroll, C. Bizer, P. Hayes, and P. Stickler, "Named graphs, provenance and trust," in *Proceedings of the 14th International Conference on the World Wide Web*, 2005, pp. 613–622.

[25] J. Cheney, "A formal framework for provenance security," in *2011 IEEE 24th Computer Security Foundations Symposium*. IEEE, 2011, pp. 281–293.

[26] R. Khan, M. Haque, and R. Hasan, "A secure location proof generation scheme for supply chain integrity preservation," in *Proceedings of the 2013 IEEE International Conference on Technologies for Homeland Security*, vol. 13, 2013, pp. 446–450.

[27] L. Sturm, C. Williams, J. Camelio, J. White, and R. Parker, "An analysis of cyber physical vulnerabilities in additive manufacturing," in *Proceedings of the Cybersecurity for Direct Digital Manufacturing (DDM) Symposium*, 2015.

[28] K. Zetter, "An unprecedented look at Stuxnet, the world's first digital weapon," *Wired*, 2014.

[29] D. Storm, "Hackers exploit SCADA holes to take full control of critical infrastructure," *Computerworld*, vol. 15, 2014.

[30] R. McMillan, "CIA says hackers have cut power grid: Several cities outside the US have sustained attacks on utility systems and extortion demands," 2008.

[31] Hyperledger, "Hyperledger whitepaper," last accessed 2017-10-17. [Online]. Available: http://www.the-blockchain.com/docs/HyperledgerWhitepaper.pdf

[32] J. Sevareid, *Use Case Inventory*, Hyperledger Requirements Working Group (WG), 2017, last updated 2016-11-01. [Online]. Available: https://wiki.hyperledger.org/groups/requirements/use-case-inventory

[33] I. Eyal, A. E. Gencer, E. G. Sirer, and R. V. Renesse, "Bitcoin-NG: A scalable blockchain protocol," in *13th USENIX Symposium on Networked Systems Design and Implementation (NSDI 16)*. Santa Clara, CA: USENIX Association, 2016. [Online]. Available: https://www.usenix.org/conference/nsdi16/technical-sessions/presentation/eyal pp. 45–59.

[34] J. Barr, "Create write-once-read-many archive storage with Amazon Glacier," last updated 2016-11-10. [Online]. Available: https://aws.amazon.com/blogs/aws/glacier-vault-lock/

[35] Dell Inc, "Dell EMC Unity: File-Level Retention (FLR)," Dell Inc., Tech. Rep., Jan 2019, last accessed 2022-01-17. [Online]. Available: http://www.the-blockchain.com/docs/HyperledgerWhitepaper.pdf

[36] J. Barr, "Create write-once-read-many archive storage with amazon glacier," *Amazon Web Services blog*, vol. 8, 2015.

[37] D. Asonov and R. Agrawal, "Keyboard acoustic emanations," in *IEEE Symposium on Security and Privacy*, 2004.

[38] D. Foo Kune and Y. Kim, "Timing attacks on PIN input devices," in *ACM Conference on Computer and Communications Security*. ACM, 2010, pp. 678–680.

[39] G. Goller and G. Sigl, "Side channel attacks on smartphones and embedded devices using standard radio equipment," in *Constructive Side-Channel Analysis and Secure Design*. Springer, 2015, pp. 255–270.

[40] D. X. Song, D. Wagner, and X. Tian, "Timing analysis of keystrokes and timing attacks on SSH," in *USENIX Security Symposium*, 2001.

[41] M. Vuagnoux and S. Pasini, "Compromising electromagnetic emanations of wired and wireless keyboards," in *USENIX Security Symposium*, 2009, pp. 1–16.

[42] L. Zhuang, F. Zhou, and J. D. Tygar, "Keyboard acoustic emanations revisited," *ACM Transactions on Information and System Security*, vol. 13, no. 1, 2009.

[43] D. Genkin, I. Pipman, and E. Tromer, "Get your hands off my laptop: Physical side-channel key-extraction attacks on PCs," *Journal of Cryptographic Engineering*, vol. 5, no. 2, pp. 95–112, 2015.

[44] P. Kocher, J. Jaffe, B. Jun, and P. Rohatgi, "Introduction to differential power analysis," *Journal of Cryptographic Engineering*, vol. 1, no. 1, pp. 5–27, 2011.

[45] P. C. Kocher, "Timing attacks on implementations of Diffie-Hellman, RSA, DSS, and other systems," in *Advances in Cryptology*. Springer, 1996, pp. 104–113.

[46] T. Bifano and Y. Yi, "Acoustic emission as an indicator of material-removal regime in glass micro-machining," *Precision Engineering*, vol. 14, no. 4, pp. 219–228, 1992.

[47] R. Y. Chiou and S. Y. Liang, "Analysis of acoustic emission in chatter vibration with tool wear effect in turning," *International Journal of Machine Tools and Manufacture*, vol. 40, no. 7, pp. 927–941, 2000.

[48] S. Hayashi, C. Thomas, D. Wildes, and G. Tlusty, "Tool break detection by monitoring ultrasonic vibrations," *CIRP Annals–Manufacturing Technology*, vol. 37, no. 1, pp. 61–64, 1988.

[49] B. Kim, "Punch press monitoring with acoustic emission (AE) part I: signal characterization and stock hardness effects," *Journal of Engineering Materials and Technology*, vol. 105, no. 4, pp. 295–300, 1983.

[50] S. Liang and D. Dornfeld, "Tool wear detection using time series analysis of acoustic emission," *Journal of Engineering for Industry*, vol. 111, no. 3, pp. 199–205, 1989.

[51] J. K. Nelson, "Acoustic emission detection of metals and alloys during machining operations," Master's thesis, Purdue University, 2012.

[52] K. Uehara and Y. Kanda, "Identification of chip formation mechanism through acoustic emission measurements," *CIRP Annals-Manufacturing Technology*, vol. 33, no. 1, pp. 71–74, 1984.

[53] "APT1: Exposing one of China's cyber espionage units," Mandiant Intelligence Center, 2013. [Online]. Available: intelreport.mandiant.com

[54] "Iranian cyber attack on New York dam shows future of war," Time, 2016, [Accessed 13-May-2016]. [Online]. Available: http://goo.gl/0FxOXo

[55] K. Zetter, "Meet 'Flame,' the massive spy malware infiltrating Iranian computers," *Wired*, 2012.

[56] L. Cai, S. Machiraju, and H. Chen, "Defending against sensor-sniffing attacks on mobile phones," in *ACM Workshop on Networking, Systems, and Applications for Mobile Handhelds*. ACM, 2009, pp. 31–36.

[57] M. A. Al Faruque, S. R. Chhetri, A. Canedo, and J. Wan, "Acoustic side-channel attacks on additive manufacturing systems," in *International Conference on Cyber-Physical Systems*, 2016.

[58] H.-C. Chen, K.-C. Lee, and J.-H. Lin, "Electromagnetic and electrostatic shielding properties of co-weaving-knitting fabrics reinforced composites," *Composites Part A: Applied Science and Manufacturing*, vol. 35, no. 11, pp. 1249–1256, 2004.

[59] Y. Yang, M. C. Gupta, K. L. Dudley, and R. W. Lawrence, "Novel carbon nanotube-polystyrene foam composites for electromagnetic interference shielding," *Nano Letters*, vol. 5, no. 11, pp. 2131–2134, 2005.

[60] F. Bacon, *New Atlantis*. Phoemixx Classics Ebooks, 2021.

[61] W. J. Elliot, "A survey of residential speaking tubes." [Online]. Available: https://acoustics.org/pressroom/httpdocs/162nd/Elliot_1aAA10.html

[62] J. Wolfe, "Open vs closed pipes (flutes vs clarinets)." [Online]. Available: https://newt.phys.unsw.edu.au/jw/flutes.v.clarinets.html

[63] R. G. Acevedo, A. L. Méndez, E. Á. Álvarez, S. Suárez, M. Lastra, and A. Gutiérrez-Trashorras, "Acoustic communications in water pipes: An experimental approach," in *1st International Congress on Water, Waste and Energy Management, Salamanca, Spain*, 2012.

[64] Y. Wu, K. Kim, M. F. Henry, and K. Youcef-Toumi, "Design of a leak sensor for operating water pipe systems," in *2017 IEEE/RSJ International Conference on Intelligent Robots and Systems (IROS)*, 2017, pp. 6075–6082.

[65] Y. Jin, Y. Ying, and D. Zhao, "Data communications using guided elastic waves by time reversal pulse position modulation: Experimental study," *Sensors*, vol. 13, no. 1, pp. 8352–8376, july 2013. [Online]. Available: https://pdfs.semanticscholar.org/be09/50068f696c94b83d9fe4ab6a7b74d45198b7.pdf

[66] Nan Su, Jianyan Liu, Qiang Liu, and Weijiang Wang, "A robust underwater acoustic communication approach for pipeline transmission," in *2016 IEEE International Conference on Signal Processing, Communications and Computing (ICSPCC)*, 2016, pp. 1–6.

[67] R. Long, P. Cawley, and M. Lowe, "Acoustic wave propagation in buried iron water pipes," *Proceedings of the Royal Society of London. Series A: Mathematical, Physical and Engineering Sciences*, vol. 459, no. 2039, pp. 2749–2770, 2003.

[68] A. Kondis, "Acoustical wave propagation in buried water filled pipes," Ph.D. dissertation, Massachusetts Institute of Technology, 2005.

[69] D. A. Maltseva, V. A. Zibrov, and A. G. Iliev, "Hydro-acoustic communication channel in the underground pipeline," in *2018 19th International Conference of Young Specialists on Micro/Nanotechnologies and Electron Devices (EDM)*, 2018, pp. 367–371.

[70] M. Conti, R. Di Pietro, L. V. Mancini, and A. Mei, "(old) distributed data source verification in wireless sensor networks," *Inf. Fusion*, vol. 10, no. 4, pp. 342–353, 2009.

[71] S. Yang and A. C. Singer, "Energy efficient ultrasonic communication on steel pipes," in *2016 IEEE International Workshop on Signal Processing Systems, SiPS 2016, Dallas, TX, USA, October 26-28, 2016*. IEEE, 2016. [Online]. Available: https://doi.org/10.1109/SiPS.2016.59 pp. 297–302.

[72] N. D. Nguyen, D. V. Le, N. Meratnia, and P. J. M. Havinga, "In-pipe wireless communication for underground sampling and testing," *GLOBECOM 2017 - 2017 IEEE Global Communications Conference*, pp. 1–7, 2017.

[73] G. Kantaris and N. Makris, "Underwater wireless in-pipe communications system," *2015 IEEE International Conference on Industrial Technology (ICIT)*, pp. 1945–1950, 2015.

[74] S. He, G. Zhang, and G. Song, "Design of a networking stress wave communication method along pipelines," *Mechanical Systems and Signal Processing*, vol. 164, p. 108192, 2022. [Online]. Available: https://www.sciencedirect.com/science/article/pii/S0888327021005689

[75] S. Chakraborty, G. J. Saulnier, K. W. Wilt, R. B. Litman, and H. A. Scarton, "Low-rate ultrasonic communication axially along a cylindrical pipe," in *2014 IEEE International Ultrasonics Symposium*, 2014, pp. 547–551.

[76] S. Chakraborty, G. J. Saulnier, K. W. Wilt, E. Curt, H. A. Scarton, and R. B. Litman, "Low-power, low-rate ultrasonic communications system transmitting axially along a cylindrical pipe using transverse waves," *IEEE Transactions on Ultrasonics, Ferroelectrics, and Frequency Control*, vol. 62, no. 10, pp. 1788–1796, 2015.

[77] V. Doychinov, S. A. Zaidi, N. Chudpooti, P. Akkaraekthalin, N. Somjit, I. D. Robertson, K. V. Horoshenkov, and J. Wakeling, "A study of wireless communications systems for robotic communications in underground pipes and ducts," in *18th International Conference on Electrical Engineering/Electronics, Computer, Telecommunications and Information Technology (ECTI-CON)*, 2021, pp. 209–213.

[78] X. Huang, J. Saniie, S. Bakhtiari, and A. Heifetz, "Applying EMAT for ultrasonic communication through steel plates and pipes," in *2018 IEEE International Conference on Electro/Information Technology (EIT)*, 2018, pp. 0379–0383.

[79] A. Heifetz, D. Shribak, X. Huang, B. Wang, J. Saniie, J. Young, S. Bakhtiari, and R. B. Vilim, "Transmission of images with ultrasonic elastic shear waves on a metallic pipe using amplitude shift keying protocol," *IEEE Transactions on Ultrasonics, Ferroelectrics, and Frequency Control*, vol. 67, no. 6, pp. 1192–1200, 2020.

[80] A. Heifetz, D. Shribak, X. Huang, B. Wang, J. Saniie, R. Ponciroli, E. R. Koehl, S. Bakhtiari, and R. B. Vilim, "Transmission of images on high-temperature nuclear-grade metallic pipe with ultrasonic elastic waves," *Nuclear Technology*, vol. 207, no. 4, pp. 604–616, 2021. [Online]. Available: https://doi.org/10.1080/00295450.2020.1782626

[81] P. Getreuer, C. Gnegy, R. F. Lyon, and R. A. Saurous, "Ultrasonic communication using consumer hardware," *IEEE Transactions on Multimedia*, vol. 20, no. 6, pp. 1277–1290, 2018.

[82] G. Trane, R. Mijarez, and J. A. Pérez-Díaz, "Automatic guided waves data transmission system using an oil industry multiwire cable," *Sensors*, vol. 20, no. 3, 2020. [Online]. Available: https://www.mdpi.com/1424-8220/20/3/868

[83] C. Kexel, M. Mälzer, and J. Moll, "Guided wave based acoustic communications in structural health monitoring systems in the presence of structural defects," in *2018 IEEE International Symposium on Circuits and Systems (ISCAS)*, 2018, pp. 1–4.

[84] F. Zonzini, L. D. Marchi, N. Testoni, and A. Marzani, "Direct spread spectrum modulation and dispersion compensation for guided wave-based communication systems," in *2019 IEEE International Ultrasonics Symposium (IUS)*, 2019, pp. 2500–2503.

[85] M. Mälzer, C. Kexel, T. Maetz, and J. Moll, "Combined inspection and data communication network for lamb-wave structural health monitoring," *IEEE Transactions on Ultrasonics, Ferroelectrics, and Frequency Control*, vol. 66, no. 10, pp. 1625–1633, 2019.

[86] L. Yuan, Y. Yang, X. Dang, and J. He, "Ultrasonic guided wave communication based on pulse position modulation in railways," in *Proceedings of the 5th International Conference on Electrical Engineering and Information Technologies for Rail Transportation (EITRT) 2021, Lecture Notes in Electrical Engineering*, vol. 868. Springer, 2022.

[87] K. T. Erickson, A. Miller, E. K. Stanek, C. Wu, and S. Dunn-Norman, "Pipelines as communication network links," University of Missouri-Rolla (US), Tech. Rep., 2005.

[88] C. Kexel, N. Testoni, F. Zonzini, J. Moll, and L. D. Marchi, "Low-power MIMO guided-wave communication," *IEEE Access*, vol. 8, pp. 217 425–217 436, 2020. [Online]. Available: https://doi.org/10.1109/ACCESS.2020.3042440

[89] M. Guri, Y. Solewicz, and Y. Elovici, "Mosquito: Covert ultrasonic transmissions between two air-gapped computers using speaker-to-speaker communication," in *2018 IEEE Conference on Dependable and Secure Computing (DSC)*, 2018, pp. 1–8.

[90] B. Carrara and C. Adams, "On acoustic covert channels between air-gapped systems," in *International Symposium on Foundations and Practice of Security*. Springer, 2014, pp. 3–16.

[91] M. Guri, Y. Solewicz, A. Daidakulov, and Y. Elovici, "Fansmitter: Acoustic data exfiltration from (speakerless) air-gapped computers," *preprint arXiv:1606.05915*, 2016.

[92] M. Guri, Y. Solewicz, A. Daidakulov, and Y. Elovici, "Acoustic data exfiltration from speakerless air-gapped computers via covert hard-drive noise ('diskfiltration')," in *European Symposium on Research in Computer sSecurity*. Springer, 2017, pp. 98–115.

[93] J. de Gortari Briseno, A. D. Singh, and M. Srivastava, "Inkfiltration: Using inkjet printers for acoustic data exfiltration from air-gapped networks," *ACM Transactions on Privacy and Security*, vol. 25, no. 2, pp. 1–26, 2022.

[94] M. Guri, "CD-leak: Leaking secrets from audioless air-gapped computers using covert acoustic signals from CD/DVD drives," in *2020 IEEE 44th Annual Computers, Software, and Applications Conference (COMPSAC)*. IEEE, 2020, pp. 808–816.

[95] M. Guri, "Gairoscope: Leaking data from air-gapped computers to nearby smartphones using speakers-to-gyro communication," in *2021 18th International Conference on Privacy, Security and Trust (PST)*. IEEE, 2021, pp. 1–10.

[96] Y. Michalevsky, D. Boneh, and G. Nakibly, "Gyrophone: Recognizing speech from gyroscope signals," in *23rd USENIX Security Symposium (USENIX Security 14)*. San Diego, CA: USENIX Association, Aug. 2014. [Online]. Available: https://www.usenix.org/conference/usenixsecurity14/technical-sessions/presentation/michalevsky pp. 1053–1067.

[97] Z. Ba, T. Zheng, X. Zhang, Z. Qin, B. Li, X. Liu, and K. Ren, "Learning-based practical smartphone eavesdropping with built-in accelerometer," in *Network and Distributed System Security Symposium*, 2020.

[98] J. Han, A. J. Chung, and P. Tague, "Pitchln: eavesdropping via intelligible speech reconstruction using non-acoustic sensor fusion," in *Proceedings of the 16th ACM/IEEE International Conference on Information Processing in Sensor Networks*, 2017, pp. 181–192.

[99] S. A. Anand and N. Saxena, "Speechless: Analyzing the threat to speech privacy from smartphone motion sensors," in *2018 IEEE Symposium on Security and Privacy (SP)*. IEEE, 2018, pp. 1000–1017.

[100] L. Zhang, P. H. Pathak, M. Wu, Y. Zhao, and P. Mohapatra, "Accelword: Energy efficient hotword detection through accelerometer," in *Proceedings of the 13th Annual International Conference on Mobile Systems, Applications, and Services*, 2015, pp. 301–315.

[101] C. Song, F. Lin, Z. Ba, K. Ren, C. Zhou, and W. Xu, "My smartphone knows what you print: Exploring smartphone-based side-channel attacks against 3d printers," in *Proceedings of the 2016 ACM SIGSAC Conference on Computer and Communications Security*, 2016, pp. 895–907.

[102] M. Guri, "Air-viber: Exfiltrating data from air-gapped computers via covert surface vibrations," *preprint arXiv:2004.06195*, 2020.

[103] Murray Associates, "Laser beam eavesdropping – sci-fi bugs?" 2022, [Online; accessed 14-August-2022]. [Online]. Available: https://counterespionage.com/laser-beam-eavesdropping/

[104] Wikipedia contributors, "Photophone — Wikipedia, the free encyclopedia," 2022, [Accessed 16-August-2022]. [Online]. Available: https://en.wikipedia.org/w/index.php?title=Photophone&oldid=1086878337

[105] Wikipedia contributors, "Laser microphone — Wikipedia, the free encyclopedia," 2022, [Accessed 14-August-2022]. [Online]. Available: https://en.wikipedia.org/w/index.php?title=Laser_microphone&oldid=1066626794

[106] R. P. Muscatell, "Laser microphone," *The Journal of the Acoustical Society of America*, vol. 76, no. 4, pp. 1284–1284, 1984.

[107] Detective Store, "Laser listening device - Spectra Laser Microphone M+," 2022, [Accessed 14-August-2022]. [Online]. Available: https://www.detective-store.com/laser-listening-device-spectra-laser-microphone-m-458.html

[108] Bioboy725, "Laser microphone," 2022, [Accessed 14-August-2022]. [Online]. Available: https://www.instructables.com/LASER-MICROPHONE

[109] M. Chounlakone and J. Alverio, "The laser microphone," 2002.

[110] A. Davis, M. Rubinstein, N. Wadhwa, G. Mysore, F. Durand, and W. T. Freeman, "The visual microphone: Passive recovery of sound from video," *ACM Transactions on Graphics (Proc. SIGGRAPH)*, vol. 33, no. 4, pp. 79:1–79:10, 2014.

[111] B. Nassi, Y. Pirutin, R. Swisa, A. Shamir, Y. Elovici, and B. Zadov, "Lamphone: Passive sound recovery from a desk lamp's light bulb vibrations," in *31st USENIX Security Symposium (USENIX Security 22)*. Boston, MA: USENIX Association, Aug. 2022. [Online]. Available: https://www.usenix.org/conference/usenixsecurity22/presentation/nassi pp. 4401–4417.

[112] M. Guri, "Beatcoin: Leaking private keys from air-gapped cryptocurrency wallets," in *2018 IEEE International Conference on Internet of Things (iThings) and IEEE Green Computing and Communications (GreenCom) and IEEE Cyber, Physical and Social Computing (CPSCom) and IEEE Smart Data (SmartData)*. IEEE, 2018, pp. 1308–1316.

[113] M. Guri and Y. Elovici, "Bridgeware: The air-gap malware," *Communications of the ACM*, vol. 61, no. 4, pp. 74–82, 2018.

[114] M. Guri, G. Kedma, A. Kachlon, and Y. Elovici, "Airhopper: Bridging the air-gap between isolated networks and mobile phones using radio frequencies," in *9th International Conference on Malicious and Unwanted Software: The Americas (MALWARE)*. IEEE, 2014, pp. 58–67.

[115] M. Guri, A. Kachlon, O. Hasson, G. Kedma, Y. Mirsky, and Y. Elovici, "GSMem: Data exfiltration from air-gapped computers over GSM frequencies," in *24th USENIX Security Symposium*, 2015, pp. 849–864.

[116] M. Guri, M. Monitz, and Y. Elovici, "USBee: Air-gap covert-channel via electromagnetic emission from USB," in *2016 14th Annual Conference on Privacy, Security and Trust (PST)*. IEEE, 2016, pp. 264–268.

[117] H. Farrukh, T. Yang, H. Xu, Y. Yin, H. Wang, and Z. B. Celik, "S3: Side-channel attack on stylus pencil through sensors," *Proceedings of the ACM on Interactive, Mobile, Wearable and Ubiquitous Technologies*, vol. 5, no. 1, pp. 1–25, 2021.

[118] D. Agrawal, B. Archambeault, J. R. Rao, and P. Rohatgi, "The EM side—channel(s)," in *International Workshop on Cryptographic Hardware and Embedded Systems*. Springer, 2002, pp. 29–45.

[119] P. Cronin, X. Gao, C. Yang, and H. Wang, "Charger-surfing: Exploiting a power line side-channel for smartphone information leakage," in *30th USENIX Security Symposium*, 2021, pp. 681–698.

[120] M. Zhao and G. E. Suh, "FPGA-based remote power side-channel attacks," in *2018 IEEE Symposium on Security and Privacy (SP)*, 2018, pp. 229–244.

[121] M. Guri, B. Zadov, D. Bykhovsky, and Y. Elovici, "Powerhammer: Exfiltrating data from air-gapped computers through power lines," *IEEE Transactions on Information Forensics and Security*, vol. 15, pp. 1879–1890, 2019.

[122] B. Zhao, M. Ni, and P. Fan, "Powermitter: data exfiltration from air-gapped computer through switching power supply," *China Communications*, vol. 15, no. 2, pp. 170–189, 2018.

[123] T. Kim and Y. Shin, "Thermalbleed: A practical thermal side-channel attack," *IEEE Access*, vol. 10, pp. 25 718–25 731, 2022.

[124] M. A. Islam, S. Ren, and A. Wierman, "Exploiting a thermal side channel for power attacks in multi-tenant data centers," in *Proceedings of the 2017 ACM SIGSAC Conference on Computer and Communications Security*, 2017, pp. 1079–1094.

[125] M. Guri, M. Monitz, Y. Mirski, and Y. Elovici, "Bitwhisper: Covert signaling channel between air-gapped computers using thermal manipulations," in *IEEE 28th Computer Security Foundations Symposium*. IEEE, 2015, pp. 276–289.

[126] Eurocodes, "Eurocodes: Building the future," 2008. [Online]. Available: https://eurocodes.jrc.ec.europa.eu/showpage.php?id=13

[127] NFPA, *NFPA Standard for the Installation of Sprinkler Systems*. National Fire Protection Association, 2022. [Online]. Available: https://www.nfpa.org/codes-and-standards/all-codes-and-standards/list-of-codes-and-standards/detail?code=13

[128] ICC, *2018 International Fire Code*. International Code Council, Aug 2017. [Online]. Available: https://www.ci.independence.mo.us/userdocs/ComDev/2018%20INTL%20FIRE%20CODE.pdf

[129] ICC, *2018 International Building Code*. International Code Council, April 2018. [Online]. Available: https://www.iccsafe.org/products-and-services/i-codes/2018-i-codes/ibc

[130] ICC, *2018 International Residential Code*. International Code Council, Sept 2018. [Online]. Available: https://www.iccsafe.org/products-and-services/i-codes/2018-i-codes/irc/

[131] PRC, *Code for design of sprinkler systems: National standard of the People's Republic of China*. Ministry of Housing and Urban-Rural Development of PRC, May 2017. [Online]. Available: https://books.google.com/books/about/GB_50084_2017_Translated_English_of_Chin.html?id=7JNXDwAAQBAJ

[132] NFPA, "Myths vs facts about home fire sprinklers," *NFPA's Fire Sprinkler Initiative*, Dec 2019. [Online]. Available: https://www.nfpa.org/Public-Education/Staying-safe/Safety-equipment/Home-fire-sprinklers/Fire-Sprinkler-Initiative/Take-action/Free-downloads/Myths-vs-facts

[133] J. P. Siegenthaler, "10 things to avoid when designing hydronic heating systems," *Plumbing and Mechanical Engineer*, 2003. [Online]. Available: https://www.pmengineer.com/articles/88321-10-things-to-avoid-when-designing-hydronic-heating-systems

[134] S. Rosen and P. Howell, *Signals and systems for speech and hearing*. Brill, 2011, vol. 29.

[135] S. A. Gelfand, *Essentials of audiology*. Thieme New York, 1997.

[136] D. Purves, G. J. Augustine, D. Fitzpatrick, L. C. Katz, A.-S. LaMantia, J. O. McNamara, and S. M. Williams, "The audible spectrum," *Neuroscience, 6th edition*, 2017.

[137] K. Ashihara, "Hearing thresholds for pure tones above 16 khz," *The Journal of the Acoustical Society of America*, vol. 122, no. 3, pp. EL52–EL57, 2007.

[138] A. Rodríguez Valiente, A. Trinidad, J. García Berrocal, C. Górriz, and R. Ramírez Camacho, "Extended high-frequency (9–20 khz) audiometry reference thresholds in 645 healthy subjects," *International Journal of Audiology*, vol. 53, no. 8, pp. 531–545, 2014.

[139] H. Taub and D. L. Schilling, *Principles of Communication Systems*. McGraw-Hill, 1986.

[140] Jake, "The water-filling algorithm: in-depth explanation," Apr 2022, accessed 2022-11-19. [Online]. Available: https://scicoding.com/water-filling-algorithm-in-depth-explanation/

[141] Jake, "Water-filling algorithm explained and implemented in python," Aug 2021, accessed 2022-11-19. [Online]. Available: https://scicoding.com/waterfilling/

[142] The Motorship: Marine Technology, Noise and vibration attenuation in pipework systems, August 2013, accessed 2022-01-10. [Online]. Available: https://www.motorship.com/noise-and-vibration-attenuation-in-pipework-systems/418141.article

[143] Victaulic Company Inc., Victaulic Couplings Vibration Attenuation Characteristics, Design Data, Publication 26.04, October 2014, last accessed 2022-01-10. [Online]. Available: https://www.victaulic.com/assets/uploads/literature/26.04.pdf

[144] A. Saxena and A. Y. Ng, "Learning sound location from a single microphone," in *2009 IEEE International Conference on Robotics and Automation*. IEEE, 2009, pp. 1737–1742.

[145] A. Das, N. Borisov, and M. Caesar, "Do you hear what I hear? Fingerprinting smart devices through embedded acoustic components," in *Proceedings of the 2014 ACM SIGSAC Conference on Computer and Communications Security*, 2014, pp. 441–452.

[146] K. Chen, S. Lu, and H. Teng, "Adaptive real-time anomaly detection using inductively generated sequential patterns,"," in *Fifth Intrusion Detection Workshop, SRI International, Menlo Park, CA*, 1990.

[147] D. E. Denning, "An intrusion-detection model," *IEEE Transactions on Software Engineering*, no. 2, pp. 222–232, 1987.

[148] F. Djebbar, B. Ayad, K. A. Meraim, and H. Hamam, "Comparative study of digital audio steganography techniques," *EURASIP Journal on Audio, Speech, and Music Processing*, vol. 2012, no. 1, pp. 1–16, 2012.

[149] S. Viswanathan, R. Tan, and D. K. Y. Yau, "Exploiting power grid for accurate and secure clock synchronization in industrial IoT," in *IEEE Real-Time Systems Symposium (RTSS)*, 2016, pp. 146–156.

Appendix A: RESIDENTIAL GAS PIPE MEASUREMENTS (RG)

		Distance	20ft_vol100		30ft_vol100		40ft_vol100	
		Values	Rx_max_freq	Max_rx_mag	Rx_max_freq	Max_rx_mag	Rx_max_freq	Max_rx_mag
Tx_freq	Bandwidth	Attenuation/ft						
100	FALSE	NA	5.00	7.73	0.00	65.87	0.00	52.56
200	FALSE	NA	4.67	10.44	3.00	11.05	1.67	10.10
300	FALSE	NA	2.67	6.81	6.67	8.70	2.00	9.83
400	FALSE	NA	4000.06	13.91	9.33	7.90	3.00	11.36
500	FALSE	NA	4000.06	13.27	3.67	12.30	1.67	10.00
600	FALSE	NA	6.00	11.86	2.33	9.11	9.00	8.51
700	FALSE	NA	1.67	8.36	4200.06	11.42	3.67	12.31
800	FALSE	NA	800.01	15.58	800.01	10.75	2.67	7.97
900	FALSE	NA	1.67	8.07	2.00	9.69	900.01	12.68
1000	FALSE	NA	4000.06	14.55	1000.02	11.17	1000.02	12.10
1100	TRUE	3.13	1100.02	16.33	1100.02	13.27	1100.02	13.20
1200	TRUE	-4.91	1200.02	13.99	1200.02	10.43	1200.02	18.90
1300	TRUE	33.66	1300.02	84.57	1300.02	26.97	1300.02	50.91
1400	FALSE	NA	1.33	8.69	1400.02	28.87	1400.02	30.16
1500	TRUE	17.81	1500.02	30.76	1500.02	12.94	1500.02	12.95
1600	TRUE	14.55	1600.02	48.91	1600.02	110.78	1600.02	34.36
1700	TRUE	45.12	1700.03	88.48	1700.03	156.98	1700.03	43.36
1800	TRUE	162.39	1800.03	185.32	1800.03	117.54	1800.03	22.93
1900	TRUE	-53.62	1900.03	15.09	1900.03	99.01	1900.03	68.71
2000	TRUE	7.22	2000.03	67.35	2000.03	98.72	2000.03	60.12
2100	TRUE	24.72	2100.03	50.43	2100.03	105.68	2100.03	25.71
2200	TRUE	8.98	2200.03	48.43	2200.03	69.66	2200.03	39.45
2300	TRUE	21.49	2300.03	131.52	2300.03	55.96	2300.03	110.03
2400	TRUE	-7.13	2400.04	22.22	2400.04	57.50	2400.04	29.35
2500	TRUE	60.86	2500.04	88.42	2500.04	87.27	2500.04	27.56
2600	FALSE	NA	2600.04	24.39	3.00	9.52	2600.04	32.98
2700	TRUE	92.34	2700.04	120.47	2700.04	109.17	2700.04	28.13
2800	TRUE	-1.58	2800.04	23.44	2800.04	55.57	2800.04	25.02
2900	TRUE	34.97	2900.04	84.69	2900.04	166.04	2900.04	49.72
3000	TRUE	-16.16	3000.05	61.38	3000.05	30.12	3000.05	77.54
3100	TRUE	-45.91	3100.05	38.22	3100.05	24.93	3100.05	84.13
3200	TRUE	37.71	3200.05	110.76	3200.05	87.23	3200.05	73.05
3300	TRUE	-39.74	3300.05	147.15	3300.05	252.91	3300.05	186.88
3400	TRUE	-107.65	3400.05	127.44	3400.05	201.57	3400.05	235.09
3500	TRUE	-17.56	3500.05	207.06	3500.05	411.10	3500.05	224.61
3600	TRUE	-110.38	3600.05	85.33	3600.05	96.80	3600.05	195.72
3700	TRUE	-30.50	3700.06	180.30	3700.06	45.24	3700.06	210.80
3800	TRUE	200.02	3800.06	338.38	3800.06	40.23	3800.06	138.36
3900	TRUE	-305.88	3900.06	720.28	3900.06	125.29	3900.06	1026.16
4000	TRUE	183.00	4000.06	701.69	4000.06	448.65	4000.06	518.69
4100	TRUE	-373.27	4100.06	314.13	4100.06	116.94	4100.06	687.40
4200	TRUE	66.76	4200.06	174.86	4200.06	583.52	4200.06	108.10
4300	TRUE	8.82	4300.07	79.45	4300.07	465.19	4300.07	70.63
4400	TRUE	11.55	4400.07	76.60	4400.07	149.02	4400.07	65.05
4500	TRUE	90.18	4500.07	185.20	4500.07	101.82	4500.07	95.02
4600	TRUE	-110.47	4600.07	218.34	4600.07	349.54	4600.07	328.81
4700	TRUE	-618.52	4700.07	48.96	4700.07	564.38	4700.07	667.48
4800	TRUE	-131.16	4800.07	181.65	4800.07	88.73	4800.07	312.81
4900	TRUE	-516.47	4900.07	73.43	4900.07	318.33	4900.07	589.90
5000	TRUE	-436.56	5000.08	21.40	5000.08	218.74	5000.08	457.95
5100	TRUE	-32.62	5100.08	95.32	5100.08	175.95	5100.08	127.94
5200	TRUE	-586.31	5200.08	28.73	5200.08	211.52	5200.08	615.04
5300	TRUE	-433.27	5300.08	52.91	5300.08	254.16	5300.08	486.18
5400	TRUE	-93.11	5400.08	52.91	5400.08	86.16	5400.08	146.02
5500	TRUE	-78.42	5500.08	34.09	5500.08	115.42	5500.08	112.51
5600	FALSE	NA	2.33	11.44	5600.08	196.91	5600.08	373.78
5700	TRUE	-234.14	5700.09	34.33	5700.09	23.55	5700.09	268.47
5800	TRUE	-391.97	5800.09	58.68	5800.09	81.16	5800.09	450.65
5900	TRUE	-256.52	5900.09	33.28	5900.09	133.74	5900.09	289.80
6000	TRUE	-142.99	6000.09	32.67	6000.09	133.26	6000.09	175.66
6100	TRUE	-169.08	6100.09	41.18	6100.09	85.27	6100.09	210.26
6200	TRUE	5.00	6200.09	39.28	6200.09	52.92	6200.09	34.28
6300	TRUE	-72.02	6300.10	10.66	6300.10	37.34	6300.10	82.67
6400	TRUE	-178.23	6400.10	49.00	6400.10	56.02	6400.10	227.22
6500	TRUE	-83.35	6500.10	97.10	6500.10	73.65	6500.10	180.45
6600	TRUE	-62.67	6600.10	54.45	6600.10	21.40	6600.10	117.11
6700	TRUE	-243.95	6700.10	13.46	6700.10	75.82	6700.10	257.41
6800	TRUE	-143.10	6800.10	44.21	6800.10	25.78	6800.10	187.32
6900	TRUE	4.80	6900.10	36.07	6900.10	18.94	6900.10	31.27
7000	TRUE	3.21	7000.11	37.34	7000.11	90.68	7000.11	34.13
7100	TRUE	125.79	7100.11	232.04	7100.11	77.55	7100.11	106.26
7200	TRUE	-123.31	7200.11	61.00	7200.11	162.13	7200.11	184.31
7300	TRUE	-112.70	7300.11	138.33	7300.11	134.74	7300.11	251.03
7400	TRUE	-24.83	7400.11	55.55	7400.11	33.53	7400.11	80.38
7500	TRUE	-67.24	7500.11	44.51	7500.11	24.77	7500.11	111.75
7600	TRUE	-16.21	7600.11	39.54	7600.11	77.73	7600.11	55.76
7700	TRUE	9.23	7700.12	58.29	7700.12	111.08	7700.12	49.06
7800	TRUE	-48.82	7800.12	168.79	7800.12	88.39	7800.12	217.61

Table A.1: Residential Gas Pipe Peak Signal Frequency and Magnitude. “Bandwidth” column indicates whether the Bandwidth Condition is satisfied

		Distance	20ft_vol100		30ft_vol100		40ft_vol100	
		Values	Rx_max_freq	Max_rx_mag	Rx_max_freq	Max_rx_mag	Rx_max_freq	Max_rx_mag
Tx_freq	Bandwidth	Attenuation/ft						
7900	TRUE	-20.34	7900.12	28.87	7900.12	81.64	7900.12	49.20
8000	TRUE	-7.60	8000.12	42.50	8000.12	19.10	8000.12	50.10
8100	TRUE	86.11	8100.12	109.77	8100.12	35.71	8100.12	23.66
8200	TRUE	78.24	8200.12	128.24	8200.12	74.27	8200.12	50.00
8300	TRUE	36.16	8300.13	66.53	8300.13	127.25	8300.13	30.37
8400	TRUE	-24.72	8400.13	14.23	8400.13	32.38	8400.13	38.95
8500	TRUE	3.01	8500.13	32.80	8500.13	49.65	8500.13	29.79
8600	TRUE	-4.76	8600.13	23.97	8600.13	11.21	8600.13	28.73
8700	TRUE	-23.59	8700.13	18.41	8700.13	62.76	8700.13	42.00
8800	TRUE	8.24	8800.13	52.23	8800.13	60.19	8800.13	43.99
8900	TRUE	16.51	8900.13	46.82	8900.13	54.33	8900.13	30.31
9000	TRUE	24.52	9000.14	93.52	9000.14	74.03	9000.14	69.00
9100	TRUE	-22.26	9100.14	19.74	9100.14	96.15	9100.14	42.00
9200	TRUE	-1.11	9200.14	26.98	9200.14	47.30	9200.14	28.09
9300	TRUE	17.13	9300.14	47.10	9300.14	74.92	9300.14	29.97
9400	TRUE	-49.20	9400.14	16.83	9400.14	85.99	9400.14	66.03
9500	TRUE	39.70	9500.14	52.27	9500.14	80.19	9500.14	12.57
9600	TRUE	1.49	9600.15	46.79	9600.15	43.83	9600.15	45.30
9700	TRUE	-25.85	9699.81	8.10	9700.15	67.57	9700.15	33.94
9800	TRUE	27.06	9800.15	88.96	9800.15	62.29	9800.15	61.90
9900	TRUE	17.41	9900.15	50.78	9900.15	23.86	9900.15	33.37
10000	TRUE	53.84	10000.15	76.39	10000.15	80.77	10000.15	22.54
10100	TRUE	-10.34	10100.15	78.25	10100.15	73.65	10100.15	88.58
10200	TRUE	27.74	10200.15	38.90	10200.15	44.97	10200.15	11.15
10300	TRUE	7.54	10300.16	37.21	10300.16	37.82	10300.16	29.66
10400	TRUE	16.09	10400.16	36.43	10400.16	26.16	10400.16	20.34
10500	TRUE	11.11	10500.16	34.40	10500.16	40.75	10500.16	23.29
10600	TRUE	16.43	10600.16	45.95	10600.16	37.35	10600.16	29.52
10700	TRUE	-23.00	10700.16	25.71	10700.16	28.61	10700.16	48.70
10800	TRUE	15.22	10800.16	32.43	10800.16	22.57	10800.16	17.20
10900	TRUE	-11.13	10900.16	39.82	10900.16	30.87	10900.16	50.95
11000	TRUE	-35.94	11000.17	18.34	11000.17	66.92	11000.17	54.28
11100	TRUE	0.85	11100.17	30.09	11100.17	34.25	11100.17	29.24
11200	TRUE	0.40	11200.17	35.44	11200.17	31.34	11200.17	35.04
11300	TRUE	-1.08	11300.17	28.49	11300.17	34.28	11300.17	29.58
11400	FALSE	NA	11400.17	29.67	11400.17	28.49	2.67	9.52
11500	TRUE	-6.92	11500.17	32.49	11500.17	33.78	11500.17	39.41
11600	TRUE	-1.38	11600.18	28.33	11600.18	36.02	11600.18	29.71
11700	TRUE	-0.63	11700.18	31.61	11700.18	26.22	11700.18	32.25
11800	TRUE	11.21	11800.18	32.50	11800.18	34.67	11800.18	21.29
11900	TRUE	-1.00	11900.18	26.07	11900.18	34.17	11900.18	27.08
12000	TRUE	-6.59	12000.18	33.44	12000.18	27.86	12000.18	40.03
12100	TRUE	0.48	12100.18	31.42	12100.18	32.69	12100.18	30.94
12200	TRUE	3.78	12200.18	32.37	12200.18	30.27	12200.18	28.60
12300	TRUE	2.59	12300.19	33.58	12300.19	34.96	12300.19	30.99
12400	TRUE	-0.56	12400.19	31.81	12400.19	35.64	12400.19	32.37
12500	TRUE	-1.92	12500.19	29.45	12500.19	30.28	12500.19	31.37
12600	TRUE	-0.29	12600.19	31.01	12600.19	32.02	12600.19	31.30
12700	TRUE	1.99	12700.19	32.89	12700.19	31.04	12700.19	30.90
12800	TRUE	1.18	12800.19	29.47	12800.19	31.09	12800.19	28.30
12900	TRUE	0.01	12900.20	31.52	12900.20	31.57	12900.20	31.50
13000	TRUE	-0.55	13000.20	31.02	13000.20	30.84	13000.20	31.57
13100	TRUE	-1.34	13100.20	32.99	13100.20	31.04	13100.20	34.33
13200	TRUE	2.68	13200.20	26.97	13200.20	30.73	13200.20	24.29
13300	TRUE	-1.14	13300.20	31.18	13300.20	30.83	13300.20	32.32
13400	TRUE	-0.08	13400.20	31.32	13400.20	30.77	13400.20	31.41
13500	TRUE	-1.50	13500.20	30.16	13500.20	31.27	13500.20	31.66
13600	TRUE	2.72	13600.21	32.03	13600.21	31.52	13600.21	29.30
13700	TRUE	1.29	13700.21	31.94	13700.21	31.53	13700.21	30.65
13800	TRUE	-1.21	13800.21	30.19	13800.21	32.15	13800.21	31.39
13900	TRUE	3.56	13900.21	33.91	13900.21	31.47	13900.21	30.35
14000	TRUE	-1.36	14000.21	30.73	14000.21	30.78	14000.21	32.09
14100	TRUE	-0.26	14100.21	31.16	14100.21	30.99	14100.21	31.42
14200	TRUE	1.67	14200.21	32.20	14200.21	32.02	14200.21	30.53
14300	TRUE	-0.10	14300.22	31.03	14300.22	31.28	14300.22	31.13
14400	TRUE	0.23	14400.22	31.38	14400.22	31.42	14400.22	31.15
14500	TRUE	1.81	14500.22	32.31	14500.22	31.00	14500.22	30.49
14600	TRUE	0.72	14600.22	31.30	14600.22	31.92	14600.22	30.58
14700	TRUE	0.07	14700.22	31.20	14700.22	31.95	14700.22	31.13
14800	TRUE	-0.45	14800.22	30.31	14800.22	30.56	14800.22	30.77
14900	TRUE	-0.46	14900.23	30.91	14900.23	30.83	14900.23	31.38
15000	TRUE	-0.13	15000.23	31.35	15000.23	31.30	15000.23	31.48
15100	TRUE	0.60	15100.23	32.00	15100.23	31.46	15100.23	31.40
15200	TRUE	0.70	15200.23	30.84	15200.23	32.49	15200.23	30.14
15300	TRUE	-1.06	15300.23	31.34	15300.23	31.64	15300.23	32.40
15400	TRUE	-0.01	15400.23	34.43	15400.23	34.02	15400.23	34.44
15500	TRUE	0.53	15500.23	31.76	15500.23	32.16	15500.23	31.23
15600	TRUE	-1.16	15600.24	30.69	15600.24	31.14	15600.24	31.85

Table A.1: Residential Gas Pipe Peak Signal Frequency and Magnitude. “Bandwidth” column indicates whether the Bandwidth Condition is satisfied (cont.)

		Distance	20ft_vol100		30ft_vol100		40ft_vol100	
		Values	Rx_max_freq	Max_rx_mag	Rx_max_freq	Max_rx_mag	Rx_max_freq	Max_rx_mag
Tx_freq	Bandwidth	Attenuation/ft						
15700	TRUE	-3.56	15700.24	27.58	15700.24	30.73	15700.24	31.14
15800	TRUE	1.55	15800.24	35.14	15800.24	32.19	15800.24	33.59
15900	TRUE	6.87	15900.24	35.98	15900.24	30.74	15900.24	29.11
16000	TRUE	0.20	16000.24	31.81	16000.24	33.80	16000.24	31.61
16100	TRUE	6.02	16100.24	31.61	16100.24	31.34	16100.24	25.59
16200	TRUE	-4.27	16200.24	40.04	16200.24	23.98	16200.24	44.31
16300	TRUE	5.97	16300.25	35.26	16300.25	42.02	16300.25	29.29
16400	TRUE	-0.85	16400.25	35.41	16400.25	31.87	16400.25	36.25
16500	TRUE	5.49	16500.25	44.99	16500.25	28.60	16500.25	39.51
16600	TRUE	-2.47	16600.25	25.33	16600.25	39.62	16600.25	27.79
16700	TRUE	0.44	16700.25	32.58	16700.25	31.05	16700.25	32.14
16800	TRUE	1.08	16800.25	30.73	16800.25	29.97	16800.25	29.65
16900	TRUE	0.04	16900.26	34.38	16900.26	35.43	16900.26	34.35
17000	TRUE	19.14	17000.26	35.02	17000.26	27.21	17000.26	15.88
17100	TRUE	-7.70	17100.26	29.07	17100.26	24.38	17100.26	36.76
17200	TRUE	4.72	17200.26	36.73	17200.26	34.09	17200.26	32.01
17300	TRUE	2.70	17300.26	35.23	17300.26	31.98	17300.26	32.54
17400	TRUE	-6.22	17400.26	25.35	17400.26	32.70	17400.26	31.57
17500	TRUE	2.07	17500.26	34.64	17500.26	34.90	17500.26	32.57
17600	TRUE	-6.97	17600.27	26.79	17600.27	34.08	17600.27	33.75
17700	TRUE	-2.35	17700.27	28.75	17700.27	38.43	17700.27	31.10
17800	TRUE	7.93	17800.27	41.62	17800.27	26.41	17800.27	33.69
17900	TRUE	-1.82	17900.27	28.61	17900.27	32.01	17900.27	30.43
18000	TRUE	6.57	18000.27	37.89	18000.27	32.91	18000.27	31.33
18100	TRUE	-6.85	18100.27	28.87	18100.27	27.88	18100.27	35.72
18200	TRUE	4.06	18200.28	34.27	18200.28	32.40	18200.28	30.21
18300	TRUE	12.42	18300.28	53.36	18300.28	40.44	18300.28	40.94
18400	TRUE	-2.97	18400.28	29.48	18400.28	36.05	18400.28	32.44
18500	TRUE	2.83	18500.28	28.16	18500.28	32.97	18500.28	25.33
18600	TRUE	6.49	18600.28	37.96	18600.28	30.32	18600.28	31.47
18700	FALSE	NA	2.00	12.33	18700.28	40.68	18700.28	32.34
18800	TRUE	12.59	18800.28	43.61	18800.28	39.28	18800.28	31.02
18900	TRUE	-3.18	18900.29	28.93	18900.29	35.74	18900.29	32.11
19000	TRUE	3.84	19000.29	36.75	19000.29	32.18	19000.29	32.91
19100	TRUE	-1.31	19100.29	30.41	19100.29	33.67	19100.29	31.72
19200	TRUE	10.21	19200.29	39.14	19200.29	32.18	19200.29	28.92
19300	TRUE	9.35	19300.29	47.99	19300.29	30.71	19300.29	38.64
19400	TRUE	7.84	19400.29	40.10	19400.29	33.77	19400.29	32.26
19500	TRUE	4.93	19500.29	35.60	19500.29	30.14	19500.29	30.67
19600	TRUE	11.17	19600.30	42.07	19600.30	30.97	19600.30	30.89
19700	TRUE	8.27	19700.30	43.56	19700.30	25.90	19700.30	35.29
19800	TRUE	-16.54	19800.30	23.10	19800.30	25.79	19800.30	39.64
19900	TRUE	15.04	19900.30	48.36	19900.30	33.42	19900.30	33.31
20000	TRUE	-10.53	20000.30	23.09	20000.30	28.47	20000.30	33.62

Table A.1: Residential Gas Pipe Peak Signal Frequency and Magnitude. “Bandwidth” column indicates whether the Bandwidth Condition is satisfied (cont.)

Appendix B: RESIDENTIAL WATER SUPPLY PIPE MEASUREMENTS (RW)

		Distance	20ft_vol100		30ft_vol100		40ft_vol100	
		Values	Rx_max_freq	Max_rx_mag	Rx_max_freq	Max_rx_mag	Rx_max_freq	Max_rx_mag
Tx_freq	Bandwidth	Attenuation/ft						
100	FALSE	NA	1.67	11.15	3.67	8.78	0.67	11.20
200	FALSE	NA	2200.03	15.99	4.33	9.04	2000.03	16.64
300	FALSE	NA	2100.03	25.01	2100.03	12.33	1800.03	18.26
400	FALSE	NA	2400.04	19.34	1.33	11.69	2000.03	39.31
500	FALSE	NA	2500.04	33.18	8.00	7.20	2000.03	44.00
600	FALSE	NA	3000.05	12.09	1800.03	17.39	1800.03	78.59
700	FALSE	NA	2100.03	91.38	2100.03	45.85	2100.03	31.22
800	FALSE	NA	2400.04	119.98	2400.04	37.08	2400.04	40.29
900	FALSE	NA	900.01	29.03	900.01	12.28	1800.03	201.69
1000	FALSE	NA	2000.03	25.96	1000.02	9.43	2000.03	190.26
1100	FALSE	NA	2200.03	33.03	5.00	8.45	2200.03	111.84
1200	FALSE	NA	2400.04	50.47	1200.02	59.63	2400.04	69.20
1300	FALSE	NA	1300.02	153.47	1300.02	60.27	2600.04	126.79
1400	TRUE	-31.83	1400.02	107.19	1400.02	68.21	1400.02	139.02
1500	FALSE	NA	3000.05	12.46	1500.02	17.53	1500.02	43.63
1600	TRUE	61.79	1600.02	143.72	1600.02	79.95	1600.02	81.94
1700	TRUE	-395.01	1700.03	82.25	1700.03	106.23	1700.03	477.26
1800	TRUE	-1142.04	1800.03	232.70	1800.03	326.97	1800.03	1374.75
1900	TRUE	-942.84	1900.03	847.78	1900.03	1072.57	1900.03	1790.63
2000	TRUE	-298.68	2000.03	939.79	2000.03	345.21	2000.03	1238.47
2100	TRUE	1426.77	2100.03	1783.18	2100.03	856.19	2100.03	356.42
2200	TRUE	575.42	2200.03	1088.45	2200.03	139.51	2200.03	513.03
2300	TRUE	760.55	2300.03	897.25	2300.03	229.60	2300.03	136.70
2400	TRUE	1690.04	2400.04	2145.47	2400.04	691.44	2400.04	455.42
2500	TRUE	802.79	2500.04	1736.79	2500.04	187.54	2500.04	934.00
2600	TRUE	-721.55	2600.04	171.23	2600.04	131.98	2600.04	892.78
2700	TRUE	-210.80	2700.04	263.52	2700.04	217.66	2700.04	474.32
2800	TRUE	-81.59	2800.04	158.94	2800.04	337.90	2800.04	240.53
2900	TRUE	-57.19	2900.04	619.71	2900.04	620.42	2900.04	676.90
3000	TRUE	316.48	3000.05	480.75	3000.05	119.26	3000.05	164.26
3100	TRUE	509.59	3100.05	730.01	3100.05	140.93	3100.05	220.42
3200	TRUE	213.29	3200.05	360.23	3200.38	27.30	3200.05	146.93
3300	TRUE	212.21	3300.05	309.95	3300.05	33.89	3300.05	97.74
3400	TRUE	129.03	3400.05	328.13	3400.05	88.81	3400.05	199.10
3500	TRUE	30.08	3500.05	135.47	3500.39	9.72	3500.05	105.39
3600	TRUE	52.99	3600.05	131.81	3600.05	31.67	3600.05	78.82
3700	TRUE	352.64	3700.06	499.33	3700.06	28.02	3700.06	146.69
3800	TRUE	35.09	3800.06	90.70	3800.06	60.96	3800.06	55.61
3900	TRUE	43.19	3900.06	57.12	3900.06	38.01	3900.06	13.92
4000	TRUE	177.01	4000.06	452.95	4000.06	527.56	4000.06	275.93
4100	TRUE	47.39	4100.06	229.18	4100.06	128.35	4100.06	181.78
4200	TRUE	183.23	4200.06	279.98	4200.06	197.59	4200.06	96.75
4300	TRUE	216.89	4300.07	239.61	4300.07	52.16	4300.07	22.71
4400	TRUE	114.01	4400.07	218.32	4400.07	57.34	4400.07	104.31
4500	TRUE	49.03	4500.07	111.53	4500.07	33.82	4500.07	62.49
4600	TRUE	76.16	4600.07	187.16	4600.07	50.11	4600.07	111.01
4700	TRUE	92.89	4700.07	218.33	4700.07	157.10	4700.07	125.44
4800	FALSE	NA	4800.07	347.43	2.67	10.04	4800.07	90.88
4900	TRUE	129.40	4900.07	177.76	4900.07	129.68	4900.07	48.36
5000	TRUE	0.78	5000.08	48.83	5000.08	56.87	5000.08	48.05
5100	TRUE	161.66	5100.08	209.56	5100.08	44.77	5100.08	47.90
5200	TRUE	143.83	5200.08	168.43	5200.08	117.12	5200.08	24.60
5300	TRUE	133.49	5300.08	191.89	5300.08	71.97	5300.08	58.40
5400	TRUE	69.30	5400.08	107.28	5400.08	45.84	5400.08	37.98
5500	TRUE	214.13	5500.08	228.72	5500.08	41.39	5500.08	14.60
5600	TRUE	27.11	5600.08	71.19	5600.08	57.75	5600.08	44.07
5700	TRUE	32.62	5700.09	77.16	5700.09	28.98	5700.09	44.55
5800	TRUE	30.41	5800.09	67.88	5800.09	13.65	5800.09	37.47
5900	TRUE	-3.83	5900.09	18.21	5900.09	40.12	5900.09	22.04
6000	TRUE	-10.91	6000.09	25.22	6000.09	82.37	6000.09	36.13

Table B.1: Residential Water Supply Pipe Peak Signal Frequency and Magnitude. “Bandwidth” column indicates whether the Bandwidth Condition is satisfied

		Distance	20ft_vol100		30ft_vol100		40ft_vol100	
		Values	Rx_max_freq	Max_rx_mag	Rx_max_freq	Max_rx_mag	Rx_max_freq	Max_rx_mag
Tx_freq	Bandwidth	Attenuation/ft						
6100	TRUE	11.95	6100.09	53.32	6100.09	57.13	6100.09	41.37
6200	TRUE	39.41	6200.09	81.82	6200.09	59.28	6200.09	42.41
6300	TRUE	14.87	6300.10	73.92	6300.10	43.61	6300.10	59.05
6400	TRUE	44.42	6400.10	119.07	6400.10	24.43	6400.10	74.65
6500	TRUE	92.49	6500.10	116.76	6500.10	42.74	6500.10	24.27
6600	TRUE	-20.50	6600.10	8.54	6600.10	86.74	6600.10	29.04
6700	TRUE	11.76	6700.10	53.02	6700.10	69.81	6700.10	41.26
6800	TRUE	78.37	6800.10	109.20	6800.10	49.70	6800.10	30.84
6900	TRUE	22.58	6900.10	70.12	6900.10	55.90	6900.10	47.54
7000	TRUE	-3.72	7000.11	41.24	7000.11	72.54	7000.11	44.96
7100	TRUE	106.12	7100.11	163.33	7100.11	44.88	7100.11	57.21
7200	TRUE	2.23	7200.11	13.52	7200.11	68.35	7200.11	11.29
7300	TRUE	1.48	7300.11	56.13	7300.11	33.28	7300.11	54.65
7400	FALSE	NA	7400.11	34.95	7400.11	91.14	7.33	6.66
7500	TRUE	82.70	7500.11	134.55	7500.11	38.21	7500.11	51.84
7600	TRUE	51.07	7600.11	102.44	7600.11	98.60	7600.11	51.37
7700	TRUE	75.20	7700.12	99.71	7700.12	17.72	7700.12	24.50
7800	TRUE	45.86	7800.12	111.71	7800.12	79.26	7800.12	65.85
7900	TRUE	142.05	7900.12	182.59	7900.12	145.65	7900.12	40.53
8000	TRUE	181.09	8000.12	220.34	8000.12	49.28	8000.12	39.25
8100	TRUE	70.28	8100.12	117.57	8100.12	131.49	8100.12	47.28
8200	TRUE	9.89	8200.12	81.65	8200.12	42.18	8200.12	71.76
8300	FALSE	NA	8300.13	59.63	8300.13	123.21	3.00	9.70
8400	TRUE	96.58	8400.13	125.91	8400.13	86.62	8400.13	29.33
8500	TRUE	33.03	8500.13	87.81	8500.13	30.26	8500.13	54.78
8600	TRUE	-17.64	8600.13	95.78	8600.13	99.02	8600.13	113.42
8700	TRUE	58.52	8700.13	108.34	8700.13	40.59	8700.13	49.82
8800	TRUE	237.86	8800.13	301.58	8800.13	103.98	8800.13	63.72
8900	TRUE	-12.84	8900.13	18.21	8900.13	37.79	8900.13	31.05
9000	TRUE	48.79	9000.14	102.96	9000.14	98.18	9000.14	54.17
9100	TRUE	1.05	9100.14	85.31	9100.14	70.64	9100.14	84.26
9200	FALSE	NA	9200.14	134.85	5.67	11.46	9200.14	33.84
9300	TRUE	-7.46	9300.14	74.18	9300.14	46.22	9300.14	81.64
9400	TRUE	-10.69	9400.14	23.55	9400.14	32.81	9400.14	34.24
9500	TRUE	-24.08	9500.14	17.98	9500.14	38.59	9500.14	42.06
9600	TRUE	-7.59	9600.15	24.12	9600.15	24.58	9600.15	31.71
9700	TRUE	-53.10	9700.15	58.16	9700.15	11.06	9700.15	111.26
9800	TRUE	19.12	9800.15	58.28	9800.15	13.76	9800.15	39.15
9900	TRUE	32.70	9900.15	68.64	9900.15	38.23	9900.15	35.94
10000	TRUE	0.83	10000.15	23.95	10000.15	41.73	10000.15	23.11
10100	TRUE	23.20	10100.15	52.83	10100.15	35.58	10100.15	29.63
10200	TRUE	14.25	10200.15	45.63	10200.15	28.24	10200.15	31.38
10300	FALSE	NA	3.33	12.14	10300.16	28.92	10300.16	32.25
10400	TRUE	71.17	10400.16	110.30	10400.16	22.96	10400.16	39.13
10500	TRUE	18.55	10500.16	60.41	10500.16	29.00	10500.16	41.86
10600	TRUE	-12.42	10600.16	14.99	10600.16	30.54	10600.16	27.42
10700	TRUE	10.87	10700.16	41.76	10700.16	30.50	10700.16	30.89
10800	TRUE	12.08	10800.16	46.96	10800.16	26.22	10800.16	34.88
10900	TRUE	-6.35	10900.16	22.43	10900.16	32.01	10900.16	28.78
11000	TRUE	8.51	11000.17	38.65	11000.17	30.80	11000.17	30.14
11100	TRUE	3.58	11100.17	34.78	11100.17	30.02	11100.17	31.19
11200	TRUE	-1.93	11200.17	29.49	11200.17	33.17	11200.17	31.42
11300	TRUE	-1.62	11300.17	27.21	11300.17	32.10	11300.17	28.83
11400	TRUE	5.26	11400.17	35.01	11400.17	32.03	11400.17	29.75
11500	TRUE	-4.24	11500.17	27.15	11500.17	30.97	11500.17	31.38
11600	TRUE	4.46	11600.18	36.98	11600.18	30.13	11600.18	32.52
11700	TRUE	-5.17	11700.18	26.75	11700.18	29.59	11700.18	31.92
11800	TRUE	0.75	11800.18	33.27	11800.18	31.81	11800.18	32.52
11900	TRUE	0.64	11900.18	30.76	11900.18	31.15	11900.18	30.11
12000	TRUE	0.97	12000.18	30.92	12000.18	31.98	12000.18	29.96

Table B.1: Residential Water Supply Pipe Peak Signal Frequency and Magnitude. "Bandwidth" column indicates whether the Bandwidth Condition is satisfied (cont.)

		Distance	20ft_vol100		30ft_vol100		40ft_vol100	
		Values	Rx_max_freq	Max_rx_mag	Rx_max_freq	Max_rx_mag	Rx_max_freq	Max_rx_mag
Tx_freq	Bandwidth	Attenuation/ft						
12100	TRUE	0.84	12100.18	31.24	12100.18	29.63	12100.18	30.40
12200	TRUE	8.34	12200.18	38.44	12200.18	30.26	12200.18	30.10
12300	TRUE	-2.30	12300.19	26.93	12300.19	32.61	12300.19	29.23
12400	TRUE	1.53	12400.19	35.86	12400.19	32.75	12400.19	34.34
12500	TRUE	-0.49	12500.19	30.63	12500.19	30.51	12500.19	31.13
12600	TRUE	1.26	12600.19	33.54	12600.19	31.16	12600.19	32.28
12700	TRUE	-3.46	12700.19	28.62	12700.19	29.37	12700.19	32.09
12800	TRUE	3.44	12800.19	34.84	12800.19	29.98	12800.19	31.40
12900	TRUE	2.19	12900.20	34.44	12900.20	31.14	12900.20	32.25
13000	TRUE	7.06	13000.20	38.69	13000.20	31.03	13000.20	31.63
13100	TRUE	-4.56	13100.20	27.34	13100.20	30.48	13100.20	31.90
13200	TRUE	5.03	13200.20	35.71	13200.20	31.74	13200.20	30.68
13300	TRUE	0.48	13300.20	32.31	13300.20	32.51	13300.20	31.83
13400	TRUE	-0.78	13400.20	32.63	13400.20	29.95	13400.20	33.40
13500	TRUE	5.24	13500.20	36.97	13500.20	30.42	13500.20	31.73
13600	TRUE	5.67	13600.21	37.74	13600.21	33.34	13600.21	32.07
13700	TRUE	-1.74	13700.21	31.18	13700.21	31.20	13700.21	32.91
13800	TRUE	4.58	13800.21	35.52	13800.21	28.36	13800.21	30.94
13900	TRUE	-2.50	13900.21	30.11	13900.21	30.41	13900.21	32.60
14000	TRUE	5.63	14000.21	37.52	14000.21	31.91	14000.21	31.89
14100	TRUE	-0.82	14100.21	31.18	14100.21	32.26	14100.21	32.00
14200	TRUE	1.62	14200.21	33.96	14200.21	32.15	14200.21	32.34
14300	TRUE	1.62	14300.22	33.47	14300.22	31.30	14300.22	31.85
14400	TRUE	0.24	14400.22	32.05	14400.22	31.05	14400.22	31.81
14500	TRUE	0.24	14500.22	32.11	14500.22	31.81	14500.22	31.87
14600	TRUE	2.37	14600.22	34.06	14600.22	33.62	14600.22	31.69
14700	TRUE	-1.55	14700.22	30.17	14700.22	30.99	14700.22	31.72
14800	TRUE	-1.85	14800.22	29.88	14800.22	32.18	14800.22	31.73
14900	TRUE	1.16	14900.23	32.47	14900.23	32.00	14900.23	31.31
15000	TRUE	-1.05	15000.23	30.71	15000.23	33.70	15000.23	31.75
15100	TRUE	0.63	15100.23	32.63	15100.23	30.39	15100.23	32.00
15200	TRUE	-2.30	15200.23	30.25	15200.23	29.86	15200.23	32.55
15300	TRUE	-1.49	15300.23	30.98	15300.23	29.81	15300.23	32.48
15400	TRUE	1.38	15400.23	33.66	15400.23	32.36	15400.23	32.28
15500	TRUE	1.43	15500.23	35.00	15500.23	31.25	15500.23	33.57
15600	TRUE	-6.16	15600.24	25.14	15600.24	34.31	15600.24	31.30
15700	TRUE	-3.55	15700.24	29.51	15700.24	32.56	15700.24	33.06
15800	TRUE	1.14	15800.24	35.45	15800.24	31.49	15800.24	34.31
15900	TRUE	4.37	15900.24	36.04	15900.24	37.29	15900.24	31.67
16000	TRUE	-1.55	16000.24	29.96	16000.24	34.34	16000.24	31.51
16100	TRUE	-0.61	16100.24	32.02	16100.24	29.82	16100.24	32.63
16200	TRUE	1.39	16200.24	33.66	16200.24	30.49	16200.24	32.27
16300	TRUE	-9.51	16300.25	25.59	16300.25	30.07	16300.25	35.10
16400	TRUE	-2.93	16400.25	32.62	16400.25	28.32	16400.25	35.56
16500	TRUE	-3.80	16500.25	31.68	16500.25	35.43	16500.25	35.49
16600	TRUE	4.57	16600.25	37.51	16600.25	40.69	16600.25	32.95
16700	TRUE	-3.33	16700.25	29.75	16700.25	30.14	16700.25	33.09
16800	TRUE	1.37	16800.25	35.65	16800.25	26.53	16800.25	34.28
16900	TRUE	5.03	16900.26	37.47	16900.26	33.76	16900.26	32.44
17000	TRUE	-4.24	17000.26	29.70	17000.26	30.64	17000.26	33.93
17100	TRUE	5.60	17100.26	39.16	17100.26	33.99	17100.26	33.56
17200	TRUE	1.73	17200.26	36.23	17200.26	24.80	17200.26	34.50
17300	TRUE	-0.67	17300.26	32.49	17300.26	32.20	17300.26	33.16
17400	TRUE	1.11	17400.26	34.00	17400.26	34.15	17400.26	32.89
17500	TRUE	3.85	17500.26	35.58	17500.26	34.22	17500.26	31.73
17600	TRUE	0.14	17600.27	31.81	17600.27	33.73	17600.27	31.67
17700	TRUE	2.94	17700.27	35.42	17700.27	31.83	17700.27	32.48
17800	TRUE	-6.55	17800.27	28.07	17800.27	32.94	17800.27	34.61
17900	TRUE	2.67	17900.27	33.38	17900.27	33.14	17900.27	30.71
18000	TRUE	3.34	18000.27	34.80	18000.27	33.79	18000.27	31.47

Table B.1: Residential Water Supply Pipe Peak Signal Frequency and Magnitude. “Bandwidth” column indicates whether the Bandwidth Condition is satisfied (cont.)

		Distance	20ft_vol100		30ft_vol100		40ft_vol100	
		Values	Rx_max_freq	Max_rx_mag	Rx_max_freq	Max_rx_mag	Rx_max_freq	Max_rx_mag
Tx_freq	Bandwidth	Attenuation/ft						
18100	TRUE	5.35	18100.27	38.85	18100.27	29.29	18100.27	33.50
18200	TRUE	-11.35	18200.28	26.45	18200.28	34.30	18200.28	37.80
18300	TRUE	6.62	18300.28	39.65	18300.28	29.50	18300.28	33.03
18400	TRUE	0.81	18400.28	33.82	18400.28	32.95	18400.28	33.01
18500	TRUE	-3.80	18500.28	29.29	18500.28	30.87	18500.28	33.10
18600	TRUE	-1.12	18600.28	32.11	18600.28	32.16	18600.28	33.23
18700	TRUE	0.46	18700.28	32.50	18700.28	35.53	18700.28	32.04
18800	TRUE	-1.23	18800.28	32.05	18800.28	32.86	18800.28	33.28
18900	TRUE	5.21	18900.29	36.50	18900.29	31.07	18900.29	31.29
19000	TRUE	4.80	19000.29	36.21	19000.29	33.47	19000.29	31.40
19100	TRUE	1.86	19100.29	33.86	19100.29	35.91	19100.29	32.01
19200	TRUE	-1.08	19200.29	34.94	19200.29	33.73	19200.29	36.01
19300	TRUE	-2.61	19300.29	32.25	19300.29	30.64	19300.29	34.86
19400	TRUE	-0.85	19400.29	26.06	19400.29	31.67	19400.29	26.91
19500	TRUE	-0.09	19500.29	32.78	19500.29	35.79	19500.29	32.87
19600	TRUE	-2.46	19600.30	29.89	19600.30	33.37	19600.30	32.35
19700	TRUE	5.66	19700.30	37.21	19700.30	29.73	19700.30	31.55
19800	TRUE	-2.76	19800.30	26.20	19800.30	30.96	19800.30	28.96
19900	TRUE	5.90	19900.30	31.07	19900.30	31.06	19900.30	25.17

Table B.1: Residential Water Supply Pipe Peak Signal Frequency and Magnitude. “Bandwidth” column indicates whether the Bandwidth Condition is satisfied (cont.)

Appendix C: OLD COMMERCIAL WET SPRINKLER PIPE MEASUREMENTS (OCS)

		Distance	20ft_vol100		40ft_vol100		60ft_vol100		80ft_vol100		100ft_vol100		120ft_vol100		170ft_vol100	
		Values	Rx_max_freq	Max_rx_mag	Rx_max_freq	Max_rx_mag	Rx_max_freq	Max_rx_mag	Rx_max_freq	Max_rx_mag	Rx_max_freq	Max_rx_mag	Rx_max_freq	Max_rx_mag	Rx_max_freq	Max_rx_mag
Tx_freq	Bandwidth	Attenuation/ft														
100	FALSE	NA	1.33	11.38	4.33	10.30	3.67	8.91	1.00	12.56	4.67	11.31	3.00	9.60	4.00	10.82
200	FALSE	NA	2200.03	11.10	5.33	7.93	6.00	9.72	2.33	8.13	2.67	5.83	2.67	8.59	2.33	11.73
300	FALSE	NA	4.33	10.36	2.33	10.43	2.67	7.96	6.00	9.48	3.67	11.71	7.67	8.40	1.67	10.05
400	FALSE	NA	6.00	8.24	4.67	10.45	8.00	9.38	2.00	9.26	1.67	7.50	4.33	10.46	1.00	8.38
500	FALSE	NA	1.33	8.97	2.00	9.89	1.00	9.54	2.67	8.45	3.00	8.98	1.67	10.94	2.67	11.09
600	FALSE	NA	5.33	10.22	2.00	13.82	2.33	14.38	3.67	7.55	4.33	9.33	4.00	9.92	600.01	6.86
700	FALSE	NA	2100.03	16.60	4.33	9.73	3.67	11.43	2.67	10.97	2.33	8.91	2100.03	11.58	2.33	9.75
800	FALSE	NA	800.01	14.97	800.01	9.97	1600.02	9.54	2.33	11.76	800.01	9.32	800.01	9.45	3.33	11.27
900	FALSE	NA	900.01	13.90	900.01	13.12	900.01	13.14	5.00	8.96	900.01	15.84	4.33	12.93	900.01	10.17
1000	FALSE	NA	1000.02	12.83	1000.02	12.85	2000.03	14.97	1000.02	12.28	1000.02	12.19	1000.02	11.55	1000.02	10.32
1100	FALSE	NA	2200.03	50.41	1100.02	12.33	1100.02	17.40	1100.02	13.16	1100.02	11.85	1100.02	11.33	1100.02	12.69
1200	FALSE	NA	1200.02	16.17	1200.02	16.57	1200.02	18.41	1200.02	11.02	1200.02	11.92	1200.02	11.85	1.67	13.67
1300	TRUE	36.88	1300.02	49.00	1300.02	14.54	1300.02	53.32	1300.02	17.76	1300.02	12.81	1300.02	12.67	1300.02	12.12
1400	TRUE	0.31	1400.02	19.79	1400.02	11.80	1400.02	30.63	1400.02	10.54	1400.02	15.34	1400.02	14.07	1400.02	19.48
1500	FALSE	NA	1500.02	23.11	1500.02	16.15	1.67	9.99	1500.02	18.00	1500.02	17.40	1500.02	17.55	1500.02	13.33
1600	FALSE	NA	1600.02	52.46	1600.02	18.91	1600.02	72.53	1600.02	22.04	1.67	10.93	1600.02	18.36	1600.02	43.89
1700	TRUE	166.52	1700.03	180.57	1700.03	14.08	1700.03	59.44	1700.03	33.22	1700.03	15.57	1700.03	21.70	1700.03	14.05
1800	TRUE	60.12	1800.03	86.00	1800.03	27.97	1800.03	45.01	1800.03	69.81	1800.03	33.63	1800.03	64.42	1800.03	25.88
1900	TRUE	171.53	1900.03	216.12	1900.03	63.98	1900.03	383.30	1900.03	101.10	1900.03	93.59	1900.03	44.61	1900.03	44.59
2000	TRUE	49.16	2000.03	138.85	2000.03	49.17	2000.03	187.87	2000.03	162.21	2000.03	95.53	2000.03	230.92	2000.03	89.68
2100	TRUE	312.69	2100.03	326.38	2100.03	138.93	2100.03	109.02	2100.03	136.50	2100.03	170.86	2100.03	219.78	2100.03	13.69
2200	TRUE	547.51	2200.03	571.35	2200.03	15.96	2200.03	267.63	2200.03	273.79	2200.03	56.81	2200.03	218.45	2200.03	23.84
2300	TRUE	635.61	2300.03	672.81	2300.03	283.96	2300.03	641.45	2300.03	30.21	2300.03	40.70	2300.03	237.41	2300.03	37.19
2400	TRUE	167.42	2400.04	198.03	2400.04	42.26	2400.04	56.69	2400.04	53.30	2400.04	38.24	2400.04	37.50	2400.04	30.61
2500	TRUE	182.01	2500.04	207.42	2500.04	18.15	2500.04	39.48	2500.04	13.07	2500.04	66.49	2500.04	19.64	2500.04	25.41
2600	TRUE	154.42	2600.04	195.48	2600.04	188.57	2600.04	70.97	2600.04	89.02	2600.04	24.55	2600.04	70.95	2600.04	41.06
2700	TRUE	80.83	2700.04	137.53	2700.04	58.67	2700.04	57.86	2700.04	47.88	2700.04	38.49	2700.04	46.33	2700.04	56.70
2800	TRUE	-4.64	2800.04	25.83	2800.04	22.38	2800.04	63.10	2800.04	49.53	2800.04	28.64	2800.04	34.65	2800.04	30.47
2900	TRUE	25.32	2900.04	97.79	2900.04	89.75	2900.04	25.86	2900.04	56.39	2900.04	114.05	2900.04	26.23	2900.04	72.47
3000	TRUE	-7.63	3000.05	25.74	3000.05	96.34	3000.05	33.00	3000.05	72.24	3000.05	13.82	3000.05	72.65	3000.05	33.38
3100	TRUE	63.86	3100.05	181.28	3100.05	135.94	3100.05	62.25	3100.05	93.65	3100.05	138.11	3100.05	183.83	3100.05	117.42
3200	TRUE	64.18	3200.05	94.02	3200.05	24.35	3200.05	178.78	3200.05	40.70	3200.05	66.20	3200.05	49.41	3200.05	29.83
3300	TRUE	104.77	3300.05	126.88	3300.05	80.74	3300.05	318.81	3300.05	43.45	3300.05	98.57	3300.05	86.28	3300.05	22.11
3400	TRUE	102.09	3400.05	141.82	3400.05	326.01	3400.05	101.76	3400.05	190.88	3400.05	209.16	3400.05	126.54	3400.05	39.73
3500	TRUE	90.44	3500.05	154.11	3500.05	83.84	3500.05	92.08	3500.05	204.04	3500.05	108.07	3500.05	52.37	3500.05	63.67
3600	TRUE	41.16	3600.05	54.46	3600.05	223.03	3600.05	59.90	3600.05	211.92	3600.05	54.51	3600.05	42.27	3599.72	13.30
3700	TRUE	15.83	3700.06	61.72	3700.06	124.95	3700.06	43.86	3700.06	223.79	3700.06	46.98	3700.06	46.02	3700.06	45.89
3800	TRUE	148.41	3800.06	177.53	3800.06	159.98	3800.06	154.36	3800.06	358.14	3800.06	242.76	3800.06	88.40	3800.06	29.12
3900	TRUE	41.29	3900.06	59.71	3900.06	39.59	3900.06	76.83	3900.06	177.97	3900.06	76.92	3900.06	66.80	3900.06	18.42
4000	TRUE	30.46	4000.06	55.00	4000.06	94.87	4000.06	73.23	4000.06	42.36	4000.06	72.56	4000.06	102.13	4000.06	24.54
4100	TRUE	74.65	4100.06	96.69	4100.06	172.32	4100.06	41.07	4100.06	124.40	4100.06	198.34	4100.06	104.06	4100.06	22.04
4200	TRUE	52.02	4200.06	106.94	4200.06	95.00	4200.06	214.91	4200.06	94.54	4200.06	127.71	4200.06	97.48	4200.06	54.93
4300	TRUE	-49.33	4300.07	14.66	4300.07	70.11	4300.07	157.19	4300.07	31.75	4300.07	61.01	4300.07	143.85	4300.07	63.99
4400	TRUE	-4.14	4400.07	42.75	4400.07	70.93	4400.07	226.66	4400.07	46.92	4400.07	51.57	4400.07	70.09	4400.07	46.89
4500	TRUE	184.63	4500.07	227.52	4500.07	156.93	4500.07	211.00	4500.07	86.15	4500.07	31.07	4500.07	102.24	4500.07	42.90
4600	TRUE	142.82	4600.07	159.26	4600.07	67.39	4600.07	460.80	4600.07	74.62	4600.07	38.72	4600.07	17.33	4600.07	16.44
4700	TRUE	554.47	4700.07	616.86	4700.07	69.71	4700.07	676.39	4700.07	53.42	4700.07	31.69	4700.07	20.75	4700.07	62.39
4800	TRUE	433.66	4800.07	463.77	4800.07	12.06	4800.07	511.08	4800.07	27.41	4800.07	31.80	4800.07	32.01	4800.07	30.11
4900	TRUE	354.17	4900.07	371.01	4900.07	87.52	4900.07	362.62	4900.07	38.45	4900.07	90.35	4900.07	41.04	4900.07	16.84
5000	TRUE	73.90	5000.08	93.90	5000.08	56.26	5000.08	132.29	5000.08	86.05	5000.08	138.39	5000.08	22.71	5000.08	20.00
5100	TRUE	347.44	5100.08	381.40	5100.08	56.43	5100.08	243.04	5100.08	44.25	5100.08	26.06	5100.08	26.79	5100.08	33.95
5200	TRUE	149.46	5200.08	165.81	5200.08	83.62	5200.08	302.80	5200.08	44.63	5200.08	85.96	5200.08	35.86	5200.08	16.35
5300	TRUE	-3.68	5300.08	22.01	5300.08	113.38	5300.08	141.82	5300.08	49.21	5300.08	31.26	5300.08	24.50	5300.08	25.70
5400	FALSE	NA	5400.08	145.87	5400.08	62.48	5400.08	99.56	5400.08	18.66	1.67	8.14	5400.08	37.03	5400.08	24.30
5500	TRUE	34.95	5500.08	68.16	5500.08	67.95	5500.08	31.72	5500.08	43.79	5500.08	76.00	5500.08	26.39	5500.08	33.21
5600	TRUE	84.44	5600.08	109.83	5600.08	37.82	5600.08	28.48	5600.08	24.25	5600.08	59.88	5600.08	25.49	5600.08	25.40
5700	TRUE	13.24	5700.09	46.19	5700.09	61.33	5700.09	33.27	5700.09	26.01	5700.09	69.35	5700.09	27.16	5700.09	32.95
5800	TRUE	30.14	5800.09	58.65	5800.09	70.65	5800.09	29.13	5800.09	31.56	5800.09	21.16	5800.09	26.31	5800.09	28.51
5900	TRUE	29.92	5900.09	55.99	5900.09	44.17	5900.09	19.26	5900.09	33.39	5900.09	49.51	5900.09	22.45	5900.09	26.07
6000	TRUE	-0.46	6000.09	29.04	6000.09	36.36	6000.09	42.84	6000.09	25.79	6000.09	38.97	6000.09	23.66	6000.09	29.49
6100	TRUE	18.48	6100.09	49.86	6100.09	22.74	6100.09	45.60	6100.09	21.23	6100.09	17.35	6100.09	39.08	6100.09	31.38
6200	TRUE	22.06	6200.09	52.31	6200.09	27.27	6200.09	32.24	6200.09	36.86	6200.09	23.76	6200.09	26.48	6200.09	30.25
6300	TRUE	22.70	6300.10	54.44	6300.10	22.35	6300.10	37.83	6300.10	52.88	6300.10	40.97	6300.10	53.74	6300.10	31.74
6400	TRUE	35.32	6400.10	70.82	6400.10	53.43	6400.10	45.61	6400.10	25.25	6400.10	44.78	6400.10	46.20	6400.10	35.49
6500	TRUE	3.78	6500.10	32.67	6500.10	20.84	6500.10	32.40	6500.10	23.01	6500.10	37.16	6500.10	18.14	6500.10	28.89
6600	TRUE	19.25	6600.10	45.99	6600.10	35.71	6600.10	37.76	6600.10	24.52	6600.10	18.99	6600.10	43.95	6600.10	26.74
6700	TRUE	0.18	6700.10	29.22	6700.10	24.74	6700.10	29.77	6700.10	27.19	6700.10	39.39	6700.10	33.55	6700.10	29.05
6800	TRUE	3.39	6800.10	31.79	6800.10	24.15	6800.10	27.31	6800.10	30.62	6800.10	14.57	6800.10	18.30	6800.10	28.41
6900	TRUE	13.95	6900.10	43.31	6900.10	53.21	6900.10	25.95	6900.10	28.63	6900.10	26.55	6900.10	30.57	6900.10	29.36
7000	TRUE	12.09	7000.11	41.83	7000.11	9.84	7000.11	31.88	7000.11	23.21	7000.11	29.39	7000.11	25.80	7000.11	29.74
7100	TRUE	21.92	7100.11	52.43	7100.11	35.83	7100.11	41.74	7100.11	29.97	7100.11	23.33	7100.11	26.63	7100.11	30.51
7200	TRUE	34.40	7200.11	57.29	7200.11	47.79	7200.11	35.65	7200.11	28.78	7200.11	26.22	7200.11	28.28	7200.11	22.89
7300	FALSE	NA	7300.11	35.58	4.67	10.29	7300.11	49.93	7300.11	28.79	7300.11	32.66	7300.11	31.02	7300.11	29.62
7400	FALSE	NA	4.33	9.53	7400.11	48.20	7400.11	45.50	7400.11	28.86	7400.11	30.07	7400.11	33.57	7400.11	28.73
7500	TRUE	23.44	7500.11	53.26	7500.11	21.01	7500.11	56.36	7500.11	28.56	7500.11	32.25	7500.11	27.31	7500.11	29.82
7600	TRUE	21.08	7600.11	53.72	7600.11	42.41	7600.11	49.86	7600.11	27.08	7600.11	33.59	7600.11	24.60	7600.11	32.64
7700	TRUE	-13.14	7700.12	14.55	7700.12	27.19	7700.12	25.46	7700.12	36.59	7700.12	21.17	7700.12	31.29	7700.12	27.69
7800	FALSE	NA	3.33	11.09	7800.12	13.07	7800.12	54.64	7800.12	35.29	7800.12	28.56	7800.12	21.64	7800.12	58.55
7900	TRUE	17.15	7900.12	49.74	7900.12	23.98	7900.12	39.40	7900.12	26.82	7900.12	70.23	7900.12	42.50	7900.12	32.59
8000	TRUE	-8.91	8000.12	21.08	8000.12	28.34	8000.12	20.36	8000.12	30.12	8000.12	22.51	8000.12	33.56	8000.12	29.98
8100	FALSE	NA	8100.12	35.37	6.00	9.28	8100.12	24.57	8100.12	23.52	8100.12	70.14	8100.12	27.52	8100.12	54.38
8200	TRUE	-13.53	8200.12	24.74	8200.12	24.38	8200.12	26.87	8200.12	34.41	8200.12	32.01	8200.12	56.95	8200.12	38.27
8300	TRUE	18.72	8300.13	51.95	8300.13	38.99	8300.13	29.23	8300.13	33.43	8300.13	23.73	8300.13	27.25	8300.13	33.23
8400	TRUE	5.49	8400.13	27.84	8400.13	34.48	8400.13	39.36	8400.13	37.94	8400.13	40.12	8400.13	32.90	8400.13	22.35
8500	TRUE	-31.81	8500.13	13.18	8500.13	31.83	8500.13	52.06	8500.13	32.17	8500.13	21.29	8500.13	14.44	8500.13	45.00
8600	TRUE	77.38	8600.13	107.80	8600.13	48.79	8600.13	97.40	8600.13	30.48	8600.13	28.26	8600.13	21.27	8600.13	30.41
8700	TRUE	-4.23	8700.13	69.11	8700.13	39.56	8700.13	21.03	8700.13	28.51	8700.13	34.64	8700.13	40.02	8700.13	73.34
8800	FALSE	NA	8800.13	27.00	4.67	7.69	8800.13	34.51	8800.13	31.56	8800.13	42.92	8800.13	49.60	8800.13	20.13
8900	TRUE	58.98	8900.13	78.59	8900.13	19.88	8900.13	58.89	8900.13	31.53	8900.13	29.94	8900.13	53.83	8900.13	19.61
9000	TRUE	18.98	9000.14	73.80	9000.14	23.54	9000.14	56.15	9000.14	17.60	9000.14	42.20	9000.14	103.36	9000.14	54.82
9100	TRUE	-15.77	9100.14	38.40	9100.14	38.04	9100.14	34.25	9100.14	37.97	9100.14	11.53	9100.14	44.10	9100.14	54.18
9200	FALSE	NA	9200.14	37.04	9200.14	47.92	9200.14	41.64	2.33	8.87	9200.14	25.74	9200.14	41.21	9200.14	33.54
9300	TRUE	73.33	9300.14	104.51	9300.14	34.47	9300.14	12.27	9300.14	25.90	9300.14	64.11	9300.14	17.15	9300.14	31.17
9400	TRUE	20.16	9400.14	45.24	9400.14	69.25	9400.14	25.56	9400.14	45.92	9400.14	62.60	9400.14	38.68	9400.14	25.08
9500	TRUE	23.95	9500.14	50.00	9500.14	40.10	9500.14	11.65	9500.14	44.46	9500.14	39.30	9500.14	25.14	9500.14	26.05
9600	TRUE	2.12	9600.15	30.02	9600.15	37.25	9600.15	24.06	9600.15	42.31	9600.15	27.08	9600.15	30.46	9600.15	27.90
9700	TRUE	13.37	9700.15	43.93	9700.15	42.50	9700.15	34.90	9700.15	57.15	9700.15	33.24	9700.15	36.78	9700.15	30.56
9800	TRUE	-3.82	9800.15	25.67	9800.15	22.65	9800.15	37.93	9800.15	35.29	9800.15	31.81	9800.15	31.96	9800.15	29.49
9900	TRUE	-4.45	9900.15	27.87	9900.15	38.10	9900.15	29.91	9900.15	36.14	9900.15	39.61	9900.15	29.58	9900.15	32.33
10000	TRUE	11.65	10000.15	41.81	10000.15	24.49	10000.15	28.88	10000.15	37.60	10000.15	33.84	10000.15	34.97	10000.15	30.15
10100	TRUE	-1.67	10100.15	32.30	10100.15	42.13	10100.15	41.00	10100.15	40.24	10100.15	35.98	10100.15	38.07	10100.15	33.97
10200	TRUE	-6.73	10200.15	25.91	10200.15	36.32	10200.15	37.24	10200.15	18.13	10200.15	30.51	10200.15	29.68	10200.15	32.64
10300	TRUE	1.62	10300.16	33.14	10300.16	28.89	10300.16	36.29	10300.16	28.07	10300.16	32.57	10300.16	30.91	10300.16	31.51
10400	TRUE	1.81	10400.16	33.36	10400.16	34.11	10400.16	33.32	10400.16	31.59	10400.16	35.92	10400.16	31.58	10400.16	31.55
10500	TRUE	1.23	10500.16	32.61	10500.16	30.88	10500.16	30.29	10500.16	30.68	10500.16	28.64	10500.16	31.69	10500.16	31.37
10600	TRUE	-1.15	10600.16	30.85	10600.16	32.50	10600.16	31.85	10600.16	30.10	10600.16	33.11	10600.16	31.08	10600.16	32.00
10700	TRUE	2.11	10700.16	33.84	10700.16	33.21	10700.16	31.55	10700.16	34.06	10700.16	33.14	10700.16	30.55	10700.16	31.74
10800	TRUE	3.18	10800.16	34.93	10800.16	31.84	10800.16	33.01	10800.16	29.73	10800.16	33.50	10800.16	31.95	10800.16	31.75
10900	TRUE	-1.27	10900.16	30.66	10900.16	32.57	10900.16	31.63	10900.16	31.31	10900.16	31.22	10900.16	32.11	10900.16	31.93

Table C.1: Old Commercial Wet Sprinkler Pipe Peak Signal Frequency and Magnitude. “Bandwidth” column indicates whether the Bandwidth Condition is satisfied

		Distance	20ft_vol100		40ft_vol100		60ft_vol100		80ft_vol100		100ft_vol100		120ft_vol100		170ft_vol100	
		Values	Rx_max_freq	Max_rx_mag	Rx_max_freq	Max_rx_mag	Rx_max_freq	Max_rx_mag	Rx_max_freq	Max_rx_mag	Rx_max_freq	Max_rx_mag	Rx_max_freq	Max_rx_mag	Rx_max_freq	Max_rx_mag
Tx_freq	Bandwidth	Attenuation/ft														
11000	TRUE	-0.16	11000.17	31.61	11000.17	31.27	11000.17	30.64	11000.17	32.77	11000.17	32.09	11000.17	31.82	11000.17	31.77
11100	TRUE	-1.25	11100.17	30.57	11100.17	31.94	11100.17	31.78	11100.17	31.59	11100.17	31.48	11100.17	32.52	11100.17	31.82
11200	TRUE	1.20	11200.17	33.00	11200.17	31.70	11200.17	31.52	11200.17	31.31	11200.17	32.22	11200.17	32.04	11200.17	31.80
11300	TRUE	1.58	11300.17	33.28	11300.17	32.34	11300.17	31.53	11300.17	31.54	11300.17	31.60	11300.17	32.03	11300.17	31.70
11400	TRUE	-0.55	11400.17	31.33	11400.17	32.38	11400.17	31.71	11400.17	31.27	11400.17	31.97	11400.17	32.16	11400.17	31.88
11500	TRUE	-0.31	11500.17	31.62	11500.17	31.63	11500.17	32.90	11500.17	31.08	11500.17	31.88	11500.17	32.17	11500.17	31.93
11600	TRUE	5.01	11600.18	36.74	11600.18	29.69	11600.18	33.55	11600.18	30.59	11600.18	31.81	11600.18	32.29	11600.18	31.73
11700	TRUE	1.55	11700.18	33.48	11700.18	31.57	11700.18	31.72	11700.18	31.91	11700.18	32.12	11700.18	32.63	11700.18	31.92
11800	TRUE	-5.12	11800.18	26.81	11800.18	36.67	11800.18	28.74	11800.18	31.61	11800.18	32.32	11800.18	32.63	11800.18	31.92
11900	TRUE	8.97	11900.18	41.05	11900.18	32.14	11900.18	31.93	11900.18	31.68	11900.18	32.48	11900.18	32.33	11900.18	32.08
12000	TRUE	-0.45	12000.18	31.55	12000.18	33.47	12000.18	31.52	12000.18	31.59	12000.18	31.59	12000.18	31.89	12000.18	32.00
12100	TRUE	-0.43	12100.18	31.66	12100.18	33.08	12100.18	33.55	12100.18	31.40	12100.18	32.35	12100.18	32.39	12100.18	32.10
12200	TRUE	1.24	12200.18	33.41	12200.18	31.99	12200.18	33.41	12200.18	31.76	12200.18	32.28	12200.18	32.56	12200.18	32.17
12300	TRUE	0.50	12300.19	33.59	12300.19	33.63	12300.19	32.94	12300.19	32.62	12300.19	33.10	12300.19	33.48	12300.19	33.09
12400	TRUE	0.35	12400.19	35.44	12400.19	35.17	12400.19	35.16	12400.19	34.77	12400.19	35.14	12400.19	35.55	12400.19	35.09
12500	TRUE	0.25	12500.19	32.71	12500.19	32.66	12500.19	32.57	12500.19	31.92	12500.19	32.31	12500.19	32.96	12500.19	32.47
12600	TRUE	1.17	12600.19	33.54	12600.19	32.68	12600.19	32.59	12600.19	31.57	12600.19	32.27	12600.19	32.71	12600.19	32.37
12700	TRUE	0.28	12700.19	32.58	12700.19	32.44	12700.19	33.21	12700.19	31.71	12700.19	31.98	12700.19	33.32	12700.19	32.31
12800	TRUE	0.66	12800.19	33.05	12800.19	32.27	12800.19	32.18	12800.19	32.32	12800.19	32.71	12800.19	32.39	12800.19	32.39
12900	TRUE	1.28	12900.20	33.97	12900.20	32.87	12900.20	32.35	12900.20	32.21	12900.20	32.68	12900.20	33.16	12900.20	32.68
13000	TRUE	0.47	13000.20	32.98	13000.20	32.83	13000.20	32.12	13000.20	32.49	13000.20	32.33	13000.20	32.74	13000.20	32.51
13100	TRUE	0.27	13100.20	32.71	13100.20	32.58	13100.20	33.61	13100.20	32.07	13100.20	32.03	13100.20	32.87	13100.20	32.45
13200	TRUE	-0.62	13200.20	31.86	13200.20	32.91	13200.20	32.05	13200.20	32.29	13200.20	32.65	13200.20	33.29	13200.20	32.48
13300	TRUE	0.13	13300.20	32.73	13300.20	34.18	13300.20	32.99	13300.20	32.06	13300.20	32.77	13300.20	33.14	13300.20	32.60
13400	TRUE	0.31	13400.20	33.05	13400.20	33.19	13400.20	32.39	13400.20	32.69	13400.20	32.51	13400.20	33.34	13400.20	32.73
13500	TRUE	0.88	13500.20	33.49	13500.20	32.42	13500.20	30.66	13500.20	32.49	13500.20	32.38	13500.20	33.34	13500.20	32.61
13600	TRUE	1.63	13600.21	34.41	13600.21	32.85	13600.21	33.53	13600.21	32.43	13600.21	32.76	13600.21	33.49	13600.21	32.78
13700	TRUE	0.83	13700.21	33.63	13700.21	32.57	13700.21	32.27	13700.21	32.48	13700.21	33.27	13700.21	33.53	13700.21	32.80
13800	TRUE	0.84	13800.21	33.58	13800.21	33.12	13800.21	32.81	13800.21	32.31	13800.21	32.79	13800.21	33.35	13800.21	32.73
13900	TRUE	1.90	13900.21	34.70	13900.21	32.90	13900.21	31.79	13900.21	32.53	13900.21	32.79	13900.21	33.20	13900.21	32.80
14000	TRUE	-0.19	14000.21	32.65	14000.21	34.08	14000.21	32.81	14000.21	32.49	14000.21	32.78	14000.21	33.27	14000.21	32.84
14100	TRUE	1.33	14100.21	34.14	14100.21	31.24	14100.21	28.40	14100.21	32.47	14100.21	32.79	14100.21	33.17	14100.21	32.81
14200	TRUE	-0.09	14200.21	32.69	14200.21	32.69	14200.21	32.76	14200.21	32.51	14200.21	32.83	14200.21	33.18	14200.21	32.78
14300	TRUE	-1.50	14300.22	31.19	14300.22	32.42	14300.22	32.00	14300.22	32.31	14300.22	32.86	14300.22	33.27	14300.22	32.70
14400	TRUE	2.88	14400.22	35.70	14400.22	32.71	14400.22	31.08	14400.22	32.60	14400.22	33.04	14400.22	33.28	14400.22	32.83
14500	TRUE	0.23	14500.22	33.12	14500.22	33.11	14500.22	33.91	14500.22	32.49	14500.22	32.94	14500.22	33.41	14500.22	32.90
14600	TRUE	-3.25	14600.22	29.58	14600.22	32.04	14600.22	32.55	14600.22	32.28	14600.22	32.65	14600.22	33.53	14600.22	32.82
14700	TRUE	0.95	14700.22	33.85	14700.22	33.28	14700.22	28.87	14700.22	33.21	14700.22	33.13	14700.22	33.30	14700.22	32.90
14800	TRUE	0.43	14800.22	33.31	14800.22	33.17	14800.22	30.60	14800.22	32.55	14800.22	33.00	14800.22	33.34	14800.22	32.89
14900	TRUE	-0.06	14900.23	32.73	14900.23	33.09	14900.23	36.02	14900.23	32.69	14900.23	32.91	14900.23	33.62	14900.23	32.80
15000	TRUE	-0.24	15000.23	32.72	15000.23	32.51	15000.23	37.53	15000.23	32.57	15000.23	32.94	15000.23	33.63	15000.23	32.96
15100	TRUE	-6.89	15100.23	26.11	15100.23	36.64	15100.23	33.63	15100.23	32.58	15100.23	32.95	15100.23	33.37	15100.23	33.00
15200	TRUE	0.73	15200.23	33.98	15200.23	35.69	15200.23	33.66	15200.23	35.36	15200.23	32.56	15200.23	33.92	15200.23	33.25
15300	TRUE	-1.82	15300.23	32.20	15300.23	33.48	15300.23	35.27	15300.23	34.23	15300.23	33.50	15300.23	34.56	15300.23	34.02
15400	TRUE	-0.48	15400.23	35.74	15400.23	35.92	15400.23	43.17	15400.23	36.49	15400.23	36.72	15400.23	36.61	15400.23	36.22
15500	TRUE	-0.58	15500.23	33.02	15500.23	32.23	15500.23	30.28	15500.23	33.64	15500.23	33.70	15500.23	34.72	15500.23	33.61
15600	TRUE	-1.21	15600.24	31.77	15600.24	34.52	15600.24	28.75	15600.24	32.12	15600.24	33.98	15600.24	32.95	15600.24	32.98
15700	TRUE	0.96	15700.24	32.93	15700.24	34.72	15700.24	37.59	15700.24	33.96	15700.24	32.93	15700.24	31.50	15700.24	31.97
15800	TRUE	8.09	15800.24	40.84	15800.24	29.98	15800.24	36.13	15800.24	32.23	15800.24	33.24	15800.24	33.85	15800.24	32.74
15900	TRUE	-1.35	15900.24	32.87	15900.24	33.51	15900.24	33.61	15900.24	32.29	15900.24	31.48	15900.24	35.97	15900.24	34.22
16000	TRUE	1.60	16000.24	35.09	16000.24	33.86	16000.24	33.12	16000.24	32.42	16000.24	33.41	16000.24	34.29	16000.24	33.49
16100	TRUE	2.13	16100.24	35.75	16100.24	35.05	16100.24	35.79	16100.24	33.83	16100.24	33.39	16100.24	34.38	16100.24	33.62
16200	TRUE	0.37	16200.24	33.58	16200.24	32.58	16200.24	35.12	16200.24	30.27	16200.24	33.93	16200.24	34.01	16200.24	33.21
16300	TRUE	-0.67	16300.25	32.48	16300.25	34.59	16300.25	35.22	16300.25	32.85	16300.25	33.43	16300.25	34.67	16300.25	33.15
16400	TRUE	2.89	16400.25	36.67	16400.25	33.44	16400.25	36.24	16400.25	33.08	16400.25	33.44	16400.25	34.28	16400.25	33.78
16500	TRUE	1.46	16500.25	35.70	16500.25	31.57	16500.25	32.40	16500.25	32.66	16500.25	34.03	16500.25	36.01	16500.25	34.24
16600	TRUE	1.73	16600.25	35.31	16600.25	33.59	16600.25	33.85	16600.25	33.37	16600.25	33.89	16600.25	34.36	16600.25	33.58
16700	TRUE	0.26	16700.25	33.73	16700.25	33.97	16700.25	33.28	16700.25	32.88	16700.25	34.21	16700.25	33.93	16700.25	33.47
16800	TRUE	-1.02	16800.25	32.89	16800.25	33.74	16800.25	33.49	16800.25	32.89	16800.25	33.05	16800.25	34.36	16800.25	33.91
16900	TRUE	1.79	16900.26	35.34	16900.26	34.26	16900.26	32.07	16900.26	33.22	16900.26	33.87	16900.26	34.15	16900.26	33.55
17000	TRUE	-1.43	17000.26	32.20	17000.26	35.30	17000.26	31.32	17000.26	33.29	17000.26	33.50	17000.26	34.81	17000.26	33.63
17100	TRUE	1.41	17100.26	35.20	17100.26	32.95	17100.26	33.91	17100.26	33.27	17100.26	33.98	17100.26	34.17	17100.26	33.80
17200	TRUE	1.51	17200.26	35.18	17200.26	32.11	17200.26	36.73	17200.26	33.23	17200.26	33.84	17200.26	34.34	17200.26	33.67
17300	TRUE	-4.54	17300.26	29.94	17300.26	33.28	17300.26	36.56	17300.26	33.12	17300.26	33.29	17300.26	34.94	17300.26	34.48
17400	TRUE	1.66	17400.26	35.64	17400.26	34.70	17400.26	30.54	17400.26	33.23	17400.26	35.46	17400.26	34.46	17400.26	33.98
17500	TRUE	-1.49	17500.26	32.34	17500.26	34.79	17500.26	33.39	17500.26	33.40	17500.26	34.25	17500.26	34.49	17500.26	33.84
17600	TRUE	-0.77	17600.27	32.72	17600.27	34.11	17600.27	33.95	17600.27	33.55	17600.27	34.56	17600.27	34.67	17600.27	33.49
17700	TRUE	-1.27	17700.27	32.57	17700.27	32.06	17700.27	33.98	17700.27	33.48	17700.27	34.35	17700.27	34.00	17700.27	33.85
17800	TRUE	-5.37	17800.27	28.35	17800.27	32.29	17800.27	34.48	17800.27	33.64	17800.27	34.13	17800.27	34.52	17800.27	33.72
17900	TRUE	-1.12	17900.27	32.59	17900.27	34.31	17900.27	36.36	17900.27	33.48	17900.27	34.02	17900.27	34.21	17900.27	33.71
18000	TRUE	-0.57	18000.27	33.24	18000.27	34.79	18000.27	34.41	18000.27	33.64	18000.27	34.17	18000.27	34.62	18000.27	33.81
18100	TRUE	1.09	18100.27	35.11	18100.27	34.22	18100.27	33.93	18100.27	34.19	18100.27	33.95	18100.27	34.87	18100.27	34.03
18200	TRUE	1.67	18200.28	35.78	18200.28	34.08	18200.28	34.32	18200.28	33.94	18200.28	33.74	18200.28	34.74	18200.28	34.11
18300	TRUE	-0.46	18300.28	33.72	18300.28	34.97	18300.28	33.94	18300.28	34.19	18300.28	33.94	18300.28	34.89	18300.28	34.18
18400	TRUE	6.70	18400.28	41.11	18400.28	33.97	18400.28	36.18	18400.28	34.05	18400.28	34.83	18400.28	35.13	18400.28	34.41
18500	TRUE	-4.49	18500.28	29.84	18500.28	33.56	18500.28	35.49	18500.28	34.61	18500.28	34.44	18500.28	35.11	18500.28	34.33
18600	TRUE	0.81	18600.28	35.03	18600.28	34.92	18600.28	35.50	18600.28	35.07	18600.28	35.13	18600.28	35.78	18600.28	34.22
18700	TRUE	-0.16	18700.28	33.89	18700.28	35.69	18700.28	35.91	18700.28	34.33	18700.28	34.50	18700.28	35.37	18700.28	34.05
18800	TRUE	0.73	18800.28	35.03	18800.28	34.86	18800.28	33.46	18800.28	34.70	18800.28	34.91	18800.28	35.47	18800.28	34.30
18900	TRUE	2.44	18900.29	36.80	18900.29	35.01	18900.29	35.36	18900.29	34.44	18900.29	34.64	18900.29	36.04	18900.29	34.36
19000	TRUE	4.59	19000.29	38.96	19000.29	34.85	19000.29	34.56	19000.29	33.56	19000.29	34.75	19000.29	35.09	19000.29	34.37
19100	TRUE	1.47	19100.29	35.83	19100.29	35.12	19100.29	35.05	19100.29	34.24	19100.29	34.74	19100.29	36.53	19100.29	34.36
19200	TRUE	1.33	19200.29	36.32	19200.29	34.60	19200.29	32.52	19200.29	34.89	19200.29	33.17	19200.29	37.89	19200.29	34.99
19300	TRUE	1.85	19300.29	36.20	19300.29	35.21	19300.29	33.07	19300.29	33.19	19300.29	34.59	19300.29	34.87	19300.29	34.35
19400	TRUE	3.45	19400.29	37.25	19400.29	34.87	19400.29	32.66	19400.29	33.34	19400.29	33.57	19400.29	35.21	19400.29	33.79
19500	TRUE	0.41	19500.29	34.39	19500.29	32.78	19500.29	34.19	19500.29	33.91	19500.29	31.82	19500.29	34.82	19500.29	33.99
19600	TRUE	2.02	19600.30	35.77	19600.30	32.97	19600.30	32.79	19600.30	33.01	19600.30	28.83	19600.30	34.31	19600.30	33.75
19700	TRUE	1.11	19700.30	34.53	19700.30	32.85	19700.30	33.44	19700.30	32.51	19700.30	33.59	19700.30	33.94	19700.30	33.43
19800	TRUE	0.17	19800.30	33.14	19800.30	32.65	19800.30	32.73	19800.30	31.11	19800.30	34.20	19800.30	33.74	19800.30	32.96
19900	TRUE	3.54	19900.30	35.58	19900.30	32.90	19900.30	32.04	19900.30	30.45	19900.30	32.96	19900.30	33.17	19900.30	32.04
20000	TRUE	1.74	20000.30	33.17	20000.30	30.99	20000.30	31.85	20000.30	30.47	20000.30	32.43	20000.30	32.07	20000.30	31.43

Table C.1: Old Commercial Wet Sprinkler Pipe Peak Signal Frequency and Magnitude. “Bandwidth” column indicates whether the Bandwidth Condition is satisfied (cont.)

Appendix D: OLD COMMERCIAL DRY SPRINKLER PIPE MEASUREMENTS (OCDS)

		Distance	20ft_vol100		50ft_vol100		60ft_vol100		90ft_vol100	
		Values	Rx_max_freq	Max_rx_mag	Rx_max_freq	Max_rx_mag	Rx_max_freq	Max_rx_mag	Rx_max_freq	Max_rx_mag
Tx_freq	Bandwidth	Attenuation/ft								
100	FALSE	NA	60.00	9.33	2.00	11.61	1.67	14.87	0.00	51.49
200	FALSE	NA	60.00	10.35	3.00	9.67	2.00	7.72	3.00	9.43
300	FALSE	NA	60.00	9.12	4.00	9.54	8.00	7.78	4.00	12.40
400	FALSE	NA	1.33	8.44	2400.04	9.88	3.00	9.89	3.00	9.85
500	FALSE	NA	2.33	13.72	2500.04	17.21	3.67	9.01	7.67	7.91
600	FALSE	NA	3600.05	12.67	2.00	13.45	1.67	9.93	1.67	8.93
700	FALSE	NA	4900.07	27.24	3.67	11.57	4.00	9.58	3.00	11.15
800	FALSE	NA	4800.07	39.94	2400.04	26.47	800.01	9.08	2.67	9.44
900	FALSE	NA	900.01	10.09	2700.04	23.80	900.01	10.42	2.00	11.10
1000	FALSE	NA	3.33	10.44	4.33	11.18	1000.02	10.35	3.00	10.92
1100	FALSE	NA	1100.02	13.08	1100.02	12.14	1100.02	13.13	3.33	13.25
1200	FALSE	NA	4800.07	34.46	2400.04	50.26	1200.02	12.23	1200.02	12.03
1300	FALSE	NA	1300.02	12.52	3.33	15.07	1300.02	12.88	1300.02	12.47
1400	FALSE	NA	1400.02	14.59	2800.04	46.64	1400.02	13.70	1400.02	12.25
1500	TRUE	0.21	1500.02	15.91	1500.02	16.52	1500.02	15.50	1500.02	15.70
1600	FALSE	NA	4800.07	38.95	1600.02	26.70	1600.02	14.85	1600.02	14.11
1700	TRUE	-0.25	1700.03	15.91	1700.03	16.89	1700.03	15.77	1700.03	16.16
1800	TRUE	-2.79	1800.03	14.95	1800.03	14.13	1800.03	17.29	1800.03	17.74
1900	FALSE	NA	1900.03	19.69	1900.03	15.89	2.67	18.79	1900.03	18.63
2000	TRUE	-7.21	2000.03	15.10	2000.03	20.86	2000.03	16.44	2000.03	22.31
2100	FALSE	NA	2100.03	21.99	2100.03	12.14	2100.03	19.72	2.33	12.88
2200	TRUE	0.97	2200.03	20.01	2200.03	24.09	2200.03	19.33	2200.03	19.04
2300	TRUE	-5.57	2300.03	17.55	2300.03	22.84	2300.03	16.98	2300.03	23.12
2400	FALSE	NA	4800.07	27.97	2400.04	87.09	2400.04	25.11	2400.04	18.58
2500	TRUE	2.40	2500.04	16.86	2500.04	65.35	2500.04	24.03	2500.04	14.46
2600	TRUE	5.43	2600.04	35.98	2600.37	17.36	2600.04	28.20	2600.04	30.55
2700	TRUE	3.21	2700.04	34.72	2700.04	40.41	2700.04	16.24	2700.04	31.51
2800	TRUE	0.00	2800.04	22.24	2800.04	44.52	2800.04	27.07	2800.04	22.23
2900	FALSE	NA	2900.04	30.30	2900.04	63.42	2900.04	21.25	3.00	11.17
3000	TRUE	-12.26	3000.05	13.66	3000.05	19.20	3000.05	25.71	3000.05	25.92
3100	TRUE	-0.16	3100.05	40.10	3100.05	42.57	3100.05	34.91	3100.05	40.26
3200	FALSE	NA	60.00	9.29	3200.05	36.88	3200.05	14.60	2.33	11.53
3300	TRUE	25.83	3300.05	46.12	3300.05	33.30	3300.05	18.88	3300.05	20.28
3400	TRUE	-19.98	3400.05	12.19	3400.05	25.25	3400.05	25.94	3400.05	32.17
3500	TRUE	6.46	3500.05	28.58	3500.05	24.11	3500.05	19.94	3500.05	22.12
3600	TRUE	-9.17	3600.05	17.63	3600.05	14.87	3600.05	42.58	3600.05	26.80
3700	TRUE	7.92	3700.06	33.64	3700.06	20.84	3700.06	29.40	3700.06	25.71
3800	TRUE	-2.24	3800.06	24.85	3800.06	22.90	3800.06	22.20	3800.06	27.09
3900	FALSE	NA	3900.06	73.58	1.33	7.56	3900.06	17.52	3900.06	22.59
4000	FALSE	NA	4.00	10.93	4000.06	12.17	4000.06	30.08	4000.06	27.76
4100	TRUE	-5.31	4100.06	21.48	4100.06	24.99	4100.06	29.42	4100.06	26.78
4200	TRUE	9.50	4200.06	36.77	4200.06	26.00	4200.06	25.96	4200.06	27.27
4300	TRUE	-12.34	4300.07	11.51	4300.07	25.86	4300.07	26.25	4300.07	23.85
4400	TRUE	-0.66	4400.07	26.08	4400.07	28.12	4400.07	27.74	4400.07	26.74
4500	TRUE	3.98	4500.07	31.26	4500.07	25.81	4500.07	25.80	4500.07	27.29
4600	TRUE	3.10	4600.07	30.56	4600.07	32.57	4600.07	27.01	4600.07	27.46
4700	TRUE	47.75	4700.07	73.57	4700.07	22.00	4700.07	27.76	4700.07	25.83
4800	TRUE	76.88	4800.07	108.36	4800.07	30.18	4800.07	33.16	4800.07	31.48
4900	TRUE	128.57	4900.07	154.92	4900.07	31.13	4900.07	31.55	4900.07	26.35
5000	TRUE	-12.09	5000.08	14.46	5000.08	26.95	5000.08	27.92	5000.08	26.55
5100	TRUE	-5.25	5100.08	20.38	5100.08	36.06	5100.08	28.15	5100.08	25.63
5200	TRUE	-12.94	5200.08	15.78	5200.08	30.43	5200.08	29.68	5200.08	28.71
5300	TRUE	-14.91	5300.08	13.22	5300.08	36.45	5300.08	29.63	5300.08	28.13
5400	TRUE	9.91	5400.08	36.17	5400.08	26.48	5400.08	26.91	5400.08	26.26
5500	TRUE	-1.50	5500.08	25.26	5500.08	27.72	5500.08	27.44	5500.08	26.76
5600	TRUE	22.40	5600.08	54.94	5600.08	27.43	5600.08	27.07	5600.08	32.54
5700	FALSE	NA	1.33	10.66	5700.09	26.98	5700.09	26.33	5700.09	27.53
5800	TRUE	10.14	5800.09	37.58	5800.09	26.25	5800.09	26.34	5800.09	27.45
5900	TRUE	8.49	5900.09	38.13	5900.09	27.36	5900.09	31.65	5900.09	29.64
6000	TRUE	-16.49	6000.09	10.60	6000.09	25.56	6000.09	29.92	6000.09	27.09
6100	TRUE	-1.44	6100.09	28.56	6100.09	27.59	6100.09	30.36	6100.09	30.00
6200	TRUE	5.36	6200.09	33.39	6200.09	28.43	6200.09	29.10	6200.09	28.03
6300	TRUE	-7.20	6300.10	22.20	6300.10	30.03	6300.10	30.23	6300.10	29.40
6400	TRUE	3.53	6400.10	34.07	6400.10	31.49	6400.10	33.06	6400.10	30.54
6500	TRUE	-0.14	6500.10	28.57	6500.10	29.65	6500.10	29.99	6500.10	28.71
6600	TRUE	-2.88	6600.10	25.59	6600.10	29.44	6600.10	29.53	6600.10	28.48
6700	TRUE	4.57	6700.10	33.32	6700.10	28.97	6700.10	29.61	6700.10	28.75
6800	TRUE	-9.58	6800.10	19.34	6800.10	29.72	6800.10	29.34	6800.10	28.91
6900	TRUE	-0.03	6900.10	29.02	6900.10	29.65	6900.10	29.36	6900.10	29.05
7000	TRUE	4.23	7000.11	33.25	7000.11	34.05	7000.11	28.89	7000.11	29.02
7100	TRUE	0.23	7100.11	28.48	7100.11	21.76	7100.11	30.28	7100.11	28.25
7200	TRUE	-2.89	7200.11	26.32	7200.11	22.11	7200.11	28.86	7200.11	29.20

Table D.1: Old Commercial Dry Sprinkler Pipe Peak Signal Frequency and Magnitude. "Bandwidth" column indicates whether the Bandwidth Condition is satisfied

		Distance	20ft_vol100		50ft_vol100		60ft_vol100		90ft_vol100	
		Values	Rx_max_freq	Max_rx_mag	Rx_max_freq	Max_rx_mag	Rx_max_freq	Max_rx_mag	Rx_max_freq	Max_rx_mag
Tx_freq	Bandwidth	Attenuation/ft								
7300	TRUE	3.75	7300.11	32.96	7299.78	13.80	7300.11	29.52	7300.11	29.21
7400	TRUE	3.58	7400.11	33.38	7400.11	52.96	7400.11	29.67	7400.11	29.79
7500	TRUE	-2.40	7500.11	26.94	7500.11	47.21	7500.11	29.96	7500.11	29.34
7600	TRUE	12.24	7600.11	41.83	7600.11	32.71	7600.11	29.19	7600.11	29.59
7700	TRUE	-0.10	7700.12	29.61	7700.12	33.95	7700.12	30.49	7700.12	29.72
7800	TRUE	13.58	7800.12	44.19	7800.12	17.13	7800.12	30.78	7800.12	30.61
7900	TRUE	12.67	7900.12	45.83	7900.12	26.56	7900.12	33.80	7900.12	33.16
8000	TRUE	-3.12	8000.12	26.99	8000.12	33.67	8000.12	29.71	8000.12	30.11
8100	TRUE	-2.41	8100.12	27.31	8100.12	26.43	8100.12	30.59	8100.12	29.73
8200	TRUE	2.45	8200.12	32.62	8200.12	32.55	8200.12	30.29	8200.12	30.17
8300	TRUE	-6.99	8300.13	23.32	8300.13	33.48	8300.13	29.94	8300.13	30.31
8400	TRUE	-0.07	8400.13	30.16	8400.13	27.64	8400.13	29.82	8400.13	30.23
8500	TRUE	28.94	8500.13	59.49	8500.13	40.69	8500.13	28.32	8500.13	30.54
8600	TRUE	12.06	8600.13	42.46	8600.13	34.92	8600.13	30.68	8600.13	30.40
8700	TRUE	1.83	8700.13	32.29	8700.13	33.05	8700.13	31.85	8700.13	30.46
8800	FALSE	NA	8800.13	34.66	1.67	13.78	8800.13	34.93	8800.13	30.49
8900	TRUE	6.88	8900.13	37.64	8900.13	38.67	8900.13	31.79	8900.13	30.76
9000	TRUE	2.01	9000.14	32.50	9000.14	48.30	9000.14	30.63	9000.14	30.49
9100	TRUE	-5.09	9100.14	25.45	9100.14	35.05	9100.14	32.33	9100.14	30.54
9200	TRUE	6.58	9200.14	36.68	9200.14	31.71	9200.14	36.76	9200.14	30.10
9300	TRUE	9.44	9300.14	40.01	9300.14	41.63	9300.14	33.35	9300.14	30.57
9400	TRUE	15.20	9400.14	46.20	9400.14	31.39	9400.14	31.36	9400.14	31.00
9500	TRUE	1.76	9500.14	33.03	9500.14	28.92	9500.14	34.23	9500.14	31.27
9600	TRUE	-11.34	9600.15	19.69	9600.15	30.05	9600.15	31.96	9600.15	31.03
9700	TRUE	-2.11	9700.15	28.84	9700.15	34.69	9700.15	31.51	9700.15	30.95
9800	TRUE	12.50	9800.15	43.32	9800.15	33.46	9800.15	30.95	9800.15	30.82
9900	TRUE	-5.82	9900.15	25.44	9900.15	30.14	9900.15	31.31	9900.15	31.26
10000	TRUE	-10.24	10000.15	21.23	10000.15	33.05	10000.15	32.27	10000.15	31.47
10100	TRUE	9.99	10100.15	44.24	10100.15	37.13	10100.15	34.86	10100.15	34.25
10200	TRUE	-7.00	10200.15	25.24	10200.15	32.83	10200.15	32.86	10200.15	32.24
10300	TRUE	-4.53	10300.16	27.07	10300.16	31.68	10300.16	32.34	10300.16	31.61
10400	TRUE	13.96	10400.16	45.52	10400.16	30.73	10400.16	32.16	10400.16	31.56
10500	TRUE	-2.11	10500.16	29.16	10500.16	27.90	10500.16	31.72	10500.16	31.27
10600	TRUE	5.14	10600.16	36.54	10600.16	32.90	10600.16	31.91	10600.16	31.40
10700	TRUE	-0.49	10700.16	31.10	10700.16	34.28	10700.16	32.30	10700.16	31.58
10800	TRUE	-3.67	10800.16	27.81	10800.16	28.69	10800.16	31.63	10800.16	31.48
10900	TRUE	11.69	10900.16	43.12	10900.16	32.06	10900.16	32.55	10900.16	31.43
11000	TRUE	-5.49	11000.17	26.12	11000.17	33.65	11000.17	32.19	11000.17	31.60
11100	TRUE	-0.92	11100.17	30.63	11100.17	30.01	11100.17	31.86	11100.17	31.54
11200	TRUE	-3.59	11200.17	27.87	11200.17	30.30	11200.17	32.28	11200.17	31.46
11300	TRUE	8.78	11300.17	40.27	11300.17	31.43	11300.17	32.04	11300.17	31.49
11400	TRUE	0.00	11400.17	31.65	11400.17	31.11	11400.17	32.23	11400.17	31.65
11500	TRUE	2.50	11500.17	34.19	11500.17	31.65	11500.17	32.26	11500.17	31.69
11600	TRUE	0.08	11600.18	31.66	11600.18	31.78	11600.18	32.06	11600.18	31.59
11700	TRUE	-0.49	11700.18	31.24	11700.18	28.97	11700.18	32.74	11700.18	31.72
11800	TRUE	-0.21	11800.18	31.47	11800.18	33.02	11800.18	32.00	11800.18	31.68
11900	TRUE	-0.06	11900.18	31.69	11900.18	32.13	11900.18	32.35	11900.18	31.74
12000	TRUE	-1.31	12000.18	30.62	12000.18	32.43	12000.18	31.91	12000.18	31.93
12100	TRUE	0.71	12100.18	32.53	12100.18	32.63	12100.18	32.48	12100.18	31.82
12200	TRUE	-1.74	12200.18	30.07	12200.18	32.26	12200.18	32.60	12200.18	31.82
12300	TRUE	-0.62	12300.19	32.15	12300.19	33.33	12300.19	33.43	12300.19	32.78
12400	TRUE	-0.98	12400.19	33.78	12400.19	35.31	12400.19	35.39	12400.19	34.76
12500	TRUE	-0.84	12500.19	31.26	12500.19	33.14	12500.19	32.58	12500.19	32.10
12600	TRUE	-1.16	12600.19	30.95	12600.19	32.69	12600.19	32.63	12600.19	32.11
12700	TRUE	-1.53	12700.19	30.42	12700.19	33.29	12700.19	32.71	12700.19	31.95
12800	TRUE	-0.78	12800.19	31.32	12800.19	32.89	12800.19	32.73	12800.19	32.11
12900	TRUE	0.70	12900.20	32.84	12900.20	32.75	12900.20	32.95	12900.20	32.14
13000	TRUE	-0.87	13000.20	31.42	13000.20	32.81	13000.20	32.92	13000.20	32.29
13100	TRUE	-0.29	13100.20	31.95	13100.20	32.69	13100.20	32.89	13100.20	32.24
13200	TRUE	3.13	13200.20	35.52	13200.20	32.29	13200.20	32.68	13200.20	32.39
13300	TRUE	-0.36	13300.20	32.00	13300.20	32.90	13300.20	33.04	13300.20	32.37
13400	TRUE	-0.46	13400.20	31.90	13400.20	32.66	13400.20	33.06	13400.20	32.36
13500	TRUE	2.40	13500.20	34.74	13500.20	33.21	13500.20	33.05	13500.20	32.34
13600	TRUE	-4.00	13600.21	28.42	13600.21	33.79	13600.21	33.21	13600.21	32.42
13700	TRUE	3.34	13700.21	35.81	13700.21	32.93	13700.21	33.05	13700.21	32.47
13800	TRUE	-0.45	13800.21	32.01	13800.21	32.60	13800.21	33.23	13800.21	32.46
13900	TRUE	0.49	13900.21	32.86	13900.21	33.18	13900.21	32.99	13900.21	32.37
14000	TRUE	-1.50	14000.21	31.01	14000.21	32.97	14000.21	33.27	14000.21	32.51
14100	TRUE	-0.67	14100.21	31.79	14100.21	32.88	14100.21	33.11	14100.21	32.46
14200	TRUE	-2.18	14200.21	30.27	14200.21	33.37	14200.21	32.94	14200.21	32.45
14300	TRUE	0.99	14300.22	33.50	14300.22	33.44	14300.22	33.18	14300.22	32.52
14400	TRUE	3.05	14400.22	35.55	14400.22	33.05	14400.22	33.21	14400.22	32.51

Table D.1: Old Commercial Dry Sprinkler Pipe Peak Signal Frequency and Magnitude. "Bandwidth" column indicates whether the Bandwidth Condition is satisfied (cont.)

		Distance	20ft_vol100		50ft_vol100		60ft_vol100		90ft_vol100	
		Values	Rx_max_freq	Max_rx_mag	Rx_max_freq	Max_rx_mag	Rx_max_freq	Max_rx_mag	Rx_max_freq	Max_rx_mag
Tx_freq	Bandwidth	Attenuation/ft								
14500	TRUE	-1.62	14500.22	30.93	14500.22	32.93	14500.22	33.33	14500.22	32.55
14600	TRUE	2.85	14600.22	35.38	14600.22	32.94	14600.22	33.22	14600.22	32.54
14700	TRUE	-3.84	14700.22	28.73	14700.22	33.03	14700.22	32.84	14700.22	32.56
14800	TRUE	-0.52	14800.22	32.05	14800.22	33.25	14800.22	33.14	14800.22	32.57
14900	TRUE	4.01	14900.23	36.57	14900.23	32.73	14900.23	33.15	14900.23	32.55
15000	TRUE	-2.36	15000.23	30.23	15000.23	33.06	15000.23	33.27	15000.23	32.59
15100	TRUE	-0.62	15100.23	32.08	15100.23	33.69	15100.23	33.41	15100.23	32.70
15200	TRUE	-2.10	15200.23	30.64	15200.23	33.27	15200.23	33.38	15200.23	32.75
15300	TRUE	-1.35	15300.23	32.35	15300.23	34.56	15300.23	34.42	15300.23	33.71
15400	TRUE	1.39	15400.23	37.15	15400.23	36.25	15400.23	36.35	15400.23	35.76
15500	TRUE	-1.10	15500.23	31.86	15500.23	33.60	15500.23	33.55	15500.23	32.96
15600	TRUE	-0.26	15600.24	32.62	15600.24	33.61	15600.24	33.62	15600.24	32.88
15700	TRUE	-0.43	15700.24	32.56	15700.24	33.32	15700.24	33.53	15700.24	32.99
15800	TRUE	-0.37	15800.24	32.67	15800.24	33.22	15800.24	33.40	15800.24	33.04
15900	TRUE	-0.12	15900.24	32.99	15900.24	33.48	15900.24	33.68	15900.24	33.10
16000	TRUE	0.34	16000.24	33.55	16000.24	33.66	16000.24	33.77	16000.24	33.21
16100	TRUE	0.23	16100.24	33.37	16100.24	33.33	16100.24	33.73	16100.24	33.14
16200	TRUE	-0.31	16200.24	32.85	16200.24	33.57	16200.24	33.80	16200.24	33.16
16300	TRUE	-1.16	16300.25	32.14	16300.25	33.52	16300.25	33.87	16300.25	33.30
16400	TRUE	-0.56	16400.25	32.80	16400.25	33.61	16400.25	33.93	16400.25	33.36
16500	TRUE	-0.66	16500.25	32.67	16500.25	33.70	16500.25	33.94	16500.25	33.34
16600	TRUE	-0.08	16600.25	33.37	16600.25	33.79	16600.25	34.08	16600.25	33.45
16700	TRUE	0.48	16700.25	33.86	16700.25	33.64	16700.25	33.93	16700.25	33.38
16800	TRUE	-0.39	16800.25	33.00	16800.25	33.69	16800.25	34.02	16800.25	33.39
16900	TRUE	-0.87	16900.26	32.56	16900.26	33.81	16900.26	33.99	16900.26	33.44
17000	TRUE	-1.18	17000.26	32.35	17000.26	33.88	17000.26	34.04	17000.26	33.54
17100	TRUE	-0.68	17100.26	32.86	17100.26	33.88	17100.26	34.05	17100.26	33.55
17200	TRUE	-0.45	17200.26	33.08	17200.26	33.83	17200.26	34.05	17200.26	33.53
17300	TRUE	0.25	17300.26	33.82	17300.26	33.76	17300.26	34.01	17300.26	33.57
17400	TRUE	-0.43	17400.26	33.16	17400.26	33.94	17400.26	34.03	17400.26	33.59
17500	TRUE	-0.08	17500.26	33.53	17500.26	33.85	17500.26	34.07	17500.26	33.61
17600	TRUE	-0.15	17600.27	33.38	17600.27	33.79	17600.27	34.05	17600.27	33.54
17700	TRUE	-1.26	17700.27	32.34	17700.27	33.95	17700.27	34.04	17700.27	33.60
17800	TRUE	-0.34	17800.27	33.26	17800.27	33.91	17800.27	34.04	17800.27	33.60
17900	TRUE	-0.33	17900.27	33.37	17900.27	34.03	17900.27	34.24	17900.27	33.70
18000	TRUE	-0.22	18000.27	33.51	18000.27	34.11	18000.27	34.26	18000.27	33.74
18100	TRUE	0.54	18100.27	34.33	18100.27	34.10	18100.27	34.37	18100.27	33.79
18200	TRUE	-1.04	18200.28	32.72	18200.28	34.10	18200.28	34.49	18200.28	33.76
18300	TRUE	-0.07	18300.28	33.74	18300.28	34.41	18300.28	34.56	18300.28	33.81
18400	TRUE	-0.59	18400.28	33.33	18400.28	34.36	18400.28	34.60	18400.28	33.92
18500	TRUE	2.59	18500.28	36.57	18500.28	34.52	18500.28	34.77	18500.28	33.99
18600	TRUE	-0.63	18600.28	33.42	18600.28	34.14	18600.28	34.84	18600.28	34.05
18700	TRUE	-1.77	18700.28	32.31	18700.28	34.87	18700.28	34.79	18700.28	34.08
18800	TRUE	-0.87	18800.28	33.21	18800.28	34.70	18800.28	34.89	18800.28	34.09
18900	TRUE	0.53	18900.29	34.63	18900.29	34.86	18900.29	34.94	18900.29	34.10
19000	TRUE	0.99	19000.29	35.15	19000.29	34.77	19000.29	35.03	19000.29	34.16
19100	TRUE	0.52	19100.29	34.56	19100.29	34.69	19100.29	34.83	19100.29	34.04
19200	TRUE	0.43	19200.29	34.35	19200.29	34.17	19200.29	34.91	19200.29	33.92
19300	TRUE	-2.16	19300.29	31.72	19300.29	34.45	19300.29	34.77	19300.29	33.87
19400	TRUE	-0.26	19400.29	33.51	19400.29	34.36	19400.29	34.42	19400.29	33.77
19500	TRUE	6.05	19500.29	39.58	19500.29	34.16	19500.29	34.30	19500.29	33.53
19600	TRUE	-1.03	19600.30	32.20	19600.30	33.48	19600.30	34.11	19600.30	33.23
19700	TRUE	-3.25	19700.30	29.52	19700.30	33.36	19700.30	33.61	19700.30	32.77
19800	TRUE	-2.33	19800.30	29.88	19800.30	32.65	19800.30	33.10	19800.30	32.21
19900	TRUE	-1.38	19900.30	30.28	19900.30	32.32	19900.30	32.52	19900.30	31.65
20000	TRUE	-0.88	20000.30	30.13	20000.30	31.34	20000.30	31.82	20000.30	31.01

Table D.1: Old Commercial Dry Sprinkler Pipe Peak Signal Frequency and Magnitude. "Bandwidth" column indicates whether the Bandwidth Condition is satisfied (cont.)

Appendix E: NEW COMMERCIAL WET SPRINKLER PIPE MEASUREMENTS (NCS)

		Distance	10ft_same_branch_vol100		50ft_same_branch_vol100		80ft_same_branch_vol100		116ft_same_branch_vol100		161ft_across_cross_mains_vol100	
		Values	Rx_max_freq	Max_rx_mag	Rx_max_freq	Max_rx_mag	Rx_max_freq	Max_rx_mag	Rx_max_freq	Max_rx_mag	Rx_max_freq	Max_rx_mag
tx_freq	bandwidth	Attenuation/ft										
100	FALSE	NA	2.33	14.33	1.00	20.46	3.00	8.34	4.67	8.07	2.00	8.33
200	FALSE	NA	2.00	9.47	3.33	9.32	2.33	8.03	9.00	7.81	1.67	9.07
300	FALSE	NA	2.67	13.12	3.67	9.31	8.67	8.04	2.00	7.64	9.33	7.50
400	FALSE	NA	2400.04	13.05	3.67	9.41	2.67	7.82	5.67	8.52	4.67	10.42
500	FALSE	NA	2.67	7.93	2.33	7.72	3.00	9.24	3.67	10.20	2.67	6.77
600	FALSE	NA	2400.04	14.57	1.33	12.05	1.67	14.72	5400.08	17.87	4.67	8.04
700	FALSE	NA	3500.05	11.41	1.33	9.69	6.00	9.24	2.33	10.00	700.01	8.34
800	FALSE	NA	1600.02	33.01	3.67	9.58	800.01	8.97	4800.07	25.47	800.01	9.25
900	FALSE	NA	6300.10	21.63	900.01	10.69	1800.03	13.56	5400.08	25.03	900.01	10.24
1000	FALSE	NA	1.67	12.31	3.00	12.30	2.33	11.66	1000.02	18.34	3.00	10.90
1100	FALSE	NA	2200.03	65.65	2.33	13.11	1100.02	12.75	1100.02	22.06	1100.02	14.10
1200	FALSE	NA	2400.04	355.94	4.33	10.02	1200.02	24.10	1200.02	11.59	1200.02	13.09
1300	FALSE	NA	2600.04	64.40	1300.02	13.42	2600.04	18.71	1300.02	14.21	1300.02	13.36
1400	TRUE	46.20	1400.02	59.19	1400.02	18.03	1400.02	12.26	1400.02	14.24	1400.02	12.99
1500	FALSE	NA	6000.09	19.40	1.67	9.71	3000.05	67.20	1500.02	14.12	1500.02	16.28
1600	FALSE	NA	1600.02	287.31	1600.02	12.54	3200.05	45.72	1600.02	12.45	1600.02	12.62
1700	FALSE	NA	3400.05	48.50	1700.03	45.33	1700.03	29.27	1700.03	15.12	1700.03	17.81
1800	FALSE	NA	3600.05	25.98	1800.03	18.91	1800.03	64.08	1800.03	20.50	1800.03	36.35
1900	TRUE	40.24	1900.03	59.70	1900.03	49.61	1900.03	67.54	1900.03	18.62	1900.03	19.46
2000	TRUE	208.56	2000.03	228.67	2000.03	136.26	2000.03	28.43	2000.03	21.10	2000.03	20.10
2100	TRUE	348.75	2100.03	376.47	2100.03	98.14	2100.03	27.01	2100.03	17.86	2100.03	27.72
2200	TRUE	451.57	2200.03	469.02	2200.03	133.14	2200.03	111.72	2200.03	26.71	2200.03	17.45
2300	TRUE	591.12	2300.03	614.09	2300.03	39.88	2300.03	31.81	2300.03	14.88	2300.03	22.97
2400	TRUE	2715.20	2400.04	2739.92	2400.04	37.00	2400.04	16.10	2400.04	19.00	2400.04	24.71
2500	TRUE	1200.93	2500.04	1219.75	2500.04	25.07	2500.04	16.91	2500.04	14.58	2500.04	18.82
2600	TRUE	714.18	2600.04	741.78	2600.04	110.68	2600.04	113.63	2600.04	24.71	2600.04	27.60
2700	TRUE	213.88	2700.04	227.00	2700.04	71.39	2700.04	79.22	2700.04	14.51	2700.04	13.12
2800	TRUE	46.50	2800.04	58.12	2800.04	71.13	2800.04	86.69	2800.04	24.56	2800.04	11.63
2900	FALSE	NA	2900.04	156.35	4.33	10.38	2900.04	60.19	2900.04	25.53	2900.04	18.89
3000	TRUE	10.00	3000.05	30.00	3000.05	30.12	3000.05	50.44	3000.05	31.28	3000.05	20.01
3100	TRUE	-12.91	3100.05	13.65	3100.05	107.78	3100.05	46.67	3100.05	32.60	3100.05	26.57
3200	TRUE	132.03	3200.05	157.41	3200.05	69.64	3200.05	38.30	3200.05	26.89	3200.05	25.37
3300	FALSE	NA	3300.05	203.49	3.00	8.09	3300.05	38.23	3300.05	52.19	3300.05	24.64
3400	TRUE	35.67	3400.05	64.38	3400.05	16.24	3400.05	32.66	3400.05	29.75	3400.05	28.71
3500	TRUE	209.57	3500.05	234.01	3500.05	24.14	3500.05	24.25	3500.39	10.24	3500.05	24.44
3600	TRUE	42.29	3600.05	66.20	3600.05	34.79	3600.05	26.32	3600.05	29.81	3600.05	23.92
3700	TRUE	58.34	3700.06	83.44	3700.06	25.46	3700.06	25.75	3700.06	27.33	3700.06	25.11
3800	FALSE	NA	7600.11	14.76	3800.06	37.64	3800.06	31.37	3800.06	19.10	3800.06	25.49
3900	TRUE	94.66	3900.06	120.63	3900.06	25.74	3900.06	23.27	3900.06	24.62	3900.06	25.97
4000	TRUE	-4.92	4000.06	20.96	4000.06	23.63	4000.06	29.61	4000.06	35.25	4000.06	25.89
4100	FALSE	NA	4100.06	110.11	4100.06	34.70	4100.06	30.06	5.00	9.44	4100.06	28.25
4200	TRUE	90.88	4200.06	116.18	4200.06	25.07	4200.06	31.28	4200.06	22.31	4200.06	25.30
4300	TRUE	48.32	4300.07	73.86	4300.07	38.31	4300.07	27.65	4300.07	27.46	4300.07	25.54
4400	TRUE	163.92	4400.07	189.74	4400.07	24.26	4400.07	25.64	4400.07	37.39	4400.07	25.82
4500	TRUE	107.50	4500.07	134.12	4500.07	24.77	4500.07	25.57	4500.07	13.66	4500.07	26.62
4600	TRUE	10.89	4600.07	36.98	4600.07	24.36	4600.07	26.91	4600.07	25.96	4600.07	26.09
4700	TRUE	73.13	4700.07	100.22	4700.07	31.99	4700.07	28.32	4700.07	27.26	4700.07	27.09
4800	TRUE	454.55	4800.07	480.68	4800.07	22.98	4800.07	28.72	4800.07	40.46	4800.07	26.13
4900	TRUE	82.83	4900.07	110.04	4900.07	30.26	4900.07	27.76	4900.07	37.74	4900.07	27.21
5000	TRUE	194.89	5000.08	222.37	5000.08	29.29	5000.08	27.90	5000.08	22.30	5000.08	27.48
5100	TRUE	127.11	5100.08	154.52	5100.08	21.09	5100.08	26.00	5100.08	27.65	5100.08	27.41
5200	TRUE	1.23	5200.08	30.83	5200.08	30.94	5200.08	31.62	5200.08	33.39	5200.08	29.60
5300	TRUE	209.25	5300.08	238.52	5300.08	30.09	5300.08	30.18	5300.08	20.08	5300.08	29.27
5400	TRUE	322.29	5400.08	350.77	5400.08	29.77	5400.08	27.21	5400.08	23.43	5400.08	28.48
5500	TRUE	232.63	5500.08	261.16	5500.08	30.29	5500.08	28.21	5500.08	45.20	5500.08	28.53
5600	TRUE	-5.55	5600.08	23.20	5600.08	29.16	5600.08	28.89	5600.08	28.83	5600.08	28.75
5700	TRUE	135.76	5700.09	164.62	5700.09	28.98	5700.09	29.01	5700.09	28.33	5700.09	28.85
5800	TRUE	96.89	5800.09	125.79	5800.09	28.99	5800.09	29.29	5800.09	28.64	5800.09	28.90
5900	TRUE	42.29	5900.09	71.42	5900.09	29.27	5900.09	30.80	5900.09	30.98	5900.09	29.14
6000	TRUE	237.49	6000.09	266.67	6000.09	29.04	6000.09	29.29	6000.09	27.08	6000.09	29.18
6100	TRUE	216.62	6100.09	245.92	6100.09	28.83	6100.09	28.42	6100.09	31.85	6100.09	29.29
6200	TRUE	130.78	6200.09	160.12	6200.09	28.69	6200.09	29.06	6200.09	29.19	6200.09	29.34
6300	TRUE	500.01	6300.10	530.27	6300.10	30.73	6300.10	31.44	6300.10	30.61	6300.10	30.26
6400	TRUE	110.40	6400.10	142.67	6400.10	32.32	6400.10	32.70	6400.10	32.89	6400.10	32.28
6500	TRUE	-1.54	6500.10	28.26	6500.10	29.69	6500.10	29.47	6500.10	29.35	6500.10	29.80
6600	TRUE	42.71	6600.10	72.40	6600.10	32.81	6600.10	30.91	6600.10	34.55	6600.10	29.70
6700	TRUE	57.75	6700.10	87.61	6700.10	32.47	6700.10	29.69	6700.10	30.23	6700.10	29.86
6800	TRUE	39.20	6800.10	69.03	6800.10	30.25	6800.10	30.18	6800.10	30.79	6800.10	29.83
6900	TRUE	163.85	6900.10	193.74	6900.10	31.84	6900.10	31.19	6900.10	32.11	6900.10	29.88
7000	TRUE	25.20	7000.11	55.45	7000.11	30.76	7000.11	31.14	7000.11	30.82	7000.11	30.25
7100	TRUE	55.41	7100.11	85.78	7100.11	30.32	7100.11	30.78	7100.11	29.81	7100.11	30.37
7200	TRUE	19.51	7200.11	49.85	7200.11	31.21	7200.11	31.98	7200.11	29.48	7200.11	30.33
7300	TRUE	58.50	7300.11	89.01	7300.11	29.40	7300.11	31.65	7300.11	31.00	7300.11	30.51
7400	TRUE	10.28	7400.11	40.92	7400.11	30.77	7400.11	31.60	7400.11	30.93	7400.11	30.64
7500	TRUE	61.60	7500.11	92.33	7500.11	31.56	7500.11	31.81	7500.11	31.20	7500.11	30.74
7600	TRUE	130.99	7600.11	161.87	7600.11	32.12	7600.11	31.24	7600.11	35.07	7600.11	30.88
7700	TRUE	73.04	7700.12	103.96	7700.12	30.58	7700.12	31.60	7700.12	31.84	7700.12	30.93
7800	TRUE	-7.40	7800.12	24.50	7800.12	32.18	7800.12	32.67	7800.12	32.72	7800.12	31.90
7900	TRUE	7.29	7900.12	41.09	7900.12	34.63	7900.12	34.72	7900.12	34.70	7900.12	33.80
8000	TRUE	-15.77	8000.12	15.49	8000.12	32.05	8000.12	32.06	8000.12	31.91	8000.12	31.26
8100	TRUE	10.77	8100.12	41.98	8100.12	32.22	8100.12	31.99	8100.12	31.82	8100.12	31.21
8200	TRUE	76.04	8200.12	107.21	8200.12	32.05	8200.12	32.31	8200.12	31.66	8200.12	31.17
8300	TRUE	107.73	8300.13	138.95	8300.13	32.54	8300.13	32.16	8300.13	32.26	8300.13	31.22
8400	TRUE	74.01	8400.13	105.28	8400.13	33.01	8400.13	32.15	8400.13	32.04	8400.13	31.26
8500	TRUE	28.48	8500.13	59.84	8500.13	32.21	8500.13	32.47	8500.13	31.62	8500.13	31.36
8600	TRUE	-17.46	8600.13	13.96	8600.13	32.15	8600.13	32.59	8600.13	31.39	8600.13	31.42
8700	TRUE	13.04	8700.13	44.47	8700.13	32.48	8700.13	32.60	8700.13	32.45	8700.13	31.43

Table E.1: New Commercial Wet Sprinkler Pipe Peak Signal Frequency and Magnitude. "Bandwidth" column indicates whether the Bandwidth Condition is satisfied

		Distance	10ft_same_branch_vol100		50ft_same_branch_vol100		80ft_same_branch_vol100		116ft_same_branch_vol100		161ft_across_cross_mains_vol100	
		Values	Rx_max_freq	Max_rx_mag	Rx_max_freq	Max_rx_mag	Rx_max_freq	Max_rx_mag	Rx_max_freq	Max_rx_mag	Rx_max_freq	Max_rx_mag
tx_freq	bandwidth	Attenuation/ft										
8800	TRUE	-3.01	8800.13	28.46	8800.13	33.07	8800.13	32.70	8800.13	32.41	8800.13	31.47
8900	TRUE	82.99	8900.13	114.59	8900.13	30.80	8900.13	33.24	8900.13	33.35	8900.13	31.60
9000	TRUE	-0.69	9000.14	30.94	9000.14	32.80	9000.14	32.88	9000.14	32.36	9000.14	31.63
9100	TRUE	0.89	9100.14	32.63	9100.14	33.44	9100.14	33.15	9100.14	33.34	9100.14	31.73
9200	TRUE	132.35	9200.14	164.14	9200.14	32.77	9200.14	33.33	9200.14	32.86	9200.14	31.79
9300	TRUE	159.28	9300.14	191.14	9300.14	32.95	9300.14	33.29	9300.14	32.99	9300.14	31.86
9400	TRUE	25.43	9400.14	57.29	9400.14	33.12	9400.14	33.34	9400.14	33.16	9400.14	31.86
9500	TRUE	89.85	9500.14	121.96	9500.14	33.30	9500.14	33.77	9500.14	33.28	9500.14	32.11
9600	TRUE	22.13	9600.15	54.26	9600.15	32.21	9600.15	34.21	9600.15	33.28	9600.15	32.13
9700	TRUE	1.90	9700.15	34.00	9700.15	33.45	9700.15	33.86	9700.15	33.48	9700.15	32.09
9800	TRUE	-1.99	9800.15	30.16	9800.15	33.69	9800.15	33.91	9800.15	33.71	9800.15	32.15
9900	TRUE	32.83	9900.15	65.17	9900.15	33.84	9900.15	34.03	9900.15	33.77	9900.15	32.34
10000	TRUE	7.21	10000.15	39.77	10000.15	33.95	10000.15	34.28	10000.15	34.17	10000.15	32.56
10100	TRUE	78.03	10100.15	113.36	10100.15	37.01	10100.15	37.28	10100.15	36.99	10100.15	35.34
10200	TRUE	34.42	10200.15	67.82	10200.15	34.62	10200.15	35.32	10200.15	35.04	10200.15	33.40
10300	TRUE	14.04	10300.16	46.58	10300.16	34.22	10300.16	34.22	10300.16	34.19	10300.16	32.54
10400	TRUE	20.16	10400.16	52.77	10400.16	34.04	10400.16	34.42	10400.16	34.01	10400.16	32.61
10500	TRUE	-4.56	10500.16	28.07	10500.16	34.04	10500.16	34.45	10500.16	34.12	10500.16	32.63
10600	TRUE	-8.83	10600.16	23.89	10600.16	34.57	10600.16	34.68	10600.16	34.63	10600.16	32.72
10700	TRUE	38.82	10700.16	71.42	10700.16	34.03	10700.16	34.52	10700.16	34.12	10700.16	32.60
10800	TRUE	0.46	10800.16	33.17	10800.16	34.26	10800.16	34.56	10800.16	34.35	10800.16	32.71
10900	TRUE	-8.55	10900.16	24.11	10900.16	34.28	10900.16	34.67	10900.16	33.85	10900.16	32.67
11000	TRUE	-16.11	11000.17	16.70	11000.17	34.40	11000.17	34.72	11000.17	34.59	11000.17	32.81
11100	TRUE	2.37	11100.17	35.14	11100.17	34.39	11100.17	34.81	11100.17	34.50	11100.17	32.77
11200	TRUE	-4.37	11200.17	28.27	11200.17	34.45	11200.17	34.76	11200.17	34.50	11200.17	32.64
11300	TRUE	-4.70	11300.17	28.04	11300.17	34.43	11300.17	34.86	11300.17	34.57	11300.17	32.75
11400	TRUE	5.31	11400.17	38.10	11400.17	34.65	11400.17	34.96	11400.17	34.50	11400.17	32.79
11500	TRUE	-7.30	11500.17	25.57	11500.17	34.76	11500.17	35.05	11500.17	34.69	11500.17	32.87
11600	TRUE	0.59	11600.18	33.36	11600.18	34.86	11600.18	34.99	11600.18	34.64	11600.18	32.77
11700	TRUE	-15.01	11700.18	17.82	11700.18	34.73	11700.18	35.14	11700.18	34.88	11700.18	32.83
11800	TRUE	5.09	11800.18	37.98	11800.18	34.77	11800.18	35.11	11800.18	34.93	11800.18	32.89
11900	TRUE	4.80	11900.18	37.79	11900.18	35.02	11900.18	35.38	11900.18	35.15	11900.18	33.00
12000	TRUE	-9.49	12000.18	23.50	12000.18	34.92	12000.18	35.39	12000.18	35.15	12000.18	33.00
12100	TRUE	-0.67	12100.18	32.41	12100.18	35.02	12100.18	35.50	12100.18	35.17	12100.18	33.09
12200	TRUE	1.10	12200.18	34.22	12200.18	35.12	12200.18	35.56	12200.18	35.27	12200.18	33.12
12300	TRUE	0.40	12300.19	34.49	12300.19	36.37	12300.19	36.67	12300.19	36.37	12300.19	34.08
12400	TRUE	-3.21	12400.19	32.94	12400.19	38.65	12400.19	38.99	12400.19	38.65	12400.19	36.15
12500	TRUE	-1.94	12500.19	31.51	12500.19	35.75	12500.19	36.03	12500.19	35.71	12500.19	33.45
12600	TRUE	-2.89	12600.19	30.46	12600.19	35.52	12600.19	35.95	12600.19	35.75	12600.19	33.36
12700	TRUE	-3.33	12700.19	30.04	12700.19	35.70	12700.19	36.03	12700.19	35.74	12700.19	33.37
12800	TRUE	-1.31	12800.19	32.15	12800.19	35.80	12800.19	36.12	12800.19	35.82	12800.19	33.47
12900	TRUE	-1.80	12900.20	31.76	12900.20	35.90	12900.20	36.29	12900.20	35.99	12900.20	33.55
13000	TRUE	-8.88	13000.20	24.81	13000.20	36.05	13000.20	36.40	13000.20	36.15	13000.20	33.70
13100	TRUE	2.06	13100.20	35.67	13100.20	35.73	13100.20	36.40	13100.20	36.13	13100.20	33.62
13200	TRUE	-1.98	13200.20	31.66	13200.20	36.06	13200.20	36.50	13200.20	36.17	13200.20	33.64
13300	TRUE	-0.09	13300.20	33.56	13300.20	35.99	13300.20	36.54	13300.20	36.25	13300.20	33.66
13400	TRUE	-2.87	13400.20	30.86	13400.20	36.29	13400.20	36.72	13400.20	36.40	13400.20	33.73
13500	TRUE	-0.06	13500.20	33.72	13500.20	36.36	13500.20	36.78	13500.20	36.35	13500.20	33.77
13600	TRUE	-0.31	13600.21	33.52	13600.21	36.59	13600.21	36.80	13600.21	36.51	13600.21	33.82
13700	TRUE	-6.06	13700.21	27.76	13700.21	36.27	13700.21	36.89	13700.21	36.52	13700.21	33.82
13800	TRUE	-2.67	13800.21	31.10	13800.21	36.57	13800.21	36.92	13800.21	36.59	13800.21	33.77
13900	TRUE	-0.91	13900.21	32.86	13900.21	36.61	13900.21	37.02	13900.21	36.68	13900.21	33.77
14000	TRUE	-4.25	14000.21	29.64	14000.21	36.71	14000.21	37.08	14000.21	36.73	14000.21	33.88
14100	TRUE	-7.06	14100.21	26.83	14100.21	36.68	14100.21	37.13	14100.21	36.77	14100.21	33.89
14200	TRUE	-0.81	14200.21	33.03	14200.21	36.72	14200.21	37.14	14200.21	36.79	14200.21	33.84
14300	TRUE	-6.54	14300.22	27.34	14300.22	36.62	14300.22	37.19	14300.22	36.82	14300.22	33.87
14400	TRUE	-3.46	14400.22	30.48	14400.22	36.85	14400.22	37.30	14400.22	36.96	14400.22	33.94
14500	TRUE	-1.71	14500.22	32.31	14500.22	36.98	14500.22	37.40	14500.22	37.02	14500.22	34.01
14600	TRUE	-3.37	14600.22	30.51	14600.22	36.93	14600.22	37.35	14600.22	37.02	14600.22	33.88
14700	TRUE	-1.74	14700.22	32.20	14700.22	36.94	14700.22	37.49	14700.22	37.10	14700.22	33.94
14800	TRUE	2.32	14800.22	36.29	14800.22	37.06	14800.22	37.53	14800.22	37.10	14800.22	33.96
14900	TRUE	0.20	14900.23	34.25	14900.23	37.17	14900.23	37.68	14900.23	37.27	14900.23	34.05
15000	TRUE	-7.29	15000.23	26.76	15000.23	37.27	15000.23	37.72	15000.23	37.29	15000.23	34.05
15100	TRUE	0.37	15100.23	34.51	15100.23	37.21	15100.23	37.88	15100.23	37.42	15100.23	34.14
15200	TRUE	-6.99	15200.23	27.13	15200.23	37.50	15200.23	37.94	15200.23	37.47	15200.23	34.11
15300	TRUE	-1.22	15300.23	33.98	15300.23	38.61	15300.23	39.15	15300.23	38.64	15300.23	35.20
15400	TRUE	2.96	15400.23	40.27	15400.23	41.00	15400.23	41.56	15400.23	41.07	15400.23	37.31
15500	TRUE	-6.48	15500.23	27.99	15500.23	37.94	15500.23	38.42	15500.23	37.92	15500.23	34.47
15600	TRUE	-0.43	15600.24	33.89	15600.24	37.87	15600.24	38.40	15600.24	37.92	15600.24	34.32
15700	TRUE	-0.46	15700.24	33.91	15700.24	37.89	15700.24	38.49	15700.24	39.54	15700.24	34.37
15800	TRUE	-0.38	15800.24	34.09	15800.24	38.06	15800.24	38.63	15800.24	40.43	15800.24	34.47
15900	TRUE	-1.48	15900.24	33.06	15900.24	38.18	15900.24	38.76	15900.24	40.66	15900.24	34.55
16000	TRUE	-3.51	16000.24	31.15	16000.24	38.39	16000.24	38.91	16000.24	40.72	16000.24	34.66
16100	TRUE	-3.32	16100.24	31.31	16100.24	38.35	16100.24	39.00	16100.24	40.64	16100.24	34.63
16200	TRUE	-0.40	16200.24	34.30	16200.24	38.40	16200.24	39.10	16200.24	40.77	16200.24	34.70
16300	TRUE	0.46	16300.25	35.20	16300.25	38.51	16300.25	39.20	16300.25	40.85	16300.25	34.73
16400	TRUE	-5.45	16400.25	29.38	16400.25	38.73	16400.25	39.39	16400.25	41.10	16400.25	34.83
16500	TRUE	-3.35	16500.25	31.50	16500.25	38.75	16500.25	39.40	16500.25	40.59	16500.25	34.86
16600	TRUE	-2.10	16600.25	32.86	16600.25	38.90	16600.25	39.56	16600.25	40.68	16600.25	34.96
16700	TRUE	-3.81	16700.25	31.14	16700.25	38.91	16700.25	39.57	16700.25	41.57	16700.25	34.95
16800	TRUE	-5.17	16800.25	29.83	16800.25	38.86	16800.25	39.67	16800.25	41.66	16800.25	35.00
16900	TRUE	-5.73	16900.26	29.24	16900.26	38.99	16900.26	39.77	16900.26	41.38	16900.26	34.97
17000	TRUE	-6.35	17000.26	28.82	17000.26	39.11	17000.26	39.85	17000.26	41.53	17000.26	35.16
17100	TRUE	-1.20	17100.26	33.96	17100.26	39.05	17100.26	39.98	17100.26	41.60	17100.26	35.16
17200	TRUE	-5.27	17200.26	29.86	17200.26	39.10	17200.26	39.97	17200.26	41.57	17200.26	35.13
17300	TRUE	1.36	17300.26	36.51	17300.26	39.09	17300.26	40.04	17300.26	41.61	17300.26	35.15
17400	TRUE	-0.89	17400.26	34.38	17400.26	39.22	17400.26	40.12	17400.26	41.80	17400.26	35.26

Table E.1: New Commercial Wet Sprinkler Pipe Peak Signal Frequency and Magnitude. "Bandwidth" column indicates whether the Bandwidth Condition is satisfied (cont.)

		Distance	10ft_same_branch_vol100		50ft_same_branch_vol100		80ft_same_branch_vol100		116ft_same_branch_vol100		161ft_across_cross_mains_vol100	
		Values	Rx_max_freq	Max_rx_mag	Rx_max_freq	Max_rx_mag	Rx_max_freq	Max_rx_mag	Rx_max_freq	Max_rx_mag	Rx_max_freq	Max_rx_mag
tx_freq	bandwidth	Attenuation/ft										
17500	TRUE	-8.55	17500.26	26.77	17500.26	39.26	17500.26	40.25	17500.26	41.96	17500.26	35.32
17600	TRUE	-7.27	17600.27	28.04	17600.27	39.34	17600.27	40.22	17600.27	41.92	17600.27	35.31
17700	TRUE	1.39	17700.27	36.72	17700.27	39.33	17700.27	40.35	17700.27	42.04	17700.27	35.34
17800	TRUE	1.86	17800.27	37.29	17800.27	39.50	17800.27	40.40	17800.27	42.13	17800.27	35.43
17900	TRUE	-13.60	17900.27	21.92	17900.27	39.44	17900.27	40.55	17900.27	42.42	17900.27	35.52
18000	TRUE	-8.87	18000.27	26.66	18000.27	39.72	18000.27	40.62	18000.27	42.49	18000.27	35.53
18100	TRUE	-2.28	18100.27	33.35	18100.27	39.90	18100.27	40.73	18100.27	42.64	18100.27	35.63
18200	TRUE	-3.22	18200.28	32.42	18200.28	39.86	18200.28	40.81	18200.28	42.75	18200.28	35.63
18300	TRUE	0.29	18300.28	36.00	18300.28	40.00	18300.28	40.91	18300.28	42.94	18300.28	35.70
18400	TRUE	0.82	18400.28	36.61	18400.28	40.14	18400.28	40.98	18400.28	43.35	18400.28	35.79
18500	TRUE	-0.91	18500.28	35.01	18500.28	40.29	18500.28	41.22	18500.28	43.35	18500.28	35.92
18600	TRUE	-3.66	18600.28	32.28	18600.28	40.43	18600.28	41.27	18600.28	43.50	18600.28	35.94
18700	TRUE	-3.35	18700.28	32.60	18700.28	40.45	18700.28	41.30	18700.28	43.57	18700.28	35.94
18800	TRUE	-0.44	18800.28	35.46	18800.28	40.60	18800.28	41.37	18800.28	43.58	18800.28	35.91
18900	TRUE	-1.36	18900.29	34.68	18900.29	40.58	18900.29	41.54	18900.29	43.74	18900.29	36.04
19000	TRUE	-10.55	19000.29	25.48	19000.29	40.77	19000.29	41.59	19000.29	43.84	19000.29	36.03
19100	TRUE	-2.12	19100.29	33.78	19100.29	40.65	19100.29	41.42	19100.29	43.75	19100.29	35.90
19200	TRUE	-2.74	19200.29	33.22	19200.29	40.56	19200.29	41.51	19200.29	43.71	19200.29	35.96
19300	TRUE	-0.56	19300.29	35.15	19300.29	40.62	19300.29	41.38	19300.29	43.67	19300.29	35.71
19400	TRUE	-6.35	19400.29	29.22	19400.29	40.49	19400.29	41.24	19400.29	43.56	19400.29	35.58
19500	TRUE	-7.06	19500.29	28.21	19500.29	40.12	19500.29	41.01	19500.29	44.43	19500.29	35.27
19600	TRUE	-6.18	19600.30	28.83	19600.30	39.90	19600.30	40.72	19600.30	50.79	19600.30	35.01
19700	TRUE	4.84	19700.30	39.38	19700.30	39.43	19700.30	40.21	19700.30	48.77	19700.30	34.54
19800	TRUE	3.68	19800.30	37.75	19800.30	38.90	19800.30	39.70	19800.30	51.82	19800.30	34.07
19900	TRUE	-14.11	19900.30	19.27	19900.30	38.18	19900.30	38.95	19900.30	46.62	19900.30	33.38
20000	TRUE	10.20	20000.30	42.95	20000.30	37.48	20000.30	38.24	20000.30	45.19	20000.30	32.75

Table E.1: New Commercial Wet Sprinkler Pipe Peak Signal Frequency and Magnitude. "Bandwidth" column indicates whether the Bandwidth Condition is satisfied (cont.)

Appendix F: NEW COMMERCIAL RISER STANDPIPE MEASUREMENTS (NCR)

		Distance	30.3ft_5th_to_3rd_vol100		45.6ft_5th_to_2nd_vol100		61.2ft_5th_to_1st_vol100	
		Values	Rx_max_freq	Max_rx_mag	Rx_max_freq	Max_rx_mag	Rx_max_freq	Max_rx_mag
Tx_freq	Bandwidth	Attenuation/ft						
1000	FALSE	NA	2.67	9.02	0.00	71.28	3.33	7.46
2000	FALSE	NA	2.00	10.91	2000.03	28.01	2000.03	9.25
3000	TRUE	2.26	3000.05	17.08	3000.05	107.11	3000.05	14.82
4000	TRUE	6.01	4000.06	23.70	4000.06	25.12	4000.06	17.69
5000	TRUE	0.78	5000.08	21.01	5000.08	23.33	5000.08	20.24
6000	TRUE	-8.36	6000.09	19.61	6000.09	28.54	6000.09	27.97
7000	TRUE	1.43	7000.11	20.85	7000.11	19.26	7000.11	19.41
8000	TRUE	2.48	8000.12	21.59	8000.12	33.15	8000.12	19.10
9000	TRUE	-0.06	9000.14	19.20	9000.14	17.47	9000.14	19.27
10000	TRUE	0.00	10000.15	20.55	10000.15	32.00	10000.15	20.56
11000	TRUE	-0.10	11000.17	16.68	11000.17	32.30	11000.17	16.77
12000	TRUE	-0.06	12000.18	16.99	12000.18	32.47	12000.18	17.05
13000	TRUE	0.08	13000.20	10.83	13000.20	33.12	13000.20	10.74
14000	FALSE	NA	1.67	11.65	14000.21	21.21	4.00	11.90
15000	TRUE	-0.92	15000.23	10.94	15000.23	33.82	15000.23	11.87
16000	FALSE	NA	2.33	11.08	1.33	8.96	7.33	7.54
17000	FALSE	NA	7.33	7.60	1.33	8.55	3.33	10.02
18000	FALSE	NA	2.67	11.20	1.00	10.46	6.00	8.84
19000	FALSE	NA	2.33	9.29	10.00	7.39	2.33	12.55
20000	FALSE	NA	1.67	11.35	3.33	9.13	18.00	7.35

Table F.1: New Commercial Riser Pipe Peak Signal Frequency and Magnitude. "Bandwidth" column indicates whether the Bandwidth Condition is satisfied

Appendix G: BLACK STEEL PIPE OUTDOOR LABORATORY SETTING MEASUREMENTS WITH VICTAULIC 005 RIGID COUPLINGS

		Distance	0ft_vol100		10ft_vol100		20ft_vol100		22.75ft_vol100		30ft_vol100		40ft_vol100		42.5ft_vol100	
		Values	Rx_max_freq	Max_rx_mag	Rx_max_freq	Max_rx_mag	Rx_max_freq	Max_rx_mag	Rx_max_freq	Max_rx_mag	Rx_max_freq	Max_rx_mag	Rx_max_freq	Max_rx_mag	Rx_max_freq	Max_rx_mag
Tx_freq	Bandwidth	Attenuation/ft														
100	FALSE	NA	60.00	12.88	60.00	10.04	2.33	18.53	60.00	10.70	2.67	11.04	2.00	15.77	60.00	20.46
200	FALSE	NA	200.00	11.57	200.00	13.45	60.00	14.70	200.00	10.80	200.00	12.73	200.00	12.13	200.00	19.37
300	FALSE	NA	300.00	15.28	300.00	18.44	60.00	20.81	300.00	16.19	300.00	17.60	300.00	17.70	300.00	28.63
400	TRUE	-17.81	400.01	21.03	400.01	23.71	400.01	27.36	400.01	21.93	400.01	22.80	400.01	23.82	400.01	38.85
500	TRUE	-24.65	500.01	24.19	500.01	27.40	500.01	31.87	500.01	25.14	500.01	26.99	500.01	25.98	500.01	48.84
600	TRUE	-31.52	600.01	29.71	600.01	32.65	600.01	39.64	600.01	30.91	600.01	33.84	600.01	33.15	600.01	61.23
700	TRUE	-33.25	700.01	33.25	700.01	36.41	700.01	44.52	700.01	34.36	700.01	36.67	700.01	37.00	700.01	66.51
800	TRUE	-21.10	800.01	37.90	800.01	41.99	800.01	49.85	800.01	38.27	800.01	40.92	800.01	40.85	800.01	59.00
900	TRUE	-9.28	900.01	44.87	900.01	47.57	900.01	57.27	900.01	43.71	900.01	46.83	900.01	46.94	900.01	54.15
1000	TRUE	2.39	1000.02	46.15	1000.02	50.30	1000.02	59.88	1000.02	45.88	1000.02	49.62	1000.02	48.43	1000.02	43.76
1100	TRUE	5.70	1100.02	54.60	1100.02	58.76	1100.02	67.87	1100.02	54.34	1100.02	57.56	1100.02	58.28	1100.02	48.89
1200	TRUE	5.71	1200.02	50.73	1200.02	56.46	1200.02	67.37	1200.02	51.21	1200.02	55.07	1200.02	54.78	1200.02	45.02
1300	TRUE	5.13	1300.02	53.52	1300.02	59.18	1300.02	72.22	1300.02	53.72	1300.02	58.71	1300.02	58.08	1300.02	48.39
1400	TRUE	5.04	1400.02	56.76	1400.02	62.87	1400.02	77.21	1400.02	58.05	1400.02	62.52	1400.02	61.77	1400.02	51.72
1500	TRUE	7.19	1500.02	66.11	1500.02	72.47	1500.02	88.45	1500.02	67.19	1500.02	72.35	1500.02	71.27	1500.02	58.91
1600	TRUE	3.83	1600.02	62.04	1600.02	65.46	1600.02	86.10	1600.02	62.90	1600.02	67.28	1600.02	67.91	1600.02	58.22
1700	TRUE	5.66	1700.03	63.43	1700.03	70.92	1700.03	87.62	1700.03	66.22	1700.03	70.68	1700.03	69.31	1700.03	57.77
1800	TRUE	5.95	1800.03	67.83	1800.03	75.37	1800.03	95.16	1800.03	70.54	1800.03	75.22	1800.03	74.16	1800.03	61.88
1900	TRUE	5.83	1900.03	74.10	1900.03	84.07	1900.03	102.19	1900.03	77.62	1900.03	83.34	1900.03	81.88	1900.03	68.28
2000	TRUE	4.46	2000.03	69.91	2000.03	79.65	2000.03	99.46	2000.03	72.86	2000.03	80.02	2000.03	78.08	2000.03	65.45
2100	TRUE	4.42	2100.03	71.87	2100.03	82.02	2100.03	96.88	2100.03	75.67	2100.03	81.59	2100.03	79.57	2100.03	67.45
2200	TRUE	5.88	2200.03	74.30	2200.03	83.74	2200.03	105.51	2200.03	77.74	2200.03	83.54	2200.03	81.46	2200.03	68.42
2300	TRUE	6.51	2300.03	76.40	2300.03	85.28	2300.03	107.46	2300.03	80.32	2300.03	85.17	2300.03	82.24	2300.03	69.89
2400	TRUE	7.43	2400.04	78.57	2400.04	87.03	2400.04	111.03	2400.04	82.10	2400.04	86.65	2400.04	83.68	2400.04	71.14
2500	TRUE	8.63	2500.04	80.88	2500.04	87.63	2500.04	114.54	2500.04	84.43	2500.04	87.96	2500.04	84.81	2500.04	72.25
2600	TRUE	10.73	2600.04	89.52	2600.04	97.01	2600.04	122.69	2600.04	93.84	2600.04	95.93	2600.04	94.66	2600.04	78.79
2700	TRUE	8.23	2700.04	85.83	2700.04	94.53	2700.04	119.71	2700.04	90.09	2700.04	94.44	2700.04	92.24	2700.04	77.60
2800	TRUE	5.85	2800.04	84.88	2800.04	96.10	2800.04	116.13	2800.04	89.47	2800.04	96.35	2800.04	92.89	2800.04	79.03
2900	TRUE	5.58	2900.04	87.55	2900.04	99.70	2900.04	117.41	2900.04	90.97	2900.04	99.75	2900.04	97.29	2900.04	81.97
3000	TRUE	7.79	3000.05	90.57	3000.05	102.22	3000.05	122.10	3000.05	92.28	3000.05	102.05	3000.05	96.21	3000.05	82.78
3100	TRUE	8.38	3100.05	92.59	3100.05	102.00	3100.05	126.54	3100.05	94.12	3100.05	102.79	3100.05	98.42	3100.05	84.21
3200	TRUE	7.72	3200.05	93.41	3200.05	104.66	3200.05	127.88	3200.05	95.45	3200.05	103.89	3200.05	102.78	3200.05	85.69
3300	TRUE	6.15	3300.05	97.26	3300.05	111.99	3300.05	137.50	3300.05	99.27	3300.05	110.11	3300.05	107.98	3300.05	91.10
3400	TRUE	4.69	3400.05	104.43	3400.05	121.70	3400.05	150.71	3400.05	107.21	3400.05	120.95	3400.05	118.95	3400.05	99.73
3500	TRUE	3.25	3500.05	96.75	3500.05	113.57	3500.05	141.62	3500.05	99.57	3500.05	113.19	3500.05	110.55	3500.05	93.51
3600	TRUE	3.19	3600.05	97.37	3600.05	114.54	3600.05	144.05	3600.05	100.09	3600.05	114.11	3600.05	111.33	3600.05	94.19
3700	TRUE	3.26	3700.06	98.05	3700.06	115.29	3700.06	144.97	3700.06	100.94	3700.06	115.07	3700.06	111.98	3700.06	94.79
3800	TRUE	3.26	3800.06	98.99	3800.06	116.56	3800.06	146.42	3800.06	101.79	3800.06	116.03	3800.06	112.92	3800.06	95.73
3900	TRUE	3.31	3900.06	99.80	3900.06	117.45	3900.06	148.36	3900.06	102.78	3900.06	117.22	3900.06	113.76	3900.06	96.49
4000	TRUE	3.36	4000.06	101.12	4000.06	118.99	4000.06	148.98	4000.06	104.08	4000.06	118.50	4000.06	115.00	4000.06	97.76
4100	TRUE	4.05	4100.06	110.69	4100.06	129.94	4100.06	163.60	4100.06	114.13	4100.06	129.61	4100.06	125.92	4100.06	106.64
4200	TRUE	4.09	4200.06	104.82	4200.06	122.97	4200.06	155.90	4200.06	107.94	4200.06	122.69	4200.06	119.08	4200.06	100.73
4300	TRUE	3.86	4300.07	102.62	4300.07	120.25	4300.07	152.04	4300.07	105.53	4300.07	120.04	4300.07	116.31	4300.07	98.76
4400	TRUE	3.78	4400.07	103.35	4400.07	121.27	4400.07	152.41	4400.07	106.14	4400.07	120.71	4400.07	117.22	4400.07	99.57
4500	TRUE	3.77	4500.07	103.70	4500.07	121.53	4500.07	154.69	4500.07	106.43	4500.07	121.13	4500.07	117.55	4500.07	99.93
4600	TRUE	3.88	4600.07	104.34	4600.07	122.34	4600.07	154.19	4600.07	106.99	4600.07	121.82	4600.07	117.99	4600.07	100.46
4700	TRUE	4.08	4700.07	104.73	4700.07	122.73	4700.07	153.48	4700.07	107.11	4700.07	121.99	4700.07	121.58	4700.07	100.65
4800	TRUE	4.14	4800.07	105.32	4800.07	123.19	4800.07	155.84	4800.07	108.36	4800.07	122.83	4800.07	122.12	4800.07	101.18
4900	TRUE	3.05	4900.07	105.41	4900.07	124.39	4900.07	156.63	4900.07	109.65	4900.07	124.01	4900.07	123.34	4900.07	102.36
5000	TRUE	1.65	5000.08	105.62	5000.08	126.39	5000.08	157.90	5000.08	110.58	5000.08	125.88	5000.08	124.92	5000.08	103.97
5100	TRUE	1.63	5100.08	105.88	5100.08	127.12	5100.08	159.70	5100.08	111.54	5100.08	126.94	5100.08	125.58	5100.08	104.25
5200	TRUE	3.09	5200.08	113.31	5200.08	134.84	5200.08	173.18	5200.08	118.79	5200.08	134.70	5200.08	133.81	5200.08	110.22
5300	TRUE	4.44	5300.08	115.10	5300.08	136.01	5300.08	174.25	5300.08	119.54	5300.08	135.32	5300.08	134.03	5300.08	110.66
5400	TRUE	3.76	5400.08	109.22	5400.08	128.82	5400.08	165.06	5400.08	113.71	5400.08	128.40	5400.08	127.66	5400.08	105.46
5500	TRUE	4.62	5500.08	110.38	5500.08	129.44	5500.08	166.13	5500.08	114.44	5500.08	129.04	5500.08	128.10	5500.08	105.76
5600	TRUE	4.94	5600.08	111.41	5600.08	129.59	5600.08	166.66	5600.08	114.64	5600.08	129.24	5600.08	128.26	5600.08	106.47
5700	TRUE	-16.77	5700.09	112.64	5700.09	129.97	5700.09	167.39	5700.09	115.09	5700.09	129.80	5700.09	128.82	5700.09	129.41
5800	TRUE	-14.80	5800.09	113.71	5800.09	130.58	5800.09	167.79	5800.09	115.77	5800.09	130.29	5800.09	129.22	5800.09	128.51
5900	TRUE	-16.99	5900.09	112.67	5900.09	131.09	5900.09	168.53	5900.09	116.24	5900.09	130.83	5900.09	129.95	5900.09	129.66
6000	TRUE	-17.15	6000.09	112.70	6000.09	131.58	6000.09	169.11	6000.09	116.57	6000.09	131.10	6000.09	130.18	6000.09	129.84
6100	TRUE	-18.77	6100.09	113.41	6100.09	132.42	6100.09	170.00	6100.09	117.15	6100.09	131.71	6100.09	130.79	6100.09	132.18
6200	TRUE	-16.38	6200.09	113.25	6200.09	132.41	6200.09	170.16	6200.09	117.42	6200.09	131.93	6200.09	130.82	6200.09	129.63
6300	TRUE	-21.92	6300.10	116.76	6300.10	136.35	6300.10	175.60	6300.10	121.14	6300.10	136.16	6300.10	135.23	6300.10	138.67
6400	TRUE	-24.19	6400.10	123.76	6400.10	145.94	6400.10	187.21	6400.10	129.25	6400.10	145.24	6400.10	144.23	6400.10	147.95
6500	TRUE	-22.77	6500.10	113.94	6500.10	134.43	6500.10	172.77	6500.10	119.10	6500.10	133.97	6500.10	133.21	6500.10	136.70
6600	TRUE	-22.66	6600.10	114.16	6600.10	134.13	6600.10	172.18	6600.10	118.80	6600.10	133.77	6600.10	133.24	6600.10	136.82
6700	TRUE	-22.38	6700.10	114.52	6700.10	134.60	6700.10	172.46	6700.10	118.96	6700.10	134.25	6700.10	133.52	6700.10	136.91
6800	TRUE	-22.98	6800.10	114.52	6800.10	135.08	6800.10	172.95	6800.10	119.20	6800.10	134.75	6800.10	134.25	6800.10	137.51
6900	TRUE	-23.21	6900.10	115.07	6900.10	135.42	6900.10	173.42	6900.10	119.64	6900.10	135.67	6900.10	134.85	6900.10	138.28
7000	TRUE	-23.70	7000.11	115.57	7000.11	136.80	7000.11	174.61	7000.11	119.96	7000.11	136.23	7000.11	135.48	7000.11	139.27
7100	TRUE	-24.11	7100.11	115.80	7100.11	136.67	7100.11	175.03	7100.11	119.96	7100.11	136.33	7100.11	135.64	7100.11	139.91
7200	TRUE	-24.43	7200.11	115.88	7200.11	137.14	7200.11	175.84	7200.11	120.24	7200.11	136.76	7200.11	136.03	7200.11	140.31
7300	TRUE	-25.74	7300.11	114.80	7300.11	138.22	7300.11	176.88	7300.11	120.09	7300.11	136.89	7300.11	136.20	7300.11	140.54
7400	TRUE	-25.51	7400.11	115.49	7400.11	137.98	7400.11	178.17	7400.11	120.79	7400.11	137.40	7400.11	136.67	7400.11	141.00
7500	TRUE	-25.04	7500.11	116.02	7500.11	138.02	7500.11	178.20	7500.11	120.50	7500.11	137.43	7500.11	136.65	7500.11	141.07
7600	TRUE	-24.79	7600.11	116.75	7600.11	138.29	7600.11	179.14	7600.11	120.70	7600.11	137.98	7600.11	137.00	7600.11	141.53
7700	TRUE	-24.69	7700.12	116.93	7700.12	138.26	7700.12	179.71	7700.12	120.72	7700.12	138.02	7700.12	137.11	7700.12	141.63
7800	TRUE	-25.48	7800.12	120.47	7800.12	142.52	7800.12	185.19	7800.12	124.66	7800.12	142.08	7800.12	141.40	7800.12	145.94
7900	TRUE	-27.34	7900.12	127.91	7900.12	151.82	7900.12	196.86	7900.12	132.47	7900.12	151.17	7900.12	150.35	7900.12	155.25
8000	TRUE	-25.53	8000.12	117.30	8000.12	139.66	8000.12	181.41	8000.12	122.00	8000.12	139.11	8000.12	138.34	8000.12	142.83
8100	TRUE	-26.18	8100.12	116.35	8100.12	138.99	8100.12	180.93	8100.12	121.39	8100.12	138.70	8100.12	138.00	8100.12	142.53
8200	TRUE	-25.87	8200.12	116.46	8200.12	139.14	8200.12	180.53	8200.12	121.27	8200.12	138.36	8200.12	137.75	8200.12	142.33
8300	TRUE	-26.52	8300.13	115.97	8300.13	139.26	8300.13	180.85	8300.13	121.31	8300.13	138.56	8300.13	138.01	8300.13	142.49
8400	TRUE	-26.98	8400.13	116.16	8400.13	139.66	8400.13	181.40	8400.13	121.71	8400.13	138.76	8400.13	138.61	8400.13	143.14
8500	TRUE	-26.86	8500.13	116.60	8500.13	140.03	8500.13	181.89	8500.13	121.92	8500.13	139.04	8500.13	138.99	8500.13	143.46
8600	TRUE	-26.69	8600.13	116.57	8600.13	139.90	8600.13	181.72	8600.13	121.87	8600.13	139.35	8600.13	139.03	8600.13	143.26
8700	TRUE	-26.54	8700.13	117.08	8700.13	139.46	8700.13	181.88	8700.13	122.16	8700.13	139.37	8700.13	139.09	8700.13	143.62
8800	TRUE	-25.85	8800.13	118.05	8800.13	139.80	8800.13	182.17	8800.13	122.13	8800.13	139.59	8800.13	139.34	8800.13	143.91
8900	TRUE	-25.48	8900.13	119.06	8900.13	140.16	8900.13	182.98	8900.13	122.84	8900.13	140.30	8900.13	139.74	8900.13	144.53
9000	TRUE	-25.67	9000.14	118.84	9000.14	139.97	9000.14	183.08	9000.14	122.78	9000.14	140.22	9000.14	139.95	9000.14	144.52
9100	TRUE	-25.52	9100.14	119.64	9100.14	140.66	9100.14	183.76	9100.14	123.46	9100.14	141.20	9100.14	140.60	9100.14	145.16
9200	TRUE	-25.19	9200.14	119.98	9200.14	141.25	9200.14	183.94	9200.14	123.59	9200.14	141.09	9200.14	140.47	9200.14	145.17
9300	TRUE	-24.67	9300.14	120.73	9300.14	141.61	9300.14	184.45	9300.14	123.92	9300.14	141.48	9300.14	140.91	9300.14	145.40
9400	TRUE	-24.57	9400.14	121.06	9400.14	141.87	9400.14	184.81	9400.14	124.24	9400.14	141.74	9400.14	141.11	9400.14	145.64
9500	TRUE	-24.78	9500.14	121.47	9500.14	142.60	9500.14	185.50	9500.14	124.83	9500.14	142.24	9500.14	141.67	9500.14	146.25
9600	TRUE	-24.83	9600.15	121.45	9600.15	143.16	9600.15	185.65	9600.15	124.95	9600.15	142.42	9600.15	141.74	9600.15	146.28
9700	TRUE	-24.99	9700.15	121.38	9700.15	143.16	9700.15	185.71	9700.15	124.99	9700.15	142.40	9700.15	141.75	9700.15	146.36
9800	TRUE	-24.93	9800.15	121.62	9800.15	143.41	9800.15	185.88	9800.15	125.20	9800.15	142.56	9800.15	142.01	9800.15	146.54
9900	TRUE	-25.11	9900.15	121.84	9900.15	143.74	9900.15	186.47	9900.15	125.57	9900.15	142.86	9900.15	142.38	9900.15	146.95
10000	TRUE	-25.31	10000.15	122.50	10000.15	144.58	10000.15	187.43	10000.15	126.25	10000.15	143.73	10000.15	143.22	10000.15	147.81
10100	TRUE	-27.58	10100.15	133.27	10100.15	157.32	10100.15	203.74	10100.15	137.49	10100.15	156.30	10100.15	155.81	10100.15	160.85
10200	TRUE	-26.34	10200.15	125.24	10200.15	148.11	10200.15	192.15	10200.15	129.42	10200.15	147.16	10200.15	146.84	10200.15	151.57
10300	TRUE	-25.70	10300.16	121.60	10300.16	143.98	10300.16	186.81	10300.16	125.83	10300.16	143.10	10300.16	142.74	10300.16	147.31
10400	TRUE	-26.05	10400.16	121.55	10400.16	144.32	10400.16	187.21	10400.16	126.01	10400.16	143.38	10400.16	143.01	10400.16	147.60
10500	TRUE	-26.24	10500.16	121.29	10500.16	144.13	10500.16	187.07	10500.16	126.07	10500.16	143.16	10500.16	142.89	10500.16	147.52
10600	TRUE	-26.10	10600.16	121.55	10600.16	144.16	10600.16	187.24	10600.16	126.20	10600.16	143.31	10600.16	142.95	10600.16	147.65
10700	TRUE	-25.98	10700.16	121.49	10700.16	143.96	10700.16	187.02	10700.16	126.00	10700.16	143.07	10700.16	142.85	10700.16	147.47

Table G.1: Victaulic 005 Connected Black Steel Pipe Peak Signal Frequency and Magnitude. "Bandwidth" column indicates whether the Bandwidth Condition is satisfied

		Distance	0ft_vol100		10ft_vol100		20ft_vol100		22.75ft_vol100		30ft_vol100		40ft_vol100		42.5ft_vol100	
		Values	Rx_max_freq	Max_rx_mag	Rx_max_freq	Max_rx_mag	Rx_max_freq	Max_rx_mag	Rx_max_freq	Max_rx_mag	Rx_max_freq	Max_rx_mag	Rx_max_freq	Max_rx_mag	Rx_max_freq	Max_rx_mag
Tx_freq	Bandwidth	Attenuation/ft														
10800	TRUE	-25.76	10800.16	121.72	10800.16	144.06	10800.16	187.13	10800.16	126.01	10800.16	143.06	10800.16	142.93	10800.16	147.48
10900	TRUE	-25.07	10900.16	122.41	10900.16	143.96	10900.16	187.12	10900.16	125.95	10900.16	143.02	10900.16	142.86	10900.16	147.48
11000	TRUE	-24.29	11000.17	123.45	11000.17	144.28	11000.17	187.57	11000.17	126.22	11000.17	143.30	11000.17	143.18	11000.17	147.74
11100	TRUE	-22.85	11100.17	124.78	11100.17	144.12	11100.17	187.45	11100.17	126.11	11100.17	143.13	11100.17	143.06	11100.17	147.62
11200	TRUE	-22.05	11200.17	125.31	11200.17	143.83	11200.17	187.06	11200.17	125.91	11200.17	142.90	11200.17	142.76	11200.17	147.36
11300	TRUE	-23.00	11300.17	124.27	11300.17	143.81	11300.17	187.12	11300.17	125.77	11300.17	142.84	11300.17	142.84	11300.17	147.27
11400	TRUE	-24.05	11400.17	123.52	11400.17	144.08	11400.17	187.45	11400.17	125.99	11400.17	143.04	11400.17	143.09	11400.17	147.57
11500	TRUE	-24.75	11500.17	122.93	11500.17	144.18	11500.17	187.68	11500.17	126.09	11500.17	143.18	11500.17	143.19	11500.17	147.67
11600	TRUE	-25.08	11600.18	122.34	11600.18	143.92	11600.18	187.28	11600.18	125.83	11600.18	142.93	11600.18	142.95	11600.18	147.43
11700	TRUE	-25.28	11700.18	122.25	11700.18	144.00	11700.18	187.50	11700.18	125.87	11700.18	142.99	11700.18	143.07	11700.18	147.53
11800	TRUE	-25.42	11800.18	122.15	11800.18	144.03	11800.18	187.56	11800.18	125.88	11800.18	143.01	11800.18	143.11	11800.18	147.58
11900	TRUE	-25.48	11900.18	122.39	11900.18	144.34	11900.18	187.92	11900.18	126.10	11900.18	143.22	11900.18	143.45	11900.18	147.88
12000	TRUE	-25.52	12000.18	122.30	12000.18	144.27	12000.18	187.92	12000.18	126.10	12000.18	143.25	12000.18	143.37	12000.18	147.82
12100	TRUE	-25.57	12100.18	122.50	12100.18	144.49	12100.18	188.22	12100.18	126.33	12100.18	143.50	12100.18	143.67	12100.18	148.07
12200	TRUE	-25.78	12200.18	122.27	12200.18	144.37	12200.18	188.14	12200.18	126.23	12200.18	143.41	12200.18	143.58	12200.18	148.05
12300	TRUE	-26.30	12300.19	126.15	12300.19	148.73	12300.19	193.76	12300.19	130.12	12300.19	147.64	12300.19	147.83	12300.19	152.44
12400	TRUE	-27.73	12400.19	134.43	12400.19	158.17	12400.19	205.97	12400.19	138.83	12400.19	157.08	12400.19	157.28	12400.19	162.16
12500	TRUE	-25.58	12500.19	123.73	12500.19	145.64	12500.19	189.74	12500.19	127.68	12500.19	144.49	12500.19	144.83	12500.19	149.31
12600	TRUE	-25.22	12600.19	123.48	12600.19	145.09	12600.19	189.13	12600.19	127.44	12600.19	144.01	12600.19	144.32	12600.19	148.70
12700	TRUE	-25.17	12700.19	123.51	12700.19	145.00	12700.19	188.97	12700.19	128.27	12700.19	143.89	12700.19	144.21	12700.19	148.68
12800	TRUE	-25.15	12800.19	123.66	12800.19	145.03	12800.19	189.20	12800.19	128.53	12800.19	144.02	12800.19	144.36	12800.19	148.81
12900	TRUE	-25.13	12900.20	124.04	12900.20	145.43	12900.20	189.62	12900.20	129.13	12900.20	144.35	12900.20	144.68	12900.20	149.18
13000	TRUE	-25.00	13000.20	124.34	13000.20	145.64	13000.20	190.02	13000.20	129.81	13000.20	144.54	13000.20	144.96	13000.20	149.34
13100	TRUE	-24.93	13100.20	124.21	13100.20	145.43	13100.20	189.62	13100.20	129.86	13100.20	144.23	13100.20	144.72	13100.20	149.14
13200	TRUE	-24.69	13200.20	124.57	13200.20	145.53	13200.20	189.88	13200.20	130.21	13200.20	144.34	13200.20	144.82	13200.20	149.26
13300	TRUE	-24.83	13300.20	124.41	13300.20	145.50	13300.20	189.80	13300.20	113.21	13300.20	144.39	13300.20	144.83	13300.20	149.24
13400	TRUE	-25.08	13400.20	124.43	13400.20	145.67	13400.20	190.09	13400.20	130.02	13400.20	144.61	13400.20	145.07	13400.20	149.51
13500	TRUE	-25.42	13500.20	123.89	13500.20	145.54	13500.20	189.88	13500.20	130.79	13500.20	144.42	13500.20	144.99	13500.20	149.31
13600	TRUE	-25.39	13600.21	124.10	13600.21	145.76	13600.21	190.12	13600.21	131.07	13600.21	144.67	13600.21	145.11	13600.21	149.49
13700	TRUE	-24.82	13700.21	124.51	13700.21	145.41	13700.21	189.82	13700.21	130.65	13700.21	144.36	13700.21	144.89	13700.21	149.33
13800	TRUE	-24.86	13800.21	124.43	13800.21	145.49	13800.21	189.78	13800.21	130.64	13800.21	144.40	13800.21	144.91	13800.21	149.28
13900	TRUE	-25.31	13900.21	123.90	13900.21	145.37	13900.21	189.71	13900.21	130.81	13900.21	144.26	13900.21	144.84	13900.21	149.21
14000	TRUE	-24.75	14000.21	124.71	14000.21	145.59	14000.21	189.96	14000.21	130.95	14000.21	144.57	14000.21	145.07	14000.21	149.45
14100	TRUE	-24.64	14100.21	124.62	14100.21	145.46	14100.21	189.68	14100.21	130.84	14100.21	144.38	14100.21	144.90	14100.21	149.26
14200	TRUE	-24.57	14200.21	124.38	14200.21	145.12	14200.21	189.31	14200.21	130.61	14200.21	144.10	14200.21	144.61	14200.21	148.95
14300	TRUE	-24.22	14300.22	124.51	14300.22	145.07	14300.22	189.21	14300.22	130.71	14300.22	144.00	14300.22	144.53	14300.22	148.73
14400	TRUE	-24.17	14400.22	124.87	14400.22	145.21	14400.22	189.46	14400.22	130.91	14400.22	144.04	14400.22	144.75	14400.22	149.04
14500	TRUE	-23.85	14500.22	125.27	14500.22	145.40	14500.22	189.58	14500.22	131.11	14500.22	144.10	14500.22	144.71	14500.22	149.12
14600	TRUE	-24.94	14600.22	123.89	14600.22	144.99	14600.22	189.08	14600.22	130.93	14600.22	143.99	14600.22	144.36	14600.22	148.82
14700	TRUE	-24.47	14700.22	124.37	14700.22	144.95	14700.22	189.10	14700.22	131.11	14700.22	143.92	14700.22	144.41	14700.22	148.84
14800	TRUE	-24.50	14800.22	124.26	14800.22	145.02	14800.22	189.08	14800.22	131.12	14800.22	143.69	14800.22	144.27	14800.22	148.76
14900	TRUE	-24.16	14900.23	124.85	14900.23	145.20	14900.23	189.37	14900.23	131.42	14900.23	144.11	14900.23	144.65	14900.23	149.01
15000	TRUE	-24.06	15000.23	124.75	15000.23	145.02	15000.23	189.10	15000.23	131.31	15000.23	143.87	15000.23	144.55	15000.23	148.81
15100	TRUE	-24.13	15100.23	124.98	15100.23	145.32	15100.23	189.41	15100.23	131.59	15100.23	144.19	15100.23	144.75	15100.23	149.11
15200	TRUE	-24.05	15200.23	124.90	15200.23	145.12	15200.23	189.31	15200.23	131.50	15200.23	143.97	15200.23	144.61	15200.23	148.95
15300	TRUE	-25.35	15300.23	128.03	15300.23	149.53	15300.23	194.79	15300.23	135.38	15300.23	148.25	15300.23	148.92	15300.23	153.38
15400	TRUE	-26.88	15400.23	136.12	15400.23	158.88	15400.23	206.93	15400.23	144.09	15400.23	157.63	15400.23	158.29	15400.23	163.00
15500	TRUE	-25.14	15500.23	124.90	15500.23	146.23	15500.23	190.62	15500.23	132.60	15500.23	145.02	15500.23	145.79	15500.23	150.05
15600	TRUE	-24.85	15600.24	124.64	15600.24	145.73	15600.24	189.89	15600.24	131.92	15600.24	144.52	15600.24	145.20	15600.24	149.50
15700	TRUE	-24.48	15700.24	124.91	15700.24	145.64	15700.24	189.71	15700.24	131.80	15700.24	144.33	15700.24	145.10	15700.24	149.39
15800	TRUE	-24.66	15800.24	124.84	15800.24	145.81	15800.24	189.80	15800.24	131.88	15800.24	144.51	15800.24	145.24	15800.24	149.50
15900	TRUE	-24.70	15900.24	125.17	15900.24	145.99	15900.24	190.25	15900.24	132.39	15900.24	144.89	15900.24	145.61	15900.24	149.87
16000	TRUE	-23.92	16000.24	126.20	16000.24	146.26	16000.24	190.61	16000.24	132.88	16000.24	145.06	16000.24	145.86	16000.24	150.12
16100	TRUE	-23.57	16100.24	126.29	16100.24	146.03	16100.24	190.23	16100.24	132.63	16100.24	144.77	16100.24	145.65	16100.24	149.86
16200	TRUE	-23.33	16200.24	126.66	16200.24	146.05	16200.24	190.43	16200.24	130.70	16200.24	144.89	16200.24	145.74	16200.24	149.99
16300	TRUE	-23.33	16300.25	126.68	16300.25	146.17	16300.25	190.52	16300.25	130.83	16300.25	144.87	16300.25	145.77	16300.25	150.01
16400	TRUE	-23.28	16400.25	127.01	16400.25	146.45	16400.25	190.80	16400.25	130.92	16400.25	145.13	16400.25	146.09	16400.25	150.29
16500	TRUE	-23.29	16500.25	126.88	16500.25	146.21	16500.25	190.58	16500.25	130.81	16500.25	144.94	16500.25	145.86	16500.25	150.17
16600	TRUE	-23.45	16600.25	126.86	16600.25	146.32	16600.25	190.75	16600.25	130.81	16600.25	145.12	16600.25	146.04	16600.25	150.31
16700	TRUE	-23.69	16700.25	126.37	16700.25	146.07	16700.25	190.43	16700.25	130.69	16700.25	144.81	16700.25	145.75	16700.25	150.06
16800	TRUE	-23.82	16800.25	126.21	16800.25	146.09	16800.25	190.49	16800.25	130.67	16800.25	144.75	16800.25	145.87	16800.25	150.03
16900	TRUE	-24.07	16900.26	125.90	16900.26	145.96	16900.26	190.33	16900.26	130.45	16900.26	144.57	16900.26	145.72	16900.26	149.97
17000	TRUE	-24.19	17000.26	126.11	17000.26	146.22	17000.26	190.71	17000.26	130.76	17000.26	144.92	17000.26	145.97	17000.26	150.30
17100	TRUE	-24.32	17100.26	125.78	17100.26	146.04	17100.26	190.53	17100.26	130.52	17100.26	144.65	17100.26	145.74	17100.26	150.10
17200	TRUE	-24.46	17200.26	125.39	17200.26	145.71	17200.26	190.03	17200.26	130.13	17200.26	144.53	17200.26	145.60	17200.26	149.84
17300	TRUE	-24.38	17300.26	125.38	17300.26	145.66	17300.26	190.06	17300.26	129.95	17300.26	143.72	17300.26	145.47	17300.26	149.76
17400	TRUE	-24.41	17400.26	125.54	17400.26	145.78	17400.26	190.32	17400.26	130.10	17400.26	143.62	17400.26	145.78	17400.26	149.95
17500	TRUE	-24.26	17500.26	125.76	17500.26	145.99	17500.26	190.55	17500.26	130.20	17500.26	143.98	17500.26	145.81	17500.26	150.02
17600	TRUE	-23.71	17600.27	126.00	17600.27	145.52	17600.27	190.14	17600.27	129.78	17600.27	143.59	17600.27	145.47	17600.27	149.70
17700	TRUE	-23.51	17700.27	126.22	17700.27	145.53	17700.27	190.21	17700.27	129.86	17700.27	143.65	17700.27	145.53	17700.27	149.73
17800	TRUE	-24.82	17800.27	124.78	17800.27	145.27	17800.27	190.17	17800.27	129.70	17800.27	143.32	17800.27	145.38	17800.27	149.61
17900	TRUE	-25.37	17900.27	124.68	17900.27	145.75	17900.27	190.62	17900.27	130.10	17900.27	143.74	17900.27	145.84	17900.27	150.05
18000	TRUE	-24.73	18000.27	125.28	18000.27	145.77	18000.27	190.55	18000.27	130.08	18000.27	143.61	18000.27	145.84	18000.27	150.01
18100	TRUE	-23.60	18100.27	126.60	18100.27	146.14	18100.27	190.89	18100.27	130.34	18100.27	144.56	18100.27	146.03	18100.27	150.20
18200	TRUE	-23.17	18200.28	126.72	18200.28	146.00	18200.28	190.77	18200.28	130.07	18200.28	144.46	18200.28	145.86	18200.28	149.89
18300	TRUE	-23.15	18300.28	126.89	18300.28	145.43	18300.28	190.94	18300.28	129.97	18300.28	144.25	18300.28	145.88	18300.28	150.04
18400	TRUE	-24.11	18400.28	126.16	18400.28	145.77	18400.28	190.98	18400.28	130.28	18400.28	144.70	18400.28	146.01	18400.28	150.27
18500	TRUE	-28.44	18500.28	122.21	18500.28	146.34	18500.28	191.62	18500.28	130.60	18500.28	145.12	18500.28	146.60	18500.28	150.64
18600	TRUE	-30.69	18600.28	119.87	18600.28	146.23	18600.28	191.64	18600.28	130.53	18600.28	145.10	18600.28	146.42	18600.28	150.56
18700	TRUE	-30.90	18700.28	119.49	18700.28	145.95	18700.28	191.32	18700.28	130.42	18700.28	144.93	18700.28	146.26	18700.28	150.39
18800	TRUE	-30.45	18800.28	119.94	18800.28	143.96	18800.28	191.38	18800.28	130.43	18800.28	144.87	18800.28	146.34	18800.28	150.39
18900	TRUE	-30.88	18900.29	119.56	18900.29	146.10	18900.29	191.45	18900.29	130.53	18900.29	144.96	18900.29	146.40	18900.29	150.44
19000	TRUE	-30.76	19000.29	119.59	19000.29	145.67	19000.29	191.39	19000.29	130.45	19000.29	144.88	19000.29	146.29	19000.29	150.35
19100	TRUE	-30.11	19100.29	119.65	19100.29	144.87	19100.29	190.53	19100.29	129.87	19100.29	144.25	19100.29	145.63	19100.29	149.76
19200	TRUE	-28.65	19200.29	120.77	19200.29	144.70	19200.29	189.98	19200.29	129.61	19200.29	143.89	19200.29	145.33	19200.29	149.42
19300	TRUE	-28.37	19300.29	120.24	19300.29	143.86	19300.29	189.11	19300.29	128.96	19300.29	143.24	19300.29	144.64	19300.29	148.61
19400	TRUE	-28.12	19400.29	119.81	19400.29	143.30	19400.29	188.14	19400.29	128.33	19400.29	142.54	19400.29	144.02	19400.29	147.93
19500	TRUE	-27.66	19500.29	118.89	19500.29	142.00	19500.29	186.40	19500.29	127.18	19500.29	141.28	19500.29	142.61	19500.29	146.55
19600	TRUE	-27.29	19600.30	117.98	19600.30	140.67	19600.30	184.69	19600.30	126.08	19600.30	140.05	19600.30	141.43	19600.30	145.27
19700	TRUE	-26.88	19700.30	116.40	19700.30	138.71	19700.30	182.07	19700.30	124.28	19700.30	138.06	19700.30	139.43	19700.30	143.28
19800	TRUE	-26.49	19800.30	114.56	19800.30	136.65	19800.30	179.17	19800.30	122.29	19800.30	135.96	19800.30	137.32	19800.30	141.06
19900	TRUE	-26.10	19900.30	112.25	19900.30	134.04	19900.30	175.66	19900.30	119.95	19900.30	133.24	19900.30	134.58	19900.30	138.36
20000	TRUE	-25.08	20000.30	110.29	20000.30	131.05	20000.30	171.95	20000.30	117.41	20000.30	130.42	20000.30	131.92	20000.30	135.36

Table G.1: Victaulic 005 Connected Black Steel Pipe Peak Signal Frequency and Magnitude. "Bandwidth" column indicates whether the Bandwidth Condition is satisfied (cont.)

Appendix H: BLACK STEEL PIPE OUTDOOR LABORATORY SETTING WITH VICTAULIC 75 FLEXIBLE COUPLINGS

		Distance	0ft_vol100		10ft_vol100		20ft_vol100		22.75ft_vol100		30ft_vol100		40ft_vol100		42.5ft_vol100	
		Values	Rx_max_freq	Max_rx_mag	Rx_max_freq	Max_rx_mag	Rx_max_freq	Max_rx_mag	Rx_max_freq	Max_rx_mag	Rx_max_freq	Max_rx_mag	Rx_max_freq	Max_rx_mag	Rx_max_freq	Max_rx_mag
Tx_freq	Bandwidth	Attenuation/ft														
100	FALSE	NA	60.00	24.35	60.00	22.53	3.00	9.36	2.33	9.53	1.33	10.40	2407.37	7.44	60.00	10.66
200	FALSE	NA	60.00	27.35	60.00	20.95	200.00	11.63	200.00	11.72	200.00	11.55	200.00	12.29	200.00	11.15
300	FALSE	NA	60.00	23.38	60.00	22.11	300.00	17.27	300.00	19.41	300.00	15.30	300.00	16.75	300.00	15.85
400	FALSE	NA	60.00	23.50	60.00	22.76	400.01	21.88	400.01	22.72	400.01	22.58	400.01	21.89	400.01	21.04
500	TRUE	-0.09	500.01	23.15	500.01	24.27	500.01	25.39	500.01	26.25	500.01	25.20	500.01	25.24	500.01	23.24
600	TRUE	-1.02	600.01	28.88	600.01	29.12	600.01	31.31	600.01	31.75	600.01	30.21	600.01	30.90	600.01	29.90
700	TRUE	-0.34	700.01	32.08	700.01	32.87	700.01	35.24	700.01	35.99	700.01	34.88	700.01	35.10	700.01	32.42
800	TRUE	-0.46	800.01	36.37	800.01	36.68	800.01	39.79	800.01	40.40	800.01	39.09	800.01	39.52	800.01	36.83
900	TRUE	5.09	900.01	41.53	900.01	41.97	900.01	45.16	900.01	45.27	900.01	44.85	900.01	45.01	900.01	36.45
1000	TRUE	-1.42	1000.02	43.11	1000.02	43.24	1000.02	47.58	1000.02	47.93	1000.02	46.71	1000.02	47.51	1000.02	44.54
1100	TRUE	-0.69	1100.02	52.42	1100.02	51.47	1100.02	56.63	1100.02	57.54	1100.02	55.86	1100.02	56.87	1100.02	53.11
1200	TRUE	0.25	1200.02	49.97	1200.02	47.60	1200.02	52.59	1200.02	54.07	1200.02	52.04	1200.02	53.12	1200.02	49.73
1300	TRUE	0.84	1300.02	53.94	1300.02	50.85	1300.02	56.24	1300.02	57.41	1300.02	55.89	1300.02	57.39	1300.02	53.10
1400	TRUE	-0.85	1400.02	55.98	1400.02	54.07	1400.02	60.81	1400.02	61.65	1400.02	60.17	1400.02	61.14	1400.02	56.83
1500	TRUE	0.44	1500.02	66.66	1500.02	62.27	1500.02	69.86	1500.02	70.85	1500.02	69.67	1500.02	70.66	1500.02	66.23
1600	TRUE	-2.95	1600.02	60.07	1600.02	59.12	1600.02	67.11	1600.02	68.50	1600.02	66.53	1600.02	67.71	1600.02	63.02
1700	TRUE	-4.78	1700.03	60.66	1700.03	60.63	1700.03	69.23	1700.03	70.72	1700.03	68.45	1700.03	70.17	1700.03	65.44
1800	TRUE	-6.73	1800.03	63.54	1800.03	64.95	1800.03	74.28	1800.03	76.12	1800.03	74.10	1800.03	75.04	1800.03	70.27
1900	TRUE	-8.24	1900.03	68.96	1900.03	71.03	1900.03	81.47	1900.03	83.07	1900.03	81.41	1900.03	82.63	1900.03	77.21
2000	TRUE	-9.11	2000.03	64.03	2000.03	67.61	2000.03	77.82	2000.03	79.23	2000.03	77.21	2000.03	78.60	2000.03	73.14
2100	TRUE	-8.07	2100.03	67.50	2100.03	68.84	2100.03	79.97	2100.03	81.35	2100.03	79.39	2100.03	80.74	2100.03	75.57
2200	TRUE	-8.37	2200.03	69.69	2200.03	70.95	2200.03	82.41	2200.03	83.57	2200.03	81.68	2200.03	83.12	2200.03	78.05
2300	TRUE	-8.29	2300.03	71.91	2300.03	72.09	2300.03	84.49	2300.03	86.08	2300.03	83.88	2300.03	85.45	2300.03	80.19
2400	TRUE	-7.79	2400.04	74.48	2400.04	73.66	2400.04	86.88	2400.04	87.93	2400.04	86.11	2400.04	87.58	2400.04	82.27
2500	TRUE	-7.27	2500.04	76.90	2500.04	75.38	2500.04	89.11	2500.04	90.43	2500.04	88.39	2500.04	89.66	2500.04	84.17
2600	TRUE	-6.10	2600.04	87.65	2600.04	83.71	2600.04	99.09	2600.04	100.38	2600.04	98.27	2600.04	99.61	2600.04	93.75
2700	TRUE	-8.06	2700.04	81.93	2700.04	79.71	2700.04	94.88	2700.04	96.31	2700.04	94.23	2700.04	95.79	2700.04	89.99
2800	TRUE	-7.77	2800.04	81.41	2800.04	78.30	2800.04	94.04	2800.04	95.23	2800.04	93.30	2800.04	94.70	2800.04	89.18
2900	TRUE	-8.78	2900.04	81.98	2900.04	79.22	2900.04	96.07	2900.04	96.98	2900.04	95.10	2900.04	96.60	2900.04	90.76
3000	TRUE	-10.12	3000.05	82.20	3000.05	79.82	3000.05	96.96	3000.05	98.13	3000.05	95.98	3000.05	97.61	3000.05	92.32
3100	TRUE	-9.80	3100.05	83.57	3100.05	80.72	3100.05	98.41	3100.05	99.42	3100.05	97.54	3100.05	98.54	3100.05	93.37
3200	TRUE	-9.36	3200.05	84.95	3200.05	80.87	3200.05	98.68	3200.05	100.26	3200.05	98.09	3200.05	100.02	3200.05	94.31
3300	TRUE	-8.98	3300.05	88.75	3300.05	82.78	3300.05	102.05	3300.05	103.45	3300.05	101.23	3300.05	103.63	3300.05	97.73
3400	TRUE	-10.33	3400.05	95.63	3400.05	91.45	3400.05	108.71	3400.05	110.15	3400.05	108.65	3400.05	111.02	3400.05	105.96
3500	TRUE	-12.35	3500.05	88.70	3500.05	89.17	3500.05	101.41	3500.05	103.26	3500.05	102.45	3500.05	105.52	3500.05	101.05
3600	TRUE	-16.06	3600.05	89.21	3600.05	92.15	3600.05	105.84	3600.05	107.71	3600.05	107.17	3600.05	110.20	3600.05	105.27
3700	TRUE	-17.87	3700.06	89.85	3700.06	92.56	3700.06	110.77	3700.06	111.94	3700.06	111.04	3700.06	113.60	3700.06	107.72
3800	TRUE	-19.13	3800.06	90.40	3800.06	92.78	3800.06	113.52	3800.06	114.94	3800.06	113.10	3800.06	115.48	3800.06	109.53
3900	TRUE	-19.53	3900.06	91.38	3900.06	93.80	3900.06	114.71	3900.06	116.16	3900.06	114.69	3900.06	116.80	3900.06	110.91
4000	TRUE	-19.65	4000.06	92.52	4000.06	94.59	4000.06	115.90	4000.06	117.70	4000.06	116.16	4000.06	118.41	4000.06	112.17
4100	TRUE	-21.93	4100.06	101.33	4100.06	103.25	4100.06	127.15	4100.06	128.81	4100.06	126.81	4100.06	128.98	4100.06	123.26
4200	TRUE	-20.90	4200.06	95.79	4200.06	97.41	4200.06	120.39	4200.06	121.90	4200.06	119.81	4200.06	122.34	4200.06	116.68
4300	TRUE	-20.36	4300.07	93.70	4300.07	94.93	4300.07	117.75	4300.07	119.22	4300.07	117.08	4300.07	119.54	4300.07	114.05
4400	TRUE	-20.53	4400.07	94.29	4400.07	95.15	4400.07	118.35	4400.07	119.75	4400.07	118.07	4400.07	120.33	4400.07	114.82
4500	TRUE	-20.43	4500.07	95.22	4500.07	95.92	4500.07	119.08	4500.07	120.20	4500.07	118.38	4500.07	120.96	4500.07	115.66
4600	TRUE	-20.70	4600.07	95.50	4600.07	96.59	4600.07	119.65	4600.07	121.02	4600.07	119.01	4600.07	121.58	4600.07	116.20
4700	TRUE	-21.42	4700.07	95.20	4700.07	96.96	4700.07	120.16	4700.07	121.48	4700.07	119.31	4700.07	121.91	4700.07	116.62
4800	TRUE	-21.85	4800.07	95.48	4800.07	97.26	4800.07	120.65	4800.07	122.22	4800.07	120.16	4800.07	122.73	4800.07	117.33
4900	TRUE	-22.25	4900.07	96.00	4900.07	98.68	4900.07	121.60	4900.07	122.75	4900.07	120.83	4900.07	123.86	4900.07	118.25
5000	TRUE	-22.45	5000.08	96.74	5000.08	98.80	5000.08	123.04	5000.08	123.85	5000.08	121.94	5000.08	124.64	5000.08	119.18
5100	TRUE	-22.71	5100.08	97.15	5100.08	99.44	5100.08	122.14	5100.08	124.54	5100.08	122.32	5100.08	125.08	5100.08	119.87
5200	TRUE	-23.78	5200.08	103.78	5200.08	105.84	5200.08	129.05	5200.08	132.41	5200.08	130.24	5200.08	133.13	5200.08	127.55
5300	TRUE	-23.66	5300.08	104.51	5300.08	106.46	5300.08	130.22	5300.08	132.95	5300.08	130.76	5300.08	133.82	5300.08	128.18
5400	TRUE	-22.42	5400.08	99.32	5400.08	101.27	5400.08	124.69	5400.08	127.48	5400.08	125.28	5400.08	127.55	5400.08	121.74
5500	TRUE	-23.46	5500.08	99.45	5500.08	101.28	5500.08	125.31	5500.08	128.25	5500.08	125.32	5500.08	128.29	5500.08	122.91
5600	TRUE	-23.47	5600.08	99.87	5600.08	100.66	5600.08	125.62	5600.08	128.64	5600.08	125.83	5600.08	128.93	5600.08	123.34
5700	TRUE	-25.03	5700.09	99.16	5700.09	101.59	5700.09	126.36	5700.09	128.94	5700.09	126.53	5700.09	129.50	5700.09	124.19
5800	TRUE	-25.82	5800.09	98.94	5800.09	101.69	5800.09	127.04	5800.09	129.26	5800.09	127.06	5800.09	130.26	5800.09	124.76
5900	TRUE	-26.93	5900.09	97.78	5900.09	102.32	5900.09	127.27	5900.09	130.00	5900.09	127.62	5900.09	130.64	5900.09	124.71
6000	TRUE	-25.23	6000.09	99.92	6000.09	102.67	6000.09	128.04	6000.09	129.97	6000.09	128.11	6000.09	131.01	6000.09	125.15
6100	TRUE	-24.48	6100.09	101.51	6100.09	102.74	6100.09	128.45	6100.09	130.62	6100.09	128.65	6100.09	131.74	6100.09	125.99
6200	TRUE	-25.13	6200.09	101.01	6200.09	102.77	6200.09	128.18	6200.09	130.96	6200.09	129.01	6200.09	131.91	6200.09	126.13
6300	TRUE	-26.07	6300.10	103.90	6300.10	106.00	6300.10	131.78	6300.10	135.36	6300.10	132.78	6300.10	136.09	6300.10	129.97
6400	TRUE	-27.42	6400.10	111.12	6400.10	113.11	6400.10	141.11	6400.10	144.13	6400.10	141.65	6400.10	144.93	6400.10	138.54
6500	TRUE	-26.43	6500.10	101.31	6500.10	104.60	6500.10	130.61	6500.10	132.76	6500.10	130.45	6500.10	133.61	6500.10	127.73
6600	TRUE	-27.87	6600.10	100.10	6600.10	102.36	6600.10	129.58	6600.10	132.43	6600.10	129.79	6600.10	133.10	6600.10	127.97
6700	TRUE	-26.58	6700.10	100.87	6700.10	103.28	6700.10	130.53	6700.10	132.34	6700.10	125.66	6700.10	133.00	6700.10	127.45
6800	TRUE	-26.52	6800.10	101.37	6800.10	103.37	6800.10	130.10	6800.10	130.04	6800.10	129.90	6800.10	133.28	6800.10	127.90
6900	TRUE	-27.43	6900.10	101.42	6900.10	104.76	6900.10	130.25	6900.10	133.03	6900.10	130.48	6900.10	133.70	6900.10	128.85
7000	TRUE	-27.35	7000.11	101.83	7000.11	105.67	7000.11	130.74	7000.11	132.87	7000.11	130.84	7000.11	134.28	7000.11	129.18
7100	TRUE	-27.24	7100.11	102.05	7100.11	105.79	7100.11	130.63	7100.11	133.12	7100.11	130.83	7100.11	134.19	7100.11	129.29
7200	TRUE	-27.63	7200.11	102.28	7200.11	104.53	7200.11	131.32	7200.11	133.65	7200.11	131.52	7200.11	134.72	7200.11	129.91
7300	TRUE	-28.62	7300.11	101.98	7300.11	106.22	7300.11	132.16	7300.11	134.21	7300.11	132.14	7300.11	135.67	7300.11	130.61
7400	TRUE	-29.42	7400.11	102.16	7400.11	107.16	7400.11	133.06	7400.11	136.49	7400.11	133.34	7400.11	136.76	7400.11	131.58
7500	TRUE	-30.47	7500.11	102.05	7500.11	106.92	7500.11	133.65	7500.11	135.54	7500.11	133.98	7500.11	137.43	7500.11	132.51
7600	TRUE	-31.08	7600.11	102.34	7600.11	107.12	7600.11	134.67	7600.11	136.86	7600.11	135.15	7600.11	138.40	7600.11	133.42
7700	TRUE	-31.16	7700.12	102.43	7700.12	107.10	7700.12	134.83	7700.12	137.09	7700.12	135.25	7700.12	138.57	7700.12	133.59
7800	TRUE	-31.87	7800.12	105.68	7800.12	110.45	7800.12	139.07	7800.12	141.49	7800.12	139.43	7800.12	143.11	7800.12	137.54
7900	TRUE	-33.21	7900.12	112.81	7900.12	117.43	7900.12	147.86	7900.12	150.46	7900.12	148.25	7900.12	151.94	7900.12	146.02
8000	TRUE	-30.13	8000.12	103.90	8000.12	108.06	8000.12	136.23	8000.12	138.49	8000.12	136.39	8000.12	140.09	8000.12	134.03
8100	TRUE	-30.73	8100.12	103.58	8100.12	107.70	8100.12	135.77	8100.12	138.00	8100.12	135.83	8100.12	139.55	8100.12	134.31
8200	TRUE	-30.53	8200.12	103.72	8200.12	107.52	8200.12	135.49	8200.12	137.71	8200.12	135.92	8200.12	139.49	8200.12	134.24
8300	TRUE	-30.45	8300.13	103.94	8300.13	107.53	8300.13	135.69	8300.13	137.98	8300.13	136.34	8300.13	139.72	8300.13	134.40
8400	TRUE	-30.82	8400.13	104.14	8400.13	108.02	8400.13	136.26	8400.13	138.57	8400.13	136.36	8400.13	140.36	8400.13	134.95
8500	TRUE	-30.91	8500.13	104.45	8500.13	108.13	8500.13	136.67	8500.13	138.59	8500.13	136.93	8500.13	140.70	8500.13	135.36
8600	TRUE	-31.00	8600.13	104.30	8600.13	108.02	8600.13	136.46	8600.13	137.99	8600.13	136.79	8600.13	140.94	8600.13	135.31
8700	TRUE	-30.95	8700.13	104.64	8700.13	107.99	8700.13	136.77	8700.13	138.36	8700.13	137.31	8700.13	140.99	8700.13	135.60
8800	TRUE	-30.90	8800.13	105.02	8800.13	108.26	8800.13	137.15	8800.13	138.68	8800.13	136.81	8800.13	141.26	8800.13	135.92
8900	TRUE	-31.13	8900.13	105.19	8900.13	108.45	8900.13	137.63	8900.13	139.11	8900.13	137.44	8900.13	141.56	8900.13	136.32
9000	TRUE	-31.34	9000.14	105.00	9000.14	108.60	9000.14	138.19	9000.14	138.95	9000.14	137.62	9000.14	141.46	9000.14	136.34
9100	TRUE	-31.58	9100.14	105.20	9100.14	108.79	9100.14	138.06	9100.14	139.70	9100.14	138.23	9100.14	141.98	9100.14	136.79
9200	TRUE	-31.66	9200.14	105.11	9200.14	108.82	9200.14	137.36	9200.14	139.79	9200.14	133.69	9200.14	142.04	9200.14	136.77
9300	TRUE	-31.66	9300.14	105.41	9300.14	108.90	9300.14	137.56	9300.14	140.56	9300.14	138.33	9300.14	142.22	9300.14	137.07
9400	TRUE	-31.60	9400.14	105.70	9400.14	109.14	9400.14	138.07	9400.14	140.81	9400.14	138.59	9400.14	142.51	9400.14	137.30
9500	TRUE	-31.50	9500.14	106.12	9500.14	109.60	9500.14	136.17	9500.14	141.47	9500.14	139.20	9500.14	143.04	9500.14	137.62
9600	TRUE	-31.39	9600.15	106.26	9600.15	109.57	9600.15	129.07	9600.15	141.56	9600.15	139.25	9600.15	143.13	9600.15	137.64
9700	TRUE	-31.35	9700.15	106.20	9700.15	109.57	9700.15	129.21	9700.15	141.62	9700.15	139.44	9700.15	143.09	9700.15	137.55
9800	TRUE	-31.38	9800.15	106.29	9800.15	109.61	9800.15	130.39	9800.15	141.85	9800.15	139.50	9800.15	143.34	9800.15	137.67
9900	TRUE	-31.61	9900.15	106.58	9900.15	109.91	9900.15	133.77	9900.15	142.18	9900.15	140.02	9900.15	143.75	9900.15	138.19
10000	TRUE	-31.84	10000.15	107.25	10000.15	110.48	10000.15	132.78	10000.15	142.89	10000.15	140.63	10000.15	144.60	10000.15	139.09
10100	TRUE	-34.39	10100.15	117.00	10100.15	120.26	10100.15	143.39	10100.15	155.48	10100.15	152.90	10100.15	157.18	10100.15	151.39
10200	TRUE	-32.66	10200.15	109.87	10200.15	113.06	10200.15	134.60	10200.15	146.32	10200.15	144.08	10200.15	147.49	10200.15	142.53
10300	TRUE	-31.66	10300.16	106.85	10300.16	109.84	10300.16	131.14	10300.16	142.29	10300.16	140.04	10300.16	143.23	10300.16	138.51
10400	TRUE	-30.56	10400.16	108.26	10400.16	109.97	10400.16	131.14	10400.16	142.48	10400.16	140.38	10400.16	143.44	10400.16	138.82

Table H.1: Victaulic 75 Connected Black Steel Pipe Peak Signal Frequency and Magnitude. "Bandwidth" column indicates whether the Bandwidth Condition is satisfied

		Distance Values	0ft_vol100		10ft_vol100		20ft_vol100		22.75ft_vol100		30ft_vol100		40ft_vol100		42.5ft_vol100	
Tx_freq	Bandwidth	Attenuation/ft	Rx_max_freq	Max_rx_mag	Rx_max_freq	Max_rx_mag	Rx_max_freq	Max_rx_mag	Rx_max_freq	Max_rx_mag	Rx_max_freq	Max_rx_mag	Rx_max_freq	Max_rx_mag	Rx_max_freq	Max_rx_mag
10500	TRUE	-31.46	10500.16	107.19	10500.16	109.83	10500.16	131.21	10500.16	142.32	10500.16	140.18	10500.16	143.42	10500.16	138.65
10600	TRUE	-31.40	10600.16	107.29	10600.16	109.90	10600.16	131.44	10600.16	142.45	10600.16	140.33	10600.16	143.54	10600.16	138.69
10700	TRUE	-31.80	10700.16	107.17	10700.16	109.67	10700.16	131.19	10700.16	141.73	10700.16	140.07	10700.16	143.66	10700.16	138.97
10800	TRUE	-31.97	10800.16	107.04	10800.16	109.63	10800.16	131.07	10800.16	141.65	10800.16	140.19	10800.16	143.71	10800.16	139.02
10900	TRUE	-31.93	10900.16	107.01	10900.16	109.57	10900.16	131.15	10900.16	141.55	10900.16	140.09	10900.16	143.85	10900.16	138.93
11000	TRUE	-32.07	11000.17	107.16	11000.17	109.79	11000.17	131.71	11000.17	141.79	11000.17	140.33	11000.17	143.85	11000.17	139.23
11100	TRUE	-32.06	11100.17	107.02	11100.17	109.59	11100.17	131.60	11100.17	141.65	11100.17	140.11	11100.17	143.95	11100.17	139.07
11200	TRUE	-32.12	11200.17	106.71	11200.17	109.31	11200.17	130.64	11200.17	141.48	11200.17	139.86	11200.17	143.36	11200.17	138.83
11300	TRUE	-32.29	11300.17	106.60	11300.17	109.32	11300.17	130.52	11300.17	141.57	11300.17	139.78	11300.17	143.54	11300.17	138.89
11400	TRUE	-31.91	11400.17	106.70	11400.17	109.45	11400.17	130.93	11400.17	141.44	11400.17	140.02	11400.17	143.71	11400.17	138.61
11500	TRUE	-32.51	11500.17	106.65	11500.17	109.59	11500.17	131.06	11500.17	141.32	11500.17	140.15	11500.17	143.82	11500.17	139.15
11600	TRUE	-32.23	11600.18	106.67	11600.18	109.25	11600.18	130.72	11600.18	141.01	11600.18	139.88	11600.18	143.54	11600.18	138.90
11700	TRUE	-32.08	11700.18	106.89	11700.18	109.35	11700.18	130.78	11700.18	141.22	11700.18	139.91	11700.18	143.82	11700.18	138.97
11800	TRUE	-31.99	11800.18	107.11	11800.18	108.87	11800.18	130.70	11800.18	140.95	11800.18	139.92	11800.18	143.65	11800.18	139.10
11900	TRUE	-31.77	11900.18	107.60	11900.18	109.01	11900.18	130.74	11900.18	141.26	11900.18	140.26	11900.18	143.98	11900.18	139.38
12000	TRUE	-31.57	12000.18	107.73	12000.18	108.84	12000.18	131.57	12000.18	141.77	12000.18	140.10	12000.18	144.04	12000.18	139.30
12100	TRUE	-31.57	12100.18	107.94	12100.18	108.89	12100.18	130.83	12100.18	142.07	12100.18	140.29	12100.18	144.32	12100.18	139.52
12200	TRUE	-31.74	12200.18	107.68	12200.18	108.86	12200.18	130.57	12200.18	142.36	12200.18	140.12	12200.18	144.21	12200.18	139.42
12300	TRUE	-31.98	12300.19	111.20	12300.19	112.23	12300.19	134.44	12300.19	146.60	12300.19	144.26	12300.19	148.47	12300.19	143.18
12400	TRUE	-33.62	12400.19	119.20	12400.19	119.73	12400.19	143.30	12400.19	146.74	12400.19	153.52	12400.19	157.91	12400.19	152.82
12500	TRUE	-31.13	12500.19	109.53	12500.19	110.17	12500.19	133.14	12500.19	131.92	12500.19	141.29	12500.19	145.36	12500.19	140.65
12600	TRUE	-31.08	12600.19	109.10	12600.19	109.78	12600.19	132.57	12600.19	132.05	12600.19	140.77	12600.19	144.85	12600.19	140.19
12700	TRUE	-31.12	12700.19	108.91	12700.19	109.65	12700.19	132.39	12700.19	131.43	12700.19	140.59	12700.19	144.68	12700.19	140.04
12800	TRUE	-31.18	12800.19	109.00	12800.19	109.08	12800.19	132.39	12800.19	131.38	12800.19	140.70	12800.19	144.78	12800.19	140.18
12900	TRUE	-31.16	12900.20	109.32	12900.20	109.23	12900.20	132.71	12900.20	132.10	12900.20	141.01	12900.20	145.18	12900.20	140.47
13000	TRUE	-31.23	13000.20	109.46	13000.20	109.33	13000.20	133.30	13000.20	132.33	13000.20	141.24	13000.20	145.31	13000.20	140.69
13100	TRUE	-31.27	13100.20	109.19	13100.20	109.08	13100.20	133.76	13100.20	132.04	13100.20	140.99	13100.20	145.03	13100.20	140.46
13200	TRUE	-31.37	13200.20	109.17	13200.20	109.81	13200.20	133.42	13200.20	132.24	13200.20	141.05	13200.20	145.19	13200.20	140.54
13300	TRUE	-31.35	13300.20	109.17	13300.20	109.74	13300.20	136.66	13300.20	132.14	13300.20	141.09	13300.20	145.17	13300.20	140.52
13400	TRUE	-31.27	13400.20	109.41	13400.20	109.79	13400.20	137.63	13400.20	132.15	13400.20	141.26	13400.20	145.39	13400.20	140.68
13500	TRUE	-30.84	13500.20	109.27	13500.20	109.65	13500.20	138.21	13500.20	132.47	13500.20	141.09	13500.20	144.79	13500.20	140.11
13600	TRUE	-31.32	13600.21	108.94	13600.21	109.71	13600.21	136.38	13600.21	137.55	13600.21	141.21	13600.21	145.37	13600.21	140.26
13700	TRUE	-31.39	13700.21	108.65	13700.21	109.55	13700.21	135.65	13700.21	143.38	13700.21	140.99	13700.21	145.05	13700.21	140.03
13800	TRUE	-31.44	13800.21	108.37	13800.21	109.48	13800.21	135.19	13800.21	143.25	13800.21	141.01	13800.21	144.93	13800.21	139.81
13900	TRUE	-31.67	13900.21	108.29	13900.21	109.38	13900.21	135.14	13900.21	143.12	13900.21	140.84	13900.21	144.93	13900.21	139.96
14000	TRUE	-31.59	14000.21	108.63	14000.21	109.45	14000.21	135.21	14000.21	143.17	14000.21	141.04	14000.21	145.21	14000.21	140.22
14100	TRUE	-31.45	14100.21	108.57	14100.21	109.33	14100.21	135.22	14100.21	142.68	14100.21	140.77	14100.21	144.99	14100.21	140.01
14200	TRUE	-31.40	14200.21	108.39	14200.21	109.13	14200.21	135.03	14200.21	142.41	14200.21	140.42	14200.21	144.69	14200.21	139.79
14300	TRUE	-31.40	14300.22	108.29	14300.22	109.29	14300.22	135.07	14300.22	142.34	14300.22	140.41	14300.22	144.62	14300.22	139.69
14400	TRUE	-30.64	14400.22	108.24	14400.22	109.39	14400.22	134.27	14400.22	142.60	14400.22	140.54	14400.22	144.71	14400.22	138.89
14500	TRUE	-31.44	14500.22	108.17	14500.22	109.40	14500.22	135.05	14500.22	142.48	14500.22	140.55	14500.22	144.88	14500.22	139.61
14600	TRUE	-31.08	14600.22	108.11	14600.22	109.18	14600.22	140.62	14600.22	142.11	14600.22	140.21	14600.22	144.45	14600.22	139.19
14700	TRUE	-31.28	14700.22	108.22	14700.22	109.21	14700.22	137.97	14700.22	142.09	14700.22	140.27	14700.22	144.16	14700.22	139.50
14800	TRUE	-31.58	14800.22	107.93	14800.22	109.07	14800.22	137.58	14800.22	141.87	14800.22	140.31	14800.22	144.03	14800.22	139.50
14900	TRUE	-31.82	14900.23	108.36	14900.23	109.38	14900.23	143.42	14900.23	142.23	14900.23	140.52	14900.23	144.40	14900.23	140.19
15000	TRUE	-31.43	15000.23	108.61	15000.23	109.26	15000.23	149.39	15000.23	142.06	15000.23	140.34	15000.23	144.22	15000.23	140.03
15100	TRUE	-31.51	15100.23	108.88	15100.23	109.51	15100.23	139.28	15100.23	142.34	15100.23	140.69	15100.23	144.98	15100.23	140.39
15200	TRUE	-31.50	15200.23	108.78	15200.23	109.28	15200.23	140.51	15200.23	142.22	15200.23	140.66	15200.23	144.32	15200.23	140.28
15300	TRUE	-32.20	15300.23	112.31	15300.23	112.53	15300.23	140.93	15300.23	146.41	15300.23	144.87	15300.23	148.57	15300.23	144.51
15400	TRUE	-34.03	15400.23	119.64	15400.23	119.66	15400.23	151.43	15400.23	155.74	15400.23	153.81	15400.23	158.06	15400.23	153.66
15500	TRUE	-31.67	15500.23	109.73	15500.23	110.01	15500.23	138.68	15500.23	143.31	15500.23	141.74	15500.23	145.56	15500.23	141.40
15600	TRUE	-31.58	15600.24	109.33	15600.24	109.61	15600.24	137.53	15600.24	142.88	15600.24	141.11	15600.24	144.96	15600.24	140.91
15700	TRUE	-31.04	15700.24	109.71	15700.24	109.46	15700.24	136.82	15700.24	142.67	15700.24	140.97	15700.24	144.87	15700.24	140.76
15800	TRUE	-30.36	15800.24	110.55	15800.24	109.52	15800.24	136.65	15800.24	142.78	15800.24	141.08	15800.24	144.95	15800.24	140.91
15900	TRUE	-30.37	15900.24	110.79	15900.24	109.77	15900.24	137.05	15900.24	143.14	15900.24	141.36	15900.24	145.32	15900.24	141.17
16000	TRUE	-30.49	16000.24	110.97	16000.24	110.00	16000.24	137.25	16000.24	143.33	16000.24	141.62	16000.24	145.54	16000.24	141.46
16100	TRUE	-31.14	16100.24	110.05	16100.24	109.60	16100.24	137.05	16100.24	143.06	16100.24	141.37	16100.24	145.27	16100.24	141.19
16200	TRUE	-30.85	16200.24	110.54	16200.24	109.70	16200.24	137.10	16200.24	143.11	16200.24	141.45	16200.24	145.35	16200.24	141.39
16300	TRUE	-30.72	16300.25	110.62	16300.25	109.73	16300.25	137.38	16300.25	143.22	16300.25	141.37	16300.25	145.72	16300.25	141.34
16400	TRUE	-30.81	16400.25	110.70	16400.25	109.87	16400.25	137.45	16400.25	143.38	16400.25	141.56	16400.25	145.98	16400.25	141.51
16500	TRUE	-30.82	16500.25	110.53	16500.25	109.70	16500.25	136.99	16500.25	143.14	16500.25	141.42	16500.25	145.76	16500.25	141.35
16600	TRUE	-30.82	16600.25	110.63	16600.25	109.85	16600.25	137.15	16600.25	143.26	16600.25	141.58	16600.25	145.82	16600.25	141.45
16700	TRUE	-30.72	16700.25	110.47	16700.25	109.65	16700.25	136.82	16700.25	142.99	16700.25	141.20	16700.25	145.56	16700.25	141.18
16800	TRUE	-30.75	16800.25	110.46	16800.25	109.69	16800.25	136.86	16800.25	142.85	16800.25	141.24	16800.25	145.48	16800.25	141.21
16900	TRUE	-30.74	16900.26	110.37	16900.26	109.60	16900.26	136.47	16900.26	142.71	16900.26	141.07	16900.26	145.38	16900.26	141.12
17000	TRUE	-30.67	17000.26	110.59	17000.26	109.79	17000.26	136.58	17000.26	142.81	17000.26	141.27	17000.26	145.57	17000.26	141.26
17100	TRUE	-30.47	17100.26	110.57	17100.26	109.59	17100.26	137.23	17100.26	142.62	17100.26	140.97	17100.26	144.10	17100.26	141.04
17200	TRUE	-30.45	17200.26	110.21	17200.26	109.25	17200.26	136.61	17200.26	142.22	17200.26	140.64	17200.26	144.44	17200.26	140.66
17300	TRUE	-30.34	17300.26	110.17	17300.26	109.08	17300.26	137.48	17300.26	142.11	17300.26	140.49	17300.26	144.51	17300.26	140.51
17400	TRUE	-30.34	17400.26	110.31	17400.26	109.26	17400.26	141.10	17400.26	142.14	17400.26	140.69	17400.26	144.91	17400.26	140.65
17500	TRUE	-30.28	17500.26	110.36	17500.26	109.24	17500.26	136.48	17500.26	142.29	17500.26	140.78	17500.26	144.75	17500.26	140.64
17600	TRUE	-30.27	17600.27	110.09	17600.27	108.92	17600.27	135.21	17600.27	141.86	17600.27	140.34	17600.27	144.45	17600.27	140.36
17700	TRUE	-30.20	17700.27	110.09	17700.27	108.91	17700.27	134.63	17700.27	141.91	17700.27	140.33	17700.27	144.42	17700.27	140.29
17800	TRUE	-30.18	17800.27	110.11	17800.27	108.90	17800.27	134.97	17800.27	141.86	17800.27	140.34	17800.27	144.34	17800.27	140.29
17900	TRUE	-30.24	17900.27	110.32	17900.27	109.26	17900.27	135.28	17900.27	142.15	17900.27	140.54	17900.27	144.55	17900.27	140.56
18000	TRUE	-30.86	18000.27	109.62	18000.27	108.94	18000.27	134.54	18000.27	141.94	18000.27	140.51	18000.27	144.51	18000.27	140.48
18100	TRUE	-30.87	18100.27	109.78	18100.27	109.04	18100.27	134.70	18100.27	142.41	18100.27	140.61	18100.27	144.71	18100.27	140.65
18200	TRUE	-30.78	18200.28	109.73	18200.28	108.93	18200.28	134.63	18200.28	142.38	18200.28	140.44	18200.28	144.52	18200.28	140.51
18300	TRUE	-30.82	18300.28	109.85	18300.28	108.98	18300.28	134.75	18300.28	142.51	18300.28	140.55	18300.28	144.75	18300.28	140.67
18400	TRUE	-30.67	18400.28	109.98	18400.28	108.98	18400.28	134.92	18400.28	142.55	18400.28	140.45	18400.28	144.63	18400.28	140.64
18500	TRUE	-30.73	18500.28	110.34	18500.28	109.23	18500.28	135.17	18500.28	142.96	18500.28	140.96	18500.28	145.03	18500.28	141.07
18600	TRUE	-30.71	18600.28	110.28	18600.28	109.34	18600.28	135.07	18600.28	142.96	18600.28	140.89	18600.28	145.03	18600.28	140.99
18700	TRUE	-30.59	18700.28	110.19	18700.28	109.05	18700.28	135.06	18700.28	142.67	18700.28	140.68	18700.28	144.85	18700.28	140.78
18800	TRUE	-30.52	18800.28	110.23	18800.28	109.07	18800.28	135.07	18800.28	142.64	18800.28	140.67	18800.28	144.80	18800.28	140.74
18900	TRUE	-30.38	18900.29	110.46	18900.29	109.05	18900.29	135.19	18900.29	142.72	18900.29	140.69	18900.29	144.90	18900.29	140.85
19000	TRUE	-30.30	19000.29	110.49	19000.29	108.98	19000.29	135.01	19000.29	142.47	19000.29	140.46	19000.29	144.62	19000.29	140.78
19100	TRUE	-30.07	19100.29	110.08	19100.29	108.30	19100.29	134.64	19100.29	141.93	19100.29	140.05	19100.29	144.15	19100.29	140.14
19200	TRUE	-29.93	19200.29	109.95	19200.29	108.05	19200.29	135.05	19200.29	141.25	19200.29	139.41	19200.29	143.38	19200.29	139.88
19300	TRUE	-29.72	19300.29	109.37	19300.29	107.47	19300.29	134.21	19300.29	140.78	19300.29	138.90	19300.29	142.80	19300.29	139.09
19400	TRUE	-29.81	19400.29	108.65	19400.29	106.98	19400.29	133.63	19400.29	140.08	19400.29	138.31	19400.29	142.33	19400.29	138.46
19500	TRUE	-29.04	19500.29	107.87	19500.29	105.80	19500.29	132.50	19500.29	138.83	19500.29	137.05	19500.29	141.03	19500.29	136.91
19600	TRUE	-28.03	19600.30	107.41	19600.30	104.88	19600.30	131.38	19600.30	137.60	19600.30	135.84	19600.30	139.81	19600.30	135.44
19700	TRUE	-27.85	19700.30	105.71	19700.30	103.34	19700.30	129.49	19700.30	135.63	19700.30	133.88	19700.30	137.81	19700.30	133.55
19800	TRUE	-27.61	19800.30	103.94	19800.30	101.70	19800.30	127.45	19800.30	133.47	19800.30	131.57	19800.30	135.66	19800.30	131.55
19900	TRUE	-27.29	19900.30	101.86	19900.30	99.68	19900.30	125.06	19900.30	130.75	19900.30	128.99	19900.30	132.79	19900.30	129.15
20000	TRUE	-26.43	20000.30	100.07	20000.30	97.65	20000.30	123.33	20000.30	128.07	20000.30	126.39	20000.30	130.12	20000.30	126.50

Table H.1: Victaulic 75 Connected Black Steel Pipe Peak Signal Frequency and Magnitude. "Bandwidth" column indicates whether the Bandwidth Condition is satisfied (cont.)

Appendix I: BLACK STEEL PIPE OUTDOOR LABORATORY SETTING WITH FLEXIBLE PVC COUPLINGS

		Distance	0ft_vol100		10ft_vol100		20ft_vol100		25ft_vol100		30ft_vol100		40ft_vol100		42.5ft_vol100	
		Values	Rx_max_freq	Max_rx_mag	Rx_max_freq	Max_rx_mag	Rx_max_freq	Max_rx_mag	Rx_max_freq	Max_rx_mag	Rx_max_freq	Max_rx_mag	Rx_max_freq	Max_rx_mag	Rx_max_freq	Max_rx_mag
Tx_freq	Bandwidth	Attenuation/ft														
100	FALSE	NA	2.33	13.19	1.33	8.04	100.00	9.01	2.67	11.66	60.00	9.86	60.00	19.92	60.00	17.06
200	FALSE	NA	200.00	13.11	200.00	11.55	200.00	12.40	200.00	13.14	200.00	12.64	60.00	20.61	60.00	17.43
300	FALSE	NA	300.00	18.07	300.00	17.39	300.00	18.48	300.00	18.06	300.00	19.73	60.00	21.26	60.00	18.26
400	TRUE	0.60	400.01	24.48	400.01	23.83	400.01	23.22	400.01	23.73	400.01	25.33	400.01	23.94	400.01	23.89
500	TRUE	-0.02	500.01	27.13	500.01	26.73	500.01	27.20	500.01	26.27	500.01	29.13	500.01	27.03	500.01	27.15
600	TRUE	1.14	600.01	34.43	600.01	32.91	600.01	33.00	600.01	34.18	600.01	36.58	600.01	32.73	600.01	33.29
700	TRUE	0.10	700.01	38.44	700.01	36.93	700.01	37.12	700.01	37.44	700.01	39.92	700.01	36.98	700.01	38.34
800	TRUE	-0.22	800.01	42.94	800.01	41.33	800.01	41.32	800.01	41.44	800.01	44.61	800.01	41.99	800.01	43.16
900	TRUE	-0.10	900.01	49.48	900.01	47.67	900.01	46.84	900.01	47.45	900.01	51.51	900.01	47.74	900.01	49.58
1000	TRUE	1.10	1000.02	51.62	1000.02	49.17	1000.02	49.41	1000.02	49.71	1000.02	54.36	1000.02	49.55	1000.02	50.52
1100	TRUE	0.16	1100.02	60.97	1100.02	58.81	1100.02	58.74	1100.02	59.54	1100.02	64.59	1100.02	58.97	1100.02	60.81
1200	TRUE	-0.04	1200.02	56.85	1200.02	55.12	1200.02	55.56	1200.02	55.67	1200.02	60.33	1200.02	55.34	1200.02	56.89
1300	TRUE	-0.10	1300.02	60.20	1300.02	58.49	1300.02	58.56	1300.02	58.70	1300.02	64.90	1300.02	58.89	1300.02	60.31
1400	TRUE	-0.85	1400.02	64.33	1400.02	62.29	1400.02	62.59	1400.02	63.16	1400.02	69.74	1400.02	62.65	1400.02	65.18
1500	TRUE	-0.65	1500.02	74.03	1500.02	71.68	1500.02	72.04	1500.02	72.93	1500.02	80.12	1500.02	72.39	1500.02	74.68
1600	TRUE	-1.14	1600.02	70.25	1600.02	68.69	1600.02	68.68	1600.02	69.35	1600.02	76.65	1600.02	69.34	1600.02	71.39
1700	TRUE	-1.47	1700.03	71.88	1700.03	70.68	1700.03	70.97	1700.03	71.29	1700.03	79.04	1700.03	71.34	1700.03	73.36
1800	TRUE	-1.64	1800.03	77.18	1800.03	75.87	1800.03	75.64	1800.03	76.53	1800.03	83.56	1800.03	75.83	1800.03	78.82
1900	TRUE	-2.22	1900.03	84.42	1900.03	83.12	1900.03	83.53	1900.03	84.20	1900.03	89.97	1900.03	83.57	1900.03	86.64
2000	TRUE	-3.10	2000.03	79.32	2000.03	79.24	2000.03	79.39	2000.03	79.99	2000.03	89.78	2000.03	79.47	2000.03	82.42
2100	TRUE	-3.16	2100.03	81.45	2100.03	81.19	2100.03	81.39	2100.03	82.22	2100.03	93.16	2100.03	81.30	2100.03	84.61
2200	TRUE	-2.34	2200.03	84.22	2200.03	83.47	2200.03	83.40	2200.03	84.03	2200.03	95.69	2200.03	83.39	2200.03	86.56
2300	TRUE	-1.63	2300.03	87.42	2300.03	85.52	2300.03	85.66	2300.03	86.47	2300.03	97.89	2300.03	85.86	2300.03	89.05
2400	TRUE	-1.06	2400.04	90.13	2400.04	87.74	2400.04	88.31	2400.04	88.83	2400.04	100.53	2400.04	87.68	2400.04	91.19
2500	TRUE	-1.29	2500.04	92.51	2500.04	90.50	2500.04	90.84	2500.04	91.59	2500.04	103.41	2500.04	89.93	2500.04	93.80
2600	TRUE	-0.47	2600.04	103.16	2600.04	100.51	2600.04	101.24	2600.04	101.85	2600.04	114.07	2600.04	99.55	2600.04	103.63
2700	TRUE	-0.75	2700.04	98.67	2700.04	96.72	2700.04	96.96	2700.04	98.01	2700.04	109.00	2700.04	95.35	2700.04	99.42
2800	TRUE	0.04	2800.04	97.98	2800.04	95.63	2800.04	96.08	2800.04	96.83	2800.04	106.47	2800.04	94.36	2800.04	97.94
2900	TRUE	-0.08	2900.04	99.70	2900.04	97.44	2900.04	97.89	2900.04	98.82	2900.04	107.11	2900.04	95.89	2900.04	99.78
3000	TRUE	0.17	3000.05	101.13	3000.05	99.00	3000.05	99.28	3000.05	100.29	3000.05	108.87	3000.05	96.79	3000.05	100.97
3100	TRUE	0.42	3100.05	102.91	3100.05	100.37	3100.05	101.03	3100.05	101.86	3100.05	113.82	3100.05	98.55	3100.05	102.49
3200	TRUE	0.80	3200.05	104.08	3200.05	101.85	3200.05	102.38	3200.05	103.11	3200.05	119.60	3200.05	99.08	3200.05	103.28
3300	TRUE	1.77	3300.05	108.47	3300.05	106.30	3300.05	106.66	3300.05	107.44	3300.05	127.11	3300.05	102.40	3300.05	106.70
3400	TRUE	3.33	3400.05	116.58	3400.05	114.25	3400.05	114.80	3400.05	115.85	3400.05	138.97	3400.05	108.95	3400.05	113.26
3500	TRUE	4.79	3500.05	108.52	3500.05	106.27	3500.05	106.73	3500.05	107.78	3500.05	130.68	3500.05	99.37	3500.05	103.73
3600	TRUE	6.27	3600.05	109.15	3600.05	106.85	3600.05	107.42	3600.05	108.35	3600.05	131.85	3600.05	98.24	3600.05	102.88
3700	TRUE	2.78	3700.06	110.12	3700.06	107.73	3700.06	108.28	3700.06	109.19	3700.06	133.06	3700.06	101.11	3700.06	107.33
3800	TRUE	-3.15	3800.06	110.99	3800.06	108.65	3800.06	109.16	3800.06	110.26	3800.06	134.23	3800.06	108.74	3800.06	114.14
3900	TRUE	-5.40	3900.06	112.19	3900.06	109.79	3900.06	110.28	3900.06	111.27	3900.06	135.61	3900.06	112.38	3900.06	117.59
4000	TRUE	-5.53	4000.06	113.87	4000.06	111.26	4000.06	111.76	4000.06	112.80	4000.06	137.26	4000.06	114.08	4000.06	119.40
4100	TRUE	-5.89	4100.06	124.27	4100.06	121.74	4100.06	122.33	4100.06	123.62	4100.06	150.54	4100.06	124.36	4100.06	130.16
4200	TRUE	-5.23	4200.06	117.91	4200.06	115.52	4200.06	115.89	4200.06	117.13	4200.06	142.53	4200.06	117.02	4200.06	123.14
4300	TRUE	-4.63	4300.07	115.41	4300.07	112.93	4300.07	113.34	4300.07	114.62	4300.07	139.75	4300.07	113.79	4300.07	120.05
4400	TRUE	-4.36	4400.07	116.17	4400.07	113.69	4400.07	114.29	4400.07	115.37	4400.07	140.68	4400.07	114.14	4400.07	120.53
4500	TRUE	-3.90	4500.07	116.51	4500.07	114.48	4500.07	114.91	4500.07	115.94	4500.07	141.28	4500.07	114.01	4500.07	120.40
4600	TRUE	-3.65	4600.07	117.17	4600.07	114.91	4600.07	115.32	4600.07	116.56	4600.07	142.22	4600.07	114.49	4600.07	120.82
4700	TRUE	-4.39	4700.07	117.23	4700.07	115.44	4700.07	115.95	4700.07	117.15	4700.07	142.81	4700.07	114.94	4700.07	121.61
4800	TRUE	-4.75	4800.07	117.68	4800.07	116.03	4800.07	116.68	4800.07	117.93	4800.07	143.35	4800.07	116.25	4800.07	122.43
4900	TRUE	-5.09	4900.07	118.41	4900.07	116.57	4900.07	117.03	4900.07	118.31	4900.07	143.98	4900.07	117.21	4900.07	123.50
5000	TRUE	-5.42	5000.08	119.44	5000.08	117.44	5000.08	117.99	5000.08	119.11	5000.08	145.11	5000.08	118.24	5000.08	124.86
5100	TRUE	-5.40	5100.08	120.17	5100.08	118.12	5100.08	118.65	5100.08	119.86	5100.08	146.18	5100.08	118.98	5100.08	125.57
5200	TRUE	-6.83	5200.08	126.52	5200.08	125.55	5200.08	126.26	5200.08	127.45	5200.08	155.97	5200.08	126.29	5200.08	133.35
5300	TRUE	-7.27	5300.08	126.65	5300.08	126.39	5300.08	126.71	5300.08	128.25	5300.08	156.70	5300.08	127.00	5300.08	133.91
5400	TRUE	-6.92	5400.08	120.51	5400.08	120.03	5400.08	120.56	5400.08	121.91	5400.08	148.66	5400.08	120.93	5400.08	127.43
5500	TRUE	-7.06	5500.08	120.89	5500.08	120.59	5500.08	121.14	5500.08	122.48	5500.08	149.30	5500.08	121.08	5500.08	127.96
5600	TRUE	-7.16	5600.08	121.06	5600.08	120.89	5600.08	121.48	5600.08	122.83	5600.08	149.44	5600.08	121.32	5600.08	128.22
5700	TRUE	-6.63	5700.09	122.09	5700.09	121.32	5700.09	122.00	5700.09	123.39	5700.09	150.21	5700.09	121.67	5700.09	128.72
5800	TRUE	-6.73	5800.09	122.34	5800.09	121.83	5800.09	122.50	5800.09	123.93	5800.09	150.96	5800.09	122.01	5800.09	129.07
5900	TRUE	-6.70	5900.09	122.99	5900.09	122.51	5900.09	123.10	5900.09	124.66	5900.09	152.42	5900.09	122.61	5900.09	129.68
6000	TRUE	-5.63	6000.09	124.37	6000.09	122.83	6000.09	123.45	6000.09	124.98	6000.09	153.66	6000.09	122.79	6000.09	130.00
6100	TRUE	-6.02	6100.09	124.95	6100.09	123.38	6100.09	123.97	6100.09	125.62	6100.09	155.00	6100.09	123.18	6100.09	130.97
6200	TRUE	-5.81	6200.09	125.24	6200.09	123.65	6200.09	124.31	6200.09	125.89	6200.09	155.65	6200.09	123.37	6200.09	131.06
6300	TRUE	-5.89	6300.10	129.29	6300.10	127.62	6300.10	128.32	6300.10	129.96	6300.10	160.75	6300.10	127.31	6300.10	135.18
6400	TRUE	-6.27	6400.10	137.73	6400.10	136.05	6400.10	136.73	6400.10	138.62	6400.10	171.42	6400.10	135.81	6400.10	143.99
6500	TRUE	-5.89	6500.10	127.09	6500.10	125.39	6500.10	126.13	6500.10	127.93	6500.10	157.88	6500.10	125.21	6500.10	132.97
6600	TRUE	-5.81	6600.10	127.08	6600.10	125.25	6600.10	125.92	6600.10	127.60	6600.10	157.61	6600.10	125.07	6600.10	132.88
6700	TRUE	-5.75	6700.10	127.37	6700.10	125.38	6700.10	125.92	6700.10	127.73	6700.10	157.58	6700.10	125.43	6700.10	133.12
6800	TRUE	-5.87	6800.10	127.66	6800.10	125.58	6800.10	126.35	6800.10	128.03	6800.10	157.76	6800.10	125.86	6800.10	133.53
6900	TRUE	-6.58	6900.10	128.22	6900.10	126.07	6900.10	126.74	6900.10	128.60	6900.10	158.11	6900.10	126.39	6900.10	134.80
7000	TRUE	-7.88	7000.11	128.70	7000.11	126.45	7000.11	127.10	7000.11	128.94	7000.11	158.19	7000.11	126.88	7000.11	136.58
7100	TRUE	-14.21	7100.11	128.69	7100.11	126.40	7100.11	127.14	7100.11	128.89	7100.11	158.07	7100.11	126.68	7100.11	142.91
7200	TRUE	-14.23	7200.11	128.87	7200.11	126.66	7200.11	127.38	7200.11	129.23	7200.11	158.78	7200.11	127.20	7200.11	143.11
7300	TRUE	-14.44	7300.11	128.95	7300.11	126.89	7300.11	127.55	7300.11	129.40	7300.11	160.04	7300.11	127.53	7300.11	143.38
7400	TRUE	-14.24	7400.11	129.32	7400.11	127.28	7400.11	127.92	7400.11	129.81	7400.11	161.28	7400.11	127.68	7400.11	143.55
7500	TRUE	-15.30	7500.11	129.10	7500.11	127.26	7500.11	127.88	7500.11	129.84	7500.11	162.05	7500.11	127.81	7500.11	144.40
7600	TRUE	-15.41	7600.11	129.48	7600.11	127.63	7600.11	128.19	7600.11	130.20	7600.11	162.95	7600.11	128.03	7600.11	144.90
7700	TRUE	-16.04	7700.12	129.15	7700.12	127.38	7700.12	127.98	7700.12	130.11	7700.12	163.01	7700.12	128.21	7700.12	145.19
7800	TRUE	-16.84	7800.12	132.78	7800.12	131.31	7800.12	132.01	7800.12	133.99	7800.12	167.77	7800.12	132.46	7800.12	149.62
7900	TRUE	-19.35	7900.12	141.04	7900.12	139.67	7900.12	140.41	7900.12	142.52	7900.12	178.46	7900.12	140.94	7900.12	160.39
8000	TRUE	-17.77	8000.12	130.26	8000.12	128.62	8000.12	129.24	8000.12	131.25	8000.12	164.00	8000.12	129.59	8000.12	148.03
8100	TRUE	-17.40	8100.12	130.04	8100.12	128.13	8100.12	128.69	8100.12	130.73	8100.12	163.54	8100.12	129.10	8100.12	147.44
8200	TRUE	-17.24	8200.12	130.06	8200.12	128.12	8200.12	128.77	8200.12	130.72	8200.12	163.58	8200.12	128.90	8200.12	147.30
8300	TRUE	-15.85	8300.13	130.25	8300.13	128.22	8300.13	128.96	8300.13	130.96	8300.13	163.90	8300.13	129.12	8300.13	146.11
8400	TRUE	-15.86	8400.13	130.60	8400.13	128.62	8400.13	129.37	8400.13	131.34	8400.13	165.13	8400.13	129.61	8400.13	146.45
8500	TRUE	-15.78	8500.13	130.81	8500.13	129.06	8500.13	129.76	8500.13	131.81	8500.13	165.87	8500.13	129.97	8500.13	146.58
8600	TRUE	-15.80	8600.13	130.64	8600.13	129.00	8600.13	129.54	8600.13	131.53	8600.13	165.73	8600.13	129.67	8600.13	146.44
8700	TRUE	-15.81	8700.13	130.96	8700.13	129.14	8700.13	129.77	8700.13	131.82	8700.13	166.03	8700.13	130.04	8700.13	146.77
8800	TRUE	-17.59	8800.13	131.02	8800.13	129.29	8800.13	130.07	8800.13	132.01	8800.13	166.59	8800.13	130.26	8800.13	148.61
8900	TRUE	-17.46	8900.13	131.59	8900.13	129.81	8900.13	130.64	8900.13	132.45	8900.13	167.03	8900.13	130.80	8900.13	149.05
9000	TRUE	-18.01	9000.14	131.63	9000.14	129.88	9000.14	130.64	9000.14	132.53	9000.14	166.90	9000.14	130.99	9000.14	149.64
9100	TRUE	-18.18	9100.14	132.16	9100.14	130.33	9100.14	131.22	9100.14	133.15	9100.14	167.38	9100.14	131.45	9100.14	150.35
9200	TRUE	-18.38	9200.14	132.21	9200.14	130.55	9200.14	131.24	9200.14	133.18	9200.14	167.59	9200.14	131.54	9200.14	150.58
9300	TRUE	-18.43	9300.14	132.57	9300.14	130.82	9300.14	131.55	9300.14	133.53	9300.14	167.91	9300.14	131.94	9300.14	151.00
9400	TRUE	-18.60	9400.14	132.70	9400.14	131.04	9400.14	131.85	9400.14	133.76	9400.14	168.19	9400.14	132.86	9400.14	151.30
9500	TRUE	-18.61	9500.14	133.26	9500.14	131.61	9500.14	132.27	9500.14	134.30	9500.14	168.83	9500.14	133.28	9500.14	151.87
9600	TRUE	-18.56	9600.15	133.40	9600.15	131.73	9600.15	132.35	9600.15	134.43	9600.15	168.97	9600.15	133.38	9600.15	151.96
9700	TRUE	-18.48	9700.15	133.35	9700.15	131.72	9700.15	132.39	9700.15	134.42	9700.15	168.96	9700.15	133.29	9700.15	151.83
9800	TRUE	-18.55	9800.15	133.49	9800.15	131.96	9800.15	132.60	9800.15	134.66	9800.15	169.14	9800.15	133.40	9800.15	152.05
9900	TRUE	-18.91	9900.15	133.45	9900.15	132.31	9900.15	133.01	9900.15	135.06	9900.15	169.33	9900.15	133.79	9900.15	152.36
10000	TRUE	-19.59	10000.15	133.56	10000.15	133.08	10000.15	133.82	10000.15	135.80	10000.15	170.54	10000.15	134.48	10000.15	153.15
10100	TRUE	-20.72	10100.15	145.65	10100.15	144.80	10100.15	145.51	10100.15	147.75	10100.15	185.63	10100.15	146.21	10100.15	166.37
10200	TRUE	-19.48	10200.15	137.40	10200.15	136.42	10200.15	137.13	10200.15	139.20	10200.15	174.72	10200.15	137.72	10200.15	156.88
10300	TRUE	-18.98	10300.16	133.61	10300.16	132.73	10300.16	133.31	10300.16	135.35	10300.16	169.90	10300.16	133.90	10300.16	152.59
10400	TRUE	-18.94	10400.16	133.84	10400.16	133.03	10400.16	133.60	10400.16	135.73	10400.16	170.08	10400.16	134.26	10400.16	152.79

Table I.1: PVC Coupling Connected Black Steel Pipe Peak Signal Frequency and Magnitude. "Bandwidth" column indicates whether the Bandwidth Condition is satisfied

		Distance	0ft_vol100		10ft_vol100		20ft_vol100		22.75ft_vol100		30ft_vol100		40ft_vol100		42.5ft_vol100	
		Values	Rx_max_freq	Max_rx_mag	Rx_max_freq	Max_rx_mag	Rx_max_freq	Max_rx_mag	Rx_max_freq	Max_rx_mag	Rx_max_freq	Max_rx_mag	Rx_max_freq	Max_rx_mag	Rx_max_freq	Max_rx_mag
Tx_freq	Bandwidth	Attenuation/ft														
10500	TRUE	-18.87	10500.16	133.80	10500.16	132.98	10500.16	133.62	10500.16	135.63	10500.16	170.05	10500.16	134.08	10500.16	152.68
10600	TRUE	-18.83	10600.16	133.99	10600.16	133.42	10600.16	133.83	10600.16	135.81	10600.16	170.36	10600.16	134.30	10600.16	152.83
10700	TRUE	-18.33	10700.16	134.34	10700.16	133.34	10700.16	133.79	10700.16	135.84	10700.16	170.10	10700.16	134.06	10700.16	152.67
10800	TRUE	-17.95	10800.16	134.79	10800.16	133.59	10800.16	134.07	10800.16	136.04	10800.16	170.17	10800.16	134.08	10800.16	152.74
10900	TRUE	-17.64	10900.16	135.04	10900.16	133.73	10900.16	134.22	10900.16	136.21	10900.16	170.06	10900.16	134.01	10900.16	152.68
11000	TRUE	-17.05	11000.17	135.96	11000.17	134.23	11000.17	134.77	11000.17	136.73	11000.17	170.43	11000.17	134.14	11000.17	153.00
11100	TRUE	-16.47	11100.17	136.46	11100.17	134.27	11100.17	134.75	11100.17	136.83	11100.17	170.27	11100.17	133.63	11100.17	152.94
11200	TRUE	-15.83	11200.17	136.80	11200.17	134.14	11200.17	134.75	11200.17	136.89	11200.17	169.96	11200.17	133.35	11200.17	152.64
11300	TRUE	-15.51	11300.17	137.18	11300.17	134.28	11300.17	134.90	11300.17	137.08	11300.17	169.98	11300.17	133.31	11300.17	152.69
11400	TRUE	-15.33	11400.17	137.54	11400.17	134.55	11400.17	135.22	11400.17	137.39	11400.17	170.26	11400.17	133.73	11400.17	152.87
11500	TRUE	-15.44	11500.17	137.60	11500.17	134.68	11500.17	135.41	11500.17	137.63	11500.17	170.43	11500.17	133.87	11500.17	153.04
11600	TRUE	-15.49	11600.18	137.32	11600.18	134.52	11600.18	135.14	11600.18	137.45	11600.18	170.12	11600.18	133.64	11600.18	152.81
11700	TRUE	-16.13	11700.18	136.72	11700.18	134.52	11700.18	135.29	11700.18	137.56	11700.18	170.25	11700.18	133.68	11700.18	152.85
11800	TRUE	-16.67	11800.18	136.26	11800.18	134.53	11800.18	135.33	11800.18	137.63	11800.18	170.22	11800.18	135.26	11800.18	152.93
11900	TRUE	-16.91	11900.18	136.34	11900.18	134.80	11900.18	135.62	11900.18	137.93	11900.18	170.65	11900.18	136.73	11900.18	153.24
12000	TRUE	-16.88	12000.18	136.33	12000.18	134.77	12000.18	135.52	12000.18	137.83	12000.18	170.65	12000.18	136.54	12000.18	153.22
12100	TRUE	-16.80	12100.18	136.66	12100.18	134.96	12100.18	135.75	12100.18	138.10	12100.18	170.94	12100.18	134.90	12100.18	153.45
12200	TRUE	-16.50	12200.18	136.90	12200.18	134.85	12200.18	135.68	12200.18	138.02	12200.18	170.78	12200.18	135.68	12200.18	153.40
12300	TRUE	-17.00	12300.19	141.03	12300.19	138.83	12300.19	139.67	12300.19	142.20	12300.19	175.90	12300.19	139.37	12300.19	158.03
12400	TRUE	-17.84	12400.19	149.87	12400.19	147.60	12400.19	148.52	12400.19	151.20	12400.19	187.20	12400.19	148.11	12400.19	167.71
12500	TRUE	-16.59	12500.19	138.09	12500.19	135.79	12500.19	136.68	12500.19	139.13	12500.19	172.23	12500.19	136.39	12500.19	154.69
12600	TRUE	-16.47	12600.19	137.62	12600.19	135.37	12600.19	136.33	12600.19	138.60	12600.19	171.62	12600.19	135.93	12600.19	154.09
12700	TRUE	-16.38	12700.19	137.61	12700.19	135.16	12700.19	136.07	12700.19	138.47	12700.19	171.55	12700.19	135.71	12700.19	153.99
12800	TRUE	-16.41	12800.19	137.60	12800.19	135.42	12800.19	136.18	12800.19	138.59	12800.19	171.74	12800.19	135.94	12800.19	154.00
12900	TRUE	-16.65	12900.20	137.82	12900.20	135.80	12900.20	136.56	12900.20	138.90	12900.20	172.15	12900.20	136.21	12900.20	154.47
13000	TRUE	-16.73	13000.20	138.01	13000.20	135.99	13000.20	136.67	13000.20	139.09	13000.20	172.50	13000.20	136.39	13000.20	154.74
13100	TRUE	-16.70	13100.20	137.75	13100.20	135.76	13100.20	136.50	13100.20	138.95	13100.20	172.19	13100.20	136.18	13100.20	154.44
13200	TRUE	-16.78	13200.20	137.81	13200.20	135.89	13200.20	136.59	13200.20	139.07	13200.20	172.29	13200.20	136.40	13200.20	154.59
13300	TRUE	-16.77	13300.20	137.74	13300.20	135.79	13300.20	136.58	13300.20	139.06	13300.20	172.36	13300.20	136.37	13300.20	154.51
13400	TRUE	-16.87	13400.20	138.02	13400.20	136.07	13400.20	136.81	13400.20	139.24	13400.20	172.64	13400.20	136.64	13400.20	154.89
13500	TRUE	-16.81	13500.20	137.79	13500.20	135.92	13500.20	136.59	13500.20	139.10	13500.20	172.48	13500.20	136.49	13500.20	154.59
13600	TRUE	-16.93	13600.21	137.94	13600.21	136.05	13600.21	136.79	13600.21	139.25	13600.21	172.64	13600.21	136.63	13600.21	154.87
13700	TRUE	-16.97	13700.21	137.62	13700.21	135.80	13700.21	136.58	13700.21	138.96	13700.21	172.38	13700.21	136.36	13700.21	154.59
13800	TRUE	-17.15	13800.21	137.47	13800.21	135.70	13800.21	136.51	13800.21	138.93	13800.21	172.30	13800.21	136.37	13800.21	154.62
13900	TRUE	-17.04	13900.21	137.48	13900.21	135.56	13900.21	136.41	13900.21	138.81	13900.21	172.25	13900.21	136.27	13900.21	154.52
14000	TRUE	-17.17	14000.21	137.60	14000.21	135.80	14000.21	136.62	14000.21	139.08	14000.21	172.44	14000.21	136.66	14000.21	154.77
14100	TRUE	-17.23	14100.21	137.35	14100.21	135.58	14100.21	136.34	14100.21	138.82	14100.21	172.24	14100.21	136.40	14100.21	154.58
14200	TRUE	-17.27	14200.21	137.00	14200.21	135.30	14200.21	136.09	14200.21	138.59	14200.21	171.98	14200.21	136.42	14200.21	154.27
14300	TRUE	-17.35	14300.22	136.84	14300.22	135.27	14300.22	136.02	14300.22	138.35	14300.22	171.90	14300.22	136.15	14300.22	154.19
14400	TRUE	-17.39	14400.22	136.99	14400.22	135.41	14400.22	136.01	14400.22	138.65	14400.22	172.10	14400.22	136.38	14400.22	154.37
14500	TRUE	-17.33	14500.22	137.10	14500.22	135.44	14500.22	136.42	14500.22	138.72	14500.22	172.07	14500.22	136.41	14500.22	154.43
14600	TRUE	-17.12	14600.22	136.93	14600.22	135.07	14600.22	135.93	14600.22	138.45	14600.22	171.68	14600.22	136.03	14600.22	154.05
14700	TRUE	-16.97	14700.22	137.12	14700.22	135.17	14700.22	135.96	14700.22	138.47	14700.22	171.66	14700.22	136.10	14700.22	154.09
14800	TRUE	-17.07	14800.22	136.90	14800.22	135.07	14800.22	135.91	14800.22	138.30	14800.22	171.64	14800.22	136.05	14800.22	153.97
14900	TRUE	-17.03	14900.23	137.24	14900.23	135.35	14900.23	136.15	14900.23	138.67	14900.23	171.89	14900.23	136.34	14900.23	154.27
15000	TRUE	-17.12	15000.23	136.99	15000.23	135.22	15000.23	136.09	15000.23	138.53	15000.23	171.79	15000.23	136.18	15000.23	154.11
15100	TRUE	-17.14	15100.23	137.24	15100.23	135.51	15100.23	136.33	15100.23	138.85	15100.23	172.04	15100.23	136.43	15100.23	154.38
15200	TRUE	-17.17	15200.23	137.04	15200.23	135.38	15200.23	136.20	15200.23	138.75	15200.23	171.87	15200.23	136.32	15200.23	154.21
15300	TRUE	-18.25	15300.23	140.56	15300.23	139.44	15300.23	140.27	15300.23	142.90	15300.23	176.95	15300.23	140.37	15300.23	158.81
15400	TRUE	-19.13	15400.23	149.43	15400.23	148.30	15400.23	149.18	15400.23	151.89	15400.23	188.15	15400.23	149.43	15400.23	168.56
15500	TRUE	-18.07	15500.23	137.31	15500.23	136.47	15500.23	137.29	15500.23	139.84	15500.23	173.16	15500.23	137.57	15500.23	155.39
15600	TRUE	-18.03	15600.24	136.81	15600.24	136.06	15600.24	136.83	15600.24	139.41	15600.24	172.53	15600.24	136.99	15600.24	154.84
15700	TRUE	-17.85	15700.24	136.85	15700.24	135.93	15700.24	136.77	15700.24	139.34	15700.24	172.43	15700.24	136.90	15700.24	154.70
15800	TRUE	-17.86	15800.24	136.95	15800.24	136.07	15800.24	136.85	15800.24	139.39	15800.24	172.66	15800.24	136.97	15800.24	154.81
15900	TRUE	-17.86	15900.24	137.32	15900.24	136.36	15900.24	137.20	15900.24	139.74	15900.24	173.14	15900.24	137.29	15900.24	155.18
16000	TRUE	-17.91	16000.24	137.58	16000.24	136.71	16000.24	137.41	16000.24	139.96	16000.24	173.64	16000.24	137.54	16000.24	155.49
16100	TRUE	-17.80	16100.24	137.43	16100.24	136.33	16100.24	137.17	16100.24	139.73	16100.24	173.40	16100.24	137.33	16100.24	155.23
16200	TRUE	-17.87	16200.24	137.46	16200.24	136.45	16200.24	137.24	16200.24	139.80	16200.24	173.67	16200.24	137.45	16200.24	155.33
16300	TRUE	-17.81	16300.25	137.55	16300.25	136.42	16300.25	137.20	16300.25	139.81	16300.25	173.75	16300.25	137.47	16300.25	155.36
16400	TRUE	-17.44	16400.25	138.17	16400.25	136.63	16400.25	137.40	16400.25	140.01	16400.25	174.18	16400.25	137.71	16400.25	155.61
16500	TRUE	-17.64	16500.25	137.82	16500.25	136.37	16500.25	137.20	16500.25	139.85	16500.25	174.01	16500.25	137.57	16500.25	155.46
16600	TRUE	-17.67	16600.25	137.96	16600.25	136.54	16600.25	137.34	16600.25	139.94	16600.25	174.16	16600.25	137.72	16600.25	155.63
16700	TRUE	-17.74	16700.25	137.61	16700.25	136.28	16700.25	137.03	16700.25	139.69	16700.25	173.79	16700.25	137.51	16700.25	155.35
16800	TRUE	-17.82	16800.25	137.47	16800.25	136.26	16800.25	136.98	16800.25	139.62	16800.25	173.84	16800.25	137.43	16800.25	155.29
16900	TRUE	-17.67	16900.26	137.40	16900.26	136.10	16900.26	136.87	16900.26	139.54	16900.26	173.63	16900.26	137.35	16900.26	155.08
17000	TRUE	-17.82	17000.26	137.64	17000.26	136.26	17000.26	137.07	17000.26	139.76	17000.26	173.96	17000.26	137.54	17000.26	155.46
17100	TRUE	-17.80	17100.26	137.47	17100.26	136.00	17100.26	136.78	17100.26	139.47	17100.26	173.46	17100.26	137.44	17100.26	155.27
17200	TRUE	-17.60	17200.26	137.32	17200.26	135.72	17200.26	136.43	17200.26	139.14	17200.26	173.15	17200.26	137.14	17200.26	154.92
17300	TRUE	-17.55	17300.26	137.32	17300.26	135.56	17300.26	136.30	17300.26	139.19	17300.26	173.02	17300.26	137.07	17300.26	154.87
17400	TRUE	-17.52	17400.26	137.53	17400.26	135.74	17400.26	136.44	17400.26	139.22	17400.26	173.04	17400.26	137.31	17400.26	155.05
17500	TRUE	-18.09	17500.26	137.04	17500.26	135.75	17500.26	136.42	17500.26	139.27	17500.26	173.26	17500.26	137.42	17500.26	155.13
17600	TRUE	-17.90	17600.27	136.90	17600.27	135.43	17600.27	136.06	17600.27	138.88	17600.27	172.70	17600.27	137.11	17600.27	154.80
17700	TRUE	-17.56	17700.27	137.31	17700.27	135.45	17700.27	136.12	17700.27	138.96	17700.27	172.69	17700.27	137.15	17700.27	154.87
17800	TRUE	-17.66	17800.27	137.19	17800.27	135.34	17800.27	135.92	17800.27	138.78	17800.27	172.46	17800.27	137.17	17800.27	154.85
17900	TRUE	-17.60	17900.27	137.48	17900.27	135.73	17900.27	136.34	17900.27	139.23	17900.27	172.96	17900.27	137.46	17900.27	155.08
18000	TRUE	-16.91	18000.27	137.33	18000.27	135.62	18000.27	136.32	18000.27	139.15	18000.27	172.81	18000.27	137.24	18000.27	154.24
18100	TRUE	-17.56	18100.27	137.62	18100.27	135.89	18100.27	136.52	18100.27	139.37	18100.27	172.97	18100.27	137.34	18100.27	155.18
18200	TRUE	-17.50	18200.28	137.56	18200.28	135.75	18200.28	136.43	18200.28	139.24	18200.28	172.71	18200.28	137.42	18200.28	155.07
18300	TRUE	-17.65	18300.28	137.49	18300.28	135.77	18300.28	136.39	18300.28	139.29	18300.28	172.87	18300.28	137.44	18300.28	155.14
18400	TRUE	-17.63	18400.28	137.62	18400.28	135.98	18400.28	136.58	18400.28	139.50	18400.28	172.88	18400.28	139.36	18400.28	155.24
18500	TRUE	-17.67	18500.28	138.01	18500.28	136.41	18500.28	136.98	18500.28	139.90	18500.28	173.42	18500.28	139.65	18500.28	155.68
18600	TRUE	-18.15	18600.28	137.47	18600.28	136.44	18600.28	137.02	18600.28	139.92	18600.28	173.25	18600.28	139.69	18600.28	155.62
18700	TRUE	-17.43	18700.28	137.92	18700.28	136.22	18700.28	136.81	18700.28	139.73	18700.28	173.06	18700.28	139.52	18700.28	155.34
18800	TRUE	-17.41	18800.28	137.90	18800.28	136.27	18800.28	136.66	18800.28	139.74	18800.28	172.97	18800.28	139.48	18800.28	155.31
18900	TRUE	-17.54	18900.29	137.95	18900.29	136.21	18900.29	136.92	18900.29	139.90	18900.29	173.04	18900.29	139.42	18900.29	155.49
19000	TRUE	-17.55	19000.29	137.88	19000.29	136.25	19000.29	136.91	19000.29	139.82	19000.29	172.91	19000.29	139.58	19000.29	155.43
19100	TRUE	-17.44	19100.29	137.30	19100.29	135.74	19100.29	136.30	19100.29	139.26	19100.29	172.18	19100.29	138.98	19100.29	154.74
19200	TRUE	-17.08	19200.29	137.12	19200.29	135.47	19200.29	135.76	19200.29	138.78	19200.29	171.73	19200.29	138.53	19200.29	154.21
19300	TRUE	-17.09	19300.29	136.25	19300.29	134.58	19300.29	135.18	19300.29	138.21	19300.29	170.78	19300.29	137.78	19300.29	153.34
19400	TRUE	-17.14	19400.29	135.58	19400.29	134.04	19400.29	134.66	19400.29	137.57	19400.29	169.97	19400.29	137.30	19400.29	152.72
19500	TRUE	-17.08	19500.29	134.24	19500.29	132.82	19500.29	133.41	19500.29	136.33	19500.29	168.44	19500.29	136.02	19500.29	151.32
19600	TRUE	-16.94	19600.30	133.00	19600.30	131.59	19600.30	132.21	19600.30	135.06	19600.30	166.95	19600.30	134.81	19600.30	149.95
19700	TRUE	-16.62	19700.30	131.14	19700.30	129.67	19700.30	130.31	19700.30	133.13	19700.30	164.60	19700.30	132.90	19700.30	147.75
19800	TRUE	-16.36	19800.30	129.12	19800.30	127.62	19800.30	128.22	19800.30	131.05	19800.30	161.98	19800.30	130.83	19800.30	145.48
19900	TRUE	-16.08	19900.30	126.56	19900.30	125.01	19900.30	125.71	19900.30	128.46	19900.30	158.85	19900.30	128.35	19900.30	142.65
20000	TRUE	-15.93	20000.30	123.76	20000.30	122.40	20000.30	123.03	20000.30	125.77	20000.30	155.52	20000.30	125.59	20000.30	139.69

Table I.1: PVC Coupling Connected Black Steel Pipe Peak Signal Frequency and Magnitude. "Bandwidth" column indicates whether the Bandwidth Condition is satisfied (cont.)

Appendix J: BLACK STEEL PIPE OUTDOOR LABORATORY SETTING WITH VICTAULIC 005 COUPLINGS AND WASHER

		Distance	0ft_vol100		10ft_vol100		20ft_vol100		22.75ft_vol100		30ft_vol100		40ft_vol100		42.5ft_vol100	
		Values	Rx_max_freq	Max_rx_mag	Rx_max_freq	Max_rx_mag	Rx_max_freq	Max_rx_mag	Rx_max_freq	Max_rx_mag	Rx_max_freq	Max_rx_mag	Rx_max_freq	Max_rx_mag	Rx_max_freq	Max_rx_mag
Tx_freq	Bandwidth	Attenuation/ft														
100	FALSE	NA	60.00	31.36	60.00	15.16	60.00	19.07	60.00	12.97	60.00	14.07	2.67	12.71	1.67	17.53
200	FALSE	NA	60.00	31.91	60.00	14.50	60.00	18.45	200.00	13.55	60.00	13.85	200.00	15.57	200.00	14.77
300	TRUE	-4.22	300.00	15.92	300.00	19.41	300.00	20.13	300.00	19.80	300.00	19.44	300.00	21.72	300.00	20.14
400	TRUE	-5.29	400.01	23.42	400.01	26.92	400.01	24.13	400.01	27.00	400.01	27.55	400.01	27.18	400.01	28.71
500	TRUE	-6.18	500.01	26.36	500.01	30.63	500.01	28.07	500.01	30.14	500.01	31.57	500.01	31.38	500.01	32.54
600	TRUE	-6.07	600.01	33.34	600.01	38.56	600.01	34.44	600.01	37.89	600.01	38.05	600.01	40.50	600.01	39.42
700	TRUE	-8.67	700.01	36.21	700.01	42.94	700.01	39.45	700.01	43.06	700.01	43.64	700.01	43.81	700.01	44.88
800	TRUE	-9.14	800.01	41.12	800.01	48.82	800.01	44.77	800.01	48.47	800.01	48.53	800.01	49.85	800.01	50.26
900	TRUE	-9.38	900.01	47.74	900.01	55.72	900.01	51.31	900.01	55.50	900.01	55.62	900.01	56.52	900.01	57.12
1000	TRUE	-10.66	1000.02	50.08	1000.02	58.25	1000.02	53.16	1000.02	58.47	1000.02	58.10	1000.02	59.66	1000.02	60.74
1100	TRUE	-12.87	1100.02	59.43	1100.02	69.54	1100.02	63.30	1100.02	69.44	1100.02	68.93	1100.02	70.97	1100.02	72.30
1200	TRUE	-12.69	1200.02	55.86	1200.02	65.68	1200.02	60.24	1200.02	65.21	1200.02	65.83	1200.02	67.65	1200.02	68.54
1300	TRUE	-13.81	1300.02	59.40	1300.02	69.77	1300.02	63.68	1300.02	69.29	1300.02	69.23	1300.02	72.11	1300.02	73.22
1400	TRUE	-15.05	1400.02	63.63	1400.02	75.03	1400.02	68.37	1400.02	74.81	1400.02	74.48	1400.02	77.10	1400.02	78.68
1500	TRUE	-16.29	1500.02	74.21	1500.02	87.11	1500.02	79.11	1500.02	85.86	1500.02	85.83	1500.02	89.04	1500.02	90.50
1600	TRUE	-18.06	1600.02	70.54	1600.02	83.55	1600.02	76.08	1600.02	83.12	1600.02	82.36	1600.02	85.41	1600.02	88.59
1700	TRUE	-19.57	1700.03	73.16	1700.03	86.74	1700.03	78.56	1700.03	83.09	1700.03	82.86	1700.03	80.03	1700.03	92.74
1800	TRUE	-16.59	1800.03	78.64	1800.03	92.84	1800.03	84.21	1800.03	89.27	1800.03	90.35	1800.03	92.90	1800.03	95.23
1900	TRUE	-18.44	1900.03	86.63	1900.03	102.40	1900.03	93.32	1900.03	103.21	1900.03	100.82	1900.03	103.27	1900.03	105.06
2000	TRUE	-20.00	2000.03	81.60	2000.03	97.67	2000.03	89.80	2000.03	97.13	2000.03	97.12	2000.03	99.81	2000.03	101.60
2100	TRUE	-21.81	2100.03	83.94	2100.03	99.88	2100.03	96.25	2100.03	99.54	2100.03	100.68	2100.03	103.09	2100.03	105.76
2200	TRUE	-21.81	2200.03	86.48	2200.03	103.54	2200.03	100.71	2200.03	102.73	2200.03	102.84	2200.03	105.88	2200.03	108.28
2300	TRUE	-22.67	2300.03	89.02	2300.03	105.77	2300.03	103.54	2300.03	105.22	2300.03	106.07	2300.03	109.46	2300.03	111.69
2400	TRUE	-24.13	2400.04	91.19	2400.04	108.90	2400.04	106.50	2400.04	108.37	2400.04	108.17	2400.04	112.04	2400.04	115.32
2500	TRUE	-23.29	2500.04	93.90	2500.04	111.72	2500.04	109.25	2500.04	110.48	2500.04	111.11	2500.04	114.54	2500.04	117.19
2600	TRUE	-27.54	2600.04	104.09	2600.04	123.23	2600.04	121.55	2600.04	120.46	2600.04	122.69	2600.04	125.94	2600.04	131.62
2700	TRUE	-19.89	2700.04	100.18	2700.04	118.47	2700.04	115.62	2700.04	114.87	2700.04	116.56	2700.04	121.11	2700.04	120.07
2800	TRUE	-20.50	2800.04	99.34	2800.04	116.63	2800.04	113.28	2800.04	115.62	2800.04	115.77	2800.04	118.71	2800.04	119.84
2900	TRUE	-24.06	2900.04	99.88	2900.04	116.91	2900.04	112.81	2900.04	119.95	2900.04	117.57	2900.04	121.07	2900.04	123.94
3000	TRUE	-26.66	3000.05	101.84	3000.05	115.65	3000.05	113.03	3000.05	123.03	3000.05	122.75	3000.05	126.43	3000.05	128.50
3100	TRUE	-28.72	3100.05	103.76	3100.05	123.54	3100.05	124.00	3100.05	128.02	3100.05	126.11	3100.05	130.32	3100.05	132.47
3200	TRUE	-30.95	3200.05	105.16	3200.05	131.43	3200.05	129.73	3200.05	131.71	3200.05	131.33	3200.05	134.85	3200.05	136.10
3300	TRUE	-36.28	3300.05	109.59	3300.05	138.49	3300.05	135.91	3300.05	139.70	3300.05	140.01	3300.05	143.58	3300.05	145.87
3400	TRUE	-39.86	3400.05	119.40	3400.05	148.74	3400.05	145.94	3400.05	151.40	3400.05	152.30	3400.05	157.16	3400.05	159.26
3500	TRUE	-35.45	3500.05	114.13	3500.05	138.82	3500.05	135.80	3500.05	141.67	3500.05	142.22	3500.05	146.60	3500.05	149.58
3600	TRUE	-34.62	3600.05	116.24	3600.05	139.71	3600.05	136.31	3600.05	142.86	3600.05	143.41	3600.05	147.85	3600.05	150.86
3700	TRUE	-34.09	3700.06	118.06	3700.06	140.36	3700.06	137.29	3700.06	143.97	3700.06	144.58	3700.06	148.91	3700.06	152.15
3800	TRUE	-33.00	3800.06	120.79	3800.06	141.87	3800.06	138.93	3800.06	145.60	3800.06	145.98	3800.06	150.53	3800.06	153.79
3900	TRUE	-33.17	3900.06	122.30	3900.06	143.54	3900.06	140.66	3900.06	146.95	3900.06	147.67	3900.06	152.38	3900.06	155.46
4000	TRUE	-33.34	4000.06	124.22	4000.06	145.69	4000.06	142.49	4000.06	148.56	4000.06	149.69	4000.06	154.09	4000.06	157.56
4100	TRUE	-36.88	4100.06	135.45	4100.06	159.40	4100.06	156.19	4100.06	162.82	4100.06	163.92	4100.06	168.77	4100.06	172.33
4200	TRUE	-35.16	4200.06	128.49	4200.06	151.16	4200.06	147.50	4200.06	154.64	4200.06	155.35	4200.06	160.09	4200.06	163.65
4300	TRUE	-34.27	4300.07	125.84	4300.07	148.14	4300.07	145.37	4300.07	151.07	4300.07	151.95	4300.07	156.46	4300.07	160.11
4400	TRUE	-34.23	4400.07	126.88	4400.07	150.09	4400.07	146.88	4400.07	152.43	4400.07	153.06	4400.07	157.82	4400.07	161.11
4500	TRUE	-34.44	4500.07	127.53	4500.07	150.77	4500.07	148.14	4500.07	153.08	4500.07	153.80	4500.07	158.28	4500.07	161.96
4600	TRUE	-34.83	4600.07	128.23	4600.07	152.09	4600.07	149.51	4600.07	153.95	4600.07	154.85	4600.07	159.52	4600.07	163.06
4700	TRUE	-34.65	4700.07	128.80	4700.07	153.42	4700.07	150.24	4700.07	154.29	4700.07	155.14	4700.07	159.90	4700.07	163.45
4800	TRUE	-34.84	4800.07	129.49	4800.07	154.75	4800.07	150.96	4800.07	155.01	4800.07	155.78	4800.07	160.64	4800.07	164.33
4900	TRUE	-35.57	4900.07	130.28	4900.07	154.95	4900.07	151.44	4900.07	157.14	4900.07	157.67	4900.07	162.47	4900.07	165.85
5000	TRUE	-37.30	5000.08	131.54	5000.08	156.56	5000.08	152.68	5000.08	160.16	5000.08	160.79	5000.08	165.53	5000.08	168.84
5100	TRUE	-39.10	5100.08	132.20	5100.08	157.49	5100.08	154.36	5100.08	161.81	5100.08	162.64	5100.08	167.60	5100.08	171.30
5200	TRUE	-41.90	5200.08	140.08	5200.08	168.09	5200.08	165.07	5200.08	172.30	5200.08	173.15	5200.08	178.42	5200.08	181.97
5300	TRUE	-43.45	5300.08	139.72	5300.08	170.27	5300.08	166.62	5300.08	173.10	5300.08	174.19	5300.08	179.37	5300.08	183.17
5400	TRUE	-41.85	5400.08	132.50	5400.08	161.71	5400.08	158.46	5400.08	164.82	5400.08	165.69	5400.08	170.63	5400.08	174.35
5500	TRUE	-41.50	5500.08	133.67	5500.08	162.91	5500.08	159.51	5500.08	165.43	5500.08	166.52	5500.08	171.41	5500.08	175.18
5600	TRUE	-41.07	5600.08	134.74	5600.08	162.76	5600.08	159.56	5600.08	166.02	5600.08	166.85	5600.08	171.73	5600.08	175.81
5700	TRUE	-41.30	5700.09	135.44	5700.09	164.19	5700.09	160.26	5700.09	166.73	5700.09	167.78	5700.09	172.91	5700.09	176.74
5800	TRUE	-41.47	5800.09	135.96	5800.09	164.46	5800.09	160.77	5800.09	167.64	5800.09	168.65	5800.09	173.67	5800.09	177.44
5900	TRUE	-42.17	5900.09	136.38	5900.09	165.35	5900.09	161.44	5900.09	168.42	5900.09	169.85	5900.09	174.74	5900.09	178.56
6000	TRUE	-43.44	6000.09	135.70	6000.09	165.71	6000.09	162.02	6000.09	168.92	6000.09	169.99	6000.09	175.63	6000.09	179.14
6100	TRUE	-41.96	6100.09	137.94	6100.09	167.00	6100.09	162.80	6100.09	169.72	6100.09	170.82	6100.09	176.09	6100.09	179.90
6200	TRUE	-40.83	6200.09	139.53	6200.09	167.37	6200.09	163.19	6200.09	169.96	6200.09	171.14	6200.09	176.32	6200.09	180.36
6300	TRUE	-41.58	6300.10	144.62	6300.10	171.74	6300.10	167.96	6300.10	175.56	6300.10	176.65	6300.10	182.09	6300.10	186.20
6400	TRUE	-43.27	6400.10	154.94	6400.10	183.32	6400.10	179.39	6400.10	186.91	6400.10	188.32	6400.10	193.89	6400.10	198.20
6500	TRUE	-39.95	6500.10	143.05	6500.10	169.83	6500.10	165.47	6500.10	172.63	6500.10	173.58	6500.10	179.09	6500.10	183.00
6600	TRUE	-39.90	6600.10	142.96	6600.10	168.05	6600.10	165.49	6600.10	172.51	6600.10	173.40	6600.10	178.77	6600.10	182.86
6700	TRUE	-39.65	6700.10	143.34	6700.10	167.05	6700.10	166.24	6700.10	172.80	6700.10	173.69	6700.10	179.04	6700.10	182.99
6800	TRUE	-39.92	6800.10	143.80	6800.10	169.88	6800.10	166.35	6800.10	173.47	6800.10	174.62	6800.10	180.32	6800.10	183.72
6900	TRUE	-40.30	6900.10	144.62	6900.10	170.73	6900.10	167.25	6900.10	174.46	6900.10	175.54	6900.10	180.94	6900.10	184.92
7000	TRUE	-40.74	7000.11	145.00	7000.11	171.89	7000.11	168.99	7000.11	175.17	7000.11	176.31	7000.11	181.85	7000.11	185.74
7100	TRUE	-41.16	7100.11	144.84	7100.11	170.62	7100.11	168.38	7100.11	175.32	7100.11	176.43	7100.11	182.04	7100.11	186.00
7200	TRUE	-41.85	7200.11	145.07	7200.11	172.11	7200.11	167.88	7200.11	175.93	7200.11	177.02	7200.11	182.34	7200.11	186.91
7300	TRUE	-41.80	7300.11	145.41	7300.11	172.82	7300.11	169.22	7300.11	176.28	7300.11	177.52	7300.11	183.08	7300.11	187.20
7400	TRUE	-41.71	7400.11	146.39	7400.11	173.71	7400.11	170.58	7400.11	177.13	7400.11	178.33	7400.11	183.89	7400.11	188.10
7500	TRUE	-41.36	7500.11	146.84	7500.11	174.26	7500.11	170.60	7500.11	177.44	7500.11	178.51	7500.11	184.11	7500.11	188.20
7600	TRUE	-41.54	7600.11	147.46	7600.11	175.27	7600.11	171.81	7600.11	177.78	7600.11	179.15	7600.11	184.63	7600.11	189.00
7700	TRUE	-41.57	7700.12	147.38	7700.12	175.01	7700.12	171.76	7700.12	177.84	7700.12	179.16	7700.12	184.77	7700.12	188.95
7800	TRUE	-42.39	7800.12	152.33	7800.12	180.70	7800.12	176.94	7800.12	183.26	7800.12	184.58	7800.12	190.94	7800.12	194.71
7900	TRUE	-46.32	7900.12	160.84	7900.12	192.44	7900.12	187.58	7900.12	195.06	7900.12	196.74	7900.12	202.62	7900.12	207.16
8000	TRUE	-43.75	8000.12	147.36	8000.12	177.51	8000.12	173.75	8000.12	179.68	8000.12	180.98	8000.12	186.77	8000.12	191.11
8100	TRUE	-43.38	8100.12	147.02	8100.12	177.14	8100.12	173.85	8100.12	178.90	8100.12	180.50	8100.12	186.00	8100.12	190.40
8200	TRUE	-43.51	8200.12	146.91	8200.12	176.99	8200.12	173.73	8200.12	178.95	8200.12	180.33	8200.12	186.04	8200.12	190.41
8300	TRUE	-43.14	8300.13	147.37	8300.13	177.58	8300.13	174.19	8300.13	179.33	8300.13	180.66	8300.13	186.35	8300.13	190.51
8400	TRUE	-42.77	8400.13	148.56	8400.13	178.14	8400.13	174.64	8400.13	180.23	8400.13	181.35	8400.13	186.87	8400.13	191.33
8500	TRUE	-42.16	8500.13	149.82	8500.13	178.87	8500.13	175.12	8500.13	180.78	8500.13	182.02	8500.13	187.74	8500.13	191.98
8600	TRUE	-42.14	8600.13	149.78	8600.13	179.05	8600.13	174.64	8600.13	180.98	8600.13	182.27	8600.13	187.84	8600.13	191.93
8700	TRUE	-42.16	8700.13	150.35	8700.13	178.84	8700.13	175.30	8700.13	181.63	8700.13	182.59	8700.13	188.46	8700.13	192.51
8800	TRUE	-42.98	8800.13	150.08	8800.13	179.38	8800.13	175.62	8800.13	181.90	8800.13	183.22	8800.13	188.87	8800.13	193.06
8900	TRUE	-42.58	8900.13	151.30	8900.13	180.36	8900.13	176.56	8900.13	182.66	8900.13	183.97	8900.13	189.75	8900.13	193.88
9000	TRUE	-43.76	9000.14	150.36	9000.14	180.49	9000.14	176.46	9000.14	182.91	9000.14	184.12	9000.14	190.14	9000.14	194.12
9100	TRUE	-44.19	9100.14	151.00	9100.14	181.23	9100.14	177.46	9100.14	183.93	9100.14	185.15	9100.14	190.86	9100.14	195.19
9200	TRUE	-44.42	9200.14	151.04	9200.14	181.29	9200.14	177.46	9200.14	183.96	9200.14	185.39	9200.14	191.24	9200.14	195.47
9300	TRUE	-44.53	9300.14	151.41	9300.14	181.64	9300.14	177.82	9300.14	184.71	9300.14	185.97	9300.14	191.80	9300.14	195.94
9400	TRUE	-44.74	9400.14	151.69	9400.14	181.90	9400.14	178.13	9400.14	185.00	9400.14	186.29	9400.14	192.14	9400.14	196.43
9500	TRUE	-44.99	9500.14	152.31	9500.14	182.52	9500.14	178.81	9500.14	185.74	9500.14	187.06	9500.14	192.86	9500.14	197.30
9600	TRUE	-45.02	9600.15	152.34	9600.15	182.65	9600.15	178.83	9600.15	185.89	9600.15	187.20	9600.15	193.00	9600.15	197.36
9700	TRUE	-45.01	9700.15	152.42	9700.15	182.64	9700.15	178.84	9700.15	185.82	9700.15	187.04	9700.15	192.98	9700.15	197.42
9800	TRUE	-44.89	9800.15	152.80	9800.15	182.87	9800.15	179.05	9800.15	186.02	9800.15	187.37	9800.15	193.19	9800.15	197.68
9900	TRUE	-44.75	9900.15	153.40	9900.15	183.35	9900.15	179.56	9900.15	186.62	9900.15	187.89	9900.15	193.74	9900.15	198.15
10000	TRUE	-44.90	10000.15	154.42	10000.15	184.41	10000.15	180.56	10000.15	187.60	10000.15	188.95	10000.15	194.89	10000.15	199.32
10100	TRUE	-48.70	10100.15	167.92	10100.15	200.74	10100.15	196.45	10100.15	204.01	10100.15	205.62	10100.15	211.89	10100.15	216.62
10200	TRUE	-46.45	10200.15	157.99	10200.15	188.99	10200.15	185.07	10200.15	192.21	10200.15	193.66	10200.15	199.65	10200.15	204.44

Table J.1: Victaulic 005 and Washer Connected Black Steel Pipe Peak Signal Frequency and Magnitude. “Bandwidth” column indicates whether the Bandwidth Condition is satisfied

		Distance	0ft_vol100		10ft_vol100		20ft_vol100		22.75ft_vol100		30ft_vol100		40ft_vol100		42.5ft_vol100	
		Values	Rx_max_freq	Max_rx_mag	Rx_max_freq	Max_rx_mag	Rx_max_freq	Max_rx_mag	Rx_max_freq	Max_rx_mag	Rx_max_freq	Max_rx_mag	Rx_max_freq	Max_rx_mag	Rx_max_freq	Max_rx_mag
Tx_freq	Bandwidth	Attenuation/ft														
10300	TRUE	-44.95	10300.16	153.69	10300.16	183.82	10300.16	179.98	10300.16	187.03	10300.16	188.26	10300.16	194.24	10300.16	198.63
10400	TRUE	-45.09	10400.16	153.97	10400.16	184.35	10400.16	180.41	10400.16	187.29	10400.16	188.70	10400.16	194.50	10400.16	199.06
10500	TRUE	-45.21	10500.16	153.64	10500.16	184.02	10500.16	180.20	10500.16	187.11	10500.16	188.49	10500.16	194.39	10500.16	198.84
10600	TRUE	-45.16	10600.16	153.99	10600.16	184.36	10600.16	180.56	10600.16	187.38	10600.16	188.74	10600.16	194.71	10600.16	199.15
10700	TRUE	-45.25	10700.16	153.71	10700.16	184.20	10700.16	180.25	10700.16	187.12	10700.16	188.54	10700.16	194.48	10700.16	198.96
10800	TRUE	-45.14	10800.16	153.83	10800.16	184.21	10800.16	180.36	10800.16	187.15	10800.16	188.53	10800.16	194.65	10800.16	198.97
10900	TRUE	-45.12	10900.16	153.83	10900.16	184.14	10900.16	180.36	10900.16	187.18	10900.16	188.52	10900.16	194.44	10900.16	198.95
11000	TRUE	-45.24	11000.17	154.14	11000.17	184.56	11000.17	180.71	11000.17	187.53	11000.17	188.91	11000.17	194.87	11000.17	199.38
11100	TRUE	-45.27	11100.17	154.07	11100.17	184.55	11100.17	180.55	11100.17	187.33	11100.17	188.71	11100.17	194.64	11100.17	199.34
11200	TRUE	-45.02	11200.17	153.88	11200.17	184.05	11200.17	180.24	11200.17	187.13	11200.17	188.42	11200.17	194.36	11200.17	198.91
11300	TRUE	-44.91	11300.17	153.91	11300.17	184.16	11300.17	180.31	11300.17	186.88	11300.17	188.48	11300.17	194.39	11300.17	198.83
11400	TRUE	-44.92	11400.17	154.28	11400.17	184.46	11400.17	180.57	11400.17	187.44	11400.17	188.83	11400.17	194.76	11400.17	199.20
11500	TRUE	-44.97	11500.17	154.45	11500.17	184.63	11500.17	180.87	11500.17	187.62	11500.17	188.98	11500.17	194.89	11500.17	199.42
11600	TRUE	-44.86	11600.18	154.17	11600.18	184.29	11600.18	180.44	11600.18	187.30	11600.18	188.65	11600.18	194.53	11600.18	199.03
11700	TRUE	-44.91	11700.18	154.31	11700.18	184.50	11700.18	180.61	11700.18	187.46	11700.18	188.75	11700.18	194.82	11700.18	199.21
11800	TRUE	-44.83	11800.18	154.36	11800.18	184.45	11800.18	180.67	11800.18	187.52	11800.18	188.79	11800.18	194.76	11800.18	199.19
11900	TRUE	-45.10	11900.18	154.63	11900.18	184.85	11900.18	181.09	11900.18	188.05	11900.18	189.20	11900.18	195.15	11900.18	199.73
12000	TRUE	-44.89	12000.18	154.70	12000.18	184.85	12000.18	181.01	12000.18	187.89	12000.18	189.18	12000.18	195.08	12000.18	199.59
12100	TRUE	-45.08	12100.18	154.92	12100.18	185.18	12100.18	181.41	12100.18	188.20	12100.18	189.45	12100.18	195.51	12100.18	200.01
12200	TRUE	-45.23	12200.18	154.72	12200.18	185.09	12200.18	181.32	12200.18	188.09	12200.18	189.44	12200.18	195.35	12200.18	199.95
12300	TRUE	-46.39	12300.19	159.50	12300.19	190.65	12300.19	186.71	12300.19	193.78	12300.19	195.11	12300.19	201.20	12300.19	205.90
12400	TRUE	-48.92	12400.19	169.76	12400.19	202.80	12400.19	198.67	12400.19	205.87	12400.19	207.44	12400.19	213.84	12400.19	218.68
12500	TRUE	-45.53	12500.19	156.15	12500.19	186.68	12500.19	182.86	12500.19	189.75	12500.19	191.00	12500.19	197.07	12500.19	201.69
12600	TRUE	-45.44	12600.19	155.49	12600.19	186.01	12600.19	182.26	12600.19	189.11	12600.19	190.39	12600.19	196.40	12600.19	200.93
12700	TRUE	-45.42	12700.19	155.42	12700.19	185.98	12700.19	182.03	12700.19	188.97	12700.19	190.32	12700.19	196.24	12700.19	200.84
12800	TRUE	-45.43	12800.19	155.52	12800.19	186.11	12800.19	182.21	12800.19	189.14	12800.19	190.45	12800.19	196.40	12800.19	200.96
12900	TRUE	-45.56	12900.20	155.95	12900.20	186.59	12900.20	182.67	12900.20	189.63	12900.20	190.97	12900.20	196.87	12900.20	201.51
13000	TRUE	-45.61	13000.20	156.16	13000.20	186.95	13000.20	182.97	13000.20	189.88	13000.20	191.16	13000.20	197.20	13000.20	201.77
13100	TRUE	-45.58	13100.20	155.94	13100.20	186.63	13100.20	182.72	13100.20	189.61	13100.20	191.00	13100.20	196.89	13100.20	201.52
13200	TRUE	-45.54	13200.20	156.10	13200.20	186.88	13200.20	182.89	13200.20	189.77	13200.20	191.11	13200.20	197.00	13200.20	201.64
13300	TRUE	-45.66	13300.20	156.03	13300.20	186.86	13300.20	183.01	13300.20	189.74	13300.20	191.13	13300.20	197.09	13300.20	201.69
13400	TRUE	-45.66	13400.20	156.34	13400.20	187.17	13400.20	183.32	13400.20	190.16	13400.20	191.49	13400.20	197.42	13400.20	202.00
13500	TRUE	-45.78	13500.20	156.19	13500.20	187.12	13500.20	183.17	13500.20	189.81	13500.20	191.29	13500.20	197.14	13500.20	201.97
13600	TRUE	-45.77	13600.21	156.34	13600.21	187.27	13600.21	183.31	13600.21	190.15	13600.21	191.48	13600.21	197.54	13600.21	202.11
13700	TRUE	-45.69	13700.21	156.05	13700.21	186.91	13700.21	182.95	13700.21	189.87	13700.21	191.24	13700.21	197.17	13700.21	201.74
13800	TRUE	-45.70	13800.21	156.04	13800.21	186.96	13800.21	183.02	13800.21	189.89	13800.21	191.37	13800.21	197.19	13800.21	201.74
13900	TRUE	-45.61	13900.21	155.98	13900.21	186.83	13900.21	182.95	13900.21	189.74	13900.21	191.09	13900.21	197.04	13900.21	201.59
14000	TRUE	-45.90	14000.21	156.07	14000.21	187.11	14000.21	183.25	14000.21	190.03	14000.21	191.44	14000.21	197.36	14000.21	201.97
14100	TRUE	-45.77	14100.21	155.85	14100.21	186.83	14100.21	182.98	14100.21	189.65	14100.21	191.13	14100.21	197.08	14100.21	201.62
14200	TRUE	-45.50	14200.21	155.75	14200.21	186.42	14200.21	182.58	14200.21	189.26	14200.21	190.81	14200.21	196.65	14200.21	201.25
14300	TRUE	-45.54	14300.22	155.63	14300.22	186.45	14300.22	182.49	14300.22	189.18	14300.22	190.64	14300.22	196.43	14300.22	201.18
14400	TRUE	-45.66	14400.22	155.77	14400.22	186.58	14400.22	182.76	14400.22	189.42	14400.22	190.93	14400.22	196.91	14400.22	201.43
14500	TRUE	-45.63	14500.22	155.92	14500.22	186.66	14500.22	182.88	14500.22	189.47	14500.22	191.00	14500.22	196.97	14500.22	201.55
14600	TRUE	-45.18	14600.22	155.87	14600.22	186.27	14600.22	182.48	14600.22	189.23	14600.22	190.55	14600.22	196.57	14600.22	201.05
14700	TRUE	-45.15	14700.22	155.92	14700.22	186.26	14700.22	182.47	14700.22	189.09	14700.22	190.66	14700.22	196.56	14700.22	201.07
14800	TRUE	-45.20	14800.22	155.85	14800.22	186.19	14800.22	182.37	14800.22	189.17	14800.22	190.55	14800.22	196.48	14800.22	201.05
14900	TRUE	-45.31	14900.23	156.05	14900.23	186.52	14900.23	182.77	14900.23	189.44	14900.23	190.79	14900.23	196.78	14900.23	201.36
15000	TRUE	-45.18	15000.23	155.88	15000.23	186.40	15000.23	182.50	15000.23	189.30	15000.23	190.64	15000.23	196.53	15000.23	201.06
15100	TRUE	-45.54	15100.23	155.86	15100.23	186.69	15100.23	182.96	15100.23	189.40	15100.23	190.94	15100.23	196.78	15100.23	201.41
15200	TRUE	-45.42	15200.23	155.75	15200.23	186.38	15200.23	182.78	15200.23	189.45	15200.23	190.72	15200.23	196.61	15200.23	201.18
15300	TRUE	-46.60	15300.23	160.51	15300.23	191.99	15300.23	188.23	15300.23	194.97	15300.23	196.23	15300.23	202.39	15300.23	207.11
15400	TRUE	-48.79	15400.23	171.09	15400.23	204.08	15400.23	200.18	15400.23	207.11	15400.23	208.65	15400.23	215.00	15400.23	219.88
15500	TRUE	-45.34	15500.23	157.28	15500.23	187.97	15500.23	184.17	15500.23	190.85	15500.23	192.16	15500.23	198.03	15500.23	202.62
15600	TRUE	-44.94	15600.24	156.95	15600.24	187.30	15600.24	183.49	15600.24	190.09	15600.24	191.36	15600.24	197.38	15600.24	201.89
15700	TRUE	-44.65	15700.24	157.01	15700.24	187.08	15700.24	183.46	15700.24	190.03	15700.24	191.16	15700.24	197.13	15700.24	201.66
15800	TRUE	-44.28	15800.24	157.50	15800.24	187.27	15800.24	183.51	15800.24	190.17	15800.24	191.29	15800.24	197.27	15800.24	201.78
15900	TRUE	-44.51	15900.24	157.74	15900.24	187.67	15900.24	184.00	15900.24	190.60	15900.24	191.82	15900.24	197.77	15900.24	202.25
16000	TRUE	-44.93	16000.24	157.81	16000.24	187.96	16000.24	184.31	16000.24	191.08	16000.24	192.19	16000.24	198.17	16000.24	202.74
16100	TRUE	-44.85	16100.24	157.54	16100.24	187.71	16100.24	183.98	16100.24	190.66	16100.24	191.82	16100.24	197.86	16100.24	202.40
16200	TRUE	-44.94	16200.24	157.57	16200.24	187.82	16200.24	184.16	16200.24	190.90	16200.24	192.00	16200.24	197.99	16200.24	202.50
16300	TRUE	-45.00	16300.25	157.47	16300.25	187.82	16300.25	184.28	16300.25	190.87	16300.25	192.02	16300.25	198.07	16300.25	202.47
16400	TRUE	-44.90	16400.25	157.90	16400.25	188.25	16400.25	184.40	16400.25	191.23	16400.25	192.37	16400.25	198.37	16400.25	202.80
16500	TRUE	-44.77	16500.25	157.85	16500.25	187.83	16500.25	184.05	16500.25	190.98	16500.25	192.13	16500.25	198.14	16500.25	202.62
16600	TRUE	-44.58	16600.25	158.25	16600.25	188.00	16600.25	184.35	16600.25	191.20	16600.25	192.40	16600.25	198.37	16600.25	202.83
16700	TRUE	-44.50	16700.25	158.10	16700.25	187.61	16700.25	183.96	16700.25	190.87	16700.25	192.01	16700.25	197.97	16700.25	202.61
16800	TRUE	-44.46	16800.25	158.05	16800.25	187.70	16800.25	184.06	16800.25	190.85	16800.25	192.06	16800.25	197.82	16800.25	202.51
16900	TRUE	-44.46	16900.26	157.96	16900.26	187.56	16900.26	183.90	16900.26	190.67	16900.26	191.97	16900.26	197.84	16900.26	202.42
17000	TRUE	-44.54	17000.26	158.17	17000.26	187.80	17000.26	184.26	17000.26	190.95	17000.26	192.12	17000.26	198.15	17000.26	202.71
17100	TRUE	-44.74	17100.26	157.69	17100.26	187.37	17100.26	183.98	17100.26	190.63	17100.26	191.92	17100.26	197.85	17100.26	202.44
17200	TRUE	-44.68	17200.26	157.21	17200.26	187.25	17200.26	183.69	17200.26	190.20	17200.26	191.50	17200.26	197.45	17200.26	201.89
17300	TRUE	-45.17	17300.26	156.62	17300.26	187.08	17300.26	183.42	17300.26	190.04	17300.26	191.34	17300.26	197.36	17300.26	201.79
17400	TRUE	-45.93	17400.26	156.06	17400.26	187.36	17400.26	183.82	17400.26	190.17	17400.26	191.52	17400.26	197.43	17400.26	201.99
17500	TRUE	-46.20	17500.26	155.84	17500.26	187.40	17500.26	183.76	17500.26	190.28	17500.26	191.61	17500.26	197.48	17500.26	202.04
17600	TRUE	-45.93	17600.27	155.50	17600.27	187.17	17600.27	183.39	17600.27	189.72	17600.27	191.09	17600.27	196.93	17600.27	201.43
17700	TRUE	-45.78	17700.27	155.57	17700.27	187.05	17700.27	183.31	17700.27	189.89	17700.27	191.06	17700.27	197.03	17700.27	201.35
17800	TRUE	-45.76	17800.27	155.56	17800.27	186.87	17800.27	183.41	17800.27	189.71	17800.27	191.09	17800.27	196.90	17800.27	201.32
17900	TRUE	-45.64	17900.27	156.14	17900.27	187.36	17900.27	183.82	17900.27	190.11	17900.27	191.47	17900.27	197.25	17900.27	201.78
18000	TRUE	-45.41	18000.27	156.21	18000.27	187.26	18000.27	183.77	18000.27	190.03	18000.27	191.30	18000.27	197.20	18000.27	201.62
18100	TRUE	-45.40	18100.27	156.53	18100.27	187.61	18100.27	184.09	18100.27	190.31	18100.27	191.62	18100.27	197.52	18100.27	201.93
18200	TRUE	-45.43	18200.28	156.38	18200.28	187.51	18200.28	183.94	18200.28	189.96	18200.28	191.51	18200.28	197.25	18200.28	201.81
18300	TRUE	-45.02	18300.28	156.81	18300.28	187.53	18300.28	183.92	18300.28	190.15	18300.28	191.51	18300.28	197.32	18300.28	201.83
18400	TRUE	-44.97	18400.28	157.11	18400.28	187.85	18400.28	184.36	18400.28	190.24	18400.28	191.77	18400.28	197.55	18400.28	202.09
18500	TRUE	-44.57	18500.28	157.98	18500.28	188.34	18500.28	184.79	18500.28	190.81	18500.28	192.36	18500.28	198.15	18500.28	202.55
18600	TRUE	-44.94	18600.28	157.86	18600.28	188.34	18600.28	184.77	18600.28	190.92	18600.28	192.39	18600.28	198.11	18600.28	202.80
18700	TRUE	-44.52	18700.28	157.44	18700.28	188.06	18700.28	184.57	18700.28	190.78	18700.28	192.13	18700.28	197.85	18700.28	201.96
18800	TRUE	-44.57	18800.28	157.40	18800.28	188.02	18800.28	184.61	18800.28	190.57	18800.28	192.07	18800.28	197.84	18800.28	201.96
18900	TRUE	-44.53	18900.29	157.63	18900.29	188.20	18900.29	184.74	18900.29	190.74	18900.29	192.31	18900.29	198.09	18900.29	202.16
19000	TRUE	-44.44	19000.29	157.64	19000.29	188.09	19000.29	184.59	19000.29	190.67	19000.29	192.21	19000.29	197.95	19000.29	202.09
19100	TRUE	-44.03	19100.29	157.31	19100.29	187.28	19100.29	183.83	19100.29	189.96	19100.29	191.48	19100.29	197.17	19100.29	201.34
19200	TRUE	-43.18	19200.29	157.44	19200.29	186.73	19200.29	183.26	19200.29	189.76	19200.29	191.08	19200.29	196.54	19200.29	200.61
19300	TRUE	-43.29	19300.29	156.53	19300.29	185.77	19300.29	182.48	19300.29	188.79	19300.29	190.10	19300.29	195.79	19300.29	199.82
19400	TRUE	-43.40	19400.29	155.49	19400.29	184.97	19400.29	181.58	19400.29	187.86	19400.29	189.21	19400.29	194.85	19400.29	198.89
19500	TRUE	-43.12	19500.29	153.76	19500.29	183.07	19500.29	179.71	19500.29	186.13	19500.29	187.48	19500.29	192.92	19500.29	196.88
19600	TRUE	-43.37	19600.30	152.34	19600.30	181.61	19600.30	178.35	19600.30	184.46	19600.30	185.80	19600.30	191.30	19600.30	195.71
19700	TRUE	-42.83	19700.30	150.11	19700.30	178.99	19700.30	175.77	19700.30	181.82	19700.30	183.19	19700.30	188.59	19700.30	192.94
19800	TRUE	-42.17	19800.30	147.80	19800.30	176.16	19800.30	172.91	19800.30	178.98	19800.30	180.34	19800.30	185.65	19800.30	189.97
19900	TRUE	-41.47	19900.30	144.81	19900.30	172.68	19900.30	169.57	19900.30	175.51	19900.30	176.74	19900.30	182.01	19900.30	186.29
20000	TRUE	-40.63	20000.30	141.63	20000.30	168.96	20000.30	166.00	20000.30	171.64	20000.30	173.01	20000.30	178.18	20000.30	182.26

Table J.1: Victaulic 005 and Washer Connected Black Steel Pipe Peak Signal Frequency and Magnitude. "Bandwidth" column indicates whether the Bandwidth Condition is satisfied (cont.)

Appendix K: BLACK STEEL PIPE OUTDOOR LABORATORY SETTING WITH VICTAULIC 75 COUPLINGS AND WASHER

		Distance	0ft_vol100		10ft_vol100		20ft_vol100		22.75ft_vol100		30ft_vol100		40ft_vol100		42.5ft_vol100	
		Values	Rx_max_freq	Max_rx_mag	Rx_max_freq	Max_rx_mag	Rx_max_freq	Max_rx_mag	Rx_max_freq	Max_rx_mag	Rx_max_freq	Max_rx_mag	Rx_max_freq	Max_rx_mag	Rx_max_freq	Max_rx_mag
Tx_freq	Bandwidth?	Attenuation/ft														
100	FALSE	NA	3.33	9.68	2.00	9.71	1.33	13.20	3.33	9.84	3.33	12.02	5.67	10.55	2407.70	10.94
200	FALSE	NA	1.67	12.07	200.00	11.72	200.00	13.35	200.00	13.87	200.00	12.91	200.00	12.57	200.00	13.34
300	TRUE	-2.19	300.00	17.52	300.00	18.57	300.00	18.49	300.00	20.07	300.00	18.89	300.00	20.62	300.00	19.72
400	TRUE	-2.69	400.01	23.61	400.01	24.54	400.01	24.55	400.01	25.41	400.01	25.81	400.01	25.32	400.01	26.30
500	TRUE	-1.84	500.01	26.79	500.01	27.78	500.01	29.04	500.01	29.00	500.01	29.24	500.01	28.82	500.01	28.63
600	TRUE	-1.98	600.01	33.82	600.01	34.86	600.01	35.29	600.01	36.40	600.01	36.39	600.01	36.00	600.01	35.80
700	TRUE	-3.29	700.01	38.32	700.01	38.49	700.01	39.92	700.01	39.79	700.01	41.10	700.01	40.75	700.01	41.61
800	TRUE	-3.08	800.01	42.88	800.01	42.94	800.01	45.67	800.01	45.25	800.01	46.27	800.01	45.22	800.01	45.95
900	TRUE	-3.08	900.01	49.53	900.01	49.53	900.01	51.57	900.01	52.04	900.01	52.65	900.01	53.05	900.01	52.61
1000	TRUE	-3.46	1000.02	51.37	1000.02	52.52	1000.02	53.56	1000.02	54.24	1000.02	55.65	1000.02	55.34	1000.02	54.83
1100	TRUE	-5.27	1100.02	61.26	1100.02	61.95	1100.02	64.31	1100.02	65.54	1100.02	65.79	1100.02	65.72	1100.02	66.53
1200	TRUE	-4.07	1200.02	57.96	1200.02	57.93	1200.02	60.20	1200.02	60.85	1200.02	62.36	1200.02	61.48	1200.02	62.03
1300	TRUE	-4.47	1300.02	61.91	1300.02	62.55	1300.02	64.04	1300.02	65.35	1300.02	66.33	1300.02	65.84	1300.02	66.38
1400	TRUE	-5.19	1400.02	66.79	1400.02	67.10	1400.02	68.93	1400.02	70.39	1400.02	71.72	1400.02	71.44	1400.02	71.98
1500	TRUE	-5.22	1500.02	77.82	1500.02	76.88	1500.02	79.82	1500.02	80.47	1500.02	83.28	1500.02	80.51	1500.02	83.03
1600	TRUE	-4.09	1600.02	73.68	1600.02	73.71	1600.02	76.50	1600.02	77.59	1600.02	79.95	1600.02	79.07	1600.02	77.77
1700	TRUE	-3.70	1700.03	75.97	1700.03	76.34	1700.03	78.75	1700.03	79.94	1700.03	80.37	1700.03	81.73	1700.03	79.68
1800	TRUE	-6.04	1800.03	81.15	1800.03	82.18	1800.03	84.06	1800.03	85.32	1800.03	86.75	1800.03	87.60	1800.03	87.19
1900	TRUE	-7.38	1900.03	89.27	1900.03	90.62	1900.03	92.95	1900.03	94.02	1900.03	96.51	1900.03	95.66	1900.03	96.65
2000	TRUE	-6.53	2000.03	85.05	2000.03	85.52	2000.03	88.45	2000.03	89.53	2000.03	91.47	2000.03	91.19	2000.03	91.58
2100	TRUE	-7.14	2100.03	87.07	2100.03	88.00	2100.03	91.02	2100.03	92.47	2100.03	93.69	2100.03	93.92	2100.03	94.21
2200	TRUE	-8.72	2200.03	89.59	2200.03	90.47	2200.03	93.00	2200.03	93.82	2200.03	96.94	2200.03	97.02	2200.03	98.31
2300	TRUE	-7.94	2300.03	92.27	2300.03	93.56	2300.03	96.51	2300.03	98.64	2300.03	99.66	2300.03	99.88	2300.03	100.22
2400	TRUE	-8.50	2400.04	95.06	2400.04	96.55	2400.04	99.29	2400.04	100.76	2400.04	103.38	2400.04	103.11	2400.04	103.56
2500	TRUE	-8.48	2500.04	98.33	2500.04	99.20	2500.04	102.80	2500.04	103.81	2500.04	106.33	2500.04	106.38	2500.04	106.81
2600	TRUE	-9.10	2600.04	109.55	2600.04	110.48	2600.04	114.43	2600.04	116.79	2600.04	118.32	2600.04	118.83	2600.04	118.65
2700	TRUE	-9.30	2700.04	105.68	2700.04	105.66	2700.04	109.87	2700.04	111.94	2700.04	114.31	2700.04	114.51	2700.04	114.97
2800	TRUE	-8.90	2800.04	104.65	2800.04	105.44	2800.04	108.88	2800.04	111.02	2800.04	113.44	2800.04	113.20	2800.04	113.55
2900	TRUE	-9.49	2900.04	106.71	2900.04	108.59	2900.04	112.00	2900.04	112.84	2900.04	115.71	2900.04	115.78	2900.04	116.19
3000	TRUE	-9.68	3000.05	108.98	3000.05	109.71	3000.05	112.92	3000.05	115.05	3000.05	118.06	3000.05	117.74	3000.05	118.66
3100	TRUE	-8.39	3100.05	112.18	3100.05	112.02	3100.05	116.21	3100.05	117.34	3100.05	120.13	3100.05	118.96	3100.05	120.57
3200	TRUE	-8.06	3200.05	114.48	3200.05	113.82	3200.05	116.39	3200.05	118.89	3200.05	121.87	3200.05	121.94	3200.05	122.54
3300	TRUE	-10.48	3300.05	118.09	3300.05	118.69	3300.05	122.49	3300.05	124.16	3300.05	127.22	3300.05	127.94	3300.05	128.57
3400	TRUE	-11.13	3400.05	126.87	3400.05	128.27	3400.05	131.99	3400.05	133.86	3400.05	137.42	3400.05	137.86	3400.05	138.00
3500	TRUE	-10.12	3500.05	118.59	3500.05	118.24	3500.05	122.57	3500.05	124.49	3500.05	128.23	3500.05	128.05	3500.05	128.71
3600	TRUE	-10.71	3600.05	119.36	3600.05	120.06	3600.05	123.99	3600.05	125.68	3600.05	128.96	3600.05	129.09	3600.05	130.07
3700	TRUE	-10.29	3700.06	120.50	3700.06	121.46	3700.06	125.05	3700.06	126.94	3700.06	130.29	3700.06	130.39	3700.06	130.80
3800	TRUE	-10.73	3800.06	121.85	3800.06	122.82	3800.06	126.39	3800.06	128.36	3800.06	131.57	3800.06	132.08	3800.06	132.58
3900	TRUE	-10.67	3900.06	123.26	3900.06	123.99	3900.06	128.02	3900.06	129.92	3900.06	133.43	3900.06	133.48	3900.06	133.93
4000	TRUE	-10.78	4000.06	125.14	4000.06	125.89	4000.06	129.61	4000.06	131.54	4000.06	135.15	4000.06	135.08	4000.06	135.92
4100	TRUE	-12.03	4100.06	137.05	4100.06	138.13	4100.06	142.31	4100.06	144.39	4100.06	148.22	4100.06	148.23	4100.06	149.08
4200	TRUE	-11.52	4200.06	129.98	4200.06	130.85	4200.06	134.78	4200.06	136.90	4200.06	140.71	4200.06	141.08	4200.06	141.50
4300	TRUE	-11.11	4300.07	127.52	4300.07	128.10	4300.07	132.22	4300.07	134.20	4300.07	137.88	4300.07	138.07	4300.07	138.63
4400	TRUE	-11.36	4400.07	128.57	4400.07	129.23	4400.07	133.33	4400.07	135.37	4400.07	139.11	4400.07	139.45	4400.07	139.93
4500	TRUE	-11.54	4500.07	129.27	4500.07	130.17	4500.07	134.08	4500.07	136.22	4500.07	139.99	4500.07	140.31	4500.07	140.80
4600	TRUE	-11.31	4600.07	130.43	4600.07	131.10	4600.07	135.01	4600.07	137.19	4600.07	140.95	4600.07	141.38	4600.07	141.74
4700	TRUE	-11.76	4700.07	130.75	4700.07	131.58	4700.07	135.85	4700.07	137.68	4700.07	141.69	4700.07	142.03	4700.07	142.52
4800	TRUE	-11.43	4800.07	131.67	4800.07	132.71	4800.07	136.63	4800.07	138.59	4800.07	142.61	4800.07	143.18	4800.07	143.10
4900	TRUE	-11.67	4900.07	132.74	4900.07	133.38	4900.07	137.42	4900.07	139.54	4900.07	143.49	4900.07	143.86	4900.07	144.41
5000	TRUE	-11.83	5000.08	133.75	5000.08	134.09	5000.08	138.44	5000.08	140.72	5000.08	144.74	5000.08	145.03	5000.08	145.58
5100	TRUE	-11.89	5100.08	134.59	5100.08	135.27	5100.08	139.09	5100.08	141.38	5100.08	145.47	5100.08	145.83	5100.08	146.48
5200	TRUE	-12.67	5200.08	142.93	5200.08	143.94	5200.08	148.25	5200.08	149.89	5200.08	154.65	5200.08	155.06	5200.08	155.60
5300	TRUE	-12.39	5300.08	144.03	5300.08	144.99	5300.08	148.87	5300.08	150.79	5300.08	155.48	5300.08	156.01	5300.08	156.42
5400	TRUE	-12.04	5400.08	136.70	5400.08	137.28	5400.08	141.42	5400.08	143.79	5400.08	147.89	5400.08	148.26	5400.08	148.74
5500	TRUE	-12.01	5500.08	137.59	5500.08	138.03	5500.08	142.12	5500.08	144.30	5500.08	148.25	5500.08	149.11	5500.08	149.60
5600	TRUE	-11.80	5600.08	138.23	5600.08	138.27	5600.08	142.39	5600.08	144.64	5600.08	149.03	5600.08	149.70	5600.08	150.04
5700	TRUE	-11.42	5700.09	139.32	5700.09	139.42	5700.09	143.47	5700.09	145.48	5700.09	149.85	5700.09	150.15	5700.09	150.74
5800	TRUE	-12.85	5800.09	138.92	5800.09	140.14	5800.09	144.21	5800.09	146.34	5800.09	150.60	5800.09	151.19	5800.09	151.77
5900	TRUE	-14.51	5900.09	138.68	5900.09	141.13	5900.09	145.88	5900.09	147.45	5900.09	151.70	5900.09	152.41	5900.09	153.19
6000	TRUE	-13.46	6000.09	140.30	6000.09	141.80	6000.09	145.90	6000.09	148.04	6000.09	152.36	6000.09	153.16	6000.09	153.76
6100	TRUE	-13.41	6100.09	141.22	6100.09	142.49	6100.09	146.56	6100.09	148.95	6100.09	153.41	6100.09	153.92	6100.09	154.64
6200	TRUE	-13.53	6200.09	141.60	6200.09	142.95	6200.09	147.05	6200.09	149.40	6200.09	153.90	6200.09	154.49	6200.09	155.14
6300	TRUE	-13.87	6300.10	146.41	6300.10	147.40	6300.10	151.59	6300.10	154.72	6300.10	159.02	6300.10	159.55	6300.10	160.28
6400	TRUE	-14.79	6400.10	156.15	6400.10	157.64	6400.10	161.97	6400.10	164.96	6400.10	169.58	6400.10	170.14	6400.10	170.93
6500	TRUE	-13.51	6500.10	144.35	6500.10	145.39	6500.10	149.73	6500.10	152.24	6500.10	156.50	6500.10	157.13	6500.10	157.86
6600	TRUE	-13.69	6600.10	144.10	6600.10	144.91	6600.10	149.19	6600.10	151.90	6600.10	156.46	6600.10	156.80	6600.10	157.80
6700	TRUE	-13.71	6700.10	144.23	6700.10	145.51	6700.10	149.48	6700.10	152.17	6700.10	156.68	6700.10	157.42	6700.10	157.94
6800	TRUE	-14.35	6800.10	144.18	6800.10	146.10	6800.10	150.38	6800.10	152.44	6800.10	157.08	6800.10	157.91	6800.10	158.53
6900	TRUE	-14.05	6900.10	145.08	6900.10	146.52	6900.10	150.17	6900.10	153.09	6900.10	157.77	6900.10	158.63	6900.10	159.13
7000	TRUE	-13.70	7000.11	145.77	7000.11	146.73	7000.11	152.45	7000.11	153.71	7000.11	158.06	7000.11	158.77	7000.11	159.46
7100	TRUE	-13.48	7100.11	146.11	7100.11	147.14	7100.11	150.38	7100.11	153.71	7100.11	158.40	7100.11	158.99	7100.11	159.59
7200	TRUE	-13.69	7200.11	146.36	7200.11	147.12	7200.11	152.08	7200.11	154.27	7200.11	158.67	7200.11	159.12	7200.11	160.06
7300	TRUE	-14.31	7300.11	146.16	7300.11	147.66	7300.11	151.54	7300.11	154.43	7300.11	158.95	7300.11	159.69	7300.11	160.47
7400	TRUE	-15.71	7400.11	145.24	7400.11	146.60	7400.11	151.75	7400.11	155.05	7400.11	159.72	7400.11	161.06	7400.11	160.95
7500	TRUE	-15.77	7500.11	145.34	7500.11	148.04	7500.11	152.76	7500.11	154.98	7500.11	159.66	7500.11	160.60	7500.11	161.11
7600	TRUE	-14.96	7600.11	146.53	7600.11	149.74	7600.11	152.81	7600.11	155.33	7600.11	160.25	7600.11	160.50	7600.11	161.49
7700	TRUE	-14.54	7700.12	147.00	7700.12	149.25	7700.12	152.64	7700.12	155.45	7700.12	160.23	7700.12	160.75	7700.12	161.54
7800	TRUE	-14.72	7800.12	151.85	7800.12	153.54	7800.12	157.56	7800.12	160.16	7800.12	165.11	7800.12	165.80	7800.12	166.58
7900	TRUE	-15.63	7900.12	161.49	7900.12	162.01	7900.12	167.67	7900.12	170.32	7900.12	175.55	7900.12	176.39	7900.12	177.12
8000	TRUE	-14.62	8000.12	148.59	8000.12	149.64	8000.12	154.34	8000.12	157.11	8000.12	161.74	8000.12	162.45	8000.12	163.21
8100	TRUE	-14.65	8100.12	148.00	8100.12	149.87	8100.12	153.52	8100.12	156.34	8100.12	161.29	8100.12	161.97	8100.12	162.65
8200	TRUE	-14.48	8200.12	148.27	8200.12	149.49	8200.12	153.69	8200.12	156.22	8200.12	161.32	8200.12	161.82	8200.12	162.75
8300	TRUE	-14.45	8300.13	148.68	8300.13	149.89	8300.13	154.08	8300.13	156.74	8300.13	161.63	8300.13	162.20	8300.13	163.13
8400	TRUE	-14.26	8400.13	149.61	8400.13	150.28	8400.13	154.50	8400.13	157.15	8400.13	162.19	8400.13	162.96	8400.13	163.87
8500	TRUE	-14.20	8500.13	150.03	8500.13	150.50	8500.13	155.21	8500.13	157.79	8500.13	162.71	8500.13	163.37	8500.13	164.22
8600	TRUE	-14.05	8600.13	150.08	8600.13	150.81	8600.13	155.05	8600.13	157.78	8600.13	162.45	8600.13	163.27	8600.13	164.13
8700	TRUE	-14.40	8700.13	150.09	8700.13	151.05	8700.13	155.30	8700.13	158.04	8700.13	162.84	8700.13	163.67	8700.13	164.49
8800	TRUE	-15.10	8800.13	149.72	8800.13	151.33	8800.13	155.61	8800.13	158.47	8800.13	163.15	8800.13	163.90	8800.13	164.82
8900	TRUE	-16.71	8900.13	148.85	8900.13	151.62	8900.13	156.25	8900.13	158.86	8900.13	163.95	8900.13	164.70	8900.13	165.56
9000	TRUE	-16.18	9000.14	149.42	9000.14	152.03	9000.14	156.34	9000.14	159.21	9000.14	163.94	9000.14	164.53	9000.14	165.60
9100	TRUE	-17.30	9100.14	148.99	9100.14	152.34	9100.14	157.08	9100.14	159.57	9100.14	164.63	9100.14	165.43	9100.14	166.29
9200	TRUE	-18.02	9200.14	148.38	9200.14	152.82	9200.14	157.07	9200.14	159.93	9200.14	164.78	9200.14	165.54	9200.14	166.41
9300	TRUE	-16.66	9300.14	150.14	9300.14	153.15	9300.14	157.38	9300.14	160.22	9300.14	165.21	9300.14	166.04	9300.14	166.80
9400	TRUE	-16.09	9400.14	151.05	9400.14	153.55	9400.14	157.82	9400.14	160.54	9400.14	165.52	9400.14	166.29	9400.14	167.13
9500	TRUE	-15.22	9500.14	152.56	9500.14	154.13	9500.14	158.46	9500.14	161.21	9500.14	166.30	9500.14	166.96	9500.14	167.78
9600	TRUE	-15.02	9600.15	152.88	9600.15	154.37	9600.15	158.60	9600.15	161.47	9600.15	166.43	9600.15	167.21	9600.15	167.90
9700	TRUE	-14.94	9700.15	153.04	9700.15	154.25	9700.15	158.75	9700.15	161.50	9700.15	166.52	9700.15	167.24	9700.15	167.98
9800	TRUE	-15.05	9800.15	153.17	9800.15	154.51	9800.15	158.98	9800.15	161.71	9800.15	166.79	9800.15	167.53	9800.15	168.22
9900	TRUE	-15.22	9900.15	153.47	9900.15	155.01	9900.15	159.22	9900.15	162.34	9900.15	167.28	9900.15	168.08	9900.15	168.69
10000	TRUE	-15.24	10000.15	154.43	10000.15	155.87	10000.15	160.45	10000.15	163.22	10000.15	168.24	10000.15	168.99	10000.15	169.68
10100	TRUE	-16.03	10100.15	168.45	10100.15	169.62	10100.15	174.52	10100.15	177.53	10100.15	183.06	10100.15	183.92	10100.15	184.48
10200	TRUE	-15.16	10200.15	158.80	10200.15	159.67	10200.15	164.48	10200.15	167.29	10200.15	172.43	10200.15	173.20	10200.15	173.96
10300	TRUE	-14.91	10300.16	154.27	10300.16	155.35	10300.16	159.87	10300.16	162.71	10300.16	167.72	10300.16	168.51	10300.16	169.18
10400	TRUE	-14.96	10400.16	154.66	10400.16	155.66	10400.16	160.28	10400.16	163.04	10400.16	167.93	10400.16	168.60	10400.16	169.62
10500	TRUE	-14.75	10500.16	154.77	10500.16	155.43	10500.16	160.04	10500.16	162.93	10500.16	167.91	10500.16	168.76	10500.16	169.51
10600	TRUE	-14.48	10600.16	155.50	10600.16	155.75	10600.16	160.43	10600.16	163.24	10600.16	168.23	10600.16	169.08	10600.16	169.98
10700	TRUE	-13.90	10700.16	156.13	10700.16	155.82	10700.16	160.24	10700.16	163.15	10700.16	168.09	10700.16	168.95	10700.16	170.03
10800	TRUE	-13.44	10800.16	156.96	10800.16	156.30	10800.16	160.70	10800.16	163.35	10800.16	168.29	10800.16	169.17	10800.16	170.40
10900	TRUE	-13.34	10900.16	157.22	10900.16	155.87	10900.16	160.12	10900.16	163.42	10900.16	168.42	10900.16	169.33	10900.16	170.56

Table K.1: Victaulic 75 and Washer Connected Black Steel Pipe Peak Signal Frequency and Magnitude. “Bandwidth” column indicates whether the Bandwidth Condition is satisfied

		Distance	0ft_vol100		10ft_vol100		20ft_vol100		22.75ft_vol100		30ft_vol100		40ft_vol100		42.5ft_vol100	
		Values	Rx_max_freq	Max_rx_mag	Rx_max_freq	Max_rx_mag	Rx_max_freq	Max_rx_mag	Rx_max_freq	Max_rx_mag	Rx_max_freq	Max_rx_mag	Rx_max_freq	Max_rx_mag	Rx_max_freq	Max_rx_mag
Tx_freq	Bandwidth?	Attenuation/ft														
11000	TRUE	-14.07	11000.17	157.00	11000.17	156.52	11000.17	161.01	11000.17	163.95	11000.17	168.95	11000.17	169.82	11000.17	171.07
11100	TRUE	-14.46	11100.17	156.60	11100.17	156.47	11100.17	161.00	11100.17	163.85	11100.17	168.91	11100.17	169.83	11100.17	171.06
11200	TRUE	-14.74	11200.17	156.11	11200.17	156.23	11200.17	160.77	11200.17	163.65	11200.17	168.72	11200.17	169.69	11200.17	170.86
11300	TRUE	-15.11	11300.17	155.80	11300.17	156.20	11300.17	160.86	11300.17	163.73	11300.17	168.73	11300.17	169.75	11300.17	170.91
11400	TRUE	-15.31	11400.17	155.90	11400.17	156.51	11400.17	161.04	11400.17	164.03	11400.17	169.05	11400.17	170.05	11400.17	171.21
11500	TRUE	-15.51	11500.17	155.85	11500.17	156.69	11500.17	161.24	11500.17	164.13	11500.17	169.21	11500.17	170.21	11500.17	171.37
11600	TRUE	-15.64	11600.18	155.41	11600.18	156.38	11600.18	160.92	11600.18	163.85	11600.18	168.89	11600.18	169.82	11600.18	171.05
11700	TRUE	-15.69	11700.18	155.45	11700.18	156.44	11700.18	160.99	11700.18	163.96	11700.18	168.92	11700.18	169.91	11700.18	171.14
11800	TRUE	-15.82	11800.18	155.39	11800.18	156.52	11800.18	160.91	11800.18	163.98	11800.18	168.93	11800.18	170.06	11800.18	171.20
11900	TRUE	-15.85	11900.18	155.77	11900.18	156.88	11900.18	161.17	11900.18	164.32	11900.18	169.32	11900.18	170.39	11900.18	171.61
12000	TRUE	-15.84	12000.18	155.67	12000.18	156.89	12000.18	161.27	12000.18	164.30	12000.18	169.31	12000.18	169.92	12000.18	171.52
12100	TRUE	-16.22	12100.18	155.92	12100.18	157.35	12100.18	161.63	12100.18	164.73	12100.18	169.80	12100.18	170.78	12100.18	172.14
12200	TRUE	-16.26	12200.18	155.91	12200.18	157.34	12200.18	161.78	12200.18	164.85	12200.18	169.77	12200.18	170.79	12200.18	172.17
12300	TRUE	-16.98	12300.19	160.54	12300.19	162.24	12300.19	166.67	12300.19	169.98	12300.19	174.96	12300.19	176.21	12300.19	177.53
12400	TRUE	-18.28	12400.19	170.75	12400.19	172.90	12400.19	177.50	12400.19	180.99	12400.19	186.47	12400.19	187.66	12400.19	189.03
12500	TRUE	-16.86	12500.19	157.42	12500.19	159.40	12500.19	163.70	12500.19	166.97	12500.19	171.88	12500.19	173.10	12500.19	174.29
12600	TRUE	-16.72	12600.19	157.20	12600.19	159.05	12600.19	163.38	12600.19	166.59	12600.19	171.72	12600.19	172.79	12600.19	173.92
12700	TRUE	-16.62	12700.19	157.35	12700.19	159.16	12700.19	163.52	12700.19	166.76	12700.19	171.84	12700.19	172.94	12700.19	173.98
12800	TRUE	-16.39	12800.19	157.72	12800.19	159.54	12800.19	163.82	12800.19	167.12	12800.19	172.24	12800.19	173.37	12800.19	174.11
12900	TRUE	-16.34	12900.20	158.39	12900.20	160.01	12900.20	164.41	12900.20	167.72	12900.20	172.80	12900.20	173.95	12900.20	174.73
13000	TRUE	-16.25	13000.20	158.84	13000.20	160.41	13000.20	164.81	13000.20	168.08	13000.20	173.24	13000.20	174.39	13000.20	175.10
13100	TRUE	-16.05	13100.20	158.85	13100.20	160.22	13100.20	164.63	13100.20	167.91	13100.20	173.04	13100.20	174.20	13100.20	174.89
13200	TRUE	-15.96	13200.20	159.07	13200.20	160.38	13200.20	164.79	13200.20	168.09	13200.20	173.27	13200.20	174.37	13200.20	175.04
13300	TRUE	-15.82	13300.20	159.21	13300.20	160.35	13300.20	164.77	13300.20	168.15	13300.20	173.25	13300.20	174.34	13300.20	175.03
13400	TRUE	-16.01	13400.20	159.41	13400.20	160.71	13400.20	165.19	13400.20	168.45	13400.20	173.54	13400.20	174.65	13400.20	175.42
13500	TRUE	-15.91	13500.20	159.27	13500.20	160.52	13500.20	164.99	13500.20	168.27	13500.20	173.39	13500.20	174.45	13500.20	175.17
13600	TRUE	-16.10	13600.21	159.44	13600.21	160.69	13600.21	165.18	13600.21	168.41	13600.21	173.56	13600.21	174.65	13600.21	175.53
13700	TRUE	-15.98	13700.21	159.23	13700.21	160.45	13700.21	164.87	13700.21	168.20	13700.21	173.23	13700.21	174.46	13700.21	175.22
13800	TRUE	-16.02	13800.21	159.27	13800.21	160.41	13800.21	164.85	13800.21	168.27	13800.21	173.36	13800.21	174.24	13800.21	175.29
13900	TRUE	-16.05	13900.21	159.09	13900.21	160.46	13900.21	164.80	13900.21	168.12	13900.21	173.28	13900.21	174.42	13900.21	175.14
14000	TRUE	-15.94	14000.21	159.55	14000.21	160.87	14000.21	165.18	14000.21	168.56	14000.21	173.56	14000.21	174.87	14000.21	175.49
14100	TRUE	-16.12	14100.21	159.03	14100.21	160.25	14100.21	164.91	14100.21	168.23	14100.21	173.34	14100.21	174.68	14100.21	175.15
14200	TRUE	-16.17	14200.21	158.59	14200.21	160.11	14200.21	164.44	14200.21	167.81	14200.21	172.81	14200.21	174.18	14200.21	174.76
14300	TRUE	-16.37	14300.22	158.27	14300.22	159.93	14300.22	164.36	14300.22	167.67	14300.22	172.71	14300.22	174.10	14300.22	174.64
14400	TRUE	-16.40	14400.22	158.31	14400.22	160.08	14400.22	164.54	14400.22	167.83	14400.22	172.87	14400.22	174.34	14400.22	174.71
14500	TRUE	-16.46	14500.22	158.54	14500.22	160.17	14500.22	164.56	14500.22	167.69	14500.22	172.99	14500.22	174.43	14500.22	175.00
14600	TRUE	-16.36	14600.22	158.30	14600.22	159.85	14600.22	164.09	14600.22	167.55	14600.22	172.52	14600.22	174.12	14600.22	174.66
14700	TRUE	-16.36	14700.22	158.42	14700.22	159.91	14700.22	164.28	14700.22	167.67	14700.22	172.67	14700.22	174.19	14700.22	174.79
14800	TRUE	-16.31	14800.22	158.54	14800.22	159.93	14800.22	164.21	14800.22	167.67	14800.22	172.77	14800.22	174.27	14800.22	174.85
14900	TRUE	-16.46	14900.23	158.80	14900.23	160.35	14900.23	164.68	14900.23	168.13	14900.23	173.13	14900.23	174.69	14900.23	175.26
15000	TRUE	-16.49	15000.23	158.62	15000.23	160.25	15000.23	164.75	15000.23	168.04	15000.23	173.10	15000.23	174.69	15000.23	175.10
15100	TRUE	-16.73	15100.23	158.75	15100.23	160.66	15100.23	165.12	15100.23	168.52	15100.23	173.51	15100.23	175.17	15100.23	175.48
15200	TRUE	-17.16	15200.23	158.22	15200.23	160.52	15200.23	165.05	15200.23	168.41	15200.23	173.48	15200.23	174.92	15200.23	175.38
15300	TRUE	-17.03	15300.23	163.58	15300.23	165.72	15300.23	169.23	15300.23	173.53	15300.23	178.74	15300.23	180.31	15300.23	180.61
15400	TRUE	-17.38	15400.23	174.63	15400.23	175.89	15400.23	181.01	15400.23	184.56	15400.23	190.16	15400.23	191.65	15400.23	192.01
15500	TRUE	-15.74	15500.23	161.20	15500.23	161.67	15500.23	166.22	15500.23	170.03	15500.23	175.11	15500.23	176.52	15500.23	176.94
15600	TRUE	-13.78	15600.24	162.39	15600.24	161.46	15600.24	166.38	15600.24	169.42	15600.24	174.37	15600.24	175.97	15600.24	176.17
15700	TRUE	-13.57	15700.24	162.68	15700.24	161.97	15700.24	165.27	15700.24	169.22	15700.24	174.48	15700.24	175.95	15700.24	176.24
15800	TRUE	-16.25	15800.24	160.12	15800.24	161.57	15800.24	166.11	15800.24	169.61	15800.24	174.69	15800.24	176.20	15800.24	176.37
15900	TRUE	-16.38	15900.24	160.32	15900.24	161.98	15900.24	166.65	15900.24	170.11	15900.24	175.08	15900.24	176.70	15900.24	176.70
16000	TRUE	-16.34	16000.24	160.87	16000.24	162.20	16000.24	166.90	16000.24	170.48	16000.24	175.45	16000.24	177.13	16000.24	177.22
16100	TRUE	-15.59	16100.24	161.27	16100.24	161.84	16100.24	166.27	16100.24	170.09	16100.24	175.20	16100.24	176.72	16100.24	176.86
16200	TRUE	-15.73	16200.24	161.25	16200.24	162.07	16200.24	166.75	16200.24	170.31	16200.24	175.30	16200.24	176.84	16200.24	176.98
16300	TRUE	-14.71	16300.25	162.22	16300.25	162.14	16300.25	166.94	16300.25	170.31	16300.25	175.41	16300.25	176.82	16300.25	176.93
16400	TRUE	-12.08	16400.25	165.14	16400.25	162.15	16400.25	166.67	16400.25	170.59	16400.25	175.64	16400.25	177.19	16400.25	177.22
16500	TRUE	-8.02	16500.25	168.97	16500.25	162.29	16500.25	166.67	16500.25	170.39	16500.25	175.40	16500.25	176.86	16500.25	176.99
16600	TRUE	-6.35	16600.25	170.88	16600.25	162.91	16600.25	167.30	16600.25	170.53	16600.25	175.63	16600.25	177.12	16600.25	177.24
16700	TRUE	-5.18	16700.25	171.70	16700.25	161.87	16700.25	166.50	16700.25	170.31	16700.25	175.32	16700.25	176.71	16700.25	176.87
16800	TRUE	-7.84	16800.25	168.95	16800.25	161.68	16800.25	166.68	16800.25	170.33	16800.25	175.39	16800.25	176.83	16800.25	176.79
16900	TRUE	-12.32	16900.26	164.35	16900.26	162.04	16900.26	167.23	16900.26	170.28	16900.26	175.39	16900.26	176.74	16900.26	176.68
17000	TRUE	-15.46	17000.26	161.53	17000.26	162.31	17000.26	166.98	17000.26	170.59	17000.26	175.55	17000.26	177.04	17000.26	176.99
17100	TRUE	-16.81	17100.26	159.95	17100.26	162.00	17100.26	166.55	17100.26	170.29	17100.26	175.36	17100.26	176.82	17100.26	176.76
17200	TRUE	-16.26	17200.26	159.99	17200.26	161.70	17200.26	166.84	17200.26	169.94	17200.26	175.00	17200.26	176.40	17200.26	176.25
17300	TRUE	-15.78	17300.26	160.45	17300.26	161.66	17300.26	165.93	17300.26	169.85	17300.26	174.96	17300.26	176.25	17300.26	176.24
17400	TRUE	-15.37	17400.26	161.02	17400.26	161.84	17400.26	166.33	17400.26	170.08	17400.26	175.15	17400.26	176.48	17400.26	176.39
17500	TRUE	-15.39	17500.26	161.10	17500.26	161.99	17500.26	166.86	17500.26	170.04	17500.26	175.21	17500.26	176.52	17500.26	176.49
17600	TRUE	-15.45	17600.27	160.60	17600.27	161.37	17600.27	166.03	17600.27	169.75	17600.27	174.72	17600.27	176.11	17600.27	176.05
17700	TRUE	-15.78	17700.27	160.38	17700.27	161.56	17700.27	166.37	17700.27	169.84	17700.27	174.86	17700.27	176.19	17700.27	176.16
17800	TRUE	-16.65	17800.27	159.58	17800.27	159.54	17800.27	166.12	17800.27	169.61	17800.27	174.80	17800.27	176.18	17800.27	176.22
17900	TRUE	-17.29	17900.27	159.29	17900.27	159.78	17900.27	166.61	17900.27	170.17	17900.27	175.20	17900.27	176.53	17900.27	176.58
18000	TRUE	-16.29	18000.27	160.27	18000.27	159.98	18000.27	166.60	18000.27	170.06	18000.27	175.12	18000.27	176.46	18000.27	176.56
18100	TRUE	-15.80	18100.27	161.10	18100.27	160.15	18100.27	166.67	18100.27	170.32	18100.27	175.47	18100.27	176.78	18100.27	176.89
18200	TRUE	-15.93	18200.28	160.86	18200.28	160.17	18200.28	166.62	18200.28	170.27	18200.28	175.26	18200.28	176.64	18200.28	176.80
18300	TRUE	-16.18	18300.28	160.65	18300.28	160.03	18300.28	166.67	18300.28	170.31	18300.28	175.21	18300.28	176.72	18300.28	176.83
18400	TRUE	-15.99	18400.28	161.11	18400.28	160.12	18400.28	166.87	18400.28	170.57	18400.28	175.54	18400.28	176.97	18400.28	177.10
18500	TRUE	-16.13	18500.28	161.58	18500.28	160.54	18500.28	167.48	18500.28	171.14	18500.28	176.13	18500.28	177.56	18500.28	177.71
18600	TRUE	-16.24	18600.28	161.55	18600.28	160.59	18600.28	167.43	18600.28	171.11	18600.28	176.15	18600.28	177.62	18600.28	177.80
18700	TRUE	-16.29	18700.28	161.34	18700.28	160.53	18700.28	167.34	18700.28	170.95	18700.28	175.96	18700.28	177.43	18700.28	177.63
18800	TRUE	-16.35	18800.28	161.32	18800.28	160.48	18800.28	167.28	18800.28	170.99	18800.28	176.02	18800.28	177.50	18800.28	177.67
18900	TRUE	-16.43	18900.29	161.41	18900.29	160.66	18900.29	167.56	18900.29	171.21	18900.29	176.27	18900.29	177.67	18900.29	177.84
19000	TRUE	-16.53	19000.29	161.33	19000.29	160.21	19000.29	167.54	19000.29	171.21	19000.29	176.22	19000.29	177.67	19000.29	177.86
19100	TRUE	-16.40	19100.29	160.75	19100.29	159.76	19100.29	166.94	19100.29	170.49	19100.29	175.55	19100.29	176.98	19100.29	177.15
19200	TRUE	-16.17	19200.29	160.49	19200.29	159.24	19200.29	166.49	19200.29	170.02	19200.29	175.03	19200.29	176.62	19200.29	176.65
19300	TRUE	-15.49	19300.29	160.41	19300.29	158.40	19300.29	165.67	19300.29	169.33	19300.29	174.36	19300.29	175.71	19300.29	175.90
19400	TRUE	-15.11	19400.29	160.06	19400.29	157.79	19400.29	164.72	19400.29	168.60	19400.29	173.55	19400.29	174.97	19400.29	175.18
19500	TRUE	-14.69	19500.29	158.67	19500.29	156.36	19500.29	163.44	19500.29	167.03	19500.29	171.73	19500.29	173.44	19500.29	173.35
19600	TRUE	-14.86	19600.30	157.22	19600.30	154.97	19600.30	162.03	19600.30	165.65	19600.30	170.42	19600.30	171.98	19600.30	172.07
19700	TRUE	-14.53	19700.30	155.01	19700.30	152.72	19700.30	159.70	19700.30	163.25	19700.30	168.06	19700.30	169.46	19700.30	169.54
19800	TRUE	-14.45	19800.30	152.53	19800.30	150.75	19800.30	157.27	19800.30	160.76	19800.30	165.45	19800.30	166.90	19800.30	166.97
19900	TRUE	-14.02	19900.30	149.66	19900.30	149.35	19900.30	154.19	19900.30	157.61	19900.30	162.21	19900.30	163.66	19900.30	163.69
20000	TRUE	-13.79	20000.30	146.46	20000.30	146.29	20000.30	151.00	20000.30	154.26	20000.30	158.88	20000.30	160.13	20000.30	160.25

Table K.1: Victaulic 75 and Washer Connected Black Steel Pipe Peak Signal Frequency and Magnitude. "Bandwidth" column indicates whether the Bandwidth Condition is satisfied (cont.)

Appendix L: BLACK STEEL PIPE OUTDOOR LABORATORY SETTING WITH FLEXIBLE PVC COUPLINGS AND WASHER

		Distance	0ft_vol100		10ft_vol100		20ft_vol100		22.75ft_vol100		30ft_vol100		40ft_vol100		42.5ft_vol100	
		Values	Rx_max_freq	Max_rx_mag	Rx_max_freq	Max_rx_mag	Rx_max_freq	Max_rx_mag	Rx_max_freq	Max_rx_mag	Rx_max_freq	Max_rx_mag	Rx_max_freq	Max_rx_mag	Rx_max_freq	Max_rx_mag
Tx_freq	Bandwidth	Attenuation/ft														
100	FALSE	NA	60.00	16.70	60.00	11.81	2.33	9.61	60.00	13.68	60.00	15.07	60.00	13.47	60.00	12.77
200	FALSE	NA	60.00	15.62	200.00	12.33	60.00	13.56	200.00	13.66	60.00	14.16	200.00	13.37	60.00	14.11
300	TRUE	1.37	300.00	19.93	300.00	18.46	300.00	18.77	300.00	20.13	300.00	17.60	300.00	19.37	300.00	18.55
400	TRUE	-1.24	400.01	24.71	400.01	24.72	400.01	25.54	400.01	25.40	400.01	26.39	400.01	25.56	400.01	25.95
500	TRUE	-0.85	500.01	28.60	500.01	27.97	500.01	27.87	500.01	28.70	500.01	29.76	500.01	29.22	500.01	29.45
600	TRUE	0.95	600.01	36.79	600.01	34.79	600.01	35.57	600.01	37.16	600.01	35.79	600.01	37.50	600.01	35.84
700	TRUE	-1.27	700.01	39.75	700.01	39.03	700.01	39.73	700.01	40.32	700.01	41.55	700.01	41.37	700.01	41.02
800	TRUE	-0.39	800.01	45.59	800.01	43.92	800.01	44.76	800.01	45.93	800.01	47.02	800.01	46.95	800.01	45.98
900	TRUE	1.09	900.01	53.52	900.01	50.53	900.01	51.82	900.01	52.91	900.01	54.12	900.01	53.02	900.01	52.43
1000	TRUE	0.28	1000.02	55.47	1000.02	52.80	1000.02	54.33	1000.02	54.65	1000.02	56.07	1000.02	55.35	1000.02	55.19
1100	TRUE	0.11	1100.02	66.77	1100.02	63.07	1100.02	64.65	1100.02	65.92	1100.02	67.31	1100.02	66.76	1100.02	66.67
1200	TRUE	-0.41	1200.02	62.42	1200.02	59.03	1200.02	60.85	1200.02	61.68	1200.02	63.26	1200.02	62.92	1200.02	62.83
1300	TRUE	-0.58	1300.02	65.94	1300.02	62.83	1300.02	65.05	1300.02	66.20	1300.02	67.04	1300.02	66.77	1300.02	66.52
1400	TRUE	-0.79	1400.02	71.05	1400.02	67.22	1400.02	69.78	1400.02	70.64	1400.02	72.72	1400.02	72.28	1400.02	71.84
1500	TRUE	-2.64	1500.02	80.35	1500.02	77.96	1500.02	80.63	1500.02	81.46	1500.02	83.70	1500.02	83.53	1500.02	82.99
1600	TRUE	-5.11	1600.02	75.10	1600.02	74.77	1600.02	77.30	1600.02	79.17	1600.02	79.92	1600.02	79.93	1600.02	80.21
1700	TRUE	-4.82	1700.03	77.81	1700.03	77.23	1700.03	80.21	1700.03	81.22	1700.03	82.90	1700.03	82.33	1700.03	82.63
1800	TRUE	-4.40	1800.03	84.69	1800.03	82.94	1800.03	86.06	1800.03	86.90	1800.03	89.33	1800.03	88.71	1800.03	89.09
1900	TRUE	-4.26	1900.03	93.79	1900.03	91.74	1900.03	94.85	1900.03	96.60	1900.03	98.31	1900.03	98.08	1900.03	98.04
2000	TRUE	-3.57	2000.03	90.02	2000.03	87.29	2000.03	90.62	2000.03	92.04	2000.03	94.62	2000.03	93.79	2000.03	93.60
2100	TRUE	-3.86	2100.03	92.74	2100.03	89.72	2100.03	92.95	2100.03	94.62	2100.03	97.00	2100.03	96.38	2100.03	96.60
2200	TRUE	-4.19	2200.03	95.28	2200.03	92.27	2200.03	96.03	2200.03	97.66	2200.03	99.43	2200.03	99.48	2200.03	99.47
2300	TRUE	-4.50	2300.03	98.30	2300.03	94.94	2300.03	98.40	2300.03	100.52	2300.03	102.78	2300.03	102.57	2300.03	102.80
2400	TRUE	-4.62	2400.04	101.13	2400.04	97.67	2400.04	101.21	2400.04	103.42	2400.04	105.85	2400.04	105.51	2400.04	105.74
2500	TRUE	-4.95	2500.04	104.00	2500.04	100.14	2500.04	104.19	2500.04	106.62	2500.04	108.79	2500.04	108.36	2500.04	108.95
2600	TRUE	-6.10	2600.04	115.04	2600.04	111.16	2600.04	116.11	2600.04	118.47	2600.04	120.94	2600.04	120.87	2600.04	121.14
2700	TRUE	-6.36	2700.04	110.21	2700.04	106.66	2700.04	111.50	2700.04	113.75	2700.04	116.46	2700.04	116.16	2700.04	116.58
2800	TRUE	-7.48	2800.04	107.95	2800.04	105.71	2800.04	110.17	2800.04	112.54	2800.04	115.02	2800.04	114.61	2800.04	115.43
2900	TRUE	-8.00	2900.04	109.58	2900.04	107.52	2900.04	111.91	2900.04	114.20	2900.04	116.89	2900.04	116.66	2900.04	117.58
3000	TRUE	-6.60	3000.05	112.59	3000.05	109.36	3000.05	113.55	3000.05	116.09	3000.05	118.77	3000.05	118.25	3000.05	119.19
3100	TRUE	-6.30	3100.05	115.23	3100.05	111.32	3100.05	116.22	3100.05	118.31	3100.05	121.15	3100.05	120.70	3100.05	121.53
3200	TRUE	-6.63	3200.05	116.87	3200.05	112.66	3200.05	117.55	3200.05	120.34	3200.05	122.84	3200.05	122.64	3200.05	123.50
3300	TRUE	-9.23	3300.05	119.93	3300.05	116.88	3300.05	122.16	3300.05	125.37	3300.05	128.34	3300.05	127.91	3300.05	129.16
3400	TRUE	-12.34	3400.05	126.21	3400.05	124.47	3400.05	130.56	3400.05	134.19	3400.05	137.44	3400.05	137.48	3400.05	138.55
3500	TRUE	-7.74	3500.05	120.51	3500.05	114.51	3500.05	120.28	3500.05	123.68	3500.05	126.93	3500.05	127.10	3500.05	128.24
3600	TRUE	-2.47	3600.05	125.80	3600.05	116.86	3600.05	121.39	3600.05	124.08	3600.05	126.92	3600.05	126.90	3600.05	128.27
3700	TRUE	-0.65	3700.06	130.85	3700.06	122.89	3700.06	126.83	3700.06	128.63	3700.06	130.74	3700.06	130.24	3700.06	131.50
3800	TRUE	-3.79	3800.06	133.31	3800.06	126.85	3800.06	131.83	3800.06	133.86	3800.06	136.62	3800.06	135.86	3800.06	137.10
3900	TRUE	-6.39	3900.06	135.02	3900.06	129.05	3900.06	134.55	3900.06	137.28	3900.06	140.42	3900.06	139.80	3900.06	141.41
4000	TRUE	-7.65	4000.06	136.67	4000.06	130.90	4000.06	136.59	4000.06	139.81	4000.06	143.04	4000.06	142.68	4000.06	144.33
4100	TRUE	-8.88	4100.06	149.59	4100.06	143.36	4100.06	149.75	4100.06	153.33	4100.06	157.09	4100.06	156.67	4100.06	158.47
4200	TRUE	-8.50	4200.06	141.98	4200.06	135.72	4200.06	141.93	4200.06	145.30	4200.06	148.96	4200.06	148.68	4200.06	150.48
4300	TRUE	-8.71	4300.07	138.49	4300.07	132.75	4300.07	138.63	4300.07	142.25	4300.07	145.74	4300.07	145.32	4300.07	147.20
4400	TRUE	-8.87	4400.07	139.64	4400.07	133.55	4400.07	139.66	4400.07	143.27	4400.07	146.88	4400.07	146.50	4400.07	148.51
4500	TRUE	-8.94	4500.07	140.15	4500.07	134.07	4500.07	140.21	4500.07	143.74	4500.07	147.40	4500.07	147.04	4500.07	149.09
4600	TRUE	-8.90	4600.07	141.31	4600.07	134.68	4600.07	141.09	4600.07	144.83	4600.07	148.38	4600.07	148.03	4600.07	150.22
4700	TRUE	-8.93	4700.07	141.63	4700.07	134.97	4700.07	141.43	4700.07	145.12	4700.07	148.82	4700.07	148.55	4700.07	150.57
4800	TRUE	-9.30	4800.07	141.98	4800.07	135.80	4800.07	142.10	4800.07	145.68	4800.07	149.45	4800.07	148.97	4800.07	151.28
4900	TRUE	-9.90	4900.07	142.17	4900.07	137.02	4900.07	143.16	4900.07	146.54	4900.07	150.17	4900.07	149.91	4900.07	152.07
5000	TRUE	-11.18	5000.08	142.65	5000.08	138.43	5000.08	144.82	5000.08	148.06	5000.08	151.90	5000.08	151.39	5000.08	153.83
5100	TRUE	-12.07	5100.08	143.08	5100.08	139.48	5100.08	145.89	5100.08	149.54	5100.08	153.30	5100.08	152.75	5100.08	155.15
5200	TRUE	-13.24	5200.08	152.14	5200.08	148.51	5200.08	155.40	5200.08	159.24	5200.08	163.32	5200.08	162.81	5200.08	165.38
5300	TRUE	-14.33	5300.08	152.12	5300.08	149.37	5300.08	156.27	5300.08	160.33	5300.08	164.40	5300.08	164.05	5300.08	166.45
5400	TRUE	-13.52	5400.08	145.02	5400.08	142.37	5400.08	148.93	5400.08	152.31	5400.08	156.17	5400.08	155.88	5400.08	158.54
5500	TRUE	-12.19	5500.08	147.25	5500.08	142.56	5500.08	149.59	5500.08	153.30	5500.08	157.09	5500.08	156.73	5500.08	159.44
5600	TRUE	-10.51	5600.08	149.42	5600.08	143.05	5600.08	149.61	5600.08	153.66	5600.08	157.65	5600.08	157.29	5600.08	159.93
5700	TRUE	-9.17	5700.09	151.49	5700.09	143.69	5700.09	150.52	5700.09	154.27	5700.09	158.29	5700.09	158.00	5700.09	160.66
5800	TRUE	-9.87	5800.09	151.60	5800.09	144.20	5800.09	151.08	5800.09	154.89	5800.09	159.03	5800.09	158.67	5800.09	161.46
5900	TRUE	-10.49	5900.09	152.04	5900.09	144.97	5900.09	151.93	5900.09	156.10	5900.09	159.87	5900.09	159.58	5900.09	162.53
6000	TRUE	-10.88	6000.09	152.08	6000.09	145.34	6000.09	152.41	6000.09	156.37	6000.09	160.53	6000.09	160.15	6000.09	162.97
6100	TRUE	-11.00	6100.09	152.68	6100.09	145.91	6100.09	153.17	6100.09	157.22	6100.09	161.40	6100.09	160.89	6100.09	163.68
6200	TRUE	-11.35	6200.09	152.91	6200.09	146.20	6200.09	153.32	6200.09	157.46	6200.09	161.68	6200.09	161.78	6200.09	164.25
6300	TRUE	-11.97	6300.10	157.52	6300.10	150.89	6300.10	158.20	6300.10	162.29	6300.10	166.72	6300.10	166.43	6300.10	169.49
6400	TRUE	-13.26	6400.10	167.25	6400.10	160.94	6400.10	168.62	6400.10	173.16	6400.10	177.67	6400.10	177.40	6400.10	180.51
6500	TRUE	-11.95	6500.10	154.63	6500.10	148.23	6500.10	155.48	6500.10	159.51	6500.10	163.81	6500.10	163.45	6500.10	166.58
6600	TRUE	-12.02	6600.10	154.19	6600.10	148.01	6600.10	155.14	6600.10	159.33	6600.10	163.46	6600.10	163.15	6600.10	166.21
6700	TRUE	-12.10	6700.10	154.18	6700.10	148.13	6700.10	155.39	6700.10	159.43	6700.10	163.64	6700.10	163.14	6700.10	166.28
6800	TRUE	-12.16	6800.10	154.61	6800.10	148.61	6800.10	155.74	6800.10	159.92	6800.10	163.97	6800.10	163.61	6800.10	166.76
6900	TRUE	-12.02	6900.10	155.54	6900.10	149.13	6900.10	156.49	6900.10	160.49	6900.10	164.67	6900.10	164.54	6900.10	167.56
7000	TRUE	-12.03	7000.11	156.09	7000.11	149.69	7000.11	156.88	7000.11	160.97	7000.11	165.24	7000.11	164.76	7000.11	168.12
7100	TRUE	-11.80	7100.11	156.23	7100.11	150.14	7100.11	157.18	7100.11	160.96	7100.11	165.18	7100.11	164.73	7100.11	168.04
7200	TRUE	-11.84	7200.11	156.85	7200.11	151.19	7200.11	158.22	7200.11	161.89	7200.11	165.91	7200.11	165.37	7200.11	168.70
7300	TRUE	-12.31	7300.11	157.49	7300.11	152.05	7300.11	159.22	7300.11	162.94	7300.11	167.15	7300.11	166.46	7300.11	169.80
7400	TRUE	-13.30	7400.11	158.26	7400.11	153.01	7400.11	160.43	7400.11	164.51	7400.11	168.65	7400.11	168.05	7400.11	171.56
7500	TRUE	-13.80	7500.11	158.62	7500.11	153.35	7500.11	161.07	7500.11	165.15	7500.11	169.54	7500.11	169.01	7500.11	172.42
7600	TRUE	-13.85	7600.11	159.58	7600.11	153.99	7600.11	161.63	7600.11	165.91	7600.11	170.36	7600.11	169.80	7600.11	173.43
7700	TRUE	-14.06	7700.12	159.60	7700.12	154.02	7700.12	161.72	7700.12	166.04	7700.12	170.58	7700.12	170.03	7700.12	173.66
7800	TRUE	-14.15	7800.12	164.81	7800.12	158.85	7800.12	166.77	7800.12	171.03	7800.12	175.79	7800.12	175.26	7800.12	178.96
7900	TRUE	-14.93	7900.12	175.40	7900.12	169.01	7900.12	177.46	7900.12	182.20	7900.12	187.15	7900.12	186.67	7900.12	190.34
8000	TRUE	-13.60	8000.12	161.95	8000.12	155.79	8000.12	163.48	8000.12	167.84	8000.12	172.43	8000.12	171.90	8000.12	175.55
8100	TRUE	-13.32	8100.12	161.76	8100.12	155.41	8100.12	163.02	8100.12	167.36	8100.12	171.90	8100.12	171.39	8100.12	175.09
8200	TRUE	-13.27	8200.12	161.81	8200.12	155.19	8200.12	163.02	8200.12	167.26	8200.12	171.85	8200.12	171.39	8200.12	175.09
8300	TRUE	-13.17	8300.13	162.06	8300.13	155.41	8300.13	163.10	8300.13	167.43	8300.13	172.09	8300.13	171.39	8300.13	175.23
8400	TRUE	-13.40	8400.13	162.53	8400.13	156.00	8400.13	163.63	8400.13	167.90	8400.13	172.74	8400.13	171.87	8400.13	175.94
8500	TRUE	-13.41	8500.13	162.97	8500.13	156.51	8500.13	164.37	8500.13	168.61	8500.13	173.19	8500.13	172.55	8500.13	176.38
8600	TRUE	-13.41	8600.13	162.99	8600.13	156.52	8600.13	164.38	8600.13	168.69	8600.13	173.04	8600.13	172.33	8600.13	176.40
8700	TRUE	-13.45	8700.13	163.30	8700.13	156.72	8700.13	164.57	8700.13	169.03	8700.13	173.67	8700.13	173.01	8700.13	176.75
8800	TRUE	-13.61	8800.13	163.65	8800.13	157.06	8800.13	165.18	8800.13	169.26	8800.13	174.01	8800.13	173.07	8800.13	177.26
8900	TRUE	-13.67	8900.13	164.24	8900.13	157.97	8900.13	165.74	8900.13	170.08	8900.13	174.76	8900.13	174.04	8900.13	177.91
9000	TRUE	-13.86	9000.14	164.33	9000.14	157.75	9000.14	165.76	9000.14	170.01	9000.14	174.71	9000.14	173.93	9000.14	178.19
9100	TRUE	-14.04	9100.14	164.86	9100.14	158.56	9100.14	166.56	9100.14	170.85	9100.14	175.59	9100.14	174.88	9100.14	178.90
9200	TRUE	-14.08	9200.14	164.92	9200.14	158.53	9200.14	166.55	9200.14	170.93	9200.14	175.60	9200.14	174.97	9200.14	178.99
9300	TRUE	-14.56	9300.14	164.95	9300.14	158.96	9300.14	166.88	9300.14	171.27	9300.14	176.06	9300.14	175.34	9300.14	179.51
9400	TRUE	-14.59	9400.14	165.16	9400.14	159.10	9400.14	167.09	9400.14	171.57	9400.14	176.34	9400.14	175.69	9400.14	179.75
9500	TRUE	-14.70	9500.14	165.82	9500.14	159.68	9500.14	167.71	9500.14	172.22	9500.14	177.04	9500.14	176.35	9500.14	180.51
9600	TRUE	-14.78	9600.15	165.96	9600.15	159.79	9600.15	167.86	9600.15	172.31	9600.15	177.06	9600.15	176.45	9600.15	180.74
9700	TRUE	-14.75	9700.15	165.92	9700.15	159.90	9700.15	167.85	9700.15	172.33	9700.15	177.13	9700.15	176.43	9700.15	180.67
9800	TRUE	-14.77	9800.15	166.22	9800.15	160.14	9800.15	168.15	9800.15	172.60	9800.15	177.47	9800.15	176.68	9800.15	180.98
9900	TRUE	-14.79	9900.15	166.72	9900.15	160.62	9900.15	168.67	9900.15	173.19	9900.15	177.95	9900.15	177.27	9900.15	181.51
10000	TRUE	-14.89	10000.15	167.72	10000.15	161.57	10000.15	169.69	10000.15	174.18	10000.15	179.04	10000.15	178.31	10000.15	182.61
10100	TRUE	-16.39	10100.15	182.16	10100.15	175.93	10100.15	184.73	10100.15	189.65	10100.15	194.89	10100.15	194.12	10100.15	198.55
10200	TRUE	-15.48	10200.15	171.82	10200.15	165.65	10200.15	173.89	10200.15	178.60	10200.15	183.75	10200.15	182.84	10200.15	187.30

Table L.1: Flexible PVC Coupling and Washer Connected Black Steel Pipe Peak Signal Frequency and Magnitude. “Bandwidth” column indicates whether the Bandwidth Condition is satisfied

		Distance	0ft_vol100		10ft_vol100		20ft_vol100		22.75ft_vol100		30ft_vol100		40ft_vol100		42.5ft_vol100	
		Values	Rx_max_freq	Max_rx_mag	Rx_max_freq	Max_rx_mag	Rx_max_freq	Max_rx_mag	Rx_max_freq	Max_rx_mag	Rx_max_freq	Max_rx_mag	Rx_max_freq	Max_rx_mag	Rx_max_freq	Max_rx_mag
Tx_freq	Bandwidth	Attenuation/ft														
10300	TRUE	-15.04	10300.16	167.13	10300.16	161.07	10300.16	169.12	10300.16	173.71	10300.16	178.54	10300.16	177.82	10300.16	182.17
10400	TRUE	-15.09	10400.16	167.43	10400.16	161.39	10400.16	169.49	10400.16	173.95	10400.16	178.91	10400.16	178.15	10400.16	182.53
10500	TRUE	-15.06	10500.16	167.30	10500.16	161.44	10500.16	169.29	10500.16	173.84	10500.16	178.74	10500.16	177.95	10500.16	182.36
10600	TRUE	-15.14	10600.16	167.49	10600.16	161.78	10600.16	169.53	10600.16	174.04	10600.16	179.00	10600.16	178.17	10600.16	182.63
10700	TRUE	-15.03	10700.16	167.31	10700.16	161.62	10700.16	169.36	10700.16	173.79	10700.16	178.69	10700.16	177.99	10700.16	182.34
10800	TRUE	-15.07	10800.16	167.39	10800.16	161.67	10800.16	169.33	10800.16	173.81	10800.16	178.69	10800.16	177.99	10800.16	182.46
10900	TRUE	-15.03	10900.16	167.29	10900.16	161.59	10900.16	169.30	10900.16	173.79	10900.16	178.72	10900.16	177.98	10900.16	182.32
11000	TRUE	-15.13	11000.17	167.58	11000.17	161.90	11000.17	169.68	11000.17	174.26	11000.17	179.06	11000.17	178.38	11000.17	182.72
11100	TRUE	-15.11	11100.17	167.47	11100.17	161.79	11100.17	169.55	11100.17	173.99	11100.17	178.89	11100.17	178.20	11100.17	182.58
11200	TRUE	-15.06	11200.17	167.19	11200.17	161.54	11200.17	169.18	11200.17	173.67	11200.17	178.65	11200.17	177.85	11200.17	182.25
11300	TRUE	-15.09	11300.17	167.23	11300.17	161.56	11300.17	169.28	11300.17	173.74	11300.17	178.67	11300.17	177.92	11300.17	182.33
11400	TRUE	-15.20	11400.17	167.44	11400.17	161.78	11400.17	169.56	11400.17	174.00	11400.17	178.96	11400.17	178.22	11400.17	182.64
11500	TRUE	-15.19	11500.17	167.68	11500.17	161.94	11500.17	169.74	11500.17	174.23	11500.17	179.15	11500.17	178.37	11500.17	182.87
11600	TRUE	-15.21	11600.18	167.28	11600.18	161.69	11600.18	169.47	11600.18	173.92	11600.18	178.82	11600.18	178.02	11600.18	182.49
11700	TRUE	-15.23	11700.18	167.43	11700.18	161.86	11700.18	169.56	11700.18	174.07	11700.18	178.90	11700.18	178.09	11700.18	182.66
11800	TRUE	-15.15	11800.18	167.52	11800.18	161.90	11800.18	169.65	11800.18	174.08	11800.18	179.14	11800.18	178.31	11800.18	182.67
11900	TRUE	-15.25	11900.18	167.79	11900.18	162.21	11900.18	169.91	11900.18	174.57	11900.18	179.44	11900.18	178.62	11900.18	183.03
12000	TRUE	-15.20	12000.18	167.77	12000.18	162.15	12000.18	169.82	12000.18	174.43	12000.18	179.38	12000.18	178.67	12000.18	182.98
12100	TRUE	-15.39	12100.18	167.97	12100.18	162.46	12100.18	170.25	12100.18	174.70	12100.18	179.68	12100.18	178.93	12100.18	183.37
12200	TRUE	-15.35	12200.18	167.92	12200.18	162.37	12200.18	170.10	12200.18	174.72	12200.18	179.55	12200.18	178.79	12200.18	183.27
12300	TRUE	-15.78	12300.19	172.94	12300.19	167.22	12300.19	175.23	12300.19	179.72	12300.19	185.07	12300.19	184.21	12300.19	188.72
12400	TRUE	-16.79	12400.19	183.70	12400.19	177.92	12400.19	186.37	12400.19	191.35	12400.19	196.76	12400.19	195.96	12400.19	200.49
12500	TRUE	-15.38	12500.19	169.36	12500.19	163.77	12500.19	171.58	12500.19	176.09	12500.19	181.07	12500.19	180.34	12500.19	184.74
12600	TRUE	-15.40	12600.19	168.73	12600.19	163.30	12600.19	170.99	12600.19	175.58	12600.19	180.49	12600.19	179.77	12600.19	184.13
12700	TRUE	-15.21	12700.19	168.63	12700.19	163.09	12700.19	170.91	12700.19	175.43	12700.19	180.38	12700.19	179.64	12700.19	183.83
12800	TRUE	-15.16	12800.19	168.84	12800.19	163.22	12800.19	171.04	12800.19	175.61	12800.19	180.60	12800.19	179.79	12800.19	184.00
12900	TRUE	-15.07	12900.20	169.30	12900.20	163.70	12900.20	171.42	12900.20	175.97	12900.20	180.98	12900.20	180.48	12900.20	184.37
13000	TRUE	-15.12	13000.20	169.60	13000.20	164.03	13000.20	171.78	13000.20	176.29	13000.20	181.34	13000.20	180.42	13000.20	184.72
13100	TRUE	-15.10	13100.20	169.29	13100.20	163.69	13100.20	171.47	13100.20	176.05	13100.20	181.05	13100.20	180.25	13100.20	184.39
13200	TRUE	-15.11	13200.20	169.37	13200.20	163.88	13200.20	171.60	13200.20	176.14	13200.20	181.11	13200.20	180.39	13200.20	184.48
13300	TRUE	-15.13	13300.20	169.39	13300.20	163.81	13300.20	171.58	13300.20	176.19	13300.20	181.23	13300.20	180.45	13300.20	184.52
13400	TRUE	-15.09	13400.20	169.62	13400.20	164.01	13400.20	171.83	13400.20	176.32	13400.20	181.60	13400.20	180.69	13400.20	184.72
13500	TRUE	-15.10	13500.20	169.45	13500.20	163.90	13500.20	171.72	13500.20	176.43	13500.20	181.36	13500.20	180.45	13500.20	184.55
13600	TRUE	-15.02	13600.21	169.69	13600.21	164.06	13600.21	171.90	13600.21	176.50	13600.21	181.53	13600.21	180.72	13600.21	184.71
13700	TRUE	-14.99	13700.21	169.31	13700.21	163.85	13700.21	171.61	13700.21	176.21	13700.21	181.23	13700.21	180.41	13700.21	184.30
13800	TRUE	-14.90	13800.21	169.32	13800.21	163.61	13800.21	171.62	13800.21	176.21	13800.21	181.25	13800.21	180.35	13800.21	184.22
13900	TRUE	-15.03	13900.21	169.12	13900.21	163.78	13900.21	171.50	13900.21	176.10	13900.21	181.14	13900.21	180.29	13900.21	184.16
14000	TRUE	-14.84	14000.21	169.62	14000.21	164.10	14000.21	171.83	14000.21	176.40	14000.21	181.45	14000.21	180.68	14000.21	184.46
14100	TRUE	-14.87	14100.21	169.25	14100.21	163.80	14100.21	171.67	14100.21	176.14	14100.21	181.22	14100.21	180.55	14100.21	184.12
14200	TRUE	-14.87	14200.21	168.94	14200.21	163.58	14200.21	171.26	14200.21	175.81	14200.21	180.85	14200.21	180.08	14200.21	183.81
14300	TRUE	-14.87	14300.22	168.85	14300.22	163.47	14300.22	171.20	14300.22	175.75	14300.22	180.82	14300.22	179.90	14300.22	183.72
14400	TRUE	-14.95	14400.22	169.01	14400.22	163.53	14400.22	171.46	14400.22	175.99	14400.22	180.82	14400.22	180.22	14400.22	183.96
14500	TRUE	-14.84	14500.22	169.23	14500.22	163.85	14500.22	171.52	14500.22	176.08	14500.22	181.15	14500.22	180.29	14500.22	184.07
14600	TRUE	-14.72	14600.22	168.83	14600.22	163.50	14600.22	171.14	14600.22	175.69	14600.22	180.69	14600.22	179.85	14600.22	183.54
14700	TRUE	-14.69	14700.22	168.93	14700.22	163.49	14700.22	171.24	14700.22	175.65	14700.22	180.82	14700.22	179.82	14700.22	183.62
14800	TRUE	-14.66	14800.22	168.82	14800.22	163.53	14800.22	171.22	14800.22	175.62	14800.22	180.71	14800.22	179.83	14800.22	183.48
14900	TRUE	-14.79	14900.23	169.08	14900.23	163.82	14900.23	171.46	14900.23	175.92	14900.23	181.02	14900.23	180.14	14900.23	183.87
15000	TRUE	-14.78	15000.23	168.89	15000.23	163.68	15000.23	171.25	15000.23	175.78	15000.23	180.88	15000.23	179.96	15000.23	183.67
15100	TRUE	-14.83	15100.23	169.12	15100.23	164.03	15100.23	171.66	15100.23	176.11	15100.23	181.20	15100.23	180.35	15100.23	183.95
15200	TRUE	-14.77	15200.23	169.02	15200.23	163.92	15200.23	171.43	15200.23	175.92	15200.23	181.03	15200.23	180.14	15200.23	183.79
15300	TRUE	-15.17	15300.23	174.04	15300.23	168.77	15300.23	176.71	15300.23	181.15	15300.23	186.42	15300.23	185.55	15300.23	189.22
15400	TRUE	-16.11	15400.23	184.92	15400.23	179.53	15400.23	187.84	15400.23	192.70	15400.23	198.26	15400.23	197.32	15400.23	201.03
15500	TRUE	-14.76	15500.23	170.52	15500.23	165.18	15500.23	172.97	15500.23	177.31	15500.23	182.44	15500.23	181.63	15500.23	185.28
15600	TRUE	-14.73	15600.24	169.88	15600.24	164.68	15600.24	172.35	15600.24	176.80	15600.24	181.88	15600.24	180.95	15600.24	184.61
15700	TRUE	-14.70	15700.24	169.76	15700.24	164.50	15700.24	172.17	15700.24	176.63	15700.24	181.73	15700.24	180.79	15700.24	184.46
15800	TRUE	-14.80	15800.24	169.81	15800.24	164.69	15800.24	172.32	15800.24	176.73	15800.24	181.90	15800.24	180.93	15800.24	184.61
15900	TRUE	-14.73	15900.24	170.30	15900.24	165.02	15900.24	172.74	15900.24	177.16	15900.24	182.31	15900.24	181.37	15900.24	185.03
16000	TRUE	-14.81	16000.24	170.54	16000.24	165.25	16000.24	173.07	16000.24	177.46	16000.24	182.67	16000.24	181.72	16000.24	185.35
16100	TRUE	-14.79	16100.24	170.19	16100.24	164.94	16100.24	172.63	16100.24	177.15	16100.24	182.18	16100.24	181.35	16100.24	184.98
16200	TRUE	-14.81	16200.24	170.21	16200.24	165.06	16200.24	172.78	16200.24	177.15	16200.24	182.24	16200.24	181.50	16200.24	185.02
16300	TRUE	-14.87	16300.25	170.16	16300.25	164.98	16300.25	172.69	16300.25	177.25	16300.25	182.24	16300.25	181.37	16300.25	185.03
16400	TRUE	-14.88	16400.25	170.39	16400.25	165.30	16400.25	172.96	16400.25	177.45	16400.25	182.63	16400.25	181.69	16400.25	185.27
16500	TRUE	-14.87	16500.25	170.16	16500.25	165.08	16500.25	172.75	16500.25	177.21	16500.25	182.36	16500.25	181.47	16500.25	185.03
16600	TRUE	-14.93	16600.25	170.30	16600.25	165.28	16600.25	173.03	16600.25	177.41	16600.25	182.48	16600.25	181.66	16600.25	185.23
16700	TRUE	-14.88	16700.25	169.99	16700.25	164.97	16700.25	172.63	16700.25	177.08	16700.25	182.27	16700.25	181.40	16700.25	184.87
16800	TRUE	-14.90	16800.25	169.94	16800.25	164.92	16800.25	172.68	16800.25	177.00	16800.25	182.18	16800.25	181.27	16800.25	184.84
16900	TRUE	-14.86	16900.26	169.81	16900.26	164.85	16900.26	172.51	16900.26	176.93	16900.26	182.04	16900.26	181.12	16900.26	184.67
17000	TRUE	-14.84	17000.26	170.09	17000.26	165.09	17000.26	172.74	17000.26	177.13	17000.26	182.31	17000.26	181.43	17000.26	184.94
17100	TRUE	-14.85	17100.26	169.79	17100.26	164.75	17100.26	172.46	17100.26	176.89	17100.26	181.99	17100.26	181.03	17100.26	184.64
17200	TRUE	-14.87	17200.26	169.36	17200.26	164.49	17200.26	172.08	17200.26	176.43	17200.26	181.61	17200.26	180.63	17200.26	184.22
17300	TRUE	-14.87	17300.26	169.22	17300.26	164.33	17300.26	171.93	17300.26	176.33	17300.26	181.45	17300.26	180.57	17300.26	184.09
17400	TRUE	-15.06	17400.26	169.21	17400.26	164.57	17400.26	172.22	17400.26	176.50	17400.26	181.70	17400.26	180.76	17400.26	184.27
17500	TRUE	-14.89	17500.26	169.42	17500.26	164.56	17500.26	172.24	17500.26	176.59	17500.26	181.73	17500.26	180.75	17500.26	184.31
17600	TRUE	-14.92	17600.27	168.98	17600.27	164.20	17600.27	171.87	17600.27	176.09	17600.27	181.25	17600.27	180.33	17600.27	183.90
17700	TRUE	-14.81	17700.27	169.05	17700.27	164.29	17700.27	171.82	17700.27	176.15	17700.27	181.30	17700.27	180.34	17700.27	183.86
17800	TRUE	-14.85	17800.27	168.99	17800.27	164.09	17800.27	171.85	17800.27	176.16	17800.27	181.30	17800.27	180.39	17800.27	183.84
17900	TRUE	-14.86	17900.27	169.29	17900.27	164.57	17900.27	172.20	17900.27	176.52	17900.27	181.63	17900.27	180.67	17900.27	184.16
18000	TRUE	-14.87	18000.27	169.24	18000.27	164.55	18000.27	172.15	18000.27	176.37	18000.27	181.54	18000.27	180.56	18000.27	184.11
18100	TRUE	-14.86	18100.27	169.47	18100.27	164.76	18100.27	172.40	18100.27	176.66	18100.27	181.86	18100.27	180.91	18100.27	184.33
18200	TRUE	-14.96	18200.28	169.25	18200.28	164.59	18200.28	172.24	18200.28	176.49	18200.28	181.63	18200.28	180.76	18200.28	184.21
18300	TRUE	-14.89	18300.28	169.35	18300.28	164.52	18300.28	172.18	18300.28	176.52	18300.28	181.65	18300.28	180.64	18300.28	184.25
18400	TRUE	-14.90	18400.28	169.40	18400.28	164.84	18400.28	172.35	18400.28	176.77	18400.28	181.97	18400.28	181.04	18400.28	184.31
18500	TRUE	-15.04	18500.28	169.87	18500.28	165.37	18500.28	172.76	18500.28	177.25	18500.28	182.50	18500.28	181.51	18500.28	184.91
18600	TRUE	-15.03	18600.28	169.91	18600.28	165.31	18600.28	172.91	18600.28	177.18	18600.28	182.44	18600.28	181.55	18600.28	184.94
18700	TRUE	-15.01	18700.28	169.68	18700.28	165.11	18700.28	172.70	18700.28	177.02	18700.28	182.19	18700.28	181.25	18700.28	184.69
18800	TRUE	-15.04	18800.28	169.63	18800.28	165.10	18800.28	172.64	18800.28	176.87	18800.28	182.15	18800.28	181.15	18800.28	184.67
18900	TRUE	-15.09	18900.29	169.71	18900.29	165.22	18900.29	172.72	18900.29	177.04	18900.29	182.31	18900.29	181.43	18900.29	184.80
19000	TRUE	-15.07	19000.29	169.62	19000.29	165.15	19000.29	172.46	19000.29	176.83	19000.29	182.17	19000.29	181.24	19000.29	184.69
19100	TRUE	-14.98	19100.29	168.90	19100.29	164.40	19100.29	171.84	19100.29	176.23	19100.29	181.38	19100.29	180.54	19100.29	183.88
19200	TRUE	-14.79	19200.29	168.37	19200.29	163.88	19200.29	171.36	19200.29	175.47	19200.29	180.76	19200.29	179.86	19200.29	183.16
19300	TRUE	-14.87	19300.29	167.55	19300.29	163.24	19300.29	170.55	19300.29	174.95	19300.29	180.01	19300.29	179.10	19300.29	182.42
19400	TRUE	-14.77	19400.29	166.78	19400.29	162.41	19400.29	169.73	19400.29	174.09	19400.29	179.21	19400.29	178.26	19400.29	181.55
19500	TRUE	-14.57	19500.29	165.20	19500.29	160.92	19500.29	168.21	19500.29	172.29	19500.29	177.29	19500.29	176.36	19500.29	179.77
19600	TRUE	-14.53	19600.30	163.68	19600.30	159.44	19600.30	166.64	19600.30	170.85	19600.30	175.91	19600.30	174.98	19600.30	178.21
19700	TRUE	-14.32	19700.30	161.34	19700.30	157.20	19700.30	164.23	19700.30	168.59	19700.30	173.34	19700.30	172.43	19700.30	175.65
19800	TRUE	-14.17	19800.30	158.68	19800.30	154.71	19800.30	161.62	19800.30	165.68	19800.30	170.61	19800.30	169.66	19800.30	172.85
19900	TRUE	-13.84	19900.30	155.55	19900.30	151.64	19900.30	158.34	19900.30	162.46	19900.30	167.20	19900.30	166.27	19900.30	169.39
20000	TRUE	-13.50	20000.30	152.18	20000.30	148.38	20000.30	154.98	20000.30	158.41	20000.30	163.62	20000.30	162.74	20000.30	165.68

Table L.1: Flexible PVC Coupling and Washer Connected Black Steel Pipe Peak Signal Frequency and Magnitude. "Bandwidth" column indicates whether the Bandwidth Condition is satisfied (cont.)